INTERACTIONS BETWEEN BIOACTIVE FOOD INGREDIENTS AND INTESTINAL MICROBIOTA

EDITED BY: Zheng Ruan, Xiaodong Xia, Guodong Zhang and Fengjie Sun
PUBLISHED IN: Frontiers in Microbiology

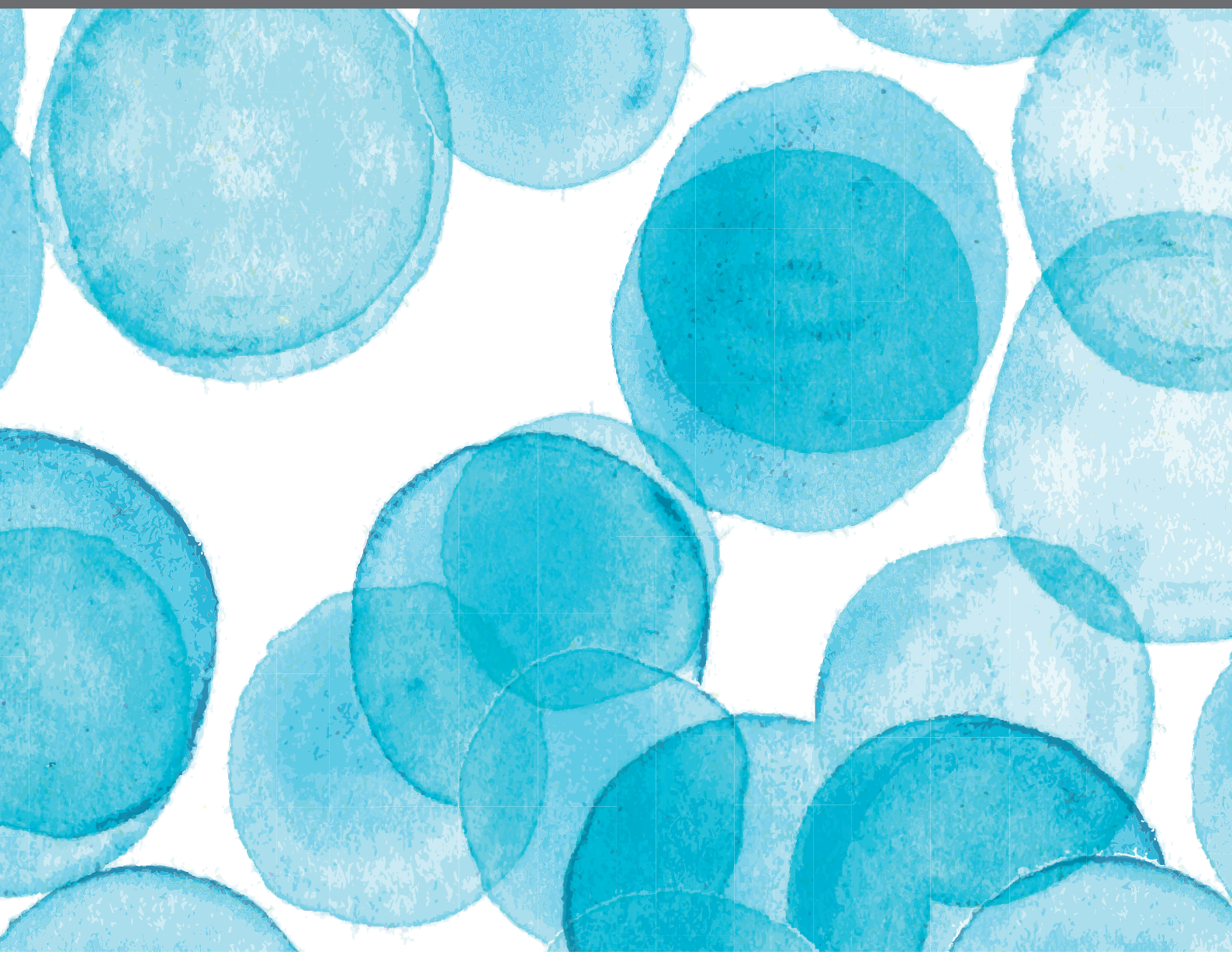

frontiers Research Topics

ISSN 1664-8714
ISBN 978-2-88976-145-6
DOI 10.3389/978-2-88976-145-6

About Frontiers

Frontiers is more than just an open-access publisher of scholarly articles: it is a pioneering approach to the world of academia, radically improving the way scholarly research is managed. The grand vision of Frontiers is a world where all people have an equal opportunity to seek, share and generate knowledge. Frontiers provides immediate and permanent online open access to all its publications, but this alone is not enough to realize our grand goals.

Frontiers Journal Series

The Frontiers Journal Series is a multi-tier and interdisciplinary set of open-access, online journals, promising a paradigm shift from the current review, selection and dissemination processes in academic publishing. All Frontiers journals are driven by researchers for researchers; therefore, they constitute a service to the scholarly community. At the same time, the Frontiers Journal Series operates on a revolutionary invention, the tiered publishing system, initially addressing specific communities of scholars, and gradually climbing up to broader public understanding, thus serving the interests of the lay society, too.

Dedication to Quality

Each Frontiers article is a landmark of the highest quality, thanks to genuinely collaborative interactions between authors and review editors, who include some of the world's best academicians. Research must be certified by peers before entering a stream of knowledge that may eventually reach the public - and shape society; therefore, Frontiers only applies the most rigorous and unbiased reviews.
Frontiers revolutionizes research publishing by freely delivering the most outstanding research, evaluated with no bias from both the academic and social point of view. By applying the most advanced information technologies, Frontiers is catapulting scholarly publishing into a new generation.

What are Frontiers Research Topics?

Frontiers Research Topics are very popular trademarks of the Frontiers Journals Series: they are collections of at least ten articles, all centered on a particular subject. With their unique mix of varied contributions from Original Research to Review Articles, Frontiers Research Topics unify the most influential researchers, the latest key findings and historical advances in a hot research area! Find out more on how to host your own Frontiers Research Topic or contribute to one as an author by contacting the Frontiers Editorial Office: frontiersin.org/about/contact

INTERACTIONS BETWEEN BIOACTIVE FOOD INGREDIENTS AND INTESTINAL MICROBIOTA

Topic Editors:
Zheng Ruan, Nanchang University, China
Xiaodong Xia, Dalian Polytechnic University, China
Guodong Zhang, University of Massachusetts Amherst, United States
Fengjie Sun, Georgia Gwinnett College, United States

Citation: Ruan, Z., Xia, X., Zhang, G., Sun, F., eds. (2022). Interactions Between Bioactive Food Ingredients and Intestinal Microbiota. Lausanne: Frontiers Media SA. doi: 10.3389/978-2-88976-145-6

Table of Contents

frontiers | Frontiers in Microbiology

EDITORIAL
published: 22 April 2022
doi: 10.3389/fmicb.2022.902962

Editorial: Interactions Between Bioactive Food Ingredients and Intestinal Microbiota

Zheng Ruan[1]*, *Fengjie Sun*[2], *Xiaodong Xia*[3] and *Guodong Zhang*[4]

[1] School of Food Science and Technology, Nanchang University, Nanchang, China, [2] School of Science and Technology, Georgia Gwinnett College, Lawrenceville, GA, United States, [3] School of Food Science and Technology, Dalian Polytechnic University, Dalian, China, [4] Department of Food Science, University of Massachusetts Amherst, Amherst, MA, United States

Keywords: Bioactive Food Ingredients, gut health, gut microbiota, polyphenol, microbe-microbe interactions, metabolomics

Editorial on the Research Topic

Interactions Between Bioactive Food Ingredients and Intestinal Microbiota

With the rapid advancement in the various "omics" technologies, a wide range of strategies (e.g., the application of dietary nutrients) have been extensively explored worldwide to improve the human health (Hasin et al., 2017; Nayak et al., 2021; Si et al., 2021). Numerous studies have shown that the microorganisms that colonize the gastrointestinal tract play important roles in not only the digestion and absorption of dietary nutrients, but also the regulation of various biological activities in hosts, e.g., metabolism, immunity, and intestinal barrier function (Wang et al., 2019: Han et al., 2021; Singh et al., 2021). Furthermore, multiple lines of evidence have suggested that food containing nutrients and polyphenols plays critical roles in determining the composition and function of the gut microbiota, ultimately directly or indirectly mediating the host's physiological activities (Ray and Mukherjee, 2021). To date, the molecular mechanisms regulating the interactions among the food nutrients/prebiotics, gut microbiota, and host health remain largely unclear.

It is commonly believed that the dietary approaches are effective to improve human health by the precision microbiome modulation (Deehan et al., 2020). Therefore, clear understanding of the molecular mechanisms that regulate the gut microbiota and its metabolic activities by dietary nutrients is beneficial in developing the dietary strategies. Delighted by these exciting achievements in the studies of the interactions among food nutrients, gut microbiota, and human health, we strongly believe it is necessary and important to further strengthen the current contributions from scholars worldwide particularly in the areas of the interactions between food nutrient and gut microbiota and the roles played by these interactions in the development of dysbiosis and low-grade inflammation during the intestinal barrier dysfunction and metabolic disorders in hosts. We here summarize the main results of the 21 out of a total of 27 submissions contributed by over 170 contributors accepted for publication in our Research Topic entitled "Interactions between Bioactive Food Ingredients and Intestinal Microbiota" in the journal *Frontiers in Microbiology*.

Briefly, these following topics are widely explored by the studies in this Research Topic: modulation of gut microbiome composition and function by food nutrients in metabolic disorders or inflammation-related intestinal diseases, the possible mechanisms for the microbial metabolites derived from dietary in mediating the physiological activities in hosts, the microbe-microbe interactions with the nutritional intervention, including the microbial communication and signaling, interactions among diet, gut microbiota, and gut health/host metabolism, development of nutritional strategies to precisely modulate gut microbiome and gut health. Most of the

OPEN ACCESS

Edited and reviewed by:
Aldo Corsetti,
University of Teramo, Italy

***Correspondence:**
Zheng Ruan
ruanzheng@ncu.edu.cn

Specialty section:
This article was submitted to Food Microbiology, a section of the journal Frontiers in Microbiology

Received: *23 March 2022*
Accepted: *04 April 2022*
Published: *22 April 2022*

Citation:
Ruan Z, Sun F, Xia X and Zhang G (2022) Editorial: Interactions Between Bioactive Food Ingredients and Intestinal Microbiota. Front. Microbiol. 13:902962. doi: 10.3389/fmicb.2022.902962

contributions collected in this Research Topic are performed based mainly on animal models, i.e., nine articles on pigs, nine on mice or rats, one on chicken, and one on bacteria, using various well-established "omics" analyses, as well as one review article. We here summarize the main results derived from these contributions.

First, in the nine contributions based on pigs, various substances have been supplemented in diet to significantly increase the growth performance and immunity and alter the composition of the gut microbiota. For example, Li et al. have shown strong evidence to suggest that as an indispensable essential micronutrient for humans and other animals, the organic selenium (i.e., 2-hydroxy-4-methylselenobutanoic acid) is capable of significantly increasing the antioxidant capacity and immune function and changing the intestinal microbiota in gilts, while the expression patterns of various genes related to selenoproteins and various cytokines are significantly regulated. This study demonstrates the potential applications of organic selenium in gilt and pig productions. Similarly, Diao et al. have shown the strong effects of dietary zinc on the growth performance and gut health in weaned piglets, as suggested by various growth performance factors and significantly regulated expressions of digestion and absorption related genes. Furthermore, several types of plant products are revealed to show the enhancing effects on the growth performance in piglets. For example, Li et al. have used the mixture of five fermented traditional Chinese medicinal herbs, including *Codonopsis pilosula* (Dangshen), *Radix astragalus* (Huangqi), *R. isatidis* (Banlangen), *R. paeoniae alba* (Baishao), and *Atractylodes macrocephala* (Baizhu), to significantly increase the growth performance and change the intestinal microbiota in piglets, while the mixture is also capable of increasing the total antioxidant capacity and decreasing the damage caused by H_2O_2 to the tight junction proteins of the porcine small intestinal epithelial cell line. Similarly, Li et al. have revealed the strong effects of the dietary fermented mao-tai lees (i.e., a by-product of Maotai liquor) on the growth performance, plasma metabolites, including various types of amino acids, and intestinal microbiota and metabolites of weaned piglets. It is interestingly noted that the amino acid metabolism is enhanced by the mao-tai lees without affecting the growth performance in the weaned piglets. Furthermore, Luo et al. and Gu et al. have shown that another two types of fermented plant products, i.e., alfalfa meal and cottonseed meal, have significantly improved the growth performance, intestinal health and immunity in weaned pigs. For example, the expressions of genes involved in immunity and intestinal barrier are significantly increased in piglets fed with alfalfa meal. These studies have provided the solid evidence to support the partial use of fermented plant products as the dietary component to ultimately reduce the consumption of grain. Moreover, Luo et al. have demonstrated that different types of dietary fibers (i.e., peahull fiber, oat bran, and the mixture of both) are revealed to show differential effects on intestinal health of growing pigs, as suggested by the varied taxonomic structures in the gut microbiota and immune-related indices. Additionally, Yu et al. have explored the alternation of the intestinal microbiota in porcine fed with the dietary manno-oligosaccharide, which is a type of prebiotic generally derived from plants or yeasts, providing novel insights into the molecular mechanisms regulating the interactions between the health and the intestinal microbiota modulated by the manno-oligosaccharide. By metagenomic sequencing, Hu et al. have investigated the effect of berberine, which is generally used as an antibacterial medicine, on the intestinal microbiome in weaned piglets. Their results have revealed significant improvements in composition, abundance, structure, and function of gut microbiome in the weaned piglets treated with berberine, providing strong evidence to support the application of berberine in human and animal health.

Second, in another nine articles based on mice or rats, various types of plant products (e.g., tea), extracts from both plants and fungi (i.e., polysaccharides, flavones, polyphenol (i.e., ellagic acid), and gastrodin), and bacteria have been used to enhance the health performance in mouse or rat models. For example, Wang et al. and Feng et al. have investigated the effects of Tibetan tea and green tea, respectively, on the gut microbiota in mouse models. Specifically, their results have revealed the protective effects on the ulcerative colitis in mice, with the expressions of genes involved in the pathways of inflammation and immune system significantly regulated, while both the β-Carotin and green tea powder have shown alleviating effects on the symptoms of gouty arthritis and have improved the gut microbiota in mice, probably attributing to the high contents of dietary fiber in both substances. Yang et al. and Fu et al. have used the plant polysaccharides derived from *Lycium barbarum* and *Portulaca oleracea* to reduce the obesity in mice fed with high-fat diet and to modulate the intestinal microbiota and inhibit the reproduction of pathogenic bacteria in aged rats, respectively. Their results have revealed that these polysaccharides may be the potential sources of prebiotics to improve the lipid metabolism and intestinal diseases. Additionally, the functions of another two types of plant extracts, i.e., gastrodin and ellagic acid, have been investigated by Wang et al. and Xu et al. in mouse models, respectively. As a type of phenolic glycoside, gastrodin is the main bioactive constituent of *Rhizoma gastrodiae*, while ellagic acid is generally found in many types of fruits and vegetables. Specifically, gastrodin has been revealed to show both the analgesic and anxiolytic effects and influence both the ferroptosis and jejunal microbiota in mice, while the ellagic acid is capable of enhancing the growth of mice, promoting the intestinal development, increasing the antioxidant capacity, and regulating the intestinal microbiota in mice. Furthermore, Xu et al. and Xu et al. have investigated the effects of the polysaccharides and flavones derived from the fungal species *Scorias spongiosa* and *Morchella importuna* on the intestinal microbiota in mice, respectively. Their results have revealed that although the polysaccharides derived from *Scorias spongiosa* have shown no significant effects on the growth performance of mice, the polysaccharides benefit the intestinal health in mice through a molecular mechanism with the involvement of elevated antioxidant and anti-inflammatory activities and significantly regulated intestinal microbiota, while the polysaccharides derived from *Morchella importuna* have shown protective effects on the damage in mice induced by

the dextran sulfate sodium through the mechanism with the inhibition of the nuclear factor kappa B and the activation of the nuclear factor erythroid 2–related factor 2 as well as the regulation of intestinal microbiota. Moreover, Xie et al. have shown that *Lactiplantibacillus plantarum* AR113 is capable of significantly accelerating the liver regeneration by regulating the gut microbiota and plasma glycerophospholipid in rats.

Third, in the only contribution based on chicken in this Research Topic, Chen et al. have performed the multi-omics analysis in chickens with the vaginal administration of *Bacteroides fragilis*. Their results have provided a theoretical basis for the application of *B. fragilis* as a potential probiotic in livestock and poultry production.

Fourth, Fan et al. have investigated the effects of osmotic pressure on the translation efficiency of *Lactobacillus rhamnosus* based on the ribosome profiling analysis at the genomic level. As a probiotic strain, *L. rhamnosus* has been widely used in various types of fermented and functional food production, playing an important role in modern biotechnological fermentation processes. The results of ribosome profiling analysis have shown that *L. rhamnosus* responds to osmotic stress by translation regulation and controls the balance between survival and growth of cells by transcription and translation.

Lastly, in the only review contribution collected in this Research Topic, Hong et al. have investigated the well-known antioxidant activities of tea polyphenols to further explore the metabolic pathways with the involvement of host-microbiota interactions. They have established the significance of several intestinal metabolites (i.e., 5-hydroxytryptamine and short-chain fatty acids) in the assessment of the tea polyphenol-mediated chronic brain diseases. This review provides novel insights into the molecular mechanisms regulating the interactions between the chronic neurological disorders and the microbial metabolites.

In summary, the collection of these front-line contributions has evidently shown not only the main advancements in these areas covered in this Research Topic to potentially make significant improvement in human health, but also the future directions with the challenges displayed for the scholars to pursue in their investigations. With the discoveries of many types of substances showing the capability of enhancing the growth performance, immunity, and the intestinal microbiota in piglets as well as the rapidly developing "omics" technologies, it is optimistically foreseen that in the near future, we would see another unprecedented wave of major achievements obtained in these areas covered in this Research Topic closely related to human health.

AUTHOR CONTRIBUTIONS

ZR and FS wrote the original draft. XX and GZ edited and reviewed the manuscript. All authors contributed to the article and approved the submitted version.

REFERENCES

Deehan, E. C., Yang, C., Perez-Muñoz, M. E., Nguyen, N., Cheng, C. C., Triador, L., et al. (2020). Precision microbiome modulation with discrete dietary fiber structures directs short-chain fatty acid production. *Cell Host Microbe* 27, 389–404. doi: 10.1016/j.chom.2020.01.006

Han, S., Lu, Y., Xie, J., Fei, Y., Zheng, G., Wang, Z., et al. (2021). Probiotic gastrointestinal transit and colonization after oral administration: a long journey. *Front. Cell. Infect. Microbiol.* 11, 609722. doi: 10.3389/fcimb.2021.609722

Hasin, Y., Seldin, M., and Lusis, A. (2017). Multi-omics approaches to disease. *Genome Biol.* 18, 83. doi: 10.1186/s13059-017-1215-1

Nayak, S. N., Aravind, B., Malavalli, S. S., Sukanth, B. S., Poornima, R., Bharati, P., et al. (2021). Omics technologies to enhance plant based functional foods: an overview. *Front. Genet.* 12, 742095. doi: 10.3389/fgene.2021.742095

Ray, S. K., and Mukherjee, S. (2021). Evolving interplay between dietary polyphenols and gut microbiota—an emerging importance in healthcare. *Front. Nutr.* 8, 634944. doi: 10.3389/fnut.2021.634944

Si, W., Zhang, Y., Li, X., Du, Y., and Xu, Q. (2021). Understanding the functional activity of polyphenols using omics-based approaches. *Nutrients* 13, 3953. doi: 10.3390/nu1311 3953

Singh, R., Zogg, H., Wei, L., Bartlett, A., Ghoshal, U. C., Rajender, S., et al. (2021). Gut microbial dysbiosis in the pathogenesis of gastrointestinal dysmotility and metabolic disorders. *J. Neurogastroenterol. Motil.* 27, 19–34. doi: 10.5056/jnm20149

Wang, G., Huang, S., Wang, Y., Cai, S., Yu, H., Liu, H., et al. (2019). Bridging intestinal immunity and gut microbiota by metabolites. *Cell. Mol. Life Sci.* 76, 3917–3937. doi: 10.1007/s00018-019-03190-6

Conflict of Interest: The authors declare that the research was conducted in the absence of any commercial or financial relationships that could be construed as a potential conflict of interest.

Publisher's Note: All claims expressed in this article are solely those of the authors and do not necessarily represent those of their affiliated organizations, or those of the publisher, the editors and the reviewers. Any product that may be evaluated in this article, or claim that may be made by its manufacturer, is not guaranteed or endorsed by the publisher.

frontiers in Microbiology

ORIGINAL RESEARCH
published: 16 August 2021
doi: 10.3389/fmicb.2021.723190

Organic Selenium Increased Gilts Antioxidant Capacity, Immune Function, and Changed Intestinal Microbiota

*Zimei Li[1†], Yanpeng Dong[1†], Sirun Chen[1], Xinlin Jia[1], Xuemei Jiang[1], Lianqiang Che[1], Yan Lin[1], Jian Li[1], Bin Feng[1], Zhengfeng Fang[1], Yong Zhuo[1], Jianping Wang[1], Haitao Xu[2], De Wu[1]*and Shengyu Xu[1]**

[1]Animal Nutrition Institute, Key Laboratory of Animal Disease-resistant Nutrition, Ministry of Education, Ministry of Agriculture and Rural Affairs, Sichuan Agricultural University, Chengdu, China, [2]Animal Husbandry Development Center of Changyi City, Shandong, China

OPEN ACCESS

Edited by:
Xiaodong Xia,
Northwest A & F University, China

Reviewed by:
Shiyu Tao,
Huazhong Agricultural University, China
Maria de los Angeles Serradell,
Consejo Nacional de Investigaciones Científicas y Técnicas (CONICET), Argentina

***Correspondence:**
Shengyu Xu
shengyu_x@hotmail.com
De Wu
wude@sicau.edu.cn

†These authors have contributed equally to this work

Specialty section:
This article was submitted to Food Microbiology, a section of the journal Frontiers in Microbiology

Received: 10 June 2021
Accepted: 21 July 2021
Published: 16 August 2021

Citation:
Li Z, Dong Y, Chen S, Jia X, Jiang X, Che L, Lin Y, Li J, Feng B, Fang Z, Zhuo Y, Wang J, Xu H, Wu D and Xu S (2021) Organic Selenium Increased Gilts Antioxidant Capacity, Immune Function, and Changed Intestinal Microbiota. Front. Microbiol. 12:723190. doi: 10.3389/fmicb.2021.723190

Selenium is an indispensable essential micronutrient for humans and animals, and it can affect biological functions by combining into selenoproteins. The purpose of this study was to investigate the effects of 2-hydroxy-4-methylselenobutanoic acid (HMSeBA) on the antioxidant performance, immune function, and intestinal microbiota composition of gilts. From weaning to the 19th day after the second estrus, 36 gilts (Duroc × Landrace × Yorkshire) were assigned to three treatments: control group, sodium selenite group (0.3 mg Se/kg Na_2SeO_3), and HMSeBA group (0.3 mg Se/kg HMSeBA). Dietary supplementation with HMSeBA improved the gilts tissue selenium content (except in the thymus) and selenoprotein P (SelP1) concentration when compared to the Na_2SeO_3 or control group. Compared with the control group, the antioxidant enzyme activity in the tissues from gilts in the HMSeBA group was increased, and the concentration of malondialdehyde in the colon had a decreasing trend ($p = 0.07$). Gilts in the HMSeBA supplemented group had upregulated gene expression of *GPX2*, *GPX4*, and *SelX* in spleen tissue, *TrxR1* in thymus; *GPX1* and *SelX* in duodenum, *GPX3* and *SEPHS2* in jejunum, and *GPX1* in the ileum tissues ($p < 0.05$). In addition, compared with the control group, the expression of *interleukin-1β* (*IL-1β*), *interleukin-6* (*IL-6*), *interleukin-8* (*IL-8*), and *monocyte chemotactic protein-1* (*MCP-1*) in the liver, spleen, thymus, duodenum, ileum, and jejunum of gilts in the HMSeBA group were downregulated ($p < 0.05$), while the expression of *interleukin-10* (*IL-10*) and *transforming growth factor-β* (TGF-*β*) in the liver, thymus, jejunum, and ileum were upregulated ($p < 0.05$). Compared with the control group and the Na_2SeO_3 group, HMSeBA had increased concentration of serum cytokines interleukin-2 (IL-2) and immunoglobulin G (IgG; $p < 0.05$), increased concentration of intestinal immunoglobulin A (sIgA; $p < 0.05$), and decreased concentration of serum IL-6 ($p < 0.05$). Dietary supplementation with HMSeBA also increased the abundance of intestinal bacteria (*Ruminococcaceae* and *Phascolarctobacterium*; $p < 0.05$) and selectively inhibited the abundance of some bacteria (*Parabacteroides* and *Prevotellaceae*; $p < 0.05$). In short, HMSeBA improves the antioxidant performance and immune function of gilts, and changed the structure of the intestinal microflora. And this study provided data support for the application of HMSeBA in gilt and even pig production.

Keywords: 2-hydroxy-4-methylselenobutanoic acid, intestinal microbiota, gilts, antioxidant capacity, immune function

INTRODUCTION

As an essential micronutrient, selenium plays an important biological role in animals and human body by participating in the composition of selenocysteine and selenoprotein (Schwarz and Fredga, 1969). Selenium is known to be the main component of 25 selenoproteins, most of which have antioxidant and immune functions (Schrauzer and Gerhard, 2000). Due to many selenoproteins having antioxidant activity, selenium has long been considered to protect the body and intestine from inflammation by reducing oxidative damage. Selenium is also an important component of glutathione peroxidase (GPH-Px) and thioredoxin reductase (TrxR) in animals, and plays an important role in antioxidation and immunity (Stadtman, 1996; Costello, 2001; Hawkes and Alkan, 2010). Studies have found that selenium deficiency has adverse effects on the growth, reproduction, and immune function of animals (Żarczyńska et al., 2013). Adding selenium and selenium products to the basic diet of animals can promote growth, improve immune function, and reduce oxidative stress (Cao et al., 2015). Margarida et al. (2020) added sodium selenite or selenium-enriched yeast to the diet of puppies and found that organic selenium reduced the DNA concentration of *Escherichia coli*, increased the DNA concentration of lactic acid bacteria, and increased the concentrations of volatile fatty acids, butyric acid, and propionic acid in puppies, which was conducive to the intestinal immunity of puppies (Margarida et al., 2020). Therefore, adding selenium to the basic diet of animals can improve immune function and change the intestinal microflora.

In animal diets, selenium mainly exists either as inorganic or organic forms. Many studies have shown that organic selenium (methionine selenium, selenium yeast, selenium enriched probiotics, etc.) has less toxicity and higher biological potency than inorganic selenium (sodium selenite and sodium selenate, etc.; Vendeland et al., 1994; Alimohamady et al., 2013; Rita and Nancy, 2015). A new organic selenium source, 2-hydroxy-4-methylselenobutanoic acid (HMSeBA) with a selenium content of 2%, is much higher than other organic selenium sources. The effectiveness of this new organic selenium source in poultry, growing pigs, and sows has been reported (Jlali et al., 2013; Chao et al., 2019). Adding HMSEBA in the diet of sows can improve the antioxidant capacity of sows and their offspring (Mou et al., 2020a). However, the effect of HMSeBA on gilts has not been extensively studied. Therefore, the purpose of this study was to investigate the effects of HMSeBA as a feed additive on the antioxidant capacity, immune function, and intestinal microbiota of gilts.

MATERIALS AND METHODS

All procedures involving animals in this study were approved by the Animal Care and Use Committee of Sichuan Agricultural University (Approval number: 20200722).

Animal and Experimental Designs

A total of 36 gilts (Duroc × Landrace × Yorkshire) with similar body weight (BW; initial body weight 5.50 ± 0.09 kg) were assigned to three treatment groups: (1) control diet (gilts were fed a basic diet from weaning to the 19th day after the second estrus, n = 12), (2) sodium selenite (Na_2SeO_3) supplemented diet (Na_2SeO_3, basal diet + Na_2SeO_3 at 0.3 mg Se/kg, n = 12), and (3) HMSeBA supplemented diet (HMSeBA, basal diet + HMSeBA at 0.3 mg Se/kg, n = 12). The powdered basal diet is presented in **Table 1**, which was formulated according to the nutrient requirements recommended by the National Research Council (2012) except for that of selenium. The dietary Se level was formulated with Na_2SeO_3 and HMSeBA

TABLE 1 | Composition and nutrient levels of the basal diet (as-fed basis).

	7–25 kg	25–75 kg	75 kg-end
Ingredient, %			
De-hulled soybean meal, 46% CP	15.00	-	-
Extruded maize meal, 8.24% CP	12.40	-	-
Expanded soybean, 35.5% CP	10.00	-	-
Whey powder, 2% CP	5.00	-	-
Sucrose	3.90	-	-
Corn, 8.24% CP	45.00	69.48	72.00
Soybean, 44% CP	-	19.00	14.00
Wheat bran, 15% CP	-	5.00	7.57
Fish meal, 62.5% CP	3.00	0.50	1.50
Soybean oil	2.00	2.00	2.00
$_L$-Lys HCl, 98%	0.60	0.49	0.28
$_{DL}$-Met, 98.5%	0.22	0.10	0.04
$_L$-Thr, 98%	0.19	0.17	0.08
$_L$-Trp, 98%	0.05	0.05	0.03
Choline chloride, 50%	0.16	0.16	0.12
Limestone	0.93	0.94	1.00
$CaHPO_4$	0.94	1.70	1.00
Sodium chloride	0.40	0.28	0.25
Mineral premix	0.32[1]	0.20[2]	0.20[2]
Vitamin premix	0.05[3]	0.03[4]	0.03[4]
Total	100.00	100.00	100.00
Nutrient level[5]			
Digestible energy, Mcal/kg	3.538	3.449	3.430
Crude protein, %	17.06	14.21	14.52
Ca, %	0.85	0.85	0.79
Total P, %	0.52	0.51	0.52
Available P, %	0.34	0.42	0.32
SID Lys, %	1.36	1.01	0.78
SID Met, %	0.50	0.33	0.27
SID Met+Cys, %	0.68	0.55	0.48
SI Thr, %	0.78	0.61	0.49
SID Trp, %	0.22	0.19	0.15

[1]*Per kilogram of diet provided: 125 mg Fe; 14 mg Cu; 30 mg Mn; 110 mg Zn; 0.30 mg I.*
[2]*Per kilogram of diet provided: 120 mg Fe; 12 mg Cu; 30 mg Mn; 100 mg Zn; 0.28 mg I.*
[3]*Per kilogram of diet provided: 12,000 IU VA; 2,400 IU VD3; 100 IU VE; 4.8 mg VK3; 2 mg VB1; 7.2 mg VB2; 3.6 mg VB6; 0.025 mg VB12; 0.48 mg biotin; 25 mg pantothenic acid; 4 mg folic acid; 40 mg niacin.*
[4]*Per kilogram of diet provided: 7,200 IU VA; 1,440 IU VD3; 60 IU VE; 2.88 mg VK3; 1.2 mg VB1; 4.32 mg VB2; 2.16 mg VB6; 0.015 mg VB12; 0.288 mg biotin; 15 mg pantothenic acid; 2.4 mg folic acid; 24 mg niacin.*
[5]*Except for the crude protein, total Ca, and P are measured values, the rest are calculated.*

according to the experimental design shown in **Table 2**. The selenium additive is added to the gilt diet in the form of a premix. And the 2-hydroxy-4-methylselenobutanoic acid (HMSeBA, Selisseo® 2% Se) was provided by Adisseo France S.A.S, and Na_2SeO_3 was provided by Chengdu Shuxing Feed Co. Ltd. (1% Se).

During the experiment, gilts were fed four times a day from weaning to 90 days of age (08:00; 12:00; 16:00; 20:00), and from 90 days to slaughter, they were fed twice a day (08: 00; 16:00). Up to 176 days of age, the gilts were fed freely; 176 days of age to slaughter, the daily feeding limit was 2.5 kg. After 180 days of age, boars were used to check for estrus twice a day (08:00; 16:00). Observation of the vulva and back pressure reflex was used to determine estrus response. On the 19th day of the third estrus period, five gilts were randomly selected from each treatment group for slaughter.

Sample Collection

Before slaughter, gilts were fasted 12 h and 5 ml of blood was collected from the anterior vena cava of the gilts. After standing for 20 min, the blood samples were centrifuged at 2,800 r/min at 4°C for 20 min. Following centrifugation serum was collected in a centrifuge tube, and stored at −20°C for further analysis.

After the gilt was slaughtered, the abdominal cavity was opened immediately, the intestines were taken out, and each intestine segment was separated. After the duodenum, jejunum, and ileum were rinsed with normal saline (0.9% NaCl), the intestinal mucosa from a 6 cm middle area was scraped off using a slide and snap-frozen in liquid nitrogen, and a 2 cm middle tissue sample was rinsed and then snap frozen in liquid nitrogen. The colonic chyme was snap-frozen in liquid nitrogen and stored at −80°C for further analysis (Wan et al., 2020).

The liver, spleen, and thymus were excised and weighed. Then the samples from liver, spleen, and thymus were rinsed in ice-cold saline (0.9% NaCl), snap frozen in liquid nitrogen, and stored at −80°C for further analysis (Mou et al., 2018).

Biochemical Analysis

Sample Preparation

The frozen tissue samples were thawed and placed in a sterile test tube containing 2 ml ice-cold PBS. Tissue specimen (g): PBS (ml) = 1:9. The mixture of the weighed tissue sample and ice-cold PBS was homogenized with a tissue homogenizer (bullet mixer). After centrifugation at 6,000 r/min 4°C for 15 min, the supernatant was divided into 200 μl sterile tubes and stored at −80°C for testing (Mou et al., 2018, 2020b).

Determination of Selenium Content

For the determination of selenium content in feed, tissue, and serum samples, we referred to the "National Food Safety Standard Determination of Selenium in Food" (GB5009.93-2017). Briefly, weighed about 1 g/1 ml of sample and added acid (nitric acid: perchloric acid = 4:1) for overnight digestion at room temperature, following digestion, the samples were heated to 365°C until the solution became clear and colorless. We then used hydrochloric acid and potassium borohydride to reduce the hexavalent selenium in the sample to hydrogen selenide in a hydrochloric acid medium. Subsequently, the total selenium content in the sample was determined by hydride atomic fluorescence spectrometry (AFS-9230, Beijing Auspicious Day Instrument Co., Ltd., Beijing, China).

Antioxidant Determination

The activities of antioxidant GPH-Px (Serial No. A005-1-2), catalase (CAT, Serial No. A064-1-1), total superoxide dismutase (T-SOD, Serial No. A001-1-2), total antioxidant capacity (T-AOC, Serial No. A015-2-1), glutathione reductase (GR, Serial No. A062-1-1), and the concentration of malondialdehyde (MDA, Serial No. A003-1-2) were analyzed using the corresponding commercial assay kit (Nanjing Institute of Jiancheng Biological Engineering, Nanjing, China) according to the manufacturer's instructions. The antioxidant activity of the above parameters was calculated based on the protein content of the tissue sample, and the assay was performed using the method described by Bradford (1976).

Serum, Intestinal Biochemical Indicators

Serum interleukin-2 (IL-2, Serial No. H003) and interleukin-6 (IL-6, Serial No. H007-1-1), immunoglobulin A (IgA, Serial No. H108-1), immunoglobulin G (IgG, Serial No. H106), immunoglobulin M (IgM, Serial No. H109), tumor necrosis factor-α (TNF-α, Serial No. H052-1), and intestinal immunoglobulin A (sIgA, Serial No. H108-2) concentrations

TABLE 2 | Selenium sources and levels in the diets.

Treatment	Diet	Supplemented Se (mg/kg)	Total Se content (mg/kg)[a]		
			5–25 kg	25–75 kg	75 kg above
Control	Basal diet	0.00	0.09	0.06	0.04
Na_2SeO_3	Basal diet + 0.3 mg Se/kg Na_2SeO_3	0.30	0.35	0.33	0.31
HMSeBA	Basal diet + 0.3 mg Se/kg HMSeBA	0.30	0.37	0.41	0.41

HMSeBA, 2-hydroxy-4-methylselenobutanoic acid; Se Selenium. [a]Analysed values.

were determined using ELISAs and the corresponding commercial assay kits (Nanjing Jiancheng Bioengineering Institute) according to the manufacturer's instructions.

Total RNA Extraction and Real-Time RT-PCR

Trizol reagent was used to extract total RNA from the frozen tissue samples. Agarose gel electrophoresis was used to check RNA integrity. RNA purity was checked using a nucleic acid/protein analyzer. A PrimeScript RT kit with gDNA eraser was used to perform genomic DNA removal and reverse transcription (RT) according to the manufacturer's instructions. A SYBR Premix Ex TaqTM kit was used for real-time PCR analysis of mRNA transcript expression. The PCR protocol was 1 cycle of 95°C for 30 s and 40 cycles of 95°C for 15 s followed by 60°C for 1 min. At the end of amplification, melting curve analysis was performed to verify specific amplifications using an ABI-7900HT Fast Real-Time PCR System (Applied Biosystems, CA, United States). Real-time PCR data were analyzed by 2-delta CT method with β-actin as the reference gene (Livak and Schmittgen, 2001) **Table 3** shows the primer sequences of individual genes (Fossum et al., 2014; Mou et al., 2020b).

TABLE 3 | Primer sequences of the target and reference genes.

Genes	Primer	Sequence (5'→3')	Accession no.
SelP 1	Forward	AACCAGAAGCGCCAGACACT	EF113596
	Reverse	TGCTGGCATATCTCAGTTCTCAGA	
GPX1	Forward	GATGCCACTGCCCTCATGA	AF532927
	Reverse	TCGAAGTTCCATGCGATGTC	
GPX2	Forward	AGAATGTGGCCTCGCTCTGA	DQ898282
	Reverse	GGCATTGCAGCTCGTTGAG	
GPX3	Forward	TGCACTGCAGGAAGAGTTTGAA	AY368622
	Reverse	CCGGTTCCTGTTTTCCAAATT	
GPX4	Forward	TGAGGCAAGACGGAGGTAAACT	NM_214407
	Reverse	TCCGTAAACCACACTCAGCATATC	
TrxR1	Forward	GATTTAACAAGCGGGTCATGGT	AF537300
	Reverse	CAACCTACATTCACACACGTTCCT	
TrxR2	Forward	TCTTGAAAGGCGGAAAAGAGAT	GU181287
	Reverse	TCGGTCGCCCTCCAGTAG	
SelK	Forward	CAGGAAACCCCCCTAGAAGAA	NM_001044553.1
	Reverse	CTCATCCACCGGCCATTG	
SelS	Forward	GAGGCAGAGGCACCTGGAT	NM_001164113.1
	Reverse	CTGCTAAAGCCTCCTGTCGTTT	
SelX	Forward	ATCCCTAAAGGCCAAGAATCATC	EF113597
	Reverse	GGCCACCAAGCAGTGTTCA	
SEPHS2	Forward	TGGCTTGATGCACACGTTTAA	NM_001093735
	Reverse	TGCGAGTGTCCCAGAATGC	
IL-1β	Forward	TCTGCCCTGTACCCCAACTG	NM_214055.1
	Reverse	CCAGGAAGACGGGCTTTTG	
IL-6	Forward	ATGCTTCCAATCTGGGTTCAA	NM_001252429.1
	Reverse	CACAAGACCGGTGGTGATTCT	
IL-8	Forward	GCAAGAGTAAGTGCAGAACTTCGA	NM_213867.1
	Reverse	GGGTGGAAAGGTGTGGAATG	
IL-10	Forward	CAGATGGGCGACTTGTTGCT	NM_214041.1
	Reverse	GGCAACCCAGGTAACCCTTAA	
TNF-α	Forward	CGACTCAGTGCCGAGATCAA	NM_214022.1
	Reverse	CCTGCCCAGATTCAGCAAAG	
TGF-β	Forward	AGGACCTGGGCTGGAAGTG	NM_214015.1
	Reverse	GGGCCCCAGGCAGAAAT	
IFN-β	Forward	TCTCTAGCACTGGCTGGAATGA	JN391525.1
	Reverse	CTGCCCATCAAGTTCCACAA	
ICAM-1	Forward	GGAGGTGCTGAAATCTCAATGTG	NM_213816.1
	Reverse	ACCTTCATGGAGCCTCCTTTG	
MCP-1	Forward	GCAAGTGTCCTAAAGAAGCAGTGA	NM_214214.1
	Reverse	GCTTGGGTTCTGCACAGATCT	
INOS-2	Forward	AGAGCCAGAAGCGCTATCATG	NM_001143690.1
	Reverse	CCCACTGCCCCCTCCTT	
β-actin	Forward	TCTGGCACCACACCTTCT	DQ178122
	Reverse	TGATCTGGGTCATCTTCTCAC	

SelP1, selenoprotein P; GPX, glutathione peroxidase; TrxR, thioredoxin reductase; SelK, selenoprotein K; SelS, selenoprotein S; SelX, selenoprotein X; SEPHS2, selenophosphate synthetase 2; IL-1β, interleukin-1β; IL-6, interleukin-6; IL-8, interleukin-8; IL-10, interleukin-10; TNF-α, tumor necrosis factor-α; TGF-β, transforming growth factor-β; IFN-β, interferon-β; ICAM-1, intercellular cell adhesion molecule-1; MCP-1, monocyte chemotactic protein-1; INOS-2, inducible nitric oxide synthase-2.

Bacterial Community Analysis

The microbial DNA of colon chyme samples was extracted using the Mo Bio Power-Fecal™ DNA Isolation Kit (MO BIO Laboratories, Carlsbad, CA, United States). A nucleic ac-id/protein analyzer (Beckman DU-800, Beckman Coulter, Inc., CA, United States) was used to determine the concentration and purity of the DNA. The DNA samples were sent to a commercial service provider (Novogene Bioinformatics Technology, Beijing, China) for pairing sequencing on the Illumina HiSeq PE250 platform and bioinformatics analyses. According to the selection of sequencing region, sample was used with forward primer 515F (5'-GTGCCAGCMGCCGCGGTAA-3') and a reverse primer 806R (5'-GGACTACHVGGGTWTCTAAT-3') to perform PCR to amplify the V4 hypervariable region of the 16S rRNA gene was used as described previously (Xu et al., 2020).

Use FLASH (V1.2.7, http://ccb.jhu.edu/software/FLASH/) to splice the reads of each sample, the resulting stitched sequence is raw tags data. Reference Qiime (V1.7.0, http://qiime.org/scripts/split_libraries_fastq.html) tags quality control process, get high quality tags data, and then remove the chimera, get the final effective data (Xu et al., 2020). Clustered into OTUs utilizing Uparse v7.0.1001[1] at 97% sequence similarity. The Ribosomal Database Project (RDP) classifier Version 2.2[2] was applied to assign taxonomy for 16S rRNA gene sequences. Species annotation was carried out on the OTUs representative sequences, and species annotation analysis was carried out using Mothur method and the SSUrNA database of SILVA[3] (set a threshold of 0.8–1) to obtain taxonomic information. A Venn diagram was generated for comparison among the OTUs of the treatments. For intestinal microbiota alpha diversity values for each sample were assessed by Qiime 1.7.0. Spearman correlation analysis was used to analyze the mutual change relationship between serum cytokines and microorganisms, and the correlation and significance between them were obtained.

Statistical Analysis

The data were analyzed using a one-way ANOVA procedure of Statistical Product and Service Solutions (SAS) statistical software (V9.4, SAS Institute Inc., Cary, NC, United States) followed by Tukey's multiple range test. The results were presented as the mean values with pooled SEM. Differences at $p < 0.05$ were considered to be statistically significant, whereas a tendency was considered when $0.05 \leq p < 0.10$.

RESULTS

Organic Selenium Increased Selenium Content and Selenoprotein Gene Expression

The results showed that adding HMSeBA to the basal diet of gilts significantly increased the total selenium content in the serum, liver, spleen, duodenum, jejunum, ileum, and colon compared with the control group ($p < 0.05$; **Table 4**). Na_2SeO_3 group increased the total selenium content in liver and colon compared with the control group ($p < 0.05$). In addition, there was no difference in total selenium content in thymus between the Na_2SeO_3 group and HMSeBA group compared with the control group (**Table 4**).

The gene expressions of *GPX2*, *GPX4*, and *SelX* in the spleen of gilts added with HMSeBA were increased ($p < 0.05$; **Figure 1A**) compared with the control group and Na_2SeO_3 group. The expressions of *SelP1*, *GPX1*, and *SelK* were higher in HMSeBA and Na_2SeO_3 groups than in the control group ($p < 0.05$). In the thymus, the expression of *TrxR1* in the HMSeBA addition group was increased compared with the control and Na_2SeO_3 groups ($p < 0.05$), the expression of *GPX1*, *GPX4*, and *SelX* were higher than the control group ($p < 0.05$), but with no difference from the Na_2SeO_3 group (**Figure 1B**).

The results showed that adding HMSeBA to the basal diet of gilts increased the expression of *GPX1* and *SelX* in the duodenum compared with control and Na_2SeO_3 groups ($p < 0.05$), the expressions of *SelP1*, *GPX3*, *TrxR2*, and *SelK* were significantly higher than those in the control group ($p < 0.05$), but no differece with Na_2SeO_3 group (**Figure 2A**). In the jejunum, the expressions of *GPX3* and *SEPHS2* in the HMSeBA addition group were higher than those in the control group and the Na_2SeO_3 group ($p < 0.05$), compared with the control group, the expression of *SelP1*, *GPX2*, *GPX4*, *TrxR2*, and *SelK* in the HMSeBA addition group significantly increased ($p < 0.05$). In addition, the expression of *TrxR1* has an increasing trend in HMSeBA group ($p = 0.05$; **Figure 2B**). The expression of *GPX1* in the ileum of gilts with the HMSeBA containing diet was higher than that of the control group and Na_2SeO_3 groups ($p < 0.05$). The expression of *SelP1*, *GPX3*, *GPX4*, *SelK*, and *SelS* in the HMSeBA and Na_2SeO_3 groups was higher than those in the control group ($p < 0.05$). The expression of *TrxR1* and *TrxR2* showed an increasing trend ($p = 0.06$, $p = 0.05$) in the HMSeBA group compared with the control group (**Figure 2C**).

TABLE 4 | HMSeBA effect on serum and tissue total selenium content of gilts.

Item	Treatment			Values of *p*
	Control	Na_2SeO_3	HMSeBA	
Serum (mg/L)	0.18 ± 0.00[b]	0.21 ± 0.00[a]	0.22 ± 0.01[a]	0.02
Liver (mg/kg)	0.46 ± 0.03[c]	0.67 ± 0.04[b]	0.91 ± 0.02[a]	<0. 01
Spleen (mg/kg)	0.30 ± 0.02[b]	0.29 ± 0.01[b]	0.48 ± 0.04[a]	<0.01
Thymus (mg/kg)	0.21 ± 0.00	0.35 ± 0.07	0.29 ± 0.01	0.24
Duodenum (mg/kg)	0.21 ± 0.02[b]	0.23 ± 0.01[b]	0.30 ± 0.01[a]	<0.01
Jejunum (mg/kg)	0.23 ± 0.00[b]	0.24 ± 0.02[b]	0.32 ± 0.01[a]	<0.01
Ileum (mg/kg)	0.20 ± 0.02[b]	0.24 ± 0.01[b]	0.39 ± 0.05[a]	<0.01
Colon (mg/kg)	0.20 ± 0.01[b]	0.32 ± 0.02[a]	0.31 ± 0.02[a]	<0.01

Data were shown as means ± SE. n = 5 in each group. Control, basal diet; Na_2SeO_3, 0.3 mg/kg Na_2SeO_3; HMSeBA, 0.3 mg/kg HMSeBA. [a,b,c]Mean values within a row with different superscript letters were significantly different (p < 0.05).

[1]http://drive5.com/uparse/
[2]http://github.com/rdpstaff/
[3]http://www.arb-silva.de/

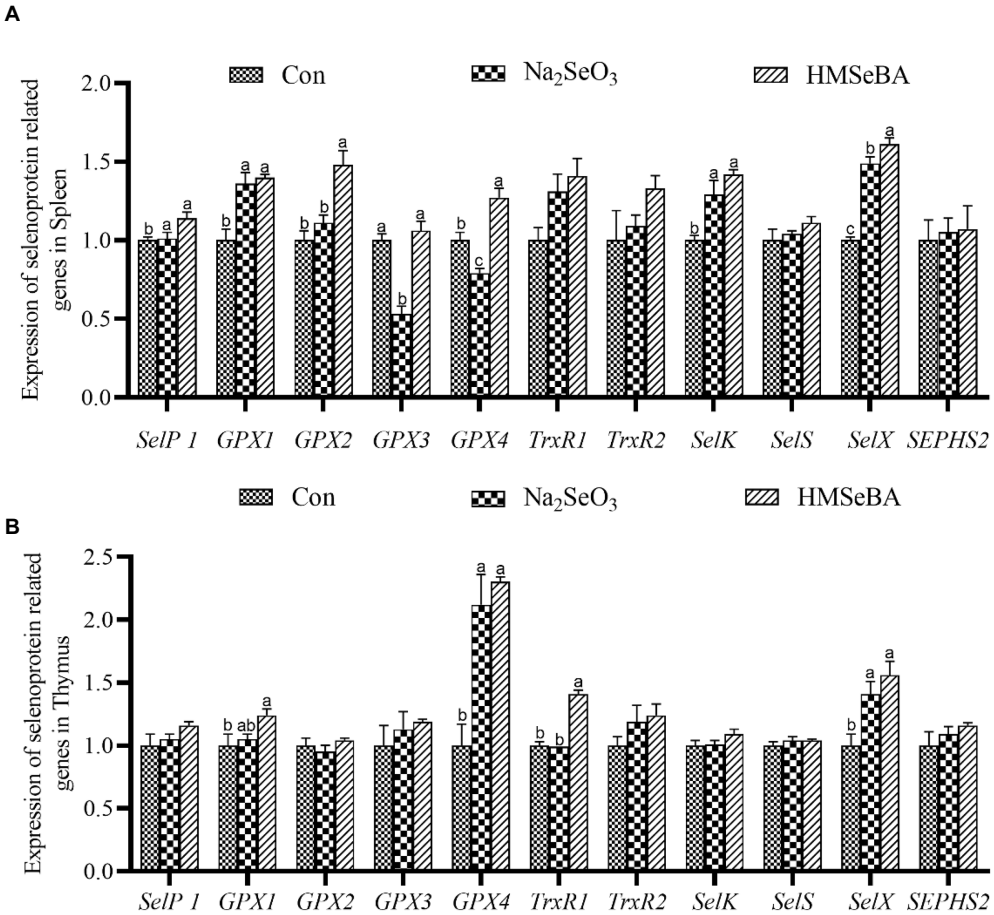

FIGURE 1 | The effect of HMSeBA on the expression of selenoprotein related genes in spleen **(A)** and thymus **(B)** of gilts. $n = 5$ in each group. Data were shown as means ± SE. $n = 5$ in each group. Control, basal diet; Na_2SeO_3, 0.3 mg Se/kg Na_2SeO_3; HMSeBA, 0.3 mg Se/kg HMSeBA. ^{a,b,c}Mean values within a row with different superscript letters were significantly different ($p < 0.05$). SelP1, selenoprotein P; GPX, glutathione peroxidase; TrxR, thioredoxin reductase; SelK, selenoprotein K; SelS, selenoprotein S; SelX, selenoprotein X; SEPHS2, selenophosphate synthetase 2.

Organic Selenium Improved the Antioxidant Capacity of Gilts

The results showed that adding HMSeBA to the basal diet of gilts increased the spleen CAT, T-SOD, and GR activity compared with the control group ($p < 0.05$), and there was no significant difference from the Na_2SeO_3 group. The activity of GSH-PX in the spleen in the HMSeBA group had an increasing trend ($p = 0.08$) compared with the control group (**Table 5**). The GR activity of the thymus in the HMSeBA group was increased ($p < 0.05$) compared with the other two groups, the activities of T-AOC, CAT, and GSH-PX were higher than those in the control group ($p < 0.05$), and there was no significant difference from the Na_2SeO_3 group. Thymus T-SOD activity in the Na_2SeO_3 group was higher than that in the control and HMSeBA groups ($p < 0.05$; **Table 5**).

Compared with the control group, gilts supplemented with HMSeBA and Na_2SeO_3 had increased GR activity in the duodenal ($p < 0.05$; **Table 6**). The T-SOD activity is decreased in Na_2SeO_3 group compared to control group and HMSeBA group. The HMSeBA group had a tendency of increased GSH-PX activity compared with the control group ($p = 0.06$). Compared with the control group and the Na_2SeO_3 group, the addition of HMSeBA resulted in increased activities of T-SOD, GSH-PX, and GR in the jejunum ($p < 0.05$). The addition of HMSeBA to the basal diet of gilts increased the activity of GSH-PX and GR in the ileum compared with the control and Na_2SeO_3 groups ($p < 0.05$), and had a tendency to increase the activity of T-SOD ($p = 0.07$). The GSH-PX activity in the colon of gilts fed diets with HMSeBA was higher than that in the control and Na_2SeO_3 groups ($p < 0.05$). Compared with the control group, the colonic T-AOC, CAT, and GR activities were significantly increased ($p < 0.05$) in the HMSeBA and Na_2SeO_3 fed groups. Dietary supplementation with HMSeBA had a tendency to decrease the MDA content ($p = 0.07$; **Table 6**).

Effects of Organic Selenium on the Expression of Inflammatory Response Related Genes in Gilts

The results showed that compared with the control and Na_2SeO_3 groups, the expression of *interleukin-1β* (*IL-1β*) and *IL-6* in the liver of gilts fed HMSeBA was significantly reduced

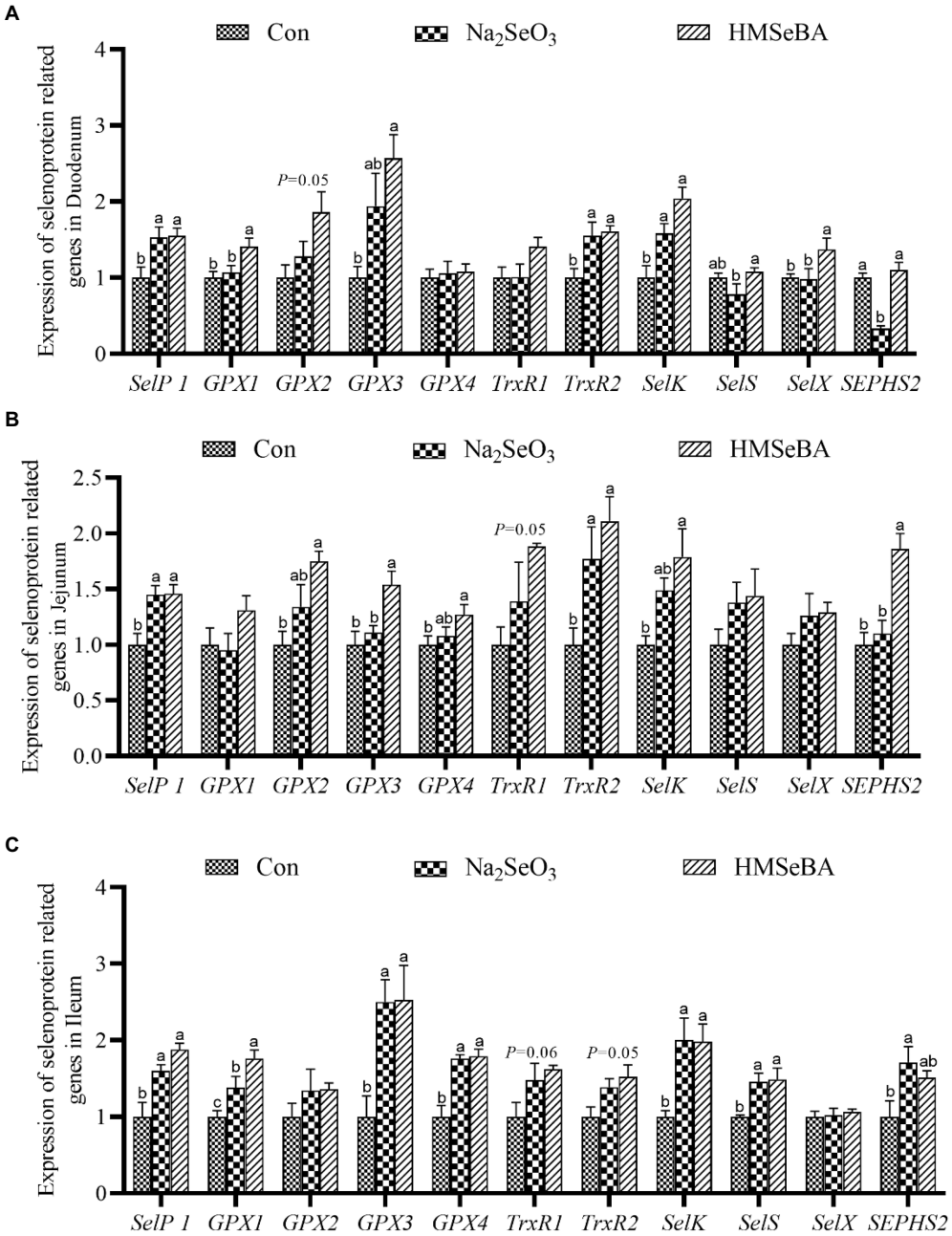

FIGURE 2 | The effect of HMSeBA on the expression of selenoprotein related genes in duodenum **(A)**, jejunum **(B)**, and ileum **(C)** of gilts. $n = 5$ in each group. Data were shown as means ± SE. $n = 5$ in each group. Control, basal diet; Na_2SeO_3, 0.3 mg Se/kg Na_2SeO_3; HMSeBA, 0.3 mg Se/kg HMSeBA. ^{a,b,c}Mean values within a row with different superscript letters were significantly different ($p < 0.05$). SelP1, selenoprotein P; GPX, glutathione peroxidase; TrxR, thioredoxin reductase; SelK, selenoprotein K; SelS, selenoprotein S; SelX, selenoprotein X; SEPHS2, selenophosphate synthetase 2.

($p < 0.05$), while the expression of *interleukin-10* (*IL-10*) and *transforming growth factor-β* (*TGF-β*) increased ($p < 0.05$), and the expression of *TNF-α* and *intercellular cell adhesion molecule-1* (*ICAM-1*) had a decreasing trend ($p = 0.08$; **Figure 3A**). In the spleen, the expression of *interleukin-8* (*IL-8*) in the HMSeBA fed group was lower than that of the control and Na_2SeO_3 groups ($p < 0.05$). Compared with the control, the expression of *IL-1β*, *IL-6*, *TNF-α*, *IFN-β*, and *monocyte chemotactic protein-1* (*MCP-1*) in the HMSeBA group was significantly decreased ($p < 0.05$), and there was no difference from the Na_2SeO_3 group. The expression of *IL-10* and *TGF-β* showed a downregulated and upregulated trend, respectively, in the HMSeBA group ($p = 0.08$, $p = 0.05$; **Figure 3B**). Dietary supplementation with HMSeBA reduced the expression of *IL-8* ($p < 0.05$; **Figure 3C**) in the thymus compared with the control and Na_2SeO_3 groups. In addition, compared with the control

TABLE 5 | Effect of HMSeBA on antioxidant capacity in gilt tissue.

Item	Treatment			Values of *p*
	Control	Na_2SeO_3	HMSeBA	
Spleen				
T-AOC (U/mg prot)	0.30 ± 0.02	0.37 ± 0.03	0.32 ± 0.04	0.31
MDA (nmol/mg prot)	2.88 ± 0.30	2.87 ± 0.18	2.63 ± 0.13	0.72
CAT (U/mg prot)	77.17 ± 4.26^{b}	87.54 ± 7.75^{ab}	102.97 ± 3.75^{a}	0.02
T-SOD (U/mg prot)	54.34 ± 11.4^{b}	69.33 ± 2.76^{a}	69.77 ± 3.02^{a}	0.01
GSH-PX (U/mg prot)	30.42 ± 1.35	36.10 ± 1.48	36.49 ± 2.64	0.08
GR (U/g prot)	0.015 ± 0.001^{b}	0.019 ± 0.002^{ab}	0.026 ± 0.003^{a}	0.02
Thymus				
T-AOC (U/mg prot)	0.28 ± 0.03^{b}	0.45 ± 0.04^{a}	0.48 ± 0.04^{a}	0.01
MDA (nmol/mg prot)	3.35 ± 0.25	2.98 ± 0.40	3.27 ± 0.26	0.56
CAT (U/mg prot)	34.37 ± 3.76^{b}	63.87 ± 4.01^{a}	57.34 ± 2.90^{a}	<0.01
T-SOD (U/mg prot)	567.83 ± 29.45^{c}	797.64 ± 0.77^{a}	694.89 ± 20.17^{b}	<0.01
GSH-PX (U/mg prot)	20.93 ± 0.23^{b}	20.44 ± 0.69^{b}	39.39 ± 2.48^{a}	<0.01
GR (U/g prot)	0.007 ± 0.002^{b}	0.012 ± 0.001^{b}	0.017 ± 0.001^{a}	<0.01

Data were shown as means ± SE. n = 5 in each group. Control, basal diet; Na_2SeO_3, 0.3 mg Se/kg Na_2SeO_3; HMSeBA, 0.3 mg Se/kg g HMSeBA. ^{a,b,c} Mean values within a row with different superscript letters were significantly different (p < 0.05). T-AOC, total antioxidant capacity; MDA, malondialdehyde; CAT, catalase; T-SOD, total superoxide dismutase; GSH-Px, glutathione peroxidase; GR, glutathione reductase.

group, the expression of *IL-10* in the HMSeBA group was increased ($p < 0.05$), the expression of *IL-6* and *ICAM-1* was decreased ($p < 0.05$), and the expression of *IL-1β* had a decreasing trend ($p = 0.09$).

The expression of *TNF-α* and *MCP-1* in the duodenum of gilts in the HMSeBA fed group was lower than those in the control and Na_2SeO_3 groups ($p < 0.05$; **Figure 4A**). In addition, the expression levels of *IL-1β*, *IL-8*, and *INOS-2* in the HMSeBA group were decreased ($p < 0.05$), and the expression of *TGF-β* tended to increase ($p = 0.09$) when compared with the control group (**Figure 4A**). Compared with the control and Na_2SeO_3 groups, the expression of *IL-8*, *ICAM-1*, and *MCP-1* in the jejunum of the HMSeBA fed group was decreased ($p < 0.05$), and the expression of *IL-10* was significantly increased ($p < 0.05$), while the expression of *IFN-β* had a decreasing trend ($p = 0.06$; **Figure 4B**). Compared with the control group, the expression of *IL-1β* in the HMSeBA and Na_2SeO_3 fed groups was significantly decreased ($p < 0.05$). In the ileum of gilts, the expression of *TGF-β* in the HMSeBA fed group was higher than that in the control and Na_2SeO_3 groups ($p < 0.05$), and the expression of *IL-1β*, *IL-6*, and *IL-8* was decreased ($p < 0.05$), the expression of *IL-10* was increased ($p < 0.05$), compared with the control group. The expression of *MCP-1* in the HMSeBA group had a decreasing trend ($p = 0.06$; **Figure 4C**).

Effect of Organic Selenium on the Inflammatory Factors and Immunoglobulins in Gilts

Serum IL-2 and IgG concentrations in the HMSeBA group were higher than those in the control and Na_2SeO_3 groups ($p < 0.05$). In addition, adding HMSeBA significantly reduced serum IL-6 and TNF-α levels compared with the control group ($p < 0.05$), while TNF-α levels showed no significant difference compared with the Na_2SeO_3 group (**Table 7**). In the duodenum, jejunum, and ileum, HMSeBA improved the intestinal sIgA level compared with the control group ($p < 0.05$; **Table 8**), while there is no significant difference in the duodenal sIgA level compared with the Na_2SeO_3 group.

Organic Selenium Supplementation Changed the Intestinal Microbiota in Gilts

The results showed that there were 10 phylum relative abundances >0.1% in colon of gilts, included Firmicutes, Bacteroidetes, Spirochaetes, Actinobacteria, Proteobacteria, Euryarchaeota, Tenericutes, unidentified_Bacteria, and Melainabacteria (**Table 9**). Compared with the control group, the HMSeBA group increased the abundance of Firmicutes and the ratio of Firmicutes/Bacteroides ($p < 0.05$), while the abundance of Bacteroides, Melainabacteria, and Spirobacteria was reduced ($p < 0.05$).

The 35 most abundant genera in all samples were detected. Compared with the control group, the gilts supplemented with HMSeBA increased the abundance of *Terrisporobacter* and *Intestinibacter* ($p < 0.05$; **Table 10**), and decreased the abundance of *Prevotellaceae* and *Megasphaera* ($p < 0.05$). There was also an increasing trend in the abundance of *Phascolarctobacterium* ($p = 0.07$), while a decreasing trend in the abundance of *Parabacteroides* ($p = 0.09$).

Relationship Between Serum Cytokines and Intestinal Microbiota

Spearman correlation analysis was used to study the relationship between environmental factors and microbial species richness, to study the mutual change relationship between environmental factors and species. At the phylum level, Fibacteria and Melainabacteria were positively correlated with the serum cytokine IL-6 ($r = 0.61$, $p < 0.05$; $r = 0.69$, $p < 0.05$; **Figure 5**), Conversely, Kiritimatiellaeota and Firmicutes were negatively correlated with the serum cytokine IL-6 ($r = -0.66$, $p < 0.05$; $r = -0.64$, $p < 0.05$). Trachelum was negatively correlated with the serum cytokine TNF-α ($r = -0.53$, $p < 0.05$).

TABLE 6 | Effect of HMSeBA on antioxidant capacity of gilt intestinal.

Item	Treatment			Values of *p*
	Control	Na_2SeO_3	HMSeBA	
Duodenum				
T-AOC (U/mg prot)	0.16 ± 0.01	0.17 ± 0.02	0.17 ± 0.02	0.95
MDA (nmol/mg prot)	2.29 ± 0.18	2.29 ± 0.09	2.03 ± 0.04	0.16
CAT (U/mg prot)	30.43 ± 7.69	48.80 ± 6.09	46.07 ± 5.27	0.15
T-SOD (U/mg prot)	901.42 ± 42.63^a	738.21 ± 37.55^b	1020.98 ± 48.62^a	<0.01
GSH-PX (U/mg prot)	17.42 ± 0.54	20.16 ± 0.82	22.03 ± 1.62	0.06
GR (U/g prot)	0.004 ± 0.001^b	0.015 ± 0.002^a	0.018 ± 0.001^a	<0.01
Jejunum				
T-AOC (U/mg prot)	0.17 ± 0.00^a	0.12 ± 0.01^b	0.17 ± 0.01^a	<0.01
MDA (nmol/mg prot)	2.37 ± 0.24	2.15 ± 0.13	2.28 ± 0.04	0.57
CAT (U/mg prot)	16.86 ± 3.22	20.61 ± 2.99	28.83 ± 3.82	0.08
T-SOD (U/mg prot)	564.81 ± 4.31^b	584.14 ± 4.06^b	668.43 ± 10.55^a	0.03
GSH-PX (U/mg prot)	28.23 ± 1.53^b	11.02 ± 0.92^c	44.79 ± 2.58^a	<0.01
GR (U/g prot)	0.012 ± 0.001^b	0.013 ± 0.001^b	0.019 ± 0.001^a	0.02
Ileum				
T-AOC (U/mg prot)	0.21 ± 0.01	0.25 ± 0.03	0.23 ± 0.01	0.51
MDA (nmol/mg prot)	2.08 ± 0.10	2.23 ± 0.19	1.84 ± 0.16	0.26
CAT (U/mg prot)	30.26 ± 5.98	37.56 ± 3.31	43.01 ± 8.20	0.43
T-SOD (U/mg prot)	801.08 ± 55.43	777.95 ± 32.28	928.37 ± 46.71	0.07
GSH-PX (U/mg prot)	24.30 ± 0.41^b	24.49 ± 1.30^b	33.04 ± 1.42^a	<0.01
GR (U/g prot)	0.013 ± 0.001^b	0.014 ± 0.001^b	0.018 ± 0.001^a	0.02
Colon				
T-AOC (U/mg prot)	0.16 ± 0.02^b	0.27 ± 0.00^a	0.25 ± 0.02^a	0.01
MDA (nmol/mg prot)	2.75 ± 0.33	2.06 ± 0.09	2.28 ± 0.07	0.07
CAT (U/mg prot)	19.30 ± 3.70^b	26.06 ± 0.41^{ab}	28.51 ± 1.22^a	0.03
T-SOD (U/mg prot)	735.12 ± 34.90	730.53 ± 25.70	763.99 ± 32.90	0.72
GSH-PX (U/mg prot)	11.27 ± 1.41^b	12.11 ± 0.93^b	16.23 ± 0.90^a	0.02
GR (U/g prot)	0.010 ± 0.001^b	0.014 ± 0.001^a	0.017 ± 0.002^a	<0.01

Data were shown as means ± SE. n = 5 in each group. Control, basal diet; Na_2SeO_3, 0.3 mg Se/kg Na_2SeO_3; HMSeBA, 0.3 mg Se/kg HMSeBA. ^{a,b,c}Mean values within a row with different superscript letters were significantly different (p < 0.05). T-AOC, total antioxidant capacity; MDA, malondialdehyde; CAT, catalase; T-SOD, total superoxide dismutase; GSH-Px, glutathione peroxidase; GR, glutathione reductase.

At the genus level, *Lacobacteria* and *Entomobacteria* were negatively correlated with the serum cytokine IL-6 ($r = -0.68$, $p < 0.05$; $r = -0.74$, $p < 0.05$; **Figure 6**), and *Prewolfella* was positively correlated with the serum cytokine IL-6 ($r = 0.81$, $p < 0.05$).

DISCUSSION

As an important part of intensive pig farms, reserve gilts are critical for both maintenance and expansion. Gilt reproduction performance is directly related to the overall level of pig production and the future of pig farms. To our knowledge, this is the first study to add HMSeBA to the basic diet of reserve gilts in order to study its effects on antioxidant capacity, immune function, and intestinal microflora. These results of current study can provide data reference and theoretical support for the application of HMSeBA in gilts, and it also have great significance to further improve the level of pig production in China, improve the breeding benefits of pig production, and improve the food composition of people.

In a general way, the level of selenium in animals mainly depends on the content of selenium in diet, and the absorption efficiency of organic selenium has proven to be superior to inorganic selenium (Juniper et al., 2008). Mou added HMSeBA to the basal diet of sows during pregnancy and lactation and found significantly increased plasma selenium concentrations in the sows and their offspring (Mou et al., 2020b). The present results showed that adding sodium selenite and HMSeBA to the diet significantly increased the selenium content in the tissues of the gilts, which was consistent with previous studies in pigs (Speight et al., 2012), poultry (Briens et al., 2013), and sheep (Faixová et al., 2016). The present study also found that the organic selenium HMSeBA significantly increased the selenium content in several tissues compared to inorganic selenium. The difference in the deposition efficiency of organic selenium and inorganic selenium may be related to their different absorption and metabolic pathways. Inorganic selenium is absorbed by animals in a passive manner and reduced to selenium by TrxR or by reaction with glutathione (Daniels, 1996). While organic selenium is actively absorbed through amino acid transport mechanisms whereby organic selenium compounds are converted to selenocysteine through the antiselenylation pathway, and selenocysteine generates selenides under the action of selenocysteine lyase

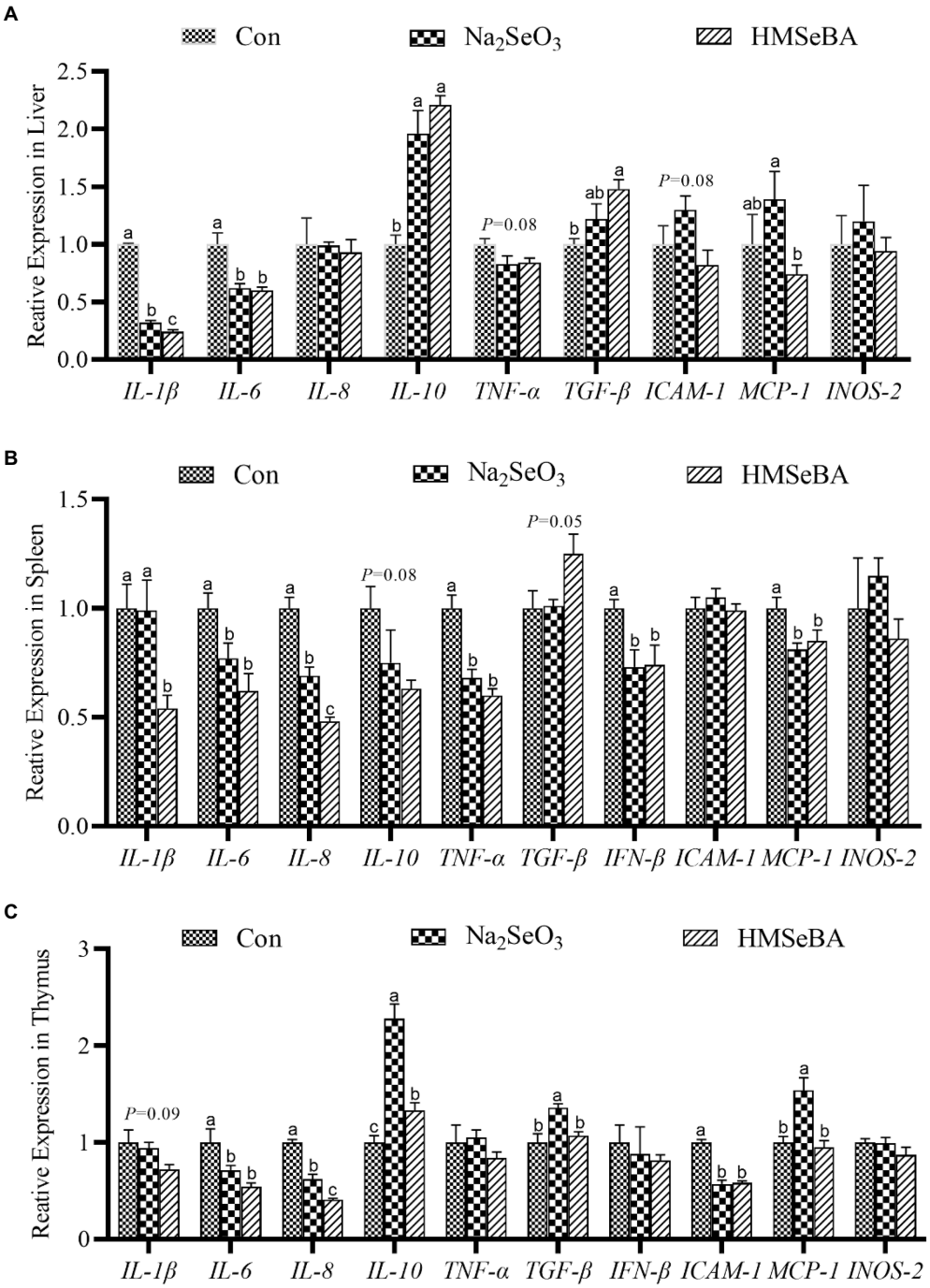

FIGURE 3 | The effect of HMSeBA on the expression of related cytokines in the liver **(A)**, spleen **(B)**, and thymus **(C)** of gilts. $n = 5$ in each group. Data were shown as means ± SE. $n = 5$ in each group. Control, basal diet; Na_2SeO_3, 0.3 mg Se/kg Na_2SeO_3; HMSeBA, 0.3 mg Se/kg HMSeBA. ^{a,b,c}Mean values within a row with different superscript letters were significantly different ($p < 0.05$). IL-1β, interleukin-1β; IL-6, interleukin-6; IL-8, interleukin-8; IL-10, interleukin-10; TNF-α, tumor necrosis factor-α; TGF-β, transforming growth factor-β; IFN-β, interferon-β; ICAM-1, intercellular cell adhesion molecule-1; MCP-1, monocyte chemotactic protein-1; INOS-2, inducible nitric oxide synthase-2.

(Fairweather-Tait et al., 2010; Mehdi et al., 2013; Burk and Hill, 2015; Shini et al., 2015). SelP1 is one of the main selenoproteins in plasma, which is composed of up to 10 selenocysteine residues and is very sensitive to changes of selenium levels. And the main function of SelP1 is to transport selenium to various tissues, selenocysteine produces selenide under the action of se cysteine lyase (Burk and Hill, 2009). In this study, the HMSeBA molecule contains 40% Se and

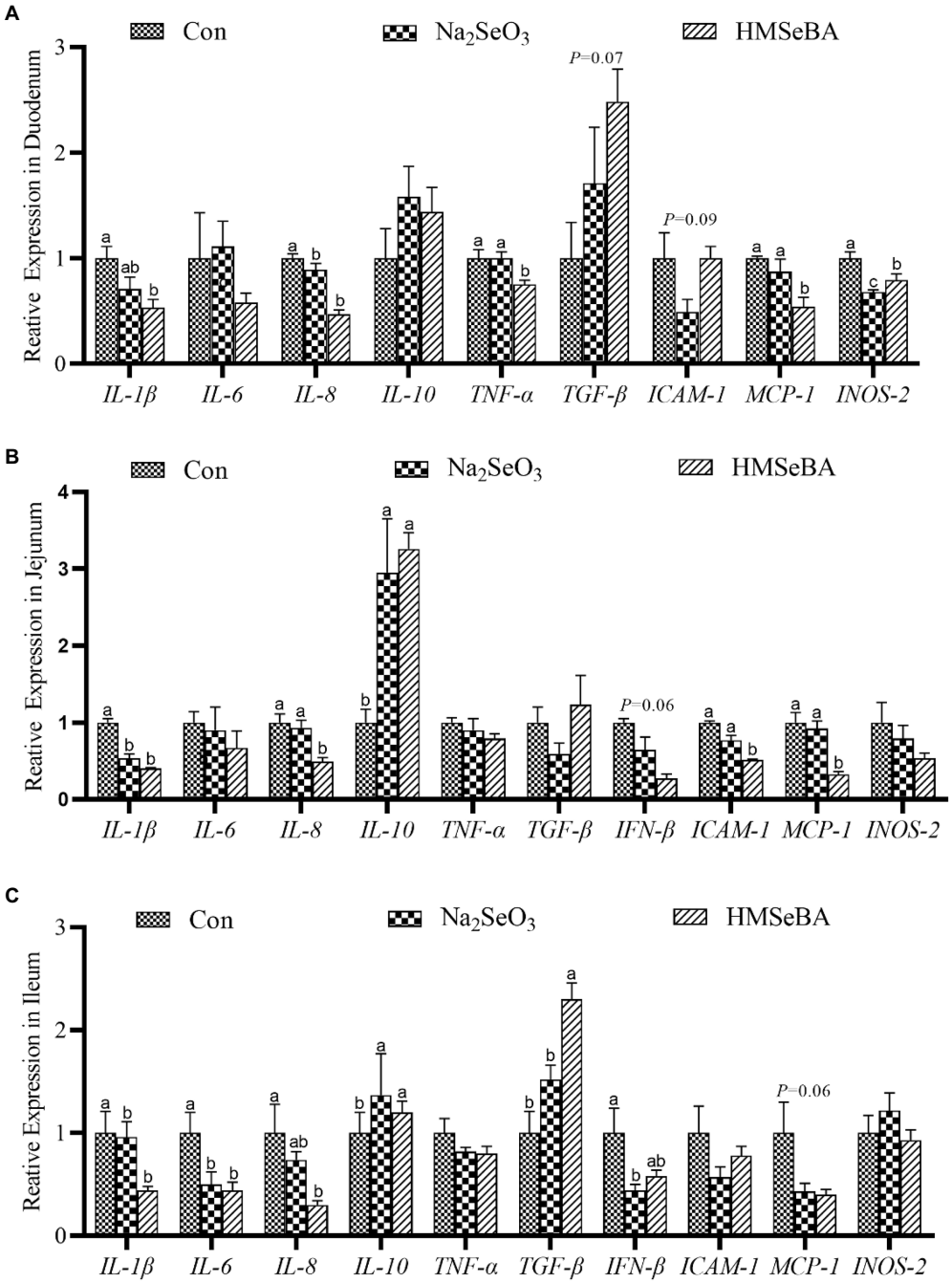

FIGURE 4 | The effect of HMSeBA on the expression of related cytokines in duodenum **(A)**, jejunum **(B)**, and ileum **(C)** of gilts. $n = 5$ in each group. Data were shown as means ± SE. $n = 5$ in each group. Control, basal diet; Na_2SeO_3, 0.3 mg Se/kg Na_2SeO_3; HMSeBA, 0.3 mg Se/kg HMSeBA. [a,b,c]Mean values within a row with different superscript letters were significantly different ($p < 0.05$). IL-1β, interleukin-1β; IL-6, interleukin-6; IL-8, interleukin-8; IL-10, interleukin-10; TNF-α, tumor necrosis factor-α; TGF-β, transforming growth factor-β; IFN-β, interferon-β; ICAM-1, intercellular cell adhesion molecule-1; MCP-1, monocyte chemotactic protein-1; INOS-2, inducible nitric oxide synthase-2.

is higher than inorganic selenium. It can be converted to selenocysteine more quickly and is rarely lost to the excretion pathway. Therefore, HMSeBA can be better absorbed and utilized by the gilts, leading to the selenium deposition effect in the tissues being more significant, and compared with control group the expression of *SelP1* in the tissues of the HMSeBA group gilts increasing.

The main antioxidant enzyme in the body is GSH-Px, whose activity will affect the level of reactive oxygen free radicals and the content of malondialdehyde and the final product of lipid

TABLE 7 | Effect of HMSeBA on serum immunity indexes and immunoglobulins of gilt.

Item	Treatment			Values of *p*
	Control	Na_2SeO_3	HMSeBA	
IL-2, pg/ml	284.95 ± 11.91[b]	227.83 ± 11.75[c]	339.88 ± 12.24[a]	<0.01
IL-6, pg/ml	48.69 ± 2.53[a]	21.59 ± 1.84[b]	20.36 ± 0.56[b]	<0.01
IgA, μg/ml	98.29 ± 2.26	100.05 ± 3.55	105.52 ± 3.25	0.26
IgG, μg/ml	559.9 ± 4.24[b]	562.27 ± 6.96[b]	670.18 ± 6.39[a]	<0.01
IgM, μg/ml	137.89 ± 2.76	140.20 ± 1.36	145.29 ± 2.34	0.10
TNF-α, pg/ml	579.55 ± 20.63[a]	517.54 ± 30.07[ab]	462.26 ± 10.57[b]	<0.01

Data were shown as means ± SE. n = 5 in each group. Control, basal diet; Na_2SeO_3, 0.3 mg Se/kg Na_2SeO_3; HMSeBA, 0.3 mg Se/kg HMSeBA. [a,b,c]Mean values within a row with different superscript letters were significantly different (p < 0.05). IL-2, Interleukin-2; IL-6, Interleukin-6; IgA, immunoglobulin A; IgG, immunoglobulin G; IgM, immunoglobulin M; TNF-α, tumor necrosis factor-α.

TABLE 8 | The effect of HMSeBA on the concentration of sIgA in the intestines of gilts.

Item	Treatment			Values of *p*
	Control	Na_2SeO_3	HMSeBA	
Duodenum, μg/ml	4.45 ± 0.71[b]	6.92 ± 0.52[a]	8.21 ± 0.28[a]	<0.01
Jejunum, μg/ml	3.59 ± 0.68[b]	4.08 ± 0.59[b]	7.83 ± 0.43[a]	<0.01
Ileum, μg/ml	2.38 ± 0.41[b]	2.58 ± 0.29[b]	5.14 ± 0.43[a]	<0.01

Data were shown as means ± SE. n = 5 in each group. Control, basal diet; Na_2SeO_3, 0.3 mg Se/kg Na_2SeO_3; HMSeBA, 0.3 mg Se/kg HMSeBA. [a,b,c]Mean values within a row with different superscript letters were significantly different (p < 0.05). sIgA, secretory immunoglobulin A.

peroxidation in the body. Selenium is a component of this enzyme and located in its active center, so the selenium status of the body directly affects the activity of GSH-Px (Brigelius-Flohé et al., 2003; Wang et al., 2011; Mistry et al., 2012). Mou et al. (2020b) fed organic selenium to pregnant sows and found this significantly increased the activity of GSH-Px in the serum and placenta of the sows, and significantly decreased the content of MDA (Mou et al., 2020b). Other studies showed that the activity of GSH-Px in the duodenum, jejunum, and rectum of chicks fed Se-deficient diets were significantly lower than those in basal diets (Ruan et al., 2018). The present study showed that HMSEBA significantly increased the activities of GSH-Px, T-SOD, and CAT in the thymus, jejunum, ileum, and colon of gilts, and the content of MDA in each tissue showed a decreasing trend. In this study, HMSEBA not only improved the antioxidant capacity of gilts, but also significantly upregulated the gene expressions of *GPX1-4* in the spleen and thymus of the gilts, as well as *GPX1*, *GPX3*, and *GPX4* in the intestinal tract of the gilts. Selenium functions mainly through selenoprotein, and *GPX1-4* plays an important role in regulating oxidative stress and inflammation in the intestinal tract (Yan and Chen, 2006; Lubos et al., 2010; Avery and Hoffmann, 2018). *GPX2* has been reported to inhibit cox-dependent PGE2 production, suggesting that *GPX2* has a potential anti-inflammatory effect within the gastrointestinal tract (Kipp et al., 2007; Banning et al., 2008). Deletion of the *GPX1* and *GPX2* genes in mice led to severe inflammation in the form of spontaneous colitis (Esworthy et al., 2011). In addition, the downregulation of *GPX3* and *GPX4* expression can also induce severe colitis and enhance tumorigenesis (Speckmann et al., 2011; Barrett et al., 2013). Therefore, supplementing selenium can upregulate the expression of *GPX*, thus preventing oxidative damage in the gastrointestinal tract and preventing inflammation.

Rats and cell culture experiments have reported that downregulation of *TrxR1* and *TrxR2* in response to selenium deficiency affects immune organs and then alters cellular signaling pathways regulated by redox, leading to increased inflammation (Flohé et al., 1997; Hirota et al., 1997; Lothrop et al., 2014). Moreover, the Ca^{2+} dependent function of SelK-deficient mice cells was decreased, and the pro-inflammatory cytokines *IL-6*, *MCP-1*, and *TNF-α* were significantly increased, while the expression of pro-inflammatory cytokines was downregulated in mice with normal *SelK* content (Nelson et al., 2011). It has been found that selenium supplementation downregulates the expression of inflammatory factors in cultured cells, and that a good selenium status can maintain the immune system under both infection and inflammatory conditions (Kudva et al., 2015). The present results showed that dietary supplementation with HMSeBA in the gilt, raised the thymus *TrxR1*, jejunum, ileum *TrxR1* and *TrxR2*, and all tissues (except the thymus) *SelK* expression, and reduced the spleen, thymus, and intestinal tissue of proinflammatory factor (*IL-1β*, *IL-6*, *TNF-α*, *IFN-β*, *MCP-1*, *ICAM-1*, and *INOS-2*) expression, increased the level of anti-inflammatory cytokines *IL-10* and the expression of *TGF-β*. Tsuji et al. also obtained similar results, by increasing selenium level in the diet, the expression levels and translation of stress-related selenoproteins *TrxR1* and *TrxR2* mRNA, as well as the expression levels and translation of genes related to inflammation and interferon-γ reaction increased, thus reduced the inflammatory response of the body and improved the immune function (Verma et al., 2011). We also found that HMSEBA significantly upregulated the expression of SEPHS2 in each intestinal segment of gilts, and SEPHS2 was mainly used as a catalyst to produce selenium phosphate and participate in the synthesis of all selenoproteins (Xu et al., 2007). Therefore, other selenoproteins in the intestine were upregulated because of the upregulated expression of *SEPHS2*, thus reducing the level of inflammation in the body and improving the immune function.

TABLE 9 | Effect of HMSeBA on the relative abundances at phyla level of colonic microbiota in gilts (%).

Item	Treatment			Values of *p*
	Control	Na_2SeO_3	HMSeBA	
Firmicutes	67.31 ± 3.49[b]	78.34 ± 1.29[a]	81.84 ± 1.45[a]	<0.01
Bacteroidetes	24.07 ± 2.82[a]	14.03 ± 0.72[b]	12.71 ± 1.37[b]	<0.01
Spirochaetes	4.42 ± 1.26	2.23 ± 0.16	2.09 ± 0.23	0.08
Actinobacteria	1.12 ± 0.28	2.43 ± 0.76	1.04 ± 0.07	0.11
Proteobacteria	1.24 ± 0.43	0.97 ± 0.25	0.55 ± 0.04	0.27
Euryarchaeota	0.34 ± 0.05	0.33 ± 0.12	0.17 ± 0.06	0.31
Tenericutes	0.36 ± 0.03	0.84 ± 0.23	1.04 ± 0.26	0.14
unidentified_Bacteria	0.10 ± 0.04	0.57 ± 0.23	0.17 ± 0.03	0.25
Melainabacteria	0.07 ± 0.00[a]	0.04 ± 0.00[b]	0.04 ± 0.00[b]	0.04
Others	0.14 ± 0.06	0.23 ± 0.05	0.28 ± 0.08	0.32
Firmicutes/Bacteroidetes	3.09 ± 0.64[b]	5.66 ± 0.39[a]	6.74 ± 0.70[a]	<0.01

Data were shown as means ± SE. n = 5 in each group. Control, basal diet; Na_2SeO_3, 0.3 mg Se/kg Na_2SeO_3; HMSeBA, 0.3 mg Se/kg HMSeBA. [a,b,c]Mean values within a row with different superscript letters were significantly different (p < 0.05).

TABLE 10 | Effect of HMSeBA on the relative abundances at genera level of colonic microbiota in gilts (%).

Item	Treatment			Values of *p*
	Control	Na_2SeO_3	HMSeBA	
Streptococcus	22.61 ± 6.26	17.54 ± 3.80	22.17 ± 5.03	0.75
Lactobacillus	4.75 ± 2.41	4.80 ± 0.37	7.82 ± 2.24	0.50
unidentified_Clostridiales	8.46 ± 0.94	9.26 ± 1.98	8.81 ± 0.46	0.92
Terrisporobacter	3.69 ± 0.25[b]	5.92 ± 0.69[ab]	8.12 ± 1.26[a]	0.01
unidentified_Ruminococcaceae	2.32 ± 0.16[b]	4.75 ± 0.92[a]	3.11 ± 0.50[ab]	0.04
Turicibacter	2.17 ± 0.28	2.40 ± 0.31	3.49 ± 0.65	0.12
Bifidobacterium	0.65 ± 0.263	1.65 ± 0.68	0.45 ± 0.08	0.14
Romboutsia	1.22 ± 0.21	1.26 ± 0.20	1.54 ± 0.29	0.59
Methanobrevibacter	0.33 ± 0.05	0.33 ± 0.12	0.17 ± 0.06	0.32
unidentified_Spirochaetaceae	1.00 ± 0.35	0.78 ± 0.18	0.62 ± 0.08	0.52
unidentified_Prevotellaceae	1.38 ± 0.17[a]	1.06 ± 0.12[ab]	0.79 ± 0.10[b]	0.03
unidentified_Lachnospiraceae	0.93 ± 0.13	1.27 ± 0.16	1.10 ± 0.11	0.24
Alloprevotella	0.45 ± 0.09	0.48 ± 0.02	0.33 ± 0.02	0.23
Mitsuokella	0.27 ± 0.07	0.67 ± 0.21	0.35 ± 0.08	0.12
Succinivibrio	0.02 ± 0.00	0.03 ± 0.00	0.04 ± 0.01	0.12
Megasphaera	0.15 ± 0.03[b]	0.53 ± 0.05[a]	0.25 ± 0.04[b]	<0.01
Phascolarctobacterium	0.22 ± 0.02	0.34 ± 0.03	0.32 ± 0.04	0.07
Anaerovibrio	0.65 ± 0.15	0.67 ± 0.14	0.61 ± 0.09	0.96
unidentified_Enterobacteriaceae	0.15 ± 0.07	0.10 ± 0.03	0.11 ± 0.02	0.70
Oscillospira	0.25 ± 0.02	0.52 ± 0.14	0.45 ± 0.04	0.14
Acetitomaculum	0.20 ± 0.02[b]	0.52 ± 0.13[a]	0.26 ± 0.04[b]	0.04
Blautia	0.15 ± 0.02	0.16 ± 0.02	0.12 ± 0.01	0.39
Oscillibacter	0.24 ± 0.01	0.34 ± 0.06	0.33 ± 0.03	0.25
Parabacteroides	0.37 ± 0.07	0.21 ± 0.04	0.26 ± 0.02	0.09
Lachnospira	0.15 ± 0.02	0.15 ± 0.00	0.16 ± 0.01	0.89
Intestinibacter	0.16 ± 0.03[b]	0.25 ± 0.04[ab]	0.34 ± 0.05[a]	0.03
Others	44.76 ± 4.46	36.08 ± 1.90	33.91 ± 2.92	0.09

Data were shown as means ± SE. n = 5 in each group. Control, basal diet; Na_2SeO_3, 0.3 mg Se/kg Na_2SeO_3; HMSeBA, 0.3 mg Se/kg HMSeBA. [a,b,c]Mean values within a row with different superscript letters were significantly different (p <0.05).

It can be seen from the above results that the immune system relies on a good selenium state to fight bacterial and viral infections, deal with oxidative damage, and regulate inflammation. It has been reported that adding selenium in the basal diet of sows effectively increased the serum IgA, IgG, and IgM concentrations of sows and their offspring (Gelderman and Clapper, 2014). When adding inorganic selenium or organic selenium to the diet, the serum IgG concentration of the ewe increased (Cabello et al., 1983). Low selenium content may also affect intestinal mucosal immunity. In commercial broilers, selenium deficiency reduced the content of soluble IgA in the duodenal mucosa and increased the level of pro-inflammatory cytokine IL-1β. In contrast, anti-inflammatory cytokines, such as TGF-β1 and IL-10, were significantly inhibited (Liu et al., 2016). In present study, the HMSeBA group increased the protein

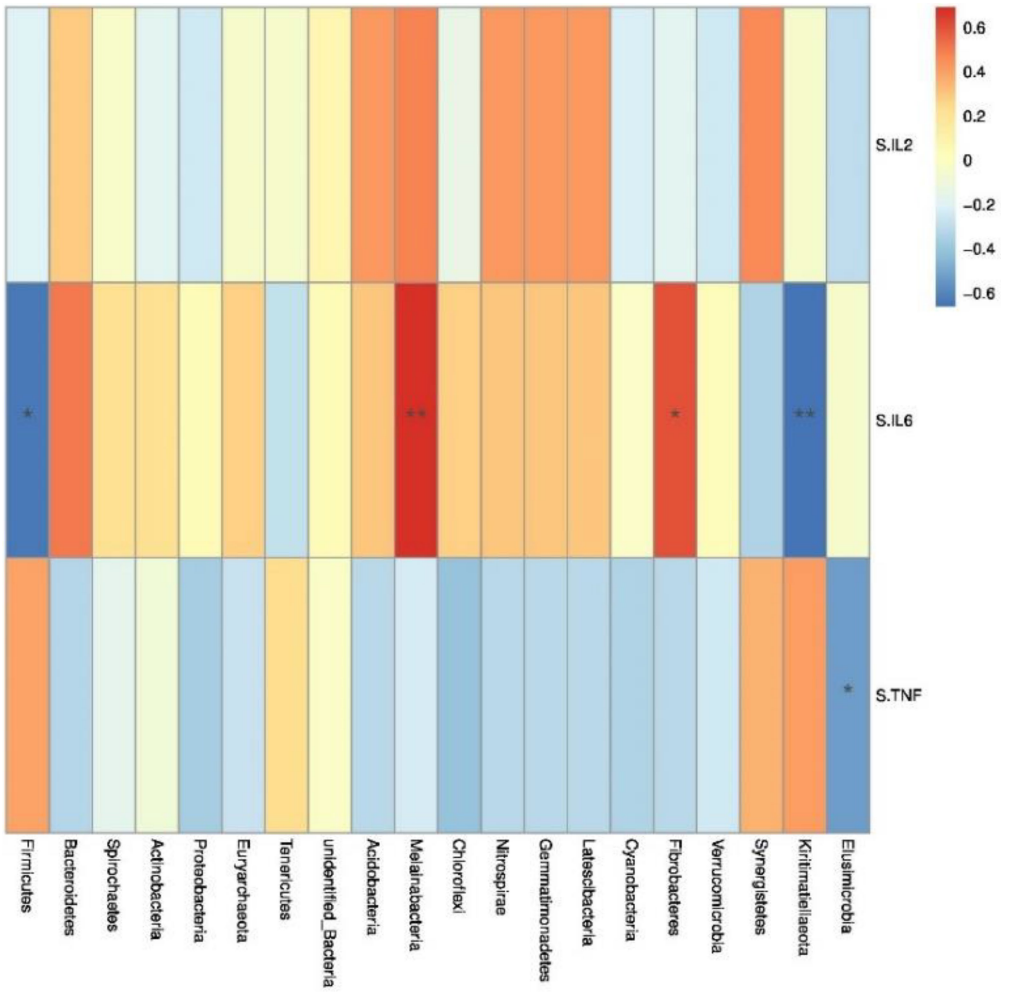

FIGURE 5 | Heat map of correlation analysis between serum cytokines and microorganisms at the phylum level. S.IL2: serum IL-2; S.IL6: serum IL-6; S.TNF: serum TNF-α. $n = 5$. Spearman diagram showed that the ordinate was environmental factor information, and the abscess was species information. The value corresponding to the middle heat map was Spearman correlation coefficient r, which was between −1 and 1. $r < 0$ was negative correlation, $r >$ was positive correlation, and the marker * indicated $p < 0.05$ for significance test.

concentrations of IL-2 and IgG in serum. And compared with the control group, the HMSeBA group decreased the protein concentrations of proinflammatory factors IL-6 and TNF-α, and increased the concentration of sIgA in the intestine. Studies have shown that low selenium leads to reduce intestinal sIgA secretion, a lower intestinal immunological barrier, and thus reduces intestinal immune function (Liu et al., 2016). The reason may be that selenium deficiency causes the increase of free radicals in the intestinal mucosa, which increases the expression of inflammatory factors, and leads to intestinal microcirculation disorders, an imbalance of T cells, blocked proliferation of lymphocytes associated with the intestine, and leads to the decrease of intestinal sIgA secretion (Hanson, 1998).

The intestinal microbiota can be regulated by dietary supplements that have the ability to stimulate the growth of beneficial bacteria and selectively inhibit the activity of pathogenic bacteria (Hrdina et al., 2009). Molan et al. found that compared with the extract without selenium, selenium extract significantly increased the number of Lactobacillus and Bifidobacterium in the cecum of rats, and reduced the number of *Escherichia coli* and Salmonella (Molan et al., 2010). The present results showed that dietary supplementation with HMSeBA reduced the number of Parabacteroides and Prevotellaceae in the intestine, and increased the number of Ruminococcaceae and Phascolarctobacterium. At the phylum level correlation analysis, Firmicutes was negatively correlated with serum levels of cytokines, 16S rRNA results showed that the HMSeBA treatment group increased the abundance of Firmicutes in the colon chyme, indicating that HMSeBA could downregulate the level of inflammatory cytokines. Meanwhile, inflammatory factor levels may also affect the abundance of microbiota, thus affecting the overall diversity of microbial communities. Dietary selenium can affect the overall diversity of existing intestinal microbiota as well as the establishment of gastrointestinal microbiota,

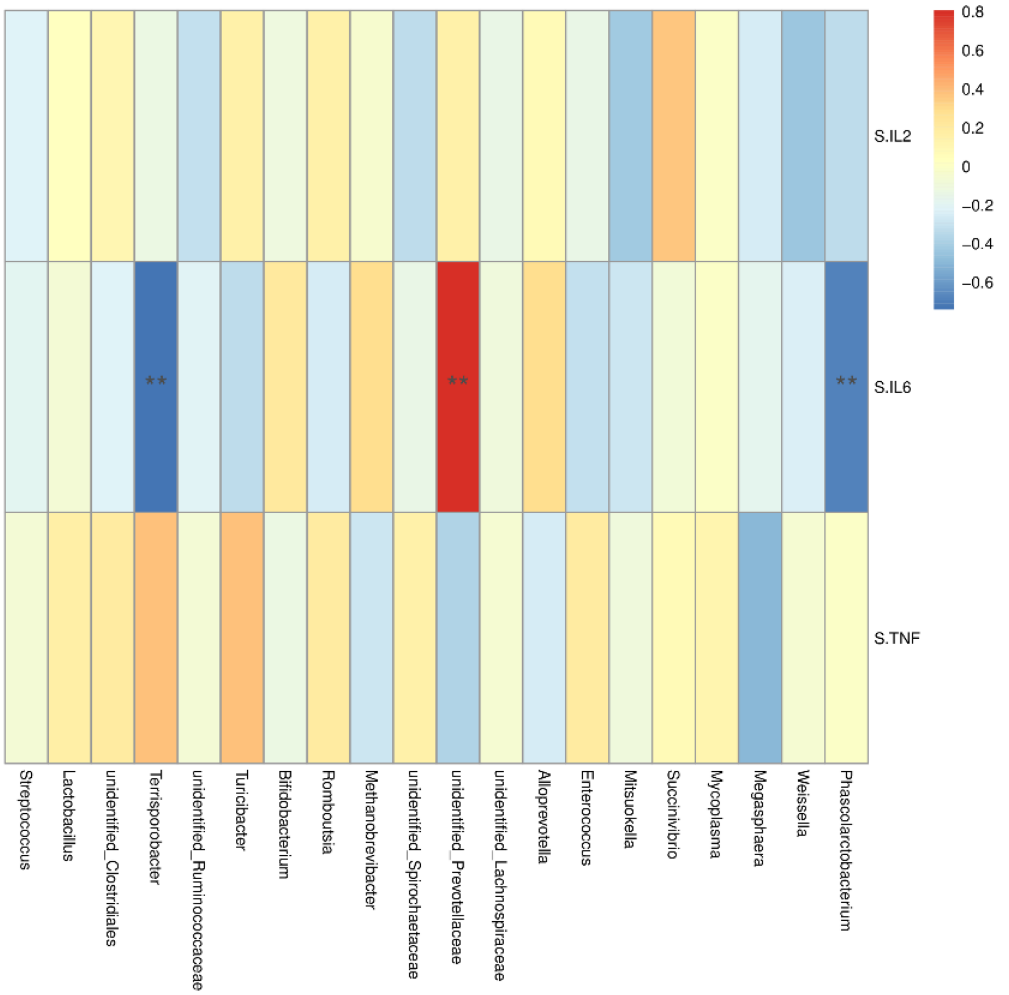

FIGURE 6 | Heat map of correlation analysis between serum cytokines and microorganisms at the genus level. S.IL2: serum IL-2; S.IL6: serum IL-6 S.TNF: serum TNF-α. $n = 5$. Spearman diagram showed that the ordinate was environmental factor information, and the abscess was species information. The value corresponding to the middle heat map was Spearman correlation coefficient r, which was between −1 and 1. $r < 0$ was negative correlation, $r >$ was positive correlation, and the marker * indicated $p < 0.05$ for significance test.

and the Parabacteroides group of Bacteroides is inversely associated with selenium supplementation. This finding might be explained by the use of selenium by various microorganisms and the toxicity of selenium to some organisms (Kasaikina and Kravtsova, 2011). The sensitivity of microorganisms to dietary selenium may be related to the regulation of host selenium status, and it has been shown that gastrointestinal microbiota affects host selenium status and selenium protein expression. Under the condition of selenium deficiency, the activities of GPX and TR in liver and intestine of germ-free (GF) mice were higher than those of conventionalized (CV) mice, and the expression of GPX1 and its mRNA in liver and colon were also higher (Hrdina et al., 2009). These results were consistent with marina's study, which found that the level of selenoprotein in GF mice was higher than that in CV mice (Fukushima et al., 2003). Therefore, dietary selenium affects the host's selenium status and the expression of selenoproteins by affecting the composition of intestinal flora, and then affects the level of inflammatory factors and immune function.

CONCLUSION

In conclusion, adding 0.3 mg Se/kg HMSeBA to the diet can improve tissue selenium content, antioxidant capacity, immunoglobulin concentration, and immune-related selenoprotein gene expression of gilts, reduce the level of proinflammatory factors, promote the growth of intestinal beneficial bacteria, and further enhance the immune function of gilts.

DATA AVAILABILITY STATEMENT

The datasets generated for this study can be found in online repositories. The names of the repository/repositories and

accession number(s) can be found at: https://www.ncbi.nlm.nih.gov/, PRJNA750710.

ETHICS STATEMENT

The animal study was reviewed and approved by All animal procedures used in this study were approved by the Animal Care and Use Committee of Sichuan Agricultural University. Written informed consent was obtained from the owners for the participation of their animals in this study.

AUTHOR CONTRIBUTIONS

SX, ZL, and DW designed the study. ZL and YD carried out the animal experiments and performed the laboratory work. ZL, YD, SC, XJia, XJian, LC, YL, JL, BF, ZF, YZ, JW, and HX performed the statistical analysis. ZL wrote the paper. SX and DW revised the manuscript. All authors contributed to the article and approved the submitted version.

FUNDING

The present study was supported by National 13th Five-Year Plan Key R&D Projects: (2018YFD0501005), Sichuan Province "145" Breeding Tackle Project (Project no. 2021YFYZ0008), and Sichuan Agricultural University Double Support Project.

ACKNOWLEDGMENTS

We thank Adisseo France S.A.S. for kindly providing HMSeBA and the 111 Project (D17015). The authors would like to thank Paul Dyce for his careful editing of this manuscript.

REFERENCES

Alimohamady, R., Aliarabi, H., Bahari, A., and Dezfoulian, A. H. (2013). Influence of different amounts and sources of selenium supplementation on performance, some blood parameters, and nutrient digestibility in lambs. *Biol. Trace Elem. Res.* 154, 45–54. doi: 10.1007/s12011-013-9698-4

Avery, J. C., and Hoffmann, P. R. (2018). Selenium, selenoproteins, and immunity. *Nutrients* 10:1203. doi: 10.3390/nu10091203

Banning, A., Florian, S., Deubel, S., Thalmann, S., Müller-Schmehl, K., Jacobasch, G., et al. (2008). GPx2 counteracts PGE2 production by dampening COX-2 and mPGES-1 expression in human colon cancer cells. *Antioxid. Redox Signal.* 10, 1491–1500. doi: 10.1089/ars.2008.2047

Barrett, C. W., Ning, W., Chen, X., Smith, J. J., Washington, M. K., Hill, K. E., et al. (2013). Tumor suppressor function of the plasma glutathione peroxidase gpx3 in colitis-associated carcinoma. *Cancer Res.* 73, 1245–1255. doi: 10.1158/0008-5472.CAN-12-3150

Bradford, M. M. (1976). A rapid and sensitive method for the quantitation of microgram quantities of protein utilizing the principle of protein-dye binding. *Anal. Biochem.* 72, 248–254. doi: 10.1016/0003-2697(76)90527-3

Briens, M. L., Mercier, Y., Rouffineau, F., Vacchina, V., and Geraert, P.-A. (2013). Comparative study of a new organic selenium source v. seleno-yeast and mineral selenium sources on muscle selenium enrichment and selenium digestibility in broiler chickens. *Br. J. Nutr.* 110, 617–624. doi: 10.1017/S0007114512005545

Brigelius-Flohé, R., Banning, A., and Schnurr, K. (2003). Selenium-dependent enzymes in endothelial cell function. *Antioxid. Redox Signal.* 5:205. doi: 10.1089/152308603764816569

Burk, R. F., and Hill, K. E. (2009). Selenoprotein P-expression, functions, and roles in mammals. *Biochim. Biophys. Acta* 1790, 1441–1447. doi: 10.1016/j.bbagen.2009.03.026

Burk, R. F., and Hill, K. E. (2015). Regulation of selenium metabolism and transport. *Annu. Rev. Nutr.* 35, 109–134. doi: 10.1146/annurev-nutr-071714-034250

Cabello, G., Levieux, D., Girardeau, J. P., and Lefaivre, J. (1983). Intestinal K99+ *Escherichia coli* adhesion and absorption of colostral IgG1 in the newborn lamb: effect of fetal infusion of thyroid hormones. *Res. Vet. Sci.* 35, 242–244. doi: 10.1016/S0034-5288(18)32187-8

Cao, J., Guo, F., Zhang, L., Dong, B., and Gong, L. (2015). Effects of dietary Selenomethionine supplementation on growth performance, antioxidant status, plasma selenium concentration, and immune function in weaning pigs. *J. Anim. Sci. Biotechnol.* 5:46. doi: 10.1186/2049-1891-5-46

Chao, Y., Yu, B., He, J., Huang, Z., Mao, X., Luo, J., et al. (2019). Effects of different levels of dietary hydroxy-analogue of selenomethionine on growth performance, selenium deposition and antioxidant status of weaned piglets. *Arch. Anim. Nutr.* 73, 1–10. doi: 10.1080/1745039X.2019.1641368

Costello, A. J. (2001). A randomized, controlled chemoprevention trial of selenium in familial prostate cancer: rationale, recruitment, and design issues. *Urology* 57, 182–184. doi: 10.1016/S0090-4295(00)00969-9

Daniels, L. A. (1996). Selenium metabolism and bioavailability. *Biol. Trace Elem. Res.* 54, 185–199. doi: 10.1007/BF02784430

Esworthy, R. S., Kim, B. W., Larson, G. P., Yip, M., Smith, D. D., Min, L., et al. (2011). Colitis locus on chromosome 2 impacting the severity of early-onset disease in mice deficient in GPX1 and GPX2. *Inflamm. Bowel Dis.* 17, 1373–1986. doi: 10.1002/ibd.21479

Fairweather-Tait, S. J., Rachel, C., and Rachel, H. (2010). Selenium bioavailability: current knowledge and future research requirements. *Am. J. Clin. Nutr.* 91, 1484S–1491S. doi: 10.3945/ajcn.2010.28674J

Faixová, Z., Piešová, E., Maková, Z., Cobanova, K., and Faix, S. (2016). Effect of dietary supplementation with selenium-enriched yeast or sodium selenite on ruminal enzyme activities and blood chemistry in sheep. *Acta Vet. Brno* 85, 185–194. doi: 10.2754/avb201685020185

Flohé, L., Brigelius-Flohé, R., Saliou, C., Traber, M. G., and Packer, L. (1997). Redox regulation of NF-kappa B activation. *Free Radic. Biol. Med.* 22, 1115–1126. doi: 10.1016/S0891-5849(96)00501-1

Fossum, C., Hjertner, B., Ahlberg, V., Charerntantanakul, W., Mcintosh, K., Fuxler, L., et al. (2014). Early inflammatory response to the saponin adjuvant matrix-M in the pig. *Vet. Immunol. Immunopathol.* 158, 53–61. doi: 10.1016/j.vetimm.2013.07.007

Fukushima, K., Ogawa, H., Takahashi, K., Naito, H., Funayama, Y., Kitayama, T., et al. (2003). Non-pathogenic bacteria modulate colonic epithelial gene expression in germ-free mice. *Scand. J. Gastroenterol.* 38, 626–634. doi: 10.1080/00365510310000376

Gelderman, A., and Clapper, J. (2014). Effects of inorganic or organic selenium on immunoglobulins in swine. *J. Anim. Sci. Biotechnol.* 4:47. doi: 10.1186/2049-1891-4-47

Hanson, L. A. (1998). Breastfeeding provides passive and likely long-lasting active immunity. *Ann. Allergy Asthma Immunol.* 81, 523–533. doi: 10.1016/S1081-1206(10)62704-4

Hawkes, W. C., and Alkan, Z. (2010). Regulation of redox signaling by selenoproteins. *Biol. Trace Elem. Res.* 134, 235–251. doi: 10.1007/s12011-010-8656-7

Hirota, K., Matsui, M., Iwata, S., Nishiyama, A., and Mori, K. (1997). AP-1 transcriptional activity is regulated by a direct association between thioredoxin and Ref-1. *Proc. Natl. Acad. Sci. U. S. A.* 94, 3633–3638. doi: 10.1073/pnas.94.8.3633

Hrdina, J., Banning, A., Kipp, A., Loh, G., Blaut, M., and Brigelius-Flohé, R. (2009). The gastrointestinal microbiota affects the selenium status and selenoprotein expression in mice. *J. Nutr. Biochem.* 20, 638–648. doi: 10.1016/j.jnutbio.2008.06.009

Jlali, M., Briens, M., Rouffineau, F., Mercerand, F., Geraert, P. A., and Mercier, Y. (2013). Effect of 2-hydroxy-4-methylselenobutanoic acid as a dietary selenium

supplement to improve the selenium concentration of table eggs. *J. Anim. Sci.* 91, 1745–1752. doi: 10.2527/jas.2012-5825

Juniper, D. T., Phipps, R. H., Ramosmorales, E., and Bertin, G. (2008). Effect of dietary supplementation with selenium-enriched yeast or sodium selenite on selenium tissue distribution and meat quality in beef cattle. *J. Anim. Sci.* 86, 3100–3109. doi: 10.2527/jas.2007-0595

Kasaikina, M., and Kravtsova, M. (2011). Dietary selenium affects host selenoproteome expression by influencing the gut microbiota. *FASEB J.* 25, 2492–2499. doi: 10.1096/fj.11-181990

Kipp, A., Banning, A., and Brigelius-Flohé, R. (2007). Activation of the glutathione peroxidase 2 (GPx2) promoter by beta-catenin. *Biol. Chem.* 388, 1027–1033. doi: 10.1515/BC.2007.137

Kudva, A. K., Shay, A. E., and Prabhu, K. S. (2015). Selenium and inflammatory bowel disease. *Am. J. Physiol. Gastrointest. Liver Physiol.* 309, G71–G77. doi: 10.1152/ajpgi.00379.2014

Liu, Z., Qu, Y., Wang, J., and Wu, R. (2016). Selenium deficiency attenuates chicken duodenal mucosal immunity via activation of the NF-κb signaling pathway. *Biol. Trace Elem. Res.* 172, 465–473. doi: 10.1007/s12011-015-0589-8

Livak, K. J., and Schmittgen, T. D. (2001). Analysis of relative gene expression data using real-time quantitative PCR and the $2^{\Delta\Delta}$ C T method. *Methods* 25, 402–408. doi: 10.1006/meth.2001.1262

Lothrop, A. P., Snider, G. W., Ruggles, E. L., Patel, A. S., Lees, W. J., and Hondal, R. J. (2014). Selenium as an electron acceptor during the catalytic mechanism of thioredoxin reductase. *Biochemistry* 53, 654–663. doi: 10.1021/bi400658g

Lubos, E., Loscalzo, J., and Handy, D. E. (2010). Glutathione peroxidase-1 in health and disease: From molecular mechanisms to therapeutic opportunities. *Antioxid. Redox Signal.* 15, 1957–1997. doi: 10.1089/ars.2010.3586

Margarida, P. A., Carlo, P., Giacomo, B., Claudio, S., Maia, M., Elisabete, M., et al. (2020). Supplemental selenium source on gut health: insights on fecal microbiome and fermentation products of growing puppies. *FEMS Microbiol. Ecol.* 96:212. doi: 10.1093/femsec/fiaa212

Mehdi, Y., Hornick, J. L., Istasse, L., and Dufrasne, I. (2013). Selenium in the environment, metabolism and involvement in body functions. *Molecules* 18, 3292–3311. doi: 10.3390/molecules18033292

Mistry, D. H., Broughton, P. F., Redman, C. W., and Poston, L. (2012). Selenium in reproductive health. *Am. J. Obstet. Gynecol.* 206, 21–30. doi: 10.1016/j.ajog.2011.07.034

Molan, A. L., Liu, Z., and Tiwari, R. (2010). The ability of green tea to positively modulate key markers of gastrointestinal function in rats. *Phytother. Res.* 24, 1614–1619. doi: 10.1002/ptr.3145

Mou, D., Ding, D., Li, S., Yan, H., Qin, B., Li, Z., et al. (2020a). Effect of maternal organic selenium supplementation during pregnancy on sow reproductive performance and long-term effect on their progeny. *J. Anim. Sci.* 98:366. doi: 10.1093/jas/skaa366

Mou, D., Ding, D., Yan, H., Qin, B., Dong, Y., Li, Z., et al. (2020b). Maternal supplementation of organic selenium during gestation improves sows and offspring antioxidant capacity and inflammatory status and promotes embryo survival. *Food Funct.* 11, 7748–7761. doi: 10.1039/d0fo00832j

Mou, D., Wang, J., Liu, H., Chen, Y., Che, L., Fang, Z., et al. (2018). Maternal methyl donor supplementation during gestation counteracts bisphenol A-induced oxidative stress in sows and offspring. *Nutrients* 45, 76–84. doi: 10.1016/j.nut.2017.03.012

National Research Council (2012). *Nutrient Requirements of Swine: Eleventh Revised Edition*. Washington, DC: The National Academies Press.

Nelson, S. M., Lei, X., and Prabhu, K. S. (2011). Selenium levels affect the IL-4-induced expression of alternative activation markers in murine macrophages. *J. Nutr.* 141, 1754–1761. doi: 10.3945/jn.111.141176

Rita, S., and Nancy, M. (2015). A review of dietary selenium intake and selenium status in Europe and the Middle East. *Nutrients* 7, 1494–1537. doi: 10.3390/nu7031494

Ruan, T., Li, L., Lyu, Y., Luo, Q., and Wu, B. (2018). Effect of methionine deficiency on oxidative stress and apoptosis in the small intestine of broilers. *Acta Vet. Hung.* 66, 52–65. doi: 10.1556/004.2018.006

Schrauzer, , and Gerhard, N. (2000). Selenomethionine: a review of its nutritional significance, metabolism and toxicity. *J. Nutr.* 130, 1653–1656. doi: 10.1093/jn/130.7.1653

Schwarz, K., and Fredga, A. (1969). Biological potency of organic selenium compounds. *J. Biol. Chem.* 244, 2103–2110. doi: 10.1016/S0021-9258(18)94372-3

Shini, S., Sultan, A., and Bryden, W. L. (2015). Selenium biochemistry and bioavailability&58; implications for animal agriculture. *Agriculture* 5, 1277–1288. doi: 10.3390/agriculture5041277

Speckmann, B., Bidmon, H. J., Pinto, A., Anlauf, M., Sies, H., and Steinbrenner, H. (2011). Induction of glutathione peroxidase 4 expression during enterocytic cell differentiation. *J. Biol. Chem.* 286, 10764–10772. doi: 10.1074/jbc.M110.216028

Speight, S. M., Estienne, M. J., Harper, A. F., Barb, C. R., and Pringle, T. D. (2012). Effects of organic selenium supplementation on growth performance, carcass measurements, tissue selenium concentrations, characteristics of reproductive organs, and testis gene expression profiles in boars. *J. Anim. Sci.* 90:533. doi: 10.2527/jas.2010-3747

Stadtman, T. (1996). A new selenoprotein from human lung adenocarcinoma cells: purification, properties, and thioredoxin reductase activity. *Proc. Natl. Acad. Sci. U. S. A.* 93, 1006–1011. doi: 10.1073/pnas.93.3.1006

Vendeland, S. C., Deagen, J. T., Butler, J. A., and Whanger, P. D. (1994). Uptake of selenite, selenomethionine and selenate by brush border membrane vesicles isolated from rat small intestine. *BioMetals* 7, 305–312. doi: 10.1007/BF00144126

Verma, S., Hoffmann, F. W., Kumar, M., Huang, Z., Roe, K., Nguyen-Wu, E., et al. (2011). Selenoprotein K knockout mice exhibit deficient calcium flux in immune cells and impaired immune responses. *J. Immunol.* 186, 2127–2137. doi: 10.4049/jimmunol.1002878

Wan, K., Li, Y., Sun, W., An, R., Tang, Z., Wu, L., et al. (2020). Effects of dietary calcium pyruvate on gastrointestinal tract development, intestinal health and growth performance of newly weaned piglets fed low-protein diets. *J. Appl. Microbiol.* 128, 355–365. doi: 10.1111/jam.14494

Wang, Y. X., Zhan, X. A., Yuan, D., Zhang, X. W., and Wu, R. J. (2011). Influence of dietary Selenomethionine supplementation on performance and selenium status of broiler breeders and their subsequent progeny. *Biol. Trace Elem. Res.* 143, 1497–1507. doi: 10.1007/s12011-011-8976-2

Xu, S., Shi, J., Dong, Y., Li, Z., and Shen, Y. (2020). Fecal bacteria and metabolite responses to dietary lysozyme in a sow model from late gestation until lactation. *Sci. Rep.* 10:3210. doi: 10.1038/s41598-020-60131-1

Xu, X. M., Carlson, B., Irons, R., Mix, H., Zhong, N., Gladyshev, V., et al. (2007). Selenophosphate synthetase 2 is essential for selenoprotein biosynthesis. *Biochem. J.* 404, 115–120. doi: 10.1042/BJ20070165

Yan, W., and Chen, X. (2006). GPX2, a direct target of p63, inhibits oxidative stress-induced apoptosis in a p53-dependent manner. *J. Biol. Chem.* 281, 7856–7862. doi: 10.1074/jbc.M512655200

Żarczyńska, K., Sobiech, P., Radwińska, J., and Rękawek, W. (2013). Effects of selenium on animal health. *J. Elem.* 18, 329–340. doi: 10.5601/jelem.2013.18.2.12

Conflict of Interest: The authors declare that the research was conducted in the absence of any commercial or financial relationships that could be construed as a potential conflict of interest.

frontiers in Microbiology

ORIGINAL RESEARCH
published: 26 August 2021
doi: 10.3389/fmicb.2021.719967

Supplementation With *Lycium barbarum* Polysaccharides Reduce Obesity in High-Fat Diet-Fed Mice by Modulation of Gut Microbiota

Mei Yang[1], Yexin Yin[1], Fang Wang[1], Haihan Zhang[1], Xiaokang Ma[1], Yulong Yin[1,2], Bie Tan[1] and Jiashun Chen[1,2]**

[1] Animal Nutritional Genome and Germplasm Innovation Research Center, College of Animal Science and Technology, Hunan Agricultural University, Changsha, China, [2] CAS Key Laboratory of Agro-ecological Processes in Subtropical Region, Institute of Subtropical Agriculture, Changsha, China

Lycium barbarum polysaccharides (LBPs) have been proved to prevent obesity and modulate gut microbiota. However, the underlying mechanisms of LBPs' regulating lipid metabolism remain entirely unclear. Therefore, the purpose of this study was to determine whether LBPs are able to modulate the gut microbiota to prevent obesity. The results showed that oral administration of LBPs alleviated dyslipidemia by decreasing the serum levels of total triglycerides, total cholesterol, and low-density lipoprotein-cholesterol and elevating the high-density lipoprotein cholesterol in obese mice. Furthermore, LBP treatment decreased the number and size of adipocytes in epididymal adipose tissues and downregulated the expression of adipogenesis-related genes, including acetyl-CoA carboxylase 1, fatty acid synthase, stearoyl-CoA desaturase 1, sterol regulatory element-binding protein-1c, peroxisome proliferator-activated receptor γ, and CCAAT/enhancer-binding protein α. 16S rRNA gene sequencing analysis showed that LBPs increased the diversity of bacteria, reduced the *Firmicutes*/*Bacteroidetes* ratio, and improved the gut dysbiosis induced by a high-fat diet; for example, LBPs increased the production of short-chain fatty acid-producing bacteria *Lacticigenium*, *Lachnospiraceae_NK4A136_group*, and *Butyricicoccus*. LBPs treatment also increased the content of fecal short-chain fatty acids, including butyric acid. These findings illustrate that LBPs might be developed as a potential prebiotic to improve lipid metabolism and intestinal diseases.

Keywords: *Lycium barbarum* polysaccharides, high-fat diet, gut microbiota, lipid metabolism, obesity

OPEN ACCESS

Edited by:
Zheng Ruan,
Nanchang University, China

Reviewed by:
Hui Yan,
Sichuan Agricultural University, China
Jin Wan,
Nanchang University, China

****Correspondence:***
Jiashun Chen
jschen@hunau.edu.cn
Yulong Yin
yinyulong@isa.ac.cn

Specialty section:
This article was submitted to Food Microbiology, a section of the journal Frontiers in Microbiology

Received: *03 June 2021*
Accepted: *09 July 2021*
Published: *26 August 2021*

Citation:
Yang M, Yin Y, Wang F, Zhang H, Ma X, Yin Y, Tan B and Chen J (2021) Supplementation With Lycium barbarum Polysaccharides Reduce Obesity in High-Fat Diet-Fed Mice by Modulation of Gut Microbiota. Front. Microbiol. 12:719967. doi: 10.3389/fmicb.2021.719967

INTRODUCTION

Obesity is an important risk factor for many chronic diseases such as type II diabetes, cardiovascular and cerebrovascular diseases, cancer, and so on (Shin and Yoon, 2018), and which has become one of the top health problems in the world. It becomes a major challenge for modern societies to decrease the incidence of obesity and its associated diseases. The pathogenesis of obesity is complex that mainly involves genetic and environmental factors (Silventoinen et al., 2007). A wealth of evidence has demonstrated that the gut microbiota plays an important role in regulating nutrient

acquisition and body weight, thus serving as a key factor to regulate obesity, and its associated disorders (Ridaura et al., 2013; Sanmiguel et al., 2015).

The gut microbiota primarily contains *Firmicutes*, *Bacteroidetes*, *Actinobacteria*, and *Proteobacteria* phyla, which are composed of more than 1,000 different bacterial species, but not all species are known to this date (Ley et al., 2005). A high-fat diet has been reported to reshape the gut microbiota, particularly by increasing the proportion of *Firmicutes* in relation to *Bacteroidetes*, which plays a significant role in the pathogenesis of obesity-induced metabolic diseases (Hildebrandt et al., 2009). Several studies provide scientific evidence that the gut microbiota is becoming a promising therapeutic target for dietary interventions to protect against obesity (Ojo et al., 2016; Zheng et al., 2018). In recent years, some plant-derived natural bioactive compounds, including polysaccharides, were reported to be helpful to reduce weight gain, and fat accumulation *via* the modulation of the gut microbiota (Shang et al., 2017; Sun et al., 2018).

Red-colored fruits of *Lycium barbarum* (Gouqizi, Fructus Lycii, or wolfberry) are used as traditional Chinese herbal medicine to promote health and longevity, and as a food supplement for 1,000 of years (Qian, 2019). *Lycium barbarum* polysaccharides (LBPs) are the main active constituents of *L. barbarum* fruits, which possess a variety of pharmacological effects, such as antioxidant, anti-stress, neuroprotective activities, anti-aging, antidiabetic activities, immune regulation, protection against liver damage, and reduction of blood glucose level (Luo et al., 2004; Ha et al., 2005). Recent studies have shown that LBPs play a vital role in regulating hepatic lipid metabolism (Jia et al., 2016). Furthermore, LBPs improve dyslipidemia, promotes energy expenditure, reduces body weight, and alleviates non-alcoholic steatohepatitis (Xiao et al., 2013, 2014). Dysfunction of hepatic energy signaling induced by a high-fat diet represents a key mechanism for hepatic insulin resistance and lipid accumulation associated with non-alcoholic fatty liver disease (Li et al., 2014). However, studies on the anti-obesogenic activity of LBPs and the related gut dysbiosis are limited. Our previous studies demonstrated that supplementation with LBPs in piglet diets stimulated the growth of beneficial gut bacteria and suppressed the growth of *Escherichia coli* (Chen et al., 2019). Although numerous health benefits of LBPs have been reported, their effects on the gut microbiota in animals with high fat-diet-induced dysbiosis are not known. Therefore, the objectives of the present study are to investigate the effects of LBPs on the gut microbiota, blood lipids, and genetic factors regarding lipid metabolism in high-fat diet-fed mice. The results will increase our understanding of how LBPs regulate gut microbiota to exert anti-obesogenic effects.

MATERIALS AND METHODS

Animals and Dietary Treatments

All procedures were approved by the Animal Care and Use Committee of Hunan Agricultural University, People's Republic of China (permit number: CACAHU 2020-0821). Three-week-old male ICR mice (specific pathogen-free) were purchased from Shanghai Laboratory Animal Central (Changsha, China). After a 1-week adaptation period, the mice were housed in a controlled environment (temperature: 23 ± 2°C, relative humidity: 50 ± 5%, and a 12-h light–dark cycle), with free access to food and drinking water during the experiment.

Thirty mice were randomly separated into three groups (n = 10), including the normal chow diet group (NC), the high-fat diet group (HFD), and the HFD-fed mice with the LBP group (HFD + LBPs). The NC group was fed with an NC diet (research diet D12450B, containing 10% kcal from fat, 3.85 total kcal/g, and Beijing Botai Hongda Biotechnology Co., Ltd.); mice in the HFD and HFD + LBP groups were fed an HFD (research diet D12492, containing 60% kcal from fat, and 5.24 total kcal/g) as model controls (Shang et al., 2017). Moreover, mice in the HFD + LBP group drank water containing 0.2% of LBPs from the beginning, and the other two groups received sterile water. In the current study, LBPs (high-performance liquid chromatography ≥ 60%) comprised D-mannose, L-rhamnose, D-glucose, D-galactosamine, and D-xylose, purchased from Xi'an ZeBang Biological Technology Co., Ltd. (Xi'an, China). Throughout the experiment, the body weight and food intake of mice were measured weekly for 10 weeks. Fecal samples were collected and stored at −80°C until further analysis. At the end of the experiment, all mice were fasted overnight and killed by cervical dislocation with sodium pentobarbital anesthesia, and all efforts were made to minimize suffering. After killing, blood, liver, epididymal adipose tissues, cecum, colon, and colon contents were collected for further analyses.

Analysis of Biochemical Parameters in Blood and Liver Samples

Blood samples were collected from the orbital venous plexus of mice under anesthesia. The serum was obtained from blood samples with the centrifugation at 4,000 × g at 4°C for 10 min and stored at −80°C for further analysis. The levels of high-density lipoprotein cholesterol (HDL-C), low-density lipoprotein cholesterol (LDL-C), total cholesterol (TC), triacylglycerols (TG), and malondialdehyde (MDA) in serum and liver were monitored by the corresponding assay kits according to the manufacturer's instructions (Nanjing Jiancheng Bioengineering Institute, China).

Histology Analysis

The liver and epididymal adipose tissues were removed and fixed in 4% formaldehyde solution, after which the fixed tissues were paraffin-embedded and the liver and epididymal adipose tissues blocks were cut into 5-μm sections, and stained with hematoxylin and eosin.

RNA Extraction and Gene Expression Analysis

Total RNA from the epididymal adipose tissues was isolated using Trizol reagent (Invitrogen, United States) and treated with DNase I (Promega Corporation, Germany) according to the manufacturer's instructions. The complementary DNA

(cDNA) was generated from total RNA according to the reverse transcription kit (TaKaRa Company, Dalian). The ABI 7900HT-polymerase chain reaction (PCR) instrument (ABI Biotechnology, United States) was used to amplify the samples by using SYBR-Green I dye (Molecular Probes, Eugene, OR, United States) and using the supporting software (Applied Biosystem, SDS2.3) for data analysis. The PCR primers sequences for the corresponding genes were listed in **Supplementary Table 1**. The PCR was performed in duplicate at 95°C for 3 min and subjected to 40 cycles of 95°C for 30 s, 55°C for 30 s, and 72°C for 45 s. The relative expression levels of target genes cDNA to β-actin cDNA were calculated as a ratio by the $2^{-\Delta\Delta Ct}$ formula.

DNA Extraction and High Throughput Sequencing

Metagenomic DNA was extracted using the E.Z.N.A.® Soil DNA Kit (Omega Bio-tek, United States) according to the manufacturer's protocols. The V3–V4 regions of the cecal microbiota 16S rRNA gene were amplified by using specific primers of (338F: 5′ ACTCCTACGGGAGGCAGCAG-3′; 806R: 5′- GGACTACHVGGGTWTCTAAT-3′) by ABI GeneAmp PCR System 9700 (Applied Biosystems, Foster City, CA, United States) in triplicate. The PCR products were examined and purified from 2% agarose gels and purified using the AxyPrep DNA Gel Extraction Kit (Axygen Biosciences, United States) and quantified by QuantiFluor™ -ST (Promega, United States). The purified amplicons were pooled in equimolar and ligated with 300-bp paired-end adapters by TruSeq™ DNA Sample Prep Kit (Illumina, United States), then sequenced on an Illumina MiSeq platform (Illumina, United States) according to the standard protocols by Majorbio Bio-Pharm Technology Co., Ltd. (Shanghai, China).

Bioinformatics Analysis

The raw sequencing data were quality trimmed and filtered by Trimmomatic and merged with FLASH according to the overlap sequences. The reads were truncated at any site accepting an average mass value less than 20 in a 50-bp sliding window (Wang W. et al., 2019). Operational taxonomic units (OTUs) were generated by clustering at 97% similarity using USEARCH v7.0,[1] and chimeric sequences were identified and removed using UCHIME (Wang S. et al., 2018). The classification of each 16S rRNA gene sequence was performed by RDP Classifier v2.11[2] according to the SILVA (Release132[3]) 16S rRNA database with a confidence threshold of 70%. Alpha diversity was analyzed using MOTHUR v1.30.2,[4] and beta diversity was determined using QIIME. Alpha diversity analysis included Shannon and Chao index. Beta diversity included unweighted unifrac distances calculated with 10 times of subsampling, and these distances were visualized by principal coordinate analysis. To identify the dimensional gut bacteria and characterize the microbial differences between different groups, the linear discriminant analysis (LDA) effect size analysis was performed. The non-parametric factorial Kruskal–Wallis sum-rank test was applied to detect features that were significantly different between assigned taxa, and the LDA was used to quantify the effect size of each feature. A significance alpha value of less than 0.05 and an effect size threshold of 3 were used for this analysis.

[1]http://drive5.com/usearch/

[2]http://sourceforge.net/projects/rdp-classifier/

[3]https://www.arb-silva.de/

[4]https://www.mothur.org/wiki/Download_mothur

Analysis of Short-Chain Fatty Acids

The contents of colon and fecal samples were collected, and a mixture of supernatant fluid and 25% metaphosphoric acid solution (4: 1 ml) was prepared for the determination of SCFAs (acetic acid, butyric acid, propionic acid, and valeric acid). Samples were incubated at room temperature and centrifuged, and the supernatants were filtered by using 0.45-μm polytetrafluoroethylene syringe filters into chromatographic glass vials (Agilent Technologies). Gas chromatography was performed using an Agilent 6890 GC system with a flame ionizable detector and an automatic liquid sampler (Agilent Technologies, Santa Clara, CA, United States) as previously described (Chen et al., 2018).

Statistical Analysis

One-way analysis of variance was used for statistical analysis using SPSS 25.0 software. Any differences among treatments were then compared using the Duncan comparison range tests. The experimental data are expressed as the means ± SEM; $P < 0.05$ among different groups were considered statistically significant.

RESULTS

Animal Weight and Food Intake

The HFD group exhibited a 14% higher final body weight as compared with the NC group (**Figure 1A**) ($P < 0.05$). The HFD-fed mice treated with LBPs reduced body weight by 7% compared with the HFD group (**Figure 1A**) ($P > 0.05$). LBP supplementation slightly decreased the body weight gain in mice with HFD feeding (**Figure 1B**) ($P > 0.05$). Supplementation with LBPs has no significant effect on food intake in HFD-fed mice (**Figure 1C**) ($P > 0.05$). The weight of total cecum and cecum in the HFD group was lower than that of the NC group (**Figures 1D,E**) ($P < 0.05$). In addition, LBP treatment improved the weight of the cecum in the HFD group (**Figure 1E**) ($P < 0.05$).

Serum and Liver Lipid Content

The consumption of dietary fat induces anomalous changes in lipid content, including TG, TC, HDL-C, and LDL-C. Compared with the NC group, HFD-fed mice had reduced HDL-C levels along with increased TG, and TC levels in serum ($P < 0.05$). Supplementation with LBPs increased HDL-C level and reduced the levels of TG, TC, and MDA in HFD-fed mice (**Figure 2A**) ($P < 0.05$). However, the TG, TC, and MDA contents in the liver were decreased after LBP administration in comparison with the HFD group (**Figure 2B**) ($P < 0.05$).

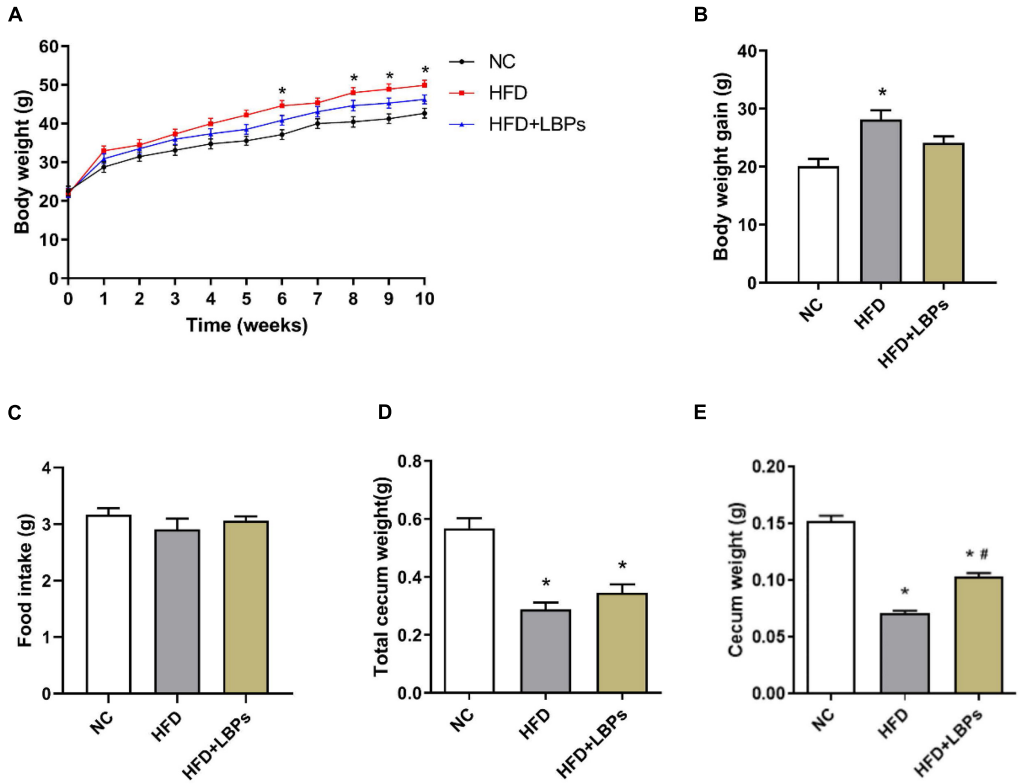

FIGURE 1 | Effects of *Lycium barbarum* polysaccharides (LBPs) on **(A)** body weight, **(B)** weight gain, **(C)** food intake, **(D)** total cecum, and **(E)** cecum tissues in HFD-fed mice. $^{*}P < 0.05$ vs. NC group and $^{\#}P < 0.05$ vs. HFD group.

Lipid Accumulation and Metabolism in Liver and Epididymal Adipose Tissues

Compared with the NC group, the HFD group increased the weight of liver, and epididymal adipose tissues. Treatment with LBPs reduced this parameter in the HFD + LBP group compared with the HFD group (**Figures 3A–C**) ($P < 0.05$). Histology analysis revealed that fat accumulation occurred in the HFD group. LBP administration decreased the fat accumulation, and the size and number of adipocytes in adipose tissues were near to the NC group (**Figures 3B–D**).

Adipogenesis-Related Gene Expression in the Epididymal Adipose Tissues

Administration of LBPs downregulated expression levels of adipogenesis-related gene including acetyl coenzyme A carboxylase 1 (ACC1), fatty acid synthase (FAS), synthesis *via* stearoyl-CoA desaturase 1 (SCD1), sterol regulatory element-binding protein 1c (SREBP-1c), peroxisome proliferator-activated receptor-γ (PPARγ), and CCAAT/enhancer-binding protein alpha (C/EBPα) in epididymal adipose tissue compared with HFD group (**Figure 4**) ($P < 0.05$).

Gut Microbiota

Compared with the NC group, the Shannon index was decreased in the HFD, whereas the administration of LBPs reversed these indexes in HFD-fed mice ($P < 0.05$). LBP administration did not significantly influence the bacterial richness compared with the HFD group (**Figure 5A**) ($P > 0.05$). The analysis of OTU in the fecal showed that 335 OTUs were common between HFD + LBP and NC groups, whereas 42 OTUs were unique in the HFD group compared with 98 in the NC group. LBP administration increased the number of shared OTU from 335 to 358 (**Figure 5B**). For unweighted unifrac distance metrics, the NC group exhibited clustering of microbiota composition distinctly different from the HFD group. LBP treatment increased the similarity between the overall gut microbiota compositions of the HFD + LBP and NC groups, indicating that LBPs improved the structure of gut microbiota in HFD-fed mice (**Figure 5C**).

At the phylum level, the top six phyla in the microbial communities included *Firmicutes*, *Desulfobacterota*, *Actinobacteriota*, *Bacteroidetes*, *Campilobacterota*, and *Proteobacteria* in the three groups, accounting for almost 99% of total bacteria. The HFD group reduced the relative abundance of *Bacteroidetes* and increased the relative abundance of *Firmicutes* ($P < 0.05$). After LBPs treatment, *Firmicutes* was reduced by 1.07-fold, whereas *Bacteroidetes* was increased by 2.73-fold in the HFD-fed mice compared with non-treatment mice. The *Firmicutes*/*Bacteroidetes* ratio was significantly increased by the HFD ($P < 0.05$). Differing from the HFD group, LBP administration significantly reduced the ratio of *Firmicute/Bacteroidetes* (**Figure 6A**)

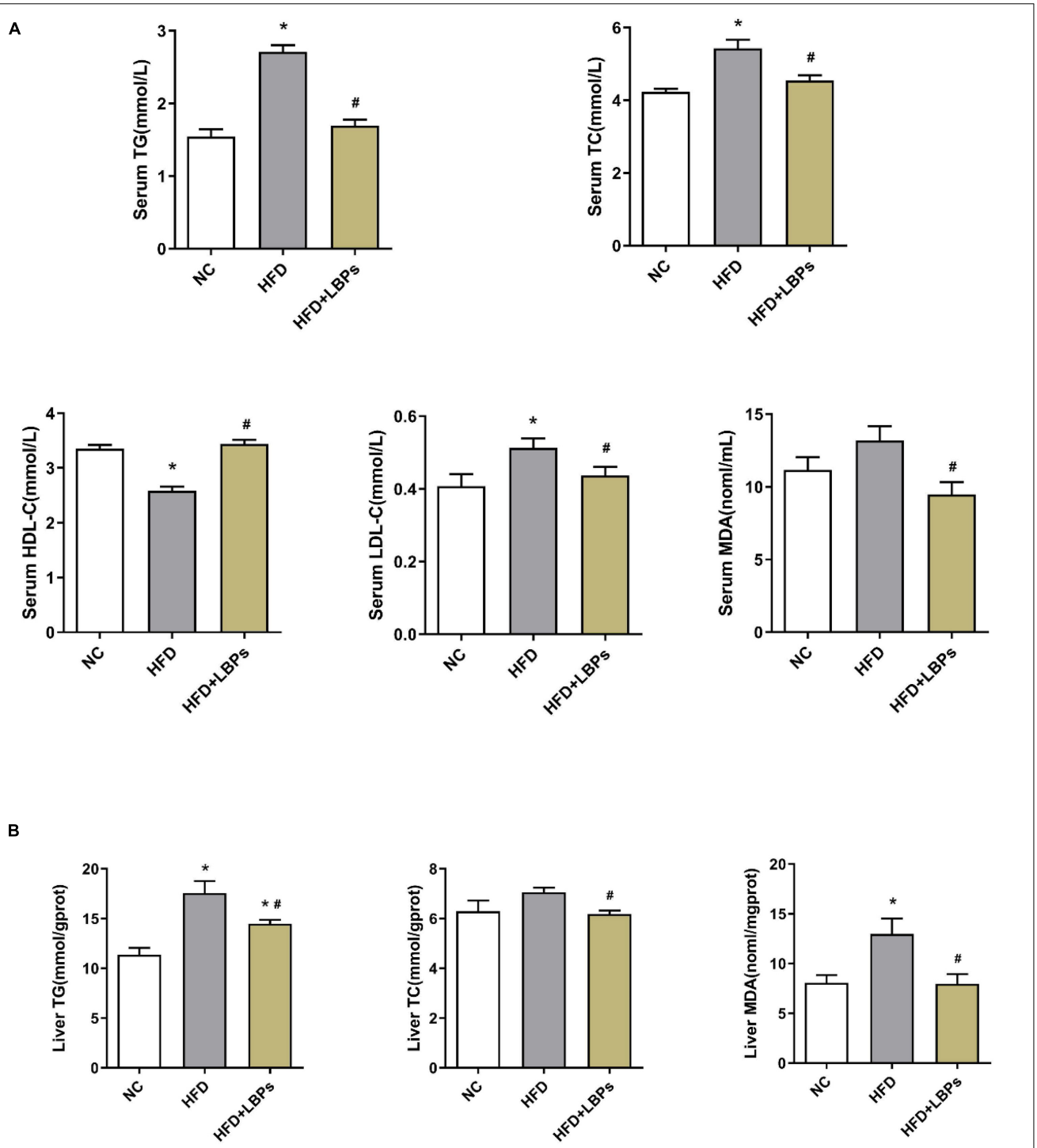

FIGURE 2 | Effects of *Lycium barbarum* polysaccharides (LBPs) on **(A)** serum and **(B)** liver lipids profile in HFD-fed mice. $^{*}P < 0.05$ vs. NC group and $^{\#}P < 0.05$ vs. HFD group.

($P < 0.05$). At the genus level, *Lactobacillus*, *Faecalibaculum*, *norank_f__Desulfovibrionaceae*, and *Bifidobacterium* were the dominant genera in the HFD + LBP group. HFD markedly increased the relative abundance of *Lactobacillus* and reduced the relative abundance of *Bacteroides* compared with the NC group ($P < 0.05$). After LBP treatment, the abundance of *Lactobacillus* and *Faecalibaculum* decreased by 1.16 and 1.27-fold, respectively, whereas *Bacteroides* was increased by 4.19-fold compared with the non-treatment group (**Figure 6B**). LDA effect size uses LDA to estimate the impact of abundance

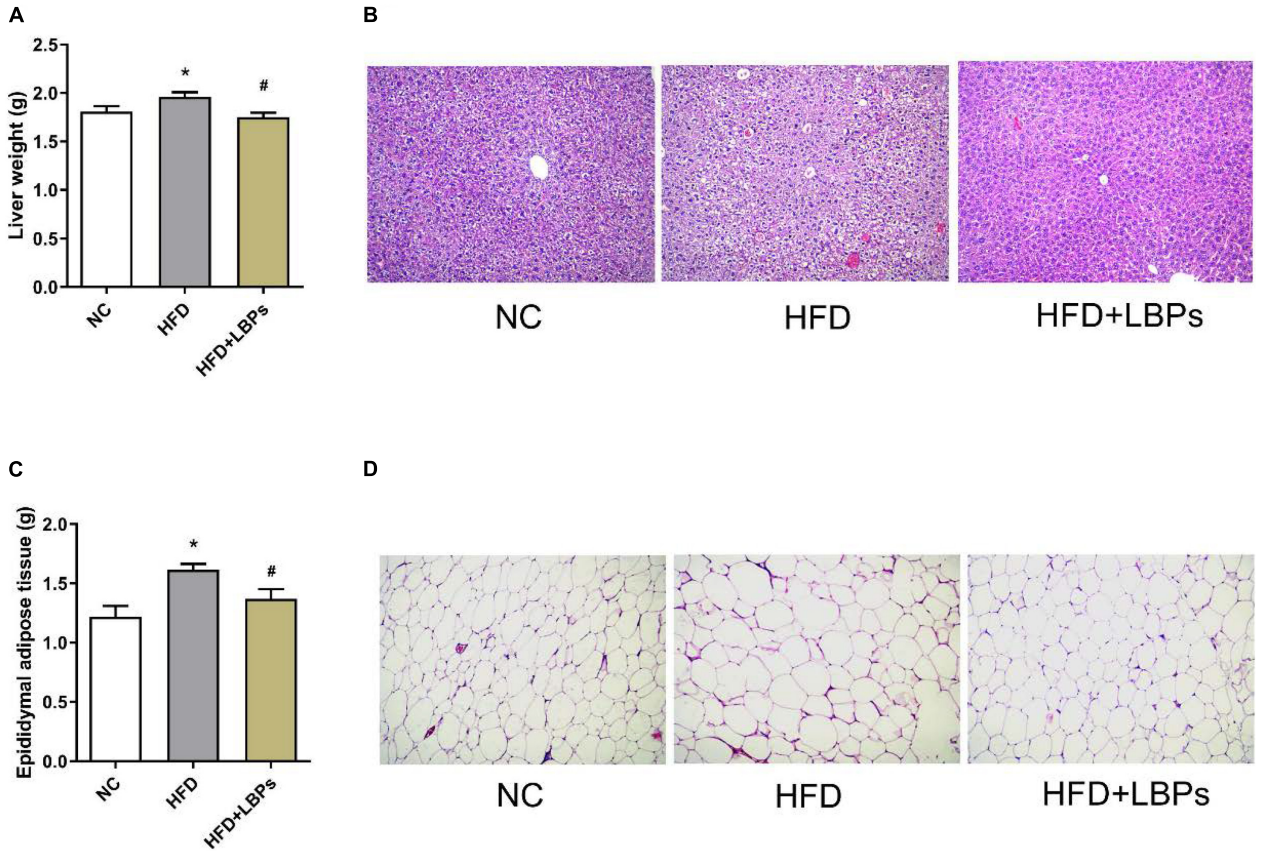

FIGURE 3 | Effects of LBPs on fat accumulation in liver and adipose tissues in HFD-fed mice. **(A)** Liver weight, **(B)** histology analysis of liver, **(C)** epididymal adipose tissues weight, and **(D)** histology analysis of epididymal adipose tissue. $^{*}P < 0.05$ vs. NC group and $^{\#}P < 0.05$ vs. HFD group.

of each component on the different effects. Fifteen taxa were detected in the NC group. The *Bacteroides*, belonging to the phylum *Bacteroidetes*, produced a large effect on the dominant community, and was markedly enriched in the NC group. The HFD group was characterized by an increased amount of *Clostridium_sensu_stricto_1*, indicating a disruption of gut symbiosis. The genera of *Lachnospiraceae_NK4A136_group, Marvinbryantia*, *Butyricicoccus*, and *Lacticigenium* were the dominant phylotypes that contributed to the differences between the gut microbiota of HFD + LBP and HFD groups (**Figure 6C**).

Short-Chain Fatty Acid Production in Colonic and Fecal Contents

Colonic propionic acid and butyric acid concentrations in the former were reduced by 11.45 and 19.55%, respectively, in the HFD group compared with those in the NC group. LBP treatment increased the levels of colonic acetic acid (by 1.42%), propionic acid (by 8.67%), butyric acid (by 11.31%) and fecal acetic acid (by 19.80%), propionic acid (by 4.87%), and butyric acid (by 57.95%) compared with those in the HFD group (**Figures 7A,B**) ($P > 0.05$). The levels of fecal butyric acid were found to be higher in the HFD + LBPs group than in the HFD group (**Figure 7B**) ($P < 0.05$).

Correlation Between the Gut Microbiota and Obesity-Related Parameters

To further identify the potential correlation between gut microbiota and obesity-related parameters, a heatmap of Spearman's correlation between the dominant genera, and obesity-related parameters was generated. A significant correlation was observed between the parameters and some specific taxa, such as *Bacteroides*, *Clostridium_sensu_stricto_1*, and *Lacticigenium* ($P < 0.05$). Among the specific genera, *Bacteroides* were negatively correlated with parameters such as epididymal adipose tissues weight, serum TG, serum LDL-C, liver TC, and liver MDA and positively correlated with serum HDL-C, colon acetic acid, colon propionic acid, and colon butyric acid. *Clostridium_sensu_stricto_1* was positively correlated with serum TC. *Lacticigenium* was positively correlated with SCFAs in the colon, suggesting it may be a probiotic that produces short-chain fatty acids (**Figure 8**).

DISCUSSION

Obesity is strongly associated with lipid metabolism, hepatic manifestation, metabolic abnormalities, and the composition of the gut microbiota (Parry and Hodson, 2017; Li et al., 2019;

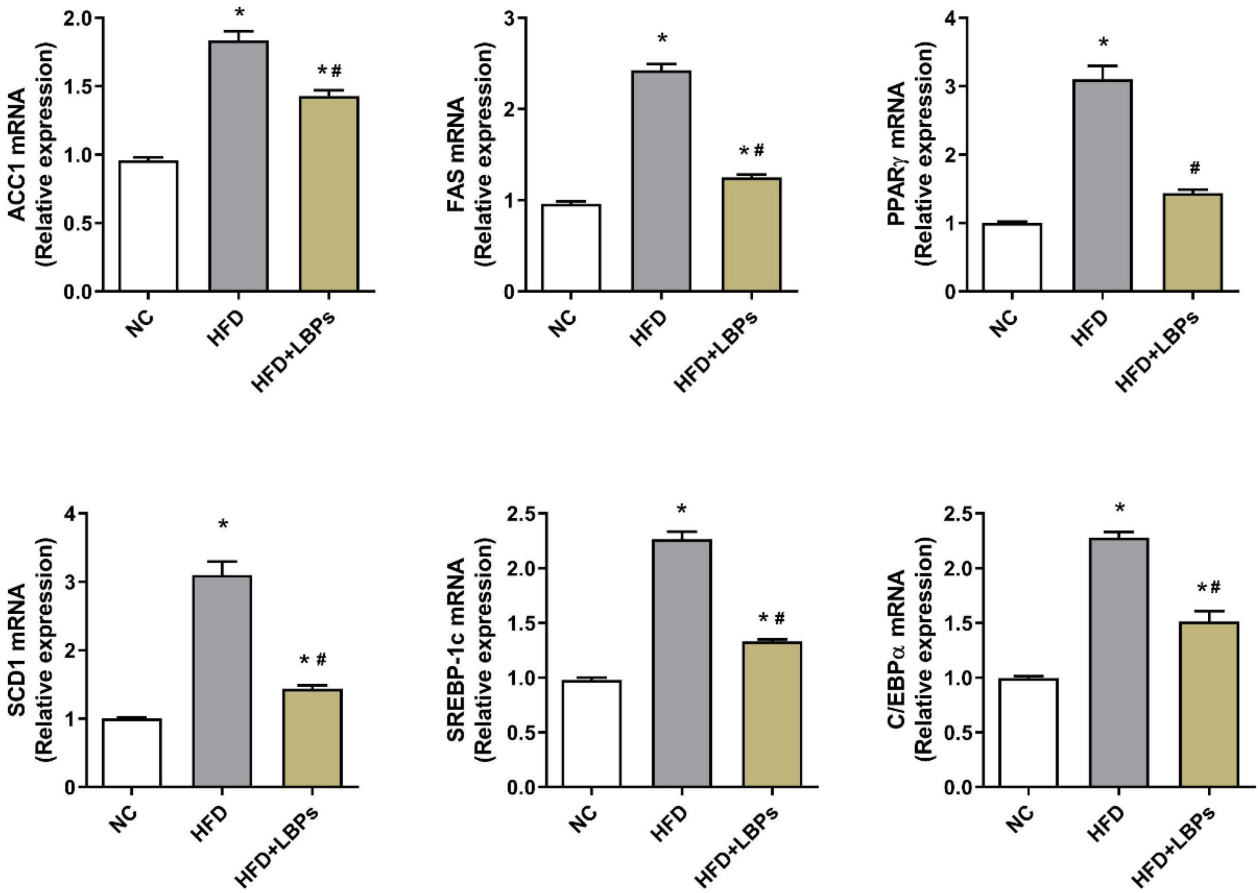

FIGURE 4 | Effects of *Lycium barbarum* polysaccharides (LBPs) on expression of lipid-related genes (ACC1, FAS, PPARγ, SCD1, SREBP-1c, and C/EBPα) in epididymal adipose tissues in HFD-fed mice. $^{*}P < 0.05$ vs. NC group and $^{\#}P < 0.05$ vs. HFD group.

Zhi et al., 2019). LBPs have been reported to play an important role in anti-inflammatory (Wu et al., 2020), immunomodulatory (Zhu et al., 2020), and anti-obesity (Jia et al., 2016). We have previously shown that dietary LBP supplementation can improve intestinal microbial populations in early-weaned pigs (Chen et al., 2019). However, the effect of dietary LBPs on lipid metabolism and the modulation of gut microbiota have not been fully investigated in HFD-induced obese animal models. In the present study, we explored how the oral administration of LBPs regulates lipid metabolism *via* modulation in high-fat diet-fed mice.

In the current study, we found that HFD feeding increased the body weight, serum lipid profile, adipose tissue, and hepatic lipid accumulation in mice compared with the NC group for 10 weeks. These findings were consistent with some previous studies on the acceleration effect of HFD feeding on body weight and fat accumulation (Duan et al., 2019; Kong et al., 2019). We also found that LBP administration effectively alleviated HFD-induced dyslipidemia and hepatic lipid accumulation through decreasing TG, TC, LDL-C, and MDA in the serum and TG, TC, and MDA levels in the liver and increasing the serum HDL-C level in HFD feeding mice. These results are similar to the previous reports that found crude polysaccharide extracts (crude LBP), okra [*Abelmoschus esculentus* (L.) Moench] polysaccharides, *Grifola frondosa* polysaccharides, and *Cipangopaludina chinensis* polysaccharides reduced the level of serum lipids in the HFD model (Luo et al., 2004; Li et al., 2019; Liao et al., 2019; Xiong et al., 2019). The possible mechanism of LBP supplementation alleviating hepatic triglyceride production and accumulation is through upregulating lipolysis-degraded enzyme, and boosting fatty acid β-oxidation and inhibiting lipogenic enzyme production in the liver (Xiao et al., 2013; Jia et al., 2016). Furthermore, dysregulated lipid metabolism may induce lipid peroxidation, directly leading to oxidative stress (Xiao et al., 2014). We found that LBPs reduced the MDA levels in serum and liver. These hepatoprotective effects of LBPs were partly attributed to the activation of nuclear factor kappa B and the inhibition of the nucleotide-binding and oligomerization domain-like receptor protein 3/6 inflammasome pathway (Xiao et al., 2018). These data indicated that LBPs showed a vital role in alleviating HFD-induced anomalous changes of lipid profile and thus preventing lipid metabolic disorders.

Adipose tissue is known as an important energy reservoir and an essential regulator of energy homeostasis (Stolarczyk, 2017).

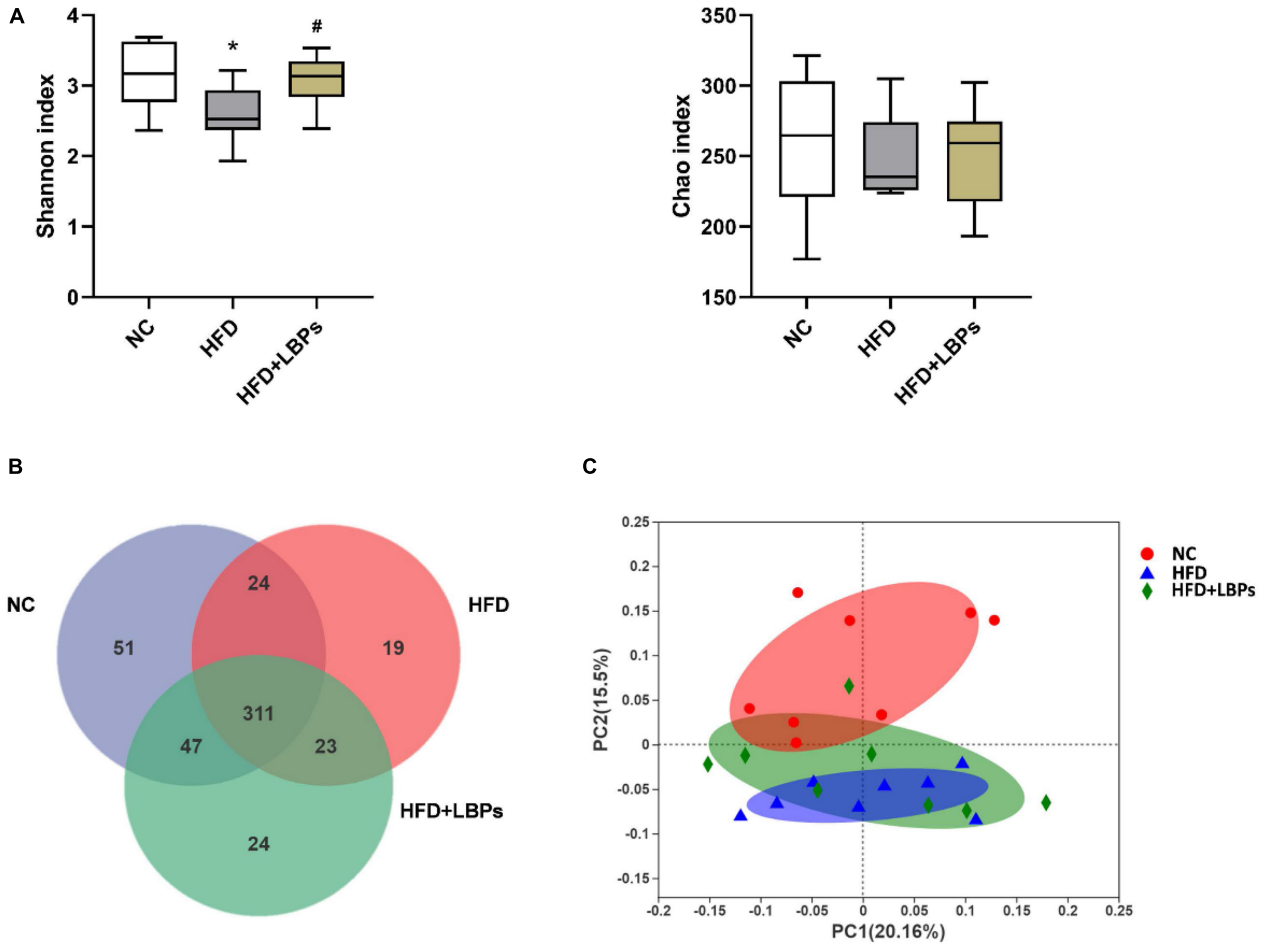

FIGURE 5 | Effects of *Lycium barbarum* polysaccharides (LBPs) on diversity of modulation of gut microbiota. **(A)** Alpha diversity analysis, including Shannon, and Chao index. **(B)** Venn diagram of OTUs. **(C)** Principal coordinate analysis plot of gut microbiota based on unweighted unifrac metric. $^{*}P < 0.05$ vs. NC group and $^{\#}P < 0.05$ vs. HFD group.

Obesity is characterized by increased adipose tissue mass, which is caused by the increased number, and size of fat cells (Yang and Kim, 2015). Our results indicated that LBP treatment decreased the weight of adipose tissues and the size of adipocytes in epididymal adipose tissues in HFD-fed mice, which was consistent with the previous study that LBPs, and fermented *Momordica charantia* polysaccharides decreased fat accumulation in epididymal adipose tissues of HFD-fed mice (Zhao et al., 2016; Wen et al., 2019). Dysfunction and excessive accumulation of lipid in adipose tissue induce obesity, which is associated with atherosclerosis, cardiovascular diseases, dyslipidemia, and other metabolic syndromes (Moseti et al., 2016). Thus, reducing fat deposit and adipogenesis in the adipose tissue can prevent the development of obesity, and its associated diseases. Additionally, in the current study, LBP supplementation suppressed the upregulated expression level of ACC1, FAS, PPARγ, SCD1, SREBP-1c, and C/EBPα in adipose tissues of HFD-fed mice. PPARγ has been verified to be a ligand-activated transcription factor that can mediate the expression of fat-related genes and facilitate the process of adipogenesis (Lee et al., 2018). C/EBPα is considered an essential regulator that can induce adipocyte differentiation and adipogenesis through PPARγ (Lee et al., 2019). SREBP-1c can mediate the expression of fatty acid synthesis genes and activates lipogenic transcription factors such as ACC-1, FAS, and SCD1, which subsequently induces lipogenesis and the accumulation of lipid (Linden et al., 2018; Terzo et al., 2018). In addition, a recent study found that LBPs inhibited ACC and FAS expression by activating the SIRT1/adenosine monophosphate-activating protein kinase pathway and reducing lipid synthesis (Jia et al., 2016). It is worth noting that HFD feeding decreases PPARγ and C/EBPα expression, whereas *Polygonatum odoratum* polysaccharides increase PPARγ, and C/EBPα messenger RNA expression compared with that in HFD-fed mice (Wang Y. et al., 2018). The reason for inconsistent results may be partially lie in treatment conditions, diet ingredients, experimental duration, and species. Our findings fit well with previous studies reporting that *Gracilaria lemaneiformis* polysaccharides downregulate PPARγ and C/EBPα expression in the adipocyte tissues of HFD-fed mice (Sun et al., 2018). Therefore, the

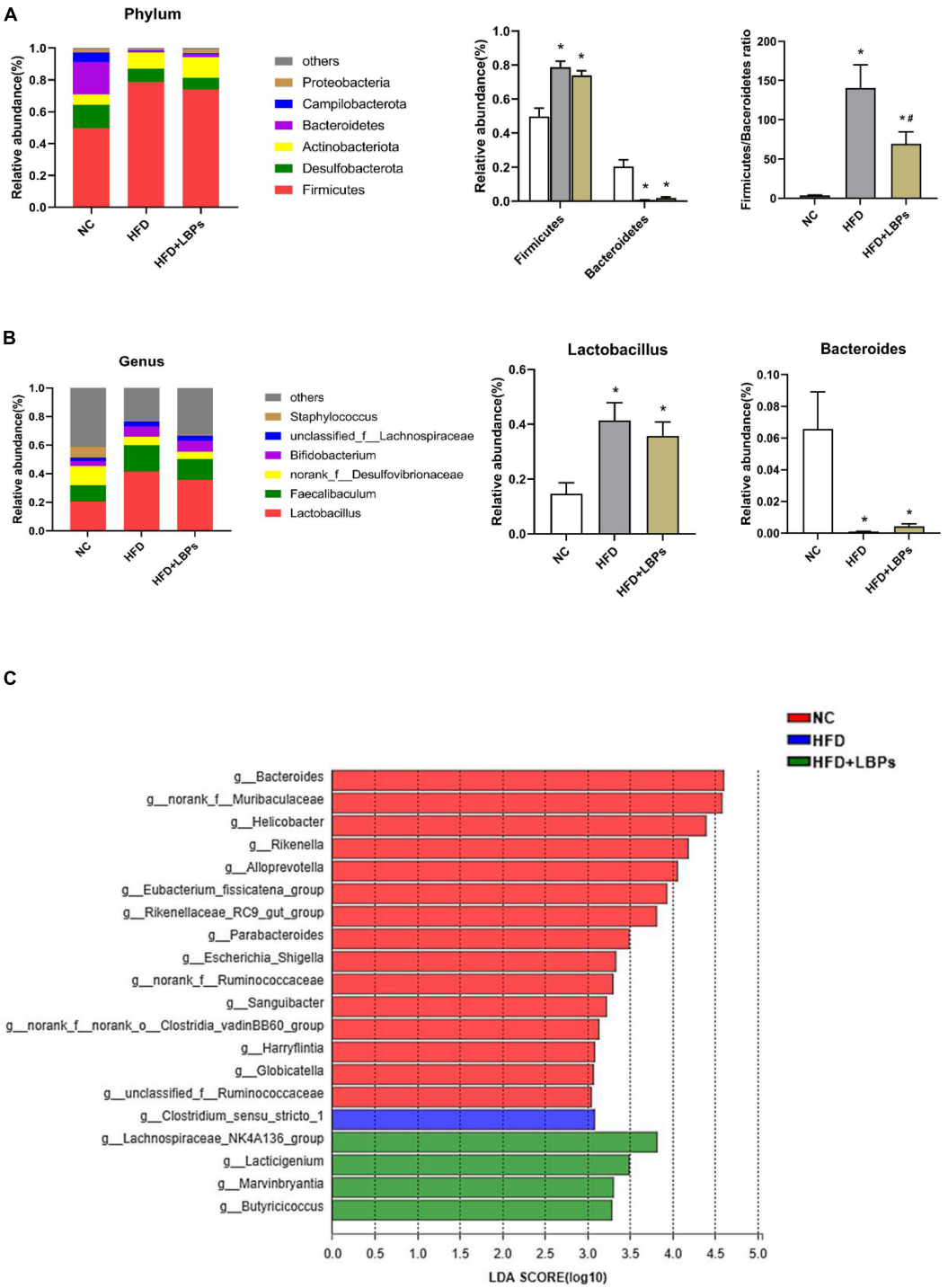

FIGURE 6 | Effects of *Lycium barbarum* polysaccharides (LBPs) on composition of gut microbiota. **(A)** Composition of gut microbiota at phylum level and differences in relative abundance of *Firmicutes* and *Bacteroidetes* at phylum level. **(B)** Composition of gut microbiota at genus level and differences in relative abundance of *Lactobacillus*, and *Bacteroides*. LDA score plot with LDA scores (log 10) higher than 3 **(C)**. $^{*}P < 0.05$ vs. NC group and $^{\#}P < 0.05$ vs. HFD group.

results showed that LBPs might be involved in decreasing fat adipogenesis and accumulation in epididymal adipose tissue mass by downregulating expression levels of adipogenesis-related genes.

The gut microbiota plays an important role in regulating energy homeostasis, glucose metabolism, and lipid metabolism in the host (Schoeler and Caesar, 2019). A variety of polysaccharides from plants have positive effects on modulating gut microbiota

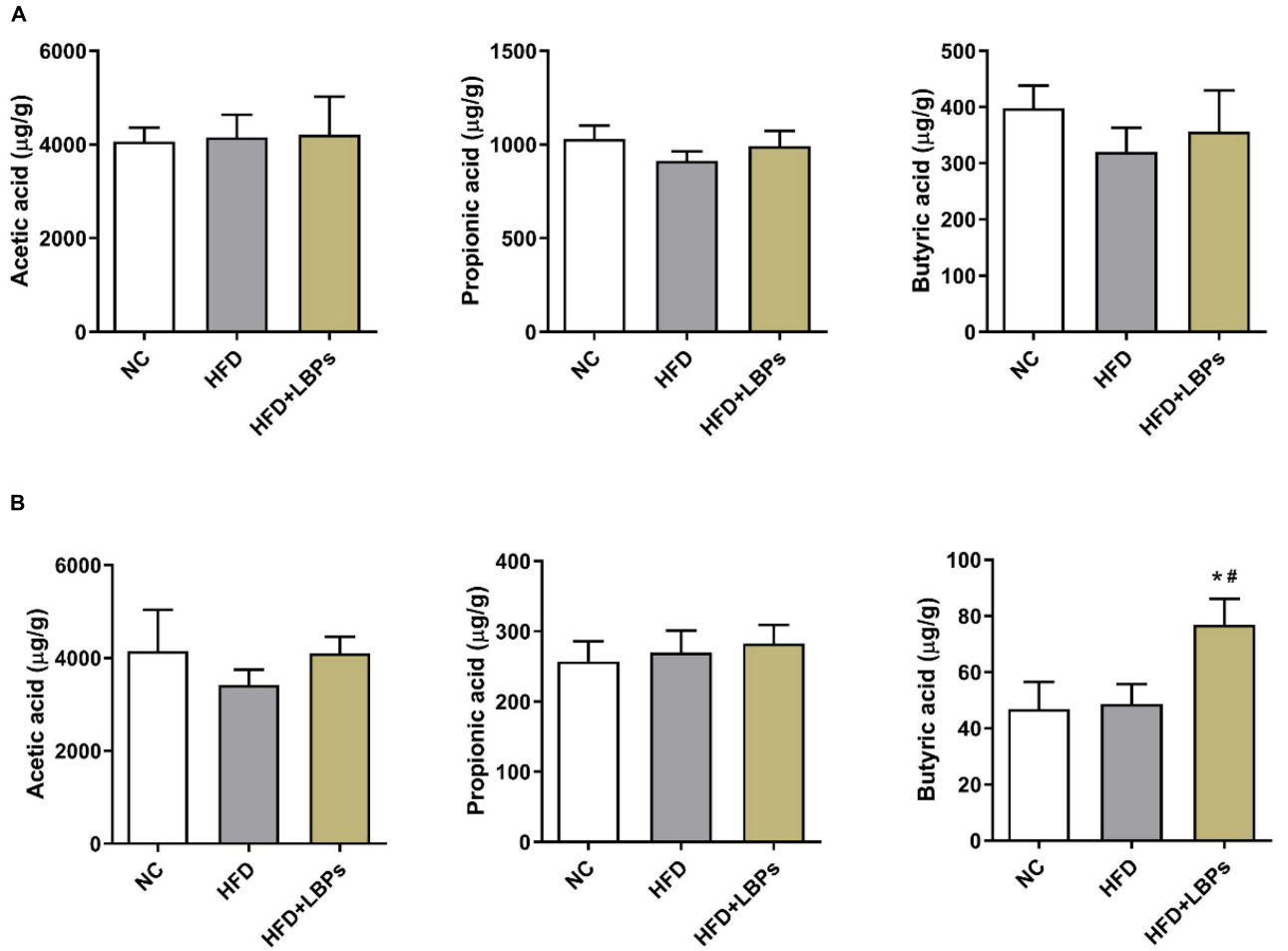

FIGURE 7 | Effects of *Lycium barbarum* polysaccharides (LBPs) on SCFAs production in **(A)** colonic, and **(B)** fecal contents. $^{*}P < 0.05$ vs. NC group and $^{\#}P < 0.05$ vs. HFD group.

and preventing the development of obesity (Wang X. et al., 2018). Lower diversity of bacterial is associated with the probability of obesity and non-alcoholic fatty liver disease (Schwimmer et al., 2019; Chen et al., 2020). In our study, the administration of LBPs increased the diversity of bacteria by increasing the Shannon index, appearing to be a positive effect on the structure of the gut microbiota in obese mice. Numerous reports have shown that an increased *Firmicutes*/*Bacteroidetes* ratio promotes more lipid production and induces the development of abnormal weight gain, and chronic metabolic disease (Liu et al., 2019; Lu et al., 2019). Based on the heatmap of Spearman's correlation, the relative abundance of *Bacteroides* was negatively associated with obesity cytokines, illustrating the potential ability to inhibit fat deposition in obese mice. In the present study, HFD consumption induced an increase in the *Firmicutes*/*Bacteroidetes* ratio, which is consistent with the previous study (Li J. et al., 2020). By contrast, oral administration of LBPs reduced the *Firmicutes*/*Bacteroidetes* ratio in HFD-fed mice, which might be a mechanism to explain the improvement of LBPs in HFD induced lipid accumulation in epididymal adipose tissues and liver. At the genus level, the HFD increased the proportions of *Clostridium_sensu_stricto_1*. LBP supplementation modulated gut microbiota and ameliorated intestinal dysbiosis by increasing the abundance of *Lachnospiraceae_NK4A136_group*, *Marvinbryantia*, *Butyricicoccus*, and *Lacticigenium* in HFD fed mice. *Clostridium_sensu_stricto_1* is generally perceived as pathogenic bacteria and interpreted as indicators of a less healthy microbiota (Huart et al., 2019; Shi et al., 2019). Some studies have reported that the proliferation of *Clostridium_sensu_stricto_1* was correlated with obesity, rheumatoid arthritis-associated atherosclerosis, dyslipidemia, and necrotic enteritis (Shi et al., 2019; Yang et al., 2019; Zeng et al., 2019). In the current study, the relative abundance of *Clostridium_sensu_stricto_1* was positively correlated with obesity, and the administration of LBPs decreased the relative abundance of *Clostridium_sensu_stricto_1*. The genus *Lachnospiraceae_NK4A136_group* was generally considered to be an SCFA producer, and its abundance was negatively correlated to inflammation (Wang J. et al., 2018). The genera *Marvinbryantia* are positively correlated to intestinal epithelial

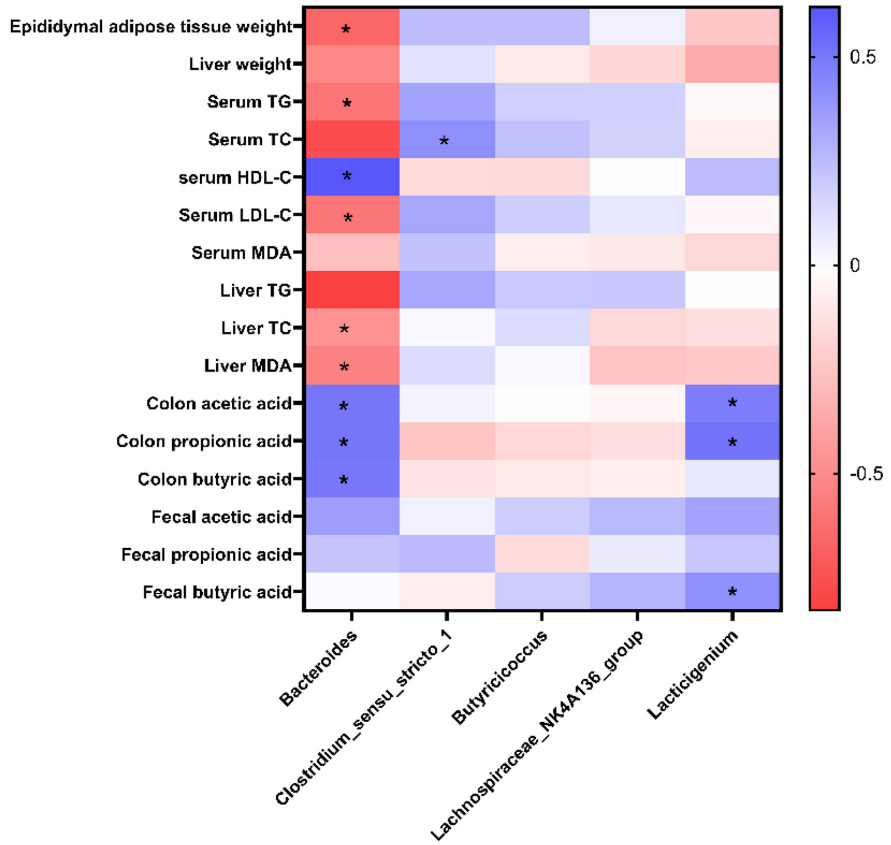

FIGURE 8 | Heatmap of Spearman's correlation between dominant genera and obesity-related parameters. *Significance was set at $P < 0.05$.

cell energy metabolism and butyrate production (Li A. L. et al., 2020). A butyrate-producing bacterium *Butyricicoccus* acts as a biomarker to predict obesity-related metabolic abnormalities, and the interventions of *Butyricicoccus* might be beneficial to weight loss and metabolic risk improvement (Luo et al., 2019; Zeng et al., 2019). It was reported that *Lacticigenium*, a lactic acid bacterium, produced acetic acids in addition to L-lactic acid (Iino et al., 2009). *Lacticigenium* showed a strong positive correlation with the produce of SCFAs. These studies support that supplementation of LBPs can promote the growth of beneficial bacteria and might contribute to improving gut dysbiosis induced by HFD.

Dietary polysaccharides can be fermented by gut microbiota provided with SCFAs, such as acetate, propionate, and butyrate (Shang et al., 2018). SCFAs are used as endogenous signaling molecules that could activate the G-protein-coupled receptor GPR43 associated with energy expenditure, leptin hormone secretion, and lipid metabolism (Hills et al., 2019; Schoeler and Caesar, 2019). Especially, butyric acid is able to mediate hepatic lipogenesis and fat oxidation (Li P. et al., 2020). In the present study, we found that LBPs increased the concentration of butyric acid in the feces of HFD-fed mice. Similar findings have been reported that some polysaccharides can increase SCFA production (Wang X. et al., 2019; Gu et al., 2020). Butyrate has the capacity to stimulate glucagon-like peptide-1 production and activate brown fat tissue, leading to sustained satiety and fat oxidation enhancement, thereby effectively preventing diet-induced obesity, insulin resistance, hypertriglyceridemia, and hepatic steatosis (Li et al., 2018; Vallianou et al., 2019). In particular, butyrate has been demonstrated to ameliorate insulin resistance and fatty acid oxidation, activate the adenosine monophosphate-activating protein kinase–acetyl–coenzyme A carboxylase pathway, and promote lipid metabolism (Mollica et al., 2017). Interestingly, some SCFA-producing intestinal microorganisms, such as *Lachnospiraceae_NK4A136_group* and *Lacticigenium*, and were enriched in the LBP-treated mice. All these results indicated that LBPs could increase SCFA production in the gut and thus benefit gut health, and prevent HFD-induced obesity.

CONCLUSION

Lycium barbarum polysaccharide supplementation attenuated epididymal and liver fat accumulation and expression levels of adipogenesis genes in adipocytes. Furthermore, LBPs increased the relative abundance of SCFA-producing bacteria and increased SCFA production in HFD-induced mice. It implied that LBPs might be regarded as a potential functional food ingredient to prevent hyperlipidemia and modulate gut microbiota dysbiosis.

DATA AVAILABILITY STATEMENT

The datasets presented in this study can be found in online repositories. The names of the repository/repositories and accession number(s) can be found below: https://www.ncbi.nlm.nih.gov/bioproject/, PRJNA735319.

ETHICS STATEMENT

The animal study was reviewed and approved by the Animal Care and Use Committee of the Hunan Agricultural University.

AUTHOR CONTRIBUTIONS

MY collected the data and drafted the manuscript. YxY and FW contributed to the animal sampling. HZ and XM performed the statistical analysis. YlY, BT, and JC provided resources and reviewed the manuscript. All authors contributed to the manuscript revision and approved the submitted version.

FUNDING

This work was supported by funding from the Youth Science Foundation Project of Hunan Agricultural University (19QN01) and the Open Foundation of CAS Key Laboratory of Agro-ecological Processes in Subtropical Region, Institute of Subtropical Agriculture (ISA2020101).

SUPPLEMENTARY MATERIAL

The Supplementary Material for this article can be found online at: https://www.frontiersin.org/articles/10.3389/fmicb.2021.719967/full#supplementary-material

REFERENCES

Chen, J., Kang, B., Zhao, Y., Yao, K., and Fu, C. (2018). Effects of natural dietary supplementation with *Macleaya cordata* extract containing sanguinarine on growth performance and gut health of early-weaned piglets. *J. Anim. Physiol. Anim. Nutr.* 102, 1666–1674. doi: 10.1111/jpn.12976

Chen, J., Long, L., Jiang, Q., Kang, B., Li, Y., and Yin, J. (2019). Effects of dietary supplementation of *Lycium barbarum* polysaccharides on growth performance, immune status, antioxidant capacity and selected microbial populations of weaned piglets. *J. Anim. Physiol. Anim. Nutr.* 106, 1106–1115. doi: 10.1111/jpn.13247

Chen, X., Sun, H., Jiang, F., Shen, Y., Li, X., Hu, X., et al. (2020). Alteration of the gut microbiota associated with childhood obesity by 16S rRNA gene sequencing. *PeerJ* 8:e8317. doi: 10.7717/peerj.8317

Duan, Y., Zhong, Y., Xiao, H., Zheng, C., Song, B., Wang, W., et al. (2019). Gut microbiota mediates the protective effects of dietary ß-hydroxy−β−methylbutyrate (HMB) against obesity induced by high-fat diets. *FASEB J.* 33, 10019–10033. doi: 10.1096/fj.201900665rr

Gu, W., Wang, Y., Zeng, L., Dong, J., Bi, Q., Yang, X., et al. (2020). Polysaccharides from *Polygonatum kingianum* improve glucose and lipid metabolism in rats fed a high fat diet. *Biomed. Pharmacother.* 125:109910. doi: 10.1016/j.biopha.2020.109910

Ha, K., Yoon, S., Choi, D., Kim, D., Kim, J., and Kim, C. (2005). Protective effect of *Lycium chinense* fruit on carbon tetrachloride-induced hepatotoxicity. *J. Ethnopharmacol.* 96, 529–535. doi: 10.1016/j.jep.2004.09.054

Hildebrandt, M. A., Hoffmann, C., Sherrill Mix, S. A., Keilbaugh, S. A., Hamady, M., Chen, Y. Y., et al. (2009). High-fat diet determines the composition of the murine gut microbiome independently of obesity. *Gastroenterology* 137, 1716–1724. doi: 10.1053/j.gastro.2009.08.042

Hills, R. D., Pontefract, B. A., Mishcon, H. R., Black, C. A., Sutton, S. C., and Theberge, C. R. (2019). Gut microbiome: profound implications for diet and disease. *Nutrients* 11:1613. doi: 10.3390/nu11071613

Huart, J., Leenders, J., Taminiau, B., Descy, J., Saint-Remy, A., Daube, G., et al. (2019). Gut microbiota and fecal levels of short-chain fatty acids differ upon 24-hour blood pressure levels in men. *Hypertension* 74, 1005–1013. doi: 10.1161/hypertensionaha.118.12588

Iino, T., Suzuki, K., and Harayama, S. (2009). Lacticigenium naphtae gen. nov., sp. nov., a halotolerant and motile lactic acid bacterium isolated from crude oil. *Int. J. Syst. Evol. Microbiol.* 59, 775–780. doi: 10.1099/ijs.0.003293-0

Jia, L., Li, W., Li, J., Li, Y., Song, H., Luan, Y., et al. (2016). *Lycium barbarum* polysaccharide attenuates high-fat diet-induced hepatic steatosis by up-regulating SIRT1 expression and deacetylase activity. *Sci. Rep.* 6:36209.

Kong, C., Gao, R., Yan, X., Huang, L., and Qin, H. (2019). Probiotics improve gut microbiota dysbiosis in obese mice fed a high-fat or high-sucrose diet. *Nutrition* 60, 175–184. doi: 10.1016/j.nut.2018.10.002

Lee, H. J., Le, B., Lee, D., Choi, B., and Yang, S. H. (2018). *Cissus quadrangularis* extract (CQR-300) inhibits lipid accumulation by downregulating adipogenesis and lipogenesis in 3T3-L1 cells. *Toxicol. Rep.* 5, 608–614. doi: 10.1016/j.toxrep.2018.02.008

Lee, J., Schmidt, H., Lai, B., and Ge, K. (2019). Transcriptional and epigenomic regulation of adipogenesis. *Mol. Cell Biol.* 39, e601–e618. doi: 10.1128/MCB.00601-18

Ley, R. E., Bäckhed, F., Turnbaugh, P., Lozupone, C. A., Knight, R. D., and Gordon, J. I. (2005). Obesity alters gut microbial ecology. *Proc. Natl. Acad. Sci. U.S.A.* 102, 11070–11075.

Li, A. L., Ni, W. W., Zhang, Q. M., Li, Y., Zhang, X., Wu, H. Y., et al. (2020). Effect of cinnamon essential oil on gut microbiota in the mouse model of dextran sodium sulfate-induced colitis. *Microbiol. Immunol.* 64, 23–32. doi: 10.1111/1348-0421.12749

Li, J., Pang, B., Shao, D., Jiang, C., Hu, X., and Shi, J. (2020). Artemisia sphaerocephala Krasch polysaccharide mediates lipid metabolism and metabolic endotoxaemia in associated with the modulation of gut microbiota in diet-induced obese mice. *Int. J. Biol. Macromol.* 147, 1008–1017. doi: 10.1016/j.ijbiomac.2019.10.069

Li, L., Guo, W. L., Zhang, W., Xu, J. X., Qian, M., Bai, W. D., et al. (2019). Grifola frondosa polysaccharides ameliorate lipid metabolic disorders and gut microbiota dysbiosis in high-fat diet fed rats. *Food Funct.* 10, 2560–2572. doi: 10.1039/C9FO00075E

Li, P., Huang, J., Xiao, N., Cai, X., Yang, Y., Deng, J., et al. (2020). Sacha inchi oil alleviates gut microbiota dysbiosis and improves hepatic lipid dysmetabolism in high-fat diet-fed rats. *Food Funct.* 11, 5827–5841. doi: 10.1039/d0fo01178a

Li, W., Li, Y., Wang, Q., and Yang, Y. (2014). Crude extracts from *Lycium barbarum* suppress SREBP-1c expression and prevent diet-induced fatty liver through AMPK activation. *Biomed. Res. Int.* 2014:196198.

Li, Z., Yi, C., Katiraei, S., Kooijman, S., Zhou, E., Chung, C. K., et al. (2018). Butyrate reduces appetite and activates brown adipose tissue via the gut-brain neural circuit. *Gut* 67, 1269–1279. doi: 10.1136/gutjnl-2017-314050

Liao, Z., Zhang, J., Liu, B., Yan, T., Xu, F., Xiao, F., et al. (2019). Polysaccharide from okra (*Abelmoschus esculentus* (L.) Moench) improves antioxidant capacity via PI3K/AKT pathways and Nrf2 translocation in a type 2 diabetes model. *Molecules* 24:1906. doi: 10.3390/molecules24101906

Linden, A. G., Li, S., Choi, H. Y., Fang, F., and Liang, G. (2018). Interplay between ChREBP and SREBP-1c coordinates postprandial glycolysis and lipogenesis in livers of mice. *J. Lipid Res.* 59:M81836.

Liu, S., Qin, P., and Wang, J. (2019). High-fat diet alters the intestinal microbiota in streptozotocin-induced type 2 diabetic mice. *Microorganisms* 7:176. doi: 10.3390/microorganisms7060176

Lu, X., Liu, J., Zhang, N., Fu, Y., and Cao, Y. (2019). Ripened pu-erh tea extract protects mice from obesity by modulating gut microbiota composition. *J. Agric. Food Chem.* 67, 6978–6994. doi: 10.1021/acs.jafc.8b04909

Luo, Q., Cai, Y., Yan, J., Sun, M., and Corke, H. (2004). Hypoglycemic and hypolipidemic effects and antioxidant activity of fruit extracts from *Lycium barbarum*. *Life Sci.* 76, 137–149. doi: 10.1016/j.lfs.2004.04.056

Luo, S., Wen, R., Wang, Q., Zhao, Z., Nong, F., Fu, Y., et al. (2019). Rhubarb peony decoction ameliorates ulcerative colitis in mice by regulating gut microbiota to restoring Th17/Treg balance. *J. Ethnopharmacol.* 231, 39–49. doi: 10.1016/j.jep.2018.08.033

Mollica, M. P., Raso, G. M., Cavaliere, G., Trinchese, G., De Filippo, C., Aceto, S., et al. (2017). Butyrate regulates liver mitochondrial function, efficiency, and dynamics in insulin-resistant obese mice. *Diabetes* 66, 1405–1418. doi: 10.2337/db16-0924

Moseti, D., Regassa, A., and Kim, W. (2016). Molecular regulation of adipogenesis and potential anti-adipogenic bioactive molecules. *Int. J. Mol. Sci.* 17:124. doi: 10.3390/ijms17010124

Ojo, B., El-Rassi, G. D., Payton, M. E., Perkins-Veazie, P., Clarke, S., Smith, B. J., et al. (2016). Mango supplementation modulates gut microbial dysbiosis and short-chain fatty acid production independent of body weight reduction in C57BL/6 mice fed a high-fat diet. *J. Nutr.* 146, 1483–1491. doi: 10.3945/jn.115.226688

Parry, S. A., and Hodson, L. (2017). Influence of dietary macronutrients on liver fat accumulation and metabolism. *J. Invest. Med.* 65, 1102–1115. doi: 10.1136/jim-2017-000524

Qian, L. (2019). Modulation of cytokine level and sperm quality of mice by *Lycium barbarum* polysaccharides. *Int. J. Biol. Macromol.* 126, 475–477. doi: 10.1016/j.ijbiomac.2018.12.250

Ridaura, V. K., Faith, J. J., Rey, F. E., Cheng, J., Duncan, A. E., Kau, A. L., et al. (2013). Gut microbiota from twins discordant for obesity modulate metabolism in mice. *Science* 341:1241214.

Sanmiguel, C., Gupta, A., and Mayer, E. A. (2015). Gut microbiome and obesity: a plausible explanation for obesity. *Curr. Obes. Rep.* 4, 250–261. doi: 10.1007/s13679-015-0152-0

Schoeler, M., and Caesar, R. (2019). Dietary lipids, gut microbiota and lipid metabolism. *Rev. Endocr. Metab. Disord.* 20, 461–472. doi: 10.1007/s11154-019-09512-0

Schwimmer, J. B., Johnson, J. S., Angeles, J. E., Behling, C., Belt, P. H., Borecki, I., et al. (2019). Microbiome signatures associated with steatohepatitis and moderate to severe fibrosis in children with nonalcoholic fatty liver disease. *Gastroenterology* 157, 1109–1122.

Shang, Q., Jiang, H., Cai, C., Hao, J., Li, G., and Yu, G. (2018). Gut microbiota fermentation of marine polysaccharides and its effects on intestinal ecology: an overview. *Carbohyd. Polym.* 179, 173–185. doi: 10.1016/j.carbpol.2017.09.059

Shang, Q., Song, G., Zhang, M., Shi, J., Xu, C., Hao, J., et al. (2017). Dietary fucoidan improves metabolic syndrome in association with increased Akkermansia population in the gut microbiota of high-fat diet-fed mice. *J. Funct. Foods* 28, 138–146. doi: 10.1016/j.jff.2016.11.002

Shi, N., Zhang, S., Silverman, G., Li, M., Cai, J., and Niu, H. (2019). Protective effect of hydroxychloroquine on rheumatoid arthritis-associated atherosclerosis. *Anim. Model. Exp. Med.* 2, 98–106. doi: 10.1002/ame2.12065

Shin, S. S., and Yoon, M. (2018). Korean red ginseng (Panax ginseng) inhibits obesity and improves lipid metabolism in high fat diet-fed castrated mice. *J. Ethnopharmacol.* 210, 80–87. doi: 10.1016/j.jep.2017.08.032

Silventoinen, K., Pietiläinen, K. H., Tynelius, P., Sørensen, T. I., Kaprio, J., and Rasmussen, F. (2007). Genetic and environmental factors in relative weight from birth to age 18: the Swedish young male twins study. *Int. J. Obesity* 31, 615–621. doi: 10.1038/sj.ijo.0803577

Stolarczyk, E. (2017). Adipose tissue inflammation in obesity: a metabolic or immune response? *Curr. Opin. Pharmacol.* 37, 35–40. doi: 10.1016/j.coph.2017.08.006

Sun, X., Duan, M., Liu, Y., Luo, T., Ma, N., Song, S., et al. (2018). The beneficial effects of *Gracilaria lemaneiformis* polysaccharides on obesity and the gut microbiota in high fat diet-fed mice. *J. Funct. Foods* 46, 48–56. doi: 10.1016/j.jff.2018.04.041

Terzo, S., Caldara, G., Ferrantelli, V., Puleio, R., Cassata, G., Mulè, F., et al. (2018). Pistachio consumption prevents and improves lipid dysmetabolism by reducing the lipid metabolizing gene expression in diet-induced obese mice. *Nutrients* 10:1857. doi: 10.3390/nu10121857

Vallianou, N., Stratigou, T., Christodoulatos, G. S., and Dalamaga, M. (2019). Understanding the role of the gut microbiome and microbial metabolites in obesity and obesity-associated metabolic disorders: current evidence and perspectives. *Curr. Obes. Rep.* 8, 317–332. doi: 10.1007/s13679-019-00352-2

Wang, J., Qin, C., He, T., Qiu, K., Sun, W., Zhang, X., et al. (2018). Alfalfa-containing diets alter luminal microbiota structure and short chain fatty acid sensing in the caecal mucosa of pigs. *J. Anim. Sci. Biotechnol.* 9:11.

Wang, S., Huang, M., You, X., Zhao, J., Chen, L., Wang, L., et al. (2018). Gut microbiota mediates the anti-obesity effect of calorie restriction in mice. *Sci. Rep.* 8:13037.

Wang, W., Zhai, S., Xia, Y., Wang, H., Ruan, D., Zhou, T., et al. (2019). Ochratoxin A induces liver inflammation: involvement of intestinal microbiota. *Microbiome* 7:151.

Wang, X., Shi, L., Wang, X., Feng, Y., and Wang, Y. (2019). MDG-1, an Ophiopogon polysaccharide, restrains process of non-alcoholic fatty liver disease via modulating the gut-liver axis. *Int. J. Biol. Macromol.* 141, 1013–1021. doi: 10.1016/j.ijbiomac.2019.09.007

Wang, X., Wang, X., Jiang, H., Cai, C., Li, G., Hao, J., et al. (2018). Marine polysaccharides attenuate metabolic syndrome by fermentation products and altering gut microbiota: an overview. *Carbohyd. Polym.* 195, 601–612. doi: 10.1016/j.carbpol.2018.05.003

Wang, Y., Fei, Y., Liu, L., Xiao, Y., Pang, Y., Kang, J., et al. (2018). *Polygonatum odoratum* polysaccharides modulate gut microbiota and mitigate experimentally induced obesity in rats. *Int. J. Mol. Sci.* 19:3587. doi: 10.3390/ijms19113587

Wen, J., Gao, H., Hu, J., Nie, Q., Chen, H., Xiong, T., et al. (2019). Polysaccharides from fermented *Momordica charantia* ameliorate obesity in high-fat induced obese rats. *Food Funct.* 10, 448–457. doi: 10.1039/c8fo01609g

Wu, Q., Liu, L., Wang, X., Lang, Z., Meng, X., Guo, S., et al. (2020). *Lycium barbarum* polysaccharides attenuate kidney injury in septic rats by regulating Keap1-Nrf2/ARE pathway. *Life Sci.* 242:117240. doi: 10.1016/j.lfs.2019.117240

Xiao, J., Liong, E. C., Ching, Y. P., Chang, R., Fung, M. L., Xu, A. M., et al. (2013). *Lycium barbarum* polysaccharides protect rat liver from non-alcoholic steatohepatitis-induced injury. *Nutr. Diabetes* 3:e81. doi: 10.1038/nutd.2013.22

Xiao, J., Wang, F., Liong, E. C., So, K., and Tipoe, G. L. (2018). *Lycium barbarum* polysaccharides improve hepatic injury through NFkappa-B and NLRP3/6 pathways in a methionine choline deficient diet steatohepatitis mouse model. *Int. J. Biol. Macromol.* 120, 1480–1489. doi: 10.1016/j.ijbiomac.2018.09.151

Xiao, J., Xing, F., Huo, J., Fung, M. L., Liong, E. C., Ching, Y. P., et al. (2014). *Lycium barbarum* polysaccharides therapeutically improve hepatic functions in non-alcoholic steatohepatitis rats and cellular steatosis model. *Sci. Rep.* 4:5587. doi: 10.1038/srep05587

Xiong, Q., Zhu, L., Zhang, F., Li, H., Wu, J., Liang, J., et al. (2019). Protective activities of polysaccharides from Cipangopaludina chinensis against high-fat-diet-induced atherosclerosis via regulating gut microbiota in ApoE-deficient mice. *Food Funct.* 10, 6644–6654. doi: 10.1039/c9fo01530b

Yang, J., and Kim, S. S. (2015). Ginsenoside Rc promotes anti-adipogenic activity on 3T3-L1 adipocytes by down-regulating C/EBPα and PPARγ. *Molecules* 20, 1293–1303. doi: 10.3390/molecules20011293

Yang, W., Lee, Y., Lu, H., Chou, C., and Wang, C. (2019). Analysis of gut microbiota and the effect of lauric acid against necrotic enteritis in *Clostridium perfringens* and Eimeria side-by-side challenge model. *PLoS One* 14:e205784. doi: 10.1371/journal.pone.0205784

Zeng, Q., Li, D., He, Y., Li, Y., Yang, Z., Zhao, X., et al. (2019). Discrepant gut microbiota markers for the classification of obesity-related metabolic abnormalities. *Sci. Rep.* 9:13424.

Zhao, R., Gao, X., Zhang, T., and Li, X. (2016). Effects of *Lycium barbarum*. polysaccharide on type 2 diabetes mellitus rats by regulating biological rhythms. *Iran J. Basic Med. Sci.* 19:1024.

Zheng, S., Huang, K., Zhao, C., Xu, W., Sheng, Y., Luo, Y., et al. (2018). Procyanidin attenuates weight gain and modifies the gut microbiota in high fat diet induced obese mice. *J. Funct. Foods* 49, 362–368. doi: 10.1016/j.jff.2018.09.007

Zhi, C., Huang, J., Wang, J., Cao, H., Bai, Y., Guo, J., et al. (2019). Connection between gut microbiome and the development of obesity. *Eur. J. Clin. Microbiol. Infect. Dis.* 38, 1987-1998.

Zhu, W., Zhou, S., Liu, J., McLean, R. J., and Chu, W. (2020). Prebiotic, immunostimulating and gut microbiota-modulating effects of *Lycium barbarum* polysaccharide. *Biomed. Pharmacother.* 121:109591. doi: 10.1016/j.biopha.2019.109591

Conflict of Interest: The authors declare that the research was conducted in the absence of any commercial or financial relationships that could be construed as a potential conflict of interest.

frontiers in Microbiology

ORIGINAL RESEARCH
published: 01 September 2021
doi: 10.3389/fmicb.2021.734389

Fermented Cottonseed Meal as a Partial Replacement for Soybean Meal Could Improve the Growth Performance, Immunity and Antioxidant Properties, and Nutrient Digestibility by Altering the Gut Microbiota Profile of Weaned Piglets

*Xueling Gu, Zhiqing Li, Jing Wang, Jiashun Chen, Qian Jiang, Nian Liu, Xiang Liu, Fan Zhang, Bie Tan, Hao Li and Xiaokang Ma**

College of Animal Science and Technology, Hunan Agricultural University, Changsha, China

The study investigated the impact of fermented cottonseed meal (FCSM) on growth performance, immunity and antioxidant properties, nutrient digestibility, and gut microbiota of weaned piglets by replacing soybean meal with FCSM in the diet. The experimental piglets were fed with either the soybean meal diet (SBM group) or fermented cottonseed meal diet (FCSM group) for 14 days after weaning. The digestibility of dry matter (DM), organic matter (OM), crude protein (CP), gross energy (GE), amino acids and nitrogen was higher in the FCSM diet than those in the SBM diet ($p < 0.05$). The piglets in the FCSM group showed greater growth performance and lower diarrhea rate than those in the SBM group ($p < 0.05$). The concentration of serum immunoglobulin G (IgG) and antioxidase, intestinal and hepatic antioxidase were increased and the concentration of malondialdehyde (MDA) in the serum was decreased in those piglets in the FCSM group compared to those piglets in the SBM group ($p < 0.05$). The piglets in the FCSM group had a higher concentration of volatile fatty acids (VFAs) in their ileum and cecum and a higher Simpson index of ileum than piglets in the SBM group ($p < 0.05$). The relative abundance of *Lactobacillus* and *[Ruminococcus]_torques_group* in ileum and *Intestinibacter*, *norank_f_Muribaculaceae*, *unclassified_o_Lactobacillales* and *[Eubacterium]_coprostanoligenes_group* in cecum were enhanced in piglets fed with the FCSM diet, whereas the relative abundance of *Sarcina* and *Terrisporobacter* were increased in piglets fed with the SBM diet. Overall, FCSM replacing SBM improved the growth performance, immunity and antioxidant properties, and nutrient digestibility; possibly *via* the alterant gut microbiota and its metabolism of weaned piglets.

Keywords: fermented cottonseed meal, growth performance, immunity and antioxidant capacity, gut microbiota, weaned piglets

OPEN ACCESS

Edited by:
Zheng Ruan,
Nanchang University,
China

Reviewed by:
Yehui Duan,
Institute of Subtropical Agriculture,
Chinese Academy of Sciences (CAS),
China
Shihai Zhang,
South China Agricultural University,
China
Shad Mahfuz,
Sylhet Agricultural University,
Bangladesh

****Correspondence:***
Xiaokang Ma
maxiaokang@hunau.edu.cn

Specialty section:
This article was submitted to Food Microbiology, a section of the journal Frontiers in Microbiology

Received: *01 July 2021*
Accepted: *05 August 2021*
Published: *01 September 2021*

Citation:
Gu XL, Li ZQ, Wang J, Chen JS, Jiang Q, Liu N, Liu X, Zhang F, Tan BE, Li H and Ma XK (2021) Fermented Cottonseed Meal as a Partial Replacement for Soybean Meal Could Improve the Growth Performance, Immunity and Antioxidant Properties, and Nutrient Digestibility by Altering the Gut Microbiota Profile of Weaned Piglets. Front. Microbiol. 12:734389. doi: 10.3389/fmicb.2021.734389

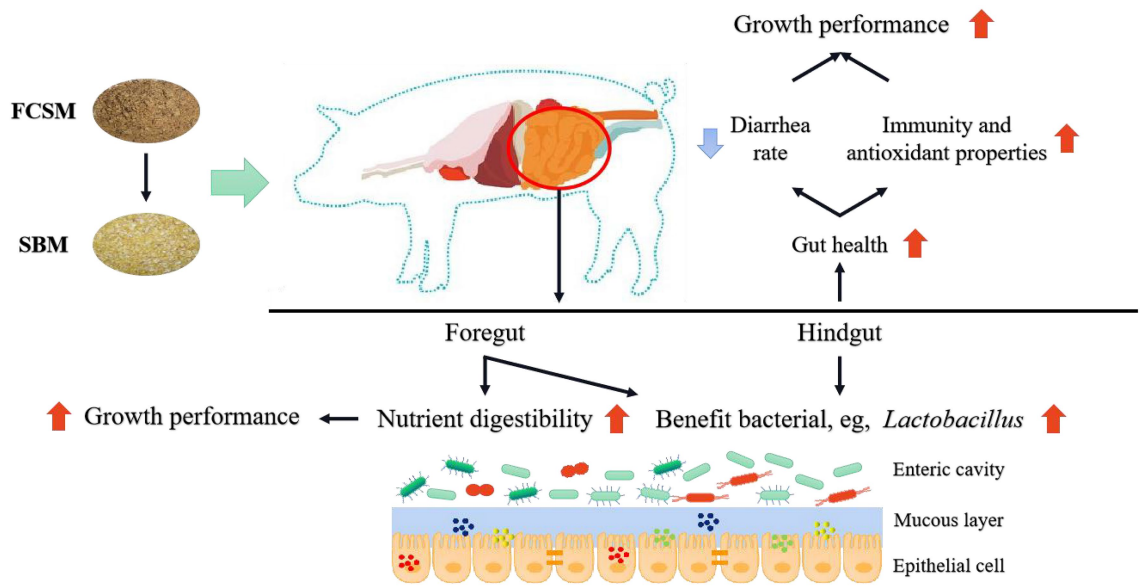

GRAPHICAL ABSTRACT | Fermented cottonseed meal as a partial replacement for soybean meal could improve the growth performance, immunity and antioxidant properties, and nutrient digestibility by altering the gut microbiota profile of weaned piglets. SBM, soybean meal; FCSM, fermented cottonseed meal.

INTRODUCTION

Soybean meal (SBM), an important protein source in the livestock industry, is highly recognized for its significant protein content and widespread availability (Azarm and Lee, 2014; Kim, 2014). However, the price of SBM has increased dramatically and the supply of high-quality protein feeding ingredients (such as SBM and fish meal) has been deficient in recent years. This leads to a higher livestock breeding expense and restricts the development of animal husbandry. Therefore, there is an urgent need for more alternative high-quality protein feeding ingredients to solve the protein source crisis in animal husbandry.

Cottonseed meal (CSM), a by-product obtained from the process of extracting the oil from cotton seed, is an attractive alternative protein source for livestock diets (Nagalakshmi et al., 2007). However, compared to SBM, the application of CSM as a feed ingredient in animal husbandry is limited due to the presence of anti-nutritional factors (Lordelo et al., 2007; Tang et al., 2012) such as free gossypol, cyclopropenoic fatty acids, and crude fiber, which may cause negative effects on growth performance and organ functionality (Nie et al., 2015; Świątkiewicz, 2016). Fermented cottonseed meal (FCSM), a product produced by mixing solid CSM with liquid phases and then inoculating the mixture with beneficial microorganisms (Sun et al., 2014), can reduce free gossypol and improve the protein quality of CSM with solid state fermentation (Zhang et al., 2007). It has been suggested that the FCSM partial replacing SBM (about 6–8%) not only can improve the growth performance, immune and antioxidant capacity, and digestibility in broiler chickens (Sun et al., 2013; Nie et al., 2015; Wang et al., 2017; Niu et al., 2020), but also can reduce the F:G (the ratio of feed and gain weight) and diarrhea rate in nursery pigs, growing pigs and finishing pigs (Guan et al., 2017), which indicated that the FCSM has the potential to be a high-quality protein source.

Weaned piglet is a critical group in whole pig production, which consumes a large amount of high-quality protein ingredients. However, there is a lack of relevant research on the application of FCSM in weaned piglets. Therefore, the present study aimed to compare the effects of dietary SBM and FCSM on growth performance, immunity and antioxidant properties, nutrient digestibility, and gut microbiota of weaned piglets.

Abbreviations: BW, Body weight; ADG, Average daily gain; ADFI, Average daily feed intake; G:F, Gain to feed ratio; IgA, Immunoglobulin A; IgG, Immunoglobulin G; IgM, Immunoglobulin M; SOD, Superoxide dismutase; GSH-Px, Glutathione peroxidase; T-AOC, Total antioxidant capacity; MDA, Malondialdehyde; CAT, Catalase; AA, Amino acid; HPLC, High Performance Liquid Chromatography; AIA, Acid insoluble ash; AID, Apparent ileal digestibility; VFAs, Volatile fatty acids; SCFAs, Short chain fatty acids; BCFAs, Branched chain fatty acids; PCR, Polymerase chain reaction; OTUs, Operational taxonomic units; PCoA, Principal co-ordinates analysis; LDA, Linear discriminant analysis; LEfSe, Linear discriminant analysis effect size; PICRUSt, Phylogenetic investigation of communities by reconstruction of unobserved states.

MATERIALS AND METHODS

The animal handling and all procedures of this study received approval from the Animal Care and Use Ethics Committee of the Hunan Agricultural University (Changsha). The FCSM used in this experiment was provided by the Tycoon Group (Xinjiang, China). The SBM used in this experiment was provided by Hunan Lifeng Biological Technology Co., Ltd. (Hunan, China). **Table 1** shows the nutrient composition of SBM and FCSM.

TABLE 1 | Analyzed composition of the fermented cottonseed meal and soybean meal (%, as-fed basis).

Item	SBM	FCSM
Dry matter	89.95	93.06
Crude protein	45.11	50.20
Ether extract	1.92	1.36
Neutral detergent fiber	13.86	19.45
Acid detergent fiber	9.75	11.70
Ash	6.21	6.65
Calcium	0.35	0.37
Phosphorus	0.69	0.98
GE, MJ/kg	17.55	17.81
Indispensable AA		
Arginine	3.36	6.09
Histidine	1.28	1.59
Isoleucine	1.89	1.52
Leucine	3.29	2.84
Lysine	2.86	2.36
Methionine	0.63	0.67
Phenylalanine	2.20	2.81
Threonine	1.72	1.78
Tryptophan	0.45	0.63
Valine	2.06	2.14
Dispensable amino acids		
Alanine	2.16	1.97
Aspartate	5.21	4.88
Cystine	0.61	0.79
Glutamine	7.34	10.05
Glycine	1.89	1.92
Proline	2.06	2.46
Serine	2.31	2.25
Tyrosine	1.68	1.49

Analysis conducted in duplicates. SBM, soybean meal; FCSM, fermented cottonseed meal.

Animal Treatment and Experimental Design

A total of 32 Duorc × (Landrace × Yorkshire) growing barrows, with an average initial body weight (BW) of 7.85 ± 0.49 kg, were allotted to two dietary treatments in a completely randomized design with 16 repetitions per treatment according to their body weight. The dietary treatments include SBM diet and FCSM diet: the FCSM diet was formulated by adding 6% FCSM to replace the SBM compared with the SBM diet, and corn and soy oil was changed to balance the energy and protein levels (**Table 2**). The experimental diets and vitamin-mineral premix were configured to meet the nutritional needs of nursery piglets as recommended by the NRC (2012). The experimental period lasted for 14 days. The house, feed trough and drinker were thoroughly cleaned and disinfected before starting the experiment. The temperature of the pig house was kept at 24–28°C, and the relative humidity was controlled at 60–70%. All the pigs were provided *ad libitum* access to water and feed. The daily feed intake and BW of each pig were recorded on day 0 and day 14 to calculate the average daily gain (ADG), average daily feed intake (ADFI) and feed conversion rate (ADG:ADFI, G:F). A scoring system was applied to indicate the presence and severity of diarrhea as following: 1 = hard feces; 2 = slightly soft feces; 3 = soft, partially formed feces; 4 = loose, semiliquid feces; and 5 = watery, mucous-like feces.

TABLE 2 | Ingredients composition and nutrient levels of the experimental diets (%, as-fed basis).

Ingredients	SBM	FCSM
Corn	42.02	41.55
Soybean meal	20.00	14.00
Extruded full-fat soybean	12.00	12.00
Soy protein concentrate	4.00	4.00
Fermented cottonseed meal	0.00	6.00
Whey powder	8.00	8.00
Soy oil	4.61	5.02
Sucrose	5.38	5.38
Dicalcium phosphate	1.26	1.29
Limestone	0.99	0.98
Salt	0.30	0.30
Lysine	0.41	0.45
Methionine	0.13	0.13
Threonine	0.13	0.13
Tryptophan	0.02	0.02
Chromic oxide	0.25	0.25
Vitamin-mineral premix[1], no antibiotic	0.50	0.50
Calculated nutrient levels		
Metabolized energy, kcal/kg	3,400	3,400
Crude protein	20.04	20.32
Standardized ileal digestible lysine	1.35	1.35
Standardized ileal digestible methionine	0.39	0.39
Standardized ileal digestible threonine	0.79	0.79
Standardized ileal digestible tryptophan	0.22	0.22

[1]*The components and contents of the premix providing nutrients for per kg feed are as follows: Vitamin A, 12,000IU; Vitamin D3, 2,500IU; Vitamin E, 30IU; Vitamin K3, 30mg; Vitamin B12, 12μg; Riboflavin, 4mg; Pantothenic acid, 15mg; Niacin, 40mg; Choline chloride, 400mg; Folic acid, 0.7mg; Vitamin B1, 1.5mg; Vitamin B6, 3mg; Biotin, 0.1mg; Manganese, 40mg; Iron, 90mg; Zinc, 100mg; Copper, 8.8mg; Iodine, 0.35mg; Selenium, 0.3mg. SBM, soybean meal; FCSM, fermented cottonseed meal.*

Sample Collection

By the end of the experiment, six samples of blood (10 ml) were collected from the precaval veins of each group of piglets after fasting for 12 h. After standing the blood samples for 1 h at 4°C, they were centrifuged at 3,000 × *g* for 15 min at 4°C, whereupon the serum samples obtained were immediately stored at −80°C for immunoglobulin and antioxidant indices analysis including immunoglobulin A (IgA), immunoglobulin G (IgG), immunoglobulin M (IgM), superoxide dismutase (SOD), glutathione peroxidase (GSH-Px), total antioxidant capacity (T-AOC), and malondialdehyde (MDA). After the blood collection, six piglets closest to the average BW from each group were slaughtered, and then the jejunum, ileum and liver, were sampled through a sterile laparotomy, which was collected in centrifuge tubes and immediately placed in liquid nitrogen and then stored at the temperature of −80°C for analysis of antioxidant indices levels of SOD, GSH-Px, catalase (CAT), T-AOC and MDA in jejunal, ileal and liver tissue. Besides, the ileum and cecum segments were isolated to collect the digesta samples using centrifuge tubes and a part of them

immediately placed in liquid nitrogen and then stored at the temperature of −80°C for analysis of microbiome and metabolite. The rest of samples were stored at −20°C for subsequent chemical composition analysis to calculate nutrient digestibility.

Determination of the Digestibility of Nutrients and Amino Acids

The feed samples and ileal digesta after freeze-drying were weighed in parallel samples for analysis and determination. Dry matter (DM), organic matter (OM), crude protein (CP), and gross energy (GE) contents were determined following the AOAC (2006) procedures. The amino acid (AA) profiles were detected by High Performance Liquid Chromatography (HPLC; Agilent 1200, Agilent Technologies, United States). Lysine and threonine were detected after hydrolyzing with 6 mol/L HCl at 105°C for 24 h. Methionine was analyzed as methionine sulfone after cold performic acid oxidation overnight before hydrolysis. Tryptophan was determined after hydrolyzing with 4 mol/L LiOH at 110°C for 20 h. The contents of acid insoluble ash (AIA) were determined in according to the method of Keulen and Young (1977) and the apparent ileal digestibility (AID) of amino acids and nitrogen was calculated as described by Stein et al. (2007).

Immunoglobulin and Antioxidant Indices Analysis

Frozen jejunal, ileal and liver tissue (2 mg) in 2 ml of phosphate-buffered saline was homogenized on ice with an Ultra-Turrax homogenizer (Bioblock Scientific, Illkirch, France) for 10 s at 6,800 rpm. The homogenate was centrifuged at 950 × *g* for 10 min at 4°C, and the supernatant was stored in a 2-ml centrifuge tube at −80°C until analysis. The GSH-Px and CAT activities, T-AOC, and MDA concentrations in the jejunal, ileal and liver tissue and serum were assayed using a UV/visible spectrophotometer (UV-2450; Shimadzu, Kyoto, Japan). The assays were conducted using assay kits purchased from Nanjing Jiancheng Institute of Bioengineering (Nanjing, Jiangsu, China) and conducted according to the manufacturer's instructions. All samples were measured in triplicate, at appropriate dilutions, and the activities of the enzymes were estimated from the linear range of standard curves constructed with the pure enzymes. The protein concentration of the supernatants was determined using Coomassie Brilliant Blue G250 (BlueGene, Shanghai, China).

Analysis for VFAs Using a Gas Chromatographic Method

The concentration of volatile fatty acids (VFAs) including short chain fatty acids (SCFAs) and branched chain fatty acids (BCFAs) in digesta were analyzed using a gas chromatographic method. Briefly, approximately 1.0 g of digesta samples were first homogenized in the 1.5 ml deionized water. After being centrifuged at 15,000 × *g* at 4°C for 10 min, supernatants (1 ml of each) were acidified with 25% metaphosphoric acid at a 1:5 ratio (1 volume of acid for 5 volumes of sample) for 30 min while on ice. The sample was injected into a GC 2010 series gas chromatograph (Shimadzu, Japan) equipped with a CP-Wax 52 CB column 30.0 m × 0.53 mm i.d (Chrompack, Netherlands). The injector and detector temperatures were 75 and 280°C, respectively. All procedures were performed in triplicate and total VFAs were determined as the sum of analyzed SCFAs (acetate, propionate, butyrate, and valerate) and BCFAs (isobutyrate and isovalerate).

Analysis for Bacterial Microbiota by 16S RNA

Total genomic DNA of 12 digesta samples were extracted using a Stool DNA Isolation Kit (Tiangen Biotech Co., Ltd., Beijing, China) following the manufacturer's instructions. The quantity and quality of extracted DNAs were measured using a NanoDrop ND-1000 spectrophotometer (Thermo Fisher Scientific, United States) and agarose gel electrophoresis, respectively. The genes of bacteria 16S ribosomal RNA in the region of V4–V5 were amplified by using polymerase chain reaction (PCR) with primers (515F 5'-barcode- GTGCCAGCMGCCGCGG)-3' and (907R 5'-120CCGTCAATTCMTTTRAGTTT-3'). Electrophoresis was applied to analyze the integrity of PCR amplicons by using a Tapestation Instruction (Agilent technologies, United States). AxyPrep DNA Gel 122 Extraction Kit was chosen to extract and purify PCR amplicons using 2% agarose gels (Axygen 123Biosciences, Union City, CA, United States) and then the production was quantified using QuantiFluor™ -ST and sequenced on an Illumina MiSeq system. QIIME software was used to demultiplex and quality-filtered raw Illumina fastq files. Operational taxonomic units (OTUs) were defined as a similarity threshold of 0.97 using UPARSE. Then UCHIME was applied to identify and delete the abnormal gene sequences. RDP database[1] was also referenced to take the taxonomy-based analysis for OUTs using RDP classifier at a 90% confidence level. The α-diversity indices including Simpson and Chao1 were analyzed by Mothur v.1.30.2. Principal co-ordinates analysis (PCoA) tools in R language were used for PCoA. The histogram of linear discriminant analysis (LDA) distribution was implemented using LDA effect size analysis (LEfSe) software.

Statistical Analysis

All data were analyzed by the GLM procedure of SPSS 21.0 (SPSS Inc., Chicago, IL, United States), and each piglet was regarded as a statistical unit. Data are showed as Mean values with standard error of the total mean (SEM). For all tests, $p < 0.05$ was considered as significant difference, while $0.05 < p < 0.10$ as a tendency.

RESULTS

Growth Performance

Over the experimental period, it has been noticed that piglets in the FCSM treatment had higher the final BW, ADG, and G:F ($p < 0.05$) and lower diarrhea incidence compared to those in the SBM treatment ($p < 0.05$; **Table 3**). No difference was observed in ADFI between the two dietary treatments (**Table 3**).

[1]http://rdp.cme.msu.edu/

TABLE 3 | Effects of two protein source on performance of weaned piglets.

Items	SBM	FCSM	SEM	*p*
Initial BW, kg	7.79	7.78	0.04	0.89
Final BW, kg	11.68	12.04	0.08	0.03
ADG, g	277.86	304.29	7.12	0.04
ADFI, g	441.05	454.16	9.17	0.46
G:F	0.63	0.67	0.01	0.03
Diarrhea incidence, %	4.78	2.42	0.47	0.02

Data were shown as the mean with the SEM (n = 16). BW, body weight; ADG, average daily gain; ADFI, average daily feed intake; G:F, ADG:ADFI; SBM, soybean meal; FCSM, fermented cottonseed meal.

Nutrient Digestibility

As shown in **Table 4**, the FCSM diet had higher apparent total tract digestibility and ileal digestibility of nutrients in terms of DM, OM, CP, and GE than the SBM diet ($p < 0.05$). Moreover, higher AID of essential AA including histidine, isoleucine, leucine, phenylalanine, valine, and nonessential AA including asparagine were discovered in the FCSM group compared to that in the SBM group ($p < 0.05$, **Table 5**). Furthermore, the AID of total nitrogen was enhanced in the FCSM group in comparison with the SBM group ($p < 0.05$).

Immunity and Antioxidant Properties

The results have shown that piglets in the FCSM group had higher serum IgG ($p < 0.05$) than those in the SBM group (**Table 6**). However, no significant difference was observed in terms of serum IgA and IgM ($p > 0.05$) of weaned piglets between the two groups. The effects of FCSM and SBM on serum, intestine and liver antioxidant enzyme activity and oxidant products on weaned piglets has been shown in **Table 7**. Compared with the SBM group, the SOD and GSH-Px in serum, jejunum, and ileum were improved on the piglets in the FCSM group ($p < 0.05$). Moreover, the jejunal T-AOC and the liver GSH-Px were enhanced on the piglets in the FCSM group ($p < 0.05$). Furthermore, the serum MDA was reduced on the piglets in the FCSM group ($p < 0.05$).

VFAs Composition

The VFAs composition in ileal and cecal digesta of weaned piglets were obtained in **Table 8**. Compared with the SBM group, the concentration of acetate, propionate, butyrate, isobutyrate, isovalerate, and total VFAs in ileal digesta of weaned piglets were increased in the FCSM group ($p < 0.05$). Similarly, the concentration of acetate, propionate, valerate, isobutyrate, isovalerate, and total VFAs in cecal digesta of weaned piglets were higher ($p < 0.05$) and the concentration of butyrate had a tendency to increase in the FCSM group ($0.05 < p < 0.1$).

Gut Microbiota Diversity

The OTUs of the ileal digesta from SBM and FCSM groups were 152 and 169, respectively, among which 82 common OTUs have been identified (**Figure 1A**). On the other hand, the OTUs of the cecal digesta from SBM and FCSM groups were 743 and 656, respectively, wherein 544 common OTUs have been identified (**Figure 1B**). The α-diversity of ileal and cecal microbiota including Simpson index and Chao1 index were presented in **Figures 2A–D**. The FCSM diet induced higher Simpson index of ileum than the SBM ($p < 0.05$), whereas no difference was shown in the other index between the two dietary treatments neither in the ileum nor cecum ($p > 0.05$). The β-diversity of bacterial community between SBM and FCSM was presented with PCoA (**Figures 2E,F**), showing a tendency of different clustering of microbial communities in cecum ($0.05 < p < 0.1$, **Figure 2F**).

TABLE 4 | Effects of two protein source on apparent total tract digestibility and ileal digestibility of nutrients of weaned piglets (%).

Item	SBM	FCSM	SEM	*p*
Apparent total tract digestibility of nutrients				
DM	84.24	85.55	0.22	0.01
OM	86.08	87.53	0.23	0.01
CP	77.81	80.08	0.23	0.01
GE	84.01	85.35	0.22	0.01
Apparent ileal digestibility of nutrients				
DM	86.24	87.85	0.22	0.01
OM	87.88	89.83	0.23	0.01
CP	79.41	82.18	0.23	0.01
GE	85.40	87.55	0.22	0.01

Data were shown as the mean with the SEM (n = 6). DM, dry matter; OM, organic matter; CP, crude protein; GE, gross energy; SBM, soybean meal; FCSM, fermented cottonseed meal.

At the phylum level, Firmicutes and Bacteroidetes were the dominant bacteria in both ileum and cecum. There was no difference found by the students' tests in microbiota at the phylum level between the two treatment groups in ileum ($p > 0.05$; **Figure 3A**). However, the proportion of cecal Proteobacteria was decreased ($p < 0.05$) in the FCSM group compared with the SBM group (**Figure 3C**). Besides, at the genus level (**Figures 3B,D**), the proportion of ileal *Lactobacillus* was enhanced but the ileal *unclassified_p_Firmicutes* and cecal *Ruminococcus_1* was decreased in the piglets in the FCSM group rather than that in the SBM group ($p < 0.05$).

The LEfSe analysis was used to identify the significantly different bacteria in the ileum and cecum between the two treatment groups from the phylum to genus level (**Figures 3E,F**). The relative abundance of *Lactobacillus* and *[Ruminococcus]_torques_group* in ileum and *Intestinibacter*, *norank_f_Muribaculaceae*, *unclassified_o_Lactobacillales* and *[Eubacterium]_coprostanoligenes_group* in cecum were enhanced in piglets fed with the FCSM diet than those fed with SBM diet, whereas the relative abundance of *Sarcina* and *Terrisporobacter* in ileum were decreased in piglets fed with the FCSM diet.

DISCUSSION

Cottonseed meal has not been widely used because it contains a large number of anti-nutritional factors, which result negative effects on growth performance, immune and antioxidant capacity and nutrient digestibility in animals (Nagalakshmi et al., 2007; Nie et al., 2015; Świątkiewicz, 2016). After going through solid

TABLE 5 | Effects of two protein source on apparent ileal digestibility of amino acids and nitrogen of weaned piglets (%).

Items	SBM	FCSM	SEM	*p*
Essential AA (%)				
Arginine	84.39	89.10	2.64	0.25
Histidine	93.01	96.48	0.77	0.02
Isoleucine	75.80	82.45	1.69	0.03
Leucine	75.45	81.22	1.43	0.02
Lysine	90.50	93.21	1.21	0.16
Methionine	90.84	93.12	1.16	0.21
Phenylalanine	94.06	96.26	0.62	0.04
Threonine	77.21	78.65	0.51	0.09
Tryptophan	78.38	79.06	1.03	0.65
Valine	80.60	86.79	1.34	0.01
Nonessential AA (%)				
Alanine	71.55	75.48	1.50	0.11
Asparagine	66.16	72.31	1.51	0.02
Cystine	61.97	63.49	2.74	0.71
Glutamine	86.67	89.86	1.57	0.20
Glycine	63.56	64.73	1.17	0.50
Proline	85.28	85.28	1.79	0.99
Serine	80.98	82.85	1.42	0.39
Tyrosine	75.73	81.27	1.85	0.07
Total nitrogen (%)	79.41	82.18	0.22	< 0.01

Data were shown as the mean with the SEM (n = 6). AA, amino acid; SBM, soybean meal; FCSM, fermented cottonseed meal.

TABLE 6 | Effects of two protein source on serum immune of weaned piglets (%).

Items	SBM	FCSM	SEM	*p*
IgG (g/L)	7.82	9.27	0.38	0.03
IgA (g/L)	1.07	1.06	0.04	0.86
IgM (g/L)	0.84	0.91	0.06	0.59

Data were shown as the mean with the SEM (n = 6). IgG, immunoglobulin G; IgA, immunoglobulin A; IgM, immunoglobulin M; SBM, soybean meal; FCSM, fermented cottonseed meal.

state fermentation, FCSM has much less free gossypol and other anti-nutritional factors, and definitively improved protein quality (Zhang et al., 2006, 2007; Sun et al., 2014; Wang et al., 2017). Sun et al. (2013) reported that the appropriate inclusion of FCSM replacing SBM improved the growth of yellow-feathered broiler chickens. Similarly, FCSM supplementation improved the ADG and G:F ratio of yellow-feathered broilers from the 43rd to 64th and the 21st to 64th day, respectively (Nie et al., 2015), which indicated that FCSM is beneficial for broilers as it enhanced their growth performance and digestion. Consistently, the current study showed that the piglets in the FCSM group presented greater growth performance and a lower diarrhea rate than those in the SBM group. The fermentation process of CSM might be one of the reasons, which effectively decreases free gossypol level, and increases acid-soluble protein level in CSM, and therefore further improves the digestive enzyme activity and nutrient digestibility in weaned piglets (Sun et al., 2014; Wang et al., 2017). This explanation has been confirmed by the nutrient digestibility of weaned piglets in FCSM and SBM treatments. The present results demonstrated that the apparent total tract digestibility and ileal digestibility of nutrients, essential and nonessential AA have been enhanced in piglets within the FCSM group.

Moreover, the microbial fermentation process can produce many beneficial substances, such as small-size peptides, exoenzymes, vitamins, organic acids, which can promote the

TABLE 7 | Effects of two protein source on serumal, intestinal and hepatic antioxidant enzyme activity and oxidant products of weaned piglets.

Items	SBM	FCSM	SEM	*p*
Serum				
SOD (U/ml)	110.38	142.56	4.25	0.03
GSH-Px (U/ml)	724.89	796.57	18.26	0.02
T-AOC (U/ml)	7.38	8.44	0.54	0.21
MDA (nmol/ml)	4.92	2.87	0.32	0.02
Jejunum				
SOD (U/mg prot)	129.51	206.25	10.30	0.01
GSH-Px (U/mg prot)	248.40	361.90	15.75	0.01
CAT (U/mg prot)	45.43	44.33	2.08	0.72
T-AOC (U/mg prot)	54.05	81.28	4.12	0.01
MDA (nmol/mg prot)	3.92	3.17	0.66	0.45
Ileum				
SOD (U/mg prot)	144.49	184.88	6.06	0.01
GSH-Px (U/mg prot)	275.33	394.29	28.60	0.02
CAT (U/mg prot)	47.23	39.27	3.86	0.19
T-AOC (U/mg prot)	45.06	60.60	6.03	0.11
MDA (nmol/mg prot)	5.31	4.60	0.43	0.29
Liver				
SOD (U/mg prot)	27.65	34.88	3.47	0.18
GSH-Px (U/mg prot)	96.34	124.23	6.93	0.02
CAT (U/mg prot)	9.13	11.81	1.53	0.26
T-AOC (U/mg prot)	26.09	31.18	3.42	0.33
MDA (nmol/mg prot)	4.38	3.21	0.46	0.11

Data were shown as the mean with the SEM (n = 6). SOD, superoxide dismutase; GSH-Px, glutathione peroxidase; CAT, catalase; T-AOC, total antioxidant capacity; MDA, malondialdehyde; SBM, soybean meal; FCSM, fermented cottonseed meal.

TABLE 8 | Effects of protein source on volatile fatty acids composition in ileal and cecal digesta of weaned pigs (mg/g digesta).

Items	SBM	FCSM	SEM	*p*
Ileum				
Acetate	0.70	0.83	0.02	0.01
Propionate	0.35	0.42	0.01	0.01
Butyrate	0.31	0.40	0.01	<0.01
Valerate	0.26	0.26	0.01	0.47
Isobutyrate	0.09	0.05	0.01	<0.01
Isovalerate	0.22	0.17	0.01	<0.01
Total VFAs[1]	1.93	2.13	0.01	<0.01
Cecum				
Acetate	3.79	4.43	0.07	<0.01
Propionate	2.72	3.36	0.18	0.04
Butyrate	1.77	2.03	0.09	0.07
Valerate	0.75	0.99	0.05	0.02
Isobutyrate	0.41	0.31	0.02	0.01
Isovalerate	0.61	0.47	0.02	0.01
Total VFAs[1]	10.06	11.60	0.27	0.01

[1]Total VFAs = Acetate + Propionate + Butyrate + Valerate + Isobutyrate + Isovalerate. Data were shown as the mean with the SEM (n = 6). VFAs, volatile fatty acids; SBM, soybean meal; FCSM, fermented cottonseed meal.

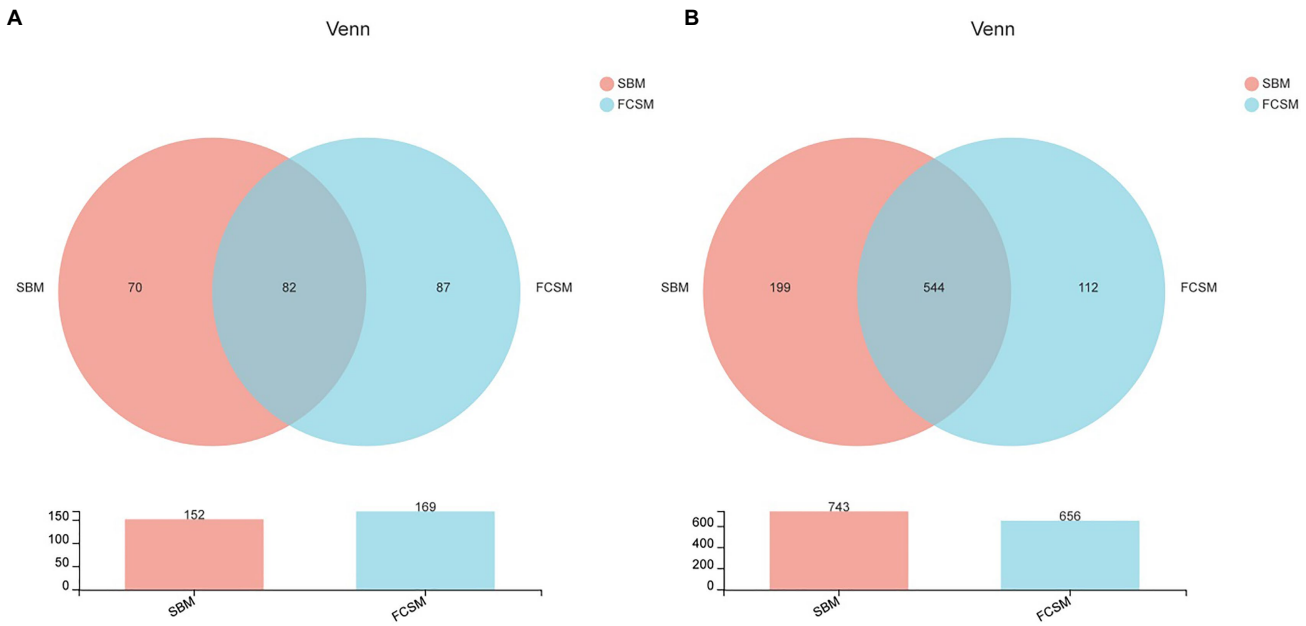

FIGURE 1 | Effects of two protein sources on the ileac **(A)** and cecal **(B)** microbes at the operational taxonomic unit (OTU) in piglets. The individual minipig was regarded as the experimental unit ($n = 6$). SBM, soybean meal; FCSM, fermented cottonseed meal.

immunity of animals (Johnson, 2013; Zhao et al., 2016). A study have reported that fermentation with *Bacillus subtilis BJ-1* can reduce free gossypol level in CSM and dietary inclusion of 12% FCSM can improve immunity (Tang et al., 2012). Wang et al. (2017) reported that the dietary supplementation of FCSM increased serum IgM and IgG levels compared with SBM groups in broilers. In the present study, the concentration of serumal IgG was increased in piglets in the FCSM group in comparison with those in the SBM group, which might be due to the live microbes in FCSM acting as probiotics to enhance the humoral immune response of the animals (Latesh et al., 2013; Stašová et al., 2015).

The immunity of piglets is highly related to antioxidant capacity (Liu et al., 2021). Besides, antioxidase can improve the immunity by promoting the bacterial clearance and regulates phagocyte numbers (Peterman et al., 2015). In addition, a microbial FCSM increased the antioxidant activity in diets for Nile tilapia (Lim and Lee, 2011). Similarly, the present study showed that the antioxidation-related enzymes in serum, jejunum, ileum and liver were improved in piglets in the FCSM group compared with that in the SBM group. Additionally, the serum MDA was reduced in piglets in the FCSM group, which indicated that FCSM improved the antioxidative abilities compared with SBM (Wang et al., 2017). This may be one of the reasons that the improvement of growth performance in piglets has found in the FCSM group (Ma, X. et al., 2019; Ma, X. K. et al., 2019).

Many studies suggest that food or feeds fermented by probiotics may be potentially an effective strategy to regulate the gut microbiota and its metabolites (Azad et al., 2020; Niu et al., 2020; Gu et al., 2021; Li et al., 2021). The VFAs, especially butyric acid, as a microbial metabolite, can not only improve the growth performance, but also boost the immunity of piglets (Fang et al., 2014; Zhao et al., 2018). Zhao et al. (2018) reported that dietary fiber increases the butyrate-producing bacteria and improves growth performance of weaned piglets. Tsai et al. (2019) discovered that feeding sodium butyrate during the nursery phase tended to alter blood cell count and improve growth performance of weaned pigs. In the present study, the VFAs of ileum and cecum were increased in the FCSM group than that in the SBM group. This may explain the improved growth performance of piglets. Moreover, VFAs, as important intermediate products during anaerobic digestion, may influence the fermentation characteristics of hindgut (Jha and Berrocoso, 2016; Seradj et al., 2018). The protein fermentation metabolites in the hindgut are amines, SCFAs and BCFAs, among which amines must be converted from nitrogen-containing groups, while BCFAs are only produced from the fermentation of three branched chain amino acids, leucine, isoleucine and valine (Jha and Berrocoso, 2016; Seradj et al., 2018). Over-fermentation of protein in the hindgut is an important cause of diarrhea in piglets. The current study found that FCSM replacing SBM decreased the isobutyrate and isovalerate of the cecum, suggesting that FCSM reduced hindgut fermentation, which may be responsible for the reduced diarrhea rate in piglets.

In recent years, the interaction and connections between dietary protein, gut microbe and host has received increasing attention. Segmented exogenous microbiota transplantation proved the spatial heterogeneity of bacterial colonization along the gastrointestinal tract, i.e., the microbiota from one specific location selectively colonizes its homologous gut region (Li et al., 2020). The number of microorganisms in the hindgut was higher than that in the foregut (Jamet et al., 2011), which is consistent with the result in the present study. It has been previously shown that FCSM enhanced the Simpson index of

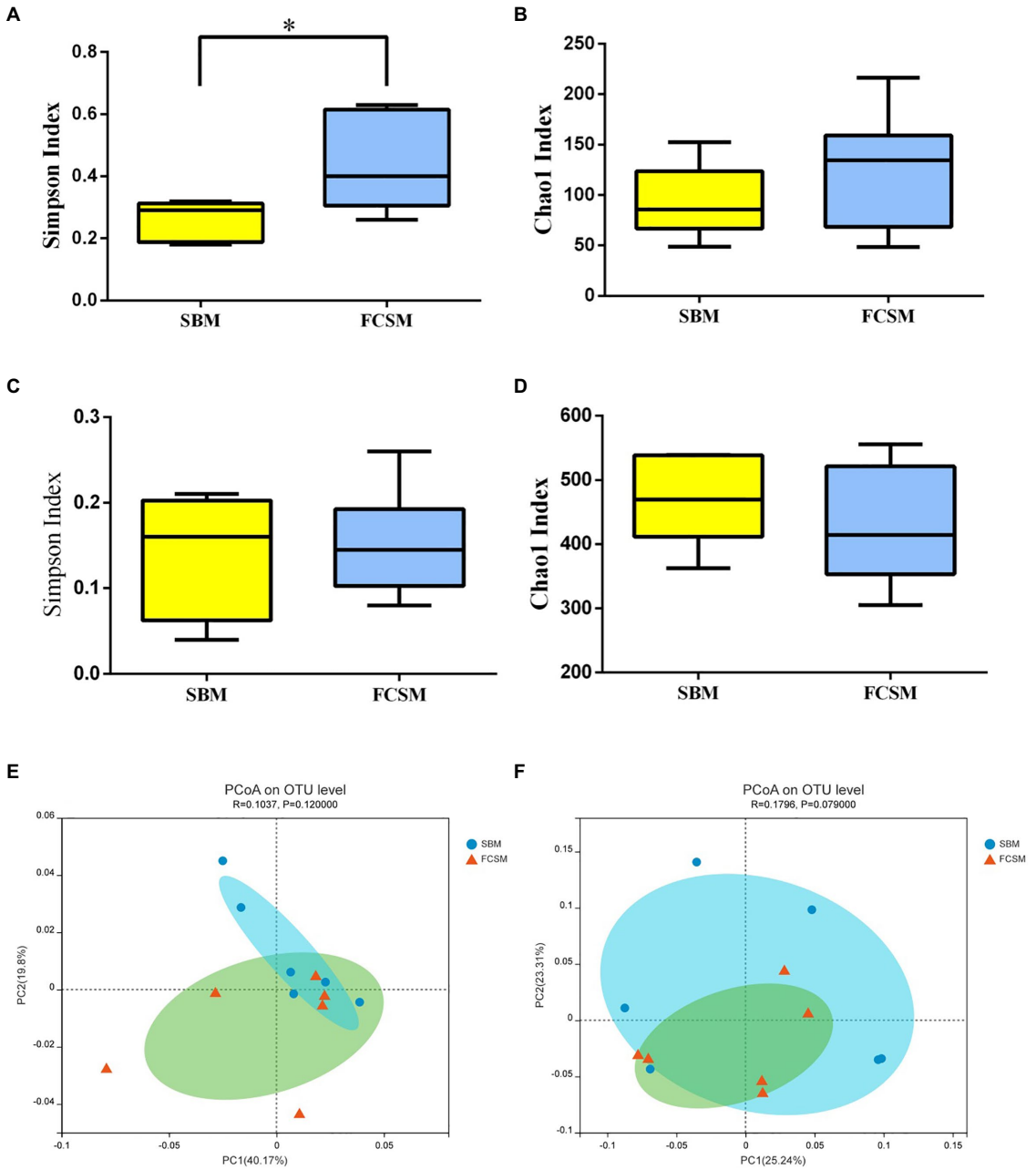

FIGURE 2 | Effects of two protein sources on the α-diversity indexes including Simpson index of ileac **(A)** and cecal **(C)** microbes, Chao1 index of the ileac **(B)** and cecal **(D)** microbes, β-diversity of the ileac **(E)** and cecal **(F)** microbes in piglets. The individual minipig was regarded as the experimental unit ($n = 6$). SBM, soybean meal; FCSM, fermented cottonseed meal. $^{*}p < 0.05$.

ileum in piglets, which has a great contribution towards the improvement of intestinal health and maturation in piglets (Wang, X. et al., 2019). Lower protein concentration or better protein sources in the diets can improve hindgut health by preventing the proliferation of pathogenic bacteria and reduced the risk of colitis (Vidal-Lletjós et al., 2017; Najafabadi et al., 2019). Studies have shown that protein fermentation can change the composition and function of intestinal flora (Lu et al., 2019; Wang, H. et al., 2019). Consistently, in the present study, the analysis of the PCoA has shown that the microbial composition between the SBM and FCSM groups are slightly different.

Firmicutes and Bacteroidetes were the most dominant phyla in the pig (Chen et al., 2017). In our study, Firmicutes is the most dominant phyla in ileum and Firmicutes and Bacteroidetes in cecum. *Lactobacillus*, as a potential probiotic, possesses the resistance to pathogen, anti-inflammatory and antioxidant capacity, and ability to improve of gut microbiota

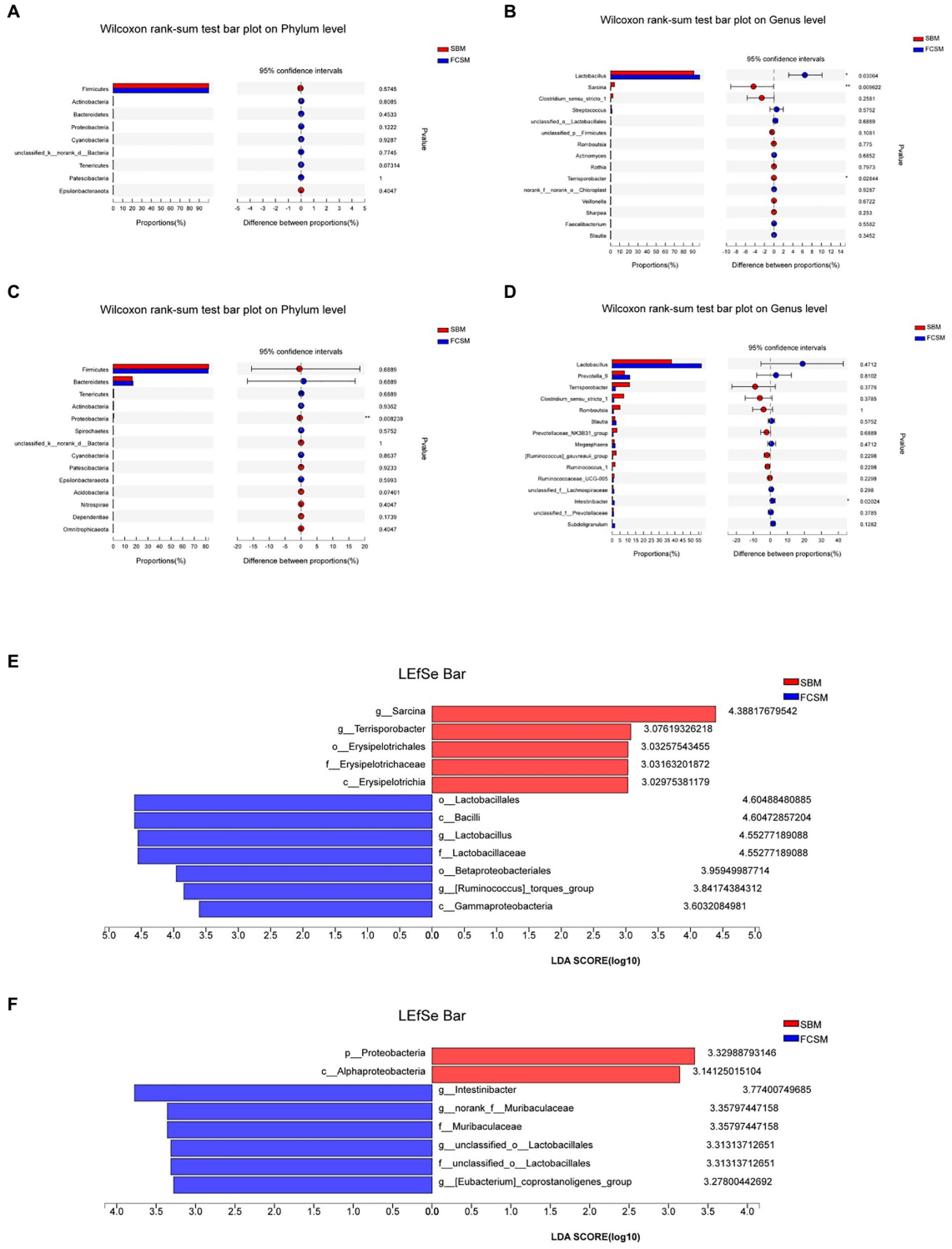

FIGURE 3 | Different microbiota comparison by the student *t*-test on Phylum and Genus of ileum **(A,B)** and cecum **(C,D)** was shown in **(A–D)**. LDA effect size analysis (LEfSe) analysis showed significantly changed bacteria between SBM and FCSM group in ileum **(E)** and cecum **(F)**. The individual minipig was regarded as the experimental unit ($n = 6$). SBM, soybean meal; FCSM, fermented cottonseed meal.

profile (He et al., 2019; Yang et al., 2020). Wang et al. (2017) has discovered that *Lactobacilli* and total anaerobic bacteria counts in ceca digesta of birds fed FCSM were improved compared with birds fed CSM on days 21 and 42. Likewise, the FCSM replacing the SBM has also enhanced the relative abundance of *Lactobacillus* of ileum and cecum

in the present study. He et al. (2019) has found that *Lactobacillus johnsonii L531* reduced pathogen load and helped maintain SCFA levels in the intestine of pigs challenged with *Salmonella enterica Infantis*. Therefore, this might be one of the reasons that piglets in the FCSM group had higher level of VFAs than that in the SBM group. On the other hand, proteobacteria is the largest phylum of bacteria, including many pathogenic bacteria, such as *Escherichia coli*, *Salmonella*, *Vibrio cholerae*, *Helicobacter pylori* and other well-known species. In the current study, the relative abundance of Proteobacteria was decreased in piglets in the FCSM group, suggesting that the FCSM has the potential function to inhibit harmful bacteria, and improves the gut microbiota profile than SBM (Wang et al., 2017). In conclusion, FCSM replacing SBM improved the growth performance, immunity and antioxidant properties, nutrients digestibility possibly *via* the altering gut microbiota profile and its metabolites in weaned piglets.

DATA AVAILABILITY STATEMENT

The data presented in the study are deposited in the (NCBI SRA) repository, accession number (PRJNA743130).

ETHICS STATEMENT

The animal study was reviewed and approved by Animal Care and Use Ethics Committee of the Hunan Agricultural University.

AUTHOR CONTRIBUTIONS

XG and XM: conceptualization, methodology, and software. ZL, NL, XL, and FZ: literature collection. XG and JW: writing–original draft preparation. JC, QJ, and BT: writing–reviewing and editing. XM: funding acquisition. All authors contributed to the article and approved the submitted version.

FUNDING

This review is funded by Scientific Research Fund of Hunan Provincial Education Department (19B267) and the Youth Science Foundation Project of Hunan Agricultural University (19QN01), and the Open Foundation of CAS Key Laboratory of Agro-ecological Processes in Subtropical Region, Institute of Subtropical Agriculture (ISA2020101).

REFERENCES

Azad, M. A. K., Gao, J., Ma, J., Li, T., Tan, B., Huang, X., et al. (2020). Opportunities of prebiotics for the intestinal health of monogastric animals. *Anim. Nutr.* 6, 379–388. doi: 10.1016/j.aninu.2020.08.001

Azarm, H. M., and Lee, S. M. (2014). Effects of partial substitution of dietary fish meal by fermented soybean meal on growth performance, amino acid and biochemical parameters of juvenile black sea bream acanthopagrus schlegeli. *Aquac. Res.* 45, 994–1003. doi: 10.1111/are.12040

Chen, L., Xu, Y., Chen, X., Fang, C., Zhao, L., and Chen, F. (2017). The maturing development of gut microbiota in commercial piglets during the weaning transition. *Front. Microbiol.* 8:1688. doi: 10.3389/fmicb.2017.01688

Fang, C. L., Sun, H., Wu, J., Niu, H. H., and Feng, J. (2014). Effects of sodium butyrate on growth performance, haematological and immunological characteristics of weanling piglets. *J. Anim. Physiol. An. N.* 98, 680–685. doi: 10.1111/jpn.12122

Gu, X. L., Chen, J., Li, H., Song, Z. H., Chang, L., He, X., et al. (2021). Isomaltooligosaccharide and bacillus regulate the duration of farrowing and weaning-estrous interval in sows during the perinatal period by changing the gut microbiota of sows. *Anim. Nutr.* 7, 72–83. doi: 10.1016/j.aninu.2020.06.010

Guan, H., Wang, J., Zhang, D., Ma, J., and Zheng, W. (2017). Effects of fermented cottonseed meal on production performance and health status of nursery pig, growing pig and finishing pig. *Swine Production* 4, 9–11. doi: 10.13257/j.cnki.21-1104/s.2017.04.003

He, T., Zhu, Y. H., Yu, J., Xia, B., Liu, X., Yang, G. Y., et al. (2019). *Lactobacillus johnsonii L531* reduces pathogen load and helps maintain short-chain fatty acid levels in the intestines of pigs challenged with *salmonella enterica Infantis*. *Vet. Microbiol.* 230, 187–194. doi: 10.1016/j.vetmic.2019.02.003

Jamet, A., Mérieux, A., Cultrone, A., Torrejon, A., Cara, C., Friss, C., et al. (2011). Enterotypes of the human gut microbiome. *Nature* 473, 174–180. doi: 10.1038/nature09944

Jha, R., and Berrocoso, J. F. D. (2016). Dietary fiber and protein fermentation in the intestine of swine and their interactive effects on gut health and on the environment: a review. *Anim. Feed Sci. Technol.* 212, 18–26. doi: 10.1016/j.anifeedsci.2015.12.002

Johnson, E. A. (2013). Biotechnology of non-saccharomyces yeasts-the basidiomycetes. *Appl. Microbiol. Biotechnol.* 97, 503–517. doi: 10.1007/s00253-012-4497-y

Keulen, J. V., and Young, B. A. (1977). Evaluation of acid-insoluble ash as a natural marker in ruminant digestibility studies. *J. Anim. Sci.* 44, 282–287. doi: 10.2527/jas1977.442282x

Kim, S. W. (2014). Identification of a second major antigenic epitope in the α-subunit of soy β-conglycinin. *Food Agric. Immunol.* 25, 311–321. doi: 10.1080/09540105.2013.791969

Latesh, K., Singh, P. K., and Manoj, K. (2013). Effect of dietary supplementation of combination of probiotics on the growth performance and immune response of broiler chickens. *Anim. Nutr. Feed. Technol.* 13, 15–25. doi: 10.1080/09064702.2013.877520

Li, H., Yin, J., He, X., Li, Z., Tan, B., Jiang, Q., et al. (2021). Enzyme-treated soybean meal replacing extruded full-fat soybean affects nitrogen digestibility, cecal fermentation characteristics and bacterial community of newly weaned piglets. *Front. Vet. Sci.* 8:639039. doi: 10.3389/fvets.2021.639039

Li, N., Zuo, B., Huang, S., Zeng, B., and Wang, J. (2020). Spatial heterogeneity of bacterial colonization across different gut segments following inter-species microbiota transplantation. *Microbiome* 8:161. doi: 10.1186/s40168-020-00917-7

Lim, S., and Lee, K. (2011). A microbial fermentation of soybean and cottonseed meal increases antioxidant activity and gossypol detoxification in diets for *Nile tilapia*, *Oreochromis niloticus*. *J. World Aquacult. Soc.* 42, 494–503. doi: 10.1111/j.1749-7345.2011.00491.x

Liu, L., Chen, D., Yu, B., Luo, Y., and He, H. (2021). Influences of selenium-enriched yeast on growth performance, immune function, and antioxidant capacity in weaned pigs exposure to oxidative stress. *Biomed. Res. Int.* 2021:5533210. doi: 10.1155/2021/5533210

Lordelo, M. M., Calhoun, M. C., Dale, N. M., Dowd, M. K., and Davis, A. J. (2007). Relative toxicity of gossypol enantiomers in laying and broiler breeder hens. *Poult. Sci.* 86, 582–590. doi: 10.1093/ps/86.3.582

Lu, J., Zhang, X., Liu, Y., Cao, H., and Shi, X. (2019). Effect of fermented corn-soybean meal on serum immunity, the expression of genes related to gut immunity, gut microbiota, and bacterial metabolites in grower-finisher pigs. *Front. Microbiol.* 10:2620. doi: 10.3389/fmicb.2019.02620

Ma, X., Shang, Q., Hu, J., Liu, H., Brøkner, C., and Piao, X. (2019). Effects of replacing soybean meal, soy protein concentrate, fermented soybean meal or fish meal with enzyme-treated soybean meal on growth performance,

nutrient digestibility, antioxidant capacity, immunity and intestinal morphology in weaned pigs. *Livest. Sci.* 225, 39–46. doi: 10.1016/j.livsci.2019.04.016

Ma, X. K., Shang, Q. H., Wang, Q. Q., Hu, J. X., and Piao, X. S. (2019). Comparative effects of enzymolytic soybean meal and antibiotics in diets on growth performance, antioxidant capacity, immunity, and intestinal barrier function in weaned pigs. *Anim. Feed Sci. Technol.* 248, 47–58. doi: 10.1016/j.anifeedsci.2018.12.003

Nagalakshmi, D., Rao, S. V. R., Panda, A. K., and Sastry, V. R. B. (2007). Cottonseed meal in poultry diets: a review. *J. Poult. Sci.* 44, 119–134. doi: 10.2141/jpsa.44.119

Najafabadi, Z. S., Nielsen, T. S., and Hedemann, M. S. (2019). Dietary protein source and butyrylated high-amylose maize starch included in a high-protein diet determines the urinary metabolome of rats. *Int. J. Food Sci. Nutr.* 70, 255–266. doi: 10.1080/09637486.2018.1499711

Nie, C., Zhang, W., Wenxia, G. E., Wang, Y., Liu, Y., and Liu, J. (2015). Effects of fermented cottonseed meal on the growth performance, apparent digestibility, carcass traits, and meat composition in yellow-feathered broilers. *Turk. J. V. Anim. Sci.* 39, 350–356. doi: 10.3906/vet-1410-65

Niu, J. L., Zhang, J., Wei, L. Q., Ma, X., Zhang, W. J., and Nie, C. X. (2020). Cottonseed meal fermented by Candida tropical reduces the fat deposition in white-feather broilers through cecum bacteria-host metabolic cross-talk. *Appl. Microbiol. Biotechnol.* 104, 4345–4357. doi: 10.1007/s00253-020-10538-7

NRC (2012). Nutrient Requirements of Swine. Washington, DC: National Academy Press.

Peterman, E. M., Sullivan, C., Goody, M. F., Rodriguez-Nunez, I., Yoder, J. A., and Kim, C. H. (2015). Neutralization of mitochondrial superoxide by superoxide dismutase 2 promotes bacterial clearance and regulates phagocyte numbers in zebrafish. *Infect. Immun.* 83, 430–440. doi: 10.1128/IAI.02245-14

Seradj, A. R., Balcells, J., Morazan, H., Alvarez-Rodriguez, J., Babot, D., and De la Fuente, G. (2018). The impact of reducing dietary crude protein and increasing total dietary fiber on hindgut fermentation, the methanogen community and gas emission in growing pigs. *Anim. Feed Sci. Technol.* 245, 54–66. doi: 10.1016/j.anifeedsci.2018.09.005

Stašová, D., Husáková, E., Bobíková, K., Karaffová, V., Levkutová, M., and Levkut, M. (2015). Expression of cytokines in chicken peripheral blood mononuclear cells after stimulation by probiotic bacteria and campylobacter jejuni in vitro. *Food Agric. Immunol.* 26, 813–820. doi: 10.1080/09540105.2015.1036356

Stein, H. H., Fuller, M. F., Moughan, P. J., Sève, B., Mosenthin, R., Jansman, A. J. M., et al. (2007). Definition of apparent, true, and standardized ileal digestibility of amino acids in pigs. *Livest. Sci.* 109, 282–285. doi: 10.1016/j.livsci.2007.01.019

Sun, H., Tang, J., Yao, X., Wu, Y., Wang, X., and Feng, J. (2013). Effects of dietary inclusion of fermented cottonseed meal on growth, cecal microbial population, small intestinal morphology, and digestive enzyme activity of broilers. *Trop. Anim. Health Prod.* 45, 987–993. doi: 10.1007/s11250-012-0322-y

Sun, H., Yao, X., Wang, X., Wu, Y., Liu, Y., Tang, J., et al. (2014). Chemical composition and in vitro antioxidant property of peptides produced from cottonseed meal by solid-state fermentation. *CYTA J. Food* 13, 264–272. doi: 10.1080/19476337.2014.948072

Świątkiewicz, S. (2016). The use of cottonseed meal as a protein source for poultry: an updated review. *Worlds Poult. Sci. J.* 72, 473–484. doi: 10.1017/S0043933916000258

Tang, J. W., Sun, H., Yao, X. H., Wu, Y. F., Wang, X., and Feng, J. (2012). Effects of replacement of soybean meal by fermented cottonseed meal on growth performance, serum biochemical parameters and immune function of yellow-feathered broilers. *Asian Aust. J. Anim. Sci.* 25, 393–400. doi: 10.5713/ajas.2011.11381

Tsai, T. C., Stein, H. H., Bradley, C. L., Blavi, L., Bottoms, K., Knapp, J., et al. (2019). Effect of sodium butyrate (SB) on growth performance and complete blood cell count in nursery pigs: two facility study. *J. Anim. Sci.* 97, 76–77. doi: 10.1093/jas/skz122.141

Vidal-Lletjós, S., Beaumont, M., Tomé, D., Benamouzig, R., Blachier, F., and Lan, A. (2017). Dietary protein and amino acid supplementation in inflammatory bowel disease course: what impact on the colonic mucosa. *Nutrients* 9:310. doi: 10.3390/nu9030310

Wang, Y., Deng, Q., Song, D., Wang, W., Zhou, H., Wang, L., et al. (2017). Effects of fermented cottonseed meal on growth performance, serum biochemical parameters, immune functions, antioxidative abilities, and cecal microflora in broilers. *Food Agric. Immunol.* 28, 725–738. doi: 10.1080/09540105.2017.1311308

Wang, H., Shen, J., Pi, Y., Gao, K., and Zhu, W. (2019). Low-protein diets supplemented with casein hydrolysate favor the microbiota and enhance the mucosal humoral immunity in the colon of pigs. *J. Anim. Sci. Biotechnol.* 10:79. doi: 10.1186/s40104-019-0387-9

Wang, X., Tsai, T., Deng, F., Wei, X., and Zhao, J. (2019). Longitudinal investigation of the swine gut microbiome from birth to market reveals stage and growth performance associated bacteria. *Microbiome* 7:109. doi: 10.1186/s40168-019-0721-7

Yang, G. Y., Xia, B., Su, J. H., He, T., Liu, X., Guo, L., et al. (2020). Anti-inflammatory effects of *Lactobacillus johnsonii* L531 in a pig model of *Salmonella Infantis* infection involves modulation of CCR6 + T cell responses and ER stress. *Vet. Res.* 51, 26–39. doi: 10.1186/s13567-020-00754-4

Zhang, W. J., Xu, Z. R., Sun, J. Y., and Yang, X. (2006). Effect of selected fungi on the reduction of gossypol levels and nutritional value during solid substrate fermentation of cottonseed meal. *J. Zhejiang Univ. Sci. B* 7, 690–695. doi: 10.1631/jzus.2006.B0690

Zhang, W. J., Xu, Z. R., Zhao, S. H., Sun, J. Y., and Yang, X. (2007). Development of a microbial fermentation process for detoxification of gossypol in cottonseed meal. *Anim. Feed Sci. Technol.* 135, 176–186. doi: 10.1016/j.anifeedsci.2006.06.003

Zhao, J., Ping, L., Wu, Y., Guo, P., Liu, L., Ma, N., et al. (2018). Dietary fiber increases the butyrate-producing bacteria and improves growth performance of weaned piglets. *J. Agric. Food Chem.* 66, 7995–8004. doi: 10.1021/acs.jafc.8b02545

Zhao, C. J., Schieber, A., and Gänzle, M. G. (2016). Formation of taste-active amino acids, amino acid derivatives and peptides in food fermentations-a review. *Food Res. Int.* 89, 39–47. doi: 10.1016/j.foodres.2016.08.042

Conflict of Interest: The authors declare that the research was conducted in the absence of any commercial or financial relationships that could be construed as a potential conflict of interest.

Publisher's Note: All claims expressed in this article are solely those of the authors and do not necessarily represent those of their affiliated organizations, or those of the publisher, the editors and the reviewers. Any product that may be evaluated in this article, or claim that may be made by its manufacturer, is not guaranteed or endorsed by the publisher.

frontiers in Microbiology

ORIGINAL RESEARCH
published: 06 September 2021
doi: 10.3389/fmicb.2021.742033

Morchella importuna Flavones Improve Intestinal Integrity in Dextran Sulfate Sodium-Challenged Mice

Yingyin Xu[1], Liyuan Xie[1], Jie Tang[1], Xiaolan He[1], Zhiyuan Zhang[1], Ying Chen[1], Jie Zhou[1], Bingcheng Gan[2] and Weihong Peng[1]**

[1] National-Local Joint Engineering Laboratory of Breeding and Cultivation of Edible and Medicinal Fungi, Institute of Agricultural Resources and Environment, Sichuan Academy of Agricultural Sciences, Chengdu, China, [2] Institute of Urban Agriculture, Chinese Academy of Agricultural Sciences, Chengdu, China

Morchella importuna, as an edible fungus, has various health benefits. However, the effects of *M. importuna* on intestinal health are rarely investigated. Hence, this study aims to ascertain the influences of flavones from the fruiting bodies of *M. importuna* (hereinafter abbreviated as MIF) on dextran sulfate sodium (DSS)-induced damage to intestinal epithelial barrier in C57BL/6J mice. In this (14-day) study, 144 C57BL/6J mice were divided into four groups: (1) Control; (2) DSS treatment; (3) DSS treatment + 100 mg/kg MIF (LMIF); (4) DSS treatment + 200 mg/kg MIF (HMIF). On days 8-14, mice in the challenged groups were challenged with 3.5% DSS, while the control group received an equal volume of normal saline. Then, serum and intestinal samples were obtained from all mice. The results showed that MIF ingestion enhanced intestinal integrity in DSS-challenged mice, as evinced by the elevated ($p < 0.05$) abundances of occludin, claudin-1, and zonula occludens-1 proteins. Meanwhile, MIF ingestion reduced ($p < 0.05$) the colonic interleukin-1β (IL-1β), tumor necrosis factor-α (TNF-α), and interferon-γ (IFN-γ) concentrations and increased the superoxide dismutase and catalase activities and Shannon and Simpson indices in DSS-challenged mice. Moreover, MIF ingestion reduced ($p < 0.05$) the abundance of phospho-nuclear factor (NF)-κB and increased the abundance of phospho-Nrf2 in DSS-challenged mice. Taken together, MIF protects against intestinal barrier injury in C57BL/6J mice *via* a mechanism that involves inhibiting NF-κB activation and promoting Nrf2 activation, as well as regulating intestinal microbiota.

Keywords: ***Morchella importuna*, intestinal barrier function, intestinal microbiota, inflammatory responses, C57BL/6 mice**

OPEN ACCESS

Edited by:
Zheng Ruan,
Nanchang University, China

Reviewed by:
Junqiu Luo,
Sichuan Agricultural University, China
Xiao Xu,
Wuhan Polytechnic University, China

****Correspondence:***
Bingcheng Gan
ganbingcheng@caas.cn
Weihong Peng
whpeng768@163.com

Specialty section:
This article was submitted to Food Microbiology, a section of the journal Frontiers in Microbiology

Received: *15 July 2021*
Accepted: *02 August 2021*
Published: *06 September 2021*

Citation:
Xu Y, Xie L, Tang J, He X, Zhang Z, Chen Y, Zhou J, Gan B and Peng W (2021) Morchella importuna Flavones Improve Intestinal Integrity in Dextran Sulfate Sodium-Challenged Mice. Front. Microbiol. 12:742033. doi: 10.3389/fmicb.2021.742033

INTRODUCTION

The intestinal epithelial barrier is a single layer of cells lining the gut that comprises the apical cell membrane and intercellular tight junctions of intestinal epithelial cells (Ulluwishewa et al., 2011; Peterson and Artis, 2014). It acts as a selective barrier that allows the absorption of nutrient substances while inhibiting the translocation of luminal pathogens (Halpern and Denning, 2015;

Wang et al., 2015). Hence, treatments aimed at decreasing intestinal permeability contribute to improved health. Nowadays, dietary bioactive substances have been found to improve intestinal barrier function by strengthening the intestinal barrier, attenuating the inflammatory responses and modulating microbiota composition (Yang et al., 2012; Tian et al., 2019; Wan et al., 2020).

The *Morchella* mushroom, a type of edible ascomycetous mushroom, has a unique flavor, as well as a high nutritional value (Tietel and Masaphy, 2018). Interestingly, some bioactive compounds have been found in the *Morchella* mushroom fruiting body, such as polysaccharides, ergosterol derivatives, microthecin, and so on (Wang et al., 2019). Modern medical research demonstrated that the *Morchella* mushrooms confer antimicrobial, antioxidant, anti-inflammatory, and antitumor activities (Kim et al., 2011; Huang et al., 2012; Heleno et al., 2013). Therefore, the mature fruiting body of *Morchella* mushrooms have been used as a traditional herbal medicine in Asian countries, such as China, India, and Japan (Mau et al., 2004; Xiong et al., 2017). However, to the best of our knowledge, the ameliorative effects of *Morchella* mushrooms on intestinal barrier function have not been investigated and warrant exploration.

In the present work, the flavones from the fruiting bodies of *M. importuna* (MIF) were prepared. Then, the protective effects and possible mechanisms of MIF against the intestinal barrier injury *in vivo* were investigated using a sodium glucose sulfate [dextran sulfate sodium (DSS)]-challenged mouse model.

MATERIALS AND METHODS

Preparation of the Fruiting Bodies of *Morchella importuna*

In this study, the MIF were collected from the experimental field of Sichuan Academy of Agricultural Sciences (Chengdu, China). The MIF were dried at 37°C, and then 200 g of MIF were immersed in proportions of 1:20 (w/v) in ethanol at 60°C for 6 h. After centrifugation at 6,000 × g for 15 min, the sediment was discarded. Thereafter, the resulting MIF was dried at 60°C and stored at −20°C before use.

Preliminary Characterization of the Fruiting Bodies of *Morchella importuna*

The molecular weight distribution of MIF was determined by high-performance gel permeation chromatography (HP-GPC). The operating procedures were Waters 515, high-performance liquid chromatography equipped with laser detector (LS), and differential refractive index (DRI); Shodex OHpak series SB-806 gel chromatographic column (300 mm × 7.8 mm); column temperature 40°C ± 0.1°C. The mobile phase was 0.05 M NaH_2PO_4-NaH_2PO_4 buffer (pH 6.7, with 0.02% NaN_3). The flow rate was 0.5 ml/min. The loading amount was 500 μl. Then, 0.05 M NaH_2PO_4-NaH_2PO_4 buffer (pH 6.7, with 0.02% NaN_3) is used to dissolve polysaccharide standards with the molecular weights of 738, 5,800, 1.22×10^4, 2.37×10^4, 4.8×10^4, 1.0×10^5, 1.86×10^5, 3.8×10^5, and 8.53×10^5 g/mol, respectively. After being filtered with 0.45-μm membrane, the determination was performed according to the above chromatographic conditions. According to the molecular weight and retention time of standards, the standard curve was drawn, and then the molecular weight was calculated according to the retention time.

Animals, Management, and Diet

A total of 144 C57BL/6J mice (initial mass 18.02 ± 0.36 g), obtained from Dashuo Experimental Animal Co., Ltd. (Chengdu, China), were divided into four treatments with six pens per treatment (six mice per pen): (1) Control (fed a normal diet); (2) DSS treatment (fed a normal diet); (3) DSS treatment + 100 mg/kg MIF (LMIF; fed a normal diet + 100 mg/kg MIF); (4) DSS treatment + 200 mg/kg MIF (HMIF; fed a normal diet + 200 mg/kg MIF). On days 8–14, mice in the challenged groups were orally administered 3.5% DSS in drinking water, while other mice were administered normal saline (Bassaganya-Riera and Hontecillas, 2006). Moreover, all mice were individually caged under a controlled environment room.

Slaughter and Sample Collection

At the end of the experiment, after 12-h starvation and ether anesthesia, blood samples from six mice with the average body weight in each group were collected, centrifuged at 1,500 × g (15 min) to obtain serum, and then stored at −20°C. Subsequently, the same mice were sacrificed, about 2-cm segments of the colon were isolated, gently flushed with normal saline, and then fixed in paraformaldehyde solution (4%) for morphological analysis. Finally, about 5-cm colonic tissues were collected and stored at −80°C until analyses.

Serum Biochemical Analysis

The serum diamine oxidase (DAO) activity and D-lactate concentration were assessed using commercial kits purchased from Jiancheng Bioengineering Institute (Nanjing, China). All measurements were performed according to the manufacturer's instructions.

Intestinal Morphology Analysis

After a 48-h fixation, the colonic segments were dehydrated using a graded series of alcohol and cleaned with xylene, embedded in paraffin, cut into cross sections of 5-μm thickness, and then stained with H&E (Fang et al., 2017). Then, the villus height and crypt depth were measured, and the ratio of villus height to crypt depth (VCR) was calculated from the value obtained above.

Intestinal Cytokine Concentration Determinations

The colonic mucosa was homogenized with normal saline (1:9), and the homogenate was centrifuged at 1,500 × g (15 min) to attain supernatant. Then, the concentrations of interleukin-1β (IL-1β), IL-6, IL-10, tumor necrosis factor-α (TNF-α), and interferon-γ (IFN-γ) in the colonic mucosal supernatant were

assayed by ELISA kits (Zhuo Cai Biotechnology Co., Ltd., Shanghai, China).

Intestinal Antioxidant Capacity Measurements

Superoxide dismutase (SOD) activity, catalase (CAT) activity, malondialdehyde (MDA) content, and total antioxidant capacity (T-AOC) in the colonic homogenates were measured. Measurements were performed by the spectrophotometric method using commercially available kits (Nanjing Jiancheng Bioengineering Institute).

Intestinal Microbiota Analysis

Total gDNA from digesta samples was extracted using a Stool DNA Isolation Kit (Tiangen Biotech Co., Ltd., Beijing, China), following the manufacturer's directions. The genes of bacterial 16S rRNA in the region of V4 were amplified by using PCR with primers (515F/806R). The PCR products were subjected to electrophoresis on 2% agarose gel, and the mixed PCR products were purified with AxyPrep DNA Gel Extraction Kit (Axygen Biosciences, Union City, CA, United States) for sequencing on an Illumina MiSeq system. All 16S rRNA gene sequencing data were saved in the National Center for Biotechnology Information and can be accessed in the Short Read Archive under the accession number PRJNA679459.[1]

Quality filtering on the raw reads was performed under specific filtering conditions to obtain the high-quality clean reads according to the Cutadapt quality-controlled process (Martin, 2011). The reads were compared with the reference database using UCHIME algorithm (Edgar et al., 2011), to detect chimera sequences, and then removed to get the clean reads (Haas et al., 2011). Clustered into operational taxonomic units (OTUs) utilizing Uparse v7.0.1001 at 97% sequence similarity (Edgar, 2013). Species annotation was carried out on the OTU representative sequences. For colonic bacteria, α-diversity index was assessed using QIIME 1.7.0. Principal coordinate analysis (PCoA) tools in R language were used for PCoA.

Western Blot Assay

Protein samples were extracted from colonic tissues using lysis buffer (Beyotime Institute of Biotechnology, Shanghai, China). The lysates were centrifuged at 12,000 × g for 10 min at 4°C, and the supernatant was collected. A bicinchoninic acid (BCA) protein assay kit (Beyotime Institute of Biotechnology) was used to determine the protein concentration in the supernatant. Thereafter, 30 μg of protein extractions were separated by 10% sodium dodecyl sulfate (SDS)–polyacrylamide gel electrophoresis (PAGE) and then transferred to a polyvinyldifluoride (PVDF) membrane (Merck Millipore Ltd., Tullagreen, Ireland) using wet Trans-Blot System (Bio-Rad Laboratories, Inc., Hercules, CA, United States). After blocking with Tris-buffered saline Tween 20 (TBS/T) containing 5% bovine serum albumin (BSA) at room temperature for 1 h, the membranes were incubated with primary antibodies at 4°C overnight against phospho-Nrf2 (Sigma-Aldrich, St. Louis, MO, United States), Keap1 (Sigma-Aldrich), heme oxygenase-1 (HO-1; Sigma-Aldrich), NAD(P)H dehydrogenase (quinone 1) (NQO-1; Sigma-Aldrich), occludin (Sigma-Aldrich), claudin-1 (Proteintech Group, Inc., Wuhan, China), zonula occludens-1 (ZO-1; Sigma-Aldrich), ZO-2 (Sigma-Aldrich), Toll-like receptor 4 (TLR4; Proteintech Group, Inc.), MyD88 (Proteintech Group, Inc.), IL-1 receptor-associated kinase 1 (IRAK1; Proteintech Group, Inc.), TNF receptor-associated factor 6 (TRAF6; Proteintech Group, Inc.), phospho-NF-κB (Proteintech Group, Inc.), or β-actin (Proteintech Group, Inc.). The polyvinylidene fluoride (PVDF) membranes were washed thrice with TBS/T, then incubated with second antibodies at room temperature for 2 h, and washed thrice with TBS/T again. BeyoECL Moon (Beyotime Institute of Biotechnology) was used to visualize signals. The Image Lab software (Bio-Rad Laboratories, Inc.) was utilized to quantify protein abundance.

Statistical Analysis

Individual rat was used as the experimental unit, and all data were analyzed by SPSS 20.0 (SPSS, Inc., Chicago, IL, United States). Statistical differences between groups were determined by Student's *t*-test, while among groups, differences were determined by Tukey's multiple-range test. Results were presented as means ± standard deviations. Differences were taken to indicate significance when $p < 0.05$.

RESULTS

Molecular Weight and Its Distribution of *Morchella importuna* Flavones

From the results of HP-GPC detection, the mass average molar mass (Mw) of MIF was 6.666×10^5 g/mol, the number average Molecular Weight (Mn) was 6.118×10^5 g/mol, and the D value (Mw/Mn) was 1.09. The dispersity ratio was close to 1, and the molecular weight distribution was narrow, indicating that the MIF was relatively pure (**Table 1**).

TABLE 1 | Molecular weight and its distribution of *Morchella importuna* flavones.

Item	MIF
Mw, g/moL	6.666×10^5
Mn, g/moL	6.118×10^5
Mw/Mn	1.09
Molecular weight distribution, %	
500000.0-522000.0 g/moL	5.30
522000.0-558000.0 g/moL	44.80
558000.0-805000.0 g/moL	37.20
805000.0-1170000.0 g/moL	7.20
1170000.0-2012949.0 g/moL	5.60

MIF, fruiting bodies of M. importuna.

[1] http://www.ncbi.nlm.nih.gov/bioproject/679459

TABLE 2 | Effects of *Morchella importuna* flavones on the serum DAO activity and D-lactate concentration in DSS-challenged mice.

Item	Treatment†			
	CON	DSS	DSS + LMIF	DSS + HMIF
DAO, U/L	10.15 ± 3.33	15.86 ± 4.92*	11.15 ± 4.87	11.12 ± 2.98*
D-Lactate, pg/ml	14.91 ± 3.71	24.49 ± 5.28**	16.29 ± 3.84	11.72 ± 2.47**

*$p < 0.05$ or **$p < 0.01$.
†*CON, control; DSS, dextran sulfate sodium (DSS) treatment; DSS + LMIF, DSS treatment + 100 mg/kg fruiting bodies of M. importuna (MIF); DSS + HMIF, DSS treatment + 200 mg/kg MIF. DAO, diamine oxidase.*

Serum Indices

DSS challenge enhanced ($p < 0.05$) the DAO activity and increased the concentration of D-lactate in C57BL/6J mice (**Table 2**). Dietary 200 mg/kg MIF inclusion reduced ($p < 0.05$) the serum D-lactate concentration in DSS-challenged mice.

Intestinal Morphology

Relative to the control mice, DSS challenge was found to reduce ($p < 0.05$) the colonic villus height without affecting crypt depth and VCR (**Figure 1**). Between the DSS-challenged mice, 100 and 200 mg/kg MIF supplementation increased ($p < 0.05$) the colonic villus height, and 200 mg/kg MIF supplementation additionally increased colonic VCR.

Intestinal Antioxidant Capacity

According to **Table 3**, it is found that DSS challenge decreased ($p < 0.05$) the SOD, CAT, and T-AOC activities and increased the MDA content in the colon of C57BL/6J mice. Supplementation with 100 and 200 mg/kg MIF increased ($p < 0.05$) the colonic SOD and CAT activities in DSS-challenged mice.

Intestinal Cytokine Concentration

Dietary 200 mg/kg MIF ingestion reduced ($p < 0.05$) the contents of the IL-1β, TNF-α, and IFN-γ and increased ($p < 0.05$) the IL-10 content in colonic mucosa of DSS-challenged mice (**Table 4**). Moreover, 100 mg/kg MIF supplementation increased ($p < 0.05$) the colonic mucosal IL-10 concentration in DSS-challenged mice.

Tight Junction Protein Abundances

Figure 2 shows the effects of MIF on tight junction protein (occludin, claudin-1, ZO-1, and ZO-2) abundances in DSS-challenged mice. DSS challenge decreased ($p < 0.05$) the abundances of occludin, claudin-1, and ZO-1 proteins. Dietary supplementation with 100 and 200 mg/kg MIF elevated ($p < 0.05$) the abundance of claudin-1 protein, and 200 mg/kg MIF also increased ($p < 0.05$) the abundances of occludin and ZO-1 proteins in DSS-challenged mice.

Nrf2 Pathway-Related Protein Abundances

The differences in colonic Nrf2 pathway-related protein abundances among the four groups are shown in **Figure 3**. The colonic protein abundances of p-Nrf2 and HO-1 were lower in the DSS group ($p < 0.05$) than that in the control group. However, supplementation with 100 and 200 mg/kg MIF increased ($p < 0.05$) the colonic protein abundances of p-Nrf2 and HO-1 in DSS-challenged mice. Neither DSS nor MIF affected ($p > 0.05$) the Keap1 and NQO-1 protein abundances in C57BL/6J mice.

NF-κB Pathway-Related Protein Abundances

Figure 4 shows that the DSS challenge elevated ($p < 0.05$) the TLR4, MyD88, IRAK1, TRAF6, and p-NF-κB protein abundances, whereas supplementation with 200 mg/kg MIF reduced ($p < 0.05$) the TLR4, MyD88, IRAK1, TRAF6, and p-NF-κB p65 protein abundances in DSS-challenged mice. Moreover, 100 mg/kg MIF downregulated ($p < 0.05$) the TLR4 protein abundance in DSS-challenged mice.

Intestinal Microbial Diversity

According to **Table 5**, it is found that DSS treatment decreased ($p < 0.05$) the Shannon index and Simpson index of bacteria in C57BL/6J mice. Supplementation with 200 mg/kg MIF increased ($p < 0.05$) the Shannon index and Simpson index of bacteria in DSS-challenged mice. Neither DSS nor MIF affected ($p > 0.05$) the Chao1 index or abundance-based coverage estimators (ACE) index of bacteria in C57BL/6J mice.

As shown in **Figure 5**, the PCoA revealed that microbial community was significantly altered after DSS challenge or MIF supplementation, with an evident separation ($p < 0.05$) among the three groups.

Intestinal Microbiota Composition

The bacterial composition was assessed at different taxonomic levels (**Figure 6** and **Supplementary Table 1**). At the phylum level, the dominant bacterial groups were *Bacteroidetes*, *Firmicutes*, and *Proteobacteria*; these were followed by the bacteria from phyla *Verrucomicrobia*, *Fusobacteria*, *Actinobacteria*, *Deferribacteres*, *Tenericutes*, and *Melainabacteria*. DSS challenge decreased ($p < 0.05$) the abundances of *Bacteroidetes* and *Verrucomicrobia*, increased ($p < 0.05$) the abundances of *Firmicutes*, *Proteobacteria*, *Deferribacteres*, and *Melainabacteria*. However, 200 mg/kg MIF supplementation increased ($p < 0.05$) the abundances of *Proteobacteria*, *Deferribacteres*, and *Melainabacteria*.

DISCUSSION

Villus height, crypt depth, and VCR serve as criteria that reflect gross intestinal morphology (Liu et al., 2008; Qin et al., 2018). At present, the DSS challenge decreased colonic villus height, which suggests that DSS caused acute damage to intestinal mucosa. MIF supplementation increased colonic villus height and VCR, which implies that MIF improved intestinal structure. The maintenance of intestinal integrity primarily depends on the tight junctions between the enterocytes. Tight junctions are composed of several tight junction proteins, such as occludin and claudins, as well as cytoplasmic ZOs (Anderson et al., 1993).

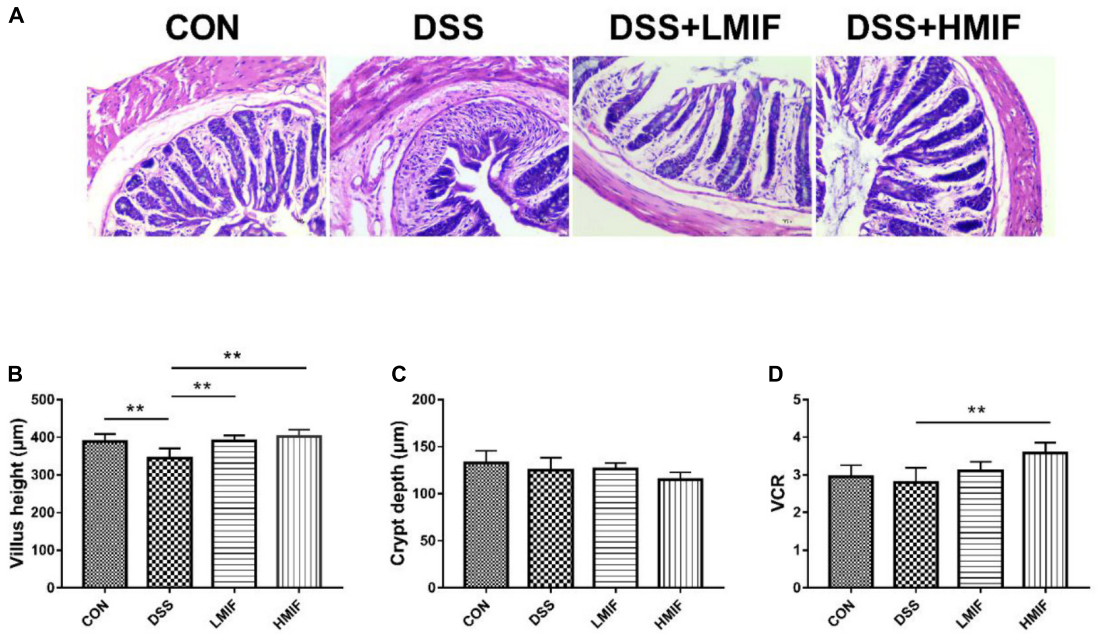

FIGURE 1 | Effects of *Morchella importuna* flavones on colonic morphologies in dextran sulfate sodium (DSS)-challenged mice. **(A)** Colonic morphological image; **(B)** villus height; **(C)** crypt depth; **(D)** ratio of villus height to crypt depth (VCR). CON, control; DSS, DSS treatment; LMIF, DSS treatment + 100 mg/kg fruiting bodies of *Morchella importuna* (MIF); HMIF, DSS treatment + 200 mg/kg MIF. $^{**}p < 0.01$.

TABLE 3 | Effects of *Morchella importuna* flavones on the colonic antioxidant capacity in DSS-challenged mice.

Item	Treatment†			
	CON	DSS	DSS + LMIF	DSS + HMIF
SOD, U/ml	145.20 ± 2.30	93.43 ± 4.69**	118.46 ± 5.54**	117.49 ± 2.37**
CAT, U/ml	89.34 ± 0.88	65.10 ± 4.16**	84.70 ± 3.26**	88.01 ± 1.53**
T-AOC, U/ml	10.49 ± 0.51	4.80 ± 0.60**	5.70 ± 0.35	4.67 ± 0.61
MDA, nmol/ml	3.59 ± 0.24	4.54 ± 0.32*	4.14 ± 0.27	4.08 ± 0.15

*$p < 0.05$ or **$p < 0.01$.
†*CON, control; DSS, dextran sulfate sodium (DSS) treatment; DSS + LMIF, DSS treatment + 100 mg/kg fruiting bodies of M. importuna (MIF); DSS + HMIF, DSS treatment + 200 mg/kg MIF. CAT, catalase; MDA, malondialdehyde; SOD, superoxide dismutase; T-AOC, total antioxidant capacity.*

TABLE 4 | Effects of *Morchella importuna* flavones on the colonic cytokine concentrations in DSS-challenged mice.

Item	Treatment†			
1.	CON	DSS	DSS + LMIF	DSS + HMIF
IL-1β, pg/ml	8.77 ± 1.09	15.02 ± 2.50**	12.51 ± 1.43	10.01 ± 1.34**
IL-6, pg/ml	11.30 ± 1.77	19.53 ± 4.64**	14.95 ± 3.26	13.45 ± 2.41*
IL-10, pg/ml	55.74 ± 5.24	38.70 ± 3.74**	50.49 ± 2.88**	53.79 ± 4.72**
TNF-α, pg/ml	83.07 ± 5.20	117.79 ± 7.30**	108.86 ± 7.36	107.51 ± 6.86*
IFN-γ, pg/ml	49.61 ± 5.33	77.37 ± 9.97**	68.91 ± 8.16	65.15 ± 7.65*

*$p < 0.05$ or **$p < 0.01$.
†*CON, control; DSS, dextran sulfate sodium (DSS) treatment; DSS + LMIF, DSS treatment + 100 mg/kg fruiting bodies of M. importuna (MIF); DSS + HMIF, DSS treatment + 200 mg/kg MIF. IFN, interferon; IL, interleukin; TNF, tumor necrosis factor.*

Of them, occludin and claudins are considered to be the major integral membrane proteins forming continuous tight junction strands (Furuse et al., 1993; Furuse et al., 1998). Here, we found that MIF supplementation increased the abundances of occludin, claudin-1, and ZO-1 proteins in the colon of DSS-challenged mice, indicating that MIF improved the intestinal barrier integrity. Furthermore, intestinal integrity can be assessed by many markers, such as DAO activity and D-lactate

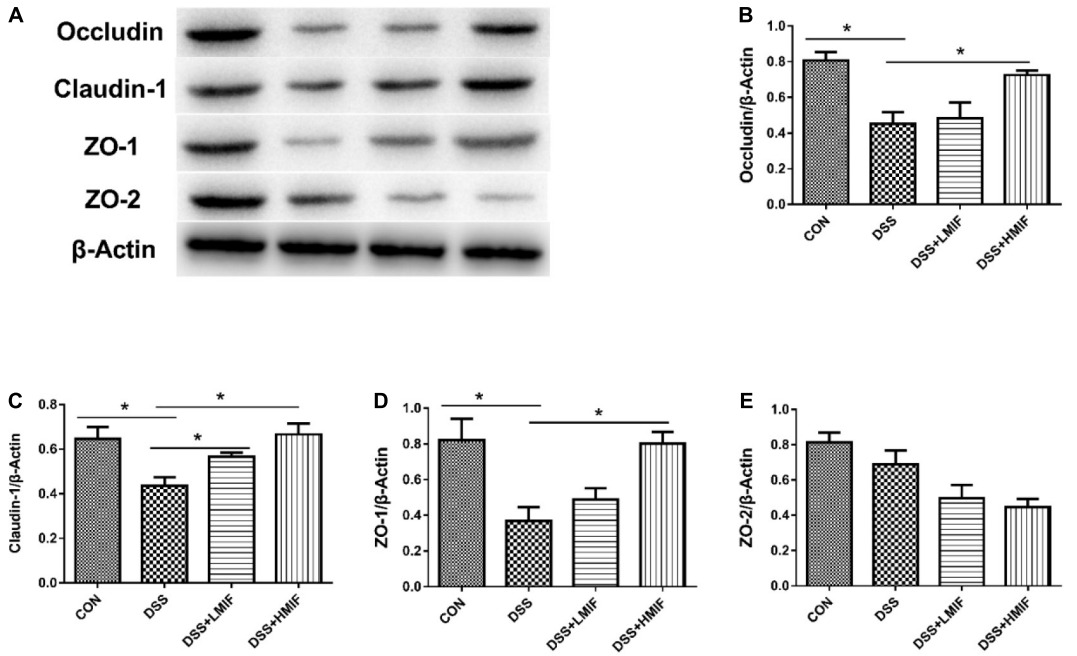

FIGURE 2 | Effects of *Morchella importuna* flavones on the abundances of the colonic tight junction proteins in dextran sulfate sodium (DSS)-challenged mice. **(A)** Representative Western blot picture; **(B)** occludin; **(C)** claudin-1; **(D)** zonula occludens-1 (ZO-1); **(E)** ZO-2. CON, control; DSS, DSS treatment; LMIF, DSS treatment + 100 mg/kg fruiting bodies of *Morchella importuna* (MIF); HMIF, DSS treatment + 200 mg/kg MIF. *$p < 0.05$.

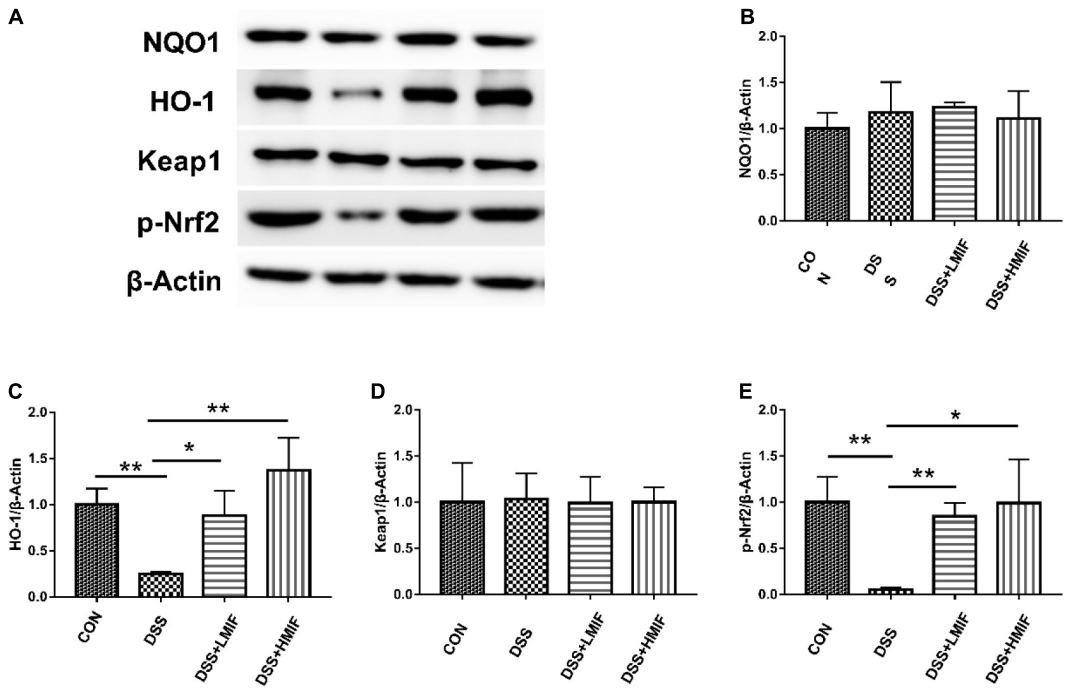

FIGURE 3 | Effects of *Morchella importuna* flavones on the abundances of the colonic Nrf2 signaling pathway-related proteins in dextran sulfate sodium (DSS)-challenged mice. **(A)** Representative Western blot picture; **(B)** NAD(P)H dehydrogenase (quinone 1) (NQO-1); **(C)** heme oxygenase-1 (HO-1); **(D)** Keap1; **(E)** p-Nrf2. CON, control; DSS, DSS treatment; LMIF, DSS treatment + 100 mg/kg fruiting bodies of *Morchella importuna* (MIF); HMIF, DSS treatment + 200 mg/kg MIF. *$p < 0.05$ or **$p < 0.01$.

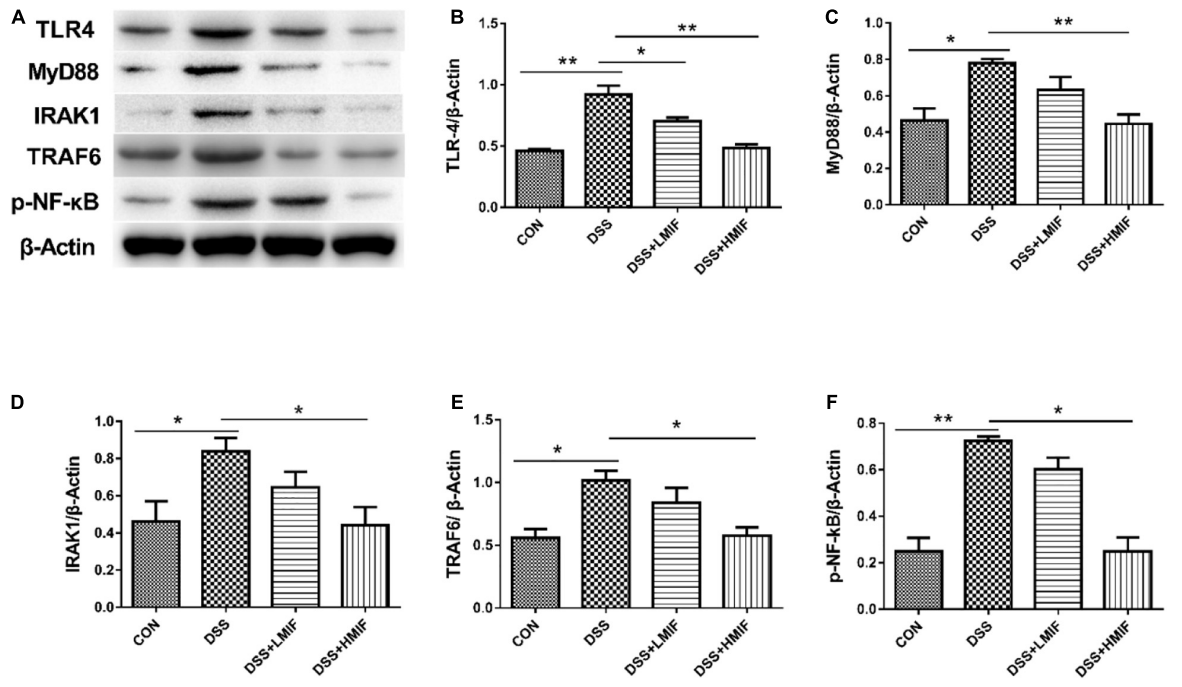

FIGURE 4 | Effects of *Morchella importuna* flavones on the abundances of the colonic Toll-like receptor 4 (TLR4) signaling pathway-related proteins in dextran sulfate sodium (DSS)-challenged mice. **(A)** Representative Western blot picture; **(B)** TLR4; **(C)** MyD88; **(D)** IL-1 receptor-associated kinase 1 (IRAK1); **(E)** TNF receptor-associated factor 6 (TRAF6); **(F)** p-NF-κB p65. CON, control; DSS, DSS treatment; LMIF, DSS treatment + 100 mg/kg fruiting bodies of *Morchella importuna* (MIF); HMIF, DSS treatment + 200 mg/kg MIF. $^{*}p < 0.05$ or $^{**}p < 0.01$.

TABLE 5 | Effects of ethanol extracts from *Morchella importuna* on the α-diversity indexes in the colon of DSS-challenged mice.

Item	Treatment†		
	CON	DSS	DSS + HMIF
Chao1 index	393.09 ± 30.64	371.89 ± 24.59	364.72 ± 12.33
ACE index	390.55 ± 23.95	374.08 ± 24.29	369.79 ± 13.76
Shannon index	6.27 ± 0.07	5.71 ± 0.20**	6.04 ± 0.04**
Simpson index	0.97 ± 0.00	0.94 ± 0.01**	0.96 ± 0.00**

$^{**}p < 0.01$.

†*CON, control; DSS, dextran sulfate sodium (DSS) treatment; DSS + HMIF, DSS treatment + 200 mg/kg fruiting bodies of M. importuna (MIF).*

concentration (Nielsen et al., 2011; Liu et al., 2012). Consistent with improved intestinal barrier function, MIF improved colonic barrier integrity in DSS-challenged mice, as evinced by decreased serum DAO activity and D-lactate concentration.

Intestinal antioxidant activity is closely related to intestinal health, which in turn is considered to be associated with intestinal structure (Jia et al., 2019). SOD and CAT are important antioxidant enzymes that can scavenge free radicals to defend against oxidative injury (Slavić et al., 2006; Lestaevel et al., 2009). We found lower SOD and CAT activities in DSS-challenged mice than in control mice, indicating that DSS challenge causes severe oxidative damage to the colon in mice. However, MIF attenuated the DSS-induced reduction of SOD and CAT activities in the colon, implying that MIF exerts a protective effect against intestinal oxidative damage caused by DSS challenge. The elevated antioxidant capacity was also supported by the expression of several critical antioxidant genes. Nrf2, one of the key transcription factors, plays a vital role in maintaining the activities of antioxidant enzymes (Cheng et al., 2015). The HO-1 is located downstream of the Nrf2 and acts as one of the key antioxidant enzymes (Han et al., 2017). In this study, MIF significantly elevated the protein levels of p-Nrf2 and HO-1 in the DSS-challenged mice, further indicating the antioxidant capacity of MIF in DSS-challenged mice. These results could determine that dietary MIF supplementation maintained the intestinal barrier function of mice under DSS challenge, to some extent, by enhancing intestinal antioxidant ability.

The unsettled balance between anti- and pro-inflammatory cytokines has been found to induce intestinal inflammatory injury in the DSS-challenged mice (Choi et al., 2017; Yin et al., 2020). In this study, MIF treatment inhibited inflammatory responses as evinced by decreasing pro-inflammatory cytokine (IL-1β, TNF-α, and IFN-γ) concentrations in the colon following DSS treatment. Contrary to the aforementioned cytokines, IL-10, as an anti-inflammatory cytokine, has been demonstrated to protect colonic inflammatory injury (Hasnain et al., 2013). Interestingly, MIF treatment also elevated the IL-10 concentration in the colon after DSS challenge. These results suggest that the beneficial effects of MIF against DSS-induced intestinal inflammatory injury were related to the regulation of the production of pro-inflammatory and anti-inflammatory cytokines. To elucidate the molecular

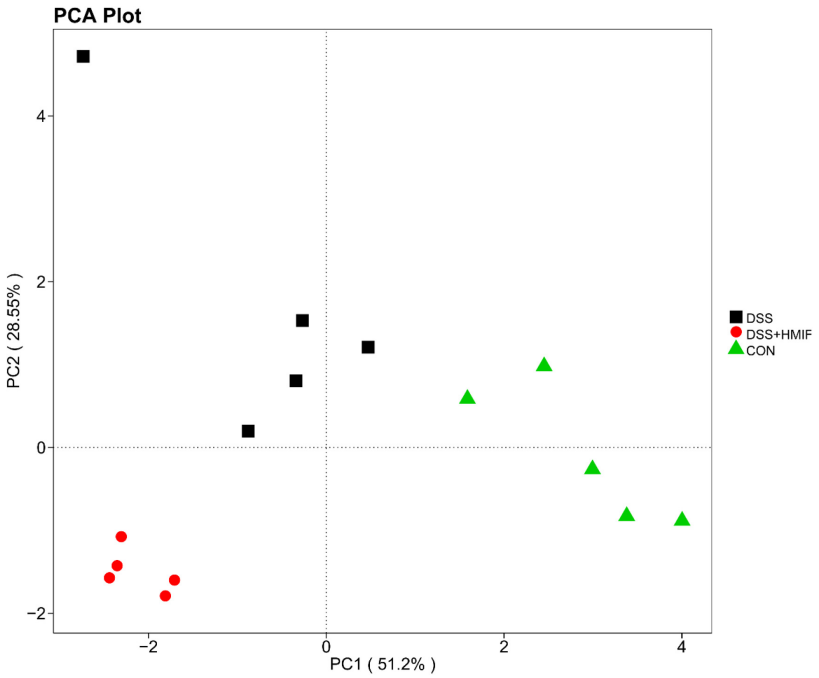

FIGURE 5 | Comparison of the colonic microbiota composition among the three groups. A principal coordinate analysis (PCoA) was used to visualize the weighted UniFrac distances of the fecal samples from the C57BL/6J mice. CON, control; DSS, dextran sulfate sodium (DSS) treatment; HMIF, DSS treatment + 200 mg/kg fruiting bodies of *Morchella importuna* (MIF).

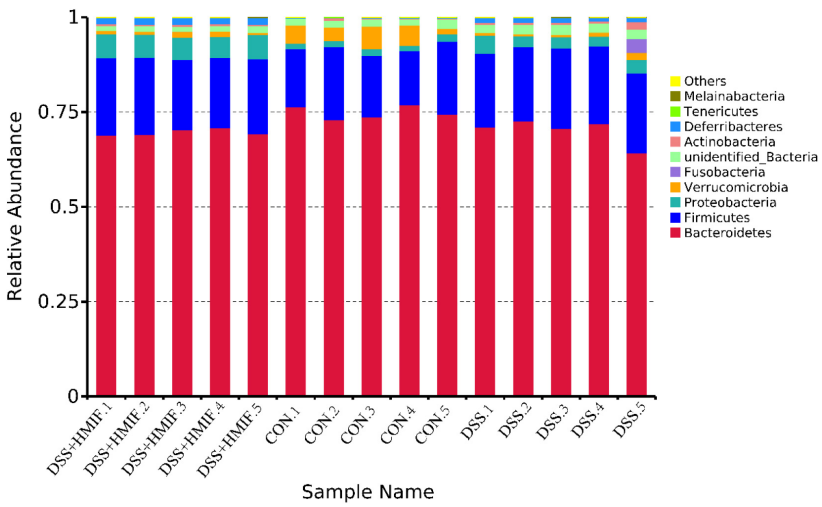

FIGURE 6 | Relative abundances of the dominant bacteria at phylum level in the colon of C57BL/6J mice among the three groups. CON, control; DSS, dextran sulfate sodium (DSS) treatment; HMIF, DSS treatment + 200 mg/kg fruiting bodies of *Morchella importuna* (MIF).

mechanisms by which MIF attenuates intestinal inflammatory responses, we investigated the TLR4 signaling pathway-related protein expression.

Activation of TLR4 signaling pathway plays an important role in defensive responses against invading pathogens *via* triggering the secretion of pro-inflammatory cytokines (Wang et al., 2017). However, the aberrant activation of TLR4 signaling pathway elicits collateral host intestinal injury (Coll and O'Neill, 2010). In the present study, we observed that colonic protein abundances of TLR4 and its downstream signals, such as MyD88, IRAK1, and TRAF6, were reduced in MIF-treated DSS-challenged mice. NF-κB is a critical nuclear transcription factor downstream of the TLR4 signaling pathway that regulates the production of pro-inflammatory cytokines (Sabroe et al., 2008). The inactivation of NF-κB has been proven to be able to alleviate the severity of intestinal inflammatory injury (Kang et al., 2017;

Wan et al., 2019). Here, the colonic protein abundance of p-NF-κB p65 in DSS-challenged mice was also decreased by MIF supplementation. These results suggest that MIF attenuates DSS-induced intestinal inflammatory injury *via* decreasing pro-inflammatory cytokine release through inhibiting the TLR4/NF-κB signaling pathway.

Although the exact pathogenesis of inflammatory bowel disease is complex, intestinal microbiota disorder is one of the most important observations (Zhai et al., 2019). As noted previously, the species, richness, and abundance of intestinal microbiota were markedly decreased in patients with inflammatory bowel disease (Zmora et al., 2019). In this study, we found that colonic microbiota in DSS-treated mice following MIF supplementation exhibit more diversity of evenness and richness than those in DSS-treated mice, as they have higher Shannon and Simpson indices. Low microbial diversity is often regarded as being associated with some infective intestinal disease, such as inflammatory bowel disease (Manichanh et al., 2006). Thus, the increase in microbial diversity induced by MIF may play a positive role in the colonic health of mice, which partly elucidates the alleviation of intestinal inflammatory injury in these mice. Furthermore, we found that MIF increased the abundances of *Proteobacteria*, *Deferribacteres*, and *Melainabacteria*, suggesting that these bacteria may play an essential role in MIF treatment of inflammatory bowel disease.

CONCLUSION

To summarize, our findings indicate that MIF have beneficial effects on modulating intestinal barrier function and microbiota in DSS-challenged mice. The reduced inflammatory factor production and enhanced antioxidant capacity caused by MIF may be associated with inhibited NF-κB signaling pathway and activated Nrf2 signaling pathway, respectively. These results offer a molecular basis for the potential contribution of MIF to the prevention of intestinal barrier injury.

DATA AVAILABILITY STATEMENT

The datasets presented in this study can be found in online repositories. The names of the repository/repositories and accession number(s) can be found in the article/ **Supplementary Material**.

ETHICS STATEMENT

The animal study was reviewed and approved by the Animal Care and Use Committee of Sichuan Academy of Agricultural Sciences (Chengdu, China).

AUTHOR CONTRIBUTIONS

BG and WP conceived this study. YX wrote the manuscript. LX, JT, XH, ZZ, YC, and JZ carried out the experiments and performed data analyses. All authors contributed to the article and approved the submitted version.

FUNDING

This study was financially supported by the special fund of Chengdu Local Finance (NASC2020AR06) and the Key Research and Development Project of Sichuan Science and Technology Plan (2021YFN0094).

SUPPLEMENTARY MATERIAL

The Supplementary Material for this article can be found online at: https://www.frontiersin.org/articles/10.3389/fmicb.2021.742033/full#supplementary-material

REFERENCES

Anderson, J. M., Balda, M. S., and Fanning, A. S. (1993). The structure and regulation of tight junctions. *Curr. Opin. Cell Biol.* 5, 772–778.

Bassaganya-Riera, J., and Hontecillas, R. (2006). CLA and n-3 PUFA differentially modulate clinical activity and colonic PPAR-responsive gene expression in a pig model of experimental IBD. *Clin. Nut.* 25, 454–465. doi: 10.1016/j.clnu.2005.12.008

Cheng, L., Jin, Z., Zhao, R., Ren, K., Deng, C., and Yu, S. (2015). Resveratrol attenuates inflammation and oxidative stress induced by myocardial ischemia-reperfusion injury: role of Nrf2/ARE pathway. *Int. J. Clin. Exp. Med.* 8:10420.

Choi, J. H., Chung, K. S., Jin, B. R., Cheon, S. Y., Nugroho, A., Roh, S. S., et al. (2017). Anti-inflammatory effects of an ethanol extract of Aster glehni via inhibition of NF-κB activation in mice with DSS-induced colitis. *Food Function* 8, 2611–2620. doi: 10.1039/c7fo00369b

Coll, R. C., and O'Neill, L. A. (2010). New insights into the regulation of signalling by toll-like receptors and nod-like receptors. *J. Innate Immunity* 2, 406–421. doi: 10.1159/000315469

Edgar, R. C. (2013). UPARSE: highly accurate OTU sequences from microbial amplicon reads. *Nat. Methods* 10, 996–998. doi: 10.1038/nmeth.2604

Edgar, R. C., Haas, B. J., Clemente, J. C., Quince, C., and Knight, R. (2011). UCHIME improves sensitivity and speed of chimera detection. *Bioinformatics* 27, 2194–2200. doi: 10.1093/bioinformatics/btr381

Fang, T., Wu, X., Cao, W., Jia, G., Zhao, H., Chen, X., et al. (2017). Effects of dietary fiber on the antioxidant capacity, immune status, and antioxidant-relative signaling molecular gene expression in rat organs. *RSC Adv.* 7, 19611–19620. doi: 10.1039/c7ra02464a

Furuse, M., Fujita, K., Hiiragi, T., Fujimoto, K., and Tsukita, S. (1998). Claudin-1 and-2: novel integral membrane proteins localizing at tight junctions with no sequence similarity to occludin. *J. Cell Biol.* 141, 1539–1550. doi: 10.1083/jcb.141.7.1539

Furuse, M., Hirase, T., Itoh, M., Nagafuchi, A., Yonemura, S., Tsukita, S., et al. (1993). Occludin: a novel integral membrane protein localizing at tight junctions. *J. Cell Biol.* 123, 1777–1788. doi: 10.1083/jcb.123.6.1777

Haas, B. J., Gevers, D., Earl, A. M., Feldgarden, M., Ward, D. V., Giannoukos, G., et al. (2011). Chimeric 16S rRNA sequence formation and detection in Sanger and 454-pyrosequenced PCR amplicons. *Genome Res.* 21, 494–504. doi: 10.1101/gr.112730.110

Halpern, M. D., and Denning, P. W. (2015). The role of intestinal epithelial barrier function in the development of NEC. *Tissue Barriers* 3:e1000707. doi: 10.1080/21688370.2014.1000707

Han, D., Chen, W., Gu, X., Shan, R., Zou, J., Liu, G., et al. (2017). Cytoprotective effect of chlorogenic acid against hydrogen peroxide-induced oxidative stress in MC3T3-E1 cells through PI3K/Akt-mediated Nrf2/HO-1 signaling pathway. *Oncotarget* 8:14680. doi: 10.18632/oncotarget.14747

Hasnain, S. Z., Tauro, S., Das, I., Tong, H., Chen, A. C. H., Jeffery, P. L., et al. (2013). IL-10 promotes production of intestinal mucus by suppressing protein misfolding and endoplasmic reticulum stress in goblet cells. *Gastroenterology* 144, 357–368.e359.

Heleno, S. A., Stojković, D., Barros, L., Glamočlija, J., Soković, M., Martins, A., et al. (2013). A comparative study of chemical composition, antioxidant and antimicrobial properties of Morchella esculenta (L.) Pers. from Portugal and Serbia. *Food Res. Int.* 51, 236–243. doi: 10.1016/j.foodres.2012.12.020

Huang, M., Zhang, S., Zhang, M., Ou, S., and Pan, Z. (2012). Effects of polysaccharides from morchella conica on nitric oxide production in lipopolysaccharide-treated macrophages. *Appl. Microbiol. Biotechnol.* 94, 763–771. doi: 10.1007/s00253-011-3711-7

Jia, Z., Wu, A., He, M., Zhang, L., Wang, C., and Chen, A. (2019). Metabolites of stable fly reduce diarrhea in mice by modulating the immune system, antioxidants, and composition of gut microbiota. *Microbial. Pathog.* 134:103557. doi: 10.1016/j.micpath.2019.103557

Kang, J. H., Choi, S., Jang, J. E., Ramalingam, P., Ko, Y. T., Kim, S. Y., et al. (2017). Wasabia japonica is a potential functional food to prevent colitis via inhibiting the NF-κB signaling pathway. *Food Function* 8, 2865–2874. doi: 10.1039/c7fo00576h

Kim, J. A., Lau, E., Tay, D., and De Blanco, E. J. C. (2011). Antioxidant and NF-κB inhibitory constituents isolated from *Morchella esculenta*. *Nat. Product Res.* 25, 1412–1417. doi: 10.1080/14786410802425746

Lestaevel, P., Romero, E., Dhieux, B., Soussan, H. B., Berradi, H., Dublineau, I., et al. (2009). Different pattern of brain pro-/anti-oxidant activity between depleted and enriched uranium in chronically exposed rats. *Toxicology* 258, 1–9. doi: 10.1016/j.tox.2008.12.021

Liu, Y., Chen, F., Odle, J., Lin, X., Jacobi, S. K., Zhu, H., et al. (2012). Fish oil enhances intestinal integrity and inhibits TLR4 and NOD2 signaling pathways in weaned pigs after LPS challenge. *J. Nut.* 142, 2017–2024.

Liu, Y., Huang, J., Hou, Y., Zhu, H., Zhao, S., Ding, B., et al. (2008). Dietary arginine supplementation alleviates intestinal mucosal disruption induced by *Escherichia coli* lipopolysaccharide in weaned pigs. *Br. J. Nut.* 100, 552–560. doi: 10.1017/s0007114508911612

Manichanh, C., Rigottier-Gois, L., Bonnaud, E., Gloux, K., Pelletier, E., Frangeul, L., et al. (2006). Reduced diversity of faecal microbiota in Crohn's disease revealed by a metagenomic approach. *Gut* 55, 205–211. doi: 10.1136/gut.2005.073817

Martin, M. (2011). Cutadapt removes adapter sequences from high-throughput sequencing reads. *EMBnet. J.* 17, 10–12. doi: 10.14806/ej.17.1.200

Mau, J. L., Chang, C. N., Huang, S. J., and Chen, C. C. (2004). Antioxidant properties of methanolic extracts from *Grifola frondosa*, *Morchella esculenta* and *Termitomyces albuminosus* mycelia. *Food Chem.* 87, 111–118. doi: 10.1016/j.foodchem.2003.10.026

Nielsen, C., Lindholt, J. S., Erlandsen, E. J., and Mortensen, F. V. (2011). D-lactate as a marker of venous-induced intestinal ischemia: an experimental study in pigs. *Int. J. Surg.* 9, 428–432. doi: 10.1016/j.ijsu.2011.04.004

Peterson, L. W., and Artis, D. (2014). Intestinal epithelial cells: regulators of barrier function and immune homeostasis. *Nat. Rev. Immunol.* 14, 141–153. doi: 10.1038/nri3608

Qin, Q., Xu, X., Wang, X., Wu, H., Zhu, H., Hou, Y., et al. (2018). Glutamate alleviates intestinal injury, maintains mTOR and suppresses TLR4 and NOD signaling pathways in weanling pigs challenged with lipopolysaccharide. *Sci. Rep.* 8, 1–10.

Sabroe, I., Parker, L., Dower, S., and Whyte, M. K. B. (2008). The role of TLR activation in inflammation. *J. Pathol.* 214, 126–135. doi: 10.1002/path.2264

Slavić, M., Slavić, M., Slavić, M., Appiah, I., Appiah, I., Appiah, I., et al. (2006). The anti-oxidative defence system in the isolated rat uterus during spontaneous rhythmic activity. *Acta Physiol. Hung.* 93, 335–339. doi: 10.1556/aphysiol.93.2006.4.9

Tian, S., Wang, J., Yu, H., Wang, J., and Zhu, W. Y. (2019). Changes in ileal microbial composition and microbial metabolism by an early-life galacto-oligosaccharides intervention in a neonatal porcine model. *Nutrients* 11:1753. doi: 10.3390/nu11081753

Tietel, Z., and Masaphy, S. (2018). True morels (Morchella)Nutritional and phytochemical composition, health benefits and flavor: a review. *Crit. Rev. Food Sci. Nut.* 58, 1888–1901. doi: 10.1080/10408398.2017.1285269

Ulluwishewa, D., Anderson, R. C., Mcnabb, W. C., Moughan, P. J., Wells, J. M., and Roy, N. C. (2011). Regulation of tight junction permeability by intestinal bacteria and dietary components. *J. Nut.* 141, 769–776. doi: 10.3945/jn.110.135657

Wan, J., Zhang, J., Chen, D., Yu, B., Huang, Z., Mao, X., et al. (2020). Alterations in intestinal microbiota by alginate oligosaccharide improve intestinal barrier integrity in weaned pigs. *J. Funct. Foods* 71:104040. doi: 10.1016/j.jff.2020.104040

Wan, J., Zhang, J., Wu, G., Chen, D., Yu, B., Huang, Z., et al. (2019). Amelioration of enterotoxigenic *Escherichia coli*-induced intestinal barrier disruption by low-molecular-weight chitosan in weaned pigs is related to suppressed intestinal inflammation and apoptosis. *Int. J. Mol. Sci.* 20:3485. doi: 10.3390/ijms20143485

Wang, B., Wu, G., Zhou, Z., Dai, Z., Sun, Y., Ji, Y., et al. (2015). Glutamine and intestinal barrier function. *Amino Acids* 47, 2143–2154.

Wang, H., Liu, Y., Shi, H., Wang, X., Zhu, H., Pi, D., et al. (2017). Aspartate attenuates intestinal injury and inhibits TLR4 and NODs/NF-κB and p38 signaling in weaned pigs after LPS challenge. *Eur. J. Nut.* 56, 1433–1443. doi: 10.1007/s00394-016-1189-x

Wang, J., Xiao, J., Geng, F., Li, X., Yu, J., Zhang, Y., et al. (2019). Metabolic and proteomic analysis of morel fruiting body (*Morchella importuna*). *J. Food Composit. Anal.* 76, 51–57. doi: 10.1016/j.jfca.2018.12.006

Xiong, C., Luo, Q., Huang, W. L., Li, Q., Chen, C., Chen, Z. Q., et al. (2017). The potential neuritogenic activity of aqueous extracts from *Morchella importuna* in rat pheochromocytoma cells. *Food Sci. Biotechnol.* 26, 1685–1692. doi: 10.1007/s10068-017-0224-x

Yang, C., Ferket, P. R., Hong, Q., Zhou, J., Cao, G., Zhou, L., et al. (2012). Effect of chito-oligosaccharide on growth performance, intestinal barrier function, intestinal morphology and cecal microflora in weaned pigs. *J. Animal Sci.* 90, 2671–2676. doi: 10.2527/jas.2011-4699

Yin, S., Yang, H., Tao, Y., Wei, S., Li, L., Liu, M., et al. (2020). Artesunate ameliorates DSS-induced ulcerative colitis by protecting intestinal barrier and inhibiting inflammatory response. *Inflammation* 43, 1–12.

Zhai, Z., Zhang, F., Cao, R., Ni, X., Xin, Z., Deng, J., et al. (2019). Cecropin a alleviates inflammation through modulating the gut microbiota of C57BL/6 mice with DSS-induced IBD. *Front. Microbiol.* 10:1595.

Zmora, N., Suez, J., and Elinav, E. (2019). You are what you eat: diet, health and the gut microbiota. *Nat. Rev. Gastroenterol. Hepatol.* 16, 35–56. doi: 10.1038/s41575-018-0061-2

Conflict of Interest: The authors declare that the research was conducted in the absence of any commercial or financial relationships that could be construed as a potential conflict of interest.

Publisher's Note: All claims expressed in this article are solely those of the authors and do not necessarily represent those of their affiliated organizations, or those of the publisher, the editors and the reviewers. Any product that may be evaluated in this article, or claim that may be made by its manufacturer, is not guaranteed or endorsed by the publisher.

frontiers in Microbiology

ORIGINAL RESEARCH
published: 26 October 2021
doi: 10.3389/fmicb.2021.725196

Mixture of Five Fermented Herbs (*Zhihuasi Tk*) Alters the Intestinal Microbiota and Promotes the Growth Performance in Piglets

*Yong Li[1†], Tiehu Sun[2†], Yuxuan Hong[3,4†], Tong Qiao[5], Yongsheng Wang[2], Wei Li[1], Shi Tang[1], Xin Yang[2], Jie Li[2], Xiaowen Li[5], Zutao Zhou[3,4] and Yuncai Xiao[3,4]**

[1]COFCO Feed Co., Ltd., Beijing, China, [2]COFCO Nutrition and Health Research Institute, Beijing, China, [3]College of Veterinary Medicine, Huazhong Agricultural University, Wuhan, China, [4]State Key Laboratory of Agricultural Microbiology, Huazhong Agricultural University, Wuhan, China, [5]Hubei Huada Real Science & Technology Co., Ltd., Wuhan, China

OPEN ACCESS

Edited by:
Fengjie Sun,
Georgia Gwinnett College,
United States

Reviewed by:
Tingjun Hu,
Guangxi University, China
Tao Wu,
Wuhan Polytechnic University, China

***Correspondence:**
Yuncai Xiao
xyc88@mail.hzau.edu.cn

[†]These authors have contributed equally to this work and share first authorship

Specialty section:
This article was submitted to Food Microbiology, a section of the journal Frontiers in Microbiology

Received: 15 June 2021
Accepted: 16 July 2021
Published: 26 October 2021

Citation:
Li Y, Sun T, Hong Y, Qiao T, Wang Y, Li W, Tang S, Yang X, Li J, Li X, Zhou Z and Xiao Y (2021) Mixture of Five Fermented Herbs (Zhihuasi Tk) Alters the Intestinal Microbiota and Promotes the Growth Performance in Piglets
Front. Microbiol. 12:725196.
doi: 10.3389/fmicb.2021.725196

To explore the feasibility of using fermented Chinese herbal mixture *Zhihuasi Tk* (*Z. Tk*) supplementation to increase the swine production, the protective effect of dietary supplementation with *Z. Tk* on the intestinal oxidative stress model and the regulation of both growth performance and intestinal microbiota of weaned piglets were investigated *in vitro*. Our results showed that the addition of *Z. Tk* increased the cell viability, prevented the decrease of glutathione peroxidase, and significantly increased the total antioxidant capacity and reduced the damage caused by H_2O_2 to the tight junction proteins of the porcine small intestinal epithelial cell line (IPEC-J2). Furthermore, weaned piglets supplemented with either 2 kg/ton zinc oxide (ZnO) or 4 kg/ton of *Z. Tk* in the diet increased body weight as well as average daily feed intake and daily gain, while the feed conversion rate and diarrhea rate decreased within 0–35 days. Results of the taxonomic structure of the intestinal microbiota showed that, in 21 days after weaning, the Firmicutes/Bacteroidetes ratio in experimental group was increased, while the abundance of beneficial bacteria such, as *Lactobacillus*, was increased by *Z. Tk*, showing inhibitory effect on pathogenic bacteria such as members of Proteobacteria. In summary, dietary supplementation with *Z. Tk* maintained the intestinal microbiota in a favorable state for the host to effectively reduce the abnormal changes in the intestinal microbial structure and improved growth performance of weaned piglets. Therefore, *Z. Tk* may potentially function as a substitute for ZnO in feed additives for weaned piglets in modern husbandry.

Keywords: weaned piglets, fermented Chinese herbal mixture, antioxidant, growth performance, intestinal microbiota

INTRODUCTION

In order to meet the production goals in the swine industry, piglets are generally weaned early prior to the establishment of a constant microbiota and a fully developed immune system (Odle et al., 1996). As one of the most traumatic stresses in a pig's life, weaning can disrupt the gut microbial environment and increase susceptibility to post-weaning diarrhea caused by

bacteria, ultimately leading to significant morbidity and mortality (Frydendahl, 2002; Campbell et al., 2013). To relieve the adverse effect of the anxiety on weaned piglets, effective strategies are needed to enhance gut health and improve the growth performance of weaned piglets while maintaining the standard of safety for consumers and farmer's productivity (Xu et al., 2018; Chen et al., 2020).

Zinc is an essential trace element for animals. Due to its high efficiency and appropriate price, zinc is commonly used in the form of ZnO in high doses (2,000–3,000 mg/kg diet) for weaned piglets as an alternative to antibiotics to prevent intestinal inflammation and increase body weight (Hu et al., 2012; Kociova et al., 2020). However, the large amount of zinc cannot be fully utilized by animals, causing severe environmental pollution (Kociova et al., 2020) and affect the intestinal microbiota by promoting the antimicrobial resistance (Bednorz et al., 2013; Rensing et al., 2018). Therefore, it is urgent to identify the safe alternatives of zinc to enhance the protection of both animals and environments (Liu et al., 2020).

Traditional Chinese medicine (TCM) commonly used in feed additives can not only effectively treat various types of medical disorders but also maintain general health and prevent disease in animals (Cao et al., 2015; Du et al., 2018; Li et al., 2019). Studies have shown that *Codonopsis pilosula*, as one of the traditional Chinese medicinal plants, has been used to effectively enhance immunity and improve microcirculation (Fu et al., 2018), while another popular medicinal herbal plant *Radix astragalus* has shown pharmaceutical effects on immunomodulation and anti-oxidation activation (Gong et al., 2018). It has been reported that the extract of *R. isatidis* showed the antioxidant and anti-inflammatory effects *in vitro* (Xiao et al., 2014). As the active ingredients of *Atractylodes macrocephala*, Atractylenolides contain the antioxidant and anti-inflammatory properties (Bailly, 2020). Studies have shown that *R. paeoniae alba* contains a large number of pharmacological properties including anti-inflammatory, antioxidation, improving immunity (Li et al., 2011; Su-Hong et al., 2015), and hepatoprotective effect (Zhao et al., 2020). It has been demonstrated that the mixture of herbal extracts contains an enhanced biological efficiency than a single extract because of the synergetic effects between the bioactive constituents of herbal mixture (Lan et al., 2017). Due to multiple pathogenic factors regulating many diseases, it is generally challenging to deal with these medical disorders. Furthermore, the functions of a single herbal medicine are often limited in treating these complicated diseases, incapable of efficiently addressing the multivariate conditions in patients. In the practice of traditional Chinese medicine, in order to achieve the enhanced therapeutic effect, several herbal medicines are commonly combined based on their medicinal properties to achieve the synergetic functions in treating the complicated diseases. To date, the explicit molecular mechanisms of herbal compatibility are still not fully elucidated. Studies have shown that the synergistic effects of herbal medicines are achieved by applying a pair of herbs with ingredients of similar therapeutic functions. For example, the active ingredients in one herbal medicine enhance the therapeutic effects of the ingredients in the other herbal medicine by regulating their absorption, distribution, metabolism, and excretion (Wang et al., 2012). Moreover, the inactive ingredients in the herbal medicines used individually become active used in combination (Wang et al., 2012). These results suggest that the therapeutic effects observed in our study are likely achieved by the combined application of these five herbal medicines.

The gut microbiota regulates physiological functions related to metabolism, biotransformation, and biosynthesis of biological ingredients (Krishnan et al., 2015; Kawai et al., 2018). Medical studies have demonstrated that microbial regulation may play an important role in the treatment of TCMs (Xu et al., 2015; Tong et al., 2018). For example, the gut microbiota may enhance the bioavailability and therapeutic effects of TCMs by regulating their transformation and absorption from the intestine into the blood, indicating that TCMs function depending on specific components of the gut microbiota (Zhang et al., 2020). Furthermore, TCMs may alter the taxonomic structure and metabolic production of the gut microbiota. For example, studies have shown that TCMs change the relative abundance of the gut microbiota at various taxonomic levels (Wei et al., 2018; Chen et al., 2018b). Therefore, it is highly speculated that the therapeutic efficiency of TCMs are, at least partially, attributed to the alteration in the gut microbiota.

A type of TCM called *Zhihuasi Tk* (*Z. Tk*) is a mixture of five well-known Chinese herbal medicines, including *Codonopsis pilosula* (Dangshen), Radix astragalus (Huangqi), R. isatidis (Banlangen), R. paeoniae alba (Baishao), and Atractylodes macrocephala (Baizhu), fermented first with probiotics and then dried and crushed. The purpose of microbial fermentation is usually to decompose or convert undesired substances into compatible materials, ultimately enhancing the product properties by increasing the amount of biologically effective compounds (Ugural and Akyol, 2020). Furthermore, the fermentation is revealed to strengthen the antioxidant effects of some plants (Kusznierewicz et al., 2008; Ugural and Akyol, 2020). For example, fermentation increases the content of phenolic in some plant products (Đorđević et al., 2010), and it is reported that the polyphenols are positively correlated with the antioxidant activities in medicinal herbs (Shan et al., 2005). Recently, the Chinese herbs have attracted growing attention as feed additives in animal production. However, studies on the effects of Chinese herbs on weaned piglets are sparse. The main purpose of this study was to explore the protective effect of *Z. Tk* on the oxidative damage of the epithelial cell barrier and to investigate the potential effect of this feed additive on improving the intestinal microbiota and the growth performance of weaned piglets.

Abbreviations: Z. Tk, Fermented Chinese herbal mixture *Zhihuasi Tk*; ZnO, Zinc oxide; TCM, Traditional Chinese medicine; IPEC-J2, The porcine small intestinal epithelial cell line; GSH-Px, Glutathione peroxidase; T-AOC, Total antioxidant capacity; BW, Body weight; ADG, Average daily gain; ADFI, Average daily feed intake; FCR, Feed conversion rate; F/B, Ratio of Firmicutes/Bacteroidetes.

MATERIALS AND METHODS

Preparation of *Zhihuasi Tk* Extracts

The *Zhihuasi Tk* (*Z. Tk*) is a mixed combination of five commonly used TCMs with different proportions including *Codonopsis pilosula* (20%), *Radix astragalus* (30%), *R. isatidis* (15%), *R. paeoniae alba* (25%), and *Atractylodes macrocephalae* (10%). The mixture was infiltrated in water to 50% moisture, heated to 80°C for 1 h, and then cooled to 37°C. Three species of probiotics (*Bacillus subtilis*, *Enterococcus faecalis*, and *Saccharomyces cerevisiae*) were simultaneously added into the processed Chinese herbal mixture, which was fermented for 72 h, then dried, and crushed into powder. We selected the fermentation based on multi-strain probiotics, instead of a single-strain probiotics, due to the more comprehensive effects of multiple bacteria and enzymes, providing higher fermentation efficiency and richer fermentation products, in particular with the medicinal fungi and probiotics. The three species of probiotics (i.e., *Bacillus subtilis*, *Enterococcus faecalis*, and *Saccharomyces cerevisiae*) used in our study are commonly applied in the fermentation of Chinese herbal medicines with sound probiotic properties (Li et al., 2020).

To investigate the effects of *Z. Tk* on the porcine small intestinal epithelial cell line (IPEC-J2), a total of 10 g of *Z. Tk* powder were submerged into 200 μl 100°C sterilized ultrapure water and incubated for 30 min in a water bath of 100°C. The large debris in the supernatant was filtered using a 300-mesh filter and then centrifuged for 30 min at 100 *g* to remove the small debris. Then, the supernatant was filtered with a 100-mesh cell sieve and used for cell culture.

IPEC-J2 Cell Culture

The IPEC-J2 cell lines were provided by the College of Veterinary Medicine, Huazhong Agricultural University. These cells were maintained in the Dulbecco's Modified Eagle Medium/Nutrient Mixture F-12, containing 10% fetal bovine serum and 1% penicillin–streptomycin (Gibco BRL Co., Ltd., United States), and cultured in an incubator with constant temperature (37°C) and atmosphere of 5% CO_2. The medium was replaced every 3 days. Then, the cells were subcultured with 0.05% trypsin (Gibco BRL Co., Ltd., United States). The monolayers of cells were collected after 3 days of incubation for further experiments.

IPEC-J2 Cell Proliferation

The IPEC-J2 cells grown at logarithmic phase were treated with 0.1% trypsin to prepare a single cell suspension and then seeded in a 96-well cell culture plate. The number of seeding was 1×10^4 cells/well and cultivated for 24 h in an incubator (37°C) with constant concentration of CO_2 (5%). Then, the medium was discarded, the wells were washed with sterile PBS, added with medium containing 0, 1, 5, 10, 50, 100, 200, 500, 800, and 1,000 μM/L H_2O_2, respectively, and cultured for 24 h (six replicate wells per group). For each well, the culture medium was discarded, added with 100 μl of medium containing 10% Cell Counting Kit-8 (Biosharp, China), and incubated for 2 h at 37°C. The OD_{450} value was measured with a microplate reader. The concentration of H_2O_2 applied in the subsequent experiments was determined based on its reduction of cell viability by 50% with the cells treated with H_2O_2 for 24 h to establish a cellular oxidative stress model. For the treatment of *Z. Tk*, the cells were treated with the medium containing 1×10^{-2}, 5×10^{-3}, 1×10^{-3}, 5×10^{-4}, 1×10^{-4}, and 5×10^{-5} dilutions of *Z. Tk* extracts for 3 h, then added 100 μl of medium containing 10% Cell Counting Kit-8 (Biosharp, China), incubated at 37°C for 2 h, and the OD_{450} values were measured with a microplate reader.

Cellular Antioxidant Assay

Based on different treatments, the IPEC-J2 cells were separated into four groups, including the control group, the H_2O_2 oxidative stress group (treated with H_2O_2 for 24 h), the *Z. Tk* group (treated with *Z. Tk* for 3 h), and the *Z. Tk* + H_2O_2 group (treated with *Z. Tk* for 3 h and then H_2O_2 for 24 h) with each group containing three replicate wells and cultivated for 24 h. The cell culture fluid was collected to detect the total antioxidant capacity (T-AOC) and measure the content of glutathione peroxidase (GSH-Px) using the total antioxidant capacity test kit (Shanghai Biyuntian Biotechnology Company, Shanghai, China) and the glutathione peroxidase test kit (Shanghai Biyuntian Biotechnology Company, Shanghai, China) following the manufacturer's instructions, respectively. The total RNA was extracted using the Total RNA Kit (R6812, U.S. Omega Bio-Tek Company) and used to synthesize cDNA using the FastKing reverse transcription kit (KR118-02, Beijing Tiangen Biological Co., Ltd., Beijing, China). The expressions of three genes (*ZO-1*, *occludin*, and *claudin*) encoding the tight junction proteins in IPEC-2 cells were determined using qPCR method with the primers shown in **Table 1**.

Laboratory Animals

Our study was performed in accordance with the Guide for the Care and Use of Laboratory Animals Monitoring Committee of Hubei Province, China with the protocols approved by the Committee on the Ethics of Animal Experiments of the College of Veterinary Medicine, Huazhong Agricultural University (No. HZAUSW-2020-0001).

A total of 135 healthy Duroc × Landrace × Yorkshine hybrid (Du Changda) weaned boars (weaned at 23 days of age) were selected and evenly divided into three groups based on their body weight (BW) with each group of nine replicates and five piglets per replicate. The negative control (NC) group was fed with basal diet, the positive control (PC) group was fed with basal diet plus 2 kg/ton zinc oxide (ZnO), and the experimental group was fed with the basal diet plus 4 kg/ton of *Z. Tk*. The pharmacological dose of 2 kg/ton to feed the weaned piglets as a positive control was based on a previous study (Wang et al., 2019). Results of our preliminary experiments using the concentrations of 1 kg/ton, 2 kg/ton, and 4 kg/ton showed that 4 kg/ton generated the highest economic benefit. Therefore, we used 4 kg/ton as the concentration of *Z. Tk* in our experiments. No animals were fed with antibiotics. The nutrient levels of crude protein, calcium, and total phosphorus

TABLE 1 | Primer sequences for genes amplified in this study. F, forward primer; R, reverse primer.

Gene	Primer sequence (5′-3′)	Amplified fragment (bp)
ß-*Actin*	F: TGCGGGACATCAAGGAGAAG R: AGTTGAAGGTGGTCTCGTGG	92
claudin	F: GGCCCTTACCTTTCGCCTGA R: GCCTCAGGGCTTGGTGTTCT	99
occludin	F: ATCAACAAAGGCAACTCT R: GCAGCAGCCATGTACTCT	74
ZO-1	F: GCCTCAGGGCTTGGTGTTCT R: GGCCCTTACCTTTCGCCTGA	87

in the diets of each group were consistent and in accordance with both the NRC (2012) and the Chinese Pig Feeding Standard (2004). The detailed feed formula and the nutritional levels were shown in **Supplementary Tables S1 and S2**, respectively.

The experiments were carried out at the experimental base of the Feed Research Institute of the Chinese Academy of Agricultural Sciences for a total of 35 days. A fully enclosed pig house was adopted with the temperature (24~26°C), humidity, ventilation intensity, and the carbon dioxide and ammonia concentrations in the house automatically controlled. The piglets were raised in pens each of 1.5 m × 1.5 m in size equipped with slatted plastic spray floor, adjustable stainless steel troughs, and nipple drinkers. Animals were fed with pellets and were free to eat and drink.

Growth Performance

On days 0, 7, 21, and 35, the weaned piglets and feed were weighed to calculate the growth indices, including average daily gain (ADG), average daily feed intake (ADFI), and feed conversion rate (FCR) as follows: ADG = (end weight − initial weight)/days of experiment, ADFI = (feed amount provided during the test period − the remaining amount of feed during the test period)/days of experiment, and FCR = average daily feed intake/average daily gain of weight.

For the first 3 weeks, the condition of diarrhea of piglets was recorded twice a day to calculate the diarrhea rate based on the diarrhea score of each group of piglets. Specifically, 0 point was scored based on the cylindrical shaped soft stools, mild to moderate diarrhea (showing irregular loose stools with high water content) was scored as 1 point, and severe diarrhea characterized as having liquid, irregular, and watery loose stools was scored as 2 points. The diarrhea rate was calculated as the (number of piglets with diarrhea)/(number of piglets tested × total days) × 100%.

Sample Collection, DNA Extraction, and Sequencing

On days 21 and 35, the feces of the piglets with the same ear size were collected from nin replicates of the three groups by rectal massage. The samples were immediately divided into the cryopreservation tubes and kept in liquid nitrogen tank (−196°C) for storage.

The total genomic DNA from fecal samples of the weaned piglets was extracted based on CTAB method (Ahrens, 1992), examined by 1% agarose gel electrophoresis, and diluted to 1 ng/μl with sterile water. PCR amplification of the V3–V4 region of the bacterial 16S rRNA gene was performed with the forward primer 341F (5′-CCTAYGGGRBGCASCAG-3′) and the reverse primer 806R (5′-GGACTACHVGGGTWTCTAAT-3′) with barcodes. PCR reactions contained 15 μl of Phusion® High-Fidelity PCR Master Mix (New England Biolabs), ~10 ng template DNA, and 2 μM of both forward and reverse primers. PCR procedures were as follows: initial denaturation at 98°C for 1 min, followed by 30 cycles of "denaturation at 98°C for 10 s, annealing at 50°C for 30 s, and elongation at 72°C for 30 s" with the final extension of 5 min at 72°C. The PCR products mixed with the same volume of 1X loading buffer (containing SYBR green) were detected using electrophoresis on 2% agarose gel. Then, the mixture of PCR products of equidensity ratios was purified with Qiagen Gel Extraction Kit (Qiagen, Germany).

Libraries for high-throughput sequencing were constructed using the TruSeq® DNA PCR-Free Sample Preparation Kit (Illumina, United States) following manufacturer's protocols with index codes added. The quality of the sequencing libraries was evaluated by the Qubit@ 2.0 Fluorometer (Thermo Scientific) and Agilent Bioanalyzer 2,100 system (Agilent Technologies, United States). Samples with PCR amplified fragment size and PCR product volume not meeting the requirements for library construction were eliminated; samples with QC30 > 90% were selected for further analysis. The library was sequenced on an Illumina next-generation sequencing platform NovaSeq to generate the 250 bp paired-end reads. Furthermore, to avoid the inclusion of inappropriate genomic data to interfere the reliability of subsequent analyses, the results of the relative abundance and beta diversity analysis were used to eliminate samples showing significant differences within the group.

Sequencing Data Analysis

Paired-end reads were aligned to samples based on their unique barcodes with the barcode and primer sequences removed. The reads were merged using FLASH V1.2.7 (Magoč and Salzberg, 2011). The high-quality clean reads were obtained by filtering the raw reads using the QIIME V1.9.1 with filtering conditions set as previously reported (Caporaso et al., 2010). The final set of effective reads was obtained by comparing the clean reads with the reference database SILVA using the UCHIME algorithm (Edgar et al., 2011) to remove the chimera sequences (Haas et al., 2011).

Sequences with ≥ 97% similarity were assigned to the same Operational Taxonomic Units (OTUs) using Uparse v7.0.1001 (Edgar, 2013). Further annotation was performed on the representative sequence of each OTU screened using the SSUrRNA database (Wang et al., 2007) of SILVA (Quast et al., 2013) using the Mothur algorithm with the threshold set at 0.8–1.0. Taxonomic rank and the microbial composition of each sample at seven ranks of classification (i.e., kingdom, phylum, class, order, family, genus, and species) were obtained

to evaluate the difference between groups using T-test. Multiple sequence alignment was performed based on the MUSCLE Version 3.8.31 (Edgar, 2004) to investigate the phylogenetic relationship among OTUs and the variations of the abundant taxa in different samples and groups. The normalization of the abundance of OTUs was performed prior to the subsequent analyses of alpha diversity and beta diversity of the gut microbiota.

The complexity of species diversity was evaluated by generating alpha diversity indices, including the observed-species, the Chao1 estimator, and the Shannon index using QIIME Version 1.7.0 with the results (i.e., the dilution curve, the species accumulation curve, and the rank abundance curve) displayed with R software Version 2.15.3, which was also used to draw the dilution curve, the rank abundance curve, and the species accumulation curve. The Wilcox test in R software was used to analyze the difference of the alpha diversity indices between groups.

Beta diversity analyses on both weighted and unweighted UniFrac were conducted to evaluate the differences of samples in species complexity using QIIME Version 1.9.1. The principal coordinate analysis (PCoA) was performed to evaluate the principal coordinates and visualize the multidimensional data. A distance matrix of weighted or unweighted UniFrac among samples was generated to establish a new set of orthogonal coordinates, with the maximum variation factor demonstrated by the first principal coordinate, the second maximum variation factor by the second principal coordinate, and so on. The results of the PCoA analysis were displayed by WGCNA, stat, and ggplot2 packages in R software Version 2.15.3. The unweighted pair-group method with arithmetic means (UPGMA) analysis was performed based on the average linkage as a type of hierarchical clustering method to explain the distance matrix by QIIME Version 1.9.1.

Statistical Analyses

Statistical analyses were performed using SPSS for Windows, version 22 (SPSS, Inc., Chicago, IL, United States). Graphs were generated using GraphPad Prism 5 software (GraphPad, Inc., California, United States). The data were presented as the mean ± standard error of the mean (SEM) with the significance levels for all analyses set as $p < 0.05$ (*) and $p < 0.01$ (**).

RESULTS

Effects of H_2O_2 and *Z. Tk* on Cell Viability of IPEC-J2

The oxidative stress model of IPEC-J2 cells was established by the induction of H_2O_2. Results showed that the cell viability was significantly reduced under the treatment of 100 μM H_2O_2, while the IPEC-J2 cell viability was reduced to below 50% treated by H_2O_2 of 500–1,000 μM for 24 h in comparison to the control group (**Figure 1A**). Therefore, the concentration of 500 μM was chosen as the optimal content of H_2O_2 for the following experiments.

Results of the effect of *Z. Tk* on the viability of IPEC-J2 cells showed that both the high concentration of *Z. Tk* extract (i.e., 1×10^{-2}) and longer incubation time inhibited cell proliferation (**Figure 1B**), while low concentrations of *Z. Tk* extract (e.g., 5×10^{-4} and 1×10^{-4}) stimulated cells and significantly increased cell viability. Specifically, the cell viability was significantly improved by the stimulation of 3 h of all three dilutions of *Z. Tk* (i.e., 1×10^{-3}, 5×10^{-4}, and 1×10^{-4}), with the dilution of 5×10^{-4} achieving the highest cell viability. Therefore, the dilution of 5×10^{-4} of *Z. Tk* and stimulation time for 3 h were selected for subsequent experiments.

Antioxidant Effect of *Z. Tk*

Results of the protective effects of *Z. Tk* on the IPEC-J2 cells under oxidative stress showed that after H_2O_2 stimulation, the content of GSH-Px in the supernatant of IPEC-J2 cells was decreased significantly in comparison to that of the control group, while the treatment of both *Z. Tk* and H_2O_2 significantly reduced the detrimental effect of H_2O_2, indicating that *Z. Tk* could protect the epithelium of the small intestine to prevent the decrease of GSH-Px (**Figure 2A**). Furthermore, the *Z. Tk* significantly improved the T-AOC of IPEC-J2 cells (**Figure 2B**). The expressions of three genes (*ZO-1*, *occludin*, and *claudin*) encoding the tight junction proteins were significantly reduced in IPEC-J2 cells treated with H_2O_2 in comparison to the control group, while *Z. Tk* significantly increased the expression of

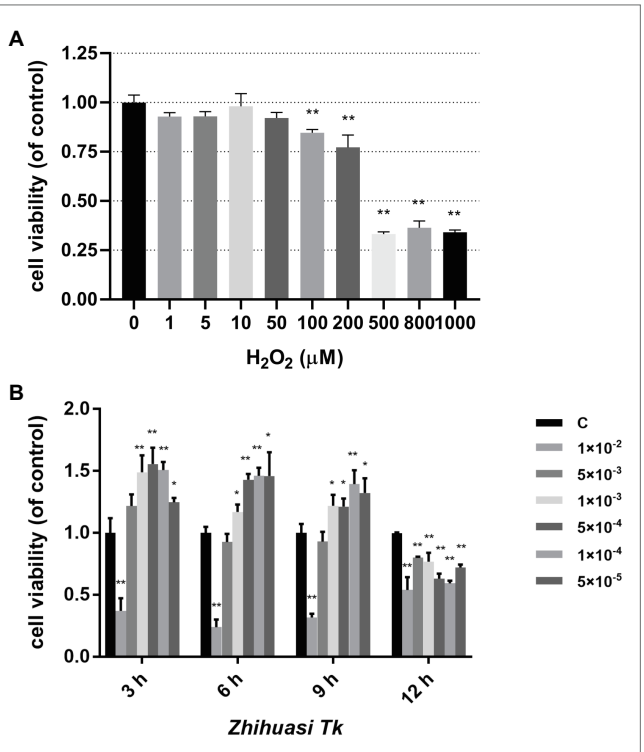

FIGURE 1 | Effects of H_2O_2 **(A)** and *Z. Tk* **(B)** of different concentrations on the viability of IPEC-J2 cells treated with different times. Symbols "*" and "**" indicate the significant differences compared with the control group set at the values of *p* of 0.05 and 0.01, respectively.

these genes, alleviating the detrimental effects of H_2O_2 on the tight junction proteins (**Figure 2C**). It was noted that the herbal extracts and H_2O_2 were not mixed throughout the entire process of treatment "*Z. Tk* + H_2O_2" group.

Growth Performance of Piglets

The results of growth performance in the piglets are shown in **Table 2**. The initial weights of the weaned piglets remained the same among the three groups of animals. On days 21 and 35, the BW of the experimental group was significantly higher than that of the NC group ($p < 0.05$). On day 35, the BW increased on average by 17.31 and 13.77% in the experimental and PC groups, respectively, compared with the NC group, although the difference was not statistically significant in PC group. In 1–7, 8–21, and 1–35 days, the experimental group showed significantly higher ADG than that of the NC group ($p < 0.05$). In 35 days, the ADG of both the PC and experimental groups increased by 20.53 and 25.65%, respectively, in comparison to the NC group. Compared with the NC group, both the experimental and the PC groups showed increased trend of the ADFI and decreased trend of diarrhea rate in 1–35 days although the

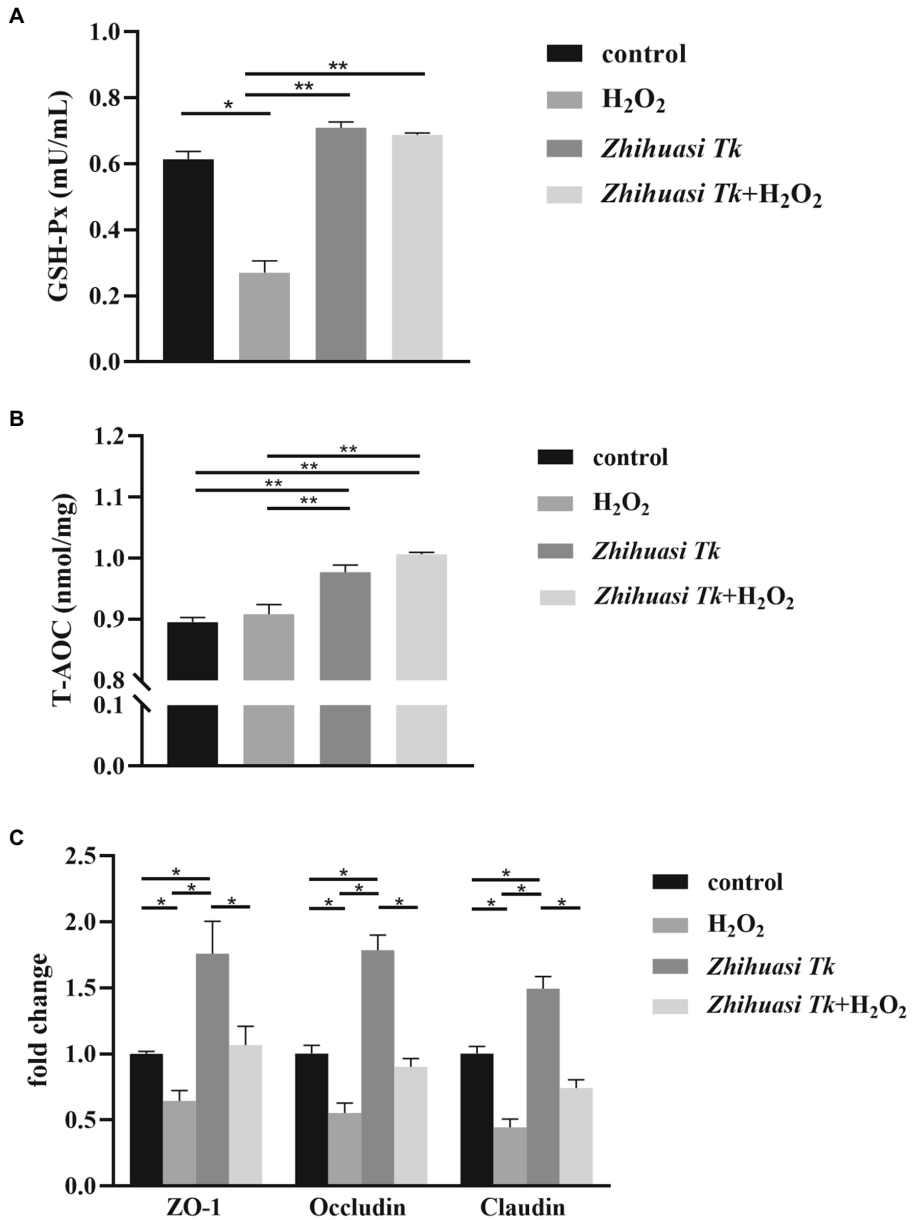

FIGURE 2 | Protective effects of *Z. Tk* on IPEC-J2 cells under oxidative stress as indicated by the content of GSH-Px **(A)**, the T-AOC **(B)** in the supernatant of IPEC-J2 cells, and the expression of genes (i.e., *ZO-1*, *occluding*, and *claudin*) encoding the tight junction proteins in IPEC-J2 cells **(C)**. Symbols "*" and "**" indicate the significant differences set at the values of *p* of 0.05 and 0.01, respectively.

difference was not statistically significant. Both the experimental group ($p < 0.05$) and PC group ($p < 0.01$) showed significantly decreased FCR at 1–35 days, compared to the NC group.

Effect of *Z. Tk* on the Diversity of the Intestinal Microbiota of Weaned Piglets

To further explore the effects of *Z. Tk* on the intestinal microbiota of weaned piglets, the V3-V4 regions of the 16S rRNA gene were sequenced based on the genomic DNA extracted from feces of the weaned piglets. A total of 2,991,714 clean reads were obtained after screening and splicing of the raw reads with an average of 55,402 ± 835 reads per sample and an average length of 414 bp per read (**Supplementary Table S3**).

The representative sequences of OTUs were obtained based on the clustered clean reads with 97% similarity. The rarefaction curve of each sample was generally flat, suggesting that the depth of sequencing was sufficient to cover all species in the sample (**Supplementary Figure S1**). Alpha diversity analyses were conducted based on the OTUs to determine three alpha diversity parameters, including the observed-species to show the observed OTUs (**Figure 3A**), the Chao1 index to estimate the community richness (**Figure 3B**), and the Shannon's diversity index to evaluate the community diversity indices (**Figure 3C**).

TABLE 2 | Growth performance in three groups of weaned piglets at different times.

	Negative control group	Positive control group	Test group
BW (kg)			
1 d	7.43 ± 0.45	7.46 ± 0.37	7.46 ± 0.37
7 d	9.27 ± 0.50	10.12 ± 0.52	10.29 ± 0.56
21 d	14.23 ± 0.85^{a}	16.32 ± 0.77^{ab}	16.89 ± 0.72^{b}
35 d	21.14 ± 1.14^{a}	24.05 ± 0.80^{ab}	24.80 ± 1.12^{b}
ADG (g/d)			
1–7 d	262.90 ± 19.92^{A}	379.21 ± 25.89^{B}	404.65 ± 28.69^{B}
8–21 d	354.31 ± 27.30^{a}	438.49 ± 23.44^{b}	462.91 ± 26.66^{b}
22–35 d	493.53 ± 37.61	552.23 ± 17.83	565.18 ± 31.71
1–35 d	391.71 ± 22.69^{a}	472.13 ± 14.65^{b}	492.17 ± 24.01^{b}
ADFI (g/d)			
1–7 d	427.73 ± 20.31	478.21 ± 22.97	465.48 ± 25.29
8–21 d	527.42 ± 37.23	596.90 ± 30.87	614.75 ± 36.64
22–35 d	810.66 ± 44.08	883.56 ± 30.00	953.38 ± 65.27
1–35 d	620.78 ± 32.55	687.83 ± 27.65	720.35 ± 44.60
FCR			
1–7 d	1.70 ± 0.15^{Aa}	1.29 ± 0.07^{ABb}	1.16 ± 0.04^{Bab}
8–21 d	1.51 ± 0.07	1.36 ± 0.03	1.34 ± 0.06
22–35 d	1.65 ± 0.05	1.61 ± 0.05	1.69 ± 0.06
1–35 d	1.59 ± 0.04^{Aa}	1.45 ± 0.02^{Bab}	1.46 ± 0.03^{ABb}
Diarrhea rate (%)			
1–7 d	11.38 ± 4.91	8.16 ± 3.83	6.786 ± 2.22
8–14 d	11.16 ± 5.13	7.41 ± 3.76	6.65 ± 1.72
15–21 d	10.63 ± 3.43	4.11 ± 2.69	4.64 ± 2.47
1–21 d	6.93 ± 2.45	4.29 ± 2.02	3.96 ± 1.28

BW, body weight; ADG, average daily gain; ADFI, average daily feed intake; FCR, feed conversion rate. Superscript letters a and b and superscript letters A and B in the same row indicate significant differences at p < 0.05 and p < 0.01, respectively.

Result revealed no significant difference in Shannon diversity among the NC, PC, and experimental groups on either day 21 or day 35 ($p > 0.05$), while the NC group on day 35 showed significantly lower Shannon's diversity index than that on day 21 ($p < 0.01$). For the community richness comparison, no significant difference was revealed in the number of observed species (OTUs) and estimated community richness (Chao1 index) among the NC, PC, and experimental groups on either day 21 or 35 ($p > 0.05$), while the observed-species ($p < 0.01$) and the Chao1 indices ($p < 0.05$) in the PC group changed significantly between days 21 and 35. Compared with the 21-day-old piglets, the community richness and the observed-species of PC group decreased significantly on day 35.

The effects of *Z. Tk* on the intestinal microflora profile of weaned piglets were further investigated using the PCoA based on weighted UniFrac of OTUs (**Figure 4A**). Results showed that in 21 days, the experimental group was relatively separated from the NC and PC groups on the PCoA scatter plot. In 35 days, no clear separation was observed among the three groups of animals, indicating the similarities among the three groups of gut microbiota. The UPGMA clustering tree based on weighted UniFrac showed that the six groups of fecal microbial communities were revealed on two branches corresponding to the ages (i.e., 21 and 35 days) of the piglets (**Figure 4B**). In 21 days, the microbial community in the feces of the NC group was closely related to that of the PC group. This result was consistent with that revealed by the PCoA. In 35 days, the NC and experimental groups were clustered into the same branch. The close relationship between the PC and NC groups indicated that *Z. Tk* significantly altered the composition of the intestinal microbiota of weaned piglets in their early weaning phases.

Effects of *Z. Tk* on the Taxonomic Composition of the Intestinal Microbiota in Weaned Piglets

The taxa with relative high abundance in the three groups of piglets were analyzed to characterize the changes of the composition in the gut microbiota. The intestinal bacterial composition of each of the three groups of piglets was categorized at the phylum level (**Figure 5A**). Firmicutes and Bacteroidetes were the two most abundant bacterial phyla in all groups of piglets. Among the top five abundant phyla (**Figure 5B**), the relative abundance of Firmicutes in the experimental group was significantly increased compared with that of the NC group ($p < 0.05$) in 21 days, while the relative abundance of Actinobacteriota was increased and other three phyla (i.e., Bacteroidota, Proteobacteria, and Euryarchaeota) was decreased in the experimental group compared to those of the NC group ($p > 0.05$). In comparison with the NC group, the relative abundance of three phyla (i.e., Firmicutes, Proteobacteria, and Actinobacteriota) in the PC group showed an increasing trend, while the relative abundance of the other two phyla (i.e., Bacteroidota and Euryarchaeota) showed a decreasing trend. At the age of 35 days, no significant difference was revealed in the bacterial composition among the three groups of intestinal microbiota. However, the relative abundance of Firmicutes and

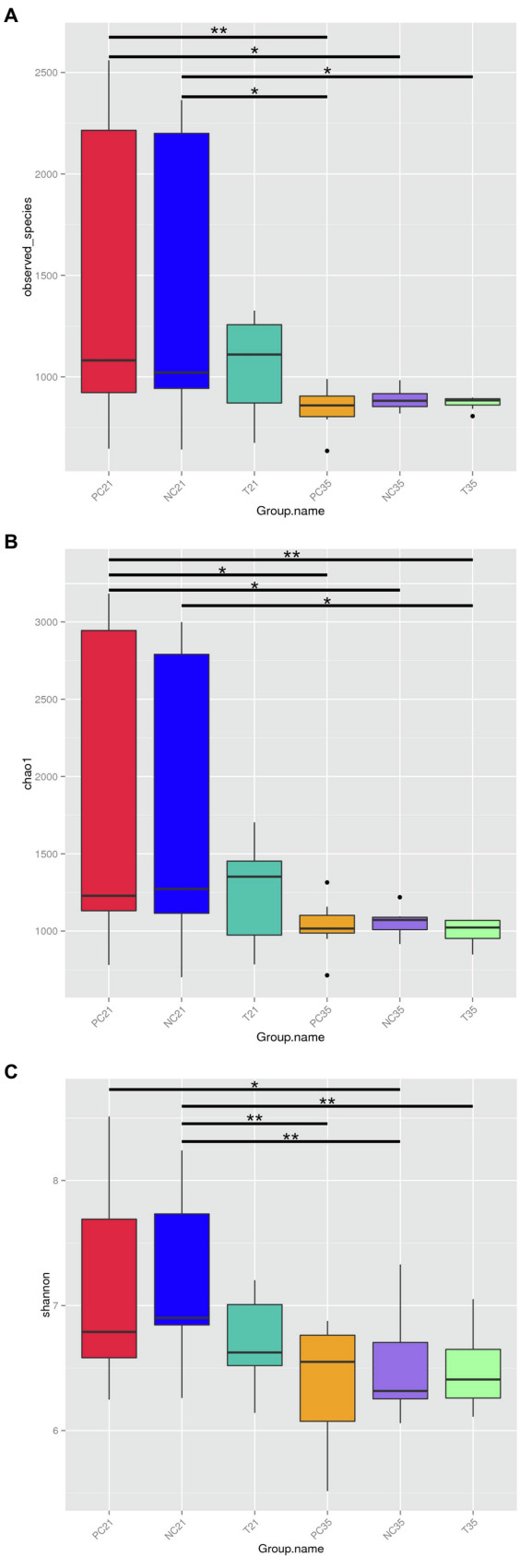

(Continued)

FIGURE 3 | Effects of *Z. Tk* and ZnO on the intestinal microbiota diversity in weaned piglets in 21 and 35 days based on alpha diversity parameters of observed species **(A)**, Chao1 index **(B)**, and the Shannon index **(C)**. Symbols "*" and "**" indicate significant differences at $p < 0.05$ and $p < 0.01$, respectively. Each of the nine samples is selected from each of the three groups of piglets, i.e., the positive control (PC), the negative control (NC), and the test groups, on days 21 and 35, respectively.

Actinobacteriota in the experimental group increased compared with that of the NC group. Proteobacteria and Euryarchaeota showed increased relative abundance in the PC group compared with the NC group, and the relative abundance of Bacteroidota in the experimental and PC groups decreased in comparison to the NC group. On day 21, the gut microbiota of the experimental group was characterized by an increased Firmicutes/Bacteroidetes ratio (F/B) in comparison to those of the PC and NC groups ($p < 0.05$; **Figure 5C**). On day 35, the difference in F/B of the three groups was not significantly different.

The effects of *Z. Tk* on the fecal microbiota in the three groups of weaned piglets were further evaluated based on the top 30 genera with the highest relative abundance (**Figure 6**). The results showed that at the genus level, the taxonomic structure of the intestinal microbiota of weaned piglets altered with ages and was impacted by both *Z. Tk* and zinc oxide (ZnO). On day 21, the PC group showed increased relative abundance in five genera (i.e., *Clostridium_sensu_stricto_1*, *Terrisporobacter*, *Succinivibrio*, *Olsenella*, and *Agathobacter*) and decreased relative abundance in other six genera (i.e., *Prevotella*, *Lactobacillus*, *Sarcina*, *Methanobrevibacter*, *Megasphaera*, and *Treponema*). In the experimental group, five genera (*Prevotella*, *Clostridium_sensu_stricto_1*, *Methanobrevibacter*, *Treponema*, and *Rikenellaceae_RC9_gut_group*) showed decreased relative abundance, while other five genera (*Lactobacillus*, *Sarcina*, *Terrisporobacter*, *Olsenella*, and *Agathobacter*) showed increased relative abundance compared to that of the NC group. On day 35, the proportions of abundant bacteria in the three groups of piglets altered evidently. For example, three genera (i.e., *Clostridium_sensu_stricto_1*, *Methanobrevibacter*, and *Succinivibrio*) in the PC group showed increased relative abundance, while seven genera (*Prevotella*, *Lactobacillus*, *Sarcina*, *Megasphaera*, *Treponema*, *Rikenellaceae_RC9_obacter group,* and *Agathellaceae_RC9_obacter*) showed decreased relative abundance, compared with that of the NC group. In the test group, seven genera (*Prevotella*, *Clostridium_sensu_stricto_1*, *Lactobacillus*, *Sarcina*, *Methanobrevibacter*, *Terrisporobacter*, and *Olsenella*) and four genera (*Megasphaera*, *Treponema*, *Rikenellaceae_RC9_gut_group*, and *Agathobacter*) showed increased and decreased relative abundance, respectively, in comparison to that of the NC group.

DISCUSSION

Chinese herbal feed additives have recently gained increasing attention due to their caability of enhancing growth performance by nourshing a healthy gut ecosystem in pigs. Furthermore, the feed additives of plant resources improve both the activity of digestive enzymes in the gastrointestinal

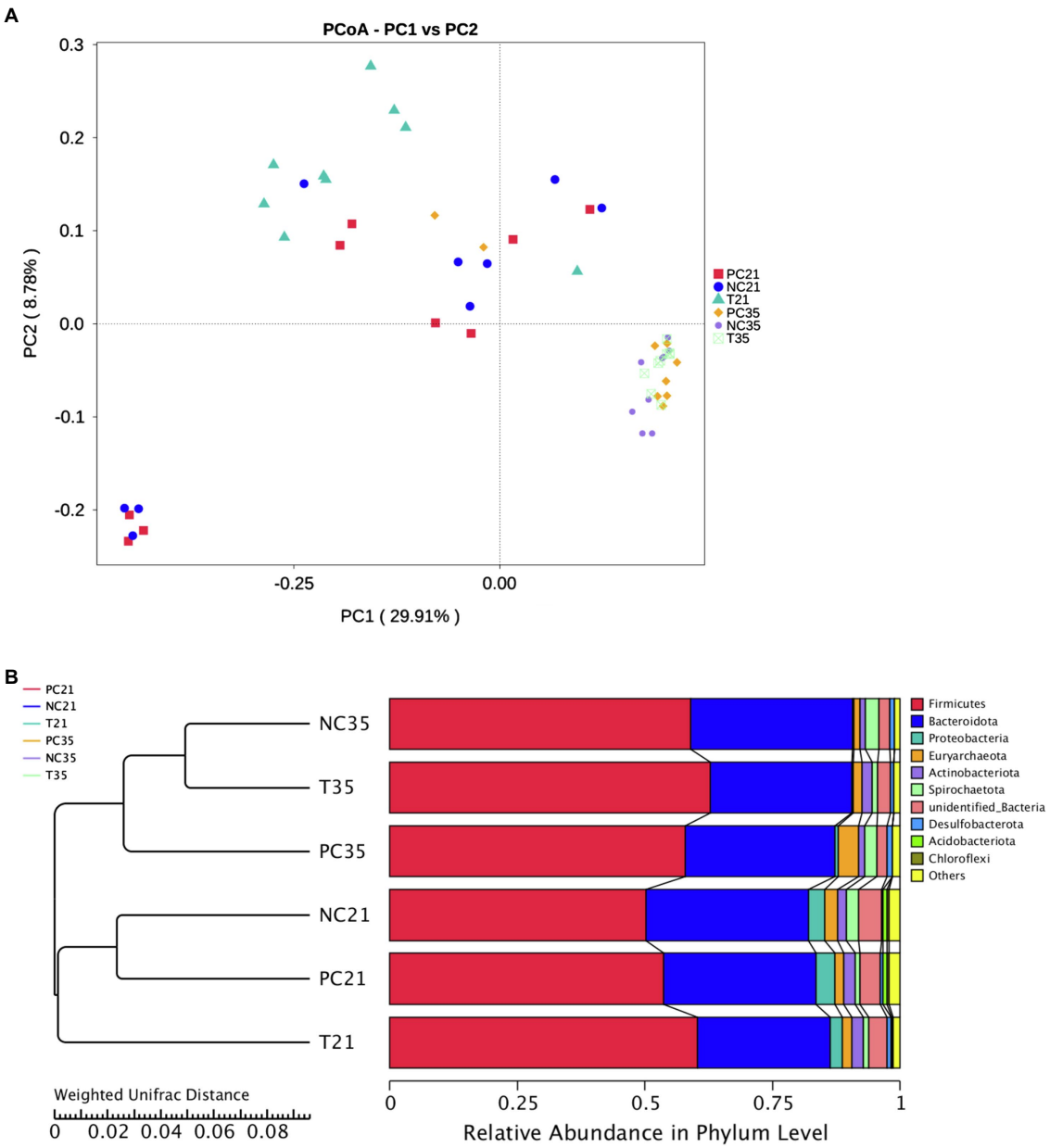

FIGURE 4 | Effects of *Z. Tk* and ZnO on the intestinal microbial diversity in weaned piglets in 21 and 35 days based on beta diversity analyses of principal coordinate analysis **(A)** and UPGMA clustering analysis **(B)** based on weighted UniFrac. Each of the nine samples is selected from each of the three groups of piglets, i.e., the positive control (PC), the negative control (NC), and the test groups, on days 21 and 35, respectively.

tract and the nutrient absorption in pigs (Zhou et al., 2015). Chinese herbal medicines are generally the most economical and labor-effective additives due to their convenient preparation and low cost (Lin et al., 2020). The effect of the fermented herbal additive mixture *Z. Tk* containing *Codonopsis pilosula*, *Radix astragalus*, *R. isatidis*, *R. paeoniae alba*, and *Atractylodes macrocephala* on pig production is unclear. Our study was designed to investigate the effects of *Z. Tk* on the antioxidant capacity, growth performance, and intestinal microbiota of weaned piglets.

Studies have shown that the five herbs used in the mixture in our study contain various types of ingredients with strong antioxidant effects. Specifically, the pectic polysaccharides in *Codonopsis pilosula* could significantly ameliorate the cellular damage caused by H_2O_2 treatment and increase the activity of antioxidant enzymes (Zou et al., 2020b). Similarly, the main biologically active components of *Radix astragalus* (e.g., polysaccharides, astragaloside, flavonoids, and saponins) have been revealed to show antioxidant effects (Gong et al., 2018). It has been reported that extracts of *R. astragalus* can decrease

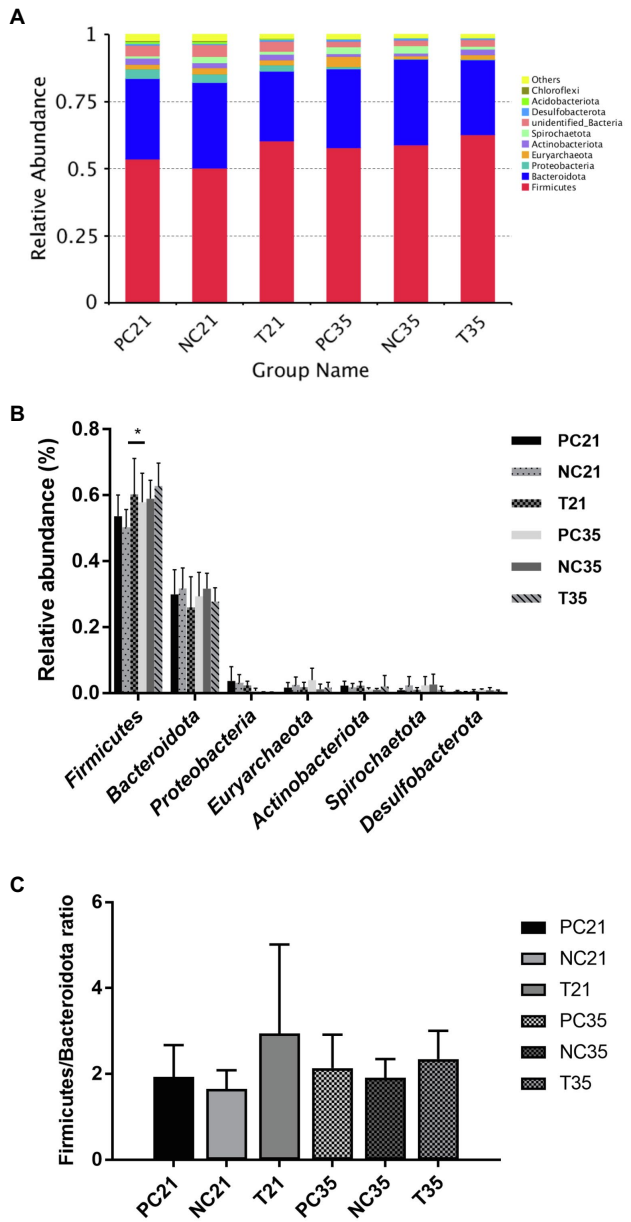

FIGURE 5 | Effects of *Z. Tk* and ZnO on the intestinal microbiota structure at the phylum level in weaned piglets characterized by the taxonomic distributions of the microbial communities in feces at phylum level **(A)**, the top five relatively abundant bacterial phyla detected in fecal samples **(B)**, and the Firmicutes/Bacteroidetes ratio (F/B; **C**). Symbol "*" indicates the significant difference set at the values of p of 0.05. Each of the nine samples is selected from each of the three groups of piglets, i.e., the positive control (PC), the negative control (NC), and the test groups, on days 21 and 35, respectively.

the inflammatory response induced by lipopolysaccharide in *Escherichia coli*, while decreasing the release of reactive oxygen species (ROS) and increasing the activation of nuclear factor and the expression of antioxidant cytoprotective factors in cells (Adesso et al., 2018). As the other ingredient in the mixture of *Z. Tk*, *Radix isatidis* is well-known for its broad antiviral activities and antioxidant properties. For example, it was reported that the proteins in *R isatidis* could eliminate the damage of free radicals, showing a strong antioxidant effect *in vivo* (Xiao et al., 2019). Furthermore, ingredients, such as white peony polyphenols, isolated from *R. paeoniae alba* (Zhou et al., 2019) and atractylenolides isolated from *Atractylodes macrocephalae* (Bailly, 2020) are also effective antioxidants. Studies have shown that polysaccharides from *Codonopsis pilosula* can protect the intestinal mucosal immune barrier, potentially maintaining the intestinal microbiota by stimulating the growth of *Lactobacillus* (Fu et al., 2018). The combination of total polysaccharides of *Radix astragalus* and *C. pilosula* was applied to treat 2.5% dextran sulfate sodium induced acute colitis in mice to restore the structure of the intestinal microbiota, increasing the level of *Bacteroidetes* and decreasing the levels of *Firmicutes* and *Proteobacteria* (Tang et al., 2021). The antiviral activities of *R. isatidis* mostly depend on the water-soluble active ingredients, e.g., amino acids, nucleosides, and sulfur-containing alkaloids, to eradicate pathogenic viruses and regulate the immune system (Zhou and Zhang, 2013). Furthermore, the main chemical components of *R. isatidis* (i.e., syringic acid, 2-amino-benzoic acid, and salicylic acid) have shown strong antibacterial activities against the growth of *Escherichia coli*, *Staphylococcus aureus*, and *Shigella dysenteriae* (Kong et al., 2008a,b). Studies have shown that the effective ingredients in *R. paeoniae alba* include paeoniflorin, tannin, and paeonol (Yan et al., 2018). As the most abundant compound reported in *R. paeoniae rubra*, paeoniflorin has been shown strong anti-inflammatory, hepatoprotective, and neuroprotective effects (Yan et al., 2018), displaying an inhibitory effect on biofilm formation of carbapenem-resistant *Klebsiella pneumoniae* (Qian et al., 2020). The sesquiterpenoids, polyacetylenes, and polysaccharides are the most abundant bioactive constituents in *Atractylodes macrocephalae*, which has been traditionally used to treat gastrointestinal hypofunction due to its potential functions of invigorating the spleen and adjusting disordered intestinal microbiota (Zhu et al., 2018). In rat models with disrupted intestinal microbiota, an administration of polysaccharides in *A. macrocephalae* significantly improved the rat vigor and body weight, promoting the ability of intestinal bacteria to digest sugars (Wang et al., 2014). These results suggest that the biologically active ingredients of the five traditional Chinese medicines mixed in *Z. Tk* are of significant importance for adjusting the function of gastrointestinal tract, affecting the structure of the intestinal microbiota, and reducing diarrhea caused by weaning stress in the weaned piglets.

Antioxidant Effect of *Z. Tk*

Weaning stress causes several health problems (e.g., diarrhea, growth restriction, and intestinal dysfunction) in piglets, as the animals are rapidly forced to adjust to the nutritional, immunological, and psychological changes (Cao et al., 2018). Furthermore, weaning stress disrupts free-radical metabolism and antioxidative system, causing severe oxidative stress in animals (Yin et al., 2014; Cao et al., 2018). The intestines are the main digestive and absorptive organ for nutrients, providing a selective blockage preventing various types of antigens. It

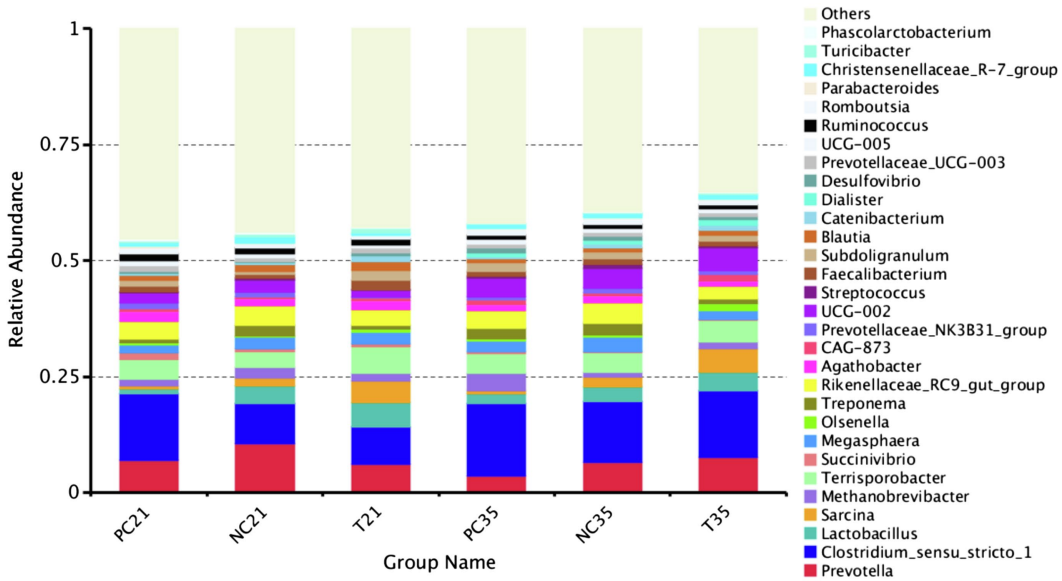

FIGURE 6 | Effects of *Z. Tk* and ZnO on the composition of gut microbiota at the genus level in three groups of piglets on days 21 and 35. Each of the nine samples is selected from each of the three groups of piglets, i.e., the positive control (PC), the negative control (NC), and the test groups, on days 21 and 35, respectively.

has been reported that a healthy intestinal environment plays an essentially important role in maintaining an organism's healthy condition (Thoo et al., 2019; Wan et al., 2019), while the oxidative stress is generally considered as a critical factor involved in the disruption of a healthy intestinal ecosystem. Therefore, it is practically important to identify appropriate natural feed additives as therapeutic agents to lessen the diseases related to oxidative stress (Zhuang et al., 2019).

Our results showed that the treatment of *Z. Tk* with appropriate concentrations and treatment time significantly increased the IPEC-J2 cell viability. H_2O_2 significantly downregulated the expression of GSH-Px, while *Z. Tk* significantly improved the T-AOC and the expression of GSH-Px in IPEC-J2 cells. These results are consistent with those reported previously, suggesting that the maintenance of strong antioxidant activities in weaned piglets is beneficial to support the intestinal barrier function (Chen et al., 2018a). Furthermore, a healthy intestinal environment relies on the tight junction proteins, which are the major factors determining the intestinal barrier function by sealing the paracellular space among epithelial cells (Nunes et al., 2019). In our study, the expression of three genes (i.e., *occludin*, *claudin*, and *ZO-1*) encoding three major intestinal barrier proteins (Liao et al., 2017) was significantly decreased by the treatment of H_2O_2 in the IPEC-J2 cells. These similar results were also reported previously (Cao et al., 2020). The *Z. Tk* significantly attenuated the dysfunction of the intestinal barrier by upregulating the expression of genes encoding the tight junction proteins under H_2O_2-induced oxidative stress in the IPEC-J2 cells. In short, the *Z. Tk* significantly decreased the H_2O_2-induced cell damage by increasing the cell viability and improving the antioxidant capacity in IPEC-J2 cells. It was reported that two types of polysaccharides isolated from *Codonopsis pilosula* (one of the five species of Chinese medicinal herbs used to make the mixture of *Z. Tk*) showed antioxidant ability against intestinal epithelial cells and proved to be effective prebiotics (Zou et al., 2020c). These results demonstrated that *Z. Tk* has shown the potential to attenuate intestinal injury (i.e., the intestinal barrier disruption) mainly by upregulating the oxidative status in the cells.

Effects of *Z. Tk* on Growth Performance in Piglets

In the swine industry, the feed efficiency is very important for the growth and fattening of animals. It is desired to generate a large amount of meat with less consumption of feed. We investigated the effect of *Z. Tk* on the growth performance of weaned piglets was investigagted with the goal to use it as a substitute for ZnO as a feed additive for weaned piglets. In our study, the addition of ZnO ($p < 0.01$) and *Z. Tk* ($p < 0.05$) to the feed both significantly improved the FCR of weaned piglets during the 1–35 days of post-weaning period, which effectively improved the economic benefits. Furthermore, the addition of *Z. Tk* to the feed significantly increased the BW at 21 and 35 days ($p < 0.05$). Our findings showed that the dietary supplementation of *Z. Tk* significantly improved the growth performance of early weaned piglets as demonstrated by several indicators, including the BW, ADG, ADFI, FCR, and diarrhea rate, suggesting that *Z. Tk* effectively helps piglets overcome the weaning stress at the early production stages. The similar results were reported previously, suggesting a positive effect of a diet supplemented with a mixture of Chinese herbal medicines on the growth performance of pigs (Yeh et al., 2011; Abdallah et al., 2019). Lan et al. (2017) reported that the

dietary supplementation of a mixture containing *Astragalus*, *Codonopsis*, and allicin increased the growth performance, the nutrient digestibility, the intestinal microbial balance (i.e., increased amount of *Lactobacillus* and decreased amount of *E. coli*), the immune response, and the meat quality of pigs.

The application of microbial fermentation to Chinese herbal medicines largely upgrades the functions of microorganisms and Chinese herbal medicines, showing enhanced effects when used in combination than applied alone. The active ingredients in the Chinese herbal medicines are released in the presence of enzymes provided by the microorganisms, effectively improving the efficacy of the herbal medicines (Ai et al., 2019; Li et al., 2020). Furthermore, after the microbial fermentation, the active macromolecular substances in the herbal medicines are transformed into small molecules that can be directly absorbed in the animal's intestines and fully metabolized in the body. Therefore, the drug residues are partly avoided (Ai et al., 2019; Li et al., 2020). The prebiotics produced by the herbal medicines after fermentation promote the reproduction of microorganisms, while the microorganisms improve the absorption of the herbal medicines in the body, complementing each other and ultimately enhancing the therapeutic effect (Ai et al., 2019). Furthermore, the process of inactivation of probiotics and degradation of metabolites after fermentation may affect the active ingredients in the herbal medicines, which is unfavorable in practice and should be avoided.

Effects of *Z. Tk* on the Microbial Diversity of the Intestinal Microbiota in Piglets

The understanding of the relationship among gut microbiota and growth performance will help us to effectively enhance the porcine growth and fattening performance of pigs. The bacterial communities of the fecal samples were compared among the NC, PC, and experimental groups of piglets on days 21 and 35 in our study. Results showed that no significant difference of the alpha diversities was revealed between the three groups of animals (**Figure 3**), suggesting that species richness and diversity of the bacterial communities were not affected significantly by either ZnO or *Z. Tk* during the entire experiment of this study. However, as the animals aged, the alpha diversity indices (i.e., Chao1, Shannon, and observed-species) of weaned piglets decreased. Studies have reported various types of changing patterns in alpha diversity indices. For example, the alpha diversities of gut microbiota increased with aging in pigs (Upadrasta et al., 2013; Niu et al., 2015), while Frese et al. (2015) reported that the alpha diversities initially increased gradually from birth to 21 days and then plateaued from 21 to 42 days. Furthermore, Arfken et al. (2020) reported that the microbial diversity and species richness and evenness were stable or showed slight decline 24 days after birth. These results suggested that the increase in the diversity and richness of the intestinal flora of piglets mainly occurs before the 21st day of birth and tends to stabilize or decrease slightly after weaning. In our study, the microbial alpha index of piglets at 35 days after weaning (56 days of age) decreased compared with that of 21 days after weaning (42 days of age). Results of beta diversity analysis showed evidently the differences between the NC and experimental groups based on the PCoA. For example, the NC and PC groups were closely related to each other on day 21, while the three groups of piglets were clustered together on day 35, indicating that the influential effects of *Z. Tk* on the taxonomic structure of the intestinal microbiota on day 21 gradually became less evident as the age increased to 35 days.

Effects of *Z. Tk* on Taxonomic Composition of the Intestinal Microbiota in Piglets

Our results revealed that all samples were relatively dominated by Firmicutes, Bacteroidota, and Proteobacteria at the phylum level, similar to the results previously reported (Han et al., 2017), and were dominated by *Prevotella*, *Clostridium_sensu_stricto_1*, and *Lactobacillus* at the genus level. Studies have shown that the taxa of Firmicutes and Bacteroidetes dominate the human, mouse, and pig microbiota (Ley et al., 2005), while lean and obese pigs contain different proportions of Firmicutes and Bacteroidetes (Guo et al., 2008). Specifically, the levels of Bacteroidetes and Bacteroides were lower in obese pigs than those of the lean pigs, while significant difference of the level of Firmicutes was not revealed between obese and lean pigs. Furthermore, the levels of Bacteroidetes and Firmicutes in the ceca also differ between obese and lean mice with the genetically obese mice showing 50% decrease in the abundance of Bacteroidetes and a proportional increase in the level of Firmicutes, in comparison to lean mice (Ley et al., 2005). It was reported that the microbiota of obese mice enhanced energy generation from ingested diet (Turnbaugh et al., 2006), while the overweight and obese subjects presented low level of Bacteroidetes (Ley et al., 2006). Generally considered as a biomarker to evaluate the body weight gain performance (Ding et al., 2019), the F/B is correlated with body mass index and tends to increase in stout healthy subjects compared to the lean healthy subjects (Ding et al., 2019). Similar results were revealed in our study. Specifically, the F/B of the experimental group increased significantly in animals with larger BW in 21 days of weaning. In our study, the weaned piglets supplemented with *Z. Tk* in the diet were characterized by the increased level of Firmicutes and decreased level of Bacteroides. These results were consistent with the significant increase in body weight of the weaned piglets, suggesting that the mixture of *Z. Tk* improved the weight of piglets by altering the bacterial structure of the intestinal microbiota (i.e., *Firmicutes* and *Bacteroides*).

Several studies on animals during their weaning stages have shown a decreased relative abundance of the *Lactobacillus* group, whereas the bacteria in *Clostridium*, *Prevotella,* and facultative anaerobes, such as *Proteobacteriaceae* (e.g., *E. coli*) were generally positively impacted (Gresse et al., 2017). Weaned piglets are generally supplemented with beneficial bacteria to counteract the disturbance of the intestinal microbiota. In particular, species of *Lactobacillus* are major players in disease prevention, while the rapid decrease in their relative abundance in the gut microbiota during weaning transition contributes to an increased risk of diseases (Konstantinov et al., 2006). In our study, the relative abundance of *Lactobacillus* in the experimental group of piglets fed with *Z. Tk* showed an increasing trend from days 21 to 35,

indicating that the supplementation of fermented herbal mixture is beneficial to the healthy development of the intestinal microbiota of piglets after weaning. Furthermore, the pathogenic bacteria decreased in the experimental group (**Figure 6**). For example, the relative abundance of *Proteobacteria* in the experimental group showed a decreasing state in 21 days. Studies have shown that *Proteobacteria* is significantly increased in the intestines of mice with ulcerative colitis producing a large number of pro-inflammatory cytokines (Powell et al., 2012). These results suggest that the chronic enrichment of members of *Proteobacteria* in the intestine may represent either an unbalanced and unstable microbial community structure or the unhealthy state of the host, while the supplementation of *Z. Tk* reduces the risk of intestinal diseases. In our study, *Prevotella* responded differently to the treatments of ZnO and *Z. Tk*. Specifically, the relative abundance of *Prevotella* decreased in both periods of 21 days and 35 days under the treatment of ZnO, whereas decreased in 21 days and then increased in 35 days under the treatment of *Z. Tk*. *Prevotella* contains a group of Gram-Negative and obligate anaerobic bacilli with the capability of fermenting carbohydrates to generate short chain fatty acids including acetate and butyrate, exerting an anti-inflammatory effect on immune cells and ultimately inhibiting the growth of potentially pathogenic bacteria (Rivera-Chávez et al., 2016; Zou et al., 2020a). In the PC group, the relative abundance of *Clostridium_sensu_stricto_1* and *Sarcina* showed an increasing and decreasing trends, respectively, in both periods of 21 and 35 days. However, in the experimental group, the relative abundance of *Clostridium_sensu_stricto_1* was not significantly different on either 21 or 35 days, while *Sarcina* showed an upward trend. Studies have shown that the *Clostridium_sensu_stricto_1* contains harmful bacteria with adverse effects on the intestinal tract (Lin et al., 2018; Zou et al., 2020a). Species in *Sarcina* are anaerobic Gram-positive cocci and associated with delayed gastric emptying (Lam-Himlin et al., 2011), while these microorganisms do not appear to cause direct mucosal injury but always appear in the gastrointestinal tract enrichment in the intestines of patients (Chan et al., 2020). Our results indicate that the treatment of *Z. Tk* and ZnO did not show any inhibitory effect on some Gram-positive pathogenic bacteria, such as *Clostridium_sensu_stricto_1* and *Sarcina*, while *Z. Tk* showed inhibitory effect on gram-negative pathogenic bacteria, such as Proteobacteria, simultaneously, promoting the relative abundance of beneficial bacteria, such as *Lactobacillus* and ultimately helping weaned piglets to smoothly survive the weaning stress.

CONCLUSION

In this study, we have demonstrated that the fermented Chinese herbal mixture *Z. Tk* can not only improve the intestinal antioxidant capacity and repair the intestinal cell barrier *in vitro* but also enhance the growth performance and the taxonomic structure of the intestinal microbiota of the weaned piglets. The intestinal microbiota of weaned piglets was altered by the addition of *Z. Tk*, mainly increasing the relative abundance of beneficial bacteria, such as *Lactobacillus* and inhibiting Gram-negative pathogenic bacteria such as members of *Proteobacteria*. More importantly, these bacteria helped to maintain the intestinal microbiota at a favorable state for the host, effectively reduced the abnormal changes in the intestinal structure of microbiota in weaned piglets and created a favorable microbial community for the subsequent restoration of a balanced gut microbiota. Our study demonstrates that *Z. Tk* is potentially a promising substitute of ZnO for facilitating the weaning phase and improving production efficiency of piglets. Specifically, *Z. Tk* showed significantly improved the growth performance of weaned piglets in comparison to that of ZnO additives. We note that because the weaned piglets have not been slaughtered due to the experimental conditions in this study, more studies *in vivo* are needed to verify the antioxidant capacity of *Z. Tk* revealed in this study.

DATA AVAILABILITY STATEMENT

The datasets presented in this study can be found in online repositories. The names of the repository/repositories and accession number(s) can be found at: https://www.ncbi.nlm.nih.gov/, PRJNA714150.

ETHICS STATEMENT

The animal study was reviewed and approved by Committee on the Ethics of Animal Experiments of the College of Veterinary Medicine, Huazhong Agricultural University.

AUTHOR CONTRIBUTIONS

YX and YL: conceptualization. YW, WL, ST, XY, and JL: methodology. YL and TS: resources. YH: data curation and writing – original draft preparation. YH and YX: writing – review and editing. YX: supervision and funding acquisition. YL, TS, ZZ, and YX: project administration. All authors contributed to the article and approved the submitted version.

FUNDING

This research was funded by the Innovative Job Funds of Agricultural Science and Technology of Hubei Province, grant number 2019-620-000-001-30.

ACKNOWLEDGMENTS

We thank the editor and reviewers for providing the constructive comments to improve our manuscript.

SUPPLEMENTARY MATERIAL

The Supplementary Material for this article can be found online at: https://www.frontiersin.org/articles/10.3389/fmicb.2021.725196/full#supplementary-material

Supplementary Table S1 | Feed formula of different groups of piglets.

Supplementary Table S2 | Formula nutrient values.

Supplementary Table S3 | Summary of sequencing data of each sample.

Supplementary Figure S1 | The rarefaction curve.

REFERENCES

Abdallah, A., Zhang, P., Zhong, Q., and Sun, Z. (2019). Application of traditional chinese herbal medicine by-products as dietary feed supplements and antibiotic replacements in animal production. *Curr. Drug Metab.* 20, 54–64. doi: 10.2174/1389200219666180523102920

Adesso, S., Russo, R., Quaroni, A., Autore, G., and Marzocco, S. (2018). Astragalus membranaceus extract attenuates inflammation and oxidative stress in intestinal epithelial cells via nf-κb activation and nrf2 response. *Int. J. Mol. Sci.* 19, 800. doi: 10.3390/ijms19030800

Ahrens, U. (1992). Detection of DNA of plant pathogenic mycoplasmalike organisms by a polymerase chain reaction that amplifies a sequence of the 16s rrna gene. *Phytopathology* 82, 828–832. doi: 10.1094/Phyto-82-828

Ai, S., Tang, W., Guo, R. L., Li, J. Q., Yang, W., and He, Z. G. (2019). Research progress on chinese herbal medicine fermentation and profile of active substances derived. *Zhongguo Zhong Yao Za Zhi* 44, 1110–1118. doi: 10.19540/j.cnki.cjcmm.20181227.002

Arfken, A. M., Frey, J. F., and Summers, K. L. (2020). Temporal dynamics of the gut bacteriome and mycobiome in the weanling pig. *Microorganisms* 8, 868. doi: 10.3390/microorganisms8060868

Bailly, C. (2020). Atractylenolides, essential components of atractylodes-based traditional herbal medicines: antioxidant, anti-inflammatory and anticancer properties. *Eur. J. Pharmacol.* 891, 173735. doi: 10.1016/j.ejphar.2020.173735

Bednorz, C., Oelgeschläger, K., Kinnemann, B., Hartmann, S., Neumann, K., Pieper, R., et al. (2013). The broader context of antibiotic resistance: zinc feed supplementation of piglets increases the proportion of multi-resistant *Escherichia coli in vivo*. *Int. J. Med. Microbiol.* 303, 396–403. doi: 10.1016/j.ijmm.2013.06.004

Campbell, J. M., Crenshaw, J. D., and Polo, J. (2013). The biological stress of early weaned piglets. *J. Anim. Sci. Biotechnol.* 4, 19. doi: 10.1186/2049-1891-4-19

Cao, S. T., Wang, C. C., Wu, H., Zhang, Q. H., Jiao, L. F., and Hu, C. H. (2018). Weaning disrupts intestinal antioxidant status, impairs intestinal barrier and mitochondrial function, and triggers mitophagy in piglets. *J. Anim. Sci.* 96, 1073–1083. doi: 10.1093/jas/skx062

Cao, S., Wang, C., Yan, J., Li, X., Wen, J., and Hu, C. (2020). Curcumin ameliorates oxidative stress-induced intestinal barrier injury and mitochondrial damage by promoting parkin dependent mitophagy through ampk-tfeb signal pathway. *Free Radic. Biol. Med.* 147, 8–22. doi: 10.1016/j.freeradbiomed.2019.12.004

Cao, H., Zhang, A., Zhang, H., Sun, H., and Wang, X. (2015). The application of metabolomics in traditional Chinese medicine opens up a dialogue between Chinese and western medicine. *Phytother. Res.* 29, 159–166. doi: 10.1002/ptr.5240

Caporaso, J. G., Kuczynski, J., Stombaugh, J., Bittinger, K., Bushman, F. D., Costello, E. K., et al. (2010). Qiime allows analysis of high-throughput community sequencing data. *Nat. Methods* 7, 335–336. doi: 10.1038/nmeth.f.303

Chan, M., Jain, D., Minimo, C., and Platt, A. (2020). Concomitant sarcina-associated erosive esophagitis and refractory helicobacter pylori gastritis. *ACG Case Rep. J.* 7, e00463. doi: 10.14309/crj.0000000000000463

Chen, M., Liao, Z., Lu, B., Wang, M., Lin, L., Zhang, S., et al. (2018b). Huang-lian-jie-du-decoction ameliorates hyperglycemia and insulin resistant in association with gut microbiota modulation. *Front. Microbiol.* 9:2380. doi: 10.3389/fmicb.2018.02380

Chen, J., Long, L., Jiang, Q., Kang, B., Li, Y., and Yin, J. (2020). Effects of dietary supplementation of *Lycium barbarum* polysaccharides on growth performance, immune status, antioxidant capacity and selected microbial populations of weaned piglets. *J. Anim. Physiol. Anim. Nutr.* 104, 1106–1115. doi: 10.1111/jpn.13247

Chen, J., Yu, B., Chen, D., Huang, Z., Mao, X., Zheng, P., et al. (2018a). Chlorogenic acid improves intestinal barrier functions by suppressing mucosa inflammation and improving antioxidant capacity in weaned pigs. *J. Nutr. Biochem.* 59, 84–92. doi: 10.1016/j.jnutbio.2018.06.005

Ding, X., Lan, W., Liu, G., Ni, H., and Gu, J. D. (2019). Exploring possible associations of the intestine bacterial microbiome with the pre-weaned weight gaining performance of piglets in intensive pig production. *Sci. Rep.* 9, 15534. doi: 10.1038/s41598-019-52045-4

Đorđević, T. M., Šiler-Marinković, S. S., and Dimitrijević-Branković, S. I. (2010). Effect of fermentation on antioxidant properties of some cereals and pseudo cereals. *Food Chem.* 119, 957–963. doi: 10.1016/j.foodchem.2009.07.049

Du, Z., Risu, N., Gentu, G., Jia, Y., and Cai, Y. (2018). Growth performance, apparent digestibility, and n balance in mongolian lambs and hoggs fed diets supplemented with a Chinese traditional herbal medicine complex. *Anim. Sci. J.* 89, 1451–1458. doi: 10.1111/asj.13081

Edgar, R. C. (2004). Muscle: multiple sequence alignment with high accuracy and high throughput. *Nucleic Acids Res.* 32, 1792–1797. doi: 10.1093/nar/gkh340

Edgar, R. C. (2013). Uparse: highly accurate otu sequences from microbial amplicon reads. *Nat. Methods* 10, 996–998. doi: 10.1038/nmeth.2604

Edgar, R. C., Haas, B. J., Clemente, J. C., Quince, C., and Knight, R. (2011). Uchime improves sensitivity and speed of chimera detection. *Bioinformatics* 27, 2194–2200. doi: 10.1093/bioinformatics/btr381

Frese, S. A., Parker, K., Calvert, C. C., and Mills, D. A. (2015). Diet shapes the gut microbiome of pigs during nursing and weaning. *Microbiome* 3, 28. doi: 10.1186/s40168-015-0091-8

Frydendahl, K. (2002). Prevalence of serogroups and virulence genes in *Escherichia coli* associated with postweaning diarrhoea and edema disease in pigs and a comparison of diagnostic approaches. *Vet. Microbiol.* 85, 169–182. doi: 10.1016/S0378-1135(01)00504-1

Fu, Y. P., Feng, B., Zhu, Z. K., Feng, X., Chen, S. F., Li, L. X., et al. (2018). The polysaccharides from *Codonopsis pilosula* modulates the immunity and intestinal microbiota of cyclophosphamide-treated immunosuppressed mice. *Molecules* 23, 1801. doi: 10.3390/molecules23071801

Gong, A. G. W., Duan, R., Wang, H. Y., Kong, X. P., Dong, T. T. X., Tsim, K. W. K., et al. (2018). Evaluation of the pharmaceutical properties and value of astragali radix. *Medicines* 5, 46. doi: 10.3390/medicines5020046

Gresse, R., Chaucheyras-Durand, F., Fleury, M. A., Van de Wiele, T., Forano, E., and Blanquet-Diot, S. (2017). Gut microbiota dysbiosis in postweaning piglets: understanding the keys to health. *Trends Microbiol.* 25, 851–873. doi: 10.1016/j.tim.2017.05.004

Guo, X., Xia, X., Tang, R., Zhou, J., Zhao, H., and Wang, K. (2008). Development of a real-time pcr method for firmicutes and bacteroidetes in faeces and its application to quantify intestinal population of obese and lean pigs. *Lett. Appl. Microbiol.* 47, 367–373. doi: 10.1111/j.1472-765X.2008.02408.x

Haas, B. J., Gevers, D., Earl, A. M., Feldgarden, M., Ward, D. V., Giannoukos, G., et al. (2011). Chimeric 16s rrna sequence formation and detection in sanger and 454-pyrosequenced pcr amplicons. *Genome Res.* 21, 494–504. doi: 10.1101/gr.112730.110

Han, G. G., Lee, J. Y., Jin, G. D., Park, J., Choi, Y. H., Chae, B. J., et al. (2017). Evaluating the association between body weight and the intestinal microbiota of weaned piglets via 16s rrna sequencing. *Appl. Microbiol. Biotechnol.* 101, 5903–5911. doi: 10.1007/s00253-017-8304-7

Hu, C., Song, J., You, Z., Luan, Z., and Li, W. (2012). Zinc oxide-montmorillonite hybrid influences diarrhea, intestinal mucosal integrity, and digestive enzyme activity in weaned pigs. *Biol. Trace Elem. Res.* 149, 190–196. doi: 10.1007/s12011-012-9422-9

Kawai, K., Kamochi, R., Oiki, S., Murata, K., and Hashimoto, W. (2018). Probiotics in human gut microbiota can degrade host glycosaminoglycans. *Sci. Rep.* 8, 10674. doi: 10.1038/s41598-018-28886-w

Kociova, S., Dolezelikova, K., Horky, P., Skalickova, S., Baholet, D., Bozdechova, L., et al. (2020). Zinc phosphate-based nanoparticles as alternatives to zinc oxide in diet of weaned piglets. *J. Anim. Sci. Biotechnol.* 11, 59. doi: 10.1186/s40104-020-00458-x

Kong, W., Zhao, Y., Shan, L., Xiao, X., and Guo, W. (2008a). Microcalorimetric studies of the action on four organic acids in radix isatidis on the growth of microorganisms. *Sheng Wu Gong Cheng Xue Bao* 24, 646–650. doi: 10.1016/s1872-2075(08)60033-3

Kong, W. J., Zhao, Y. L., Shan, L. M., Xiao, X. H., and Guo, W. Y. (2008b). Investigation on the spectrum-effect relationships of etoac extract from radix

isatidis based on hplc fingerprints and microcalorimetry. *J. Chromatogr. B Anal. Technol. Biomed. Life Sci.* 871, 109–114. doi: 10.1016/j.jchromb.2008.06.053

Konstantinov, S. R., Awati, A. A., Williams, B. A., Miller, B. G., Jones, P., Stokes, C. R., et al. (2006). Post-natal development of the porcine microbiota composition and activities. *Environ. Microbiol.* 8, 1191–1199. doi: 10.1111/j.1462-2920.2006.01009.x

Krishnan, S., Alden, N., and Lee, K. (2015). Pathways and functions of gut microbiota metabolism impacting host physiology. *Curr. Opin. Biotechnol.* 36, 137–145. doi: 10.1016/j.copbio.2015.08.015

Kusznierewicz, B., Śmiechowska, A., Bartoszek, A., and Namieśnik, J. (2008). The effect of heating and fermenting on antioxidant properties of white cabbage. *Food Chem.* 108, 853–861. doi: 10.1016/j.foodchem.2007.11.049

Lam-Himlin, D., Tsiatis, A. C., Montgomery, E., Pai, R. K., Brown, J. A., Razavi, M., et al. (2011). Sarcina organisms in the gastrointestinal tract: A clinicopathologic and molecular study. *Am. J. Surg. Pathol.* 35, 1700–1705. doi: 10.1097/PAS.0b013e31822911e6

Lan, R. X., Park, J. W., Lee, D. W., and Kim, I. H. (2017). Effects of astragalus membranaceus, codonopsis pilosula and allicin mixture on growth performance, nutrient digestibility, faecal microbial shedding, immune response and meat quality in finishing pigs. *J. Anim. Physiol. Anim. Nutr.* 101, 1122–1129. doi: 10.1111/jpn.12625

Ley, R. E., Bäckhed, F., Turnbaugh, P., Lozupone, C. A., Knight, R. D., and Gordon, J. I. (2005). Obesity alters gut microbial ecology. *Proc. Natl. Acad. Sci. U. S. A.* 102, 11070–11075. doi: 10.1073/pnas.0504978102

Ley, R. E., Turnbaugh, P. J., Klein, S., and Gordon, J. I. (2006). Microbial ecology: human gut microbes associated with obesity. *Nature* 444, 1022–1023. doi: 10.1038/4441022a

Li, L., Wang, L., Fan, W., Jiang, Y., Zhang, C., Li, J., et al. (2020). The application of fermentation technology in traditional chinese medicine: a review. *Am. J. Chin. Med.* 48, 899–921. doi: 10.1142/S0192415X20500433

Li, Y. F., Wang, M., Wang, X. Y., Yu, H. S., Kang, L. P., Ma, B. P., et al. (2011). Pharmacokinetic properties of albiflorin and paeoniflorin after oral administration of pure compound, radix paeoniae alba extract and danggui-shaoyao-san extract to rats. *J. Asian Nat. Prod. Res.* 13, 117–127. doi: 10.1080/10286020.2010.546353

Li, N., Wang, B., Wu, Y., Luo, X., Chen, Z., Sang, C., et al. (2019). Modification effects of sanwei ganjiang powder on liver and intestinal damage through reversing bile acid homeostasis. *Biomed. Pharmacother.* 116, 109044. doi: 10.1016/j.biopha.2019.109044

Liao, P., Liao, M., Li, L., Tan, B., and Yin, Y. (2017). Effect of deoxynivalenol on apoptosis, barrier function, and expression levels of genes involved in nutrient transport, mitochondrial biogenesis and function in ipec-j2 cells. *Toxicol. Res.* 6, 866–877. doi: 10.1039/C7TX00202E

Lin, C., Wan, J., Su, Y., and Zhu, W. (2018). Effects of early intervention with maternal fecal microbiota and antibiotics on the gut microbiota and metabolite profiles of piglets. *Meta* 8, 89. doi: 10.3390/metabo8040089

Lin, Z. N., Ye, L., Li, Z. W., Huang, X. S., Lu, Z., Yang, Y. Q., et al. (2020). Chinese herb feed additives improved the growth performance, meat quality, and nutrient digestibility parameters of pigs. *Ani. Mod. Exp. Med.* 3, 47–54. doi: 10.1002/ame2.12104

Liu, H., Hu, J., Mahfuz, S., and Piao, X. (2020). Effects of hydrolysable tannins as zinc oxide substitutes on antioxidant status, immune function, intestinal morphology, and digestive enzyme activities in weaned piglets. *Animals* 10, 757. doi: 10.3390/ani10050757

Magoč, T., and Salzberg, S. L. (2011). Flash: fast length adjustment of short reads to improve genome assemblies. *Bioinformatics* 27, 2957–2963. doi: 10.1093/bioinformatics/btr507

Niu, Q., Li, P., Hao, S., Zhang, Y., Kim, S. W., Li, H., et al. (2015). Dynamic distribution of the gut microbiota and the relationship with apparent crude fiber digestibility and growth stages in pigs. *Sci. Rep.* 5, 9938. doi: 10.1038/srep09938

Nunes, C., Freitas, V., Almeida, L., and Laranjinha, J. (2019). Red wine extract preserves tight junctions in intestinal epithelial cells under inflammatory conditions: implications for intestinal inflammation. *Food Funct.* 10, 1364–1374. doi: 10.1039/C8FO02469C

Odle, J., Zijlstra, R. T., and Donovan, S. M. (1996). Intestinal effects of milkborne growth factors in neonates of agricultural importance. *J. Anim. Sci.* 74, 2509–2522. doi: 10.2527/1996.74102509x

Powell, N., Walker, A. W., Stolarczyk, E., Canavan, J. B., Gökmen, M. R., Marks, E., et al. (2012). The transcription factor t-bet regulates intestinal inflammation mediated by interleukin-7 receptor+ innate lymphoid cells. *Immunity* 37, 674–684. doi: 10.1016/j.immuni.2012.09.008

Qian, W., Zhang, J., Wang, W., Wang, T., Liu, M., Yang, M., et al. (2020). Antimicrobial and antibiofilm activities of paeoniflorin against carbapenem-resistant *Klebsiella pneumoniae*. *J. Appl. Microbiol.* 128, 401–413. doi: 10.1111/jam.14480

Quast, C., Pruesse, E., Yilmaz, P., Gerken, J., Schweer, T., Yarza, P., et al. (2013). The silva ribosomal rna gene database project: improved data processing and web-based tools. *Nucleic Acids Res.* 41, D590–D596. doi: 10.1093/nar/gks1219

Rensing, C., Moodley, A., Cavaco, L. M., and McDevitt, S. F. (2018). Resistance to metals used in agricultural production. *Microbiol. Spectr.* 6, 1–24. doi: 10.1128/microbiolspec.ARBA-0025-2017

Rivera-Chávez, F., Zhang, L. F., Faber, F., Lopez, C. A., Byndloss, M. X., Olsan, E. E., et al. (2016). Depletion of butyrate-producing clostridia from the gut microbiota drives an aerobic luminal expansion of salmonella. *Cell Host Microbe* 19, 443–454. doi: 10.1016/j.chom.2016.03.004

Shan, B., Cai, Y. Z., Sun, M., and Corke, H. (2005). Antioxidant capacity of 26 spice extracts and characterization of their phenolic constituents. *J. Agric. Food Chem.* 53, 7749–7759. doi: 10.1021/jf051513y

Su-Hong, C., Qi, C., Bo, L., Jian-Li, G., Jie, S., and Gui-Yuan, L. (2015). Antihypertensive effect of radix paeoniae alba in spontaneously hypertensive rats and excessive alcohol intake and high fat diet induced hypertensive rats. *Evid. Based Complement. Alternat. Med.* 2015, 731237. doi: 10.1155/2015/731237

Tang, S., Liu, W., Zhao, Q., Li, K., Zhu, J., Yao, W., et al. (2021). Combination of polysaccharides from astragalus membranaceus and *Codonopsis pilosula* ameliorated mice colitis and underlying mechanisms. *J. Ethnopharmacol.* 264, 113280. doi: 10.1016/j.jep.2020.113280

Thoo, L., Noti, M., and Krebs, P. (2019). Keep calm: the intestinal barrier at the interface of peace and war. *Cell Death Dis.* 10, 849. doi: 10.1038/s41419-019-2086-z

Tong, X., Xu, J., Lian, F., Yu, X., Zhao, Y., Xu, L., et al. (2018). Structural alteration of gut microbiota during the amelioration of human type 2 diabetes with hyperlipidemia by metformin and a traditional chinese herbal formula: A multicenter, randomized, open label clinical trial. *MBio* 9, e02392–e02317. doi: 10.1128/mBio.02392-17

Turnbaugh, P. J., Ley, R. E., Mahowald, M. A., Magrini, V., Mardis, E. R., and Gordon, J. I. (2006). An obesity-associated gut microbiome with increased capacity for energy harvest. *Nature* 444, 1027–1031. doi: 10.1038/nature05414

Ugural, A., and Akyol, A. (2020). Can pseudocereals modulate microbiota by functioning as probiotics or prebiotics? *Crit. Rev. Food Sci. Nutr.*, 1–15. doi: 10.1080/10408398.2020.1846493

Upadrasta, A., O'Sullivan, L., O'Sullivan, O., Sexton, N., Lawlor, P. G., Hill, C., et al. (2013). The effect of dietary supplementation with spent cider yeast on the swine distal gut microbiome. *PLoS One* 8:e75714. doi: 10.1371/journal.pone.0075714

Wan, M. L. Y., Ling, K. H., El-Nezami, H., and Wang, M. F. (2019). Influence of functional food components on gut health. *Crit. Rev. Food Sci. Nutr.* 59, 1927–1936. doi: 10.1080/10408398.2018.1433629

Wang, Q., Garrity, G. M., Tiedje, J. M., and Cole, J. R. (2007). Naive bayesian classifier for rapid assignment of rrna sequences into the new bacterial taxonomy. *Appl. Environ. Microbiol.* 73, 5261–5267. doi: 10.1128/AEM.00062-07

Wang, S., Hu, Y., Tan, W., Wu, X., Chen, R., Cao, J., et al. (2012). Compatibility art of traditional chinese medicine: From the perspective of herb pairs. *J. Ethnopharmacol.* 143, 412–423. doi: 10.1016/j.jep.2012.07.033

Wang, W., Van Noten, N., Degroote, J., Romeo, A., Vermeir, P., and Michiels, J. (2019). Effect of zinc oxide sources and dosages on gut microbiota and integrity of weaned piglets. *J. Anim. Physiol. Anim. Nutr.* 103, 231–241. doi: 10.1111/jpn.12999

Wang, R., Zhou, G., Wang, M., Peng, Y., and Li, X. (2014). The metabolism of polysaccharide from atractylodes macrocephala koidz and its effect on intestinal microflora. *Evid. Based Complement. Alternat. Med.* 2014, 926381. doi: 10.1155/2014/926381

Wei, X., Tao, J., Xiao, S., Jiang, S., Shang, E., Zhu, Z., et al. (2018). Xiexin tang improves the symptom of type 2 diabetic rats by modulation of the gut microbiota. *Sci. Rep.* 8, 3685. doi: 10.1038/s41598-018-22094-2

Xiao, P., Huang, H., Chen, J., and Li, X. (2014). *In vitro* antioxidant and anti-inflammatory activities of radix isatidis extract and bioaccessibility of six bioactive compounds after simulated gastro-intestinal digestion. *J. Ethnopharmacol.* 157, 55–61. doi: 10.1016/j.jep.2014.09.005

Xiao, P., Huang, H., Li, X., Chen, J., and Duan, J. A. (2019). Characterization, evaluation of nutritional parameters of radix isatidis protein and its antioxidant activity in d-galactose induced ageing mice. *BMC Complement. Altern. Med.* 19:297. doi: 10.1186/s12906-019-2726-y

Xu, J., Li, Y., Yang, Z., Li, C., Liang, H., Wu, Z., et al. (2018). Yeast probiotics shape the gut microbiome and improve the health of early-weaned piglets. *Front. Microbiol.* 9:2011. doi: 10.3389/fmicb.2018.02011

Xu, J., Lian, F., Zhao, L., Zhao, Y., Chen, X., Zhang, X., et al. (2015). Structural modulation of gut microbiota during alleviation of type 2 diabetes with a Chinese herbal formula. *ISME J.* 9, 552–562. doi: 10.1038/ismej.2014.177

Yan, B., Shen, M., Fang, J., Wei, D., and Qin, L. (2018). Advancement in the chemical analysis of paeoniae radix (shaoyao). *J. Pharm. Biomed. Anal.* 160, 276–288. doi: 10.1016/j.jpba.2018.08.009

Yeh, H. S., Weng, B. C., and Lien, T. F. (2011). Effects of Chinese traditional herbal medicine complex supplementation on the growth performance, immunity and serum traits of pigs. *Anim. Sci. J.* 82, 747–752. doi: 10.1111/j.1740-0929.2011.00897.x

Yin, J., Wu, M. M., Xiao, H., Ren, W. K., Duan, J. L., Yang, G., et al. (2014). Development of an antioxidant system after early weaning in piglets. *J. Anim. Sci.* 92, 612–619. doi: 10.2527/jas.2013-6986

Zhang, H. Y., Tian, J. X., Lian, F. M., Li, M., Liu, W. K., Zhen, Z., et al. (2020). Therapeutic mechanisms of traditional chinese medicine to improve metabolic diseases via the gut microbiota. *Biomed. Pharmacother.* 133:110857. doi: 10.1016/j.biopha.2020.110857

Zhao, Y., Zhang, Y., Kong, H., Zhang, M., Cheng, J., Wu, J., et al. (2020). Carbon dots from paeoniae radix alba carbonisata: Hepatoprotective effect. *Int. J. Nanomedicine* 15, 9049–9059. doi: 10.2147/ijn.S281976

Zhou, Y., Tan, F., Li, C., Li, W., Liao, W., Li, Q., et al. (2019). White peony (fermented *Camellia sinensis*) polyphenols help prevent alcoholic liver injury *via* antioxidation. *Antioxidants* 8:524. doi: 10.3390/antiox8110524

Zhou, H., Wang, C., Ye, J., Chen, H., and Tao, R. (2015). Effects of dietary supplementation of fermented *Ginkgo biloba* l. Residues on growth performance, nutrient digestibility, serum biochemical parameters and immune function in weaned piglets. *Anim. Sci. J.* 86, 790–799. doi: 10.1111/asj.12361

Zhou, W., and Zhang, X. Y. (2013). Research progress of Chinese herbal medicine radix isatidis (banlangen). *Am. J. Chin. Med.* 41, 743–764. doi: 10.1142/S0192415X1350050X

Zhu, B., Zhang, Q. L., Hua, J. W., Cheng, W. L., and Qin, L. P. (2018). The traditional uses, phytochemistry, and pharmacology of atractylodes macrocephala koidz.: a review. *J. Ethnopharmacol.* 226, 143–167. doi: 10.1016/j.jep.2018.08.023

Zhuang, Y., Wu, H., Wang, X., He, J., He, S., and Yin, Y. (2019). Resveratrol attenuates oxidative stress-induced intestinal barrier injury through pi3k/akt-mediated nrf2 signaling pathway. *Oxidative Med. Cell. Longev.* 2019, 7591840. doi: 10.1155/2019/7591840

Zou, J., Shen, Y., Chen, M., Zhang, Z., Xiao, S., Liu, C., et al. (2020a). Lizhong decoction ameliorates ulcerative colitis in mice via modulating gut microbiota and its metabolites. *Appl. Microbiol. Biotechnol.* 104, 5999–6012. doi: 10.1007/s00253-020-10665-1

Zou, Y. F., Zhang, Y. Y., Paulsen, B. S., Rise, F., Chen, Z. L., Jia, R. Y., et al. (2020b). Structural features of pectic polysaccharides from stems of two species of radix codonopsis and their antioxidant activities. *Int. J. Biol. Macromol.* 159, 704–713. doi: 10.1016/j.ijbiomac.2020.05.083

Zou, Y. F., Zhang, Y. Y., Zhu, Z. K., Fu, Y. P., Paulsen, B. S., Huang, C., et al. (2020c). Characterization of inulin-type fructans from two species of radix codonopsis and their oxidative defense activation and prebiotic activities. *J. Sci. Food Agric.* 101, 2491–2499. doi: 10.1002/jsfa.10875

Conflict of Interest: YL, WL, and ST are employed by COFCO Feed Co., Ltd. TQ and XL are employed by Hubei Huada Real Science & Technology Co., Ltd.

The remaining authors declare that the research was conducted in the absence of any commercial or financial relationships that could be construed as a potential conflict of interest.

Publisher's Note: All claims expressed in this article are solely those of the authors and do not necessarily represent those of their affiliated organizations, or those of the publisher, the editors and the reviewers. Any product that may be evaluated in this article, or claim that may be made by its manufacturer, is not guaranteed or endorsed by the publisher.

frontiers in Microbiology

ORIGINAL RESEARCH
published: 28 October 2021
doi: 10.3389/fmicb.2021.771617

Effects of Dietary Zinc Sources on Growth Performance and Gut Health of Weaned Piglets

Hui Diao[1†], Jiayou Yan[1†], Shuwei Li[1,2†], Shengyao Kuang[3], Xiaolan Wei[1], Mengjia Zhou[1], Jinxiu Zhang[1], Chongbo Huang[1], Peng He[1] and Wenjie Tang[1]*

[1]Animal Breeding and Genetics Key Laboratory of Sichuan Province, Sichuan Academy of Animal Science, Chengdu, China, [2]Sichuan Animtech Biology Development Co., Ltd, Chengdu, China, [3]Livestock and Poultry Biological Products Key Laboratory of Sichuan Province, Sichuan Animtech Feed Co., Ltd, Chengdu, China

OPEN ACCESS

Edited by:
Zheng Ruan,
Nanchang University, China

Reviewed by:
Wenkai Ren,
South China Agricultural University, China
Tiejun Li,
Chinese Academy of Sciences, China

***Correspondence:**
Wenjie Tang
wenhan28@126.com

[†]*These authors have contributed equally to this work*

Specialty section:
This article was submitted to Food Microbiology, a section of the journal Frontiers in Microbiology

Received: *06 September 2021*
Accepted: *11 October 2021*
Published: *28 October 2021*

Citation:
Diao H, Yan J, Li S, Kuang S, Wei X, Zhou M, Zhang J, Huang C, He P and Tang W (2021) Effects of Dietary Zinc Sources on Growth Performance and Gut Health of Weaned Piglets. Front. Microbiol. 12:771617. doi: 10.3389/fmicb.2021.771617

The present study aimed to investigate the effects of dietary zinc sources on the growth performance and gut health of weaned piglets. In total, 96 Duroc × Landrace × Yorkshire (DLY) weaned piglets with an initial average body weight of 8.81 ± 0.42 kg were divided into four groups, with six replicates per treatment and four pigs per replicate. The dietary treatment groups were as follows: (1) control group, basal diet; (2) zinc sulphate (ZnSO4) group, basal diet +100 mg/kg ZnSO4; (3) glycine zinc (Gly-Zn) group, basal diet +100 mg/kg Gly-Zn and (4) zinc lactate group, and basal diet +100 mg/kg zinc lactate. The whole trial lasted for 28 days. Decreased F/G was noted in the Gly-Zn and zinc lactate groups ($p < 0.05$). The zinc lactate group had a lower diarrhea rate than the control group ($p < 0.05$). Moreover, the ZnSO4, Gly-Zn, and zinc lactate groups had significantly higher apparent total tract digestibility of dry matter (DM), crude protein (CP), ether extract (EE), crude ash, and zinc than the control group ($p < 0.05$). The Gly-Zn and zinc lactate groups had higher jejunal villus height and a higher villus height:crypt depth ratio than the control group ($p < 0.05$). In addition, the ZnSO4, Gly-Zn and zinc lactate groups had a significantly lower mRNA expression level of jejunal ZRT/IRT-like protein 4 (ZIP4) and higher mRNA expression level of jejunal interleukin-1β (IL-1β) than the control group ($p < 0.05$). The mRNA expression level of jejunal zinc transporter 2 (ZNT2) was higher and that of jejunal Bcl-2-associated X protein (Bax) was lower in the Gly-Zn and zinc lactate groups than in the control group ($p < 0.05$). Moreover, the zinc lactate group had a higher count of *Lactobacillus* spp. in the cecal digesta and higher mRNA expression levels of jejunal occludin and mucin 2 (MUC2) than the control group ($p < 0.05$). In conclusion, dietary supplementation with 100 mg/kg ZnSO4, Gly-Zn, or zinc lactate could improve the growth performance and gut barrier function of weaned piglets. Dietary supplementation with organic zinc, particularly zinc lactate, had the best effect.

Keywords: zinc source, growth performance, digestibility, gut health, weaned piglets

INTRODUCTION

In the weaning stage, piglets have weak cerebral cortex development and high metabolism and face high nutritional, environmental, and psychological stress, resulting in changes in intestinal digestion and absorption, immunity, and behavior, which manifest as diarrhea, growth retardation, and even death (Campbell et al., 2013). In recent years, weaning stress of piglets has been found to damage the intestinal mucosal barrier function of piglets and their innate immune response to pathogenic bacteria (Hu et al., 2013; Mclamb et al., 2013). The intestine is not only the main organ for the digestion and absorption of nutrients but also the largest organ in the immune system of animals. It has two critical functions: acting as a selective filter for essential nutrients and acting as a barrier against harmful substances (Karl Kunzelmann, 2002; Blikslager et al., 2007). Intestinal barrier dysfunction can cause intestinal microorganisms and endotoxins to break through the intestinal barrier and enter other organs and the circulatory system, resulting in intestinal infections and diseases, such as inflammatory bowel disease, food allergy, diarrhea, and ischemic disease (Torsten et al., 2001; Turner, 2006).

Zinc is an essential trace element that plays a crucial role in several biological processes (Bonaventura et al., 2015). It is an activator or a component of various enzymes in animals and is involved in intracellular signal transduction and cell proliferation, thereby affecting cellular function, acid–base balance, oxidation resistance, immune capacity, and reproduction (Vallee and Falchuk, 1993; Andreini et al., 2006). Moreover, zinc is beneficial for the regeneration of injured intestinal epithelial tissue and is thus necessary for normal intestinal barrier function (Alam et al., 1994). Dietary supplementation with zinc has been shown to reduce intestinal permeability and prevent the loss of intestinal integrity as a result of weaning, heat stress, malnutrition, and inflammatory bowel disease (Rodriguez et al., 1996; Zhang and Guo, 2009; Fernandez et al., 2014). Given these biological functions, zinc may be an attractive feed additive for improving gut health.

Dietary supplementation with inorganic or organic zinc is a common industry practice for meeting the dietary requirements of animals. Inorganic zinc sources, such as zinc sulphate (ZnSO4), have been used as the main nutrient source in feed for a long time (Sandra et al., 2020). In organic zinc sources, zinc binds to organic ligands, typically an organic acid, amino acid, or protein. Organic zinc sources have a relatively higher bioavailability than inorganic ones, allowing lower concentrations to be added to feed (Pearce et al., 2015; Li et al., 2018). Dietary supplementation with organic zinc has been found to improve the growth performance and intestinal health of animals (Levkut et al., 2017; Song et al., 2017; Yan et al., 2017). Zinc lactate, an organic zinc source, has been used as a new feed additive in production practices; however, the effect of zinc lactate on the intestinal health of weaned piglets has not been systematically studied. Moreover, the effects of zinc lactate on the growth performance and intestinal health of piglets need to be compared with those of other zinc sources commonly used in livestock production. Therefore, the objective of the present study was to systematically assess the effects of dietary zinc sources [ZnSO4, glycine zinc (Gly-Zn) and zinc lactate] on the growth performance, intestinal development, digestion and absorption, and intestinal barrier function of weaned piglets in order to further understand the mechanisms underlying the regulatory effects of different zinc sources on intestinal health.

MATERIALS AND METHODS

Animals, Management, and Diets

ZnSO4 was provided by Chengdu Shuxing Feed Co., Ltd. (No 147 Qingpu Road, Shouan, Sichuan, China). Gly-Zn was provided by Sichuan jilongda Biotechnology Group Co., Ltd. (No 111 Jinxing Road, Guanghan, Sichuan, China). Zinc lactate was provided by Sichuan Animtech Feed Co., Ltd. (No.7 Niusha Road, Chengdu, Sichuan, China).

In total, 96 healthy Duroc × Landrace × Yorkshire (DLY) weaned piglets (28 days old) with an initial average body weight of 8.81 ± 0.42 kg were randomly divided into four groups, with six replicates per treatment and four pigs per replicate, according to their initial body weight and sex. The dietary treatment groups were as follows: (1) control group, basal diet; (2) ZnSO4 group, basal diet +100 mg/kg ZnSO4; (3) Gly-Zn group, basal diet +100 mg/kg Gly-Zn; and (4) zinc lactate group, basal diet +100 mg/kg zinc lactate. The whole trial lasted for 28 days. On days 25–28, the digestion test was performed using acid insoluble ash (AIA) as an endogenous indicator.

The basal diets were formulated by using corn and soybean meal as the main ingredients. The experimental diet was prepared according to the nutrient recommendations of NRC (2012) for pigs weighing 7–11 kg (**Table 1**). No antibiotics were used in any diet. Piglets were penned by replicates in sties ($1.6 \times 1.5\ m^2$). The room temperature and relative humidity were controlled during the experimental period. All the piglets had *ad libitum* access to both feed and water. The health status of each pig was checked once a day.

Sample Collection

Using the quartering method, about 150 g of the experimental diet was taken for each treatment and stored in a refrigerator at −20°C until the analysis of nutrient contents. Fecal samples were collected from days 25 to 28 of the experiment to determine the apparent total tract digestibility (ATTD). After each collection, a few drops of toluene and 10% hydrochloric acid were added to the samples for antisepsis and nitrogen fixation. The fecal samples collected from days 25 to 28 from each replicate were thoroughly mixed and dried in a forced air oven at 60°C for 72 h. Following this, the dried samples were smashed and stored at −20°C to measure the nutrient contents.

At the end of day 28 of the experiment, one piglet with an average body weight was selected in each pen, anesthetized with 10 mg/kg body weight of Zoletil 50 (Beijing PET Technology Co., Ltd, Beijing, China), and slaughtered by exsanguination. Then, the abdomen was opened and the intestinal segments were rapidly separated. Following this, the intact duodenum,

TABLE 1 | Composition and nutrient level of basic diet (air dry basis %).

Ingredient	Content	Composition	Nutrient content
Corn	27.79	Calculated Composition	
Extruded corn	28.61	DE (MJ/kg)	3.55
Dehulled soybean meal	10.33	Crude protein	19.59
Extruded soybean	4.50	Calcium	0.81
Fish meal	0.50	Total phosphorus	0.57
Whey powder	8.00	Available phosphorus	0.37
Soybean protein concentrate	12.00	Lys	1.36
Soybean oil	1.90	Met+Cys	0.75
Sucrose	3.50	Thr	0.79
Limestone	0.91	Trp	0.23
Dicalcium phosphate	0.74	Analyzed composition	
Nacl	0.25	Crude protein	19.70
L-Lys-HCl (78%)	0.38	Crude ash	4.80
DL-Met (99%)	0.17	Dry matter	90.90
Trp (98%)	0.05	Ether extraction	6.20
Thr (98.5%)	0.02	Zinc[3]	0.002
Chloride choline	0.10		
Vitamin premix[1]	0.05		
Mineral premix[2]	0.20		
Total	100.00		

[1]The premix provides following per kg diet:VA 5512 IU, VD32250 IU, VE 24 mg, VK3 3 mg, VB2 6 mg, VB6 3 mg, VB12 24 μg, folic acid 1.2 mg, nicotinic acid 14 mg, biotin 150 μg, D-pantothenic acid 15 mg.

[2]The premix provides following per kg diet: Fe 100 mg, Cu 6 mg, Mn 4 mg, I 0.14 mg, Se 0.3 mg.

[3]Analyzed zinc content of experimental diets were as follows: 0.002% (Control group), 0.013% (ZnSO4 group), 0.012% (Gly-Zn group), 0.012% (Zinc lactate group), respectively.

jejunum, and ileum were taken and stored in 4% paraformaldehyde solution for intestinal morphology analysis and goblet cell number determination. The cecal digesta was then collected into sterile EP tubes for determining the bacteria count. Finally, the jejunal mucosa were separated for measuring intestinal development and barrier-related gene expression levels and immediately stored at −80°C.

Growth Performance

The body weight of each pig was recorded on days 0 and 28; weighing was performed before the pigs were fed. During the experiment, the amount of feed offered daily and the quantity remaining in the feeder the next morning were accurately recorded for each pen. Feed consumption was calculated as the amount of feed offered daily − the quantity remaining in the feeder the next morning − the amount of waste material. The values were used to calculate the average daily gain (ADG) and average daily feed intake (ADFI). The feed-to-gain ratio (F/G) was calculated on the basis of the ADG and ADFI values.

Diarrhea Rate

Diarrhea scores of all the piglets were recorded each afternoon for 28 days according to the following scoring system: 0 = normal, firm feces; 1 = possible slight diarrhea, soft and formed feces; 2 = moderate diarrhea, unformed and slightly fluid feces, and 3 = severe diarrhea, very watery feces (Hart and Dobb, 1988). Pigs with a score of 2 or 3 were considered to have diarrhea. The diarrhea rate was calculated using the following formula: diarrhea rate (%) = number of pigs with diarrhea in each pen/(number of pigs × total observation days) × 100 (Huang et al., 2004).

Histological Measurements

The duodenum, jejunum, and ileum, which were fixed in 4% paraformaldehyde solution for 8–24 h, were dehydrated, made transparent, and embedded to prepare paraffin sections with a thickness of 5 μm. Following this, the sections of the intestinal samples were stained with hematoxylin and eosin. Then, 10 well-oriented slices were selected for each sample and photographed for morphometric variables detection. The distance from the villus tip to the crypt mouth (villus height) and that from the crypt mouth to the base (crypt depth) was measured using an image processing and analysis system (Media Cybernetics, Bethesda, MD, United States). Moreover, the number of jejunal goblet cells was counted using an Olympus optical microscope after histochemical staining with Alcian blue and periodic acid-Schiff (Ab-PAS) stains (Kunert et al., 2002).

Apparent Total Tract Digestibility

Samples of the feed and feces were assessed to measure the contents of zinc (Chinese National Standard, GB/T 13885-2017), crude ash (method 942.05, AOAC, 1995), CP (method 990.03, AOAC, 1995), EE (method 945.16, AOAC, 1995), and DM (method 930.15, AOAC, 1995). The ATTD was measured using AIA as an endogenous indicator. AIA in diets and feces samples were determined by a method described by Chinese National Standard (GB/T 23742). ATTD was calculated using previously published formulae (Diao et al., 2017).

Total RNA Extraction, Reverse Transcription Reaction, and Real-Time Quantitative PCR

Total RNA was separated from frozen jejunal mucosa using TRIzol reagent (Takara Bio Inc., Dalian, China), according to the manufacturer's instructions. Following this, the RNA quality and purity were assessed by electrophoresis on 0.1% agarose gels. Subsequently, eligible RNA samples were reverse transcribed into complementary DNA using the PrimeScript™ Reverse Transcription Reagent Kit (Takara Bio Inc., Dalian, China). For the quantification of intestinal development-related genes (IGF-1, insulin-like growth factor 1; EGF, epidermal growth factor), cell apoptosis-related genes (Bcl-2, B-cell lymphoma/leukemia-2; Bax, Bcl-2-associated X protein), intestinal digestion- and absorption-related genes (SGLT-1, sodium/glucose cotransporter 1; GLUT-2, glucose transporter type 2; SLC_7A_1, solute carrier family 7; ZNT1, zinc transporter 1; ZNT2, zinc transporter 2; ZIP4, ZRT/IRT-like protein 4), and intestinal barrier-related genes (MUC1, mucin 1; MUC2, mucin 2; occludin; IL-10, interleukin-10; IL-1β, interleukin-1β), real-time PCR was performed using the CFX96 Real-Time

TABLE 2 | Primer sequences and annealing temperature of pigs.

Target gene	Forward and reverse primer (5′–3′)	Product length	Annealing temperature	Accession number
EGF	F:ATCTCAGGAATGGGAGTCAACC R: TCACTGGAGGATGGAATACAGC	165	60	NM_214020.1
IGF-1	F:CTGAGGAGGCTGGAGATGTACT R: CCTGAACTCCCTCTACTTGTGTTC	137	60	NM_001097417.1
Bax	F:AAGCGCATTGGAGATGAACT R: TGCCGTCAGCAAACATTTC	121	60	XM_013998624.1
Bcl-2	F:TGCCTTTGTGGAGCTGTATG R: GCCCGTGGACTTCACTTATG	144	60	XM_003121700.4
SGLT-1	F:GCAACAGCAAAGAGGAGCGTAT R: GCCACAAAACAGGTCATAGGTC	137	60	NM_001164021.1
GLUT-2	F:GACACGTTTTGGGTGTTCCG R: GAGGCTAGCAGATGCCGTAG	149	60	NM_001097417.1
SLC_7A_1	F:TCTTTGCAGGTCGTTTGGGA R: GGCTGATCACCTGTTGGAGT	137	60	NM_001012613.1
DMT1	F:GCAGGTGGTTGACGTCTGTA R: CACGCCCCCTTTGTAGATGT	100	60	NM_001128440.1
ZNT1	F:TGCTCTGCATGCTGTTACTGA R: TGGAAGGAGTCCGAGAGCAT	97	60	NM_001139470.1
ZNT2	F:GAGATGTGATCGTGGTGCTGATG R: CGCCCAGATATGCAGGTTGTGC	119	60	NM_001139475.1
ZIP4	F:CAGGGTCATCTGGGAAAGGAAGC R: CCGGCACTCAGGCACATCGTG	101	60	XM_001925360.3
Occludin	F:CAGGTGCACCCTCCAGATTG R: GGACTTTCAAGAGGCCTGGAT	110	60	NM_001163647.2
MUC1	F:GTGCCGCTGCCCACAACCTG R: AGCCGGGTACCCCAGACCCA	141	60	XM_001926883.5
MUC2	F:GGTCATGCTGGAGCTGGACAGT R: TGCCTCCTCGGGGTCGTCAC	181	60	XM_013989745.1
IL-10	F:CCTGGAAGACGTAATGCCGA R: CACGGCCTTGCTCTTGTTTT	148	60	NM_214041.1
IL-1β	F:ACGTGCAATGATGACTTTGTCTG R: AGAGCCTTCAGCATGTGTGG	113	60	NM_214055.1
β-actin	F:TCTGGCACCACACCTTCT R: TGATCTGGGTCATCTTCTCAC	114	60	DQ178122

PCR Detection System (Bio-Rad Laboratories, Richmond, CA, United States), according to a previously published method (Zhao et al., 2015). A 10 μl quantitative fluorescent PCR reaction volume was used in the present study; it consisted of 0.5 μl upstream primer, 0.5 μl downstream primer, 1 μl cDNA, 3 μl RNase-free H_2O, and 5 μl SYBR Premix Ex Taq™. The reaction cycle conditions were as follows: 30 s at 95°C, 10 s at 95°C, and 25 s at 60°C for a total of 39 cycles. Primer sequences are shown in **Table 2**; the primers were commercially synthesized by Invitrogen (Shanghai, China). The relative expression level of each gene in the jejunum was computed using β-actin as the reference gene.

Microbial Population Determination

Digesta from the cecum were collected, and bacterial DNA was extracted using commercial stool DNA kits (Omega Bio-Tek, Doraville, CA, United States). Fluorescent oligonucleotide probes and primers for total bacteria, *Lactobacillus* spp., *Escherichia coli.*, *Bifidobacterium* spp., and *Bacillus* spp. were acquired in accordance with previous reports (**Table 3**) for the quantitative detection of the aforementioned bacteria (Fierer et al., 2005; Qi et al., 2011), which were commercially synthesized by Invitrogen (Shanghai, China). Quantitative real-time PCR was performed using the CFX96 Real-Time PCR Detection System (Bio-Rad Laboratories, Richmond, CA, United States) with optical-grade 96-well plates. A 25 μl reaction mixture was used to determine the total bacterial count, and a 20 μl reaction mixture was used to determine the counts of *Lactobacillus* spp., *E. coli.*, *Bifidobacterium* spp., and *Bacillus* spp. The PCR conditions and calculation method were in accordance with those reported in a previous study (Qi et al., 2011).

Statistical Analysis

The experimental data have been tested for normality prior to one-way ANOVA was made using SAS software (version 8.2, SAS Inst. Inc., Cary, NC). When the data were recognized as normally distributed and exhibited homogeneity of variance, data were analyzed by one-way ANOVA and Duncan's multiple comparison. For data analysis, each pen was considered as an

TABLE 3 | Primes and probes for real-time PCR of bacteria.

Items	Primer/probe name and sequence(5′-3′)	Product length/bp
Escherichia coli	DC-F,CATGCCGCGTGTATGAAGAA DC-R,CGGGTAACGTCAATGAGCAAA DC-P,(FMA)AGGTATTAACTTTACTCCCTTCCTC(BHQ-1)	96
Lactobacillus	RS-F,GAGGCAGCAGTAGGGAATCTTC RS-R,CAACAGTTACTCTGACACCCGTTCTTC RS-P,(FMA)AAGAAGGGTTTCGGCTCGTAAAACTCTGTT(BHQ-1)	126
Bifidobacterium	SQ-F,CGCGTCCGGTGTGAAAG SQ-R,CTTCCCGATATCTACACATTCCA SQ-P, (FMA) ATTCCACCGTTACACCGGGAA(BHQ-1)	121
Bacillus	YB-F,GCAACGAGCGCAACCCTTGA YB-R,TCATCCCCACCTTCCTCCGGT YB-P, (FMA)CGGTTTGTCACCGGCAGTCACCT(BHQ-1)	92
Total bacteria	Eub338F,ACTCCTACGGGAGGCAGCAG Eub518R,ATTACCGCGGCTGCTGG	200

experimental unit. p values <0.05 were considered statistically significant. Results are expressed as the means and SEMs.

RESULTS

Growth Performance and Diarrhea Rate

The effects of dietary zinc sources on the growth performance and diarrhea rate in weaned piglets are shown in **Table 4**. Compared with the control group, the F/G decreased in the Gly-Zn and zinc lactate groups from days 0 to 28 ($p < 0.05$). However, a lower diarrhea rate was observed only in the zinc lactate group ($p < 0.05$). The ADG tended to be higher in the ZnSO4, Gly-Zn, and zinc lactate groups than in the control group ($p = 0.053$). No differences were observed in the ADFI among the four groups during the experimental period ($p > 0.05$).

Apparent Total Tract Digestibility

The effects of dietary zinc sources on the ATTD in weaned piglets are shown in **Table 5**. The ATTD of DM, CP, EE, and crude ash was significantly higher in the ZnSO4, Gly-Zn, and zinc lactate groups than in the control group ($p < 0.05$). The ATTD of zinc significantly differed among the three groups receiving dietary zinc supplementation; it was the highest in the zinc lactate group, followed by the Gly-Zn and ZnSO4 groups ($p < 0.05$).

Relative mRNA Expression Levels of Jejunal Transporters

As shown in **Figure 1**, the mRNA expression level of jejunal ZIP4 was significantly lower in the ZnSO4, Gly-Zn, and zinc lactate groups than in the control group ($p < 0.05$). The mRNA expression of jejunal ZNT2 was higher in the Gly-Zn and zinc lactate groups than in the control group ($p < 0.05$). However, the mRNA expression level of jejunal ZNT2 did not differ significantly between the ZnSO4 and control groups ($p > 0.05$). The mRNA expression level of jejunal ZNT1 tended to be higher in the ZnSO4, Gly-Zn, and zinc lactate groups than in the control group ($p = 0.067$). However, the mRNA expression level of jejunal GLUT-2 tended to be higher only in the Gly-Zn and zinc lactate groups than in the control group ($p = 0.064$). Moreover, the mRNA expression levels of jejunal SGLT-1 and SLC_7A_1 did not differ among the four groups ($p > 0.05$).

Intestinal Morphology

The villus height, crypt depth, and goblet cell number in small intestinal tissues are expressed in **Table 6** and **Figure 2**. The jejunal villus height and villus height:crypt depth ratio were higher in the Gly-Zn and zinc lactate groups than in the control group ($p < 0.05$). The numbers of goblet cells in the ileum ($p = 0.064$) and the villus height of the duodenum ($p = 0.094$) and ileum ($p = 0.060$) tended to be higher in the zinc lactate group than in the control group. In addition, the jejunal crypt depth tended to be lower in the ZnSO4 and zinc lactate groups than in the control group ($p = 0.079$).

Relative mRNA Expression Levels of Intestinal Development-Related Genes

The mRNA expression levels of intestinal development-related genes in the piglets are summarized in **Figure 3**. The Gly-Zn and zinc lactate groups had a lower mRNA expression level of jejunal Bax than the control group ($p < 0.05$). However, the mRNA expression level of jejunal Bax did not differ significantly between the ZnSO4 and control groups ($p > 0.05$). Moreover, the mRNA expression levels of jejunal Bcl-2, EGF, and IGF-1 did not differ among the four groups ($p > 0.05$).

Intestinal Barrier Function

As shown in **Figure 4**, the zinc lactate group had a higher mRNA expression level of the jejunal occludin gene than the control group ($p < 0.05$). Moreover, the Gly-Zn and zinc lactate groups had a higher mRNA expression level of the jejunal occludin than the ZnSO4 group ($p < 0.05$). The mRNA expression level of jejunal IL-1β was higher in the ZnSO4,

TABLE 4 | Effect of dietary zinc sources on the growth performance and diarrhea rate in weaned piglets.

Items	Control	ZnSO4	Gly-Zn	Zinc lactate	SEM	*P* values
Initial BW, kg	8.68	8.92	8.86	8.82	0.212	0.873
28-day BW, kg	17.25	18.31	17.87	17.89	0.441	0.444
ADFI (g)	517.41	534.41	496.54	508.78	16.040	0.442
ADG (g)	306.16	335.68	321.99	334.02	7.034	0.053
F/G	1.69^{a}	1.60^{ab}	1.54^{b}	1.52^{b}	0.031	0.021
Diarrhea rate	20.24^{a}	17.86^{ab}	13.53^{ab}	10.04^{b}	2.217	0.041

Control, basal diet. ZnSO4, basal diet + 100 mg/kg zinc sulphate. Gly-Zn, basal diet + 100 mg/kg glycine zinc. Zinc lactate, basal diet + 100 mg/kg zinc lactate. BW, body weight. ADFI, average daily feed intake. ADG, average daily gain. F/G, feed-to-gain ratio. SEM, standard error of the mean. a,b, Within a row, means without a common superscript letter differ (P < 0.05).

TABLE 5 | Effect of dietary zinc sources on the apparent total tract digestibility in weaned piglets.

Items	Control	ZnSO4	Gly-Zn	Zinc lactate	SEM	*P* values
EE	71.32^{b}	76.44^{a}	77.72^{a}	78.84^{a}	0.954	0.002
DM	84.56^{b}	87.59^{a}	87.60^{a}	87.71^{a}	0.344	0.001
Crude ash	60.55^{b}	67.64^{a}	69.45^{a}	70.12^{a}	0.588	<0.0001
CP	77.35^{b}	80.97^{a}	80.63^{a}	81.73^{a}	0.544	0.001
Zinc	2.08^{c}	10.27^{c}	27.91^{b}	42.95^{a}	2.212	<0.0001

Control, basal diet. ZnSO4, basal diet + 100 mg/kg zinc sulphate. Gly-Zn, basal diet + 100 mg/kg glycine zinc. Zinc lactate, basal diet + 100 mg/kg zinc lactate. EE, ether extract; DM, dry matter; CP, crude protein. SEM, standard error of the mean. a,b, Within a row, means without a common superscript letter differ (P < 0.05).

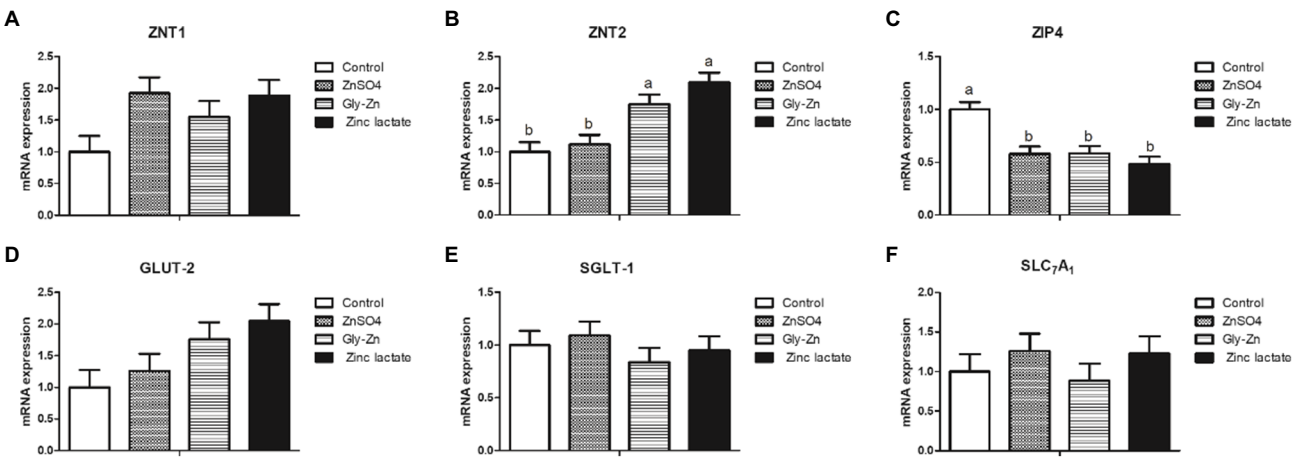

FIGURE 1 | Effect of dietary zinc sources on the relative mRNA expression levels of jejunal digestion- and absorption-related genes in weaned piglets. Control, basal diet. ZnSO4, basal diet +100 mg/kg zinc sulphate. Gly-Zn, basal diet +100 mg/kg glycine zinc. Zinc lactate, basal diet +100 mg/kg zinc lactate. The relative mRNA expression levels of jejunal zinc transporter 1 (ZNT1; **A)**, zinc transporter 2 (ZNT2; **B)**, ZRT/IRT-like protein 4 (ZIP4; **C)**, glucose transporter type 2 (GLUT-2; **D)**, sodium/glucose cotransporter 1 (SGLT-1; **E)**, and solute carrier family 7 (SLC_7A_1; **F)** were determined by real-time quantitative PCR. ^{a,b} Within a row, means without a common superscript letter differ ($p < 0.05$).

Gly-Zn, and zinc lactate groups than in the control group ($p < 0.05$). In addition, the mRNA expression level of jejunal IL-10 tended to be higher in the ZnSO4, Gly-Zn, and zinc lactate groups than in the control group ($p = 0.087$). The mRNA expression level of jejunal MUC2 was higher in the zinc lactate group than in the control group ($p < 0.05$). However, the mRNA expression level of jejunal MUC2 did not differ significantly among the ZnSO4, Gly-Zn, and control groups ($p > 0.05$).

As shown in **Table 7**, the total bacterial count in the cecal digesta was higher in the ZnSO4, Gly-Zn, and zinc lactate groups than in the control group ($p < 0.05$). The zinc lactate group had a higher count of *Lactobacillus* spp. in the cecal digesta than the control group ($p < 0.05$). However, the count of *E. coli* in the cecal digesta tended to be lower in the Gly-Zn and zinc lactate groups than in the control group ($p = 0.075$).

DISCUSSION

Zinc is a component of various enzymes in animals; it has important physiological and nutritional functions for animal growth, reproduction, and immunity. It also exhibits cell growth-promoting and antioxidant effects (Bonaventura et al., 2015). Zinc depletion tests have confirmed that zinc deficiency can result in lower ADG, decreased growth hormone synthesis, and reduced production of IGF-1 induced by growth hormone, thereby impairing the growth of piglets (Swinkels et al., 1996). In the present study, the ADG in the zinc supplementation groups (ZnSO4, Gly-Zn, and zinc lactate groups) was higher than that in the control group, indicating a beneficial effect of zinc on growth performance. On comparing different zinc sources, organic zinc sources were found to have a relatively higher bioavailability than inorganic ones (Pearce et al., 2015; Li et al., 2018). In a previous study, weaned piglets fed 20–120 mg

TABLE 6 | Effect of dietary zinc sources on the intestinal morphology and number of goblet cells in weaned piglets.

Items	Control	ZnSO4	Gly-Zn	Zinc lactate	SEM	*P* values
Duodenum						
Villus height, μm	352.75	381.74	412.31	442.35	24.132	0.094
Crypt depth, μm	145.74	139.89	142.07	144.08	6.417	0.925
Villus height: crypt depth	2.59	2.74	2.91	2.95	0.206	0.602
Jejunum						
Villus height, μm	332.86^{b}	354.33^{ab}	414.85^{a}	416.92^{a}	16.507	0.004
Crypt depth, μm	159.69	125.63	140.91	126.22	9.649	0.079
Villus height: crypt depth	2.46^{b}	2.85^{ab}	2.95^{a}	3.21^{a}	0.117	0.004
Ileum						
Villus height, μm	309.84	332.10	321.14	382.55	18.325	0.060
Crypt depth, μm	146.44	148.79	147.40	139.51	7.486	0.822
Villus height: crypt depth	2.66	2.78	2.69	3.07	0.132	0.152
Goblet cells	316.56	339.56	330.67	387.72	17.856	0.064

Control, basal diet. ZnSO4, basal diet + 100 mg/kg zinc sulphate. Gly-Zn, basal diet + 100 mg/kg glycine zinc. Zinc lactate, basal diet + 100 mg/kg zinc lactate. SEM, standard error of the mean. a,b, Within a row, means without a common superscript letter differ (P < 0.05).

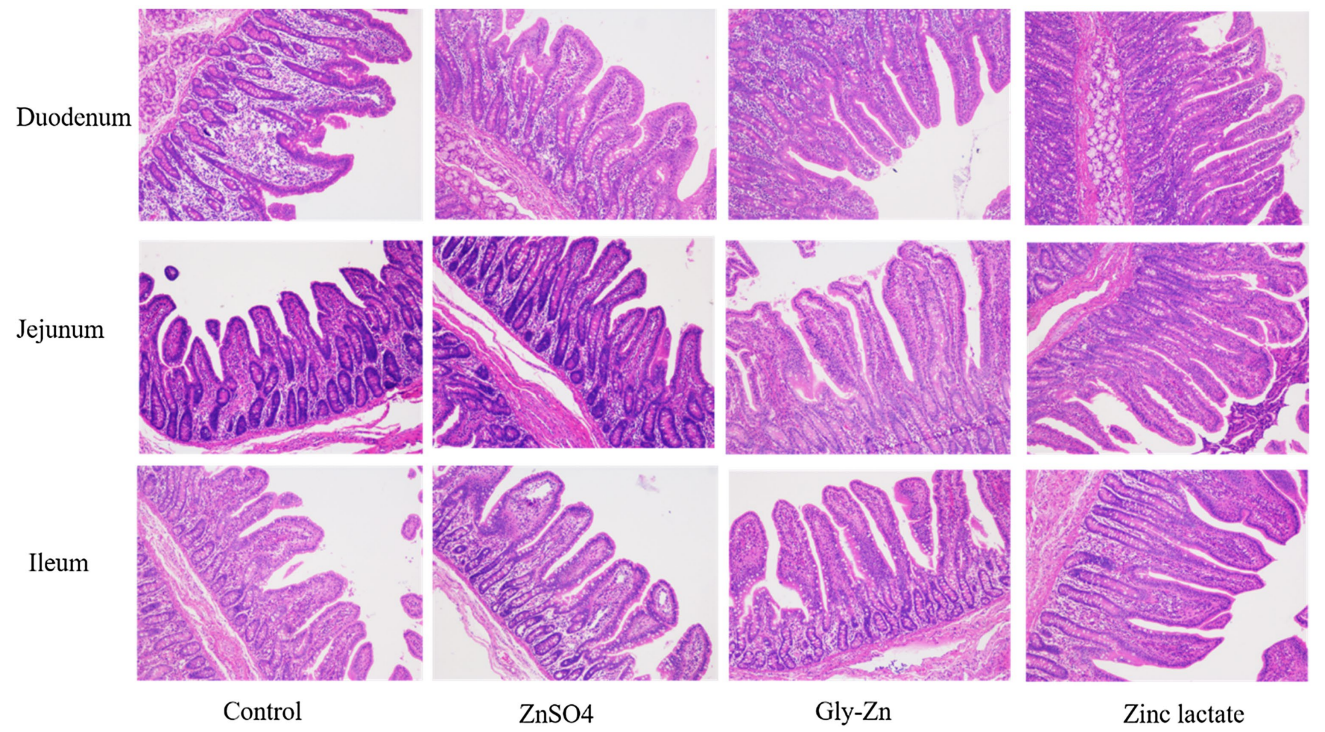

FIGURE 2 | Effect of dietary zinc sources on intestinal morphology (images) in weaned piglets. Control, basal diet. ZnSO4, basal diet +100 mg/kg zinc sulphate. Gly-Zn, basal diet +100 mg/kg glycine zinc. Zinc lactate, basal diet +100 mg/kg zinc lactate.

Zn/kg in an organic form (zinc amino acid [ZnAA]) were found to have a lower F/G than those in the unsupplemented group, while no differences were noted between the inorganic zinc-supplemented and unsupplemented groups (Zhang et al., 2017). Under nursery conditions, dietary supplementation with 500 mg/kg polysaccharide zinc complex had the same effect as that supplemented with 3,000 mg/kg pharmacological zinc oxide on enhancing the growth performance of piglets (Case and Carlson, 2002). In another study, broilers fed diets supplemented with 60 mg/kg ZnAA complexes had a lower F/G in the starter phase than those fed diets supplemented with ZnSO4 (Chand et al., 2020; Grande et al., 2020). Similarly, the organic form of zinc (zinc lactate) was found to be superior in improving the growth of young grass carp (Song et al., 2017). In the present study, compared with the control group, the F/G decreased in the organic zinc-supplemented groups (Gly-Zn and zinc lactate groups) from days 0 to 28; these findings are generally consistent with those of the aforementioned

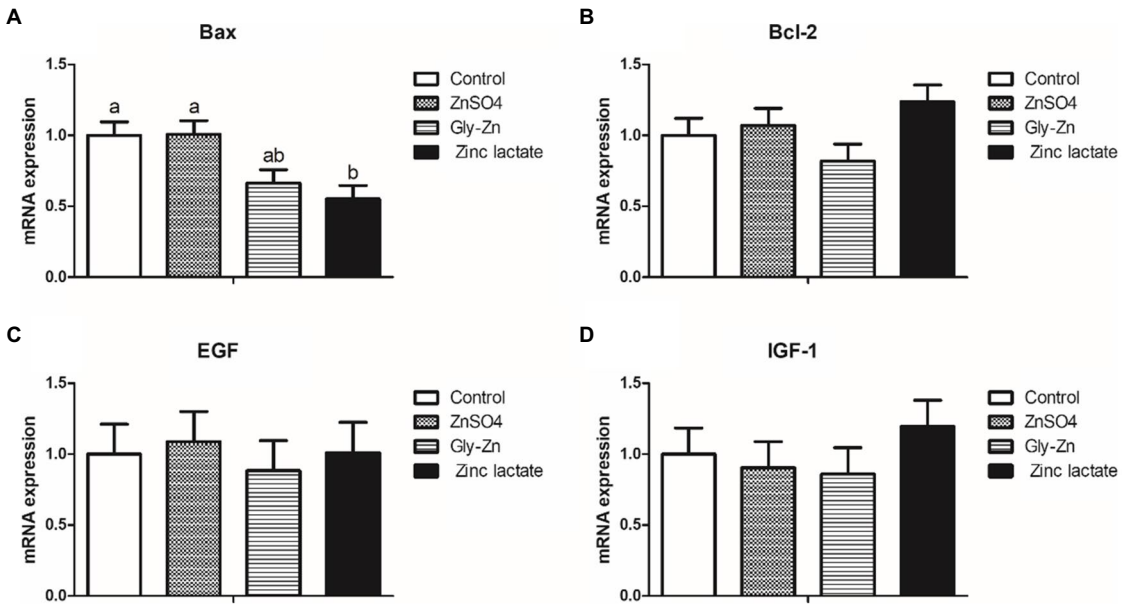

FIGURE 3 | Effect of dietary zinc sources on the relative messenger RNA (mRNA) expression levels of intestinal development-related genes in weaned piglets. Control, basal diet. ZnSO4, basal diet +100 mg/kg zinc sulphate. Gly-Zn, basal diet +100 mg/kg glycine zinc. Zinc lactate, basal diet +100 mg/kg zinc lactate. The relative mRNA expression levels of jejunal Bcl-2-associated X protein (Bax; **A)**, B-cell lymphoma/leukaemia-2 (Bcl-2; **B)**, epidermal growth factor (IGF-1; **C)**, and insulin-like growth factor-1 (IGF-1; **D)** were determined by real-time quantitative PCR. ^{a,b} Within a row, means without a common superscript letter differ ($p < 0.05$).

studies. Moreover, zinc deficiency could alter paracellular ionic conductance, cause perturbed barrier integrity and reduce Cl^- secretion, resulting in increased susceptibility to infection (Sarkar et al., 2018). Thus, adequate levels are required to maintain the gut barrier, avoid risk intestinal infections, and prevent diarrhea. However, a lower diarrhea rate was observed only in the zinc lactate group in the present study, suggesting that zinc lactate has a more beneficial effect on intestinal health than Gly-Zn.

In the present study, the ATTD of DM, CP, EE, and crude ash was found to be increased in pigs fed 100 mg/kg zinc, regardless of the zinc source. However, the ATTD of zinc significantly differed among the three groups receiving dietary zinc supplementation; it was the highest in the zinc lactate group, followed by the Gly-Zn and ZnSO4 groups. In general, the improvement in nutrient digestibility is accompanied by the elevation in growth performance; this was mutually confirmed by improved growth performance in the present study. Consistent with our result, dietary supplementation with 60 mg/kg ZnAA complexes was found to result in better digestibility of zinc than supplementation with ZnSO4 in young broilers in a previous study (Zhang et al., 2017). Supplementation with different zinc sources (zinc lactate, Gly-Zn, and ZnSO4) did not affect the digestibility of other nutrients (DM, CP, EE, and crude ash) in the present study; these findings are in accordance with those of previous studies comparing the supplementation of Gly-Zn and ZnSO4 (Ma et al., 2011; Kwiecień et al., 2017). The ZnT family, which is responsible for decreasing the concentration of zinc ions in the cytoplasm, and the ZIP family, which is responsible for increasing the concentration of zinc ions in the cytoplasm, play important roles in the absorption and transport of zinc ions (Nies, 2007). In the present study, dietary supplementation with 100 mg/kg ZnSO4, Gly-Zn, or zinc lactate decreased the mRNA expression level of jejunal ZIP4 in weaned piglets. The mRNA expression level of jejunal ZNT2 was higher in the Gly-Zn and zinc lactate groups than in the control group; these findings are consistent with those of a previous *in vitro* study (Huang et al., 2016). A study conducted using a pig model also revealed that the addition of zinc lactate to the medium could upregulate the mRNA expression level of ZNT2 and downregulate the mRNA expression level of ZIP4 (Wang et al., 2014). It has been reported that zinc has acquired an insulin-like activity (Tang and Shay, 2001). A higher mRNA expression level of jejunal GLUT-2 was observed in the Gly-Zn and zinc lactate groups in the present study, indicating that organic zinc may stimulate higher glucose transporter expression and lower blood glucose levels.

Weaning stress disturbs the intestinal health balance, which is characterized by villous atrophy and crypt hyperplasia, in addition to a reduction in epithelial brush border activity and nutrient digestibility (Montagne et al., 2003; Wang et al., 2006). Consequently, maintaining intestinal morphological properties for digesting various nutrients after weaning is important. In the present study, the jejunal villus height and villus height:crypt depth ratio were higher in the Gly-Zn and zinc lactate groups than in the control group. Moreover, the villus heights of the duodenum and ileum were higher in the zinc lactate group than in the control group. In accordance with our findings, dietary supplementation with 100 mg/kg zinc lactate was found

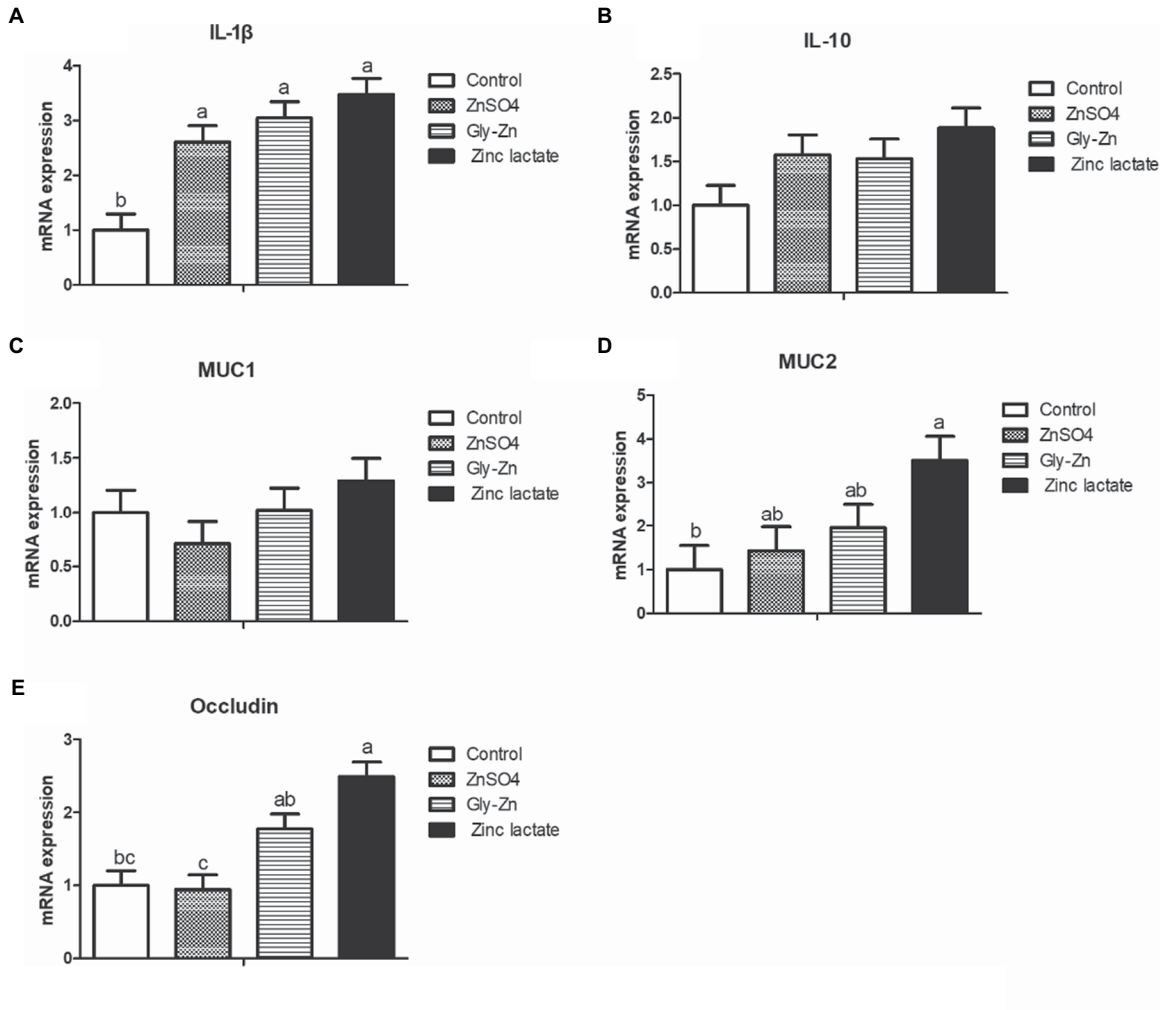

FIGURE 4 | Effect of dietary zinc sources on the relative mRNA expression levels of jejunal barrier-related genes in weaned piglets. Control, basal diet. ZnSO4, basal diet +100 mg/kg zinc sulphate. Gly-Zn, basal diet +100 mg/kg glycine zinc. Zinc lactate, basal diet +100 mg/kg zinc lactate. The relative mRNA expression levels of jejunal interleukin-1β (IL-1β; **A)**, interleukin-10 (IL-10; **B)**, mucin 1 (MUC1; **C)**, mucin 2 (MUC2; **D)**, and Occludin; **E)** were determined by real-time quantitative PCR. [a,b] Within a row, means without a common superscript letter differ ($p < 0.05$).

TABLE 7 | Effect of dietary zinc source on the numbers of *Escherichia coli*, *Lactobacilli* spp., *Bifidobacterium* spp., and *Bacillus* spp. in the cecal digesta of weaned piglets (log [copies/g]).

Items	Control	ZnSO4	Gly-Zn	Zinc lactate	SEM	*P* values
Total bacteria	9.90[b]	11.05[a]	11.04[a]	11.53[a]	0.276	0.006
Bacillus spp.	8.17	8.60	8.63	8.50	0.140	0.126
Lactobacillus spp.	6.79[b]	6.93[b]	7.50[ab]	8.03[a]	0.177	0.001
Escherichia coli	9.72	9.77	9.14	9.20	0.198	0.075
Bifidobacterium spp.	5.28	5.72	5.65	5.81	0.290	0.601

Control, basal diet. ZnSO4, basal diet + 100 mg/kg zinc sulphate. Gly-Zn, basal diet + 100 mg/kg glycine zinc. Zinc lactate, basal diet + 100 mg/kg zinc lactate. SEM, standard error of the mean. a,b Within a row, means without a common superscript letter differ (p < 0.05).

to significantly increase the villus height and decrease the crypt depth of the duodenum, jejunum, and ileum in weaned piglets in a previous study, thereby improving the morphology and function of the intestinal epithelium (Wang et al., 2014). Similarly, dietary supplementation with 90 mg/kg Gly-Zn increased the villus height of the duodenum and jejunum and decreased the crypt depth of the jejunum and ileum in 42-day-old chickens in another study (Ma et al., 2011). Intestinal morphology is directly proportional to digestibility and, consequently, to feed conversion efficiency (Collett, 2012).

Therefore, the improved intestinal morphology may partly explain the lowered F/G and increased digestibility of zinc on dietary supplementation with Gly-Zn or zinc lactate. On the other hand, the improvement in intestinal epithelial morphology caused by supplementation with organic zinc may be related to the promotion of intestinal epithelial cell development. *In vitro*, zinc lactate could significantly promote the proliferation of the porcine jejunal epithelial cells IPEC-J2 after 48 h of inoculation, and the proliferation amplitude was elevated with an increase in zinc lactate concentrations (Han et al., 2012). Meanwhile, zinc lactate could significantly reduce the cell apoptosis rate and the expression level of apoptotic protein in IPEC-J2 cells induced by hydrogen peroxide (Tang et al., 2020). In our present study, a lower mRNA expression level of jejunal *Bax* (a pro-apoptotic gene) was observed in the zinc lactate group, indicating that zinc lactate may promote intestinal morphology by promoting cell proliferation and inhibiting cell apoptosis.

Intestinal barrier integrity is primarily maintained by the tight junctions. Zinc deficiency causes the release of zinc bound to proteins and increases the content of free zinc in the cytoplasm, resulting in the inhibition of cell growth, disruption of tight junction proteins, and the subsequent impairment of intestinal barrier function (Zhong et al., 2010). In an *in vitro* study, compared with ZnSO4, 300 μmol zinc butyrate could increase transmembrane resistance and maintain the integrity of tight junctions in IPEC-J2 cells, indicating that zinc butyrate could alleviate the increased permeability of IPEC-J2 cells induced by heat stress (Mani et al., 2019). Sanz Fernandez et al. (2014) revealed that the transepithelial resistance of the ileum was 56% higher in the ZnAA complex group than in the ZnSO4 group (Fernandez et al., 2014). In grass carp, compared with the 56.9 mg/kg ZnSO4 group, dietary supplementation with 49.84 mg/kg zinc lactate upregulated the mRNA expression levels of occludin, ZO-1, claudin-B, claudin-C, claudin-F, claudin-3, claudin-7A, claudin-7B, claudin-11, claudin-12, and claudin-15A genes in the intestine (Song et al., 2017). Consistent with previous findings, we found that the mRNA expression level of the jejunal occludin was higher in the zinc lactate group than in the control and ZnSO4 groups. Myosin light-chain kinase (MLCK) is the most important calmodulin kinase affecting the barrier function of the intestinal mucosal epithelium (Nalle et al., 2011). Tumor necrosis factor-α (TNF-α) induces the expression of MLCK and phosphorylated myosin light chains, resulting in a loss of intercellular tight junctions and further increasing intestinal epithelial permeability through paracellular pathways (Mckenzie and Ridley, 2007). Previous studies have demonstrated that organic zinc can downregulate the expression of TNF-α in the intestine (Li, 2015; Song et al., 2017). Therefore, it is speculated that organic zinc can maintain the normal tight junctions of intestinal epithelial cells by inhibiting the TNF-α-induced upregulation of MLCK expression.

Among the chemical barrier components of the intestinal mucosa, MUC2, which is mainly secreted by cup cells, is the main component of intestinal mucus and plays an important role in lubricating the intestinal tract, in providing adhesion sites for intestinal antibacterial proteins and symbiotic flora and in resisting the invasion of intestinal pathogens and harmful substances (Hasnain et al., 2010). Compared with ZnSO4, protein-chelated zinc was found to significantly increase the number of intraepithelial goblet cells in the duodenum and jejunum of growing-finishing pigs (Zhou, 2009). In a previous study, dietary supplementation with 30 mg/kg Gly-Zn or ZnSO4 upregulated the mRNA expression level of jejunal *MUC2* in broilers. The mRNA expression level of *MUC2* in the Gly-Zn group tended to be higher than that in the ZnSO4 group (Levkut et al., 2017); these findings are in accordance with those of the present study. In the present study, supplementation with zinc lactate increased the number of goblet cells in the ileum and upregulated the transcription level of *MUC2* in the intestine, indicating that zinc lactate could also improve the intestinal chemical barrier function in weaned piglets.

The intestinal tract is the largest organ in the immune system of animals, and maintaining normal intestinal barrier function is extremely important for good intestinal health (Chassaing et al., 2014). Long-term zinc deficiency leads to the infiltration of inflammatory cells, particularly the uncontrolled migration of epithelial multinucleated lymphocytes, in the intestinal mucosa, thereby inducing mucosal injury and damaging the intestinal immune barrier (Finamore et al., 2008). Moreover, zinc deficiency can reduce the proliferation of T lymphocytes and B lymphocytes in mice, weaken their ability to deal with the invasion of exogenous pathogenic microorganisms and damage their immune system (Srinivas et al., 1989). Cytokines have momentous effects on immune responses and are involved in regulating intestinal barrier integrity (Al-Sadi, 2009). Zinc promotes the adhesion of monocytes to endothelial cells; this is important for the production of inflammatory cytokines, such as IL-1β, IL-6, and TNF-α (Chavakis et al., 1999). Consistently, higher mRNA expression levels of jejunal *IL-1β* and *IL-10* were observed following zinc supplementation in the present study, indicating that dietary supplementation with 100 mg/kg zinc can improve intestinal immune function in weaned piglets. Very limited studies have assessed the effects of different zinc sources on the intestinal immune barrier. In grass carp, compared with the 56.9 mg/kg ZnSO4 group, dietary supplementation with 49.84 mg/kg zinc lactate was found to upregulate the mRNA expression level of *IL-10* in the intestine (Song et al., 2017). However, there was no difference in the effect of different zinc sources on inflammatory cytokines; this could be related to zinc levels, animal species, period, and health status, among others.

The digestive tract of animals has evolved into a key site for the coexistence of nutrients and microorganisms. The intestinal biological barrier is formed by a large number of normal microflora, and the intestinal microecological balance is crucial for the normal function of the intestinal biological barrier (Shanahan, 2002). Zinc is an essential mineral element involved in the colonization and proliferation of microorganisms in the host. Chronic dietary zinc depletion induces significant

taxonomic alterations in the intestinal microflora and decreases the overall species richness and diversity, thereby establishing a microbial profile resembling that of various pathological states (Spenser et al., 2015). In the present study, dietary supplementation with 100 mg/kg zinc increased the total bacterial count in the cecal digesta of weaned piglets. As we did not assess the microbial diversity in the cecal digesta, the effects of different zinc sources on the intestinal microbial diversity need to be studied further. Another intriguing finding of the present study was that the count of *Lactobacillus* spp. in the cecal digesta was higher in the zinc lactate group than in the control group. Moreover, the count of *E. coli* in the cecal digesta was lower in the Gly-Zn and zinc lactate groups than in the control group. The alteration in and balance between beneficial bacteria (such as *Lactobacillus* spp.) and harmful bacteria (such as pathogenic *E. coli*) in the gut are associated with the gut health of the host (Diao et al., 2015). *E. coli* has been reported to destabilize and dissociate tight junction proteins (Muza-Moons et al., 2004). In the present study, the increased mRNA expression level of the occludin gene observed in the zinc lactate group was in accordance with the decreased *E. coli* count. Collectively, these findings suggest that zinc lactate could maintain the balance of the gut microbiota and improve the intestinal barrier.

CONCLUSION

In conclusion, dietary supplementation with 100 mg/kg ZnSO4, Gly-Zn, or zinc lactate could improve the growth performance of weaned pigs, at least partly, by improving the digestion of nutrients, intestinal morphology, and barrier function. Dietary supplementation with organic zinc, particularly zinc lactate, was found to have the best effect. However, the mRNA expression levels of zinc transporters were not consistent between the groups receiving dietary supplementation with inorganic and organic zinc, indicating possible differences in the absorption and transport channels.

DATA AVAILABILITY STATEMENT

The original contributions presented in the study are included in the article/supplementary material, further inquiries can be directed to the corresponding author.

ETHICS STATEMENT

The animal study was reviewed and approved by Animal Care Advisory Committee of Sichuan Academy of Animal Science.

AUTHOR CONTRIBUTIONS

HD, JY, and SL conceived the study, designed, and performed the experiments, including chemical analysis, analyzed the experimental data, and wrote the manuscript. WT was responsible for conceptualization. SK and JZ verified the validity of the experiments and checked the results. XW, MZ, CH, and PH participated in the experimental design and gave important intellectual advice for approval. All the authors read and approved the final version of the manuscript.

FUNDING

The present study was financially supported by the Sichuan Science and Technology Programmes (2020YFH0170, 2021ZHYZ0005, and 2021NZZJ0019).

ACKNOWLEDGMENTS

The authors wish to thank GW Zhang and ZG Luo from the College of Animal Science, Southwest University, for the elaborate animal examination and surgery.

REFERENCES

Alam, A. N., Sarker, S. A., Wahed, M. A., Khatun, M., and Rahaman, M. M. (1994). Enteric protein loss and intestinal permeability changes in children during acute shigellosis and after recovery: effect of zinc supplementation. *Gut* 35, 1707–1711. doi: 10.1136/gut.35.12.1707

Al-Sadi, R. (2009). Mechanism of cytokine modulation of epithelial tight junction barrier. *Front. Biosci.* 14, 2765–2778. doi: 10.2741/3413

Andreini, C., Banci, L., Bertini, I., and Rosato, A. (2006). Counting the zinc-proteins encoded in the human genome. *J. Proteome Res.* 5, 196–201. doi: 10.1021/pr050361j

AOAC. (1995). "Official methods of analysis," in *Association of Official Analytical Chemists. 16th Edn.* Washington, DC, USA.

Blikslager, A. T., Moeser, A. J., Gookin, J. L., Jones, S. L., and Odle, J. (2007). Restoration of barrier function in injured intestinal mucosa. *Physiol. Rev.* 87, 545–564. doi: 10.1152/physrev.00012.2006

Bonaventura, P., Benedetti, G., Albarède, F., and Miossec, P. (2015). Zinc and its role in immunity and inflammation. *Autoimmun. Rev.* 14, 277–285. doi: 10.1016/j.autrev.2014.11.008

Campbell, J. M., Crenshaw, J. D., and Polo, J. (2013). The biological stress of early weaned piglets. *J. Anim. Sci. Biotechnol.* 4, 45–48. doi: 10.1186/2049-1891-4-19

Case, C., and Carlson, M. (2002). Effect of feeding organic and inorganic sources of additional zinc on growth performance and zinc balance in nursery pigs. *J. Anim. Sci.* 80, 1917–1924. doi: 10.2527/2002.8071917x

Chand, N., Zahirullah, R. U. K., Shah, M., Naz, S., and Tinelli, A. (2020). Zinc source modulates zootechnical characteristics, intestinal features, humoral response, and paraoxonase (PON1) activity in broilers. *Trop. Anim. Health Prod.* 52, 511–515. doi: 10.1007/s11250-019-02036-4

Chassaing, B., Kumar, M., Baker, M. T., Singh, V., and Vijay-Kumar, M. (2014). Mammalian gut immunity, Mammalian gut immunity. *Biomed. J.* 37, 246–258. doi: 10.4103/2319-4170.130922

Chavakis, T., May, A. E., Preissner, K. T., and Kanse, S. M. (1999). Molecular mechanisms of zinc-dependent leukocyte adhesion involving the urokinase receptor and β2-Integrins. *Blood* 93, 2976–2983. doi: 10.1182/blood.V93.9.2976

Collett, S. R. (2012). Nutrition and wet litter problems in poultry. *Anim. Feed Sci. Technol.* 173, 65–75. doi: 10.1016/j.anifeedsci.2011.12.013

Diao, H., Gao, Z. B., Yu, B., Zheng, P., He, J., Yu, J., et al. (2017). Effects of benzoic acid (VevoVitall) on the performance and jejunal digestive physiology in young pigs. *J. Anim. Sci. Biotechnol.* 7, 32–160. doi: 10.1186/s40104-016-0091-y

Diao, H., Zheng, P., Yu, B., He, J., Mao, X. B., Yu, J., et al. (2015). Effects of benzoic acid and thymol on growth performance and gut characteristics of weaned piglets. *Asian Austral. J. Anim. Sci.* 28, 827–839. doi: 10.5713/ajas.14.0704

Fernandez, M. V. S., Pearce, S. C., Gabler, N. K., Patience, J. F., and Baumgard, L. H. (2014). Effects of supplemental zinc amino acid complex on gut integrity in heat-stressed growing pigs. *Animal* 8, 43–50. doi: 10.1017/S1751731113001961

Fierer, N., Jackson, J. A., Vilgalys, R., and Jackson, R. B. (2005). Assessment of soil microbial community structure by use of taxon-specific quantitative PCR assays. *Appl. Environ. Microbiol.* 71, 4117–4120. doi: 10.1128/AEM.71.7.4117-4120.2005

Finamore, A., Massimi, M., Conti Devirgiliis, L., and Mengheri, E. (2008). Zinc deficiency induces membrane barrier damage and increases neutrophil transmigration in Caco-2 cells. *J. Nutr.* 138, 1664–1670. doi: 10.1093/jn/138.9.1664

Grande, A. D., Leleu, S., Delezie, E., Rapp, C., and Ducatelle, R. (2020). Dietary zinc source impacts intestinal morphology and oxidative stress in young broilers. *Poult. Sci.* 99, 441–453. doi: 10.3382/ps/pez525

Han, G. Q., Yu, B., Chen, D. W., Xiang, Z. T., Qi, H. W., Chen, H., et al. (2012). Effect of zinc lactate on cell proliferation and related-regulator genes mRNA expression in porcine jejunal epithelial cells IPEC-J2. *Acta Veterinaria et Zootechnica Sinica.* 43, 740–747.

Hart, G. K., and Dobb, G. J. (1988). Effect of a fecal bulking agent on diarrhea during enteral feeding in the critically Ill. *JPEN-Parenter Enter.* 12, 465–468. doi: 10.1177/0148607188012005465

Hasnain, S. Z., Wang, H., Ghia, J. E., Haq, N., Deng, Y., Velcich, A., et al. (2010). Mucin gene deficiency in mice impairs host resistance to an enteric parasitic infection. *Gastroenterology* 138, 1763.e5–1771.e5. doi: 10.1053/j.gastro.2010.01.045

Hu, C. H., Xiao, K., Luan, Z. S., and Song, J. (2013). Early weaning increases intestinal permeability, alters expression of cytokine and tight junction proteins, and activates mitogen-activated protein kinases in pigs. *J. Anim. Sci.* 91, 1094–1101. doi: 10.2527/jas.2012-5796

Huang, C., Qiao, S., Li, D., Piao, X., and Ren, J. (2004). Effects of lactobacilli on the performance, diarrhea incidence, VFA concentration and gastrointestinal microbial flora of weaning pigs. *Asian Austral. J. Anim. Sci.* 17, 401–409. doi: 10.5713/ajas.2004.401

Huang, D., Zhuo, Z., Fang, S., Yue, M., and Feng, J. (2016). Different zinc sources have diverse impacts on gene expression of zinc absorption related transporters in intestinal porcine epithelial cells. *Biol. Trace Elem. Res.* 173, 325–332. doi: 10.1007/s12011-016-0655-x

Karl Kunzelmann, M. M. (2002). Electrolyte transport in the mammalian colon: mechanisms and implications for disease. *Physiol. Rev.* 82, 245–289. doi: 10.1152/physrev.00026.2001

Kunert, K. S., Tisdale, A. S., and Gipson, I. K. (2002). Goblet cell numbers and epithelial proliferation in the conjunctiva of patients with dry eye syndrome treated with cyclosporine. *Arch. Ophthalmol.* 120, 330–337. doi: 10.1001/archopht.120.3.330

Kwiecień, M. G., Winiarska-Mieczan, A., Milczarek, A., and Klebaniuk, R. (2017). Biological response of broiler chickens to decreasing dietary inclusion levels of zinc glycine chelate. *Biol. Trace Elem. Res.* 175, 204–213. doi: 10.1007/s12011-016-0743-y

Levkut, M., Husáková, E., Bobíková, K., Karaffová, V., Levkutová, M., Ivanišinová, O., et al. (2017). Inorganic or organic zinc and MUC-2, IgA, IL-17, TGF-β4 gene expression and sIgA secretion in broiler chickens. *Food Agric. Immunol.* 28, 801–811. doi: 10.1080/09540105.2017.1313202

Li, C.W. (2015). Effects of dietary zinc nutrition of the broiler breeders on the immunity function of their offsprings and the related molecular mechanism. docter's thesis. Beijing. China Agricultural University.

Li, L. L., Gong, Y. J., Zhan, H. Q., Zheng, Y. X., and Zou, X. T. (2018). Effects of dietary Zn-methionine supplementation on the laying performance, egg quality, antioxidant capacity, and serum parameters of laying hens. *Poult. Sci.* 98, 923–931. doi: 10.3382/ps/pey440

Ma, W., Niu, H., Feng, J., Wang, Y., and Feng, J. (2011). Effects of zinc glycine chelate on oxidative stress, contents of trace elements, and intestinal morphology in broilers. *Biol. Trace Elem. Res.* 142, 546–556. doi: 10.1007/s12011-010-8824-9

Mani, V., Rubach, J. K., Sanders, D. J., Pham, T., Koltes, D. A., Gabler, N. K., et al. (2019). Evaluation of the protective effects of zinc butyrate in IPEC-J2 cells and grower pigs under heat stress. *Transl. Anim. Sci.* 3, 842–854. doi: 10.1093/tas/txz023

Mckenzie, J. A. G., and Ridley, A. J. (2007). Roles of Rho/ROCK and MLCK in TNF-α-induced changes in endothelial morphology and permeability. *J. Cell. Physiol.* 213, 221–228. doi: 10.1002/jcp.21114

Mclamb, B. L., Gibson, A. J., Overman, E. L., Stahl, C., Moeser, A. J., and Colette, K. L. (2013). Early weaning stress in pigs impairs innate mucosal immune responses to enterotoxigenic *E. coli* challenge and exacerbates intestinal injury and clinical disease. *PloS One* 8:e59838. doi: 10.1371/journal.pone.0059838

Montagne, L., Pluske, J. R., and Hampson, D. J. (2003). A review of interactions between dietary fibre and the intestinal mucosa, and their consequences on digestive health in young non-ruminant animals. *Anim. Feed Sci. Technol.* 108, 95–117. doi: 10.1016/S0377-8401(03)00163-9

Muza-Moons, M. M., Schneeberger, E. E., and Hecht, G. A. (2004). Enteropathogenic Escherichia coli infection leads to appearance of aberrant tight junctions strands in the lateral membrane of intestinal epithelial cells. *Cell. Microbiol.* 6, 783–793. doi: 10.1111/j.1462-5822.2004.00404.x

Nalle, S. C., Joseph, N. E., Savage, P. A., and Turner, J. R. (2011). Intestinal damage and myosin light chain kinase (MLCK)-dependent epithelial barrier dysfunction are vital to minor mismatch graft-versus-host disease. *Gastroenterology* 140:167. doi: 10.1016/S0016-5085(11)60677-X

National Research Council. 2012. *Nutrient Requirements of Swine. 11th Edn*. Washington, DC, USA: National Academy Press.

Nies, D. H. (2007). Biochemistry. How cells control zinc homeostasis. *Science.* 317, 1695–1696. doi: 10.1126/science.1149048

Pearce, C., Fernandez, M. V. S., Torrison, J., Wilson, M. E., and Gabler, N. K. (2015). Dietary organic zinc attenuates heat stress–induced changes in pig intestinal integrity and metabolism. *J. Anim. Sci.* 93, 4702–4713. doi: 10.2527/jas.2015-9018

Qi, H. W., Xiang, Z. T., Han, G. Q., Yu, B., Huang, Z. Q., and Chen, D. W. (2011). Effects of different dietary protein sources on cecal microflora in rats. *Afri. J. Biotechnol.* 11, 3704–3708. doi: 10.1186/1472-6750-11-46

Rodriguez, P., Darmon, N., Chappuis, P., Candalh, C., Blaton, M. A., Bouchaud, C., et al. (1996). Intestinal paracellular permeability during malnutrition in Guinea pigs: effect of high dietary zinc. *Gut* 39, 416–422. doi: 10.1136/gut.39.3.416

Sandra, V. E., Laila, P. J. F. D., Anna, V., Sandra, V. K., Diego, M. D., and David, S. O. (2020). Effects of copper and zinc sources and inclusion levels of copper on weanling pig performance and intestinal microbiota. *J. Anim. Sci.* 98:117. doi: 10.1093/jas/skaa117

Sarkar, P., Saha, T., Aoun, J., Chakraborty, S. H., Chakrabarti, M. K., Dutta, S. K., et al. (2018). Evidence that zinc deficiency impairs gut epithelial barrier and intestinal immunity. *FASEB J.* 32, 716–747. doi: 10.1096/fasebj.2018.32.1_supplement.747.16

Shanahan, F. (2002). The host-microbe interface within the gut. *Best Pract. Res. Clin. Gastroenterol.* 16, 915–931. doi: 10.1053/bega.2002.0342

Song, Z. X., Jiang, W. D., Liu, Y., Wu, P., Jiang, J., Zhou, X. Q., et al. (2017). Dietary zinc deficiency reduced growth performance, intestinal immune and physical barrier functions related to NF-κB, TOR, Nrf2, JNK and MLCK signaling pathway of young grass carp (Ctenopharyngodon idella). *Fish Shellfish Immunol.* 66, 497–523. doi: 10.1016/j.fsi.2017.05.048

Spenser, R., Hadar, N., Sharon, M., Raymond, G., Omry, K., and Elad, T. (2015). Chronic zinc deficiency alters chick gut microbiota composition and function. 12th European nutrition Connference. *Nutrients* 7, 9768–9784. doi: 10.3390/nu7125497

Srinivas, U., Braconier, J. H., Jeppsson, B., and Hansson, L. (1989). Influence of zinc deficiency and malnutrition on organ uptake of *Eschericia coli* during gram-negative sepsis in the rat. *Nutr. Res.* 9, 455–463. doi: 10.1016/S0271-5317(89)80122-8

Swinkels, J. W., Kornegay, E. T., Zhou, W., Lindemann, M. D., Webb, K. E., and Verstegen, M. W. (1996). Effectiveness of a zinc amino acid chelate and zinc sulfate in restoring serum and soft tissue zinc concentrations when fed to zinc-depleted pigs. *J. Anim. Sci.* 74, 2420–2430. doi: 10.2527/1996.74102420x

Tang, W. J., Jing, L., Li, T. J., Yang, L. Y., and Yin, Y. L. (2020). The associated regulatory mechanisms of zinc lactate in redox balance and mitochondrial function of intestinal porcine epithelial cells. *Oxidative Med. Cell. Longev.* 2020, 1–15. doi: 10.1155/2020/8815383

Tang, X. H., and Shay, N. F. (2001). Zinc has an insulin-like effect on glucose transport mediated by phosphoinositol-3-kinase and akt in 3T3-L1

fibroblasts and adipocytes. *J. Nutr.* 131, 1414–1420. doi: 10.1093/jn/131.5.1414

Torsten, K., Shaun, V. W., Chen, J., Parkos, C. A., and Nusrat, A. (2001). Neutrophil transmigration in inflammatory bowel disease is associated with altered expression of intercellular junction proteins. *Am. J. Pathol.* 159, 2001–2009. doi: 10.1016/S0002-9440(10)63051-9

Turner, J. R. (2006). Molecular basis of epithelial barrier regulation: from basic mechanisms to clinical application. *Am. J. Pathol.* 169, 1901–1909. doi: 10.2353/ajpath.2006.060681

Vallee, B. L., and Falchuk, K. H. (1993). The biochemical basis of zinc physiology. *Physiol. Rev.* 73, 79–118. doi: 10.1152/physrev.1993.73.1.79

Wang, Y., Shan, T., Xu, Z., Liu, J., and Feng, J. (2006). Effect of lactoferrin on the growth performance, intestinal morphology, and expression of PR-39 and protegrin-1 genes in weaned piglets. *J. Anim. Sci.* 84, 2636–2641. doi: 10.2527/jas.2005-544

Wang, R., Xin, A., Zhang, C., Li, M. Q., Mei, W., An, Q. C., et al. (2014). Effects of zinc lactate on intestinal morphology, mRNA expressions of metallothioneins 1 in intestinal mucosa and acute phase proteins in tissues of weaner piglets. *Chin. J. Anim. Nutr.* 26, 1068–1076. doi: 10.3969/j.issn.1006-267x.2014.04.028

Yan, J. Y., Zhang, G. W., Zhang, C., Tang, L., and Kuang, S. Y. (2017). Effect of dietary organic zinc sources on growth performance, incidence of diarrhoea, serum and tissue zinc concentrations, and intestinal morphology in growing rabbits. *World Rabbit Sci.* 25, 43–49. doi: 10.4995/wrs.2017.5770

Zhang, B., and Guo, Y. (2009). Supplemental zinc reduced intestinal permeability by enhancing occludin and zonula occludens protein-1 (ZO-1) expression in weaning piglets. *Br. J. Nutr.* 102, 687–693. doi: 10.1017/S0007114509289033

Zhang, Y., Ward, T. L., Ji, F., Peng, C., and Dong, B. (2017). Effects of zinc sources and levels of zinc amino acid complex on growth performance, hematological and biochemical parameters in weanling pigs. *Asian Austral. J. Anim. Sci.* 31, 1267–1274. doi: 10.5713/ajas.17.0739

Zhao, Y., Yu, B., Mao, X., He, J., Huang, Z., Zheng, P., et al. (2015). Dietary vitamin D supplementation attenuates immune responses of pigs challenged with rotavirus potentially through the retinoic acid-inducible gene I signalling pathway. *Br. J. Nutr.* 112, 381–389. doi: 10.1017/S000711451400097X

Zhong, W., Mcclain, C. J., Cave, M., Kang, Y. J., and Zhou, Z. (2010). The role of zinc deficiency in alcohol-induced intestinal barrier dysfunction. *Am. J. Physiol. Gastrointest. Liver Physiol.* 298, G625–G633. doi: 10.1152/ajpgi.00350.2009

Zhou, L.H. (2009). Effects of copper and zinc protein chelate on immune performance in growth-finishing swine. master's thesis. Nanjing. Nanjing Agricultural University.

Conflict of Interest: Author SL was employed by company Sichuan Animtech Biology Development Co., Ltd. Author SK was employed by company Sichuan Animtech Feed Co., Ltd.

The remaining authors declare that the research was conducted in the absence of any commercial or financial relationships that could be construed as a potential conflict of interest.

Publisher's Note: All claims expressed in this article are solely those of the authors and do not necessarily represent those of their affiliated organizations, or those of the publisher, the editors and the reviewers. Any product that may be evaluated in this article, or claim that may be made by its manufacturer, is not guaranteed or endorsed by the publisher.

frontiers in Microbiology

ORIGINAL RESEARCH
published: 25 November 2021
doi: 10.3389/fmicb.2021.781454

Ribosome Profiling and RNA Sequencing Reveal Genome-Wide Cellular Translation and Transcription Regulation Under Osmotic Stress in *Lactobacillus rhamnosus* ATCC 53103

*Xuejing Fan[1], Tianyu Bao[1], Huaxi Yi[2], Zongcai Zhang[1], Kenan Zhang[1], Xin Liu[1], Xue Lin[1], Zhen Zhang[1] and Zhen Feng[1,3]**

[1] Key Laboratory of Dairy Science, Ministry of Education, College of Food Science, Northeast Agricultural University, Harbin, China, [2] College of Food Science and Engineering, Ocean University of China, Qingdao, China, [3] Spice and Beverage Research Institute, Chinese Academy of Tropical Agricultural Sciences, Wanning, China

OPEN ACCESS

Edited by:
Xiaodong Xia,
Dalian Polytechnic University, China

Reviewed by:
Jianjun Qiao,
Tianjin University, China
Zhimin Li,
East China University of Science and Technology, China

***Correspondence:**
Zhen Feng
neau_fengzhen@163.com

Specialty section:
This article was submitted to Food Microbiology, a section of the journal Frontiers in Microbiology

Received: *22 September 2021*
Accepted: *27 October 2021*
Published: *25 November 2021*

Citation:
Fan X, Bao T, Yi H, Zhang Z, Zhang K, Liu X, Lin X, Zhang Z and Feng Z (2021) Ribosome Profiling and RNA Sequencing Reveal Genome-Wide Cellular Translation and Transcription Regulation Under Osmotic Stress in Lactobacillus rhamnosus ATCC 53103. Front. Microbiol. 12:781454. doi: 10.3389/fmicb.2021.781454

To determine whether osmotic pressure affects the translation efficiency of *Lactobacillus rhamnosus*, the ribosome profiling assay was performed to analyze the changes in translation efficiency in *L. rhamnosus* ATCC 53103. Under osmotic stress, differentially expressed genes (DEGs) involved in fatty acid biosynthesis and metabolism, ribosome, and purine metabolism pathways were co-regulated with consistent expression direction at translation and transcription levels. DEGs involved in the biosynthesis of phenylalanine, tyrosine, and tryptophan, and the phosphotransferase system pathways also were co-regulated at translation and transcription levels, while they showed opposite expression direction at two levels. Moreover, DEGs involved in the two-component system, amino acid metabolism, and pyruvate metabolism pathways were only regulated at the transcription level. And DEGs involved in fructose and mannose metabolism were only regulated at the translation level. The translation efficiency of DEGs involved in the biosynthesis of amino acids was downregulated while in quorum sensing and PTS pathways was upregulated. In addition, the ribosome footprints accumulated in open reading frame regions resulted in impaired translation initiation and elongation under osmotic stress. In summary, *L. rhamnosus* ATCC 53103 could respond to osmotic stress by translation regulation and control the balance between survival and growth of cells by transcription and translation.

Keywords: *L. rhamnosus*, ribosome profiling, osmotic stress, translation regulation, translation efficiency

INTRODUCTION

Lactobacillus rhamnosus Gorbach Goldin (LGG) as a probiotic strain and starter culture strain has been widely used in various types of fermented and functional food production. Furthermore, it also plays an important role in modern biotechnological fermentation processes (Moayyedi et al., 2018). The benefits of LGG were primarily in gastrointestinal health and immune function, including

adaptation to the human intestinal environment and reproduction, prevention of colonization by pernicious organisms, regulation of human intestinal flora, prevention of diarrhea, relief of lactose intolerance, and improvement of intestinal function (Sun et al., 2019; Chandrasekharan et al., 2020; Song et al., 2020). Environmental stress is one of the greatest challenges to the production and enrichment of probiotic strains and starter culture strains, especially osmotic stress (Muruzovic et al., 2018). Osmotic stress appears with the accumulation of metabolites and continuous addition of sodium hydroxide neutralizing agent into the medium during high density culture of strains (Tian et al., 2014). Osmotic stress results in the water movement from inside the cell to the outside, changes in the cell volume intracellular solute concentration, dehydration of cells, and affects cell growth rate and metabolic activities (Lin et al., 2017; Tian et al., 2018). Osmotic stress influences the growth and robustness of probiotic strains and starter culture strains. Therefore, a clear understanding of how LGG responds to osmotic stress at the molecular level is crucial to improve the survival and growth of probiotic and starter culture strains in the fermentation process.

Many osmotic adaptation sophisticated mechanisms have been revealed at molecular and physiological levels in lactic acid bacteria (LAB). A series of anti-osmotic components, molecular chaperone proteins, genes acting as regulatory factors and sigma factors and transport proteins have been found to improve the osmotic adaptation of LAB. GroE-DnaK-DnaJ has a σ^A sigma factor promoter, which could bind the HrcA repressor to improve the adaptation of LAB under osmotic stress. F_0F_1-ATPase and K^+-ATPase involve in response to the osmotic stress in LAB. Arginine, ornithine, arginine, and lysine also involve in the regulation of osmotic stress by the arginine deiminase pathway in LAB (Bucka-Kolendo and Sokolowska, 2017). Previous researches were focused on the expression regulations of genes at transcription level and the proteins (Palomino et al., 2016; Lv et al., 2017). The regulation of protein expression levels is vital for LAB in response to osmotic stress, since most cellular processes are catalyzed by proteins. Hence, regulation of gene expression at the translation level from the mRNA pool in response to osmotic stress are indeed valuable. At present, regulation of gene expression at the translation level is not fully understood in the adaptation to osmotic stress during the fermentation of LAB.

Translation from mRNA to protein depends on cellular factors and temporally coordinated transient interactions between tRNA and the ribosome, a two-subunit protein and RNA complex that orchestrates protein synthesis in the cell (Shcherbik and Pestov, 2019). Changes in gene expression levels of specific mRNA depend on the composition of the actively translating ribosome (Genuth and Barna, 2018). Translation efficiency (TE) is the metric of ribosome quality (Brandman et al., 2012). Stresses can trigger both translation initiation and elongation through different mechanisms (Wek, 2018). Ribosome profiling focuses on measuring ribosome occupancy, delineating translation regions precisely, revealing the genome's full coding potential, and the regulation of genes expression at translation and transcription levels (Ingolia, 2016). It provides a quantitative, high-resolution translation profile, identifies previously unknown translation events through evaluating TE, and describes the specific features of translation-elongation (Lei et al., 2015). Using ribosome profiling, the reduction of 21 nt mRNA fragments (RPFs) and the formation or translocation of peptide were the major factors in the translation rate-limiting step that was revealed under hyperosmotic and oxidative stresses in *Saccharomyces cerevisiae* (Wu et al., 2019). The ribosome footprints accumulated in the initiation of open reading frame regions (ORFs) and the early translation elongation paused under heat stress in *Escherichia coli* (Zhang et al., 2017). However, there are barely studies on translation regulation under environmental stress in LAB using ribosome profiling, especially under osmotic stress.

The initial aim of this project was to reveal genome-wide cellular translation regulation under osmotic stress in *L. rhamnosus* ATCC 53103 by using RNA-seq and ribosome profiling, with the long-term goal of elucidating new strategies to increase the viability of LAB under environment stress.

MATERIALS AND METHODS

Strain, Growth Conditions, and Osmotic Stress

L. rhamnosus ATCC 53103 was from the American Type Culture Collection (Manassas, VA, United States) and cultured in MRS medium at 37℃. It was revitalized in MRS medium at 37℃ three times before use. Cultures were stored at –80℃ in MRS medium containing 10% glycerol. The growth of *L. rhamnosus* ATCC 53103 was monitored by an automatic growth curve analyzer (Bioscreen Cpro; OY Growth Curves, Finland) at 600 nm (OD_{600}). For osmotic stress, the cells (OD_{600} ∼1.8) were collected by centrifugation (6,000 × g, 10 min, 4℃) and then resuspended in MRS medium containing 0.2, 0.4, 0.6, and 0.8 M sodium lactate. The effect of osmotic stress on cell growth was further monitored by an automatic growth curve analyzer (Bioscreen Cpro; OY Growth Curves, Finland). The relevant results were shown in **Supplementary Figure 1**. Because a higher sodium lactate concentration (0.8 M) in the MRS inhibited the growth of *L. rhamnosus* ATCC 53103. When the sodium lactate concentration was 0.6 M, the growth rate of *L. rhamnosus* ATCC 53103 decreased significantly, while the viable counts reached 8.66 $\log_{10}$CFU/mL after 24 h culture. Therefore, the final concentration of sodium lactate in this study was 0.6 M.

Total RNA Extraction and Library Construction

The cultures of control group and osmotic stress group were harvested by centrifugation (6,000 × g 15 min, 4℃) after 3.5 and 6.5 h (OD_{600} ∼1.0), respectively. Total RNAs were extracted using a TRIzol-based method (Life

Technologies, CA, United States). rRNAs were removed using the Ribo-Zero Magnetic Gold Kit (Epicenter Biotechnologies, Madison, WI, United States). RNA quality was checked using the Agilent 2200 TapeStation system (Agilent Technologies, Inc., Santa Clara, CA, United States). The library was constructed using a TruSeq RNA Sample Prep Kit v2 (Illumina, San Diego, CA, United States), and then sequenced by using the Illumina HiSeqi^{TM} 2500 platform with pair-end 150 base reads.

Ribosome Profiling

For Ribo-Seq, chloramphenicol (200 μM) was added into the cultures when OD_{600} reached 1.0, and then cells were harvested by centrifugation (6,000 × g, 10 min, 4℃) after shaking for 2 min. Bacterial sludge was washed using resuspension buffer (20 mL) composed of NH_4Cl (100 mM), $MgCl_2$ (10 mM), chloramphenicol (1 mM), and Tris-HCl (pH 8.0, 20 mM). The cells were collected by centrifugation (4,000 × g, 5 min, 4℃), and then were mixed immediately with cell lysis buffer. The resuspended extracts were transferred from lysis buffer to new microtubes, pipetted several times then incubated on ice for 10 min. The cells were triturated ten times through a 26-G needle. The lysate was collected by centrifugation (20,000 × g, 10 min, 4℃. To prepare RPFs, RNase I (7.5 μL) and DNase I (5 μL) were added to lysate (300 μL) to incubate for 45 min with gentle mixing. Nuclease digestion was stopped by adding RNase inhibitor (10 μL). RPFs were isolated using the RNA Clean and Concentrator-25 Kit (R1017, Zymo Research, Orange County, CA, United States). The Ribo-seq libraries were constructed using NEBNext® Multiple Small RNA Library Prep Set from Illumina® (catalog no. E7300S, E7300L). 140–160 bp PCR products were enriched to generate cDNA libraries and then sequenced using Illumina HiSeq^{TM} 2500.

Analysis of Differentially Expressed Genes

The gene expression level was normalized by the fragments per kilobase of transcript per million (FPKM) of mapped reads to control the influence of gene lengths and amount of sequencing data in calculation of gene expression. The edgeR package[1] was used to identify DEGs across sample groups. Gene ontology (GO) annotation and Kyoto Encyclopedia for Genes and Genomes (KEGG) pathway of DEGs were analyzed. According to expressions levels in translation and transcription, DEGs were classified into five different groups: unchanged (DEGs were not regulated at both two levels), homodirection (DEGs were regulated at the two levels with consistent trends), opposite (DEGs were regulated at the two levels with opposite trends), translation (DEGs were only regulated at the translation level) and transcription (DEGs were only regulated at the transcription level).

Analysis of Differentially Expressed Gene Translation Efficiency and Its Correlation With Differentially Expressed Genes Expression at the Transcription Level

The TEs of all DEGs were identified, calculated, and compared using RiboDiff (Zhong et al., 2017). According to DEGs expression with the changes of TE at the transcription level, DEGs were classified into five different groups as described above: Unchanged; Homodirection; Opposite; TE (DEGs only had change at the TE level); and Transcription.

Data Analysis

Raw data were filtered following the previous study (Langmead and Salzberg, 2012). Trimmed reads were mapped to *L. rhamnosus* reference transcriptome[2] allowing no mismatches using Bowtie2 (version 2.2.8). Retained reads were aligned to the reference genome using Bowtie2. Genes and gene expression were identified and calculated using RSEM. Genes with$|\log_2(\text{fold change})| > 1$ and a false discovery rate (FDR) < 0.05 were considered as significant DEGs. Both Ribo-seq and RNA-seq data types had two biological duplications.

RESULTS

Analysis of Ribo-Seq and RNA-Seq Data

To systematically investigate the effect of osmotic stress on transcription and translation regulation, RNA-seq and ribosome profiling were analyzed in the same two sets of parallel populations of *L. rhamnosus* ATCC 53103 cells with two different concentrations of sodium lactate (control vs. 0.6 M). Each experiment was divided into control group (CG) and osmotic stress group (OS), respectively (**Supplementary Figure 2**). The regulation of transcription and translation under osmotic stress were examined by deep sequencing of cellular total mRNAs and RPFs, respectively. A large number of reads were produced by ribosome footprints and RNA-seq transcripts. The average read was around 30 bp.

The total reads, ranging from 11,356,406 to 81,788,555 per DNA library, were produced by deep sequencing (**Supplementary Table 1**). After filtering, around 30 and 20 million reads were generated from RPF of CG and OS samples, respectively. Around 26 and 24 million mRNA-seq reads were generated from CG and OS samples, respectively. These reads were mapped to *L. rhamnosus* reference transcriptome data. The mapping efficiency of RPF samples was ∼20%. There are high correlations between the two biological duplication (R^2>0.85) for both Ribo-seq and RNA-seq data. A total of 5578 and 5616 mapped genes were obtained from RPF samples of CG and OS, respectively. A total of 5,318 and 5,370 mapped genes were obtained from CG and OS mRNA samples, respectively.

The length of RPFs in OS and CG samples was around 30 nt (**Figures 1A,B**). The triplet periodicity between OS and CG samples were compared by scanning from the start codon to stop

[1]http://www.rproject.org/

[2]https://www.ncbi.nlm.nih.gov/nuccore/NC_013198.1

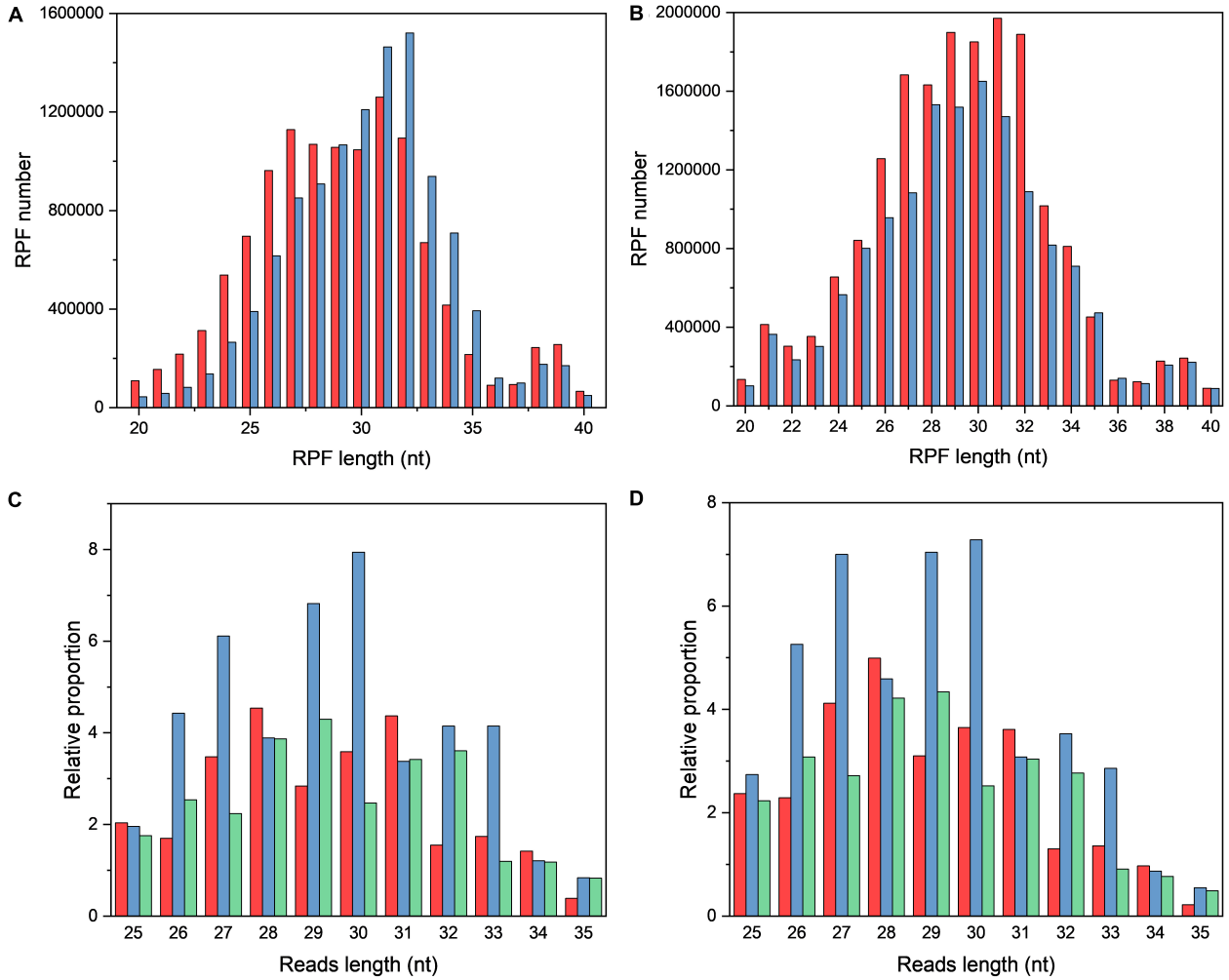

FIGURE 1 | The characteristics of ribosome profiling data in OS and CG. **(A,B)** Length distribution of RPFs in OS **(A)** and CG **(B)**. The red and blue bars refer to two biological replicates. **(C,D)** Three-nucleotide periodicity at the first 35 nt of CDS in OS **(C)** and CG **(D)**.

codon, and a strong three-nucleotide periodicity in OS and CG samples was observed (**Figures 1C,D**).

Effect of Osmotic Stress on Expression and the Function of Differentially Expressed Genes at Translation and Transcription Levels

To explore how *L. rhamnosus* ATCC 53103 cells deal with osmotic stress, both translation and transcription relative variations between CG and OS were examined. The results showed that osmotic stress changed gene expression at the translation and transcription levels (**Figure 2**). A total of 289 and 614 DEGs were upregulated while 156 and 336 DEGs were downregulated at the translation and transcription levels, respectively (**Figures 2A–C**). About a quarter (11.5 and 12.1%) of the regulated DEGs were shared between the two levels (**Figures 2D,E**). At the translation and transcription levels, the expression of genes from samples of OS was moderately correlated (R^2 = 0.7757; **Supplementary Figure 3**). GO annotation and KEGG pathway analysis also showed that DEGs largely overlapped in GO and many KEGG pathways which also illustrated a big overlap at these two levels including ABC transporters, biosynthesis of antibiotics, secondary metabolites, and metabolic pathways etc. (**Figures 3A,B**). It is worthwhile to note that large numbers of DEGs showed different expression trends and many DEGs of enriched pathways showed a different response at the two levels. These results demonstrated that the regulation of DEGs at the translation level played an important role under osmotic stress in LGG.

Effect of Osmotic Stress on the Dynamic Profiles of Translation and Transcription

To obtain the changes of gene expression trends at the translation and transcription levels simultaneously, DEGs were divided into different groups based on the fold change of gene expression

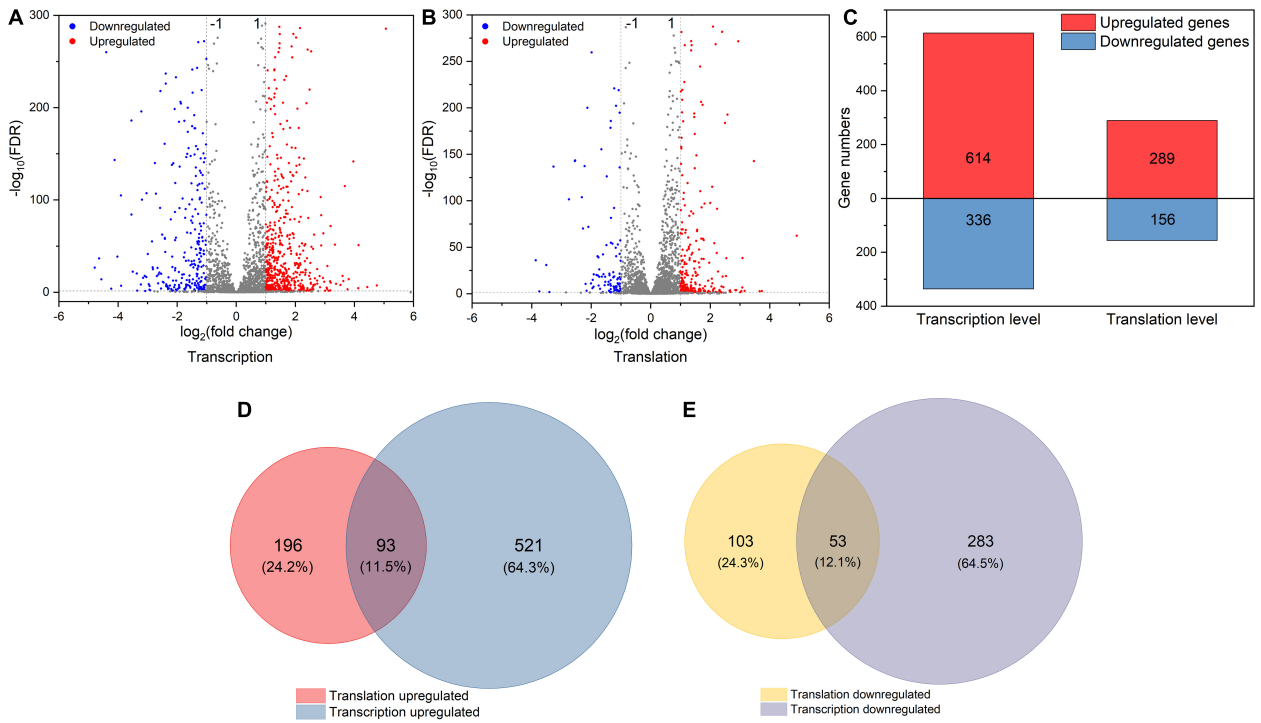

FIGURE 2 | (A,B) The volcano plot of DEGs ($|\log_2 FC| > 1$ and FDR < 0.05) at transcription and translation levels under osmotic stress. **(C)** The number of DEGs at transcription and translation levels under osmotic stress. **(D,E)** The relationship between osmotic responsive genes at transcription and translation levels. Genes analyzed in **Figure 1 (D,E)** were derived from **Figure 1 (A,B)**.

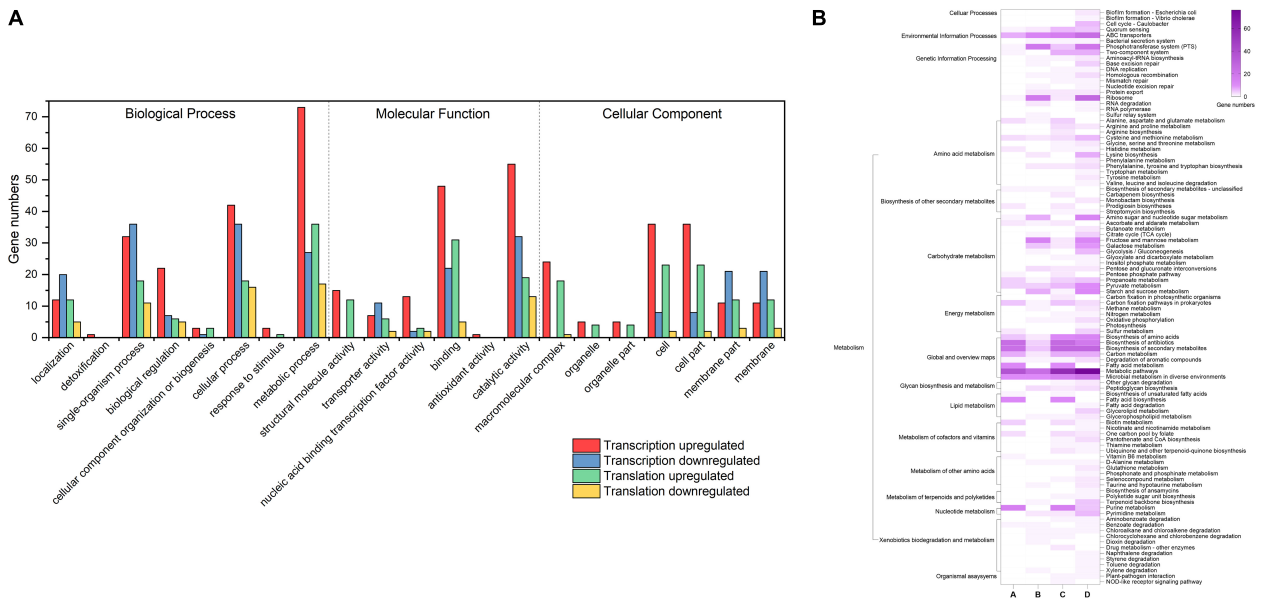

FIGURE 3 | (A) GO analysis of DEGs in OS and CG. **(B)** KEGG pathways of DEGs in OS and CG.

($|\log_2(\text{fold change})| > 1$) between CG and OS (**Figure 4** and **Supplementary Table 2**).

A total of 93 DEGs were upregulated at the two levels and 53 DEGs were downregulated at the two levels (yellow dots). These DEGs were mainly involved in the fatty acid biosynthesis and metabolism, ribosome assembly, and purine metabolism pathways. The DEGs *purD*, *purH*, *purN*, *purM*, *purQ*, *purC*, and *purK* involved in purine metabolism were downregulated

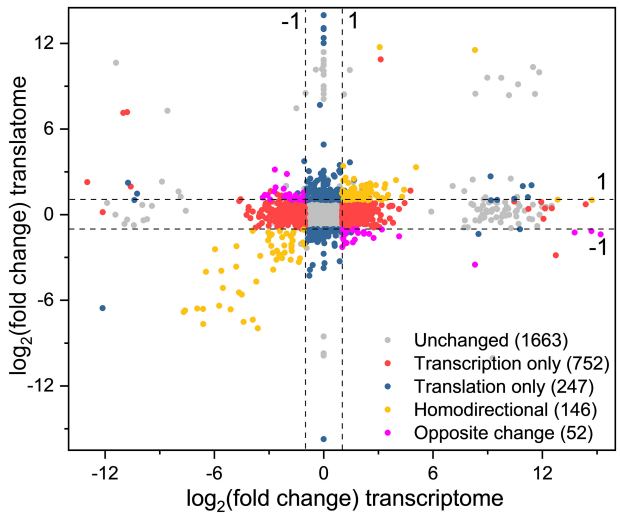

FIGURE 4 | Simultaneous monitoring of the changes at the transcription and translation levels in *L. rhamnosus* ATCC 53103 under osmotic stress. Plot of the $\log_2$fold change of RPFs (OS/CG) against the $\log_2$fold change of respective mRNAs (OS/CG). The four dash lines indicate $\log_2$fold change values -1 or + 1.

from 99.37- to 249.25-fold and from 12.25- to 205.53-fold at the translation level and transcription level, respectively. The DEGs *accA*, *accD*, *accC1*, *accB*, *pksA*, and *fabH* involved in fatty acid biosynthesis were downregulated from 4.56- to 14.47-fold and from 3.52- to 7.35-fold at the translation level and transcription level, respectively.

A total of 24 DEGs were downregulated at the transcription level and upregulated at the translation level, while 28 DEGs were upregulated at the transcription level and downregulated at the translation level (purple dots). These DEGs were mainly involved in biosynthesis of phenylalanine, tyrosine, and tryptophan, protein export, phosphotransferase system (PTS), ABC transporters, galactose metabolism, and pyrimidine metabolism pathways. The DEGs *fruA* and *lacF* involved in the PTS pathway were upregulated and downregulated from 2.09- to 2.57-fold and from 7.63- to 8.43-fold at the translation level and the transcription level, respectively.

A total of 752 DEGs were regulated at the transcription level only (red dots). These DEGs were mainly involved in biosynthesis and metabolism of amino acid, the two-component system, ABC transporters and pyruvate metabolism pathways. The DEGs *tauA*, *tauB*, *tcyJ*, and *macB2* involved in the ABC transporters were upregulated from 4.00- to 13.64-fold, respectively. The DEGs *cydA*, *ciaR*, *dltC*, *citF*, and *citC* involved in the two-component system were downregulated from 2.26- to 8.07-fold, respectively.

A total of 247 DEGs were regulated at the translation level only (blue dots). The DEGs *levE*, *fruK*, *rhaD*, *sorA*, and *rhaB* involved in fructose and mannose metabolism were upregulated. The DEGs *licB*, *bglP*, *sorA*, *manX*, and *mtlF* involved in the PTS pathway also were upregulated. The DEGs *rplL*, *rpmD*, *rplF*, *rplN*, and *rplP* involved in ribosome assembly were upregulated about 2–3-fold. The DEGs *potA* and *potB* involved in the ABC transporters pathway were upregulated by 10.42- and 7.69-fold, respectively. Meanwhile, the DEGs *cysE*, *cysK*, *hisG*, *hisZ*, *nodI*, *oppA*, and *macB* involved in biosynthesis of amino acids and antibiotics, and ABC transporters pathway also were downregulated.

Effect of Osmotic Stress on the Dynamic Profiles of Translation Efficiency and Transcription

TEs of 363 and 386 DEGs were upregulated and downregulated, respectively, which suggested that TE played an important role in response to osmotic stress in LGG (**Figure 5A** and **Supplementary Table 3**). GO annotation showed that these DEGs were mainly enriched in cell part, membrane part, binding, catalytic activity, metabolic process, biological regulation, localization, cellular, and single-organism process (**Figure 5B**). KEGG pathway analysis indicated that these DEGs were mainly involved in biosynthesis of secondary metabolites, biosynthesis of antibiotics, amino acids metabolism, pyruvate metabolism, carbon metabolism, purine metabolism, glycolysis pathway, ribosome assembly, the two-component system, ABC transporters, PTS pathways (**Supplementary Table 4**). The DEGs *rpsD*, *rpsT*, *rpmG*, *rpsQ*, *rpsC*, *rpsS*, *rpsJ*, *rpsZ*, *purD*, *purH*, *purN*, *purK*, *desR*, *yvfT*, *bceB*, *ywqE*, *iphP*, *htrA*, *opuCD*, *opuCC*, *opuCB*, and *opuCA* were involved in ribosome assembly, purine metabolism, the two-component system, and ABC transporters pathways, and their TEs were downregulated. Other DEGs, such as *secG*, *dppC*, *comA*, *yidC*, *manZ*, and *lacF* were involved in quorum sensing and PTS pathways and their TEs were upregulated.

The calculation and analysis showed that the Pearson correlation coefficient between mRNA abundance and TE was –0.5845 (**Supplementary Figure 4**). This showed that transcription abundance affected TE. Hence, the distribution of DEGs was classified into different groups based on the regulation of TE and gene expression at the transcription level (**Figure 5C**). A total of 434 DEGs were regulated only at the transcription level while their TEs were not regulated, such as *rpsN*, *rplJ*, *accA*, *fabZ*, *pksA*, *tauA*, *tcyJ*, *nodI*, *purF*, and *trpA*. They were mainly involved in the assembly of ribosomes, fatty acid biosynthesis and metabolism, PTS, ABC transporters, and metabolism of starch, sucrose, purine, fructose, mannose, amino sugar, and nucleotide sugar pathways (**Supplementary Table 5**). TEs of 233 DEGs were regulated while their expressions were not regulated at the transcription level, such as *cysE*, *cysK*, *sdaAB*, *ilvE*, *tpiA*, *glcK*, *kdgK*, *rhaD*, and *ssdA*. They were mainly involved in the metabolism of cysteine and methionine, glycolysis, and microbial metabolism in diverse environment pathways (**Supplementary Table 6**). Only 11 DEGs were regulated at the transcription level, while their TEs were also regulated, and their regulations had similar trends. These DEGs included *fhs*, *purH*, *purN*, *accD*, *accB*, *purD*, *purK*, and *potC*. They were mainly involved

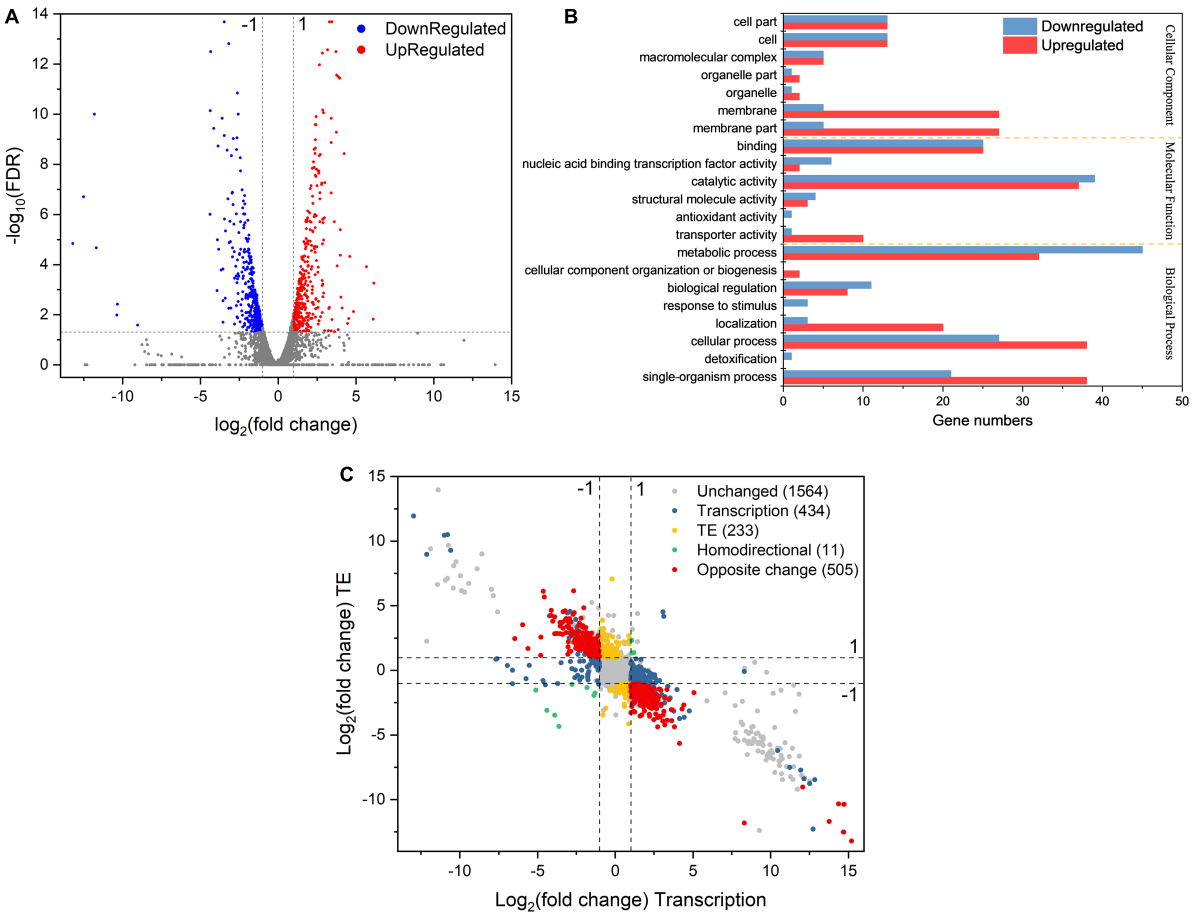

FIGURE 5 | (A) The volcano plot of DEGs' TE response under osmotic stress. **(B)** GO annotation of differentially expressed genes with largely changed translation efficiency under sodium lactate stress. **(C)** Simultaneous monitoring of the distribution of $\log_2$fold change TE and corresponding $\log_2$fold change mRNA abundance in *L. rhamnosus* ATCC 53103 under osmotic stress. The four dash lines indicate $\log_2$fold change values –1 or + 1.

in the metabolism of purine, fatty acid, propanoate, carbon, and pyruvate pathways (**Supplementary Table 7**). TEs of 286 DEGs were downregulated while their expressions were upregulated at the transcription level. These DEGs were mainly involved in pathways of biosynthesis and metabolism of amino acids, antibiotic biosynthesis, the citrate cycle, glycolysis, glutathione metabolism, carbon metabolism, amino sugar metabolism, nucleotide sugar metabolism, pyrimidine metabolism, and ribosome assembly. Such as the DEGs *dapB* and *dapH* were involved in lysine biosynthesis via the succinyl-DAP and acetyl-DAP pathways, respectively. *SpeF* was involved in arginine and proline metabolism. The DEGs *rpmG*, *rpsC*, *rpsD*, and *rpsT* were involved in ribosome functional group assembly. The mapped reads of these DEGs are shown in **Figures 6A–D**. TEs of 219 DEGs were upregulated and their expressions were downregulated at the transcription level. These DEGs mainly involved in pathways of protein export, ABC transporters, and two-component system (**Supplementary Table 8**). The DEGs included *lspA*, *yheI*, *ecfT*, and *dltC*, and the mapped reads are shown in **Figures 6E–H**.

Effects of Osmotic Stress on Ribosomes Accumulation in Open Reading Frame Regions

Codon resolution is one of the advantages of ribosome profiling. To evaluate the translation events, the average occupancy of ribosomes was calculated around the start and stop codons. The footprints increased significantly under osmotic stress in *L. rhamnosus* ATCC 53103, which mapped to the initiation region around the 5′-end approximately at the –15 position (**Figure 7A**). In addition, ribosome occupancy from the nucleotide –100 to the end codon was also higher in OS than that in CG (**Figure 7B**). A few typical DEGs had higher ribosome occupancy under osmotic stress, such as *pdhB*, *pdhD*, and *metF* (**Figures 7C–E**). TEs of these DEGs were downregulated under osmotic stress.

DISCUSSION

The total reads were obtained from CG and OS samples, and the mapping efficiency of RPF samples was relatively low (∼20%) in this study. The present result was similar to

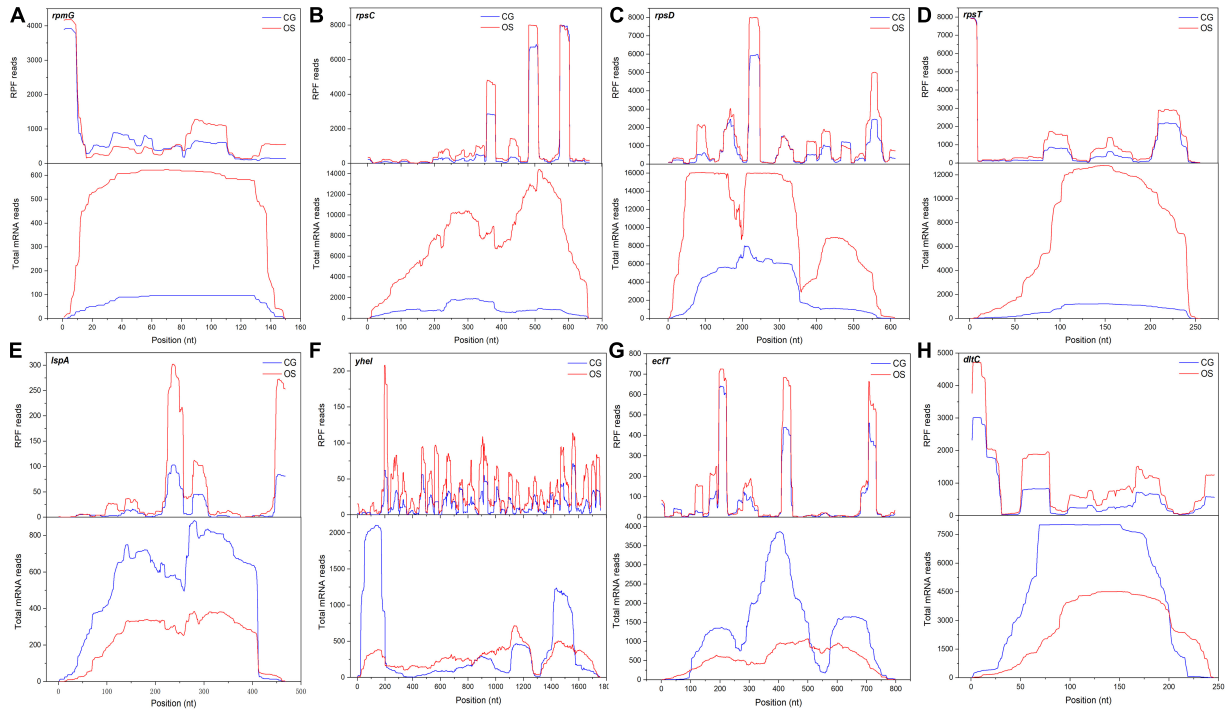

FIGURE 6 | The mapped reads of DEGs with regulated TE and transcript under osmotic stress. **(A–H)** The DEGs were *rpmG, rpsC, rpsD, rpsT, lspA, yhel, ecfT*, and *dltC*, respectively.

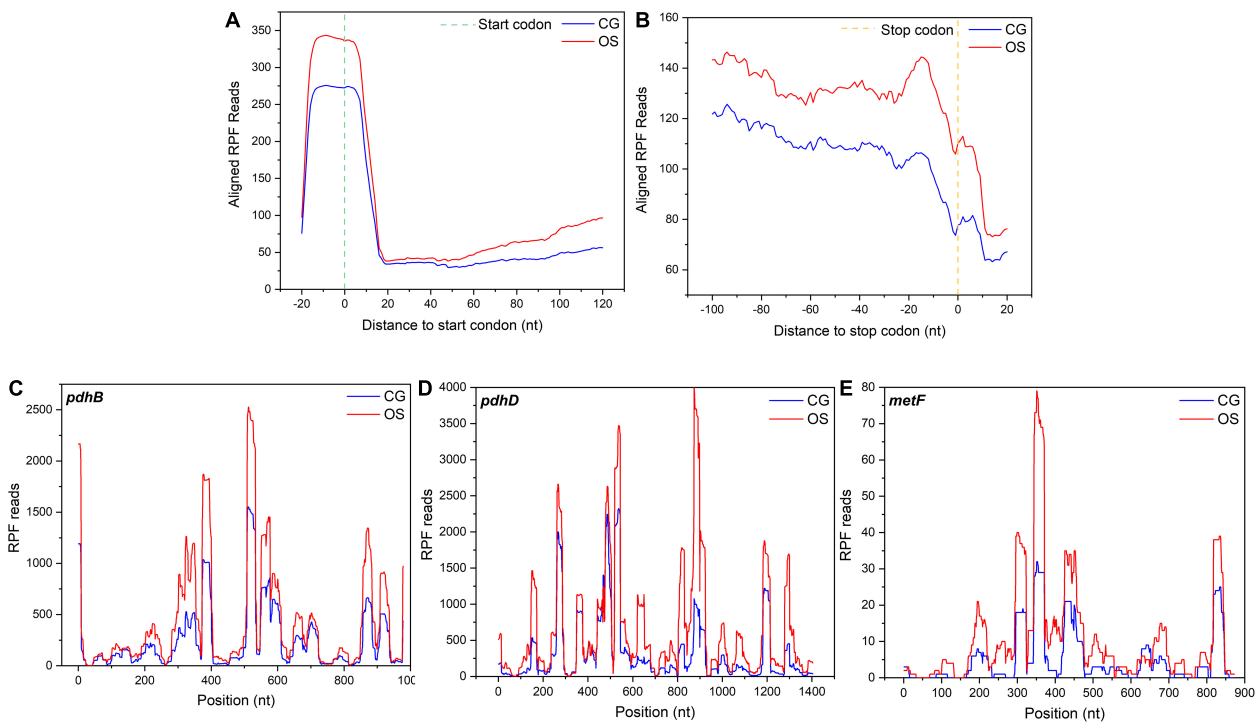

FIGURE 7 | (A) Alignments of RPF reads in the 5′UTR of all mapped genes in a 20-nucleotide distance to start codon. **(B)** Alignments of the RPF reads in 3′UTR of all mapped genes in a 20-nucleotide distance to stop codon. **(C–E)** Three representative genes, *pdhB*, *pdhD*, and *metF*, with their ribosome footprint densities increased under osmotic stress in *L. rhamnosus* ATCC 53103.

Saccharomyces cerevisiae (16%) under starvation stress (Ingolia et al., 2009). It might be due to the large number of rRNAs that were removed. During translation, ribosome read density distribution moves three nucleotides simultaneously. Hence the representative feature of read density distribution is the triplet periodicity (Ingolia et al., 2009; Guo et al., 2010; Chew et al., 2013). The three-nucleotide periodicity were clearly observed in both CG and OS samples. The present result was similar with yeast, maize, and *Arabidopsis* under starvation, drought, dark, and sublethal hypoxia conditions, respectively (Ingolia et al., 2009; Chew et al., 2013; Liu et al., 2013; Juntawong et al., 2014; Lei et al., 2015).

Using RNA sequencing coupled with ribosome profiling, the changes of genome-wide gene expression were not only explored at the translation and transcription levels but also the interactions were revealed between both regulation levels under osmotic stress in *L. rhamnosus* ATCC 53103. Many DEGs were involved in fatty acid biosynthesis and metabolism, ribosomes, purine metabolism pathways, ABC transporters, and PTS pathways at the translation and transcription levels. As a stress sensor, ribosomes mediate the synthesis and attenuation of proteins in response to stress (Shcherbik and Pestov, 2019). The DEGs involved in ribosome assembly were upregulated under osmotic stress in *L. rhamnosus* ATCC 53103. It is essential for bacterial survival to strictly regulate fatty acid biosynthesis and metabolism (Yang et al., 2019). *FabH* catalyzes the type II fatty acid initiation biosynthesis reactions (Lai and Cronan, 2003). *FabZ* codifies a dehydratase, introduces double bonds into the carbon chain, and stimulates the production of unsaturated fatty acid (Siroli et al., 2020). However, these DEGs involved in fatty acid biosynthesis and metabolism pathways were downregulated at both levels. This reflected that *L. rhamnosus* needed to save cellular metabolic energy and increase environmental adaptation by limiting fatty acid biosynthesis (Adu et al., 2018). Purine metabolism was activated in the bacteria in response to environmental stress (Goncheva et al., 2019). As the genetic information transmitters and phosphate group donors, purine intermediates were not only involved in signal mediation but also ensured the living cell energy supply in response to environment stress. *L. rhamnosus* reduced growth rate under osmotic stress, and the DEGs involved in the purine metabolism pathway were downregulated at the translation and transcription levels. The synthesis of purine is energetically expensive (Peifer et al., 2012). The reduction of synthesis of purine maintained the stability of *L. rhamnosus* ATCC 53103 intracellular pool size, helped cells save energy, and keep cells growing slowly under osmotic stress (Shimaoka et al., 2007). Similarly, downregulated DEGs in the PTS pathway at the translation level also showed that conservation of energy was beneficial for *L. rhamnosus* ATCC 53103 in response to osmotic stress (Ganesan et al., 2007).

A total of 752 DEGs only were regulated only at the transcription level and 247 DEGs were regulated only at the translation level in the present study. These results indicated that *L. rhamnosus* ATCC 53103 regulated gene expression at the two levels independently under osmotic stress. Although translation regulation was not to generate new mRNA, it could be regarded as a rapid and direct environmental response (Sonenberg and Hinnebusch, 2009). Therefore, translation regulation plays a relatively independent and fine-tuning role in response to stress (Lackner et al., 2012). Genes regulated at the transcription level can be a barometer for the follow-up translation change (Lei et al., 2015). Genes upregulated only at the transcription level showed that *L. rhamnosus* ATCC 53103 regulated mRNA abundance to recover the TE reduction under osmotic stress. The ample mRNA provided a spare pool to facilitate the translation regulation immediately when osmotic stress abates in the future (Shenton et al., 2006). The interaction between the translation and transcription response boosts the gene expression flexibility, which makes for osmotic stress adaptation of *L. rhamnosus* ATCC 53103. Severe and rapid stresses might result in response quickly and independently of gene expression at translation and transcription levels; while moderate and chronic stresses might lead to more coordinated regulation at both levels (Lei et al., 2015).

The intracellular amino acid concentration is crucial for bacteria in response to osmotic stress (Gaucher et al., 2019). The DEGs involved in the amino acid biosynthesis pathway were upregulated at the transcription level under osmotic stress in the present study. A similar phenomenon was found under stress in other LAB (Papadimitriou et al., 2016). However, the reduction of TEs of the amino acid biosynthesis gene cluster resulted in the accumulation of uncharged tRNAs, lowering its activity and reducing the rates of overall protein synthesis (Spriggs et al., 2010). TEs of DEGs related to ribosome assembly were downregulated under osmotic stress, resulting in decreasing the freely available ribosome complexes for translation, affecting the mRNA translation, thereby reducing the production of protein and altering proteome allocation by the translation regulation (Song et al., 2018). This regulation would be crucial to the conservation of energy under osmotic stress. The TEs of DEGs involved in protein export, ABC transporters, and the two-component system were upregulated. The two-component system is made up primarily of a response regulator and histidine kinase, which associate with the cell membrane. LAB often regulates the expression of genes enriched in the two-component system to cope with environmental stress (Zhang et al., 2017). Osmotic stress showed a significant correlation with biosynthesis and metabolism of secondary metabolites and antibiotics. These changes might help *L. rhamnosus* ATCC 53103 to reprogram translation to adapt to the osmotic stress. The existence of various parallel mechanisms at the transcription and translation levels were to maintain the balance between survival and growth of *L. rhamnosus* ATCC 53103 under osmotic stress (Durfee et al., 2008).

Under osmotic stress, ribosome occupancy in the initiation region from the nucleotide –100 to the end codon increased dramatically. Furthermore, it was higher than that of the normal condition in the present study. It suggested that ribosomes pausing at initiation and later elongation steps was a general ribosome reaction under osmotic stress in prokaryotes (Shalgi et al., 2013). The accumulation of ribosomes

resulted in increasing the ribosome density and the fraction of stalled bound ribosomes. This phenomenon would create traffic jams on all mRNAs and affect the TE (Zhang et al., 2017). Meanwhile, with the increase of bound ribosomes, the amount of tRNAs on mRNAs increased and the free tRNAs pool decreased. The reduction of free tRNAs pool would decrease translation initiation and elongation rates, reduce genes TE, and further retard the production of total protein (Shah et al., 2013). Therefore, translation dynamics of *L. rhamnosus* ATCC 53103 would change under osmotic stress. The global TE downregulation would provide another way to reduce the production of protein and promote survival of *L. rhamnosus* ATCC 53103 under osmotic stress.

CONCLUSION

Based on ribosome profiling and RNA-seq, the study focused on a landscape of highly dynamic translation and transcription regulation, and revealed the changes of TEs of DEGs under osmotic stress in *L. rhamnosus* ATCC 53103. The DEGs involved in the purine metabolism pathway were downregulated at the translation and transcription levels under osmotic stress. The TEs of DEGs involved in fatty acid biosynthesis and metabolism pathways were not regulated, although these DEGs were downregulated at the translation and transcription levels. Abundant DEGs involved in the biosynthesis of amino acid pathways and ribosome assembly were upregulated at the transcription level and the TEs of these DEGs were downregulated. TEs of DEGs related to protein export, ABC transporters, and the two-component system were upregulated. The ribosome footprints accumulated in the ORF regions, resulting in impaired translation initiation and elongation under osmotic stress. *L. rhamnosus* ATCC 53103 controlled the balance between cell survival and growth by using transcription and translation parallel mechanisms under osmotic stress.

DATA AVAILABILITY STATEMENT

The data presented in the study are deposited in the Gene Expression Omnibus (GEO) repository, accession number GSE188929.

AUTHOR CONTRIBUTIONS

XF conceived and supervised the study. XF, TB, and HY designed the experiments. ZoZ, KZ, and XiL performed the experiments. XuL and ZhZ analyzed the data. XF and ZF wrote the manuscript. All authors have read and approved the manuscript.

FUNDING

This work was financially supported by grants from the National Natural Science Foundation of China (31771989).

SUPPLEMENTARY MATERIAL

The Supplementary Material for this article can be found online at: https://www.frontiersin.org/articles/10.3389/fmicb.2021.781454/full#supplementary-material

Supplementary Figure 1 | Effects of different sodium lactate concentration on the growth of *L. rhamnosus* ATCC 53103. **(A)** Growth curve of *L. rhamnosus* ATCC 53103 under different sodium lactate concentration. **(B)** The viable count of *L. rhamnosus* ATCC 53103 under different sodium lactate concentration.

Supplementary Figure 2 | Overview of experimental design. RNA-seq and ribosome profiling were performed on CG and OS.

Supplementary Figure 3 | Correlation of gene expression of mRNA abundance with Ribo-seq abundance of OS.

Supplementary Figure 4 | Correlation of gene expression of mRNA abundance with gene translation efficiency of OS.

REFERENCES

Adu, K. T., Wilson, R., Nichols, D. S., Baker, A. L., Bowman, J. P., and Britz, M. L. (2018). Proteomic analysis of *Lactobacillus casei* GCRL163 cell-free extracts reveals a SecB homolog and other biomarkers of prolonged heat stress. *PLoS One* 13:e0206317. doi: 10.1371/journal.pone.0206317

Brandman, O., Stewart-Ornstein, J., Wong, D., Larson, A., Williams, C. C., Li, G. W., et al. (2012). A ribosome-bound quality control complex triggers degradation of nascent peptides and signals translation stress. *Cell* 151, 1042–1054. doi: 10.1016/j.cell.2012.10.044

Bucka-Kolendo, J., and Sokolowska, B. (2017). Lactic acid bacteria stress response to preservation processes in the beverage and juice industry. *Acta Biochim. Pol.* 64, 459–464. doi: 10.18388/abp.2017_1496

Chandrasekharan, B. P., Foster, S. L., Saeedi, B., Weinshenker, D., and Neish, A. S. (2020). Lactobacillus Rhamnosus GG (LGG)-Induced enteric neuronal differentiation attenuates opioid-induced constipation. *Gastroenterology* 158:S276. doi: 10.1016/S0016-5085(20)31374-3

Chew, G. L., Pauli, A., Rinn, J. L., Regev, A., Schier, A. F., and Valen, E. (2013). Ribosome profiling reveals resemblance between long non-coding RNAs and 5 ' leaders of coding RNAs. *Development* 140, 2828–2834. doi: 10.1242/dev.098343

Durfee, T., Hansen, A. M., Zhi, H., Blattner, F. R., and Jin, D. J. (2008). Transcription profiling of the stringent response in *Escherichia coli*. *J. Bacteriol.* 190, 1084–1096. doi: 10.1128/JB.01092-07

Ganesan, B., Stuart, M. R., and Weimer, B. C. (2007). Carbohydrate starvation causes a metabolically active but nonculturable state in *Lactococcus lactis*. *Appl. Environ. Microbiol.* 73, 2498–2512. doi: 10.1128/AEM.01832-06

Gaucher, F., Bonnassie, S., Rabah, H., Marchand, P., Blanc, P., Jeantet, R., et al. (2019). Review: adaptation of beneficial propionibacteria, *Lactobacilli*, and *Bifidobacteria* improves tolerance toward technological and digestive stresses. *Front. Microbiol.* 10:841. doi: 10.3389/fmicb.2019.00841

Genuth, N. R., and Barna, M. (2018). The discovery of ribosome heterogeneity and its implications for gene regulation and organismal life. *Mol. Cell* 71, 364–374. doi: 10.1016/j.molcel.2018.07.018

Goncheva, M. I., Flannagan, R. S., Sterling, B. E., Laakso, H. A., Friedrich, N. C., Kaiser, J. C., et al. (2019). Stress-induced inactivation of the *Staphylococcus aureus* purine biosynthesis repressor leads to hypervirulence. *Nat. Commun.* 10:775. doi: 10.1038/s41467-019-08724-x

Guo, H. L., Ingolia, N. T., Weissman, J. S., and Bartel, D. P. (2010). Mammalian microRNAs predominantly act to decrease target mRNA levels. *Nature* 466, 835–866. doi: 10.1038/nature09267

Ingolia, N. T. (2016). Ribosome footprint profiling of translation throughout the genome. *Cell* 165, 22–33. doi: 10.1016/j.cell.2016.02.066

Ingolia, N. T., Ghaemmaghami, S., Newman, J. R. S., and Weissman, J. S. (2009). Genome-wide analysis in vivo of translation with nucleotide resolution using ribosome profiling. *Science* 324, 218–223. doi: 10.1126/science.1168978

Juntawong, P., Girke, T., Bazin, J., and Bailey-Serres, J. (2014). Translational dynamics revealed by genome-wide profiling of ribosome footprints in *Arabidopsis*. *Proc. Natl. Acad. Sci. U.S.A.* 111, E203–E212. doi: 10.1073/pnas.1317811111

Lackner, D. H., Schmidt, M. W., Wu, S. D., Wolf, D. A., and Bahler, J. (2012). Regulation of transcriptome, translation, and proteome in response to environmental stress in fission yeast. *Genome Biol.* 13:R25. doi: 10.1186/gb-2012-13-4-r25

Lai, C. Y., and Cronan, J. E. (2003). β-ketoacyl-acyl carrier protein synthase III (FabH) is essential for bacterial fatty acid synthesis. *J. Biol. Chem.* 278, 51494–51503. doi: 10.1074/jbc.M308638200

Langmead, B., and Salzberg, S. L. (2012). Fast gapped-read alignment with Bowtie 2. *Nat. Methods* 9, 357–U354. doi: 10.1038/NMETH.1923

Lei, L., Shi, J. P., Chen, J., Zhang, M., Sun, S. L., Xie, S. J., et al. (2015). Ribosome profiling reveals dynamic translational landscape in maize seedlings under drought stress. *Plant J.* 84, 1206–1218. doi: 10.1111/tpj.13073

Lin, J. T., Liang, H. B., Yan, J. W., and Luo, L. X. (2017). The molecular mechanism and post-transcriptional regulation characteristic of *Tetragenococcus halophilus* acclimation to osmotic stress revealed by quantitative proteomics. *J. Proteomics* 168, 1–14. doi: 10.1016/j.jprot.2017.08.014

Liu, M. J., Wu, S. H., Wu, J. F., Lin, W. D., Wu, Y. C., Tsai, T. Y., et al. (2013). Translational landscape of photomorphogenic *Arabidopsis*. *Plant Cell* 25, 3699–3710. doi: 10.2307/23598427

Lv, L. X., Yan, R., Shi, H. Y., Shi, D., Fang, D. Q., Jiang, H. Y., et al. (2017). Integrated transcriptomic and proteomic analysis of the bile stress response in probiotic *Lactobacillus salivarius* LI01. *J. Proteomics* 150, 216–229. doi: 10.1016/j.jprot.2016.08.021

Moayyedi, M., Eskandari, M. H., Rad, A. H. E., Ziaee, E., Khodaparast, M. H. H., and Golmakani, M. T. (2018). Effect of drying methods (electrospraying, freeze drying and spray drying) on survival and viability of microencapsulated *Lactobacillus rhamnosus* ATCC 7469. *J. Funct. Food.* 40, 391–399. doi: 10.1016/j.jff.2017.11.016

Muruzovic, M. Z., Mladenovic, K. G., and Comic, L. R. (2018). In vitro evaluation of resistance to environmental stress by planktonic and biofilm form of lactic acid bacteria isolated from traditionally made cheese from Serbia. *Food Biosci.* 23, 54–59. doi: 10.1016/j.fbio.2018.03.005

Palomino, M. M., Waehner, P. M., Martin, J. F., Ojeda, P., Malone, L., Rivas, C. S., et al. (2016). Influence of osmotic stress on the profile and gene expression of surface layer proteins in *Lactobacillus acidophilus* ATCC 4356. *Appl. Microbiol. Biotechnol.* 100, 8475–8484. doi: 10.1007/s00253-016-7698-y

Papadimitriou, K., Alegria, A., Bron, P. A., De Angelis, M., Gobbetti, M., Kleerebezem, M., et al. (2016). Stress physiology of lactic acid bacteria. *Microbiol. Mol. Biol. Rev.* 80, 837–890. doi: 10.1128/MMBR.00076-15

Peifer, S., Barduhn, T., Zimmet, S., Volmer, D. A., Heinzle, E., and Schneider, K. (2012). Metabolic engineering of the purine biosynthetic pathway in *Corynebacterium glutamicum* results in increased intracellular pool sizes of IMP and hypoxanthine. *Microb. Cell. Fact.* 11:138. doi: 10.1186/1475-2859-11-138

Shah, P., Ding, Y., Niemczyk, M., Kudla, G., and Plotkin, J. B. (2013). Rate-limiting steps in yeast protein translation. *Cell* 153, 1589–1601. doi: 10.1016/j.cell.2013.05.049

Shalgi, R., Hurt, J. A., Krykbaeva, I., Taipale, M., Lindquist, S., and Burge, C. B. (2013). Widespread regulation of translation by elongation pausing in heat shock. *Mol. Cell* 49, 439–452. doi: 10.1016/j.molcel.2012.11.028

Shcherbik, N., and Pestov, D. G. (2019). The impact of oxidative stress on ribosomes: from injury to regulation. *Cells* 8:1379. doi: 10.3390/cells8111379

Shenton, D., Smirnova, J. B., Selley, J. N., Carroll, K., Hubbard, S. J., Pavitt, G. D., et al. (2006). Global translational responses to oxidative stress impact upon multiple levels of protein synthesis. *J. Biol. Chem.* 281, 29011–29021.

Shimaoka, M., Takenaka, Y., Kurahashi, O., Kawasaki, H., and Matsui, H. (2007). Effect of amplification of desensitized purF and prs on inosine accumulation in *Escherichia coli*. *J. Biosci. Bioeng.* 103, 255–261. doi: 10.1263/jbb.103.255

Siroli, L., Braschi, G., Rossi, S., Gottardi, D., Patrignani, F., and Lanciotti, R. (2020). Lactobacillus paracasei A13 and high-pressure homogenization stress response. *Microorganisms* 8:439. doi: 10.3390/microorganisms8030439

Sonenberg, N., and Hinnebusch, A. G. (2009). Regulation of translation initiation in eukaryotes: mechanisms and biological targets. *Cell* 136, 731–745. doi: 10.1016/j.cell.2009.01.042

Song, J. J., Li, Y., Li, J., Wang, H. W., Zhang, Y., and Suo, H. Y. (2020). Lactobacillus rhamnosus 2016SWU.05.0601 regulates immune balance in ovalbumin-sensitized mice by modulating expression of the immune-related transcription factors and gut microbiota. *J. Sci. Food Agric.* 100, 4930–4939. doi: 10.1002/jsfa.10554

Song, Y., Shin, J., Jin, S., Lee, J. K., Kim, D. R., Kim, S. C., et al. (2018). Genome-scale analysis of syngas fermenting acetogenic bacteria reveals the translational regulation for its autotrophic growth. *BMC Genomics* 19:837. doi: 10.1186/s12864-018-5238-0

Spriggs, K. A., Bushell, M., and Willis, A. E. (2010). Translational regulation of gene expression during conditions of cell stress. *Mol. Cell* 40, 228–237. doi: 10.1016/j.molcel.2010.09.028

Sun, J. H., Chen, H. Y., Qiao, Y. L., Liu, G. F., Leng, C., Zhang, Y. J., et al. (2019). The nutrient requirements of *Lactobacillus rhamnosus* GG and their application to fermented milk. *J. Dairy Sci.* 102, 5971–5978. doi: 10.3168/jds.2018-15834

Tian, X. W., Wang, Y. H., Chu, J., Mohsin, A., and Zhuang, Y. P. (2018). Exploring cellular fatty acid composition and intracellular metabolites of osmotic-tolerant mutant *Lactobacillus paracasei* NCBIO-M2 for highly efficient lactic acid production with high initial glucose concentration. *J. Biotechnol.* 286, 27–35. doi: 10.1016/j.jbiotec.2018.09.005

Tian, X. W., Wang, Y. H., Chu, J., Zhuang, Y. P., and Zhang, S. L. (2014). Oxygen transfer efficiency and environmental osmolarity response to neutralizing agents on L-lactic acid production efficiency by *Lactobacillus paracasei*. *Process. Biochem.* 49, 2049–2054. doi: 10.1016/j.procbio.2014.06.014

Wek, R. C. (2018). Role of eIF2 α kinases in translational control and adaptation to cellular stress. *Cold Spring Harb. Perspect. Biol.* 10:a032870. doi: 10.1101/cshperspect.a032870

Wu, C. C. C., Zinshteyn, B., Wehner, K. A., and Green, R. (2019). High-resolution ribosome profiling defines discrete ribosome elongation states and translational regulation during cellular stress. *Mol. Cell* 73, 959–970. doi: 10.1016/j.molcel.2018.12.009

Yang, X. P., Teng, K. L., Li, L. L., Su, R. N., Zhang, J., Ai, G. M., et al. (2019). Transcriptional regulator acrR increases ethanol tolerance through regulation of fatty acid synthesis in *Lactobacillus plantarum*. *Appl. Environ. Microbiol.* 85:e01690-19. doi: 10.1128/AEM.01690-19

Zhang, Y. Q., Xiao, Z. T., Zou, Q., Fang, J. H., Wang, Q. F., Yang, X. R., et al. (2017). Ribosome profiling reveals genome-wide cellular translational regulation upon heat stress in *Escherichia coli*. *Genom. Proteomics Bioinform.* 15, 324–330. doi: 10.1016/j.gpb.2017.04.005

Zhong, Y., Karaletsos, T., Drewe, P., Sreedharan, V. T., Kuo, D., Singh, K., et al. (2017). RiboDiff: detecting changes of mRNA translation efficiency from ribosome footprints. *Bioinformatics* 33, 139–141. doi: 10.1093/bioinformatics/btw585

Conflict of Interest: The authors declare that the research was conducted in the absence of any commercial or financial relationships that could be construed as a potential conflict of interest.

Publisher's Note: All claims expressed in this article are solely those of the authors and do not necessarily represent those of their affiliated organizations, or those of the publisher, the editors and the reviewers. Any product that may be evaluated in this article, or claim that may be made by its manufacturer, is not guaranteed or endorsed by the publisher.

frontiers in Microbiology

ORIGINAL RESEARCH
published: 29 November 2021
doi: 10.3389/fmicb.2021.778555

The Impacts of Dietary Fermented Mao-tai Lees on Growth Performance, Plasma Metabolites, and Intestinal Microbiota and Metabolites of Weaned Piglets

*Zhihua Li[1,2], Qian Zhu[1], Md. Abul Kalam Azad[1], Huawei Li[1], Pan Huang[1] and Xiangfeng Kong[1]**

[1]Hunan Provincial Key Laboratory of Animal Nutritional Physiology and Metabolic Process, National Engineering Laboratory for Pollution Control and Waste Utilization in Livestock and Poultry Production, Institute of Subtropical Agriculture, Chinese Academy of Sciences, Changsha, China, [2]College of Animal Science and Technology, Nanjing Agricultural University, Nanjing, China

OPEN ACCESS

Edited by:
Zheng Ruan,
Nanchang University, China

Reviewed by:
Miao Yu,
Guangdong Academy of Agricultural Sciences, China
Gang Shu,
South China Agricultural University, China

***Correspondence:**
Xiangfeng Kong
nnkxf@isa.ac.cn

Specialty section:
This article was submitted to Food Microbiology, a section of the journal Frontiers in Microbiology

Received: 17 September 2021
Accepted: 05 November 2021
Published: 29 November 2021

Citation:
Li Z, Zhu Q, Azad MAK, Li H, Huang P and Kong X (2021) The Impacts of Dietary Fermented Mao-tai Lees on Growth Performance, Plasma Metabolites, and Intestinal Microbiota and Metabolites of Weaned Piglets. Front. Microbiol. 12:778555. doi: 10.3389/fmicb.2021.778555

This study investigated the effects of dietary supplementation with fermented Mao-tai lees (FML) on growth performance, plasma metabolites, and intestinal microbiota and metabolites of weaned piglets. A total of 128 *Duroc* × *Landrace* × *Yorkshire* piglets (28-days old) were randomly assigned to one of four groups, feeding a basal diet (control group), a basal diet supplemented with 2, 4 or 6% FML, respectively, for 42 days. The results showed that dietary 4% FML supplementation had higher ($p < 0.05$) average daily gain (ADG) and plasma triglyceride concentration during days 1–14 of the trial than the other FML supplemented groups. In addition, dietary 2 and 4% FML supplementation increased ($p < 0.05$) the ADG during days 15–28 of the trial and plasma total protein concentration on day 42 of the trial compared with the 6% FML supplement. The plasma concentrations of arginine, ethanolamine, histidine, isoleucine, lysine, methionine, proline, taurine, threonine, and tyrosine were increased ($p < 0.05$) in the 4% FML group compared with the other three groups on day 14 of the trial. Dietary supplementation with 2–6% FML decreased ($p < 0.05$) the plasma urea nitrogen concentration on day 14 of the trial and the abundance of *Escherichia coli* in the colon, and dietary 2 and 4% FML supplementation decreased ($p < 0.05$) the abundance of sulfate-reducing bacteria compared with the control group. In the intestinal contents, a higher concentration of FML (6%) supplementation decreased ($p < 0.05$) the colonic acetate concentration compared with the control and 2% FML groups, while 4% FML supplementation increased ($p < 0.05$) the colonic cadaverine concentration compared with the other three groups. In conclusion, dietary 4% FML supplementation might contribute to the increased amino acids metabolism without affecting the growth performance of weaned piglets. Moreover, dietary 2 and 4% FML supplementation were also beneficial to intestinal health *via* decreasing the abundances of specific pathogens and increasing the concentrations of microbial metabolites in the gut, which provides the theoretical basis and data support for the application of FML in pigs.

Keywords: amino acids, fermented Mao-tai lees, growth performance, intestinal microbiota, weaned piglets

INTRODUCTION

To reduce production costs, livestock producers have increased the use of agricultural by-products, including distillers dried grains with soluble (DDGS) of sorghum, wheat, corn, and rye, which can replace some conventional feedstuffs. The DDGS from six different dry grind ethanol plants contains various nutrients, including 7.89–15.10% oil, 28.01–30.03% crude protein (CP), 37.51–48.74% neutral detergent fiber (NDF), 13.92–18.71% acid detergent fiber (ADF), and 3.72–4.59% ash (Singh et al., 2002). Compared with corn and soybean, the DDGS has considerably more fiber which consists predominantly of 35% insoluble dietary fiber (Stein and Shurson, 2009) with low fermentation performance, including arabinoxylans, cellulose, and lignin (Gutierrez et al., 2014). Mao-tai liquor is famous due to its unique production process, impressive liquor quality, and complex aromas (Wang et al., 2016). The production of Mao-tai liquor was 50,235.17 tons in Kweichow Moutai Co., Ltd. (2020), Guizhou, China (Annual Report, 2020), and the solid by-products (including lees) are estimated to be about 150,700 tons. After the processing and production of liquor, a large amount of solid by-products remained unused, which can cause resource waste and environmental pollution. Therefore, the comprehensive utilization of Mao-tai lees (a common DDGS) in animal feed is conducive to the sustainable development of the wine industry and solves the problem of feedstuff shortage in animal husbandry.

Piglets are vulnerable to physiological, nutritional, and environmental weaning stressors due to the transportation, mixing with other littermates, separation from the sow's milk, and changes to solid feed and ambient temperature (Tang et al., 2009; Azad et al., 2021). These abrupt changes often cause intestinal microbiota imbalance, which has been related to decreased growth rate, changes in gut morphology and microbial populations, and increased susceptibility to scouring and disease (Reilly et al., 2008). Previous studies indicated that increasing DDGS inclusion in diets resulted in the reduction of body gain to feed intake of weaned piglets, which might be due to the increasing unfermented DDGS inclusion reached to a physical limitation of the gut size, or by decreasing the density and altering the taste or smell of the diet, thus reduced the diet palatability (Avelar et al., 2010). Therefore, it is important to improve the digestibility and nutritional value of DDGS. Fermentation is a practical way to increase cellulose and hemicellulose degradation (Yang et al., 2012), lower phytic acid, and enhance protein digestibility, so fermentation of DDGS may facilitate higher inclusion levels in animal diets, especially for mono-gastric animals (Lamsal et al., 2012). Yeasts, such as *Saccharomyces boulardii,* have increasingly been used for fermenting DDGS, providing vital evidence of its efficacy as an adjuvant agent to treat diarrhea and prevent antibiotic-associated complications (Buts, 2009). Thus, microbial fermentation can improve the nutritional values and functional effects of DDGS.

Previous studies mostly focused on the effects of dietary supplementation with DDGS and fermented DDGS on the growth performance and digestibility of animals (Stein and Shurson, 2009; Gutierrez et al., 2014). However, the effects of dietary supplementation with DDGS on plasma metabolites and intestinal microbiota and their metabolites have not been elucidated yet. Our previous studies showed that supplementing 15% fermented Mao-tai lees (FML) to growing-finishing pigs' diets could improve the gut health *via* increasing the abundance of putative beneficial microbiota and straight-chain fatty acid concentrations, and decreasing the abundances of potential pathogens in the colon (Li et al., 2019). Therefore, we hypothesized that the FML could be used as a cost-effective alternative for feedstuff of weaned piglets owing to its beneficial to plasma and intestinal metabolites and intestinal microbiota. Thus, the present study determined the effects of dietary FML supplementation on growth performance, plasma metabolites, and intestinal microbiota and metabolites of weaned piglets.

MATERIALS AND METHODS

Preparation of FML

The FML was prepared by the Road Biological Environmental Co., Ltd., Sichuan, China. After sterilization, Mao-tai liquor lees containing 55% water were mixed with 5‰ *Saccharomyces cerevisia*e, 3‰ *Aspergillus niger*, and 0.6‰ *Bacillus subtilis*. The mixture was incubated at 32°C for 36 h under ventilation and at 32°C for 12 h under static and anaerobic conditions. Then, the incubated mixture was added into 0.5‰ acid protease and 0.5‰ neutral protease and further incubated at pH 5.0 and 60°C for 12 h. After fermentation, the fermented products were dried using a fluidized bed dryer at 40°C, pulverized, screened through a 0.45-mm mesh, and packed for use. The determined nutrient levels (%) of FML based on dry matter content (92.97%) were as follows: ash, 9.28; CP, 23.96; ether extract (EE), 5.39; crude fiber (CF), 17.67; ADF, 38.06; NDF, 47.28; Ca, 0.53; P, 0.55; and gross energy (GE), 18.29 MJ/Kg (Li et al., 2019).

Animals, Housing, and Treatment

A total of 128 *Duroc* × *Landrace* × *Yorkshire* piglets weaned at 21-day old were used in this study. After a 7-day adaptation period, all piglets at 28-day old with 7.94 ± 0.12 kg of average body weight (BW) were randomly assigned to one of four groups. The piglets were fed a basal diet (control group), a basal diet supplemented with 2, 4, or 6% FML, respectively. The basal diet (**Supplementary Table 1**) was formulated to meet the National Research Council (2012) nutrient requirements for weaned piglets. Each group had eight replicates (pens) with four piglets per replicate. The piglets were housed individually in an environmentally controlled room (23 ± 2°C) with a nursery facility with hard plastic completely slotted flooring. The piglets were fed twice daily (at 8:00 and 16:00), and water was available *ad libitum*. Each pen was equipped with a stainless-steel feeder and a nipple drinker. The FML was accurately weighed and fully mixed with the basal feed.

Growth Performance

Piglet BW was measured on days 14, 28, and 42 of the trial. The feed intake and number of piglets with diarrhea were recorded daily. Average daily gain (ADG), average daily feed

intake (ADFI), and the ratio of feed intake to BW gain (F/G) were calculated.

Sample Collection and Preparation

Blood samples (5 ml) were collected from the precaval vein on days 14, 28, and 42 of the trial, respectively. Plasma was obtained by centrifugation at 3,000 × g and 4°C for 10 min and then stored at −80°C until analysis. At the end of the trial, all the animals were electrically stunned (120 V, 200 HZ), exsanguinated, and eviscerated for sample collection. The contents of the ileum (10 cm above the ileo-cecal junction) and colon (middle portion) were collected and divided into two aliquots. One aliquot of the contents (1 g) was immediately snap-frozen in liquid nitrogen and then stored at −80°C for analysis of microbial DNA. The other portion (approximately 20 g) was stored at −20°C to assay the concentrations of short-chain fatty acids (SCFAs) and bioamines (only in the colon).

Analysis of Plasma Metabolites

Plasma concentrations of urea nitrogen (UN), total protein (TP), total cholesterol (TC), triglyceride (TG), high-density lipoprotein-cholesterol (HDL-C), and low-density lipoprotein-cholesterol (LDL-C) were analyzed using a Roche automatic biochemical analyzer (Cobas c311, F. Hoffmann-La Roche Ltd., Basel, Switzerland) and commercial kits (F. Hoffmann-La Roche Ltd., Basel, Switzerland) according to the manufacturers' instructions, as well as the plasma activities of alkaline phosphatase (ALP), aspartate aminotransferase (AST), and alanine aminotransferase (ALT; Kong et al., 2007).

Plasma samples (1.00 ml) were blended with the same volume of 8% 5-sulfosalicylic acid for 30 min and then centrifuged at 12,000 × g for 10 min at 4°C. The supernatant was filtered through a 0.45-μm membrane for free amino acids (AAs) analysis using an auto amino acid analyzer (L8800, Hitachi, Tokyo, Japan; Hu et al., 2019).

Determination of Microbiota Abundances in the Ileal and Colonic Contents

The abundances of the ileal and colonic microbiota were analyzed as previously described (Su et al., 2018). Briefly, the total microbial DNA was extracted and purified by a QIAamp DNA Stool Kit (Qiagen, Hilden, Germany). The specific primers (**Supplementary Table 2**) of targeted microbiota were used to amplify the targeted gene fragments. The recombinant plasmid vector of targeted microbiota was constructed and cloned according to the pMDTM19-T vector cloning kit (TaKaRa Biotechnology, Dalian, China) instructions. Quantitative real-time polymerase chain reaction (qPCR) was performed using an SYBR Green detection kit (Thermo Fisher Scientific, Waltham, MA) to determine the abundances of general microbial DNA from the intestinal contents and above recombinant DNA using a Lightcycler 480II instrument (Applied Biosystems; Su et al., 2018). The standard curves for all determined microbiota were constructed based on the recombinant DNA of representative species. The results are presented as the gene copies of microbial DNA of the intestinal contents.

Determination of Microbial Metabolites

The ileal and colonic SCFAs, including acetate, propionate, butyrate, isobutyrate, valerate, and isovalerate, were analyzed according to the method described by Zhou et al. (2014). The contents of cadaverine, phenylethylamine, putrescine, tryptamine, tyramine, spermidine, and 1,7-heptyl diamine in the colonic contents were measured as described previously (Ji et al., 2018), using an Agilent 6,890 gas chromatography (Agilent Technologies, Inc., Palo Alto, CA, United States).

Statistical Analysis

Statistical analysis was performed using SAS software version 9.2. The normal distribution and homogeneity of variance of data were evaluated by the Shapiro–Wilk method and Levene method. Then, all data were subjected to one-way ANOVA with Duncan's multiple range test. The statistical data are expressed with means and pooled standard error of the means (SEM) among the four groups. Statistical significance was defined as $p < 0.05$. Probability values between 0.05 and 0.10 were considered to be trends.

RESULTS

Effects of Dietary FML Supplementation on Growth Performance and Diarrhea Rate of Weaned Piglets

To evaluate the effects of FML on the growth performance of weaned piglets, the BW, ADFI, and F/G were measured at different stages of the trial. As shown in **Table 1**, there were no significant differences ($p > 0.05$) in the initial BW, final BW, ADFI, and F/G among the four groups. The 4% FML group had higher ($p < 0.05$) ADG during days 1–14 of the trial than the other FML supplemented groups. Moreover, the pigs supplemented with 2 and 4% FML during days 15–28 of the trial had higher ($p < 0.05$) ADG than the 6% FML group. There were no significant differences ($p > 0.05$) in the diarrhea rate of piglets among the four groups during days 1–14, 15–28, 29–42, and 1–42 of the trial (**Supplementary Table 3**).

Effects of Dietary FML Supplementation on Plasma Biochemical Parameters of Weaned Piglets

The plasma biochemical indicators of weaned piglets are shown in **Table 2**. On day 14 of the trial, the plasma UN concentration of the FML groups (2, 4, and 6%) was lower ($p < 0.05$) than the control group. The plasma TG concentration of the 4% FML group was higher ($p < 0.05$) than the 2 and 6% FML groups. On day 28 of the trial, the plasma LDL-C concentration of the 4% FML group was higher ($p < 0.05$) than the 6% FML group. The plasma TG concentration of the 4 and 6% FML groups was higher ($p < 0.05$) than the control group. Moreover, dietary

TABLE 1 | Effects of dietary supplementation with fermented Mao-tai lees (FML) on growth performance of weaned piglets.

Items	Control	Dietary FML level			SEM	*p* values
		2%	4%	6%		
Initial BW (kg)	7.93	7.93	7.95	7.95	0.12	1.00
Final BW (kg)	26.46	26.93	27.02	25.95	0.44	0.82
ADFI (g d^{-1})						
Days 1–14 of the trial	448.22	448.45	448.31	446.69	2.28	0.99
Days 15–28 of the trial	909.13	946.80	891.32	913.65	12.76	0.50
Days 29–42 of the trial	1204.95	1135.23	1224.21	1181.32	21.91	0.54
Days 1–42 of the trial	847.01	866.74	852.26	847.22	5.99	0.63
ADG (g d^{-1})						
Days 1–14 of the trial	256.67^{ab}	241.63^{b}	267.08^{a}	238.73^{b}	3.64	<0.01
Days 15–28 of the trial	510.34^{ab}	519.87^{a}	519.39^{a}	488.91^{b}	4.50	0.04
Days 29–42 of the trial	595.76	557.44	583.63	558.93	9.18	0.38
Days 1–42 of the trial	439.57	452.42	452.02	434.57	3.51	0.19
F/G (g g^{-1})						
Days 1–14 of the trial	1.82	1.86	1.79	1.84	0.02	0.38
Days 15–28 of the trial	1.79	1.82	1.78	1.87	0.03	0.64
Days 29–42 of the trial	2.04	2.03	2.08	2.12	0.02	0.82
Days 1–42 of the trial	1.94	1.89	1.92	2.00	0.02	0.15

Data are presented as means with pooled standard error of the means (SEM; n = 8). [a, b]Mean values within a row with different superscript letters were significantly different ($p < 0.05$). ADFI, average daily feed intake; ADG, average daily gain; BW, body weight; and F/G, ratio of feed to gain.

FML supplementation had a trend to decrease ($p = 0.05$) the plasma TP concentration. On day 42 of the trial, the plasma LDL-C concentration of the 6% FML group was higher ($p < 0.05$) than the 2% FML and control groups. The plasma TP concentration of the 6% FML group was lower ($p < 0.05$) than the other three groups. In addition, the plasma TC concentration of the 4 and 6% FML groups had an increasing trend ($p = 0.06$) compared with the control and 2% FML groups. However, there were no significant differences ($p > 0.05$) in plasma levels in the plasma concentrations of ALP, ALT, AST, and HDL-C during the entire trial period among the four groups.

Effects of Dietary FML Supplementation on Plasma-Free AAs in Weaned Piglets

We further investigated the effects of FML supplementation on piglet's plasma-free AAs profiles. As shown in **Table 3**, the plasma concentrations of arginine (Arg), ethanolamine (EOHNH2), histidine (His), isoleucine (Ile), lysine (Lys), methionine (Met), proline (Pro), taurine (Tau), threonine (Thr), and tyrosine (Tyr) in the 4% FML group were higher ($p < 0.05$) compared with the other three groups on day 14 of the trial. In addition, the plasma concentration of sarcosine (Sar) was higher ($p < 0.05$) in the 4 and 6% FML groups than the control and 2% FML groups. On day 28 of the trial, the plasma concentrations of cysteine (Cys; $p < 0.05$) and Tau ($p = 0.08$) of the 4% FML group were higher than the other three groups. Moreover, on day 42 of the trial, the plasma concentration of citrulline (Cit) of the 2 and 6% FML groups was lower ($p < 0.05$), as well as the plasma concentration of EOHNH2 of the three FML groups, while the plasma Pro concentration of the 2% FML group was higher ($p < 0.05$), when compared with the control group.

Effects of Dietary FML Supplementation on Microbiota Abundances in the Ileal and Colonic Contents of Weaned Piglets

The microbiota abundances in the ileal and colonic contents of weaned piglets are shown in **Table 4**. There were no significant differences ($p > 0.05$) in the abundances of *Clostridium cluster* IV, *Bacteroidetes*, *Lactobacillus*, *Escherichia coli (E. coli)*, and total bacteria in the ileal contents were observed among the four groups. The relative abundance of *Firmicutes* in the 6% FML group was lower ($p < 0.05$) compared with the control group. Meanwhile, the ratio of *Firmicutes* to *Bacteroidetes* (F/B) in the 4 and 6% FML groups was lower ($p = 0.07$) compared with the control and 2% FML groups. Dietary 4% FML supplementation increased ($p < 0.05$) the abundance of sulfate-reducing bacteria compared with the control and 2% FML groups.

In the colonic contents, dietary 4% FML supplementation increased ($p < 0.05$) the F/B ratio compared with the other three groups. In addition, the relative abundance of *E. coli* in the FML groups (2, 4, and 6%) and the relative abundance of sulfate-reducing bacteria in the 2 and 4% FML groups were lower ($p < 0.05$) compared with the control group.

Effects of Dietary FML Supplementation on Intestinal Concentrations of SCFAs and Bioamines of Weaned Piglets

Ileal and colonic SCFAs concentrations are presented in **Table 5**. The piglets fed with 6% FML had lower ($p < 0.05$) colonic acetate concentration than the control and 2% FML groups. A higher ($p = 0.09$) straight-chain fatty acid concentration in the colon was observed in the 2% FML group compared with the control and 6% FML groups. However, there were no

TABLE 2 | Effects of dietary supplementation with fermented Mao-tai less (FML) on plasma biochemical parameters in weaned piglets.

Items	Day of the trial	Control	Dietary FML level			SEM	*p* values
			2%	4%	6%		
ALP (U L^{-1})	14	509.50	463.00	425.75	357.38	26.00	0.21
	28	435.88	353.50	405.00	385.63	21.20	0.59
	42	241.33	245.17	279.83	274.00	12.78	0.65
ALT (U L^{-1})	14	47.88	56.75	45.75	52.75	2.13	0.26
	28	57.25	47.25	55.13	53.75	2.17	0.41
	42	39.33	41.17	42.17	42.50	2.44	0.33
AST (U L^{-1})	14	71.63	76.75	87.50	86.25	5.43	0.71
	28	76.50	67.38	68.38	61.38	3.10	0.40
	42	61.33	51.50	61.67	69.50	3.30	0.30
UN (mmol L^{-1})	14	3.22^{a}	2.15^{b}	2.23^{b}	2.31^{b}	0.13	<0.01
	28	2.52	2.66	2.16	2.11	0.12	0.27
	42	2.62	3.19	2.95	2.24	0.17	0.25
HDL-C (mmol L^{-1})	14	0.61	0.68	0.67	0.62	0.02	0.72
	28	0.69	0.76	0.79	0.70	0.02	0.36
	42	0.70	0.72	0.93	0.80	0.04	0.12
LDL-C (mmol L^{-1})	14	0.91	0.82	0.80	0.97	0.04	0.34
	28	1.02^{ab}	1.04^{ab}	1.17^{a}	0.91^{b}	0.03	0.04
	42	1.00^{b}	0.88^{b}	1.07^{ab}	1.36^{a}	0.06	0.02
TC (mmol L^{-1})	14	1.66	1.64	1.64	1.70	0.05	0.97
	28	1.84	1.90	2.07	1.77	0.05	0.11
	42	1.80	1.69	2.07	2.21	0.08	0.06
TG (mmol L^{-1})	14	0.39^{ab}	0.32^{b}	0.48^{a}	0.36^{b}	0.02	0.04
	28	0.40^{b}	0.44^{ab}	0.63^{a}	0.58^{a}	0.03	0.04
	42	0.27	0.40	0.39	0.26	0.03	0.29
TP (g L^{-1})	14	45.91	39.88	39.68	39.93	1.28	0.24
	28	52.64	42.96	42.53	45.83	1.35	0.05
	42	55.52^{a}	57.72^{a}	53.10^{a}	44.98^{b}	1.46	<0.01

Data are presented as means with pooled SEM (n = 8). [a, b]Mean values within a row with different superscript letters were significantly different (p < 0.05). ALP, alkaline phosphatase; ALT, alanine aminotransferase; AST, aspartate transaminase; UN, urea nitrogen; HDL-C, high-density lipoprotein-cholesterol; LDL-C, low-density lipoprotein-cholesterol; TC, total cholesterol; TG, triglyceride; and TP, total protein.

significant differences ($p > 0.05$) in the concentrations of other SCFAs among the four groups.

Colonic bioamine concentrations of piglets are presented in **Table 6**. The 4% FML group had a higher ($p < 0.05$) cadaverine concentration in the colonic contents than the other three groups. There were no significant differences ($p > 0.05$) in the concentrations of other bioamines among the four groups.

DISCUSSION

The nutritional values of DDGS may be improved by microbial fermentation or enzymatic degradation. Wiseman et al. (2017) reported that fermented DDGS is beneficial to improve the growth performance in weaned piglets, possibly due to nutrient breakdown and normal development of the gut microbiota. In the present study, dietary FML supplementation regulated plasma-free AAs metabolism and altered intestinal microbiota and metabolites of weaned piglets.

The growth performance of weaned piglets can reflect the subsequent performance and the production profitability to some extent. In the present study, although there were no statistical significances in the growth performance of piglets compared with the control group; however, the dietary supplementation with 4% FML had a higher ADG than the other three groups during days 1–14 of the trial. Several previous studies also showed that dietary DDGS supplementation with enzymes was not effective in improving the growth performance of nursery pigs (Jones et al., 2010; Kerr et al., 2013). However, other studies reported that multi-enzyme blends were tended to improve the growth performance in growing-finishing pigs fed diets with DDGS (Emiola et al., 2009; Li et al., 2012). Therefore, the inconsistency might have resulted from differences in the DDGS source, dietary level of the DDGS used, supplementing dose and types of the enzymes or microorganisms used, age of experimental animals, and the nutrient level of the experimental diet (Swiatkiewicz et al., 2016). The diarrhea rate during the nursery period is an essential indicator of the gut health status of piglets. Our results showed that the FML had no adverse side effects on the piglets' diarrhea rate. Thus, these findings indicate that the dietary FML could be used in mono-gastric animals because microbial fermentation could improve the quality of protein and decrease the CF in the Mao-tai lees.

Plasma metabolites primarily originate from the digestion and absorption of the gut. The UN and TP play a critical role in transamination and reflect the status of protein synthesis and catabolism (Liu et al., 2015). The UN is the main nitrogenous product of protein, and its concentration reflects the efficiency of protein utilization (Chen et al., 2018). Lower UN concentration

TABLE 3 | Effects of dietary supplementation with fermented Mao-tai less (FML) on plasma concentration of free amino acids in weaned piglets.

Items (μmol L^{-1})	Day of the trial	Control	Dietary FML level			SEM	*p* values
			2%	4%	6%		
Ala	14	611.14	745.97	816.85	779.94	31.57	0.10
	28	695.50	676.26	777.23	759.27	21.86	0.30
	42	381.94	590.29	574.96	603.71	34.22	0.08
Arg	14	101.06^{b}	80.45^{b}	150.10^{a}	108.69^{b}	6.83	<0.01
	28	124.91	123.27	143.54	113.44	8.05	0.63
	42	103.63	91.01	83.61	91.90	4.07	0.38
Asp	14	32.80	31.37	41.39	30.91	1.77	0.14
	28	34.95	32.08	41.26	35.58	2.52	0.65
	42	19.48	29.35	25.16	27.16	1.58	0.13
Cit	14	84.51	76.58	77.39	77.67	2.88	0.77
	28	70.08	72.65	74.10	76.54	2.07	0.75
	42	70.94^{a}	57.69^{bc}	68.46^{ab}	54.33^{c}	2.41	0.03
Cys	14	16.42	10.76	12.81	14.46	1.03	0.24
	28	13.81^{b}	11.76^{b}	23.55^{a}	13.15^{b}	1.7	0.05
	42	14.13	6.53	5.77	11.96	1.53	0.13
EOHNH2	14	2.94^{b}	3.12^{b}	5.60^{a}	1.86^{b}	0.43	0.02
	28	2.69	2.06	4.79	3.83	0.46	0.15
	42	4.79^{a}	0.92^{b}	1.54^{b}	0.78^{b}	0.42	<0.01
Glu	14	417.43	402.24	519.13	472.22	24.82	0.33
	28	361.24	372.61	444.16	373.75	18.4	0.38
	42	232.74	318.50	274.69	335.74	20.57	0.30
Gly	14	1265.73	1588.42	1337.18	1299.56	63.89	0.27
	28	1271.19	1384.78	1280.59	1222.47	44.88	0.65
	42	870.66	1026.73	993.20	972.76	48.75	0.71
His	14	11.90^{b}	11.17^{b}	20.18^{a}	12.15^{b}	1.18	0.01
	28	28.19	24.86	23.42	25.65	1.06	0.47
	42	21.19	20.60	19.18	20.35	0.66	0.76
Ile	14	113.19^{b}	107.60^{b}	144.31^{a}	116.61^{b}	4.74	0.02
	28	106.47	110.74	112.05	97.80	2.81	0.30
	42	88.34	99.06	91.50	80.23	3.57	0.35
Leu	14	115.68	107.03	139.81	115.99	5.15	0.13
	28	189.22	182.89	197.34	170.43	5.21	0.34
	42	175.80	198.00	190.53	158.17	6.59	0.17
Lys	14	187.54^{b}	199.89^{b}	303.36^{a}	207.59^{b}	13.82	<0.01
	28	300.40	275.16	308.42	310.36	13.14	0.78
	42	155.73	187.96	136.45	168.16	12.42	0.53
Met	14	51.92^{b}	44.14^{b}	87.93^{a}	59.79^{b}	4.26	<0.01
	28	58.68	55.81	53.15	53.12	2.22	0.80
	42	31.59	30.43	34.94	28.46	1.46	0.50
Orn	14	116.66	106.14	140.83	115.56	5.76	0.18
	28	137.32	147.60	130.51	122.03	4.68	0.30
	42	81.60	79.50	77.59	75.28	3.54	0.95
Phe	14	57.36^{ab}	44.83^{b}	68.82^{a}	65.25^{a}	2.85	0.01
	28	78.74	65.12	71.97	59.25	2.73	0.06
	42	64.35	62.88	62.85	60.44	2.51	0.97
Pro	14	254.18^{b}	265.42^{b}	328.20^{a}	270.46^{b}	9.05	0.01
	28	294.70	314.03	305.90	334.79	7.93	0.34
	42	202.03^{b}	281.91^{a}	258.88^{ab}	232.56^{ab}	11.12	0.04
Sar	14	30.31^{b}	34.36^{b}	47.67^{a}	45.99^{a}	2.24	0.01
	28	41.99	44.90	47.13	48.82	1.50	0.42
	42	38.40	42.35	46.41	39.26	2.30	0.62
Ser	14	198.05	247.47	267.35	244.74	11.65	0.19
	28	184.80	199.18	204.12	201.97	7.45	0.81
	42	120.94	138.06	125.36	129.5	4.42	0.58
Tau	14	95.20^{b}	92.31^{b}	164.05^{a}	104.53^{b}	7.83	<0.01
	28	122.77	100.68	142.94	91.77	7.77	0.08
	42	78.22	56.44	62.13	62.05	5.57	0.56
Thr	14	79.10^{bc}	68.20^{c}	215.14^{a}	123.57^{b}	13.48	<0.01
	28	85.69	86.64	86.31	79.46	4.50	0.94
	42	50.83	52.43	68.66	52.73	3.29	0.17
Tyr	14	61.98^{b}	54.70^{b}	97.12^{a}	67.53^{b}	4.51	<0.01

(Continued)

TABLE 3 | Continued

Items (μmol L^{-1})	Day of the trial	Control	Dietary FML level			SEM	*p* values
			2%	4%	6%		
	28	94.45	84.90	87.79	93.09	3.80	0.81
	42	68.39	74.65	59.35	54.32	3.23	0.12
Val	14	127.01	98.00	130.39	110.07	6.05	0.20
	28	159.69	150.71	157.95	155.17	5.09	0.94
	42	168.13	170.66	156.72	152.32	6.71	0.76

Data are presented as means with pooled SEM (n = 8). [a–c]Mean values within a row with different superscript letters were significantly different (p < 0.05). Ala, alanine; Arg, arginine; Asp, aspartic acid; Cit, citrulline; Cys, cysteine; EOHNH2, ethanolamine; Glu, glutamic acid; Gly, glycine; His, histidine; Ile, isoleucine; Leu, leucine; Lys, lysine; Met, methionine; Orn, ornithine; Phe, phenylalanine; Pro, proline; Sar, sarcosine; Ser, serine; Tau, taurine; Thr, threonine; Tyr, tyrosine; and Val, valine.

TABLE 4 | Effects of dietary supplementation with Fermented Mao-tai Lees (FML) on microbiota abundance in ileal and colonic contents of weaned piglets.

Items (copies g^{-1})	Control	Dietary FML level			SEM	*p* values
		2%	4%	6%		
Ileum						
Clostridium cluster IV (10^5)	2.01	2.00	1.97	0.92	0.31	0.51
Bacteroidetes (10^6)	3.80	1.85	2.79	3.07	0.60	0.76
Escherichia coli (10^6)	5.43	1.09	4.81	0.43	1.00	0.18
Firmicutes (10^9)	12.25^{a}	3.78^{ab}	4.22^{ab}	1.17^{b}	1.60	0.04
F/B	251.15	243.86	74.44	40.37	38.16	0.07
Lactobacillus (10^6)	15.06	16.09	9.50	0.34	3.18	0.29
Sulfate-reducing bacteria (10^4)	1.13^{b}	0.88^{b}	4.60^{a}	2.37^{ab}	0.51	0.04
Total bacteria (10^9)	28.35	5.39	40.13	1.93	7.28	0.18
Colon						
Clostridium cluster IV (10^7)	23.42	34.78	7.71	27.90	4.42	0.14
Bacteroidetes (10^{10})	2.51	3.56	2.58	3.81	0.33	0.46
Escherichia coli (10^6)	33.06^{a}	6.94^{b}	3.25^{b}	1.71^{b}	3.99	0.03
Firmicutes (10^9)	9.91	14.42	18.85	18.19	2.03	0.48
F/B	0.45^{b}	0.38^{b}	0.96^{a}	0.59^{b}	0.07	<0.01
Lactobacillus (10^6)	18.18	3.19	1.44	6.91	2.45	0.15
Sulfate-reducing bacteria (10^4)	9.81^{a}	1.27^{b}	2.01^{b}	5.81^{ab}	1.14	0.02
Total bacteria (10^{11})	8.59	10.70	4.43	9.88	1.71	0.58

Data are presented as means with pooled SEM (n = 8). [a, b]Mean values within a row with different superscript letters were significantly different (p < 0.05). F/B, Firmicutes/Bacteroidetes.

indicates a good balance of AAs (Hahn et al., 1995). In the present study, dietary FML supplementation decreased the plasma UN concentration on day 14 of the trial, suggesting that dietary FML improved the utilization of protein (Zhai et al., 2018). In addition, dietary 6% FML supplementation decreased the plasma TP concentration on day 42 of the trial, which may be due to that the relatively high fiber content decreased the digestion and absorption of dietary protein. The ALT and AST are transaminases which play crucial roles in protein and amino acid metabolism, and their plasma activities may increase when tissues damage and dysfunction, particularly in the liver (Canli and Canli, 2015). In the present study, dietary FML supplementation did not affect the plasma ALT and AST activities, suggesting that dietary FML had no detrimental effect on the liver tissue.

The TG plays an important role in nutrient metabolism as an energy source and transporter of dietary fat. There is no apparent relationship between the decrease in LDL-C and the increase in HDL-C (Barter et al., 2010). The LDL can antagonize the quorum sensing system that upregulates the gene expressions required for invasive *Staphylococcus aureus* infection (Peterson et al., 2008). In the present study, dietary 4% FML supplementation increased the plasma TG level on day 14 of the trial and LDL-C level on day 28 of the trial without decreasing the HDL-C level, which may be useful for promoting the ADG and inhibiting pathogenic infection.

Plasma proteins mostly exert their physiological functions in the form of AAs in the body. In the present study, dietary 4% FML supplementation increased the plasma concentrations of Arg, EOHNH2, His, Ile, Lys, Met, phenylalanine, Pro, Tau, Thr, and Tyr on day 14 of the trial. These findings indicated that the AA catabolism was improved by the FML supplementation, which may be due to high levels of acidic protein, cellulose, AAs, and organic acids in the FML. The AAs play important roles in regulating food intake and nutrient metabolism in animals (Wu et al., 2014). Several AAs (e.g.,

TABLE 5 | Effect of dietary supplementation with fermented Mao-tai less (FML) on intestinal SCFA contents of weaned piglets.

Items	Control	Dietary FML level			SEM	*p* values
		2%	4%	6%		
Ileum (mg g^{-1})						
Acetate	0.29	0.16	0.40	0.30	0.05	0.33
Propionate	0.02	0.01	0.02	0.02	0.00	0.64
Butyrate	0.03	0.01	0.04	0.03	0.01	0.53
Isobutyrate	0.006	0.009	0.007	0.006	0.00	0.92
Valerate	0.009	0.003	0.007	0.007	0.00	0.43
Isovalerate	0.008	0.01	0.009	0.014	0.00	0.19
Total straight-chain fatty acids	0.35	0.18	0.46	0.36	0.05	0.33
Total BCFA	0.01	0.02	0.02	0.03	0.00	0.57
Total SCFA	0.37	0.20	0.33	0.38	0.04	0.36
Colon (mg g^{-1})						
Acetate	3.48^{a}	3.89^{a}	3.44^{ab}	2.94^{b}	0.11	0.01
Propionate	1.76	2.33	1.86	1.83	0.11	0.18
Butyrate	1.01	1.29	1.28	1.15	0.07	0.40
Isobutyrate	0.11	0.11	0.14	0.11	0.01	0.16
Valerate	0.19	0.26	0.25	0.27	0.02	0.64
Isovalerate	0.18	0.16	0.23	0.18	0.01	0.28
Total straight-chain fatty acids	6.35	7.46	6.72	5.95	0.23	0.09
Total BCFA	0.28	0.27	0.37	0.30	0.02	0.24
Total SCFA	6.69	7.35	7.09	5.90	0.24	0.14

Data are presented as means with pooled SEM (n = 8). $^{a, b}$Mean values within a row with different superscript letters were significantly different (p < 0.05). BCFA, branched-chain fatty acid; SCFA, short-chain fatty acid.

TABLE 6 | Effects of dietary supplementation with fermented Mao-tai lees (FML) on colonic bioamine concentrations of weaned piglets.

Items (μg g^{-1})	Control	Dietary level of FML			SEM	*P* values
		2%	4%	6%		
Cadaverine	8.51^{b}	11.91^{b}	30.52^{a}	10.09^{b}	2.53	0.01
1,7-heptanediamine	1.27	0.63	0.94	0.96	0.16	0.53
Phenylethylamine	2.66	1.64	1.15	1.43	0.24	0.12
Putrescine	17.65	15.51	15.15	11.72	1.63	0.64
Spermidine	19.54	15.29	21.07	9.53	2.47	0.46
Spermine	1.05	1.06	2.05	0.75	0.27	0.51
Tryptamine	3.34	3.76	2.56	2.29	0.34	0.42
Tyramine	9.41	4.62	3.35	4.16	1.47	0.46
Total bioamine	63.08	51.80	60.76	38.86	5.17	0.36

Data are presented as means with pooled SEM (n = 8). $^{a, b}$Mean values within a row with different superscript letters were significantly different (p < 0.05).

Arg, glutamic acid, glycine, Pro, and leucine) participate in cell signal transmission and metabolic regulation (Wu et al., 2014). The Tau, a sulfated compound synthesized by the eukaryotic host, could increase the ADG and hepatic antioxidant status, while relieve lipopolysaccharide-induced inflammation of broiler chickens (Han et al., 2020). A constant supply of sufficient AAs to living cells from the blood is required to ensure protein accretion in the skeletal muscle of growing pigs (Regmi et al., 2016). This may be one of the reasons why the 4% FML supplementation increased the ADG during days 1–14 of the trial.

In the gut microbiota of pigs, *Firmicutes* and *Bacteroidetes* are the most abundant bacteria (Guo et al., 2008). The piglets with a higher F/B ratio are easier to obtain energy from food (Turnbaugh et al., 2006). The present study showed that dietary 4% FML supplementation significantly increased the F/B ratio in the colon, which may increase the energy utilization of feed. *Clostridium clusters* IV produces butyrate as a result of carbohydrate fermentation (Duytschaever et al., 2012). *Lactobacillus* is a well-known probiotic offering diverse applications. Furthermore, *Lactobacillus plantarum* plays a role in preventing diarrhea, lowering cholesterol, reducing irritable bowel syndrome symptoms, and producing plantaricins (Seddik et al., 2017). In the present study, dietary 2–6% FML supplementation had no significant effect on the abundances of *Clostridium clusters* IV and *Lactobacillus* of the weaned pigs. However, our previous studies showed that dietary 15% FML supplementation could increase the abundance of *Lactobacillus* of the growing-finishing pigs (Li et al., 2019). This discrepancy might be related to the different doses of FML supplementation and the age of pigs.

E. coli includes harmless commensal and different pathogenic variants which can cause enteric diseases, such as diarrhea or dysentery, and even lead to extra-intestinal infections (Leimbach et al., 2013). Therefore, lower levels of pathogenic *E. coli* in the gut could reduce the incidence of diarrhea in piglets. Sulfate-reducing bacteria in the large intestine can produce volatile sulfur compounds, such as hydrogen sulfide and methanethiol, which are responsible for fecal odor (Ushid et al., 2002). Sulfate-reducing bacteria are also a potential player in the etiology of intestinal disorders, inflammatory bowel diseases, and colorectal cancer in particular (Carbonero et al., 2012). In the present study, dietary 2 and 4% FML supplementation could decrease amounts of *E. coli* and sulfate-reducing bacteria in the colon. Our previous studies also confirmed that dietary 15% FML supplementation could decrease the abundance of potential pathogen *Escherichia* spp. in pigs at different ages (Li et al., 2019). These findings suggested that dietary FML supplementation, particularly 4% FML, could regulate the balance of intestinal microflora.

The SCFAs, especially butyrate, are mainly produced by microbial fermentation of carbohydrates and non-starch polysaccharides in the large intestine, where the relative abundances of microbiota are greater than those in the small intestine (Le et al., 2016). Similarly, the concentrations of individual and total SCFAs were much lower in the ileum than those in the colon. The SCFAs absorbed in the colon not only serve as an energy source but also play roles in the regulation of the immune system, colonic gene expression, gut motility, and metabolic regulation (Puertollano et al., 2014). Acetate can protect gastrointestinal mucosa from ethanol-induced injuries *via* suppressing gastrointestinal oxidation, inflammation, and apoptosis (Liu et al., 2017). In the present study, dietary 2% FML supplementation improved the levels of acetate and straight-chain fatty acids in the colonic contents than the higher percentage of FML supplementation (6%), which possibly a lower percentage of FML benefits to intestinal health of weaned piglets.

Cadaverine is synthesized from the Lys through decarboxylation by lysine decarboxylase in microbiota and ornithine decarboxylase 1 in mammalian cells (Bekebrede et al., 2020), which is essential for the maintenance of cell growth and macromolecular biosynthesis by interacting with nucleic acids, proteins, and membranes (Millerfleming et al., 2015), and can protect cells from oxidative stress by scavenging superoxide radicals (Kang et al., 2007). In addition, cadaverine can regulate the gut physiology of animals in different ways (Wang et al., 2015). In the present study, dietary 4% FML supplementation increased the colonic cadaverine content of piglets. Bioamine level could be upregulated through the phosphorylation of related enzymes by activating mTORC1 (Bekebrede et al., 2020). Therefore, the present study results suggest that the increased colonic cadaverine level in the dietary 4% FML group may be *via* regulating the mTORC1 pathway. However, the underlying mechanism needs to be further clarified.

CONCLUSION

In summary, dietary FML supplementation (2 and 4%) could partly improve plasma-free AA levels of the weaned piglets without affecting the piglets' growth performance. Furthermore, dietary 4% FML supplementation was more beneficial to intestinal health *via* decreasing the abundances of *E. coli* and sulfate-reducing bacteria, and increasing the concentration of cadaverine in the colon. This study also showed that dietary 4% FML supplementation had more distinct effects than the dietary 2 and 6% FML supplements. Thus, the FML could be used as an effective feed additive, which is not only beneficial to animal health but also resource-conserving and environment-friendly.

DATA AVAILABILITY STATEMENT

The original contributions presented in the study are included in the article/**Supplementary Material**, and further inquiries can be directed to the corresponding author.

ETHICS STATEMENT

The animal study was reviewed and approved by the Animal Care and Use Committee of the Institute of Subtropical Agriculture, Chinese Academy of Sciences.

AUTHOR CONTRIBUTIONS

ZL and XK conceived and designed the experiment. ZL, QZ, PH, and HL performed the experiment. ZL, QZ, and MA processed the data. ZL prepared and drafted the manuscript. MA and XK revised the manuscript. All authors have read and approved the final manuscript.

FUNDING

The present work was jointly supported by the National Natural Science Foundation of China (31772613) and Special Funds for Construction of Innovative Provinces in Hunan Province (2019RS3022).

ACKNOWLEDGMENTS

We thank the staff and postgraduate students of Hunan Provincial Key Laboratory of Animal Nutritional Physiology and Metabolic Process for collecting the samples, and the technicians from CAS Key Laboratory of Agro-ecological Processes in Subtropical Region for providing technical assistance.

SUPPLEMENTARY MATERIAL

The Supplementary Material for this article can be found online at: https://www.frontiersin.org/articles/10.3389/fmicb.2021.778555/full#supplementary-material

REFERENCES

Avelar, E., Jha, R., Beltranena, E., Cervantes, M., Morales, A., and Zijlstra, R. T. (2010). The effect of feeding wheat distillers dried grain with solubles on growth performance and nutrient digestibility in weaned pigs. *Anim. Feed Sci. Technol.* 160, 73–77. doi: 10.1016/j.anifeedsci.2010.06.009

Azad, M. A. K., Wang, H., Yang, H., Tan, B., and Guan, G. (2021). Effects of dietary carboxymethyl pachyman on oxidative stress and inflammation in weaned piglets challenged with diquat. *Anim. Feed Sci. Technol.* 276:114922. doi: 10.1016/j.anifeedsci.2021.114922

Barter, P. J., Brandrupwognsen, G., Palmer, M. K., and Nicholls, S. J. (2010). Effect of statins on HDL-C: a complex process unrelated to changes in LDL-C: analysis of the VOYAGER database. *J. Lipid Res.* 51, 1546–1553. doi: 10.1194/jlr.P002816

Bekebrede, A. F., Keijer, J., Gerrits, W. J. J., and Boer, V. C. J. (2020). The molecular and physiological effects of protein-derived polyamines in the intestine. *Nutrients* 12:197. doi: 10.3390/nu12010197

Buts, J. P. (2009). Twenty-five years of research on *Saccharomyces boulardii* trophic effects: updates and perspectives. *Digest. Dis. Sci.* 54, 15–18. doi: 10.1007/s10620-008-0322-y

Canli, E. G., and Canli, M. (2015). Low water conductivity increases the effects of copper on the serum parameters in fish (*Oreochromis niloticus*). *Environ. Toxicol. Phar.* 39, 606–613. doi: 10.1016/j.etap.2014.12.019

Carbonero, F., Benefiel, A. C., Alizadehghamsari, A. H., and Gaskins, H. R. (2012). Microbial pathways in colonic sulfur metabolism and links with health and disease. *Front. Physiol.* 3:448. doi: 10.3389/fphys.2012.00448

Chen, J., Su, W., Kang, B., Jiang, Q., Zhao, Y., Fu, C., et al. (2018). Supplementation with α-ketoglutarate to a low-protein diet enhances amino acid synthesis in tissues and improves protein metabolism in the skeletal muscle of growing pigs. *Amino Acids* 50, 1525–1537. doi: 10.1007/s00726-018-2618-3

Duytschaever, G., Huys, G., Bekaert, M., Boulanger, L., De, B. K., and Vandamme, P. (2012). Dysbiosis of *Bifidobacteria* and *Clostridium cluster XIVa* in the cystic fibrosis fecal microbiota. *J. Cyst. Fibros.* 12, 206–215. doi: 10.1016/j.jcf.2012.10.003

Emiola, I. A., Opapeju, F. O., Slominski, B. A., and Nyachoti, C. M. (2009). Growth performance and nutrient digestibility in pigs fed wheat distillers dried grains with solubles-based diets supplemented with a multicarbohydrase enzyme. *J. Anim. Sci.* 87, 2315–2322. doi: 10.2527/jas.2008-1195

Guo, X., Xia, X., Tang, R., Zhou, J., Zhao, H., and Wang, K. (2008). Development of a real-time PCR method for *Firmicutes* and *Bacteroidetes* in faeces and its application to quantify intestinal population of obese and lean pigs. *Lett. Appl. Microbiol.* 47, 367–373. doi: 10.1111/j.1472-765X.2008.02408.x

Gutierrez, N. A., Serão, N. V., Kerr, B. J., Zijlstra, R. T., and Patience, J. F. (2014). Relationships among dietary fiber components and the digestibility of energy, dietary fiber, and amino acids and energy content of nine corn coproducts fed to growing pigs. *J. Anim. Sci.* 92, 4505–4517. doi: 10.2527/jas.2013-7265

Hahn, J. D., Biehl, R. R., and Baker, D. H. (1995). Ideal digestible lysine level for early- and late-finishing swine. *J. Anim. Sci.* 73, 773–784. doi: 10.2527/1995.733773x

Han, H., Zhang, J., Chen, Y., Shen, M., Yan, E., Wei, C., et al. (2020). Dietary taurine supplementation attenuates lipopolysaccharide-induced inflammatory responses and oxidative stress of broiler chickens at an early age. *J. Anim. Sci.* 98:skaa311. doi: 10.1093/jas/skaa311

Hu, C. J., Li, F. N., Duan, Y. H., Zhang, T., Li, H. W., Yin, Y. L., et al. (2019). Dietary supplementation with arginine and glutamic acid alters the expression of amino acid transporters in skeletal muscle of growing pigs. *Amino Acids* 51, 1081–1092. doi: 10.1007/s00726-019-02748-9

Ji, Y., Guo, Q., Yin, Y., Blachier, F., and Kong, X. (2018). Dietary proline supplementation alters colonic luminal microbiota and bacterial metabolite composition between days 45 and 70 of pregnancy in Huanjiang mini-pigs. *J. Anim. Sci. Biotechnol.* 9:18. doi: 10.1186/s40104-018-0233-5

Jones, C. K., Bergstrom, J. R., Tokach, M. D., DeRouchey, J. M., Goodband, R. D., Nelssen, J. L., et al. (2010). Efficacy of commercial enzymes in diets containing various concentrations and sources of dried distillers grains with solubles for nursery pigs. *J. Anim. Sci.* 88, 2084–2091. doi: 10.2527/jas.2009-2109

Kang, I. H., Kim, J. S., Kim, E. J., and Lee, J. K. (2007). Cadaverine protects *Vibrio vulnificus* from superoxide stress. *J. Microbiol. Biotechnol.* 17, 176–179. doi: 10.1016/j.mimet.2006.07.012

Kerr, B. J., Weber, T. E., and Shurson, G. C. (2013). Evaluation of commercially available enzymes, probiotics, or yeast on apparent total-tract nutrient digestion and growth in nursery and finishing pigs fed diets containing corn dried distillers grains with solubles. *Appl. Anim. Sci.* 29, 508–517. doi: 10.15232/s1080-7446(15)30272-2

Kong, X. F., Wu, G. Y., Liao, Y. P., Hou, Z. P., Liu, H. J., Yin, F. G., et al. (2007). Dietary supplementation with Chinese herbal ultra-fine powder enhances cellular and humoral immunity in early-weaned piglets. *Livest. Sci.* 108, 94–98. doi: 10.1016/j.livsci.2007.01.002

Kweichow Moutai Co., Ltd. (2020). Annual Report. Available at: https://www.moutaichina.com/maotaigf/tzzgx/cwbg/index.html (Accessed November 2, 2021).

Lamsal, B. P., Pathirapong, P., and Rakshit, S. (2012). Microbial growth and modification of corn distillers dried grains with solubles during fermentation. *Ind. Crop. Prod.* 37, 553–559. doi: 10.1016/j.indcrop.2011.07.037

Le, M. H., Galle, S., Yang, Y., Landero, J. L., Beltranena, E., Gänzle, M. G., et al. (2016). Effects of feeding fermented wheat with *Lactobacillus reuteri* on gut morphology, intestinal fermentation, nutrient digestibility, and growth performance in weaned pigs. *J. Anim. Sci.* 94, 4677–4687. doi: 10.2527/jas.2016-0693

Leimbach, A., Hacker, J., and Dobrindt, U. (2013). *E. coli* as an all-rounder: the thin line between commensalism and pathogenicity. *Curr. Top. Microbiol. Immunol.* 358, 3–32. doi: 10.1007/82_2012_303

Li, H., Li, H., Xie, P., Li, Z., Yin, Y., Blachier, F., et al. (2019). Dietary supplementation with fermented Mao-tai lees beneficially affects gut microbiota structure and function in pigs. *AMB Express* 9:26. doi: 10.1186/s13568-019-0747-z

Li, G., Wang, X., Lin, M., Lu, Z., and Yao, W. (2012). Effects of corn DDGS in combination with compound enzymes on growth performance, carcass fat quality, and plasma and tissue redox homeostasis of growing-finishing pigs. *Livest. Sci.* 149, 46–52. doi: 10.1016/j.livsci.2012.06.019

Liu, Y., Kong, X., Jiang, G., Tan, B., Deng, J., Yang, X., et al. (2015). Effects of dietary protein/energy ratio on growth performance, carcass trait, meat quality, and plasma metabolites in pigs of different genotypes. *J. Anim. Sci. Biotechnol.* 6:36. doi: 10.1186/s40104-015-0036-x

Liu, J., Wang, J., Shi, Y., Su, W., Chen, J., Zhang, Z., et al. (2017). Short-chain fatty acid acetate protects against ethanol-induced acute gastric mucosal lesion in mice. *Biol. Pharm. Bull.* 40, 1439–1446. doi: 10.1248/bpb.b17-00240

Millerfleming, L., Olinsandoval, V., Campbell, K., and Ralser, M. (2015). Remaining mysteries of molecular biology: the role of polyamines in the cell. *J. Mol. Biol.* 427, 3389–3406. doi: 10.1016/j.jmb.2015.06.020

National Research Council (2012). *Nutrient Requirements of Swine. 11th Edn*. Washington, DC: National Academy Press.

Peterson, M. M., Mack, J. L., Hall, P. R., Alsup, A. A., Alexander, S. M., Sully, E. K., et al. (2008). Apolipoprotein B is an innate barrier against invasive *Staphylococcus aureus* infection. *Cell Host Microbe* 4, 555–566. doi: 10.1016/j.chom.2008.10.001

Puertollano, E., Kolida, S., and Yaqoob, P. (2014). Biological significance of short-chain fatty acid metabolism by the intestinal microbiome. *Curr. Opin. Clin. Nutr.* 17, 139–144. doi: 10.1097/MCO.0000000000000025

Regmi, N., Wang, T., Crenshaw, M. A., Rude, B. J., Wu, G., and Liao, S. F. (2016). Effects of dietary lysine levels on plasma free amino acid profile in late-stage finishing pigs. *Springerplus* 5:888. doi: 10.1186/s40064-016-2463-3

Reilly, P., O'Doherty, J. V., Pierce, K. M., Callan, J. J., O'Sullivan, J. T., and Sweeney, T. (2008). The effects of seaweed extract inclusion on gut morphology, selected intestinal microbiota, nutrient digestibility, volatile fatty acid concentrations and the immune status of the weaned pig. *Animal* 2, 1465–1473. doi: 10.1017/S1751731108002711

Seddik, H. A., Bendali, F., Gancel, F., Fliss, I., Spano, G., and Drider, D. (2017). *Lactobacillus plantarum* and its probiotic and food potentialities. *Probiotics Antimicrob.* 9, 111–122. doi: 10.1007/s12602-017-9264-z

Singh, V., Moreau, R. A., Hicks, K. B., Belyea, R. L., and Staff, C. H. (2002). Removal of fiber from distillers dried grains with solubles (DDGS) to increase value. *Trans. ASABE* 45, 389–392. doi: 10.13031/2013.8510

Stein, H. H., and Shurson, G. C. (2009). Board-invited review: The use and application of distillers dried grains with solubles in swine diets. *J. Anim. Sci.* 87, 1292–1303. doi: 10.2527/jas.2008-1290

Su, J., Zhu, Q., Zhao, Y., Han, L., Yin, Y., Blachier, F., et al. (2018). Dietary supplementation with Chinese herbal residues or their fermented products

modifies the colonic microbiota, bacterial metabolites, and expression of genes related to colon barrier function in weaned piglets. *Front. Microbiol.* 9:3181. doi: 10.3389/fmicb.2018.03181

Swiatkiewicz, S., Swiatkiewicz, M., Arczewska-Wlosek, A., and Jozefiak, D. (2016). Efficacy of feed enzymes in pig and poultry diets containing distillers dried grains with solubles: a review. *J. Anim. Physiol. Anim. Nutr.* 100, 15–26. doi: 10.1111/jpn.12351

Tang, Z., Yin, Y., Zhang, Y., Huang, R., Sun, Z., Li, T., et al. (2009). Effects of dietary supplementation with an expressed fusion peptide bovine lactoferricin-lactoferrampin on performance, immune function and intestinal mucosal morphology in piglets weaned at age 21 d. *Br. J. Nutr.* 101, 998–1005. doi: 10.1017/S0007114508055633

Turnbaugh, P. J., Ley, R. E., Mahowald, M. A., Magrini, V., Mardis, E. R., and Gordon, J. I. (2006). An obesity-associated gut microbiome with increased capacity for energy harvest. *Nature* 444, 1027–1031. doi: 10.1038/nature05414

Ushid, K., Maekawa, M., and Arakawa, T. (2002). Influence of dietary supplementation of herb extracts on volatile sulfur production in pig large intestine. *J. Nutr. Sci. Vitaminol.* 48, 18–23. doi: 10.3177/jnsv.48.18

Wang, J., Li, G. R., Tan, B. E., Xiong, X., Kong, X. F., Xiao, D. F., et al. (2015). Oral administration of putrescine and proline during the suckling period improves epithelial restitution after early weaning in piglets. *J. Anim. Sci.* 93, 1679–1688. doi: 10.2527/jas.2014-8230

Wang, Q., Zhang, H., and Liu, X. (2016). Microbial community composition associated with Maotai liquor fermentation. *J. Food Sci.* 81, M1485–M1494. doi: 10.1111/1750-3841.13319

Wiseman, M., McBride, B., Li, J., Wey, D., Zhu, J., and de Lange, C. F. M. (2017). Effects of steeped or fermented distillers dried grains with solubles on growth performance in weanling pigs. *J. Anim. Sci.* 95, 3563–3578. doi: 10.2527/jas.2017.1478

Wu, G., Bazer, F. W., Dai, Z., Li, D., Wang, J., and Wu, Z. (2014). Amino acid nutrition in animals: protein synthesis and beyond. *Annu. Rev. Anim. Biosci.* 2, 387–417. doi: 10.1146/annurev-animal-022513-114113

Yang, S. L., Junyi, L., and Wang, T. (2012). Evaluation of enzyme activity and fiber content of soybean cotyledon fiber and distiller's dried grains with solubles by solid state fermentation. *Appl. Biochem. Biotech.* 167, 109–121. doi: 10.1007/s12010-012-9665-0

Zhai, F. H., Liu, H. Y., and Han, J. R. (2018). Protein nutritional value, polyphenols and antioxidant properties of corn fermented with *Agaricus brasiliensis* and *Agaricus bisporus*. *World J. Microbiol. Biotechnol.* 34:36. doi: 10.1007/s11274-017-2399-y

Zhou, X. L., Kong, X. F., Lian, G. Q., Blachier, F., Geng, M. M., and Yin, Y. L. (2014). Dietary supplementation with soybean oligosaccharides increases short-chain fatty acids but decreases protein-derived catabolites in the intestinal luminal content of weaned Huanjiang mini-piglets. *Nutr. Res.* 34, 780–788. doi: 10.1016/j.nutres.2014.08.008

Conflict of Interest: The authors declare that the research was conducted in the absence of any commercial or financial relationships that could be construed as a potential conflict of interest.

Publisher's Note: All claims expressed in this article are solely those of the authors and do not necessarily represent those of their affiliated organizations, or those of the publisher, the editors and the reviewers. Any product that may be evaluated in this article, or claim that may be made by its manufacturer, is not guaranteed or endorsed by the publisher.

frontiers in Microbiology

ORIGINAL RESEARCH
published: 08 December 2021
doi: 10.3389/fmicb.2021.793576

Effects of Ellagic Acid Supplementation on Jejunal Morphology, Digestive Enzyme Activities, Antioxidant Capacity, and Microbiota in Mice

Qiuying Xu[1], Mingkang Shen[2], Yuxin Han[3] and Hui Diao[4]*

[1] Sichuan Nursing Vocational College, Chengdu, China, [2] School of the 1st Clinical Medical Sciences, Wenzhou Medical University, Wenzhou, China, [3] School of Nursing, Chengdu University of Traditional Chinese Medicine, Chengdu, China, [4] Animal Breeding and Genetics Key Laboratory of Sichuan Province, Sichuan Academy of Animal Science, Chengdu, China

OPEN ACCESS

Edited by:
Zheng Ruan,
Nanchang University, China

Reviewed by:
Junqiu Luo,
Sichuan Agricultural University, China
Luoyi Zhu,
Zhejiang University, China

***Correspondence:**
Qiuying Xu
xuqiuying0808@163.com

Specialty section:
This article was submitted to Food Microbiology, a section of the journal Frontiers in Microbiology

Received: *12 October 2021*
Accepted: *01 November 2021*
Published: *08 December 2021*

Citation:
Xu Q, Shen M, Han Y and Diao H (2021) Effects of Ellagic Acid Supplementation on Jejunal Morphology, Digestive Enzyme Activities, Antioxidant Capacity, and Microbiota in Mice. Front. Microbiol. 12:793576. doi: 10.3389/fmicb.2021.793576

Ellagic acid (EA), a plant polyphenol mainly found in nuts and fruits, exhibits various biological effects. However, the effects of EA on intestinal health remain poorly understood. Hence, the present study aimed to assess the effects of EA supplementation on jejunal morphology, digestive enzyme activities, antioxidant capacity, and microbiota in C57BL/6J mice. A total of 144 mice were randomly assigned to three treatments groups: the control (CON) group received a standard pellet diet, the 0.1% EA group received a standard pellet diet plus 0.1% EA, and the 0.3% EA group received a standard pellet diet plus 0.3% EA. The mice were killed at the end of the experimental period, and jejunal samples were collected. The results revealed that the mice in the 0.3% EA group had higher ($P < 0.05$) average daily gain and greater ($P < 0.05$) jejunal villus height than those in the CON group. In addition, the jejunal lactase and sucrase activities were higher ($P < 0.05$) in the 0.1% EA and 0.3% EA groups, and the alkaline phosphatase activity was higher ($P < 0.05$) in the 0.3% EA group than in the CON group. Compared with the CON group, the administration of EA increased ($P < 0.05$) the superoxide dismutase and catalase activities but decreased ($P < 0.05$) the malonaldehyde content in the jejunum. Moreover, the jejunal messenger RNA expression levels of nuclear factor-E2-related factor 2 (*Nrf2*) and haem oxygenase-1 (*HO-1*) were higher ($P < 0.05$) in the 0.3% EA group than in the CON group. Furthermore, compared with the CON group, the count of *Escherichia coli* decreased ($P < 0.05$), and that of *Lactobacillus* species increased ($P < 0.05$) in the 0.3% EA group. In general, our findings indicate that the administration of EA can enhance the growth of mice, promote intestinal development, increase the antioxidant capacity, and regulate the intestinal microbiota.

Keywords: ellagic acid, morphology, digestive enzyme activities, antioxidant, microbiota, Nrf2, HO-1

INTRODUCTION

The small intestine serves as the crucial site for nutrient digestion and absorption while simultaneously acting as an important line of defense against the invasion of antigens and pathogens (Nagler-Anderson, 2001; Hirata et al., 2007; Barszcz and Skomiał, 2011). However, the health status of the intestine in young animals could be easily deteriorated by many factors, including pathogen infection, inflammation, and oxidative stress (Liu, 2015; Wan et al., 2021); these factors lead to intestinal mucosal damage and dysfunction and, in turn, negatively affect the growth performance and health of animals (Liu et al., 2008). Interestingly, there is clear evidence that adequate nutrition can help maintain intestinal integrity in animals (He et al., 2017; Wan et al., 2018). Thus, it is extremely important to maintain the structural and functional integrity of the small intestine and to thereby ensure that its absorptive and protective functions are not compromised (Yu et al., 2010).

In recent years, there has been increasing interest in understanding the role of polyphenolic compounds and their possible mechanisms of action in maintaining intestinal health. Ellagic acid (EA), a natural phenolic phytochemical antioxidant, mainly occurs in vegetables and fruits, such as persimmon, raspberries, blackberries, and strawberries, in addition to nuts (Derosa et al., 2016). It has important biological activities, such as antioxidative (Yüce et al., 2007), anti-inflammatory (Marín et al., 2013), anticancer (Umesalma and Sudhandiran, 2011), and antidiabetic (Fatima et al., 2017) activities. Previous studies have shown that EA can scavenge free radicals (Zheng et al., 2020) and inhibit lipid peroxidation (Kilic et al., 2014). More recently, EA supplementation has been reported to improve the activity of antioxidant enzymes and ameliorate intestinal inflammation *in vivo* and *in vitro* (Han et al., 2006; Mishra and Vinayak, 2014). However, little information is available about the effects of different EA doses and their protective effects on intestinal health in mice. In light of the earlier information, we assessed the effects of EA supplementation on jejunal development and antioxidant capacity in mice.

MATERIALS AND METHODS

Animals and Treatment

The Ethics Review Committee for Animal Experimentation of Sichuan Academy of Animal Science (Chengdu, China) approved the animal experimental protocols. The animal experimental protocols were conducted in accordance with the practical animal protection law and the Guide for the Care and Use of Laboratory Animals formulated by the National Research Council (China). A total of 144 C57BL/6J mice weighing 26–30 g were obtained from Dossy Experimental Animals Co., Ltd. (Chengdu, China) and randomly divided into three groups (each group has had 48 mice): the control (CON) group received a standard pellet diet, the 0.1% EA group received a standard pellet diet plus 0.1% EA, and the 0.3% EA group received a standard pellet diet plus 0.3% EA. All the mice were maintained at 25°C with a 12-h light/dark cycle and given food and water *ad libitum* for 21 consecutive days. All the mice were weighed on the morning of days 1 and 22 to calculate the average daily gain (ADG).

Sample Collection

At the end of the experimental regimen and after 16 h of fasting, the mice were killed by ether anesthesia. The jejunum was removed, and the jejunal contents were collected and frozen at −80°C for microbial DNA analysis. Jejunal tissue samples were collected, washed in ice-cold physiological saline (0.9%), and blotted dry. Then, the jejunal section was divided into two pieces: one was fixed in 4% paraformaldehyde solution for histological studies, and the other was stored at −80°C for further analysis.

Morphological Examination

The 4% paraformaldehyde solution-fixed jejunal samples were dehydrated in ethanol and embedded in paraffin. Then, 5-μm thick transverse sections were cut and stained with hematoxylin and eosin. The villus height and crypt depth of 10 well-oriented villi were measured using a BH2 Olympus microscope (Olympus, Tokyo, Japan).

Jejunal Enzyme Activity Measurements

The jejunal mucosa was homogenized after ensuring that the weight of the intestinal mucosa (g)/volume of physiological saline pre-cooled on ice (ml) was 1:9 and was centrifuged at 2,500 × *g* for 10 min to obtain the supernatant. Then, the enzyme activities in the jejunal mucosal supernatant were measured strictly in accordance with the instructions provided in the respective kits (Nanjing Jiancheng Bioengineering Institute, Nanjing, China).

Jejunal Antioxidant Capacity Measurements

The superoxide dismutase (SOD) activity, catalase (CAT) activity, malonaldehyde (MDA) content, and total antioxidant capacity (T-AOC) in the jejunal homogenates were measured using commercially available kits (Nanjing Jiancheng Bioengineering Institute, Nanjing, China).

Messenger RNA Abundance Analysis

Total RNA was extracted from the jejunal mucosa using TRIzol reagent (Invitrogen, Carlsbad, CA, United States), according to the manufacturer's instructions. The sequences of primers used in the present study are provided in **Table 1**. The RNA concentration was measured using NanoDrop 1000 (Thermo Fisher Scientific), and the RNA integrity was assessed by electrophoresis on 1% agarose gel. The reaction mixture consisted of 5-μl fresh SYBR® Premix Ex Taq II (Tli RNase H Plus), 0.5-μl forward primer, 0.5-μl reverse primer, 1-μl complementary DNA, and 3-μl diethylpyrocarbonate-treated water. The polymerase chain reaction (PCR) protocol was as follows: 1 cycle at 95°C for 30 s, 40 cycles at 95°C for 5 s and 60°C for 34 s and 1 cycle at 95°C for 15 s, 60°C for 1 min and 95°C for 15 s. The relative expression levels of the target genes to the housekeeping gene (β-actin) were assessed using the $2^{-\Delta\Delta Ct}$ method (Che et al., 2017).

TABLE 1 | Primer sequences of target and reference genes.

Genes	Primer sequence (5′–3′)	Product (bp)	GenBank accession
Nrf2	Forward: CCATGTGTGGCAGTCCATGAT Reverse: GCAGGCATACCATTGTGGAT	183	AH006764.2
HO-1	Forward: GAAATCATCCCTTGCACGCC Reverse: CCTGAGAGGTCACCCAGGTA	122	NM_010442.2
Keap1	Forward: GAGTAGAGGTAGGGGTCGCC Reverse: TCACGGTGACTAAGCACAGC	82	NM_016679.4
NQO1	Forward: CATTGCAGTGGTTTGGGGTG Reverse: TCTGGAAAGGACCGTTGTCG	111	NM_008706.5
β-actin	Forward: TGAGCTGCGTTTTACACCCT Reverse: GCCTTCACCGTTCCAGTTTT	198	NM_007393.5

Nrf2, nuclear factor-E2-related factor 2; HO-1, heme oxygenase-1; Keap1, kelch-like epichlorohydrin-associated protein 1; NQO1, NADPH quinone acceptor oxidoreductase 1.

TABLE 2 | Primer sequences of target microbial populations in jejunal contents.

Items	Primer sequence (5′–3′)	Amplicon length (bp)
Bacteroidetes	Forward: GGARCATGTGGTTTAATTCGATGAT Reverse: AGCTGACGACAACCATGCAG	126
Escherichia coli	Forward: CATGCCGCGTGTATGAAGAA Reverse: CGGGTAACGTCAATGAGCAAA	95
Firmicutes	Forward: GGAGYATGTGGTTTAATTCGAAGCA Reverse: AGCTGACGACAACCATGCAC	126
Lactobacillus	Forward: AGCAGTAGGGAATCTTCCA Reverse: ATTCCACCGCTACACATG	345

Bacterial DNA Extraction and Real-Time Quantitative Polymerase Chain Reaction

Approximately 1-g jejunal content was used for bacterial DNA extraction using the QIAamp DNA Stool Kit (Qiagen, Hilden, Germany) according to the manufacturer's instructions. Bacterial DNA extracted from the jejunal contents was used for gene sequence amplification by quantitative PCR using the primers specified in **Table 2**. Primer specificity was assessed on the basis of the 16S rRNA gene sequence. The reaction conditions for quantitative PCR were as follows: 50°C for 2 min, 95°C for 5 min and 40 cycles of denaturation at 94°C for 20 s, primer annealing at a species-specific temperature for 30 s, and primer extension at 60°C for 1 min (Su et al., 2018).

Statistical Analysis

All results are expressed as the means ± standard errors. Data were analyzed by one-way analysis of variance using the GLM procedure of SAS software (Version 9; SAS Institute, Inc., Cary, NC, United States). All statements of statistical significance are based on a probability of $P < 0.05$.

RESULTS

Growth Performance

As shown in **Figure 1**, the mice in the 0.3% EA group had significantly higher ($P < 0.05$) ADG than those in the CON group.

Jejunal Morphology

The jejunal villus height (**Figure 2A**) was greater in the mice fed with the EA diet than those fed with the basal diet. The villus height was greater ($P < 0.05$) in the 0.3% EA group than in the CON group (**Figure 2B**). However, the crypt depth (**Figure 2C**) and villus height/crypt depth ratio (**Figure 2D**) did not differ among the three groups ($P > 0.05$).

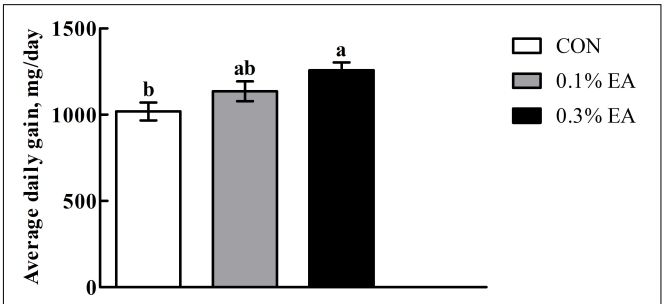

FIGURE 1 | Effects of ellagic acid (EA) supplementation on growth performance of mice. Results are presented as means ± standard errors. ^{a,b}Mean values followed by different letters within a row indicate significant differences ($P < 0.05$). CON, control group, mice received a standard pellet diet; 0.1% EA, mice received a standard pellet diet plus 0.1% EA; 0.3% EA, mice received a standard pellet diet plus 0.3% EA.

Jejunal Enzyme Activities

The jejunal enzyme activities are presented in **Table 3**. Compared with the CON group, the jejunal lactase and sucrase activities were enhanced ($P < 0.05$) in the 0.1% EA and 0.3% EA groups. Moreover, 0.3% EA supplementation was found to increase ($P < 0.05$) the jejunal alkaline phosphatase activity.

Jejunal Microbiota

The counts of Bacteroidetes and Firmicutes species in the jejunal contents did not change significantly ($P > 0.05$) after EA supplementation (**Table 4**). Compared with the CON group, the count of *Escherichia coli* decreased ($P < 0.05$), and that of *Lactobacillus* species increased ($P < 0.05$) in the 0.3% EA group.

Jejunal Antioxidant Capacity

As shown in **Table 5**, EA supplementation increased ($P < 0.05$) the SOD and CAT activities and decreased ($P < 0.05$) the MDA content in the jejunum of mice.

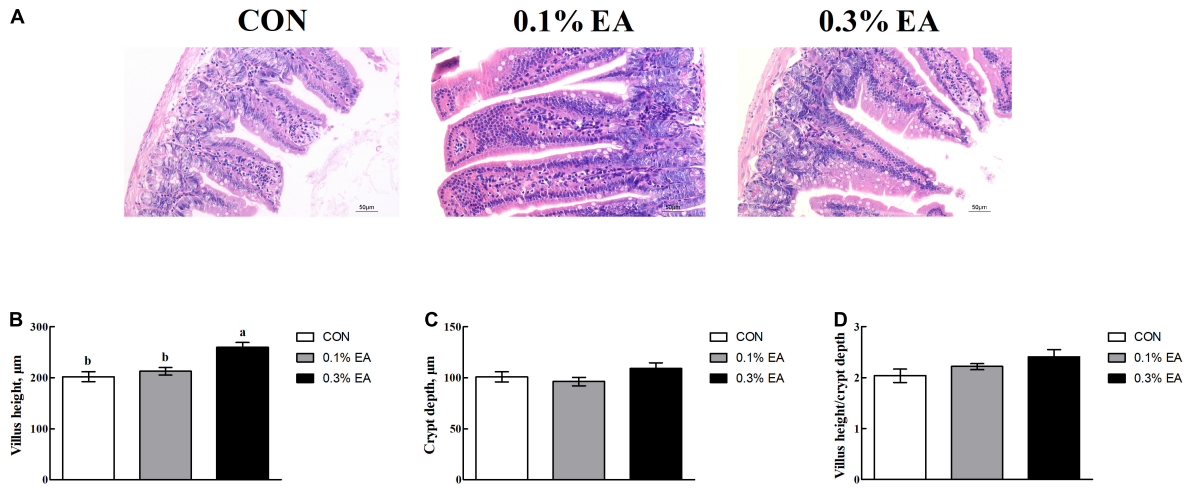

FIGURE 2 | Effects of EA supplementation on jejunal morphology in mice. **(A)** Image showing jejunal morphology (200×); **(B)** villus height; **(C)** crypt depth; **(D)** villus height/crypt depth ratio. Results are presented as means ± standard errors. ^{a,b}Mean values followed by different letters within a row indicate significant differences ($P < 0.05$). CON, control group, mice received a standard pellet diet; 0.1% EA, mice received a standard pellet diet plus 0.1% EA; 0.3% EA, mice received a standard pellet diet plus 0.3% EA.

TABLE 3 | Effects of ellagic acid (EA) supplementation on jejunal digestive enzyme activities in mice.

Items	Treatment group*			*P*-value
	CON	0.1% EA	0.3% EA	
Lactase, U/mL	1.86 ± 0.19^{c}	3.22 ± 0.25^{b}	4.90 ± 0.37^{a}	<0.001
Sucrase, U/mL	17.85 ± 0.51^{b}	50.51 ± 0.83^{a}	49.94 ± 1.39^{a}	<0.001
Alkaline phosphatase, U/mL	4.65 ± 0.10^{b}	9.75 ± 0.27^{ab}	9.87 ± 0.21^{a}	<0.001

Results are presented as means ± standard errors.
$^{a-c}$Mean values followed by different letters within a row indicate significant differences ($P < 0.05$).
**CON, control group, mice received a standard pellet diet; 0.1% EA, mice received a standard pellet diet plus 0.1% EA; 0.3% EA, mice received a standard pellet diet plus 0.3% EA.*

TABLE 4 | Effects of EA supplementation on bacteria in jejunal digesta in mice [log 10 (copies per gram)].

Items	Treatment group*			*P*-value
	CON	0.1% EA	0.3% EA	
Bacteroidetes	7.14 ± 0.54	6.72 ± 0.45	6.41 ± 0.49	0.590
Escherichia coli	8.94 ± 0.36^{a}	8.04 ± 0.29^{a}	6.73 ± 0.40^{b}	<0.001
Firmicutes	7.90 ± 0.44	7.62 ± 0.22	7.46 ± 0.26	0.620
Lactobacillus	4.39 ± 0.26^{b}	4.75 ± 0.26^{ab}	5.67 ± 0.44^{a}	0.032

Results are presented as means ± standard errors.
^{a,b}Mean values followed by different letters within a row indicate significant differences ($P < 0.05$).
**CON, control group, mice received a standard pellet diet; 0.1% EA, mice received a standard pellet diet plus 0.1% EA; 0.3% EA, mice received a standard pellet diet plus 0.3% EA.*

TABLE 5 | Effects of EA supplementation on jejunal antioxidant capacity in mice.

Items	Treatment group*			*P*-value
	CON	0.1% EA	0.3% EA	
SOD, U/ml	75.62 ± 7.71^{b}	155.57 ± 9.83^{a}	171.71 ± 9.53^{a}	<0.001
CAT, U/ml	68.07 ± 2.00^{c}	94.00 ± 2.24^{b}	107.10 ± 2.44^{a}	<0.001
T-AOC, U/ml	6.00 ± 0.98	6.52 ± 0.98	6.84 ± 0.33	0.768
MDA, nmol/ml	5.95 ± 0.36^{a}	4.22 ± 0.16^{b}	3.89 ± 0.12^{b}	<0.001

Results are presented as means ± standard errors.
$^{a-c}$Mean values followed by different letters within a row indicate significant differences ($P < 0.05$).
**CON, control group, mice received a standard pellet diet; 0.1% EA, mice received a standard pellet diet plus 0.1% EA; 0.3% EA, mice received a standard pellet diet plus 0.3% EA.*

Nuclear Factor-E2-Related Factor 2 Pathway-Related Gene Expressions Levels

The differences in jejunal nuclear factor-E2-related factor 2 (Nrf2) pathway-related gene expression levels among the three groups are presented in **Figure 3**. The jejunal messenger RNA (mRNA) expression levels of *Nrf2* and haem oxygenase-1 (*HO-1*) were higher in the 0.3% EA group ($P < 0.05$) than in the CON group. However, no significant differences ($P > 0.05$) were noted in the mRNA expression levels of *Keap1* and *NQO-1* among the three groups.

DISCUSSION

The intestine has an enormous surface area that is optimized to efficiently absorb nutrients, water, and electrolytes from food (König et al., 2016). Maintaining the normal morphology of the intestinal mucosa is essential to ensure efficient digestion and absorption in animals (Mou et al., 2019). The villus height,

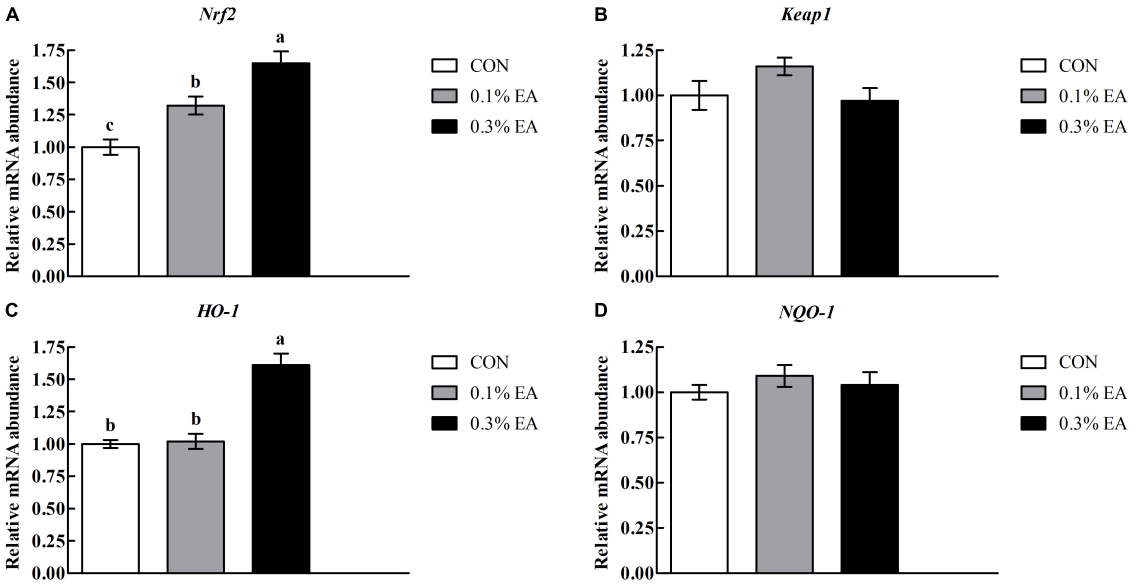

FIGURE 3 | Effects of EA supplementation on nuclear factor-E2-related factor 2 (Nrf2) pathway-related mRNA expression levels in mouse jejunum. **(A)** Nrf2; **(B)** Keap1; **(C)** HO-1; **(D)** NQO-1. Results are presented as means ± standard errors. $^{a-c}$Mean values followed by different letters within a row indicate significant differences ($P < 0.05$). CON, control group, mice received a standard pellet diet; 0.1% EA, mice received a standard pellet diet plus 0.1% EA; 0.3% EA, mice received a standard pellet diet plus 0.3% EA.

crypt depth, and villus height/crypt depth ratio are the most direct indices that can reflect the morphology of the small intestine (Qin et al., 2018). In the present study, the jejunal villus height was found to be greater in the 0.3% EA group than in the CON group. This finding was consistent with that of Sun et al. (2017), suggesting that EA administration can change the morphological structure of the mouse jejunum and can promote the development of the small intestine in mice. It is well known that digestive brush border enzymes mainly attach to the apical parts of villi (Asp et al., 1975). Moreover, the proliferation of villi helps more digestive enzymes to enter the intestine, thereby facilitating the digestion and absorption of more nutrients (Cao et al., 2015). However, changes in intestinal morphology are associated with alterations in enzyme activities (Wan et al., 2017). In the current study, we found that 0.1 or 0.3% EA supplementation enhanced the jejunal lactase, sucrase, and alkaline phosphatase activities in mice. BW changes are a comprehensive reflection of health. In our study, mice fed the 0.3% EA diet had higher ADG than those fed the basal diet. This is a comprehensive reflection of EA-induced small intestinal development and improved intestinal nutrient digestion and absorption capacity.

The intestinal antioxidant capacity is also crucial for maintaining intestinal health (Kim et al., 2021). The body has a series of defense mechanisms for controlling oxidative stress; one of these is the enzymatic antioxidant system (Pari and Sivasankari, 2008). SOD and CAT are important enzymatic antioxidants that can provide major antioxidant defenses against ROS (Bhattacharyya et al., 2014; Shen et al., 2014). In the present study, the jejunal SOD and CAT activities significantly increased, whereas the jejunal MDA content decreased in mice fed EA. These findings suggest that EA can improve the jejunal antioxidant capacity. Evidence suggests that the antioxidant effect of EA may be mediated by the stimulation of Nrf2 and the activation of antioxidant response elements, such as HO-1 (Ding et al., 2014). Nrf2 is an important transcription factor that can control the induction of antioxidant genes (Baluchnejadmojarad et al., 2017). In this study, we found that EA supplementation increased Nrf2 and HO-1 mRNA expression levels in the mouse jejunum, suggesting that EA can protect against oxidative stress *via* the Nrf2/HO-1 pathway.

The intestinal microflora plays an important role in maintaining intestinal microenvironment homeostasis (Liu et al., 2019). Previous studies have revealed an increase in the abundance of Firmicutes and *Lactobacillus* species and a decrease in the abundance of Verrucomicrobia and Bacteroidetes species in mice after polyphenols supplementation (Kim et al., 2021; Lu et al., 2021). Our results demonstrated that EA supplementation decreased the count of *E. coli* but increased the count of *Lactobacillus* species. These results may be attributed to the bacteriostatic or bactericidal action of polyphenols or their ability to inhibit the adhesion of pathogenic bacteria to the intestinal tract cells (Abu Hafsa and Ibrahim, 2018). Furthermore, the intestinal microflora has been reported to affect intestinal morphology (Forder et al., 2007). For instance, dietary *Lactobacillus casei* supplementation was found to increase the count of *Enterobacteriaceae* species and improve the intestinal villus length in mice (Allori et al., 2000). In the present study, the increased villus height noted in the 0.3% EA group was consistent with the increased *Lactobacillus* count in the jejunum, similar to previous findings.

CONCLUSION

In conclusion, the present study demonstrated that EA administration could enhance the growth of mice, promote jejunal development, improve the jejunal antioxidant capacity, and regulate the intestinal microbiota. These findings provide guidance on EA supplementation.

DATA AVAILABILITY STATEMENT

The original contributions presented in the study are included in the article/supplementary material, further inquiries can be directed to the corresponding author.

ETHICS STATEMENT

The animal study was reviewed and approved by the animal experimental protocols were approved by the Ethics Review Committee for Animal Experimentation of Sichuan Academy of Animal Science (Chengdu, China). The animal experimental protocols were conducted in accordance with the practical animal protection law and the Guide for the Care and Use of Laboratory Animals formulated by the National Research Council (China).

AUTHOR CONTRIBUTIONS

QX and HD conceived the present study and wrote the manuscript. MS and YH conducted the experiments and performed the data analysis. All authors contributed to the article and approved the submitted version.

FUNDING

This study was financially supported by the school-level project of Sichuan Nursing Vocational College (2021ZRZ02).

REFERENCES

Abu Hafsa, S. H., and Ibrahim, S. A. (2018). Effect of dietary polyphenol-rich grape seed on growth performance, antioxidant capacity and ileal microflora in broiler chicks. *J. Anim. Physiol. Anim. Nutr.* 102, 268–275. doi: 10.1111/jpn.12688

Allori, C., Agüero, G., de Ruiz Holgado, A. P., De Nader, O. M., and Perdigon, G. (2000). Gut mucosa morphology and microflora changes in malnourished mice after renutrition with milk and administration of *Lactobacillus casei*. *J. Food Prot.* 63, 83–90. doi: 10.4315/0362-028x-63.1.83

Asp, N.-G., Gudmand-Höyer, E., Andersen, B., Berg, N.-O., and Dahlqvist, A. (1975). Distribution of disaccharidases, alkaline phosphatase, and some intracellular enzymes along the human small intestine. *Scand. J. Gastroent.* 10, 647–651. doi: 10.1080/00365521.1975.12097025

Baluchnejadmojarad, T., Rabiee, N., Zabihnejad, S., and Roghani, M. (2017). Ellagic acid exerts protective effect in intrastriatal 6-hydroxydopamine rat model of Parkinson's disease: possible involvement of ERβ/Nrf2/HO-1 signaling. *Brain Res.* 1662, 23–30. doi: 10.1016/j.brainres.2017.02.021

Barszcz, M., and Skomiał, J. (2011). The development of the small intestine of piglets-chosen aspects. *J. Anim. Feed Sci.* 20, 3–15.

Bhattacharyya, A., Chattopadhyay, R., Mitra, S., and Crowe, S. E. (2014). Oxidative stress: an essential factor in the pathogenesis of gastrointestinal mucosal diseases. *Physiol. Rev.* 94, 329–354. doi: 10.1152/physrev.00040.2012

Cao, W., Liu, G. M., Fang, T. T., Wu, X. J., Jia, G., Zhao, H., et al. (2015). Effects of spermine on the morphology, digestive enzyme activities, and antioxidant status of jejunum in suckling rats. *Rsc. Adv.* 5, 76607–76614. doi: 10.1039/c5ra15793e

Che, L. Q., Xu, Q., Wu, C., Luo, Y. H., Huang, X. B., Zhang, B., et al. (2017). Effects of dietary live yeast supplementation on growth performance, diarrhoea severity, intestinal permeability and immunological parameters of weaned piglets challenged with enterotoxigenic *Escherichia coli* K88. *Br. J. Nutr.* 118, 949–958. doi: 10.1017/S0007114517003051

Derosa, G., Maffioli, P., and Sahebkar, A. (2016). Ellagic acid and its role in chronic diseases. *Adv. Exp. Med. Biol.* 928, 473–479.

Ding, Y., Zhang, B., Zhou, K. Y., Chen, M. C., Wang, M. M., Jia, Y. Y., et al. (2014). Dietary ellagic acid improves oxidant-induced endothelial dysfunction and atherosclerosis: role of Nrf2 activation. *Int. J. Cardiol.* 175, 508–514. doi: 10.1016/j.ijcard.2014.06.045

Fatima, N., Hafizur, R. M., Hameed, A., Ahmed, S., Nisar, M., and Kabir, N. (2017). Ellagic acid in *Emblica officinalis* exerts anti-diabetic activity through the action on β-cells of pancreas. *Eur. J. Nutr.* 56, 591–601. doi: 10.1007/s00394-015-1103-y

Forder, R. E. A., Howarth, G. S., Tivey, D. R., and Hughes, R. J. (2007). Bacterial modulation of small intestinal goblet cells and mucin composition during early posthatch development of poultry. *Poultry Sci.* 86, 2396–2403. doi: 10.3382/ps.2007-00222

Han, D. H., Lee, M. J., and Kim, J. H. (2006). Antioxidant and apoptosis-inducing activities of ellagic acid. *Anticancer Res.* 26, 3601–3606.

He, L. Q., Zhou, X. H., Huang, N., Li, H., Cui, Z. J., Tian, J. Q., et al. (2017). Administration of alpha-ketoglutarate improves epithelial restitution under stress injury in early-weaning piglets. *Oncotarget* 8, 91965–91978. doi: 10.18632/oncotarget.20555

Hirata, Y., Broquet, A. H., Menchén, L., and Kagnoff, M. F. (2007). Activation of innate immune defense mechanisms by signaling through RIG-I/IPS-1 in intestinal epithelial cells. *J. Immunol.* 179, 5425–5432. doi: 10.4049/jimmunol.179.8.5425

Kilic, I., Yeşiloğlu, Y., and Bayrak, Y. (2014). Spectroscopic studies on the antioxidant activity of ellagic acid. *Spectroc. Acta Pt. A Molec. Biomolec. Spectr.* 130, 447–452. doi: 10.1016/j.saa.2014.04.052

Kim, D.-H., Sim, Y., Hwang, J.-H., Kwun, I.-S., Lim, J.-H., Kim, J., et al. (2021). Ellagic acid prevents binge alcohol-induced leaky gut and liver injury through inhibiting gut dysbiosis and oxidative stress. *Antioxidants* 10:1386. doi: 10.3390/antiox10091386

König, J., Wells, J., Cani, P. D., García-Ródenas, C. L., MacDonald, T., Mercenier, A., et al. (2016). Human intestinal barrier function in health and disease. *Clin. Transl. Gastroenterol.* 7:e196.

Liu, J., Wang, H.-W., Lin, L., Miao, C.-Y., Zhang, Y., and Zhou, B.-H. (2019). Intestinal barrier damage involved in intestinal microflora changes in fluoride-induced mice. *Chemosphere* 234, 409–418. doi: 10.1016/j.chemosphere.2019.06.080

Liu, Y. L. (2015). Fatty acids, inflammation and intestinal health in pigs. *J. Anim. Sci. Biotechnol.* 6, 1–9. doi: 10.1016/j.plefa.2018.10.006

Liu, Y. L., Huang, J. J., Hou, Y. Q., Zhu, H. L., Zhao, S. J., Ding, B. Y., et al. (2008). Dietary arginine supplementation alleviates intestinal mucosal disruption induced by *Escherichia coli* lipopolysaccharide in weaned pigs. *Br. J. Nutr.* 100, 552–560. doi: 10.1017/S0007114508911612

Lu, F., Li, Y. Y., Wang, X., Hu, X. S., Liao, X. J., and Zhang, Y. (2021). Early-life polyphenol intake promotes *Akkermansia* growth and increase of host goblet cells in association with the potential synergistic effect of *Lactobacillus*. *Food Res. Int.* 149:110648. doi: 10.1016/j.foodres.2021.110648

Marín, M., Giner, R. M., Ríos, J.-L., and Recio, M. C. (2013). Intestinal anti-inflammatory activity of ellagic acid in the acute and chronic dextrane sulfate sodium models of mice colitis. *J. Ethnopharmacol.* 150, 925–934. doi: 10.1016/j.jep.2013.09.030

Mishra, S., and Vinayak, M. (2014). Ellagic acid inhibits PKC signaling by improving antioxidant defense system in murine T cell lymphoma. *Mol. Biol. Rep.* 41, 4187–4197. doi: 10.1007/s11033-014-3289-0

Mou, Q., Yang, H.-S., Yin, Y.-L., and Huang, P.-F. (2019). Amino acids influencing intestinal development and health of the piglets. *Animals* 9:302. doi: 10.3390/ani9060302

Nagler-Anderson, C. (2001). Man the barrier! Strategic defences in the intestinal mucosa. *Nat. Rev. Immunol.* 1, 59–67. doi: 10.1038/35095573

Pari, L., and Sivasankari, R. (2008). Effect of ellagic acid on cyclosporine A-induced oxidative damage in the liver of rats. *Fundam. Clin. Pharmacol.* 22, 395–401. doi: 10.1111/j.1472-8206.2008.00609.x

Qin, Q., Xu, X., Wang, X. Y., Wu, H. T., Zhu, H. L., Hou, Y. Q., et al. (2018). Glutamate alleviates intestinal injury, maintains mTOR and suppresses TLR4 and NOD signaling pathways in weanling pigs challenged with lipopolysaccharide. *Sci. Rep.* 8:15124. doi: 10.1038/s41598-018-33345-7

Shen, X. J., Yi, D., Ni, X. Q., Zeng, D., Jing, B., Lei, M. X., et al. (2014). Effects of *Lactobacillus plantarum* on production performance, immune characteristics, antioxidant status, and intestinal microflora of bursin-immunized broilers. *Can. J. Microbiol.* 60, 193–202. doi: 10.1139/cjm-2013-0680

Su, J. Y., Zhu, Q., Zhao, Y., Han, L., Yin, Y. L., Blachier, F., et al. (2018). Dietary supplementation with chinese herbal residues or their fermented products modifies the colonic microbiota, bacterial metabolites, and expression of genes related to colon barrier function in weaned piglets. *Front. Microbiol.* 9:3181. doi: 10.3389/fmicb.2018.03181

Sun, Y.-Q., Tao, X., Men, X.-M., Xu, Z.-W., and Wang, T. (2017). *In vitro* and *in vivo* antioxidant activities of three major polyphenolic compounds in pomegranate peel: ellagic acid, punicalin, and punicalagin. *J. Integr. Agric.* 16, 1808–1818.

Umesalma, S., and Sudhandiran, G. (2011). Ellagic acid prevents rat colon carcinogenesis induced by 1, 2 dimethyl hydrazine through inhibition of AKT-phosphoinositide-3 kinase pathway. *Eur. J. Pharmacol.* 660, 249–258. doi: 10.1016/j.ejphar.2011.03.036

Wan, J., Jiang, F., Xu, Q. S., Chen, D. W., Yu, B., Huang, Z. Q., et al. (2017). New insights into the role of chitosan oligosaccharide in enhancing growth performance, antioxidant capacity, immunity and intestinal development of weaned pigs. *RSC. Adv.* 7, 9669–9679. doi: 10.1039/c7ra00142h

Wan, J., Zhang, J., Chen, D. W., Yu, B., Huang, Z. Q., Mao, X. B., et al. (2018). Alginate oligosaccharide enhances intestinal integrity of weaned pigs through altering intestinal inflammatory responses and antioxidant status. *RSC. Adv.* 8, 13482–13492.

Wan, J., Zhang, J., Xu, Q. S., Yin, H., Chen, D. W., Yu, B., et al. (2021). Alginate oligosaccharide protects against enterotoxigenic *Escherichia coli*-induced porcine intestinal barrier injury. *Carbohydr. Polym.* 270:118316. doi: 10.1016/j.carbpol.2021.118316

Yu, J., Yin, P., Liu, F. H., Cheng, G. L., Guo, K. J., Lu, A., et al. (2010). Effect of heat stress on the porcine small intestine: a morphological and gene expression study. *Comp. Biochem. Physiol. A Mol. Integr. Physiol.* 156, 119–128. doi: 10.1016/j.cbpa.2010.01.008

Yüce, A., Ateşşahin, A., ÇeribaşSi, A. O., and Aksakal, M. (2007). Ellagic acid prevents cisplatin-induced oxidative stress in liver and heart tissue of rats. *Basic Clin. Pharmacol. Toxicol.* 101, 345–349. doi: 10.1111/j.1742-7843.2007.00129.x

Zheng, Y. Z., Fu, Z. M., Deng, G., Guo, R., and Chen, D. F. (2020). Free radical scavenging potency of ellagic acid and its derivatives in multiple H^+/e^- processes. *Phytochemistry.*180:112517. doi: 10.1016/j.phytochem.2020.112517

Conflict of Interest: The authors declare that the research was conducted in the absence of any commercial or financial relationships that could be construed as a potential conflict of interest.

Publisher's Note: All claims expressed in this article are solely those of the authors and do not necessarily represent those of their affiliated organizations, or those of the publisher, the editors and the reviewers. Any product that may be evaluated in this article, or claim that may be made by its manufacturer, is not guaranteed or endorsed by the publisher.

frontiers in Microbiology

ORIGINAL RESEARCH
published: 13 December 2021
doi: 10.3389/fmicb.2021.797875

Fermented Alfalfa Meal Instead of "Grain-Type" Feedstuffs in the Diet Improves Intestinal Health Related Indexes in Weaned Pigs

Yuheng Luo[1]†, Yang Liu[1]†, Yuqing Shen[1]†, Jun He[1]†, Hua Li[1], Cong Lan[1], Jiayan Li[1], Hong Chen[2], Daiwen Chen[1], Zhihua Ren[3], Bing Yu[1], Zhiqing Huang[1], Ping Zheng[1], Xiangbing Mao[1], Jie Yu[1], Junqiu Luo[1] and Hui Yan[1]*

[1] Key Laboratory for Animal Disease-Resistance Nutrition of China Ministry of Education, Key Laboratory of Animal Disease-Resistant Nutrition and Feed of China Ministry of Agriculture and Rural Affairs, Key Laboratory of Animal Disease-Resistant Nutrition of Sichuan Province, Institute of Animal Nutrition, Sichuan Agricultural University, Chengdu, China, [2] College of Food Science, Sichuan Agricultural University, Ya'an, China, [3] Sichuan Province Key Laboratory of Animal Disease and Human Health, Key Laboratory of Environmental Hazard and Human Health of Sichuan Province, College of Veterinary Medicine, Sichuan Agricultural University, Chengdu, China

OPEN ACCESS

Edited by:
Fengjie Sun,
Georgia Gwinnett College,
United States

Reviewed by:
Zhipeng Li,
Jilin Agricultural University, China
Bi E. Tan,
Hunan Agricultural University, China
Changzheng Guo,
Université Claude Bernard Lyon 1,
France

***Correspondence:**
Yuheng Luo
luoluo212@126.com

† These authors have contributed equally to this work

Specialty section:
This article was submitted to Food Microbiology, a section of the journal Frontiers in Microbiology

Received: 19 October 2021
Accepted: 15 November 2021
Published: 13 December 2021

Citation:
Luo Y, Liu Y, Shen Y, He J, Li H, Lan C, Li J, Chen H, Chen D, Ren Z, Yu B, Huang Z, Zheng P, Mao X, Yu J, Luo J and Yan H (2021) Fermented Alfalfa Meal Instead of "Grain-Type" Feedstuffs in the Diet Improves Intestinal Health Related Indexes in Weaned Pigs. Front. Microbiol. 12:797875. doi: 10.3389/fmicb.2021.797875

Corn and soybean meal are the two main components in formula feed of farm animals, leading to a serious food competition between humans and livestock. An alternative may be to encourage the utilization of unconventional feedstuff in animal diet. In the current study, we evaluated the utilization of fermented alfalfa meal (FAM) in weaned pigs. Twenty weaned piglets (separately caged) were randomly divided into two groups. Pigs in the control group (CON) were fed corn-soybean meal diet, and part of corn and soya protein concentrate in the diet of another group was replaced by 8% FAM. After 40 days of feeding, the average feed intake of FAM pigs was increased ($P > 0.05$), and the villus height (VH) of jejunum and duodenum, crypt depth (CD), and VH/CD in FAM pigs was improved compared to the CON group ($P < 0.05$). The increase ($P < 0.05$) of goblet cells in the jejunum of FAM pigs was positively correlated with the expression of *MUC-2* gene ($R = 0.9150$). The expression of genes related to immunity (*IRAK4*, *NF-κB,* and *IL-10*) and intestinal barrier (*Occludin* and *MUC-2*) in the jejunum, as well as the expression of *ZO-1* and *MUC-2* in the colon of these pigs, also showed increase ($P < 0.05$) compared to CON pigs, which was accompanied by the decrease ($P < 0.05$) of LPS concentration in the serum. The elevated proportion of $CD3^+$ and $CD8^+$ T-lymphocyte subsets in spleen ($P < 0.05$) confirmed the improvement of systemic immune function in FAM pigs. In addition, FAM pigs have a higher β-diversity of microbial community ($P < 0.05$) and promoted enrichment of probiotics such as *Lactobacillus* that positively was correlated with acetate concentration in the colon over CON pigs. In summary, partially replacement of expanded corn and soya protein concentrate with FAM (8%) may benefit the intestinal barrier and immune function of weaned pigs without affecting their growth. Our findings also provide evidence of the feasibility of FAM as a dietary component in pigs to reduce the consumption of grain.

Keywords: weaned pigs, fermented alfalfa meal, intestinal barrier, colonic microbiota, immunity

INTRODUCTION

The expanding livestock industry has led to an increase in the demand for grain and its by-products, resulting in deteriorating food competition between humans and livestock (van Kernebeek et al., 2016; van Zanten et al., 2018) and adverse environmental impacts (Schader et al., 2015). In recent years, to meet the increasing demand for high-quality meat, the swine populations in China have a rapid growth (Zhuang et al., 2020), leading to an increase in the consumption of corn-soybean meal based commercial feed. Replacing "grain-type" feedstuffs with "non-grain-type" feed resources is an effective way to ensure the sustainable development of the swine industry.

Alfalfa, especially *Medicago sativa* L., is regarded as "the queen of forages" because of its high content of protein, minerals, and vitamins and is the most common perennial legume forage in China (Shi et al., 2017). The annual global output of alfalfa is more than 300 million tons (Zheng et al., 2018). Alfalfa meal is commonly used in ruminants as a commercial feedstuff. However, due to its high content of crude fiber, alfalfa meal is not considered to be effectively used by pigs. Insoluble dietary fiber (IDF), such as cellulose, lignin, and xylan, is the main component of crude fiber in alfalfa, accounting for more than 90% of the total dietary fiber (Knudsen, 1997; Chen et al., 2013). For pigs, especially weaned piglets with limited tolerance to crude fiber, high levels of crude fiber from plant cell walls can reduce the digestibility of nutrients and the palatability of feed. We have previously reported that the solid-state fermentation by compound fungal strains can reduce the level of crude fiber in wheat bran and increase the content of soluble dietary fiber (SDF), and the supplement of fermented wheat bran in the diet can improve the intestinal health without affecting the growth performance in weaned pigs (Luo et al., 2021). The main purpose of the current study is to evaluate the feasibility of FAM replacing part of "grain-type" feedstuff in weaned pigs. Meanwhile, the growth performance, intestinal barrier, immunity related parameters, and the colonic microbiota were investigated to discuss the potential effects of FAM on intestinal health of weaned pigs.

MATERIALS AND METHODS

All experimental procedures and animal care were accomplished in accordance with the Guide for the Care and Use of Laboratory Animals provided by the Institutional Animal Care Advisory Committee for Sichuan Agricultural University. The experimental protocols used in the present study were approved by the Sichuan Agricultural University Institutional Animal Care and Use Committee No. 69130079.

Animals and Diets

A total of 20 Duroc × Landrace × Yorkshire cross-bred weaned pigs with similar initial body weight (7.20 ± 0.27 kg) were randomly allocated to two groups with 10 replicates per group and 1 pig per replicate, and each pig was raised in a 1.5 m × 0.7 m × 1.0 m metabolism cage. Pigs in the control group (CON) were fed a basal corn-soybean meal diet. For pigs in another group (FAM), a total of 7.2% expanded corn and 1.8% soya protein concentrate in the diet were replaced by equivalent FAM, respectively. FAM used in the current study was prepared according to the method established in our previous study (Luo et al., 2021). The diets were formulated to meet the nutrient recommendations of the National Research Council (2012) and no antibiotics were supplemented (**Table 1**). The whole experiment lasted for 40 days, and the diet and water were available *ad libitum*. The feed intake, mental status, and health condition of each pig were investigated and recorded every day.

Sample Collection, RNA Extraction, and Real-Time PCR

On the early morning of day 41, all pigs were weighed and 10 mL jugular blood was collected for flow cytometry and biochemical analysis. After that, pigs were sacrificed under anesthesia by lethal injection of 200 mg/kg sodium pentobarbital. The abdomen of each pig was opened immediately and approximately 2 cm of middle duodenum, jejunum, ileum, and colon was collected and fixed in 100 mL 10% formaldehyde solution for histology analysis, respectively, and the mucosa of each segment was scraped using a sterilized slide and stored in liquid nitrogen for RNA extraction. Approximate 5 g of colonic digesta was collected for the analysis of microbiota and concentration of short chain fatty acids (SCFAs), and 5 g of spleen was also collected and stored on ice for the determination of T-lymphocyte subsets.

The RNA of mucosal samples of jejunum and colon from each pig were extracted using Trizol (TAKARA, Japan). The mRNA levels of key genes of pattern recognition receptor related signaling pathway, such as *NOD1*, *NOD2*, *RIPK-2* (Wan et al., 2018a), *TLR4*, *MyD88*, *TRAF6* (Wan et al., 2019), *IRAK4* (Islam et al., 2012), and *NF-κB* (Tian et al., 2016), and cytokines and antimicrobial peptides, such as *IL-1*β, *IL-6*, *IL-10* (Feng et al., 2015), and *pBD1* (Cheng et al., 2015), as well as intestinal barrier related genes, such as *ZO-1*, *Occludin* (Wan et al., 2020), and *MUC-2* (Wan et al., 2018b), were quantified by real-time PCR and the relative expression of each gene was calculated using the $2^{-\Delta\Delta Ct}$ method (Reid et al., 2011). The extraction of RNA and procedures of real-time PCR have been described before (Luo et al., 2021).

Histological and Flow Cytometry Analysis

The villus height (VH), crypt depth (CD), and VH/CD ratio of each small intestine sample was measured. The methods of embedding, staining, and microscopic observation of paraffin sections have been described before (Luo et al., 2021). The concentrations of lipopolysaccharide (LPS) and D-lactate in each serum sample were assayed using a porcine ELISA kit purchased from Wuhan Meimian Biological Technology Co., Ltd. (Hubei, China). The proportion of $CD3^+$, $CD4^+$, and $CD8^+$T lymphocyte subsets in each blood sample was detected following our reported method (Luo et al., 2021).

TABLE 1 | The composition and the level of nutrients in the experimental diets (air-dried basis).

Item	CON	FAM
Ingredient (%)		
Expanded corn	37.19	29.99
Peeled soybean meal	20.55	20.55
corn starch	18.00	18.00
Fish meal	4.50	4.50
Soya protein concentrate	4.30	2.50
Whey powder	5.50	5.50
Sucrose	4.00	4.00
Glucose	3.00	4.00
Soybean oil	0.20	0.20
FAM	0.00	8.00
NaCl	0.30	0.30
L-Lysine·HCl	0.40	0.40
DL-Methionine	0.15	0.15
Threonine	0.14	0.14
Tryptophan	0.03	0.03
Limestone	0.60	0.60
Dicalcium phosphate	0.80	0.80
Chloride choline	0.10	0.10
Vitamin premix[1]	0.04	0.04
Mineral premix[2]	0.20	0.20
Total	100.00	100.00
Nutritional value[3]		
Digestible energy (DE, Mcal/kg)	3.53	3.55
Crude protein (CP, %)	17.45	16.66
Calcium (Ca, %)	1.00	0.79
Total phosphorus (TP, %)	0.63	0.56
Available phosphorus (AP, %)	0.43	0.40
Digestible lysine (D-Lys, %)	1.44	1.33
Digestible methionine (D-Met, %)	0.45	0.43
Methionine + Cystine (D-Met + D-Cys, %)	0.66	0.67
Digestible threonine (D-Thr, %)	0.86	0.81
Digestible tryptophan (D-Trp, %)	0.28	0.20
Crude fiber (CF, %)	1.92	6.64
Neutral detergent fiber (NDF, %)	12.12	14.12
Acid detergent fiber (ADF, %)	10.61	12.17
Soluble dietary fiber (SDF, %)	2.10	3.96
Insoluble dietary fiber (IDF, %)	7.83	8.47

[1]The vitamin premix provided Vitamin A 30,000,000 IU, Vitamin D3 10,000,000 IU, Vitamin E 80,000 IU, Vitamin K3 10,000 mg, Vitamin B1 10,000 mg, Vitamin B2 25,000 mg, Vitamin B6 12,000 mg, Vitamin B12 120 mg, D-pantothenic acid 50,000 mg, folic acid 5,000 mg, and biotin 500 mg per kg of diet.

[2]The mineral premix (7–25 kg) provided, 350 mg Fe ($FeSO_4 \cdot H_2O$), 41.67 mg Cu ($CuSO_4 \cdot 5H_2O$), 292.78 mg Zn ($ZnSO_4 \cdot 7H_2O$), 66.20 mg Mn ($MnSO_4 \cdot H_2O$), 8.31 mg I (KI), 30.61 mg Se (Na_2SeO_3), and 1209.55 mg $CaCO_3$ per kg of diet.

[3]The level of CP, CF, NDF, ADF, SDF, and IDF was measured value, while the content of DE, Ca, TP, AP, D-Lys, D-Met, D-Met + D-Cys, D-Thr, and D-Trp was calculated value.

CON, control, FAM, fermented alfalfa meal.

DNA Extraction, 16S rRNA Amplicons Sequencing, and Analysis of Short Chain Fatty Acids

The genomic DNA in each colonic sample was extracted using a bead-beating method (Zoetendal et al., 1998). The subsequent establishment of 16S rRNA amplicons library and bioinformatics analysis was performed following our described methods (Luo et al., 2017), and all reads were deposited in the National Center for Biotechnology Information (NCBI) and can be accessed in the Short Read Archive (SRA) under accession number PRJNA763735. The determination of acetate, propionate, butyrate, valerate, isobutyrate, and isovalerate concentration in colonic digesta also referred to our published methods (Luo et al., 2015). In brief, approximate 1 g of each digesta sample was suspended in 2 mL distilled water and vortexed, and then centrifuged (12,000 g) at 4°C for 10 min. The supernatant (1 mL) was then mixed with 0.2 mL metaphosphoric acid, and 1-μL supernatant was analyzed using a gas chromatograph (Varian, GC CP3800).

Statistical Analysis

An IBM SPSS Statistics 27 software was used to check normal distribution of the data. Then, differences in intestinal morphology related parameters, number of goblet cells, intestinal permeability indexes, proportion of T-lymphocyte subsets, and concentration of short-chain fatty acids (SCFAs) between CON and FAM groups were analyzed with independent sample t-test. Differences were considered statistically significant when $P < 0.05$. The correlation between the concentration of each SCFA and bacterial species was calculated using Pearson's correlational analysis and the results were visualized using the vegan, ggcor, and dplyr packages of R 4.0.1. The Pearson's correlation between the number of goblet cells and relative expression of *MUC-2* gene in jejunum was analyzed and visualized using a ggplot2 package of R 4.0.1, while the relative expression of genes in jejunum and colon of pigs in the two groups was clustered using a pheatmap package.

RESULTS

Influence of Fermented Alfalfa Meal on the Growth Performance and the Morphology of Small Intestine in Weaned Pigs

After 40 days of feeding, no difference in the final body weight (FBW), ADG, and F/G was found between the two groups ($P < 0.05$), but the ADFI of FAM pigs was increased ($P < 0.05$, **Table 2**). According to histological staining and scoring, comparing with CON pigs, the villus height (VH) in duodenum (**Figure 1A**), and the VH/CD in duodenum and jejunum (**Figures 1A,B**), except that in ileum (**Figure 1C**), was increased ($P < 0.05$). The number of goblet cells in jejunum (**Figure 1D**) was also increased ($P < 0.05$), while the crypt depth (CD) in the jejunum (**Figure 1B**) of FAM pigs was decreased ($P < 0.05$).

Effect of Fermented Alfalfa Meal on the Intestinal Barrier and Immune Related Indexes in the Intestine of the Weaned Pigs

As shown above, the feeding of FAM containing diet affected the intestinal morphology of the weaned pigs, which may further

TABLE 2 | The growth performance of the weaned pigs.

Item	CON	FAM	SD	*P*-value
IBW (kg)	7.23	7.17	0.27	0.22
FBW (kg)	19.22	17.21	2.13	0.08
ADG (g)	480.58	430.20	53.24	0.08
ADFI (g)	718.85	722.28	47.50	0.03
F/G	1.51	1.68	0.17	0.65

IBW, initial body weight; FBW, final body weight; ADG, average daily gain; ADFI, average daily feed intake; F/G, feed/gain; CON, control; FAM, fermented alfalfa meal; SD, standard deviation.

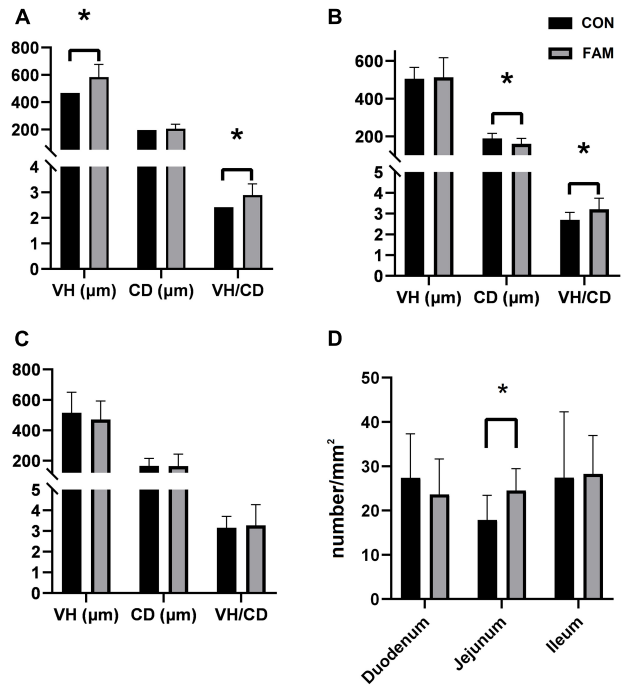

FIGURE 1 | The morphology and number of goblet cells in the small intestine of the pigs. CON, control; FAM, fermented alfalfa meal. **(A–C)** The morphology of duodenum, jejunum, and ileum of the pigs. **(D)** The number of goblet cells per square millimeter of intestinal villus in each segment. *$P < 0.05$.

influence the intestinal barrier and immune function of these animals. Because both the morphology and number of goblet cells in jejunum showed marked changes, we selected jejunum as the representative of small intestine. According to real-time PCR results, the relative expression of several intestinal barrier and immunity related genes were increased ($P < 0.01$ or 0.05) in the jejunum (**Figures 2A,B**) and colon (**Figures 2C,D**) of FAM pigs compared with CON pigs. Particularly, most of these up-regulated genes were found in the jejunum (*IRAK4*, *NF-κB*, *IL-10*, *Occludin,* and *MUC-2*) and only two (*ZO-1* and *MUC-2*) presented in the colon. Consistent with this, the concentration of LPS in the serum of FAM pigs was lower ($P < 0.05$) than that in CON pigs (**Figure 2E**). Because goblet cells are the producer of mucin in the gut (Grondin et al., 2020), we further analyzed the correlation between the number of goblet cells and the relative expression of *MUC-2* in jejunum, indicating a significant ($R = 0.92$) correlation between them (**Figure 2F**).

Effect of Fermented Alfalfa Meal on the Proportion of T-Lymphocyte Subsets in Serum and Spleen of the Weaned Pigs

The difference in the concentration of serum LPS may reflect the change in intestinal permeability and immunity of the pigs. We thus compared the proportion of T-lymphocyte subsets in the blood of pigs between the two groups. The results of flow cytometry showed that the proportion of $CD3^+$ ($P < 0.01$) and $CD8^+$ ($P < 0.05$) T lymphocyte subsets in the spleen of FAM pigs was decreased compared to CON pigs (**Figure 3B**). However, we did not observe any differences in the proportion of $CD4^+$ T-lymphocyte subsets and ratio of $CD4^+/CD8^+$ in the blood ($P > 0.05$) of pigs between the two groups (**Figure 3A**).

Effect of Fermented Alfalfa Meal on the Microbial Community and Metabolites in the Colon of the Weaned Pigs

The utilization of fiber in the hindgut of pigs mainly depends on the fermentation of microorganisms. Therefore, we examined the composition of microbial community and the concentration of main metabolites (SCFAs) in the colon of the pigs. Sequencing based on 16S rRNA amplicons showed no difference ($P > 0.05$) in the α-diversity of colonic microbial community between the two groups (**Table 3**), but a difference ($P = 0.038$) in β-diversity was found (**Figure 4A**).

Except for those unidentified phyla, a total of 22 and 25 known phyla were identified in the colonic digesta of CON and FAM pigs (**Figure 4B**), respectively. Of these phyla, Firmicutes (62.63∼70.38%), Bacteroidetes (22.01∼29.10%), and Proteobacteria (2.13∼2.60%) were the most predominant bacteria in relative abundance. The difference of colonic microbial composition between the two groups was mainly reflected in the genus level. Among the top 20 genera, the abundance of *Lactobacillus* showed significantly different ($P = 0.013$) between the two groups, which was absolutely higher in FAM (22.58%) pigs compared to CON (1.48%) pigs (**Figure 4C**). Linear discriminant analysis (LDA) and LDA coupled with effect size (LefSe, $\alpha = 0.01$, LDA score > 2.0) showed 34 and 21 taxa enriched in CON and FAM pigs (**Figure 4D**), respectively. Of these taxa, 8 known genera including *Pyramidobacter*, *Lactifluus*, *Oxalobacter*, *Buryricimonas*, *vadinCA11*, *Sutterella*, *Ruminobacter,* and *YRC22* were particularly abundant in CON pigs, while 7 other known genera, *Lysinibacillus*, *Enterococcus*, *Ureibacillus*, *Bacillus*, *Trichococcus*, *Veillonella,* and *Lactobacillus*, were specifically abundant in FAM pigs (**Figure 4D**).

Among the six measured SCFAs, the concentration of acetate showed increased ($P < 0.05$) in the colonic digesta of FAM pigs compared to CON pigs (**Figure 4E**). Further Pearson's correlation showed multiple correlations between the abundance of specifically enriched taxa and the concentration of SCFAs (**Figure 4F**), highlighting the contribution of these bacteria to microbial metabolites in the colon of these pigs.

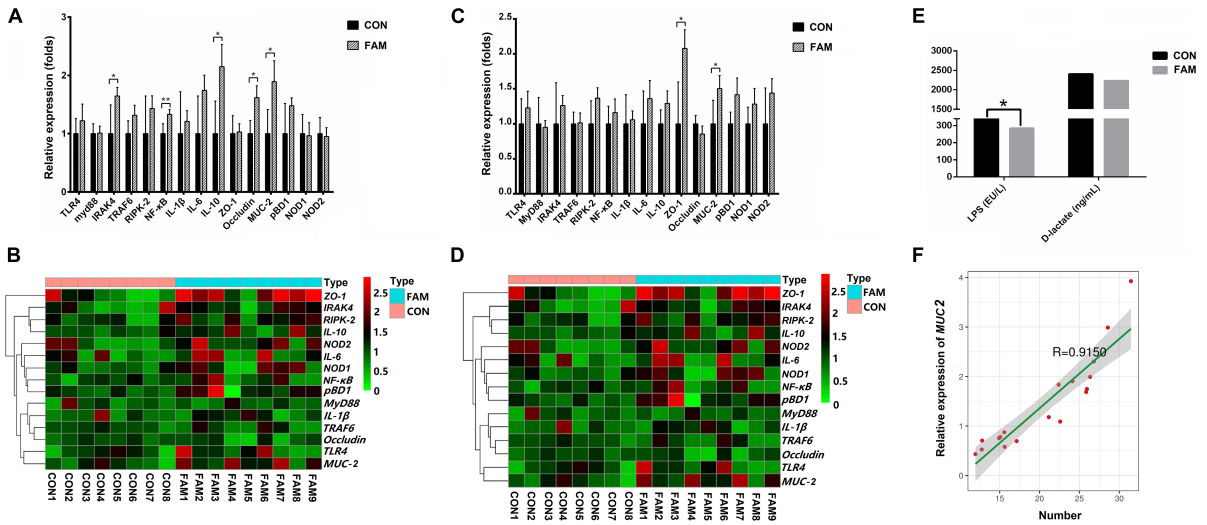

FIGURE 2 | The relative expression of barrier and immunity relating genes and the permeability of intestine in the weaned pigs. **(A)** The relative expression of genes in jejunum. **(B)** The expression of genes in the jejunum of each pig visualized by heatmap. **(C)** The relative expression of genes in colon. **(D)** The expression of genes in the colon of each pig visualized by heatmap. **(E)** The concentration of LPS and D-lactate in serum. **(F)** The correlation between the relative expression of *MUC-2* and the number of goblet cells in jejunum. $^{**}P < 0.01$ and $^{*}P < 0.05$.

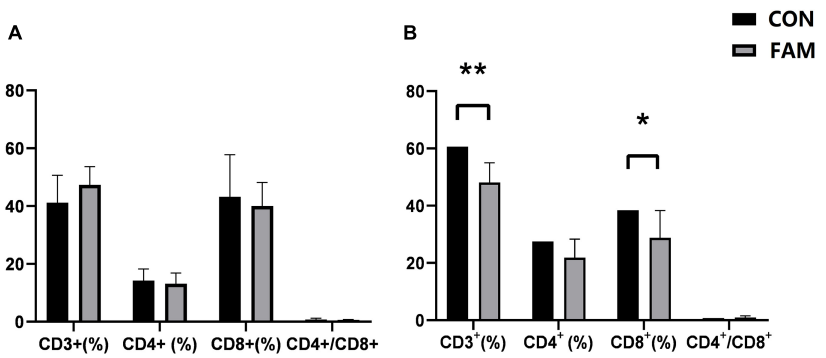

FIGURE 3 | The percentage of different T lymphocyte subsets $CD4^+/CD8^+$ ratio in the blood and spleen of the weaned pigs. CON, control; FAM, fermented alfalfa meal. **(A)** Blood. **(B)** Spleen. $^{**}P < 0.01$ and $^{*}P < 0.05$, respectively.

DISCUSSION

In the past, the application of forage grass was mostly limited to ruminants. The digestive physiological structure of monogastric livestock such as pig determines that they cannot effectively use forage. The rational development of non-grain feed resources is a feasible way to remit the contradiction between increasing population and the shortage of food. In the current study, we proved the feasibility of small-amount substitution of expanded corn and soybean protein concentrate by FAM in the feed of weaned piglets.

Limited studies focused on the utilization of alfalfa meal in swine feed. For example, the daily gain of growing pigs housed in a cold (10°C), thermoneutral (22.5°C), or hot (35°C) thermal environment can be reduced by 1, 3, and 5% by the supplement of 10% dehydrated alfalfa meal in their feed (Stahly and Cromwell, 1986). Similar result is also found in sows fed 20% alfalfa meal containing feed (Pond et al., 1980). When the proportion of alfalfa meal in feed ranges from 20 to 60%, its negative effect on daily gain and feed/gain in growing-finishing pigs is dose-dependent (Powley et al., 1981), which may be due to the high concentration of crude fiber in alfalfa meal. It is worth noting that

TABLE 3 | The α-diversity indexes of microbial community in the colonic digesta of the weaned pigs.

Index	CON	FAM	SD	*P*-value
Chao1	11825.18	10962.04	1898.304	0.55
Observed species	5088.77	5022.37	509.10	0.87
PD whole tree	310.58	309.38	28.27	0.96
Shannon	9.12	8.91	0.67	0.72

CON, control; FAM, fermented alfalfa meal; SD, standard deviation.

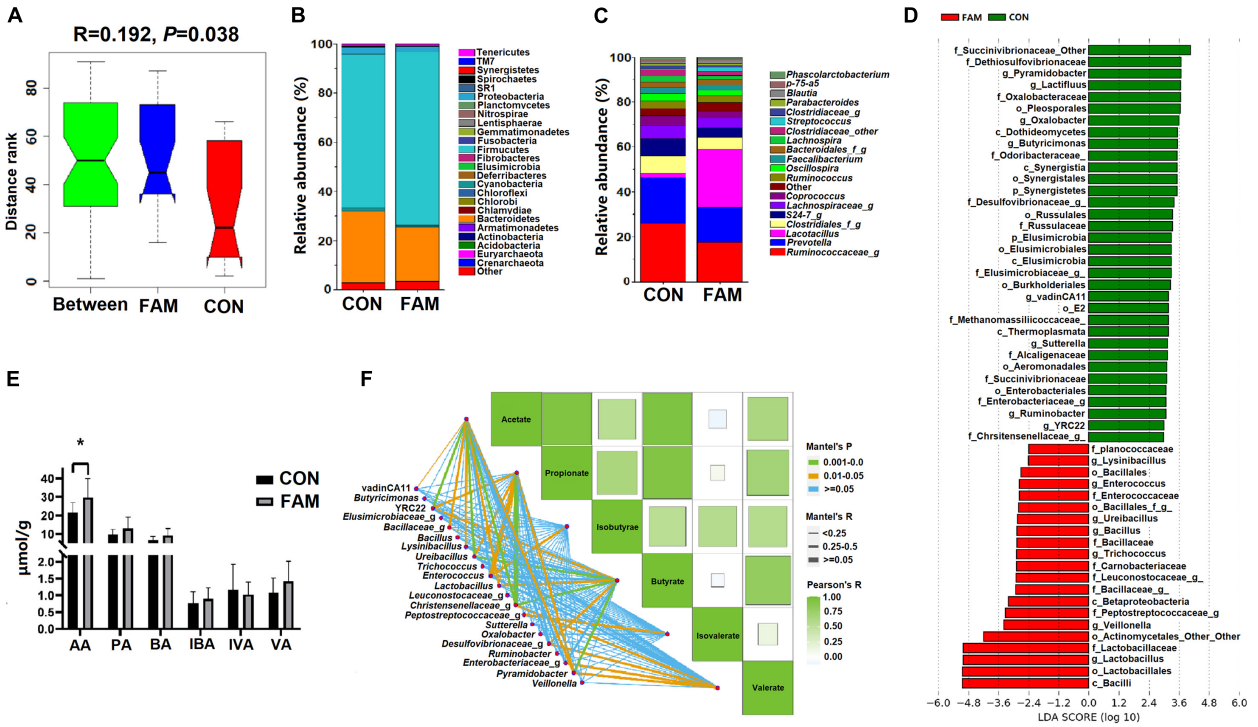

FIGURE 4 | The microbial community, concentration of SCFAs, as well as the interaction between characteristic bacteria and SCFAs in the colon of the weaned pigs. **(A)** The β-diversity of colonic microbial community based on unweighted unifrac distance. **(B)** The composition of colonic microbiota at phylum level. **(C)** The relative abundance of top 20 microbial genera in the colonic digesta. **(D)** Bacterial groups with significant differences in relative abundance in the two groups of pigs, and data shows according to the results of Lefse analysis (characteristic bacteria). **(E)** The concentration of each SCFA in the colon of the pigs. **(F)** The correlation between the concentration of SCFAs and the relative abundance of characteristic bacteria. CON, control; FAM, fermented alfalfa meal. $^*P < 0.05$.

the alfalfa meal used in these studies is not specially processed (e.g., fermentation). In this study, the proportion of FAM was 8%, resulting in an increase of crude fiber from 1.95 (CON) to 3.64 (FAM) in formula feed. Meanwhile, the concentration of extruded corn and soya protein concentrate in the feed of FAM group was 7.2 and 1.8% lower than that of CON group. However, no significant changes in most growth performance related parameters, except for increased ADFI, were found in FAM pigs after a continuous feeding for 40 days. These findings suggest that partially replacing expanded corn and soybean protein with 8% FAM has no effect on the growth of weaned pigs.

Our study highlighted the role of FAM containing diet on intestinal health of the weaned pigs. The intestinal epithelium has strong plasticity (de Sousa E Melo and de Sauvage, 2019). Changes in villus density and height, crypt depth, as well as the renewal rate of epithelium are regarded as common parameters to assess host response to nutrients, pathogens, and stress (Kopf and Sixt, 2019). Crypt in intestinal epithelium is considered as a villus workshop due to its internal stem cells (De Gregorio et al., 2018). We found that comparing with pigs fed basal diet, pigs fed FAM containing diet had higher villus height and ratio of villus height/crypt depth, especially in jejunum and duodenum, indicating a promotion of FAM on the development of villi in the small intestine. Interestingly, we further found that the number of goblet cells in the jejunum of pigs fed FAM diet is remarkably higher than that of pigs in the control group, which was positively correlated with the expression of *MUC-2* gene. It is well known that goblet cells, existing in the single columnar epithelium of small and large intestine, secrete mucin 2 (Pelaseyed et al., 2014) that works with water, inorganic salt, and antibacterial peptide to form viscous gel-like network in the gut (Kim and Ho, 2010). Our result thus suggests an enhanced intestinal mucus barrier in pigs fed FAM. In addition, the increased expression of tight junction protein (e.g., Occludin and ZO-1) genes in the jejunum and colon suggested an improved intestinal mechanical barrier in pigs fed FAM containing diet. The lower concentration of LPS in the serum provides further evidence for FAM diet improving the intestinal barrier function of these pigs.

As the "pioneer" of pathogens invading body, LPS triggers the immune response of the host by activating the signal pathway related to pattern recognition receptors such as TLR4 (Szabo et al., 2010). We found that after feeding FAM containing diet, the expression of *IRAK4*, *NF-κB*, and *IL-10* genes in the jejunum of pigs was elevated compared to the CON group. IRAK4 can activate downstream inhibitor of NF-κB kinase (IKK) and mitogen activated protein kinase (MAPK) pathway by inducing the binding of IRAK1 and tumor necrosis factor-associated factor 6 (TRAF6) (Madera-Salcedo et al., 2013), which in turn promotes the nuclear translocation of NF-κB (Sina et al., 2010). Among all NF-κB-induced cytokines, IL-10 is

a well-known anti-inflammatory cytokine that can stimulate natural and specific immunity (de Vries, 1995). Therefore, our findings indicate that the supplement of FAM in the diet may enhance the immune function of the weaned pigs through MyD88 dependent LPS/TLR4 signal pathway. This inference was also confirmed by the results of flow cytometry, that is, the proportion of $CD3^+$ and $CD8^+$ T lymphocytes in the spleen of pigs fed FAM diet was decreased compared to control.

Gut microbiota constitutes another important intestinal barrier. The composition of microflora is an important factor affecting intestinal homeostasis of the host (Ohland and Jobin, 2015). In the current study, 16S rRNA based amplicon sequencing revealed similar α-diversity but different composition of microbial community in the colon between FAM and CON pigs. Genera that may contain large amounts of probiotics, such as *Lactobacillus* and *Enterococcus*, were enriched in the colon of FAM pigs. Interestingly, *Lysinibacillus*, a genus with a strong ability to degrade lignocellulose (Ayeronfe et al., 2019), was also found more abundant in pigs fed FAM diet. It is speculated that the changed microbiota in colon of FAM pigs contributed to the fermentation ability more than CON pigs, which was confirmed by the markedly higher concentration of acetate in the colon of these pigs. A study in growing pigs also shows that with the increase of alfalfa meal in the diet, the pH value of ileal digesta and the concentration of acetate in feces is increased (Chen et al., 2013). Our results of correlation analysis proved that the distinct microbial species enriched in the colon of the pigs contributed to the different concentration and composition of SCFAs between the two groups. Moreover, although the level of crude fiber in FAM diet was as high as 6.64% (vs. 1.92% in CON diet), no decrease in the growth performance of the animals was observed in this study, which may be related to the improvement of microbial composition and metabolites in the hindgut. However, the direct effect of the dietary fiber composition of FAM on intestinal microbiota in pigs remains to be explored.

CONCLUSION

In the current study, we showed that the supplement of FAM in the diet improved the morphology and reduced the mucosal permeability of small intestine without affecting the growth of weaned piglets. The interaction between increased number of goblet cells and *MUC-2* expression in jejunum suggests that FAM containing diet may promote the secretion of mucus in the piglets. We also found that the supplement of FAM may improve the internal environment of hindgut by shape the composition and metabolites of microbiota. Our findings provide powerful evidences that FAM can be used in the feed of weaned pigs, and the proportion of FAM in the formula diet can reach at least 8% by replacing equivalent expanded corn and/or soya protein concentrate.

DATA AVAILABILITY STATEMENT

The datasets presented in this study can be found in online repositories. The names of the repository/repositories and accession number(s) can be found below: https://www.ncbi.nlm.nih.gov/genbank/, PRJNA763735.

ETHICS STATEMENT

The animal study was reviewed and approved by Institutional Animal Care Advisory Committee for Sichuan Agricultural University.

AUTHOR CONTRIBUTIONS

YuL designed the experiment, wrote the manuscript, and provided funds. YaL, YS, and JH finished the animal trial and laboratory analysis. CL, JiL, and HL finished the real-time PCR and bioinformatics analysis. HC, DC, ZR, and BY helped to design the animal trial and revise the manuscript. JH, ZH, PZ, XB, and JY helped to finish the laboratory analysis. JuL and HY helped to revise the manuscript. All authors contributed to the article and approved the submitted version.

FUNDING

This study was supported by National Natural Science Foundation of China (31872369 and 32072743) and the "Double Support Plan" Foundation of Sichuan Agricultural University.

REFERENCES

Ayeronfe, F., Kassim, A., Hung, P., Ishak, N., Syarifah, S., and Aripin, A. (2019). Evaluation of *Lysinibacillus* SP, isolated from *Coptotermes curvignathus* Gut, for the delignification of oil palm residues. *Biosci. J.* 35, 892–902. doi: 10.14393/BJ-v35n3a2019-42070

Chen, L., Zhang, H. F., Gao, L. X., Zhao, F., Lu, Q. P., and Sa, R. N. (2013). Effect of graded levels of fiber from alfalfa meal on intestinal nutrient and energy flow, and hindgut fermentation in growing pigs1. *J. Anim. Sci.* 91, 4757–4764. doi: 10.2527/jas.2013-6307

Cheng, C., Sun, W. K., Liu, R., Wang, R. M., Chen, Y. H., Wang, Y., et al. (2015). Comparison of gene expression of Toll-like receptors and antimicrobial peptides in immune organs and tissues between Yorkshire and Tibetan pigs. *Anim. Genet.* 46, 272–279. doi: 10.1111/age.12286

Feng, Z., Li, T., Wu, C., Tao, L., Blachier, F., and Yin, Y. (2015). Monosodium l -glutamate and dietary fat exert opposite effects on the proximal and distal intestinal health in growing pigs. *Appl. Physiol. Nutr. Metab.* 40, 353–363. doi: 10.1139/apnm-2014-0434

De Gregorio, V., Imparato, G., Urciuolo, F., and Netti, P. A. (2018). Micro-patterned endogenous stroma equivalent induces polarized crypt-villus architecture of human small intestinal epithelium. *Acta Biomater.* 81, 43–59. doi: 10.1016/j.actbio.2018.09.061

Grondin, J. A., Kwon, Y. H., Far, P. M., Haq, S., and Khan, W. I. (2020). Mucins in intestinal mucosal defense and inflammation: learning from clinical and experimental studies. *Front. Immunol.* 11:2054. doi: 10.3389/fimmu.2020.02054

Islam, M. A., Cinar, M. U., Uddin, M. J., Tholen, E., Tesfaye, D., Looft, C., et al. (2012). Expression of Toll-like receptors and downstream genes in lipopolysaccharide-induced porcine alveolar macrophages. *Vet. Immunol. Immunopathol.* 146, 62–73. doi: 10.1016/j.vetimm.2012.02.001

Kim, Y. S., and Ho, S. B. (2010). Intestinal goblet cells and Mucins in health and disease: recent insights and progress. *Curr. Gastroenterol. Rep.* 12, 319–330. doi: 10.1007/s11894-010-0131-2

Knudsen, K. E. B. (1997). Carbohydrate and lignin contents of plant materials used in animal feeding. *Anim. Feed Sci. Tech.* 67, 319–338. doi: 10.1016/S0377-8401(97)00009-6

Kopf, A., and Sixt, M. (2019). Gut homeostasis: active migration of intestinal epithelial cells in tissue renewal. *Curr. Biol.* 29, R1091–R1093. doi: 10.1016/j.cub.2019.08.068

Luo, Y., He, J., Li, H., Lan, C., Cai, J., Chen, H., et al. (2021). Wheat bran fermented by mixed fungal strains improves the digestibility of crude fiber and may benefit the gut health without impacting the growth performance in weaned pigs. *Food Funct.* 12, 2962–2971. doi: 10.1039/D1FO00273B

Luo, Y., Zhang, L., Li, H., Smidt, H., Wright, A.-D. G., Zhang, K., et al. (2017). Different types of dietary fibers trigger specific alterations in composition and predicted functions of colonic bacterial communities in BALB/c mice. *Front. Microbiol.* 8:966. doi: 10.3389/fmicb.2017.00966

Luo, Y.-H., Yang, C., Wright, A.-D. G., He, J., and Chen, D.-W. (2015). Responses in ileal and cecal bacteria to low and high amylose/amylopectin ratio diets in growing pigs. *Appl. Microbiol. Biotechnol.* 99, 10627–10638. doi: 10.1007/s00253-015-6917-2

Madera-Salcedo, I. K., Cruz, S. L., and Gonzalez-Espinosa, C. (2013). Morphine prevents lipopolysaccharide-Induced tnf secretion in mast cells blocking IκB kinase activation and SNAP-23 phosphorylation: correlation with the Formation of a β-Arrestin/TRAF6 complex. *J. Immunol.* 191, 3400–3409. doi: 10.4049/jimmunol.1202658

National Research Council (2012). *Nutrient Requirements of Swine*, 11th Edn. Washington, DC: National Academies Press.

Ohland, C. L., and Jobin, C. (2015). Microbial activities and intestinal homeostasis: a delicate balance between health and disease. *Cell Mol. Gastroenterol. Hepatol.* 1, 28–40. doi: 10.1016/j.jcmgh.2014.11.004

Pelaseyed, T., Bergström, J. H., Gustafsson, J. K., Ermund, A., Birchenough, G. M. H., Schütte, A., et al. (2014). The mucus and mucins of the goblet cells and enterocytes provide the first defense line of the gastrointestinal tract and interact with the immune system. *Immunol. Rev.* 260, 8–20. doi: 10.1111/imr.12182

Powley, J. S., Cheeke, P. R., England, D. C., Davidson, T. P., and Kennick, W. H. (1981). Performance of growing-finishing swine fed high levels of alfalfa meal: effects of alfalfa level, dietary additives and antibiotics. *J. Anim. Sci.* 53, 308–316. doi: 10.2527/jas1981.532308x

Reid, G., Kirschner, M. B., and van Zandwijk, N. (2011). Circulating microRNAs: association with disease and potential use as biomarkers. *Crit. Rev. Oncol. Hemat.* 80, 193–208. doi: 10.1016/j.critrevonc.2010.11.004

Schader, C., Muller, A., Scialabba, N. E.-H., Hecht, J., Isensee, A., Erb, K.-H., et al. (2015). Impacts of feeding less food-competing feedstuffs to livestock on global food system sustainability. *J. R. Soc. Interface* 12:20150891. doi: 10.1098/rsif.2015.0891

Shi, S., Nan, L., and Smith, K. (2017). The current status, problems, and prospects of alfalfa (*Medicago sativa* L.) breeding in China. *Agronomy* 7:1. doi: 10.3390/agronomy7010001

Sina, C., Arlt, A., Gavrilova, O., Midtling, E., Kruse, M.-L., Müerköster, S. S., et al. (2010). Ablation of gly96/immediate early gene-X1 (gly96/iex-1) aggravates DSS-induced colitis in mice: role for gly96/iex-1 in the regulation of NF-κB. *Inflamm. Bowel Dis.* 16, 320–331. doi: 10.1002/ibd.21066

de Sousa E Melo, F., and de Sauvage, F. J. (2019). Cellular plasticity in intestinal homeostasis and disease. *Cell Stem Cell* 24, 54–64. doi: 10.1016/j.stem.2018.11.019

Stahly, T. S., and Cromwell, G. L. (1986). Responses to dietary additions of fiber (Alfalfa Meal) in growing pigs housed in a cold, warm or hot thermal environment. *J. Anim. Sci.* 63, 1870–1876. doi: 10.2527/jas1986.6361870x

Szabo, G., Bala, S., Petrasek, J., and Gattu, A. (2010). Gut-liver axis and sensing microbes. *Dig. Dis.* 28, 737–744. doi: 10.1159/000324281

Tian, G., Liang, X., Chen, D., Mao, X., Yu, J., Zheng, P., et al. (2016). Vitamin D 3 supplementation alleviates rotavirus infection in pigs and IPEC-J2 cells *via* regulating the autophagy signaling pathway. *J. Steroid. Biochem.* 163, 157–163. doi: 10.1016/j.jsbmb.2016.05.004

van Kernebeek, H. R. J., Oosting, S. J., van Ittersum, M. K., Bikker, P., and De Boer, I. J. M. (2016). Saving land to feed a growing population: consequences for consumption of crop and livestock products. *Int. J. Life Cycle Assess.* 21, 677–687. doi: 10.1007/s11367-015-0923-6

van Zanten, H. H. E., Herrero, M., van Hal, O., Röös, E., Muller, A., Garnett, T., et al. (2018). Defining a land boundary for sustainable livestock consumption. *Glob. Chang. Biol.* 24, 4185–4194. doi: 10.1111/gcb.14321

de Vries, J. E. (1995). Immunosuppressive and anti-inflammatory properties of interleukin 10. *Ann. Med.* 27, 537–541. doi: 10.3109/07853899509002465

Pond, W. G., Yen, J. T., Lindvall, R. N., and Hill, D. (1980). Dietary alfalfa meal. For genetically obese and lean growing pigs: effect on body weight gain and on carcass and gastrointestinal tract measur ements and blood metabolites. *J. Anim. Sci.* 51, 367–373. doi: 10.1080/00071668008416704

Wan, J., Zhang, J., Chen, D., Yu, B., Huang, Z., Mao, X., et al. (2018a). Alginate oligosaccharide enhances intestinal integrity of weaned pigs through altering intestinal inflammatory responses and antioxidant status. *RSC Adv.* 8, 13482–13492. doi: 10.1039/C8RA01943F

Wan, J., Zhang, J., Chen, D., Yu, B., Mao, X., Zheng, P., et al. (2018b). Alginate oligosaccharide-induced intestinal morphology, barrier function and epithelium apoptosis modifications have beneficial effects on the growth performance of weaned pigs. *J. Anim. Sci. Biotechnol.* 9:58. doi: 10.1186/s40104-018-0273-x

Wan, J., Zhang, J., Wu, G., Chen, D., Yu, B., Huang, Z., et al. (2019). Amelioration of enterotoxigenic *Escherichia coli*-induced intestinal barrier disruption by low-molecular-weight chitosan in weaned pigs is related to suppressed intestinal inflammation and apoptosis. *IJMS* 20:3485. doi: 10.3390/ijms20143485

Wan, J., Zhang, J., Yin, H., Chen, D., Yu, B., and He, J. (2020). Ameliorative effects of alginate oligosaccharide on tumour necrosis factor-α-induced intestinal epithelial cell injury. *Int. Immunopharmacol.* 89:107084. doi: 10.1016/j.intimp.2020.107084

Zheng, M., Niu, D., Zuo, S., Mao, P., Meng, L., and Xu, C. (2018). The effect of cultivar, wilting and storage period on fermentation and the clostridial community of alfalfa silage. *Ital. J. Anim. Sci.* 17, 336–346. doi: 10.1080/1828051X.2017.1364984

Zhuang, M., Shan, N., Wang, Y., Caro, D., Fleming, R. M., and Wang, L. (2020). Different characteristics of greenhouse gases and ammonia emissions from conventional stored dairy cattle and swine manure in China. *Sci. Total Environ.* 722:137693. doi: 10.1016/j.scitotenv.2020.137693

Zoetendal, E. G., Akkermans, A. D. L., and De Vos, W. M. (1998). Temperature gradient gel electrophoresis analysis of 16S rRNA from human fecal samples reveals stable and host-specific communities of active bacteria. *Appl. Environ. Microbiol.* 64, 3854–3859. doi: 10.1128/AEM.64.10.3854-3859.1998

Conflict of Interest: The authors declare that the research was conducted in the absence of any commercial or financial relationships that could be construed as a potential conflict of interest.

Publisher's Note: All claims expressed in this article are solely those of the authors and do not necessarily represent those of their affiliated organizations, or those of the publisher, the editors and the reviewers. Any product that may be evaluated in this article, or claim that may be made by its manufacturer, is not guaranteed or endorsed by the publisher.

frontiers in Microbiology

ORIGINAL RESEARCH
published: 13 January 2022
doi: 10.3389/fmicb.2021.800470

Lactiplantibacillus plantarum AR113 Exhibit Accelerated Liver Regeneration by Regulating Gut Microbiota and Plasma Glycerophospholipid

Chunliang Xie[1†], Zhoumei Zhang[1†], Manyi Yang[3], Cha Cao[1], Yingjun Zhou[1], Zuohua Zhu[1], Wenbing Gong[1], Chao Xu[1], Li Yan[1], Zhenxiu Hu[1], Lianzhong Ai[2] and Yuande Peng[1]**

[1] Institute of Bast Fiber Crops, Chinese Academy of Agricultural Sciences, Changsha, China, [2] Shanghai Engineering Research Center of Food Microbiology, School of Medical Instrument and Food Engineering, University of Shanghai for Science and Technology, Shanghai, China, [3] Department of Hepatobiliary and Pancreatic Surgery, NHC Key Laboratory of Nanobiological Technology, Xiangya Hospital, Central South University, Changsha, China

Emerging evidence indicates that probiotics have been proved to influence liver injury and regeneration. In the present study, the effects of *Lactiplantibacillus plantarum* AR113 on the liver regeneration were investigated in 70% partial hepatectomy (PHx) rats. Sprague-Dawley (SD) rats were gavaged with *L. plantarum* AR113 suspensions (1×10^{10} CFU/mL) both before and after partial hepatectomy. The results showed that *L. plantarum* AR113 administration 2 weeks before partial hepatectomy can accelerate liver regeneration by increased hepatocyte proliferation and tumor necrosis factor-α (TNF-α), hepatocyte growth factor (HGF), and transforming growth factor-β (TGF-β) expression. Probiotic administration enriched *Lactobacillus* and *Bacteroides* and depleted *Flavonifractor* and *Acetatifactor* in the gut microbiome. Meanwhile, *L. plantarum* AR113 showed decline of phosphatidylethanolamine (PE), phosphatidylcholine (PC), phosphatidyl serine (PS), and lysophosphatidyl choline (LysoPC) levels in the serum of the rats after the *L. plantarum* AR113 administration. Moreover, *L. plantarum* AR113 treated rats exhibited higher concentrations of L-leucine, L-isoleucine, mevalonic acid, and lower 7-oxo-8-amino-nonanoic acid in plasma than that in PHx. Spearman correlation analysis revealed a significant correlation between changes in gut microbiota composition and glycerophospholipid. These results indicate that *L. plantarum* AR113 is promising for accelerating liver regeneration and provide new insights regarding the correlations among the microbiome, the metabolome, and liver regeneration.

Keywords: ***Lactiplantibacillus plantarum*, partial hepatectomy, liver regeneration, gut microbiota, plasma metabolites, glycerophospholipid**

OPEN ACCESS

Edited by:
Xiaodong Xia,
Dalian Polytechnic University, China

Reviewed by:
Fouzia Sadiq,
Shifa Tameer-e-Millat University, Pakistan
Zhaolai Dai,
China Agricultural University, China

***Correspondence:**
Lianzhong Ai
ailianzhong@hotmail.com
Yuande Peng
ibfcpyd313@126.com

[†] These authors have contributed equally to this work and share first authorship

Specialty section:
This article was submitted to Food Microbiology, a section of the journal Frontiers in Microbiology

Received: *23 October 2021*
Accepted: *29 November 2021*
Published: *13 January 2022*

Citation:
Xie C, Zhang Z, Yang M, Cao C, Zhou Y, Zhu Z, Gong W, Xu C, Yan L, Hu Z, Ai L and Peng Y (2022) Lactiplantibacillus plantarum AR113 Exhibit Accelerated Liver Regeneration by Regulating Gut Microbiota and Plasma Glycerophospholipid. Front. Microbiol. 12:800470. doi: 10.3389/fmicb.2021.800470

INTRODUCTION

Liver diseases are a major medical problem for health care systems worldwide (Chowdhury et al., 2021). Partial hepatectomy and liver transplantation are currently the only curable methods for patients with hepatocellular carcinoma and cirrhosis (Yagi et al., 2020). However, complications like biliary leakage with consecutive bacterial peritonitis have a severe negative impact on the post-operative course (Tanemura et al., 2018). Therefore, the liver's remarkable capacity to regenerate after surgery determines the long-term prognosis and quality of life of patients.

Liver regeneration is an orchestrated biological process that includes sequential changes in gene expression, growth factor production, and tissue remodeling (Michalopoulos and Bhushan, 2021). Following liver resection, hepatocytes, which are not terminally differentiated, exhibit substantial proliferative capacity. Many cytokines, notably HGF, epidermal growth factor, transforming growth factor-α (TGF-α), interleukin-6 (IL-6), and TNF-α, which are involved in liver regeneration, have been identified and extensively reviewed (Hoffmann et al., 2020). However, liver regeneration research has typically focused on signaling pathways intrinsic to the liver, overlooking those derived from the gut.

Due to the intestinal-liver axis interaction, there are natural and close links between the gut and the liver in terms of anatomical structure and physiological function. Gut microbiota play an important role in different liver diseases (such as non-alcoholic fatty liver disease, cirrhosis, hepatocellular carcinoma, alcoholic liver disease, etc.) (Trebicka et al., 2021). For example, in decompensated liver cirrhosis, gut microbiota composition is changed due to factors such as liver function decline, decreased bile secretion, and hepatic portal hypertension (Crismale and Friedman, 2020). On the contrary, intestinal mucosal permeability is increased, bacterial overgrowth and translocation of intestinal bacteria leads to endogenous infection, which is a common complication of end-stage cirrhosis (Li et al., 2018). It has been noted that liver regeneration is closely associated with alterations in gut microbiota. In the absence of gut microbiota, the normal regeneration function of the liver was significantly inhibited (Adolph et al., 2018). Gut microbiota may indirectly interfere with liver regeneration after partial hepatectomy by inducing systemic or local inflammatory responses through bacterial or endotoxin translocation (Cornide-Petronio et al., 2020). In addition, gut microbiota affects intestinal signaling and enterohepatic circulation of bile acids (BAs) which have been identified as key metabolic signals during liver regeneration (Liu et al., 2015).

Probiotics supplementation is associated with modulation of the gut microbiota to reduce the inflammation cascade and enhance the immune system associated with liver surgery (Nishida et al., 2018). *Pediococcus pentoseceus*, *Lactococcus raffinolactis*, and *Lactobacillus paracasei 19* inhibited bacterial translocations after liver resection in rats, and induced hepatocyte mitosis which was delayed by colonic anastomosis (Seehofer et al., 2004). Treatment with the Linex containing *Lactobacillus* and *Bifidobacterium* alleviated hepatic injury and restored liver function in chronic liver disease patients (Rodes et al., 2014). Although these selected strains have been shown to prevent bacterial infections following abdominal surgery, thus far, the experience with selected probiotics in patients after PHx is limited.

The present study aimed to evaluate the effects of *L. plantarum* AR113 in liver regeneration. The results showed that *L. plantarum* AR113 intervention 2 weeks prior to partial hepatectomy significantly promoted liver regeneration and reduced mortality in animals. In addition, comprehensive analyses of cytokines, gut microbiome, and serum metabolites composition were performed to explore the mechanism underlying the beneficial effects of *L. plantarum* AR113 during the late phases of liver regeneration. In general, our data suggest that *L. plantarum* AR113 administration before PHx may be a promising strategy to accelerate liver regeneration.

Abbreviations: *L. plantarum*, *Lactiplantibacillus plantarum*; PHx, 70% partial hepatectomy; SD, Sprague-Dawley; TNF-α, tumor necrosis factor-α; HGF, hepatocyte growth factor; TGF-β, transforming growth factor-β; PE, phosphatidyl ethanolamine; PC, phosphatidyl choline; PS, phosphatidyl serine; LysoPC, lysophosphatidyl choline; TGF-α, transforming growth factor-α; IL-6, interleukin-6; BAs, bile acids; MRS, Man-Rogosa-Sharpe; PBS, phosphate buffer saline; H&E, hematoxylin-eosin; TBil-V, total bilirubin; ALT, alanine aminotransferase; AST, aspartate aminotransferase; ALB II, albumin II; Glo II, globulin II; TP, total protein; PCoA, principal coordinates analysis; LEfSe, linear discriminant analysis effect size; LDA, linear discriminant analysis; PCA, principle component analysis; OPLS-DA, orthogonal partial least-squares-discriminant analysis; VIP, variable importance in the projection; KEGG, Kyoto Encyclopedia of Genes and Genomes; ANOVA, analysis of variance; Leu, leucine; Ile, isoleucine; Val, valine; PIs, glycerophosphoinositol; PCs, glycerophosphocholines; PSs, glycerophosphoserines; PGs, glycerophosphoglycerols; GPE, glycerophosphoethanolamine; GPC, glycerophosphocholine; GPCRs, G protein-coupled receptors; GPI, glycosylphosphatidylinositol; ARA, arachidonic acid; TG, triacylglycerol.

MATERIALS AND METHODS

Bacterial Cultures and Growth Conditions

Lactiplantibacillus plantarum AR113 was obtained from the Shanghai Engineering Research Center of Food Microbiology, University of Shanghai for Science and Technology (Shanghai, China), which was kept at the China General Microbiological Culture Collection Center, preservation number, CGMCC No. 13909). *L. plantarum* AR113 was stored in 30% glycerol tubes at −80°C. The bacteria were first streaked on Man-Rogosa-Sharpe (MRS) agar plates and cultured in an anaerobic station at 37°C. After 3 days of culture, single colonies of bacteria were activated in MRS liquid medium for 2 generations and cultured at 37°C for 16 h. The bacteria were centrifuged (8,000 × *g*, incubated at 4°C for 10 min) and resuspended with sterile phosphate buffer saline (PBS, pH 7.4) until the final concentration was $1*10^{10}$ CFU/mL.

Animals and Partial Hepatectomy

The animal protocol was reviewed and approved by the Animal Care Committee of Institute of Bast Fiber Crops, Chinese Academy of Agricultural Sciences (no. 2020-016). SD rats were housed in steel microisolator cages at 22°C with a 12-h light/dark cycle. Food and water were provided *ad libitum* throughout study. A total of 120 male rats were randomly

divided into five groups: (A) control, (B) sham hepatectomy, the sham hepatectomy consisted of laparotomy and mobilization of the liver, (C) PHx, 70% liver resection procedures were performed, (D) AR113+PHx, *L. plantarum* AR113 was given by gastric gavage, which was started 14 days before partial hepatectomy, and continued until 3 or 7 days after the PHx. (E) PHx+AR113, *L. plantarum* AR113 was given by gastric gavage, which was started at partial hepatectomy, and continued until 3 or 7 days after the operation. For rats in groups (C–E), 70% liver resection procedures were performed according to the method published by Higgins and Anderson (Higgins and Anderson, 1931). *L. plantarum* AR113 (suspended in physiological saline) was given to rat by oral gavage at a dose of 10^{10} CFU/mL. Rats in Groups A and B were gavaged the same volume of physiological saline. Rats were killed 3 or 7 days after 2/3 PHx surgery covering the time when hepatocytes are actively proliferating. At the end of the experiment, animals were sacrificed, and liver, blood, and fecal samples were collected.

Hepatic Regeneration Rate Measurement

The liver regeneration rate was calculated as remnant liver weight/estimated whole liver weight, which was calculated as follows:

$$\text{Liver Regeneration Rate} = [\text{Wc} - (\text{Wa} - \text{Wb})]/[\text{Wa} - \text{Wb}] \times 100$$

$$\text{Wa} = \text{Wb}/70\%$$

Where Wa is the initial weight of rat liver at the start of PHx, and Wb and Wc are the actual weights of the surgically excised liver tissue and the residual liver tissue at the time points of 3 and 7 days after reperfusion.

Liver Histology

After rats were sacrificed, a portion of each excised liver was formalin-fixed and sliced into 5 μm thick sections. The sections were then stained with Hematoxylin-Eosin (H&E) for morphological examination. Three H&E-stained levels/sections were examined per specimen. Images were then taken at 20× magnification.

Immunohistochemistry was carried out for Ki-67 to estimate liver proliferation. The sections were incubated with rabbit anti mouse Ki-67 (1:100 Abcam, Cambridge, United Kingdom) as primary antibodies overnight at 4°C. After washing, the sections were incubated with second antibodies HRP polymer detection kit. Digital images were taken around the central vein by using an AxioM1 light microscope (Carl Zeiss, Germany). The number of Ki-67-positive hepatocytes was manually counted in 20 random visual fields at 200X magnification.

Liver Biochemistry

The concentrations of liver plasma total bilirubin-V (TBil-V), alanine aminotransferase (ALT), aspartate aminotransferase (AST), IL-6, albumin II (ALB II), globulin II (Glo II), total protein (TP), TNF-α, TGF-β, and HGF were determined by using commercial kits as described in the references (Cassano and Dufour, 2019).

Analysis of the Gut Microbiota

Fecal DNA was manually extracted using QIAamp DNA Stool Mini Kit (Qiagen, Germany). The extracted DNA from each sample was used as the template to amplify the V3 and V4 hypervariable regions of ribosomal 16S rRNA genes on a 454-Junior Genome Sequencer (Roche 454 Life Sciences, Branford, CT, United States) as described. The 16S rRNA genes were amplified by the universal primers F (5′-ACTCCTACGGGAGGCAGCAG-3′) and R (5′-GGACTACHVGGGTWT-CTAAT-3′). The PCR products were purified with AMPure XP beads (Agencourt, Beckman Coulter, Brea, CA, United States) and were sequenced on an Illumina MiSeq platform (Illumina, San Diego, CA, United States). The clean data were clustered into operational taxonomic units (OTUs) with a 97% threshold by Vsearch software (v2.3.4, Vsearch). OTUs were annotated with RDP classifier as described to the Ribosomal Database Project (RDP, database v.11.3). The Chao1 index, Shannon index, and principal coordinates analysis (PCoA) were calculated by QIIME software (version 1.8.0). Linear discriminant analysis effect size (LEfSe) analysis was performed on the Galaxy web platform to identify discriminant taxa among groups. Linear discriminant analysis (LDA) score was used to estimate the effect size of different taxon. Results with LDA score greater than 3.5 were defined as discriminative taxa.

Plasma Metabolites Analysis

Each 200 μL serum was added to 600 μL pre-cooled methanol: acetonitrile (2:1 = v:v) and vortexed for 1 min. After centrifugation at 2×10^4 *g* for 20 min, supernatant was transferred to a new tube and freeze-dried. The dried samples were re-constituted with 10% aqueous methanol, filtered through 0.22 μm polyvinylidene fluoride membrane, and used for subsequent LC-MS/MS analysis.

To identify the metabolites from plasma, samples were analyzed by LC-MS/MS analysis, which was described in our previous study (Heinrich et al., 1988). The extracts were analyzed by ACQUITY UHPLC system (Waters) coupled to a Xevo G2-XS Q-TOF mass spectrometer, operating in both positive and negative ionization mode. The sample was loaded onto an ACQUITY UPLC BEH C18 (100 mm × 2.1 mm, 1.7 μm) column held at 45°C. The mobile phase consisted of 0.1% (v/v) formic acid (solution A) and acetonitrile contained 0.1% formic acid (solution B), with a flow rate of 0.4 mL/min. The elution profile was set as following: 0 min, 1% B; 1 min, 5% B; 2 min, 30% B; 3.5 min, 60% B; 7.5 min, 90% B; 9.5 min, 100% B; 12.5 min, 100% B; and 12.7 min, 1% B; 16 min, 1%, flow rate, 0.40 mL/min.

The ion source condition settings were as follows: desolvation temperature set at 350°C; capillary voltage set at 30 V; mass spectrometry data range was from 100 to 1,200 m/z. The raw data from the LC-MS/MS were analyzed using the progenesis QI software (Waters Corporation, Milford, United States). The internal standard was used for data QC to test reproducibility of analysis methods. Principle component analysis (PCA) and

orthogonal partial least-squares-discriminant analysis (OPLS-DA) were performed using SIMCA-P+12.0.1.0 chemometrics software to visualize the metabolites alterations among the samples. The statistical criteria for preliminary selection of characteristic metabolites were threshold of variable importance in the projection (VIP) from the OPLS-DA greater than 1.0 and q-value < 0.05 in a t-test. Enriched metabolic pathways were performed using MetaboAnalyst[1] based on the pathway library from Kyoto Encyclopedia of Genes and Genomes (KEGG).

Statistical Analysis

Student's t-test was used for comparisons of metabolite levels using the statistical computer package GraphPad Prism version 6 (GraphPad Software Inc., San Diego, CA, United States). Results in the present study were shown as means ± SEM. Statistical comparisons were made using two-way analysis of variance (ANOVA) with Tukey's *post hoc* test. P-values < 0.05 were considered as statistical significance. Columns with different letters differ significantly.

RESULTS

L. plantarum AR113 Administration Increased Hepatocyte Proliferation and Accelerated Liver Regeneration of 70% Partial Hepatectomy Rats

In order to investigate the effect of *L. plantarum* AR113 administration on liver regeneration, hepatocyte proliferation and hepatic regeneration rate were analyzed. The proliferation of hepatocytes at different groups after two-thirds PHx was evaluated in rats by Ki67 staining. Remarkably, pretreatment with *L. plantarum* AR113 before PHx significantly increased the cell proliferation rate compared with the PHx group at 3 days after PHx (**Supplementary Table 1**). Because the proliferation of liver cells occurs within 3 days after surgery, there was no significant difference in cell proliferation rates between the PHx group and *L. plantarum* AR113 pretreatment group at 7 days after PHx (**Supplementary Table 1**). Therefore, *in vivo* proliferation analyses demonstrated that proliferation of hepatocytes was enhanced in the presence of *L. plantarum* AR113 administration.

Rats were sacrificed 3 and 7 days after PHx and their livers were collected and analyzed. Intriguingly, **Table 1** shows that *L. plantarum* AR113 pretreatment can significantly reduce rat mortality during PHx. In addition, we also found that hepatic regeneration rate in *L. plantarum* AR113 pretreatment rats was significantly accelerated compared to PHx rats at 7 days after PHx, but there was no significant difference in the hepatic regeneration rate between these two groups at 3 days after PHx, suggesting that it takes a long time for probiotics to promote liver regeneration.

[1]www.Metaboanalyst.ca

TABLE 1 | The hepatic regeneration rate and rat mortality after PHx.

	Hepatic regeneration rate		Rat mortality (%)
	3 days after PHx	7 days after PHx	
PHx	45.5% ± 0.57^a	58.2% ± 0.83^b	40%
AR113+PHx	46.49% ± 1.09^a	67.72% ± 1.37^a	25%
PHx+AR113	40.32% ± 0.65^b	62.51% ± 0.98^a	35%

Different letters indicate significant differences, $P < 0.05$ (ANOVA followed by Tukey's HSD test).

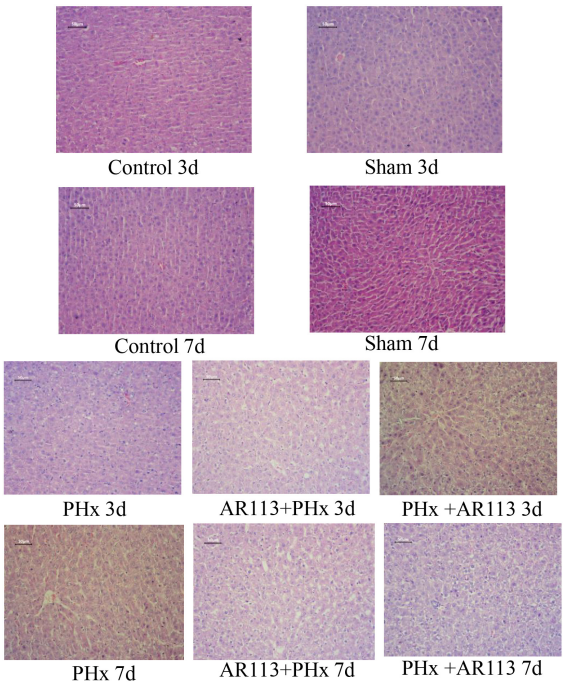

FIGURE 1 | H&E staining 3 and 7 days after PHx of the liver tissue sections of Control, Sham, PHx, AR113+PHx, and PHx+AR113 groups. Scale bar = 50 μm for H&E.

Effect of *L. plantarum* AR113 Administration on Liver Histological Changes

The liver H&E staining results of the rats in all groups are presented in **Figure 1**. In the Control and Sham groups, the liver showed a normal structure with well-preserved cell morphology and a prominent nucleus. After PHx, the liver structure showed crypt structure atrophy, mucosal epithelium impairment, and decreased goblet cells. However, the histological changes were reversed by *L. plantarum* AR113 administrations, evidenced by a loss of swollen hepatocytes, cytoplasmic vacuolization, and fat vacuoles.

Effect of *L. plantarum* AR113 Administration on Liver Function, Cytokines, and Growth Factors

In order to investigate the effect of *L. plantarum* AR113 administration on liver function, the contention of ALT, AST, TP, ALB II, TBil-V, and Glo II were detected. Compared with Control and Sham groups, the ALT, AST, and TBil-V levels in PHx rats

were significantly increased and ALB II, Glo II, and TP were significantly decreased. Serum ALT, AST, and TBil-V levels were rapidly elevated at Day 3 after PHx (**Supplementary Figure 1**), and declined at Day 7 after PHx (**Supplementary Figure 2**). In contrast, serum ALB II, Glo II, and TP were decreased sharply at Day 3 after PHx (**Supplementary Figure 1**), and could increase at Day 7 after PHx (**Supplementary Figure 2**). *L. plantarum* AR113 administration had no significant effect on liver function (**Supplementary Figure 2**).

Cytokines and growth factors have prominent roles in liver regeneration. Serum cytokine and growth factors at 3 days after PHx levels are shown in **Figure 2**. Compared with the PHx group at 3 days after PHx, TNF-α and HGF were significantly increased by AR113 pretreatment, while TGF-β and IL-6 did not change significantly. At 7 days after PHx, TNF-α, IL-6 and TGF-β were significantly increased by AR113 pretreatment compared with PHx group (**Figure 3**). Interestingly, there was no significant difference in the expression levels of TNF-α, HGF and TGF-β between the PHx group and the PHx+AR113 group.

Effect of *L. plantarum* AR113 Administration on Microbial Communities

To elucidate the effects of *L. plantarum* AR113 administration on microbial communities, analysis of the 16S rRNA gene sequences of Control, Sham, PHx, AR113+PHx, and PHx+AR113 groups at Day 3 and Day 7 after PHx was conducted. Sequencing of 16S bacterial RNA retrieved an overall number of 38,155∼41,957 reads, 26,774∼37,361 after filtering, which were clustered in 1,329 operational taxonomic units (OTUs).

Alpha diversity (Shannon and Simpson index) analysis showed that at Day 3 after PHx, the Shannon index of the Control group was significantly higher than that of the Sham, PHx, and AR113+PHx groups (**Supplementary Figure 3**), but had no significant difference as compared with PHx+AR113. However, there was no significant difference in alpha diversity between the Sham, PHx, AR113+PHx, and PHx+AR113 groups. At Day 7 after PHx, there were no significant differences in alpha diversity between groups, suggesting that the reduced diversity of microbial communities associated with PHx had returned to normal levels (**Supplementary Figure 4**).

Remarkable changes in the microbiota community structure were induced by PHx intervention. The microbes in the Control and Sham groups were more closely clustered relative to PHx and AR113+PHx groups, which is an indication that PHx surgery induced similar microbial composition changes. Distinct changes in microbiota composition have revealed a clear separation between no PHx groups (Control and Sham) and PHx groups (PHx, AR113+PHx, and PHx+AR113) after PHx at Days 3 and 7 (**Supplementary Figure 5**). *L. plantarum* AR113 treatment induced significant changes

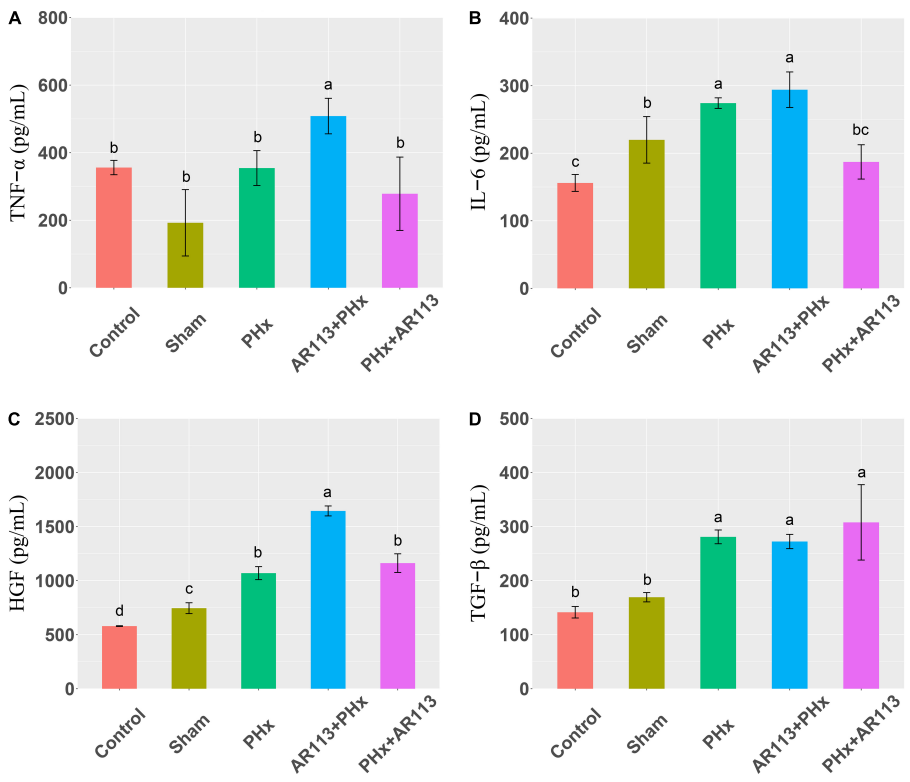

FIGURE 2 | Cytokines and growth factors at 3 days after PHx among the Control, Sham, PHx, AR113+PHx, and PHx+AR113 groups. **(A)** Changes in TNF-α levels; **(B)** Changes in IL-6 levels; **(C)** Changes in HGF levels; **(D)** Changes in HGF-β levels. Different letters indicate significant differences, $P < 0.05$ (ANOVA followed by Tukey's HSD test).

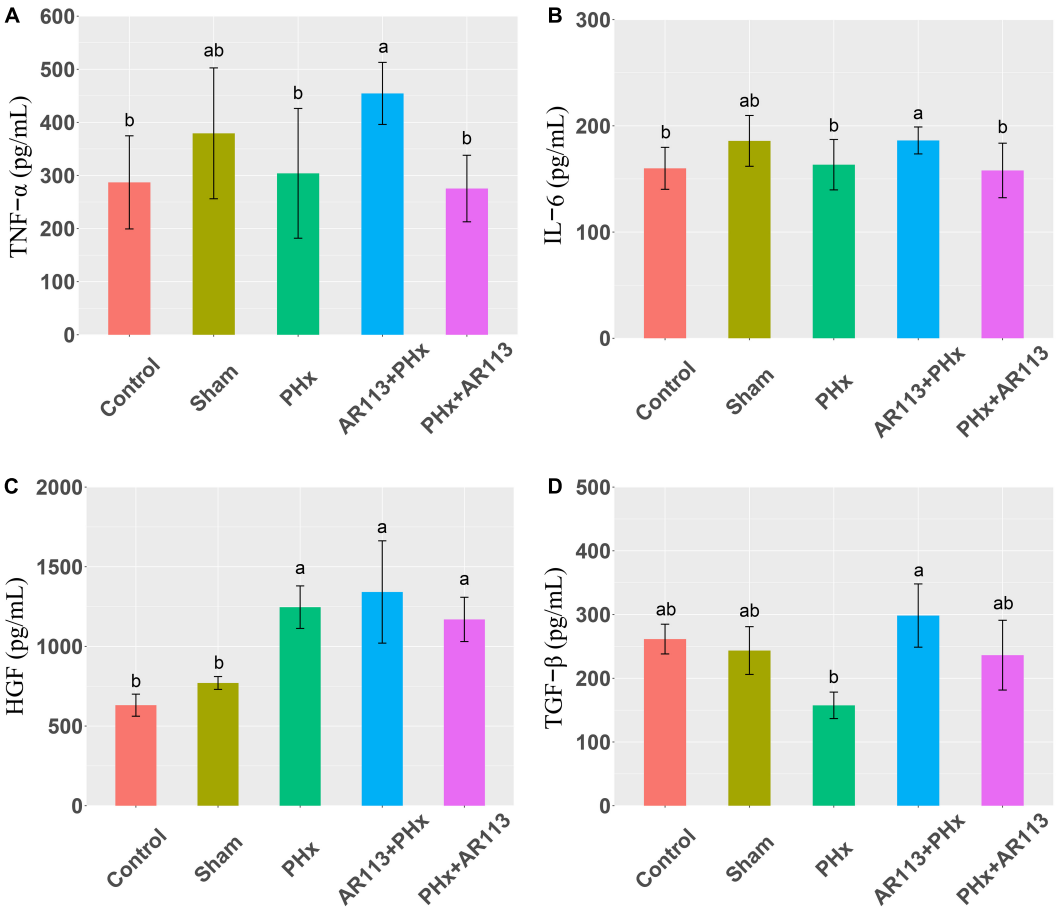

FIGURE 3 | Cytokines and growth factors at 7 days after PHx among the Control, Sham, PHx, AR113+PHx, and PHx+AR113 groups. **(A)** Changes in TNF-α levels; **(B)** Changes in IL-6 levels; **(C)** Changes in HGF levels; **(D)** Changes in HGF-β levels. Different letters indicate significant differences, $P < 0.05$ (ANOVA followed by Tukey's HSD test).

in the gut microbial community. At the phylum level, Firmicutes and Bacteroidetes are two major phyla of the domain bacteria in gut microbiota (**Figure 4**). The abundances of Firmicutes and Bacteroidetes were increased in PHx groups (PHx, AR113+PHx, and PHx+AR113 groups). The Firmicutes-to-Bacteroidetes ratio was calculated, and the results showed that the F/B ratio was elevated in the PHx and PHx+AR113 as compared with the AR113+PHx groups (**Figure 5**). Proteobacteria abundance in AR113+ PHx and Sham groups was not significantly different but decreased in both PHx and PHx+AR113 groups.

At the genus level, the abundance of *Lactobacillus* and *Bacteroides* from *L. plantarum* AR113 administration groups was higher than that of PHx and Sham groups (**Figure 6**). The abundance of *Lachnospiraceae_NK4A136_group* was increased after PHx, which may be related to liver resection. In each genus of Bacteroidetes, the abundance of *Prevotellaceae_Ga6A1_group* has the highest abundance in the AR113+PHx group. In PHx groups (PHx, AR113+PHx, and PHx+AR113), the abundance of the *Prevotella_9* genus was significantly higher than in the Sham group, while the abundance of *Helicobacter* of Proteobacteria in the Sham group was significantly higher than that in the other three groups.

We used the LEfSe analysis to identify the specific bacteria phylotypes that were differentially altered among the five groups, the LEfSe algorithm with a logarithmic LDA score cutoff ≥3.0 was then performed (**Figure 7** and **Supplementary Tables 2**, **3**). Three days after PHx, the most differentially abundant gut microbiota in group PHx were *Prevotella_9*, *Faecalibaculum*, *Dehalococcoidia*, and *661239*. The gut microbiota enriched in the AR113 administration group (AR113+PHx and PHx+AR113) were *Ruminococcus_torques_group*, *Bacteroidaceae*, *Bacteroides*, *Coprococcus_2*, *Ruminiclostridium_9*, *Ruminococcaceae_UCG_004*, *Ambiguous_taxa*, *Prevotellaceae_Ga6A1_group*, *Tannerellaceae*, *Parabacteroides*, *Mogibacterium*, and *Atopobium*. Seven days after PHx, the most differentially abundant gut microbiota in group PHx were *Clostridia*, *Clostridiales*, *Lachnospiraceae*, *Roseburia*, *Marinifilaceae*, *Oscillibacter*, *Butyricimonas*, *uncultured*, *Lachnospiraceae_UGG_001*, *PLTA13*, *Micrococcaceae*, *Ambiguous_taxa*, and *Odoribacter*. The gut microbiota enriched in the *L. plantarum* AR113 administration group were *Prevotella_1*, *Eubacterium_xylanophilum_group*,

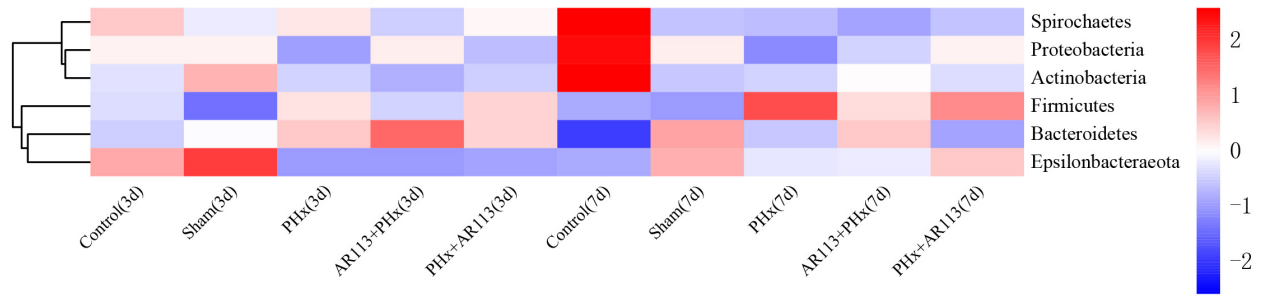

FIGURE 4 | Distribution of relative abundance at the phylum level among Control, Sham, PHx3, AR113+PHx3, and PHx3+ AR113 groups.

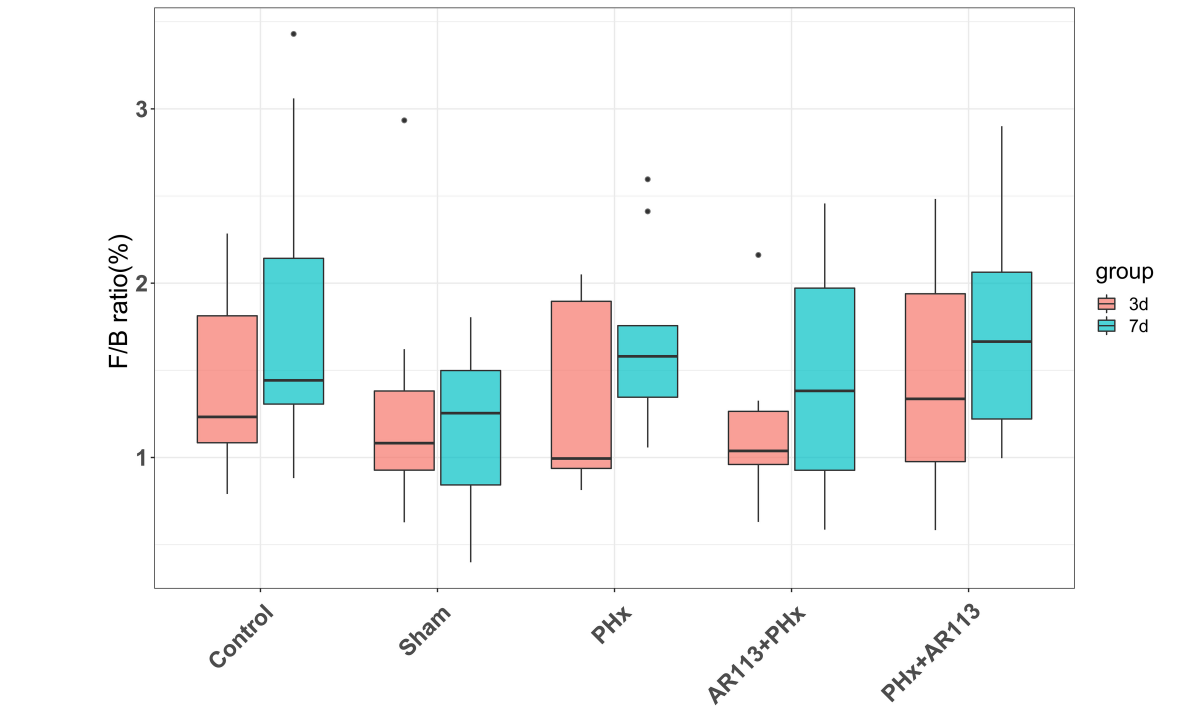

FIGURE 5 | The Firmicutes-to-Bacteroidetes ratio (F/B) of Control, Sham, PHx, AR113+PHx, and PHx+AR113 groups.

Thermotunica, *Roseiarcus*, *Vagococcus*, and *Ruminiclostridium_5*. These results suggest that administration of probiotics can significantly alter the composition of gut microbiota after PHx.

Effect of *L. plantarum* AR113 Administration on Overall Plasma Metabolite Content

The metabolic profiles were acquired using LC–MS/MS, and 4297 metabolites were identified. Then, multivariate analysis was conducted after data normalization. OPLS-DA model between the PHx and AR113+PHx groups at Day 3 and Day 7 was established and differentially abundant metabolites were derived from this model with a VIP $>$ 1 and a P-value $<$ 0.05. There were 68 and 74 differentially expressed metabolites identified between the PHx and AR113+PHx groups at Day 3 and Day 7, respectively. Ultimately, 17 metabolites differentially expressed both in Day 3 and Day 7 were selected (**Table 2**). Of these metabolites, L-isoleucine, L-leucine, 3-O-Methylniveusin A, piperidine, PA(22:0/a-25:0), PI(20:3(5Z,8Z,11Z)/20:3(8Z,11Z,14Z), and mevalonic acid showed an increase in the AR113+PHx group compared with the PHx group. 1-Arachidonoylglycerophosphoinositol, palmitic amide, 1-(6-[3]-ladderane-hexanoyl)-2-(8-[3]-ladderane-octanyl)-sn-glycerophosphoethanolamine, 7-oxo-8-amino-nonanoic acid, and 5S-HETE di-endoperoxide showed a decrease in the PHx group.

We also compared the plasma metabolite changes between the PHx and PHx+AR113 groups. There were 135 and 115 differentially expressed metabolites identified between the PHx and PHx+AR113 groups at Day 3 and Day 7, respectively. There were 26 metabolites differentially expressed

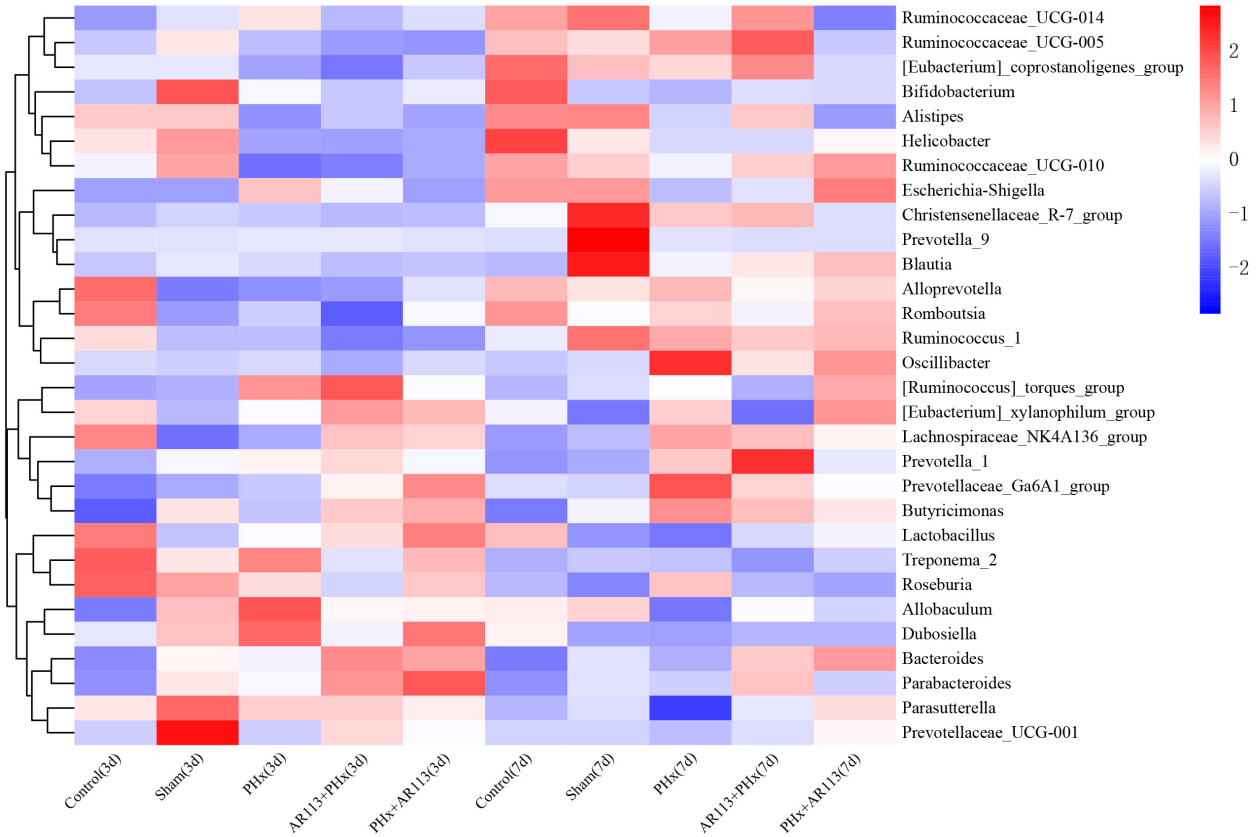

FIGURE 6 | Distribution of relative abundance at the genus level among Control, Sham, PHx3, AR113+PHx3, and PHx3+ AR113 groups.

both in Day 3 and Day 7 (**Table 3**). The probiotic group showed greater reductions in 4-phosphopantothenoylcysteine, chrycorin, PI(20:3(5Z,8Z,11Z)/20:3(8Z,11Z,14Z)), PI(20:4(5Z,8Z,11Z,14Z)/18:0), PC(22:4(7Z,10Z,13Z,16Z)/22:6(4Z,7Z,10Z,13Z,16Z,19Z)), PC(22:6(4Z,7Z,10Z,13Z,16Z,19Z)/22:4(7Z,10Z,13Z,16Z)), 1-Oleoylglycerophosphoserine, and 1-(2-methoxy-6Z-heptadecenyl)-sn-glycero-3-phosphoserine. In contrast, PE(P-16:0/0:0), sphinganine 1-phosphate, mevalonic acid, PE(18:1(9Z)/0:0), LysoPE(18:2(9Z,12Z)/0:0), LysoPE(20:4(5Z,8Z,11Z,14Z)/0:0), LysoPE(0:0/20:4(5Z,8Z,11Z,14Z)), L-leucine, and L-isoleucine were upregulated in the PHx+AR113 group compared with the PHx group.

Effect of *L. plantarum* AR113 Administration on Metabolic Pathways

The differential expressed metabolites between PHx and AR113+PHx groups or PHx and PHx+AR113 groups were mapped to the KEGG database[2] for metabolic pathway construction (**Figure 8**). Intriguingly, the differentially expressed metabolites between PHx and AR113+PHx groups were mainly associated with protein digestion and absorption, choline metabolism in cancer, glycerophospholipid metabolism, leucine (Leu) and isoleucine (Ile) biosynthesis, valine (Val), Leu and leucine degradation, and mineral absorption pathways. Besides, Val, Leu, and Ile biosynthesis, Val, Leu, and Ile degradation, protein digestion and absorption, mineral absorption, central carbon metabolism in cancer, and biosynthesis of amino acids were differentially expressed between PHx and PHx+AR113 groups. These results indicated that *L. plantarum* AR113 administration accelerated liver regeneration accompanied by a series of changes in metabolism, especially Leu and Ile biosynthesis, Val, Leu, and Ile degradation, and mineral absorption pathways.

In addition, the differentially expressed metabolites pathways between pre-probiotic (AR113+PHx) and post-probiotic (PHx+AR113) treatment groups were also discussed. It was found that different ways of probiotics administration can affect choline metabolism in cancer, glycerophospholipid metabolism, retrograde endocannabinoid signaling, sphingolipid metabolism, glycosylphosphatidylinositol (GPI)-anchor biosynthesis, autophagy, and arachidonic acid (ARA) metabolism pathways.

The Correlation Between Gut Microbiome and Plasma Metabolome

The correlations of the discriminative gut microbiome and differential plasma metabolites from Control, Sham, PHx, AR113+PHx, and PHx+AR113 were determined

[2]http://www.genome.jp/kegg/

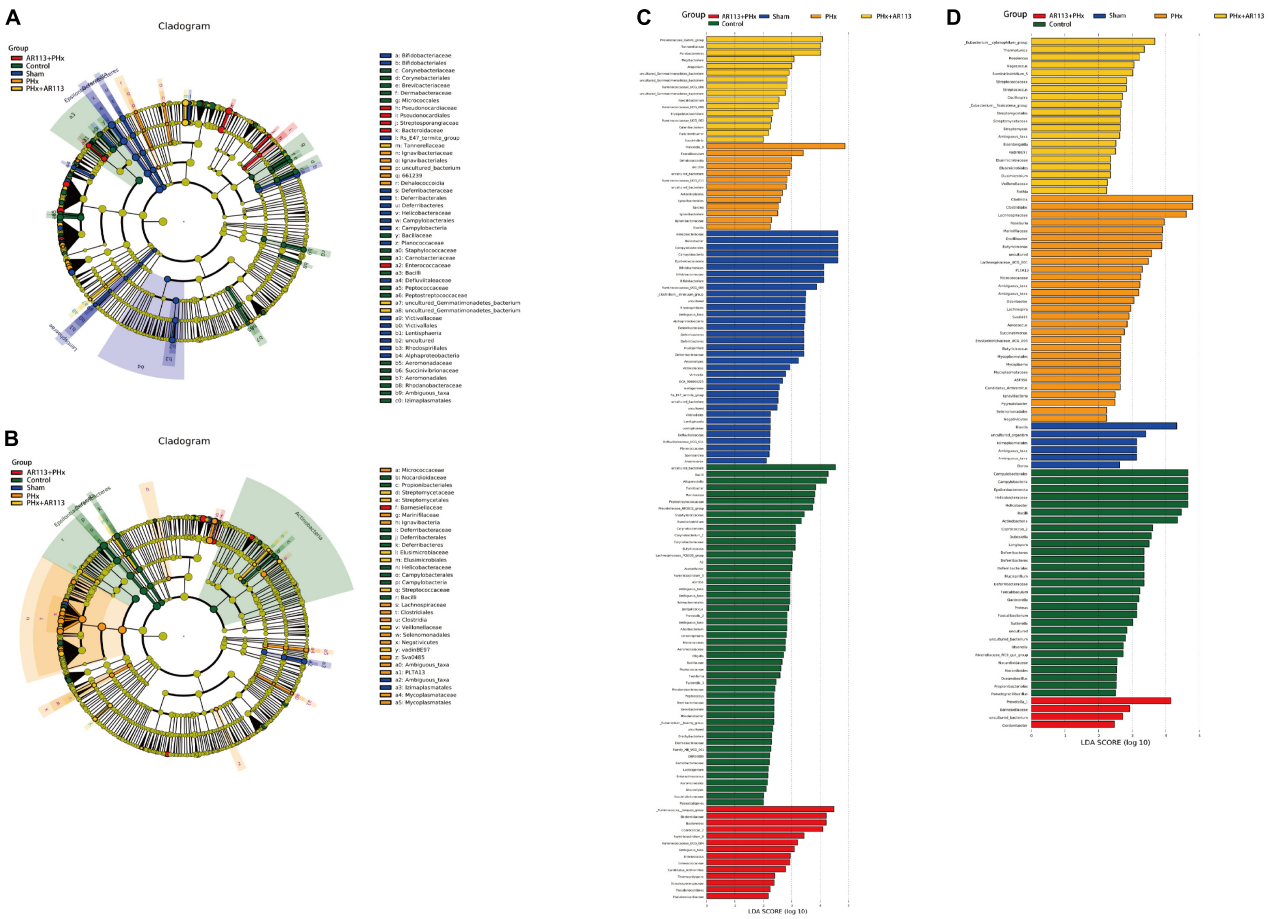

FIGURE 7 | LEfSe analysis among the Control, Sham, PHx, AR113+PHx, and PHx+AR113 groups. Cladogram displays the taxonomic tree of differentially abundant taxa. Histograms represent the LDA scores of bacteria with significant differential abundance between the compared groups, identified by different colors. Features with LDA score ≥ 3. **(A,C)**, 3 days after PHx. **(B,D)**, 7 days after PHx.

using Spearman's rank correlation analysis (**Figure 9**). Taking the correlation analysis of glycerolipids and gut microbiome as an example, the results showed that the relative abundances of *Helicobacter*, *Ruminococcus,* and *Ruminococcaceae* were negatively correlated with serum levels of LysoPE and PE in serum. In contrast, the abundance of *Lactobacillus*, *Allobaculum*, *Dubosiella*, *Prevotella*, *Roseburia*, *Butyricimonas*, *Parabacteroides*, and *Bacteroides* was positively correlated with the circulating levels of LysoPE and PE. In addition, we found PC(18:1(11Z)/18:1(11Z)), PC(22:6(4Z,7Z,10Z,13Z,16Z,19Z)/22:4(7Z,10Z,13Z,16Z), PC(22:4(7Z,10Z,13Z,16Z)/22:6(4Z,7Z,10Z,13Z,16Z,19Z)), LysoPC(20:4(8Z,11Z,14Z,17Z)), and PC(20:4(8Z,11Z,14Z,17Z)/0:0) exhibited positive correlations with *Helicobacter*, *Ruminococcus*, *Alistipes*, and *Ruminococcaceae* and negative correlations with *Lactobacillus*, *Allobaculum*, *Dubosiella*, *Bifidobacterium*, *Prevotella_9*, *Butyricimonas*, *Prevotella_1*, *[Eubacterium]_xylanophilum_group*, *[Ruminococcus]_torques_group*, *Parabacteroides*, *Bacteroides*, and *Prevotellaceae_Ga6A1_group*. Notably, PC(22:5(4Z,7Z,10Z,13Z,16Z)/0:0), PC(22:6-(4Z,7Z,10Z,13Z,16Z,19Z)/22:4(7Z,10Z,13Z,16Z)), LysoPC(22:6(4Z,7Z,10Z,13Z,16Z,19Z)), and LysoPC(18:1(11Z)) were positively correlated with *Prevotella_9*, *Treponema_2*, *Roseburia*, *Dubosiella*, and *Lactobacillus* and negatively correlated with *Escherichia–Shigella*, *Ruminococcaceae_UCG–014*, others, and *Allobaculum*. Together, these data suggested that some species of gut microbial species may modulate the levels of glycerophospholipid that are correlated with liver regeneration.

DISCUSSION

The crosstalk between the gut and liver make probiotics play an important role in the progression of liver diseases (Shavandi et al., 2020). Many studies have demonstrated the beneficial effects of probiotics on the modulation of alcohol-induced liver injury, D-galactosamine-induced rat liver injury, and chronic liver disease patients (Nardone et al., 2010). However, to the best of our knowledge, few studies have focused on its effect on liver regeneration. In our research, pretreatment with *L. plantarum* AR113 was found to have increased hepatocyte proliferation and

TABLE 2 | Summary of the differentially expressed metabolites between PHx and AR113+PHx groups.

m/z	Ion mode	Metabolites	VIP	*P*-value	FC
132.10171	Pos	L-Isoleucine	3.10	3.0952	0.77
203.08349	Neg	Phenylalanyl-Glycine	3.95	0.0218	0.80
130.08765	Neg	L-Leucine	1.99	0.0017	0.73
881.19349	Pos	[Gallocatechin(4alpha->8)]2catechin	1.50	0.0009	0.44
881.44495	Pos	1-[2,4-dihydroxy-5-(3-methylbut-2-en-1-yl)phenyl]-2-hydroxy-3-[4-hydroxy-3-methoxy-5-(3-methylbut-2-en-1-yl)phenyl]propan-1-one	1.70	0.0006	0.46
403.23215	Pos	5S-HETE di-endoperoxide	2.30	0.0000	32.63
186.11375	Neg	7-oxo-8-amino-nonanoic acid	2.57	0.0004	2.81
129.05583	Neg	Mevalonic acid	1.35	0.0255	0.69
256.26275	Pos	Palmitic amide	4.28	0.0264	1.69
881.6963	Pos	PA(22:0/a-25:0)	1.61	0.0005	0.46
763.53652	Pos	1-(6-[3]-ladderane-hexanoyl)-2-(8-[3]-ladderane-octanyl)-sn-glycerophosphoethanolamine	1.75	0.0001	1.86
619.28723	Neg	1-Arachidonoylglycerophosphoinositol	1.94	0.0005	1.53
909.54695	Neg	PI(20:3(5Z,8Z,11Z)/20:3(8Z,11Z,14Z))	1.98	0.0185	0.68
254.17573	Neg	Labienoxime	1.29	0.0000	0.34
407.17245	Neg	3-O-Methylniveusin A	2.58	0.0176	0.70
146.05992	Pos	4-formyl Indole	1.39	0.0074	0.82
86.096214	Pos	Piperidine	2.73	0.0054	0.77

Pos, positive ion mode; Neg, negative ion mode.

accelerated liver regeneration of PHx rats. The beneficial effects of *L. plantarum* AR113 were associated with increased hepatocyte proliferation, improved liver function, and modulation of gut microbiome and plasma metabolome.

It has been reported that although liver regeneration results ultimately in restoration of liver mass and function, partial hepatectomy is primarily a compensatory hyperplasia (Michalopoulos and Bhushan, 2021). To evaluate the degree of liver injury after 70% partial hepatectomy, liver function was examined. Previous research showed that serum ALT and AST activity increased rapidly and significantly after 70% partial hepatectomy on Day 1 and returned almost to pre-operative levels after 2–3 days in control rats (Yu et al., 2018). Not surprisingly, our study found that *L. plantarum* AR113 administration does not reduce serum ALT and AST activity and ALB II after PHx at Day 3 and Day 7. This is because local inflammatory reactions may occur in response to damage around the ligated area of the liver, resulting in transient increases in serum ALT and AST activity.

Cytokines such as TNF-α, IL-6, HGF, TGF-β, and TNF-α and the activation of NF-κB by cytokines were shown to be required for the initiation of liver regeneration. Several lines of evidence suggest that TNF-α and IL-6 are among the most crucial components of the early signaling pathways leading to regeneration (Fathi et al., 2021). In the liver, IL-6 is secreted by Kupffer cells, and this secretion is stimulated by TNF-α (Jin et al., 2021). HGF is a 97-kd protein that was originally isolated from the peripheral blood of animals after PHx, which is known to be essential to initiate the process of liver regeneration (Gao and Peng, 2021); it could rapidly be elevated by 10- to 20-fold at the early stage of liver injury (Shi and Line, 2020). Present study showed that *L. plantarum* AR113 given two weeks before PHx significantly increased the expression of TNF-α after PHx. but giving probiotics after PHx did not achieve the same effect. In addition, we found that TGF-β was increased in AR113+ PHx group at day 7 after PHx. TGF-β is produced principally in the hepatic stellate cells, and is a representative mitoinhibitory factor, which presumably induces the termination of liver regeneration (Masuda et al., 2020). Our study showed that whether probiotics are given before or after PHx will affect the expression of cytokine expression level.

Accumulating evidence has indicated that the gut microbiome is involved in the pathogenesis of liver diseases by influencing the host's immunity and metabolism (Lederer et al., 2017). Firmicutes and Bacteroidetes are the two most dominant bacterial phyla affecting host energy extraction efficiency and linked with excess adiposity (Behari et al., 2021). In the present study, *Lactobacillus*, *Lachnospiraceae_NK4A136*, *Ruminococcus_1,* and *[Ruminococcus]_torques* which were affected by *L. plantarum* AR113 administration belong to Firmicutes. *Prevotella_9*, *Bacteroides*, *Alloprevotella*, *Prevotellaceae_Ga6A1_group,* and *Butyricimonas* belong to Bacteroidetes. Some studies have used the ratio of the two dominant phyla (Firmicutes and Bacteroidetes) as a marker for microbial dysbiosis (Jasirwan et al., 2021). Changes in this ratio have also been found in several metabolic disorders. Our study showed that the F/B ratio in the AR113+PHx group was the lowest among all the groups, suggesting that *L. plantarum* AR113 given 2 weeks before PHx could change the microbiome composition. The depletion of genera *Alloprevotella* and *Prevotella* can contribute

TABLE 3 | Summary of the differentially expressed metabolites between PHx and PHx+ AR113 groups.

m/z	Ion mode	Metabolites	VIP	*P*-value	FC
132.10171	Pos	L-Isoleucine	3.38	0.0014	0.75
130.08765	Neg	L-Leucine	2.28	0.0083	0.70
552.27106	Neg	Vignatic acid A	3.58	0.0000	3.18
355.06781	Pos	6-[5-(2-carboxyeth-1-en-1-yl)-2,3-dihydroxyphenoxy]-3,4,5-trihydroxyoxane-2-carboxylic acid	3.87	0.0000	1.79
403.23215	Pos	5S-HETE di-endoperoxide	2.28	0.0000	21.29
186.11375	Neg	7-oxo-8-amino-nonanoic acid	2.85	0.0003	3.31
129.05583	Neg	Mevalonic acid	1.87	0.0035	0.56
506.32298	Neg	PC(17:1(10Z)/0:0)	1.33	0.0280	0.89
904.58372	Pos	PC(22:6(4Z,7Z,10Z,13Z,16Z,19Z)/22:4(7Z,10Z,13Z,16Z))	3.28	0.0004	1.99
904.5835	Pos	PC(22:4(7Z,10Z,13Z,16Z)/22:6(4Z,7Z,10Z,13Z,16Z,19Z))	1.83	0.0000	1.94
478.29196	Pos	LysoPE(18:2(9Z,12Z)/0:0)	2.93	0.0433	0.67
500.277	Neg	LysoPE(20:4(5Z,8Z,11Z,14Z)/0:0)	3.30	0.0276	0.69
438.29619	Pos	PE(P-16:0/0:0)	2.83	0.0200	0.51
500.27645	Neg	LysoPE(0:0/20:4(5Z,8Z,11Z,14Z))	1.48	0.0211	0.71
763.53652	Pos	1-(6-[3]-ladderane-hexanoyl)-2-(8-[3]-ladderane-octanyl)-sn-glycerophosphoethanolamine	1.20	0.0096	1.47
885.54815	Neg	PI(20:4(5Z,8Z,11Z,14Z)/18:0)	7.30	0.0163	1.63
909.54695	Neg	PI(20:3(5Z,8Z,11Z)/20:3(8Z,11Z,14Z))	1.29	0.0389	1.46
504.27176	Neg	1-Oleoylglycerophosphoserine	4.20	0.0000	2.42
506.28682	Neg	1-(2-methoxy-6Z-heptadecenyl)-sn-glycero-3-phosphoserine	3.08	0.0000	2.73
401.07701	Neg	4-Phosphopantothenoylcysteine	2.24	0.0463	1.39
380.25588	Neg	Sphinganine 1-phosphate	2.53	0.0277	0.55
466.33424	Pos	1alpha,25-dihydroxy-24a-homo-22-thiavitamin D3/1alpha,25-dihydroxy-24a-homo-22-thiacholecalciferol	2.23	0.0200	0.61
480.30672	Pos	PE(18:1(9Z)/0:0)	3.11	0.0143	0.61
72.080461	Pos	Pyrrolidine	2.24	0.0008	0.59
86.096214	Pos	Piperidine	3.04	0.0006	0.74
201.03839	Neg	Chrycorin	3.05	0.0007	1.42

Pos, positive ion mode; Neg, negative ion mode.

to non-alcoholic fatty liver disease and microbiome dysbiosis (Safari and Gerard, 2019). In addition, genus *Prevotella* is considered beneficial for promoting hepatic glycogen storage and improving glucose metabolism (Monga Kravetz et al., 2020). We found the expression level of *Prevotella* was decreased after AR113 administration while *Alloprevotella* was increased. Meanwhile, the overgrowth of *Ruminococcus* may lead to metabolic dysfunction and aggravation of liver injury. The genus *Ruminococcus* is considered a gut microbiota signature of non-alcoholic fatty liver disease and was positively correlated with the levels of ALT, AST, TBil-V, and TBA (Demir et al., 2020). Our study found the expression level of *Prevotella* was decreased after AR113 administration. Besides, the colonization of *L. plantarum* AR113 enriched the normal gut microbiota, especially *Lactobacillus*, which can ferment nutrients into lactic acid and benefit health. The decrease in potential pathogens and restoration of the normal gut microbiota by *L. plantarum* AR113 might improve host metabolism and accelerate liver regeneration.

Branched chain amino acids, including Leu, Ile, and Val, play critical roles in regulating metabolism of glucose, lipid, protein synthesis, intestinal health, and immunity (Hernandez-Conde et al., 2021). We found L-leucine and L-isoleucine were up regulated in the *L. plantarum* AR113 administration group compared with the PHx group. Leu was reported to have a proliferative effect on hepatocyte, suggesting that *L. plantarum* AR113 may promote liver regeneration by up-regulating serum Leu. Thus far, the effects of Ile on liver regeneration were limited.

Except for branched chain amino acids, our study also found that *L. plantarum* AR113 administration had an effect on glycerophospholipid metabolism that was evidenced by altered serum levels of glycerophosphoinositol (PIs), PCs, LysoPC, and PEs which are the fundamental components of lipid bilayers of cell membranes. Phospholipids, including PEs, PCs, glycerophosphoserines (PSs), glycerophosphoglycerols (PGs), and CLs, are the prominent membrane lipids (Xie et al., 2016). PIs were ubiquitous components of eukaryotic cells that participate in cell proliferation and survival. It was reported that liver regeneration was characterized by increases in PE, and decreases in glycerophosphoethanolamine (GPE) and glycerophosphocholine (GPC) (Zakian et al., 2005). Indeed, PHx caused a transient and reversible accumulation

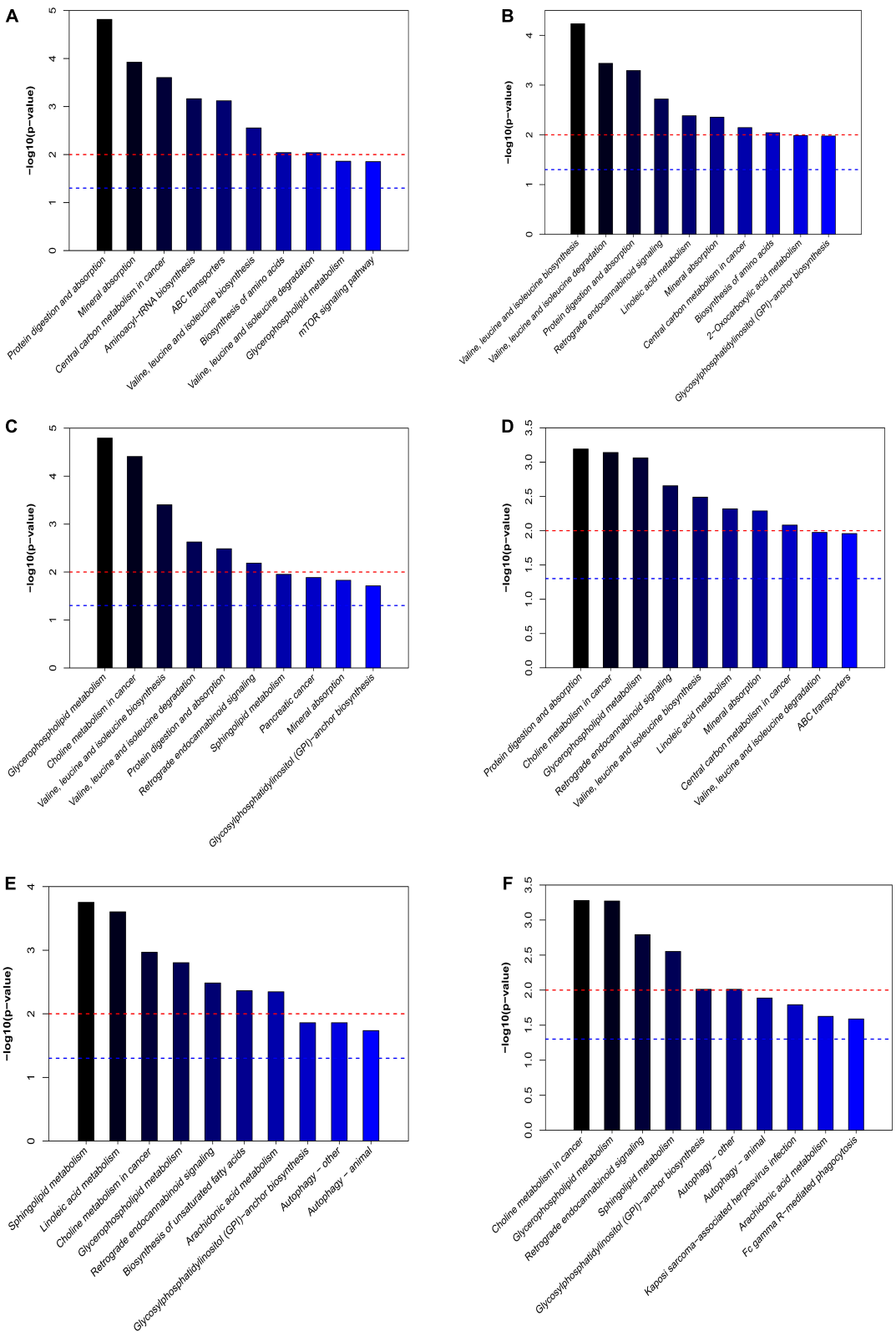

FIGURE 8 | The differentially expressed metabolic pathways among the PHx, AR113+PHx, PHx+AR113 groups of 3 or 7 days after PHx. **(A)** PHx and AR113+PHx groups of 3 days after PHx; **(B)** PHx and AR113+PHx groups of 7 days after PHx; **(C)** PHx and PHx+AR113 groups of 3 days after PHx; **(D)** PHx and PHx+AR113 groups of 7 days after PHx; **(E)** AR113+PHx and PHx+AR113 groups of 3 days after PHx; **(F)** AR113+PHx and PHx+AR113 groups of 7 days after PHx.

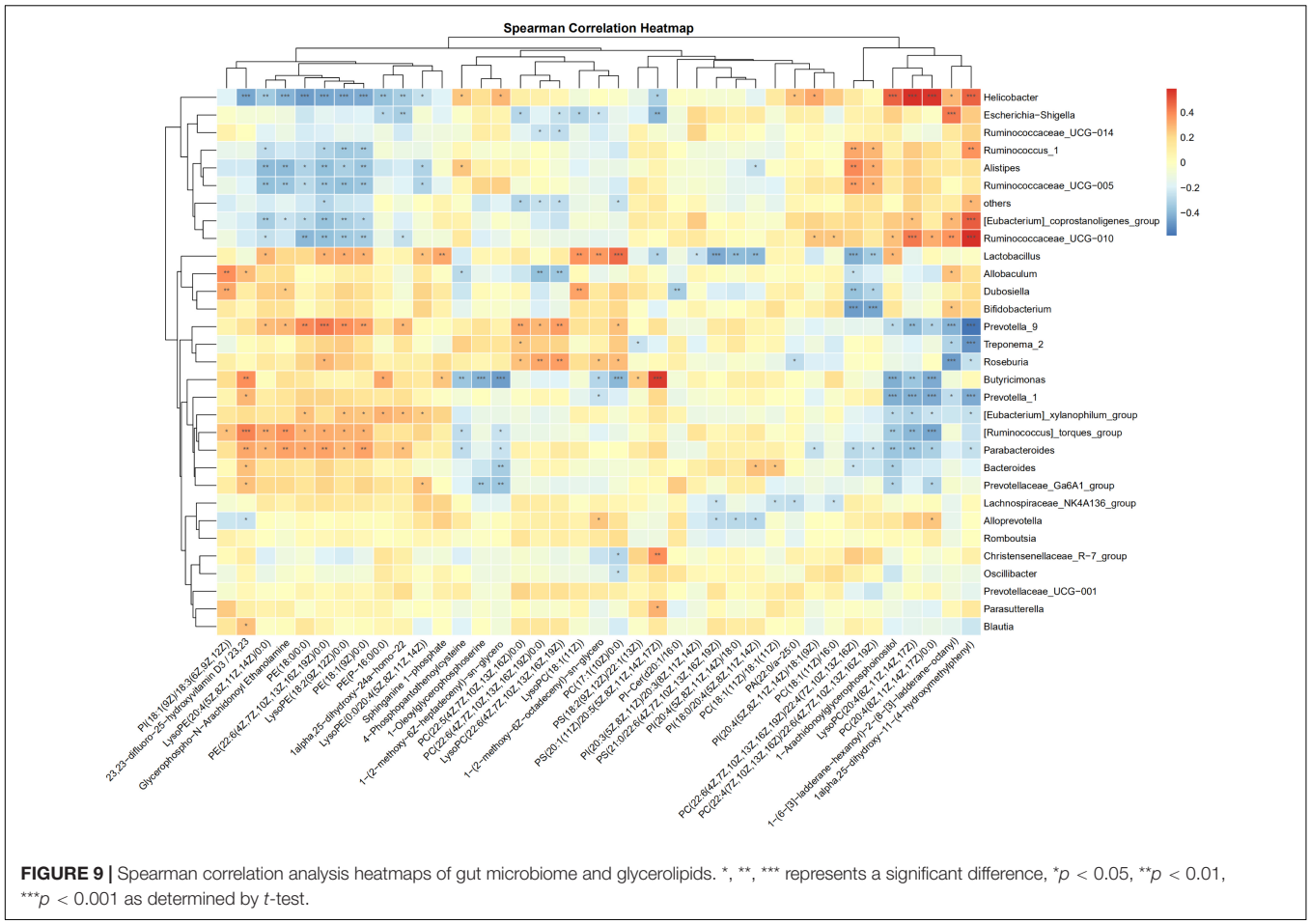

FIGURE 9 | Spearman correlation analysis heatmaps of gut microbiome and glycerolipids. *, **, *** represents a significant difference, $^{*}p < 0.05$, $^{**}p < 0.01$, $^{***}p < 0.001$ as determined by *t*-test.

of phospholipids in the liver at the early phase of liver regeneration. In our study, the probiotic treated group showed greater reductions in PI(20:3(5Z,8Z,11Z)/20:3(8Z,11Z,14Z)), PI(20:4(5Z,8Z,11Z,14Z)/18:0), PC(22:4(7Z,10Z,13Z,16Z)/22:6(4Z,7Z,10Z,13Z,16Z,19Z)), PC(22:6(4Z,7Z,10Z,13Z,16Z,19Z)/22:4(7Z,10Z,13Z,16Z)), 1-Oleoylglycerophosphoserine, and 1-(2-methoxy-6Z-heptadecenyl)-sn-glycero-3-phosphoserine, but had increased concentrations of PE(P-16:0/0:0), sphinganine 1-phosphate, PE(18:1(9Z)/0:0), LysoPE(18:2(9Z,12Z)/0:0), LysoPE(20:4(5Z,8Z,11Z,14Z)/0:0), and LysoPE(0:0/20:4(5Z,8Z,11Z,14Z)). PE is an important lipid marker of inflammation in glycerophospholipid metabolism. An increased concentrations of PE has been detected in systemic circulation of nonalcoholic steatohepatitis patients (Puri et al., 2009). LysoPE has also been shown to play a role in intercellular signaling and in the activation of signaling enzymes (Yanagida and Valentine, 2020), and has been suggested to act through putative G protein-coupled receptors (GPCRs) (Kaluarachchi et al., 2018).

Based on these results, our study found that probiotics intervention can affect the metabolic changes of rats after PHx. More importantly, we also found that *L. plantarum* AR113 administration preoperatively had different effects on liver regeneration rates and metabolites compared with probiotics given postoperatively. Except for the glycerophospholipid metabolism, retrograde endocannabinoid signaling, sphingolipid metabolism, and GPI-anchor biosynthesis pathways, we also found autophagy and ARA metabolism pathways were affected by different ways of probiotics administration. ARA is one of the most abundant polyunsaturated fatty acids present in human tissue and represents one of the pivotal signaling molecules involved in the initiation and propagation of diverse signaling cascades regulating inflammation, pain, and homeostatic function (Turolo et al., 2021). In humans and mammals, ARA has been widely observed to reduce the triacylglycerol (TG) accumulation in liver, plasma, and adipose tissue (Pei et al., 2020). At present, the relationship between ARA and liver regeneration remains unclear. In contrast to ARA metabolism pathways, autophagy was reported to be essential for liver regeneration. Autophagy is a homeostatic mechanism that regulates turnover of long-lived or damaged proteins and organelles and supplies amino acids taken from degradation products of the autolysosome (Xu et al., 2020). To our knowledge, our study first reported that different ways of probiotic administration modulate liver regeneration by affecting autophagy pathways.

Our data showed that LysoPE and PE showed a positive correlation with *Lactobacillus*, *Allobaculum*, *Dubosiella*,

Prevotella, *Roseburia*, *Butyricimonas*, *Parabacteroides*, and *Bacteroides*, but an inverse correlation with *Helicobacter*, *Ruminococcus,* and *Ruminococcaceae*. The opposite correlation pattern suggests that their counterbalancing role in modulating lipid homeostasis is beneficial for liver regeneration. Thus, the constantly changing gut flora acted as an entire system and exerted various functions on host–microbial nutritional utilization throughout the course of the liver regeneration to meet diverse cell proliferation and energy demands during the different biological processes (Macchi and Sadler, 2020).

CONCLUSION

The present study showed that *L. plantarum* AR113 administration increased hepatocyte proliferation and accelerated liver regeneration of PHx rats. Two weeks of *L. plantarum* AR113 before PHx induced decreased F/B ratio. The colonization of *L. plantarum* AR113 enriched the normal gut microbiota, especially *Lactobacillus*. The decrease in potential pathogens and restoration of the normal gut microbiota by *L. plantarum* AR113 might improve host metabolism and accelerated liver regeneration. One of the most profound changes was *L. plantarum* AR113 administration of glycerophospholipid metabolism that was evidenced by decreased serum levels of PI and PCs, and increased LysoPC and PEs. Further investigations will focus on the key metabolites and ultimately clarify the molecular basis for these microbe–host interactions during liver regeneration.

DATA AVAILABILITY STATEMENT

The original contributions presented in the study are included in the article/**Supplementary Material**, further inquiries can be directed to the corresponding author/s.

ETHICS STATEMENT

The animal study was reviewed and approved by the Hunan SJA Laboratory Animal Co., Ltd.

AUTHOR CONTRIBUTIONS

ChuX and ZhoZ conceptualized the study and wrote and prepared the original draft. MY was in charge of the project administration. CC conceptualized the study. YZ and ZuoZ designed the experiments. WG and ChaX supervised the study. LY and ZH wrote the review. LA and YP conceived and supervised the work. All authors contributed to the article and approved the submitted version.

FUNDING

This work was supported by the grant from the Central Public-Interest Scientific Institution Basal Research Fund (no. Y2019XK15), Training Program for Excellent Young Innovators of Changsha (kq 2009089), China Agriculture Research System for Bast and Leaf Fiber Crops (no. CARS-16), and Project of Scientific Elitists in National Agricultural Research and Agricultural Science and Technology Innovation Program of China (CAAS-ASTIP-2021-IBFC).

SUPPLEMENTARY MATERIAL

The Supplementary Material for this article can be found online at: https://www.frontiersin.org/articles/10.3389/fmicb.2021.800470/full#supplementary-material

REFERENCES

Adolph, T. E., Grander, C., Moschen, A. R., and Tilg, H. (2018). Liver-microbiome axis in health and disease. *Trends Immunol.* 39, 712–723. doi: 10.1016/j.it.2018.05.002

Behari, J., Graham, L., Wang, R., Schirda, C., Borhani, A. A., Methe, B. A., et al. (2021). Dynamics of hepatic steatosis resolution and changes in gut microbiome with weight loss in nonalcoholic fatty liver disease. *Obes Sci .Pract.* 7, 217–225. doi: 10.1002/osp4.476

Cassano, M., and Dufour, J. F. (2019). Inflammation and microbiota fingerprint: delphi's oracle for nonalcoholic fatty liver disease-related hepatocellular carcinoma? *Hepatology* 69, 12–15. doi: 10.1002/hep.30267

Chowdhury, M. M. H., Salazar, C. J. J., and Nurunnabi, M. (2021). Recent advances in bionanomaterials for liver cancer diagnosis and treatment. *Biomater Sci.* 9, 4821–4842. doi: 10.1039/d1bm00167a

Cornide-Petronio, M. E., Alvarez-Mercado, A. I., Jimenez-Castro, M. B., and Peralta, C. (2020). Current knowledge about the effect of nutritional status, supplemented nutrition diet, and gut microbiota on hepatic ischemia-reperfusion and regeneration in liver surgery. *Nutrients* 12:284. doi: 10.3390/nu12020284

Crismale, J. F., and Friedman, S. L. (2020). Acute liver injury and decompensated cirrhosis. *Med. Clin. North Am.* 104, 647–662. doi: 10.1016/j.mcna.2020.02.010

Demir, M., Lang, S., Martin, A., Farowski, F., Wisplinghoff, H., Vehreschild, M., et al. (2020). Phenotyping non-alcoholic fatty liver disease by the gut microbiota: ready for prime time? *J. Gastroenterol. Hepatol.* 35, 1969–1977. doi: 10.1111/jgh.15071

Fathi, F., Sanei, B., Ganjalikhani Hakemi, M., Saidi, R. F., and Rezaei, A. (2021). Liver resection promotes (regulates) proinflammatory cytokines in patients with hepatocellular carcinoma. *Can. J. Gastroenterol. Hepatol.* 2021:5593655. doi: 10.1155/2021/5593655

Gao, C., and Peng, J. (2021). All routes lead to rome: multifaceted origin of hepatocytes during liver regeneration. *Cell Regen* 10:2. doi: 10.1186/s13619-020-00063-3

Heinrich, V. R., Kneist, S., and Kunzel, W. (1988). [Limit of the reparative capacity of deciduous dental pulp]. *Zahn Mund Kieferheilkd Zentralbl* 76, 14–21.

Hernandez-Conde, M., Llop, E., Gomez-Pimpollo, L., Fernandez Carrillo, C., Rodriguez, L., Van Den Brule, E., et al. (2021). Adding branched-chain amino acids to an enhanced standard-of-care treatment improves muscle mass of cirrhotic patients with sarcopenia: a placebo-controlled trial. *Am. J. Gastroenterol.* 116, 2241–2249. doi: 10.14309/ajg.0000000000001301

Higgins, G. M., and Anderson, R. M. (1931). Experimental pathology of the liver. I: restoration of the liver of the white rat following partial surgical removal. *Arch. Path. Lab. Med.* 12, 186–202.

Hoffmann, K., Nagel, A. J., Tanabe, K., Fuchs, J., Dehlke, K., Ghamarnejad, O., et al. (2020). Markers of liver regeneration-the role of growth factors and cytokines: a systematic review. *BMC Surg.* 20:31. doi: 10.1186/s12893-019-0664-8

Jasirwan, C. O. M., Muradi, A., Hasan, I., Simadibrata, M., and Rinaldi, I. (2021). Correlation of gut firmicutes/bacteroidetes ratio with fibrosis and steatosis

stratified by body mass index in patients with non-alcoholic fatty liver disease. *Biosci. Microbiota Food Health* 40, 50–58. doi: 10.12938/bmfh.2020-046

Jin, S., Yu, C., and Yu, B. (2021). Changes of serum IL-6, IL-10 and TNF-alpha levels in patients with systemic lupus erythematosus and their clinical value. *Am. J. Transl. Res.* 13, 2867–2874.

Kaluarachchi, M., Boulange, C. L., Karaman, I., Lindon, J. C., Ebbels, T. M. D., Elliott, P., et al. (2018). A comparison of human serum and plasma metabolites using untargeted (1)H NMR spectroscopy and UPLC-MS. *Metabolomics* 14, 32. doi: 10.1007/s11306-018-1332-1

Lederer, A. K., Pisarski, P., Kousoulas, L., Fichtner-Feigl, S., Hess, C., and Huber, R. (2017). Postoperative changes of the microbiome: are surgical complications related to the gut flora? A systematic review. *BMC Surg* 17:125. doi: 10.1186/s12893-017-0325-8

Li, B., Zhang, C., and Zhan, Y. T. (2018). Nonalcoholic fatty liver disease cirrhosis: a review of its epidemiology, risk factors, clinical presentation, diagnosis, management, and prognosis. *Can J. Gastroenterol. Hepatol.* 2018:2784537. doi: 10.1155/2018/2784537

Liu, H. X., Keane, R., Sheng, L., and Wan, Y. J. (2015). Implications of microbiota and bile acid in liver injury and regeneration. *J. Hepatol.* 63, 1502–1510. doi: 10.1016/j.jhep.2015.08.001

Macchi, F., and Sadler, K. C. (2020). Unraveling the epigenetic basis of liver development, regeneration and disease. *Trends Genet.* 36, 587–597. doi: 10.1016/j.tig.2020.05.002

Masuda, A., Nakamura, T., Abe, M., Iwamoto, H., Sakaue, T., Tanaka, T., et al. (2020). Promotion of liver regeneration and antifibrotic effects of the TGFbeta receptor kinase inhibitor galunisertib in CCl4treated mice. *Int. J. Mol. Med.* 46, 427–438. doi: 10.3892/ijmm.2020.4594

Michalopoulos, G. K., and Bhushan, B. (2021). Liver regeneration: biological and pathological mechanisms and implications. *Nat. Rev. Gastroenterol. Hepatol.* 18, 40–55. doi: 10.1038/s41575-020-0342-4

Monga Kravetz, A., Testerman, T., Galuppo, B., Graf, J., Pierpont, B., Siebel, S., et al. (2020). Effect of gut microbiota and PNPLA3 rs738409 variant on nonalcoholic fatty liver disease (NAFLD) in obese youth. *J. Clin. Endocrinol. Metab.* 105:dgaa382. doi: 10.1210/clinem/dgaa382

Nardone, G., Compare, D., Liguori, E., Di Mauro, V., Rocco, A., Barone, M., et al. (2010). Protective effects of lactobacillus paracasei F19 in a rat model of oxidative and metabolic hepatic injury. *Am. J. Physiol. Gastrointest Liver Physiol.* 299, G669–G676. doi: 10.1152/ajpgi.00188.2010

Nishida, A., Inoue, R., Inatomi, O., Bamba, S., Naito, Y., and Andoh, A. (2018). Gut microbiota in the pathogenesis of inflammatory bowel disease. *Clin. J. Gastroenterol.* 11, 1–10. doi: 10.1007/s12328-017-0813-5

Pei, K., Gui, T., Kan, D., Feng, H., Jin, Y., Yang, Y., et al. (2020). An overview of lipid metabolism and nonalcoholic fatty liver disease. *Biomed Res. Int.* 2020:4020249. doi: 10.1155/2020/4020249

Puri, P., Wiest, M. M., Cheung, O., Mirshahi, F., Sargeant, C., Min, H. K., et al. (2009). The plasma lipidomic signature of nonalcoholic steatohepatitis. *Hepatology* 50, 1827–1838. doi: 10.1002/hep.23229

Rodes, L., Saha, S., Tomaro-Duchesneau, C., and Prakash, S. (2014). Microencapsulated bifidobacterium longum subsp. infantis ATCC 15697 favorably modulates gut microbiota and reduces circulating endotoxins in F344 rats. *Biomed Res. Int.* 2014:602832. doi: 10.1155/2014/602832

Safari, Z., and Gerard, P. (2019). The links between the gut microbiome and non-alcoholic fatty liver disease (NAFLD). *Cell Mol. Life Sci.* 76, 1541–1558. doi: 10.1007/s00018-019-03011-w

Seehofer, D., Rayes, N., Schiller, R., Stockmann, M., Muller, A. R., Schirmeier, A., et al. (2004). Probiotics partly reverse increased bacterial translocation after simultaneous liver resection and colonic anastomosis in rats. *J. Surg. Res.* 117, 262–271. doi: 10.1016/j.jss.2003.11.021

Shavandi, A., Saeedi, P., Gerard, P., Jalalvandi, E., Cannella, D., and Bekhit, A. E. (2020). The role of microbiota in tissue repair and regeneration. *J. Tissue Eng. Regen. Med.* 14, 539–555. doi: 10.1002/term.3009

Shi, J. H., and Line, P. D. (2020). Hallmarks of postoperative liver regeneration: an updated insight on the regulatory mechanisms. *J. Gastroenterol Hepatol* 35, 960–966. doi: 10.1111/jgh.14944

Tanemura, A., Mizuno, S., Hayasaki, A., Fujii, T., Iizawa, Y., Kato, H., et al. (2018). Biliary complications during and after donor hepatectomy in living donor liver transplantation focusing on characteristics of biliary leakage and treatment for intraoperative bile duct injury. *Transplant Proc.* 50, 2705–2710. doi: 10.1016/j.transproceed.2018.03.045

Trebicka, J., Bork, P., Krag, A., and Arumugam, M. (2021). Utilizing the gut microbiome in decompensated cirrhosis and acute-on-chronic liver failure. *Nat. Rev. Gastroenterol Hepatol* 18, 167–180. doi: 10.1038/s41575-020-00376-3

Turolo, S., Edefonti, A., Mazzocchi, A., Syren, M. L., Morello, W., Agostoni, C., et al. (2021). Role of arachidonic acid and its metabolites in the biological and clinical manifestations of idiopathic nephrotic syndrome. *Int. J. Mol. Sci.* 22:5452. doi: 10.3390/ijms22115452

Xie, T., Zhou, X., Wang, S., Lu, Y., Zhu, H., Kang, A., et al. (2016). Development and application of a comprehensive lipidomic analysis to investigate tripterygium wilfordii-induced liver injury. *Anal. Bioanal. Chem.* 408, 4341–4355. doi: 10.1007/s00216-016-9533-9

Xu, F., Hua, C., Tautenhahn, H. M., Dirsch, O., and Dahmen, U. (2020). The role of autophagy for the regeneration of the aging liver. *Int. J. Mol. Sci.* 21:3606. doi: 10.3390/ijms21103606

Yagi, S., Hirata, M., Miyachi, Y., and Uemoto, S. (2020). Liver regeneration after hepatectomy and partial liver transplantation. *Int .J. Mol. Sci.* 21:8414. doi: 10.3390/ijms21218414

Yanagida, K., and Valentine, W. J. (2020). Druggable lysophospholipid signaling pathways. *Adv. Exp. Med. Biol.* 1274, 137–176. doi: 10.1007/978-3-030-50621-6_7

Yu, L. H., Yu, W. L., Zhao, T., Wu, M. C., Fu, X. H., and Zhang, Y. J. (2018). Postoperative delayed elevation of ALT correlates with early death in patients with HBV-related hepatocellular carcinoma and post-hepatectomy liver failure. *HPB (Oxford)* 20, 321–326. doi: 10.1016/j.hpb.2017.10.001

Zakian, K. L., Koutcher, J. A., Malhotra, S., Thaler, H., Jarnagin, W., Schwartz, L., et al. (2005). Liver regeneration in humans is characterized by significant changes in cellular phosphorus metabolism: assessment using proton-decoupled 31P-magnetic resonance spectroscopic imaging. *Magn. Reson. Med.* 54, 264–271. doi: 10.1002/mrm.20560

Conflict of Interest: The authors declare that the research was conducted in the absence of any commercial or financial relationships that could be construed as a potential conflict of interest.

Publisher's Note: All claims expressed in this article are solely those of the authors and do not necessarily represent those of their affiliated organizations, or those of the publisher, the editors and the reviewers. Any product that may be evaluated in this article, or claim that may be made by its manufacturer, is not guaranteed or endorsed by the publisher.

frontiers in Microbiology

ORIGINAL RESEARCH
published: 25 January 2022
doi: 10.3389/fmicb.2022.837182

Effects of β-Carotin and Green Tea Powder Diets on Alleviating the Symptoms of Gouty Arthritis and Improving Gut Microbiota in C57BL/6 Mice

Yu Feng[1,2†], Yanbo Yu[3†], Zheng Chen[1,2], Lili Wang[4], Jingyu Ma[4], Xiaohui Bai[4], Yundong Sun[5] and Dawei Wang[1,2]*

[1]Department of Orthopedic, Shandong Provincial Hospital, Cheeloo College of Medicine, Shandong University, Jinan, China, [2]Department of Orthopedic, Shandong Provincial Hospital Affiliated to Shandong First Medical University, Jinan, China, [3]Department of Gastroenterology, Qilu Hospital, Shandong University, Jinan, China, [4]Department of Clinical Laboratory, Shandong Provincial Hospital Affiliated to Shandong First Medical University, Jinan, China, [5]Department of Microbiology, Key Laboratory for Experimental Teratology of Ministry of Education, Key Laboratory of Infection and Immunology of Shandong Province, School of Basic Medicine, Shandong University, Jinan, China

OPEN ACCESS

Edited by:
Fengjie Sun,
Georgia Gwinnett College,
United States

Reviewed by:
Hongkai Bi,
Nanjing Medical University, China
Ming Su,
Peking University People's Hospital, China

***Correspondence:**
Dawei Wang
wangdawei@sdu.edu.cn

[†]These authors have contributed equally to this work and share first authorship

Specialty section:
This article was submitted to Food Microbiology, a section of the journal Frontiers in Microbiology

Received: 16 December 2021
Accepted: 05 January 2022
Published: 25 January 2022

Citation:
Feng Y, Yu Y, Chen Z, Wang L, Ma J, Bai X, Sun Y and Wang D (2022) Effects of β-Carotin and Green Tea Powder Diets on Alleviating the Symptoms of Gouty Arthritis and Improving Gut Microbiota in C57BL/6 Mice. Front. Microbiol. 13:837182. doi: 10.3389/fmicb.2022.837182

As a chronic metabolic disease caused by disorders of purine metabolism, gout has shown increasing incidence rate worldwide. Considering that gout is not easily treated and cured, further studies are explored to prevent gout development through diet modification. Both β-carotin and green tea powder are rich in dietary fiber, which helps maintain the balance of gut microbiota in humans. The aim of this study was to investigate the effects of β-carotin and green tea powder diet on the prevention of gouty arthritis in relation to the bacterial structure of gut microbiota in mice. We successfully induced gouty arthritis in C57BL/6 mice by injecting monosodium urate (MSU) crystals and feeding high-fat diet (HFD), and further investigated the effects of additional β-carotin and green tea powder in the diets of mice on the prevention of gouty arthritis in mice. Our results showed that diet of β-carotin and green tea powder reduced the joint swelling and pain in mice with gout, reduced the levels of serum uric acid (UA) and three types of pro-inflammatory cytokines, i.e., interleukin-1β (IL-1β), interleukin-6 (IL-6), and tumor necrosis factor-α (TNF-α), improved the gut microbiota profile, and reduced the metabolic levels of purines and pyrimidines. In conclusion, our study provided evidence to support the application of β-carotin and green tea powder diet as a dietary adjustment method to prevent and treat gouty arthritis.

Keywords: β-carotin, green tea powder, gouty arthritis, gut microbiota, purine metabolism

INTRODUCTION

Gout is a chronic metabolic disease caused by disorders of purine metabolism (Kuo et al., 2015), characterized by elevated levels of uric acid (UA) in the blood to gradually form monosodium urate (MSU) crystals in the joints and soft tissues surrounding the joints, further inducing an acute inflammatory response with symptoms, such as fever, swelling, and burning

and severe pains (Rees et al., 2014; So and Martinon, 2017). Studies have shown that the prevalence and incidence rates of gout are currently rapidly increasing worldwide (Kuo et al., 2015). For example, there are ~1.4 women and 4.0 men with gout per 1,000 people (Roddy and Doherty, 2010; Abhishek et al., 2017). Risk factors that have been identified for the development of gout include poor diet, hyperuricemia, and other metabolic syndromes (Roddy and Doherty, 2010). Both allopurinol and febuxostat are effective in the treatment of gout as the first-line agents to lower the level of uric acid (Abhishek et al., 2017). However, the use of these medicines has caused many common types of side effects in gout patients with negative impact on their health, such as rash, diarrhea, and abnormal hepatic functions (Wen et al., 2021). Therefore, prevention of gouty arthritis is extremely important and novel therapeutic treatments are needed to prevent the development of gouty arthritis.

Gut microbiota play significant roles in human health (Clemente et al., 2012). In recent years, a growing number of studies have revealed a strong connection between the development of gout and gut microbes (Guo et al., 2016; Shao et al., 2017). Furthermore, there is a growing body of evidence showing that the gut microbiota are also involved in purine metabolism and inflammatory responses induced by MSU crystals (Vieira et al., 2015; Chiaro et al., 2017). Moreover, a previous study suggested that the regulation of homeostasis in gut microbiota may be a potential therapeutic strategy of treating gouty arthritis with the traditional Chinese medicine "Simiao Decoction" (Lin et al., 2020a).

Dietary patterns affect the taxonomic compositions and biological functions of gut microbiota (Scott et al., 2013). For example, a high-fat diet (HFD) affects the composition of the gut microbiota in mice (Mullin, 2010) and significantly reduces the number of Bifidobacteria (Brinkworth et al., 2009). The short-chain fatty acids (SCFAs) play an important role in maintaining lipid homeostasis and reducing tissue inflammation, while different populations of gut microbes can modulate their beneficial effects by fermenting dietary fiber to produce SCFAs (Hills et al., 2019). Furthermore, studies have shown that green tea powder is rich in dietary fiber, which can further improve lipid metabolism in mice fed with HFD by altering the structure of gut microbiota (Wang et al., 2020). Moreover, the probiotic-containing yogurt has also been shown to significantly reduce the number of intestinal pathogens (Yang et al., 2012).

Consumption of dietary fiber and prebiotics that can be metabolized by microorganisms in the gastrointestinal tract is generally considered a dietary strategy to regulate the microbiota (Holscher, 2017). Both β-carotin and green tea powder are rich in dietary fiber (Wang et al., 2020; Matsumoto et al., 2021). Therefore, we hypothesized that the addition of these two substances to mouse feed could prevent gout development in mice by affecting the taxonomic components and functions of the gut microbiota in mice. In this study, we first established the mouse models of gouty arthritis induced by MSU crystal and HFD. We then further analyzed the taxonomic structure of gut microbiota and gout symptoms with the addition of β-carotin and green tea powder added either separately and in combination in the diet for mice. Our results showed that diets of β-carotin and green tea powder alleviated the symptoms of gouty arthritis in mice, reduced the levels of serum uric acid and three type of pro-inflammatory cytokines, i.e., interleukin-1β (IL-1β), interleukin-6 (IL-6), and tumor necrosis factor-α (TNF-α), improved the gut microbiota profile, and reduced the metabolic levels of purines and pyrimidines.

MATERIALS AND METHODS

β-Carotin and Green Tea Powder

β-Carotin was purchased from Adamas Chemical Reagent Co., Ltd. (Shanghai, China, Cat. 1109142). Green tea "Longjing" was purchased from Hangzhou Zhenghao Tea Co. (Hangzhou, China). Green tea powder was made from green tea raw materials by hot water extraction, followed by dehydration and drying. The green tea ingredients were mixed in water at 90°C for 30 min and then the mixture was dewatered using a screw extruder at 0.5–1.2 MPa for 1 min, dried at 100–130°C for 3–5 h, and finally the dehydrated green tea leaves were ground into powder and stored at 4°C.

Animals

Twenty-five specific pathogen-free (SPF) male C57BL/6 mice (4–6 weeks old with an average body weigher of 15 ± 3 g) were provided by Beijing Vital River Laboratory Animal Technology Co., Ltd. (Beijing, China) and housed in the SPF environment of Shandong Provincial Hospital Laboratory Animal Research Center. The experimental procedure was approved by the Laboratory Animal Management and Ethics Review Committee of Shandong University, China (Permit No.: MECSDUMS2012056). All mice were maintained under the standard environmental conditions (12/12 h light/dark cycle and 25 ± 1°C) with constant access to food and water.

Dietary Treatments

After 1 week of rearing to adapt to the environment, all 25 mice were evenly and randomly divided into five groups, including the control group (CTL), the gouty arthritis model group (Model), the β-carotin diet group (Model + β-carotin), the green tea powder diet group (Model + GTP), and the β-carotin and green tea powder combined diet group (Model + Double). The mice in the CTL group were fed with a normal diet (containing 24% kcal from protein, 3.44 total kcal/g, and Beijing Keaoxieli Feed. Co., Ltd.) every day and were individually injected a total of 40 μl of phosphate buffered saline (PBS) into the right rear footpad once every 10 days. The other four groups of mice were fed daily with HFD (10% yeast extract) and were injected with MSU crystals (1 mg mixed in 40 μl PBS) into the right hind footpad once every 10 days (Lin et al., 2020b). The experiments lasted for 6 weeks after the mouse models of gouty arthritis were established. The proportion of green tea powder and β-carotin added to the feed was converted according to the daily weight of the oral feed. The mice in the Model + β-carotin and Model + GTP groups were supplemented with 0.05% β-carotin

and 2% green tea powder in the HFD, respectively (Wang et al., 2020; Yang et al., 2020). The mice in the Model+Double group were fed with 2% green tea powder and 0.05% β-carotin added to the HFD.

Sample Collection

Samples were collected at the end of the 6-week long experiments (i.e., 42 days). The mouse blood was collected through the orbital vein and then centrifuged at 1,300*g* and 4°C for 10 min. Subsequently, the mice were euthanized with CO_2 with the fresh fecal materials collected immediately from the colon tissue of the mice and stored at −80°C. Simultaneously, the liver and foot joint tissues were collected, quickly frozen in liquid nitrogen, and then stored at −80°C.

Preparation of the MSU Crystals

Monosodium urate crystals were prepared as described previously (Ruiz-Miyazawa et al., 2017). Briefly, the MSU (800 mg) was dissolved in boiling Milli-Q water (155 ml) and added with NaOH (5 ml), with the pH value adjusted to 7.2 using hydrochloric acid. The solution was cooled and centrifuged to collect the crystals, which were evaporated and stored after high temperature sterilization.

Evaluation of Foot Joint Hypersensitivity and Oedema

A digital caliper (Meinaite, Germany) was used to measure the thickness of the footpads of each mouse before and 4, 24, 48, and 72 h after the injection of MSU crystals into the footpads of the mice. The degree of foot swelling in mice was calculated as the ratio of Δmm/mm (at zero time point) of the joints (Lin et al., 2020b). As described previously (Chaplan et al., 1994), von Frey filaments (UGO Basile, Italy) were used to measure the mechanical retreat threshold (MWT) to estimate the foot pain threshold of mice.

Measurements of the Levels of Pro-inflammatory Cytokines and Enzymatic Activities

Thaw The samples of mouse foot joint and liver samples were thawed at room temperature and subsequently homogenized (0.05 g tissue per 1.0 ml buffer solution) and centrifuged for 10 min at 12,000 rpm and 4°C. The supernatants were assessed for the myeloperoxidase (MPO) activity in foot joint tissues and the xanthine oxidase (XOD) and adenosine deaminase (ADA) activities in hepatic tissues by following the manufacturer's instructions (Jiancheng, Nanjing, China). Both XOD and ADA were enzymes involved in purine metabolism to promote the uric acid production (Lou et al., 2020). Three types of pro-inflammatory cytokines, i.e., IL-1β, IL-6, and TNF-α, were measured in serum and foot joint supernatant using the Mouse ELISA Commercial Kit (NOVUS, Germany) according to the manufacturer's instructions of Varioskan Flash (Thermo Science, United States). The levels of serum UA in mice were measured by using TBA-40FR automated biochemical analyzer (Toshiba, Japan).

Histopathological Assessment of Foot Joint

Foot joint tissues collected from mice were first rinsed with PBS, and then fixed overnight in 10% paraformaldehyde, followed by decalcification with EDTA for 3 weeks. The decalcified foot joint tissue was embedded in paraffin for sectioning. The sections with thickness of 5 μm were stained with hematoxylin and eosin (H&E) to evaluate the changes in the morphology and inflammation levels of the foot joint tissues.

Gut Microbiota Analysis

Genomic DNA was extracted from the samples using the TIANamp Bacteria DNA Kit (Tiangen Biotechnology Co., Ltd., Beijing, China) according to the manufacturer's instructions. Primers 27F and 1492R were used for PCR amplification (10 μl system, Solexa PCR) of the target area of 16S rRNA. The sequencing libraries were quality-checked, and the high-quality sequencing libraries were subjected to barcode identification and other necessary processes to obtain the circular co-sequencing (CCS) sequences. The optimized CCSs were clustered at the level of 97% similarity (USEARCH, version 10.0) with the species classification obtained based on the sequence composition of the operational taxonomic unit (OTU). The platforms 16S: The Silva database[1] and RDP Classifier[2] were used to analyze the species annotation and taxonomy as well as the diversity of gut microbiota. Alpha diversity analysis was performed to examine the species richness and diversity with the ACE, Chao1, Shannon, and Simpson indices for each sample calculated. The differences in the community composition and structure of different samples were compared through Beta diversity analysis, i.e., the principal coordinate analysis (PCoA). Finally, Metastats analysis was performed to compare the significant differences between the groups at the genus level, and the linear discriminant analysis effect size (LEfSe) analysis was used to screen the biomarkers with statistical differences between the groups (LDA score > 4). The "cor.test" function in the statistical software R was used to calculate the Spearman correlation coefficient between the microbial community and gout symptoms, visualized with a heat map (Li et al., 2020a). PICRUSt was used to infer the metabolic functions of the intestinal microbiota and to predict the molecular function of each sample based on the sequences of 16S rRNA-tagged genes (Langille et al., 2013). These predictions were pre-calculated for the annotation of genes based on the Kyoto Encyclopedia of Genes and Genomes (KEGG) database.[3] The datasets presented in this study can be found in the National Center for Biotechnology Information (https://www.ncbi.nlm.nih.gov/sra/) database with the accession number PRJNA783957.

Statistics

The biochemical data were analyzed and plotted using GraphPad Prism 8.0. The differences in gene expression among different groups were statistically evaluated based on *t*-test. Compositional

[1]https://www.arb-silva.de/
[2]https://www.findbestopensource.com/product/rdp-classifier
[3]https://www.genome.jp/kegg/

differences in the microbiota between different groups were analyzed using the Kruskal–Wallis rank-sum test ($p < 0.05$).

RESULTS

β-Carotin and Green Tea Powder Effectively Alleviate the Symptoms of Gout in Mice

The mouse model of gouty arthritis induced by treating the mice with MSU crystals and HFD was successful established. The levels of serum UA, the footpad swelling, and the pain threshold in mice were assessed to evaluate the effect of adding β-carotin and green tea powder to the diet on gout (**Figure 1**). Compared with the mice in the CTL group, the mice in the Model group showed evident foot joint swelling, with foot joint swelling decreased significantly after feeding mice with β-carotin and green tea powder (**Figures 1A,B**). Compared with the CTL group, the footpad mechanical pain threshold was reduced in the Model group mice, while addition of β-carotin and green tea powder alleviated the MSU-induced mechanical abnormalities in pain (**Figure 1C**). When mice were given a combination of both β-carotin and green tea powder, the most pronounced decrease in foot joint swelling and footpad mechanical pain threshold was observed (**Figures 1B,C**). Furthermore, feeding both β-carotin and green tea powder to mice in the Model + Double group or the separate feeding of β-carotin and green tea powder to the mice in the Model + β-carotin and Model + GTP group significantly decreased the level of serum UA compared to the Model group (**Figure 1D**).

β-Carotin and Green Tea Powder Improves Gout-Related Inflammation Markers in Mice

To further analyze the effects of β-carotin and green tea powder on gout, the inflammation of gout sites in different treatment groups of mice was evaluated (**Figure 2**). Results of the histological analysis showed that MSU crystals significantly increased the inflammatory cell infiltration in the foot joint compared to the CTL group, while feeding mice with β-carotin and green tea powder decreased the number of inflammatory cells in the foot joint (**Figure 2A**).

Previous studies have shown that IL-6 (Cavalcanti et al., 2016), IL-1β (So and Martinon, 2017), and TNF-α (Amaral et al., 2016) were associated with inflammatory activity in patients with gout. Compared with mice in the CTL group, the levels of IL-1β, IL-6, TNF-α, and MPO activity were significantly higher in the foot joints of mice in the Model group, showing that the administration of β-carotin and green tea powder significantly decreased the levels of these inflammatory markers (**Figure 2B**).

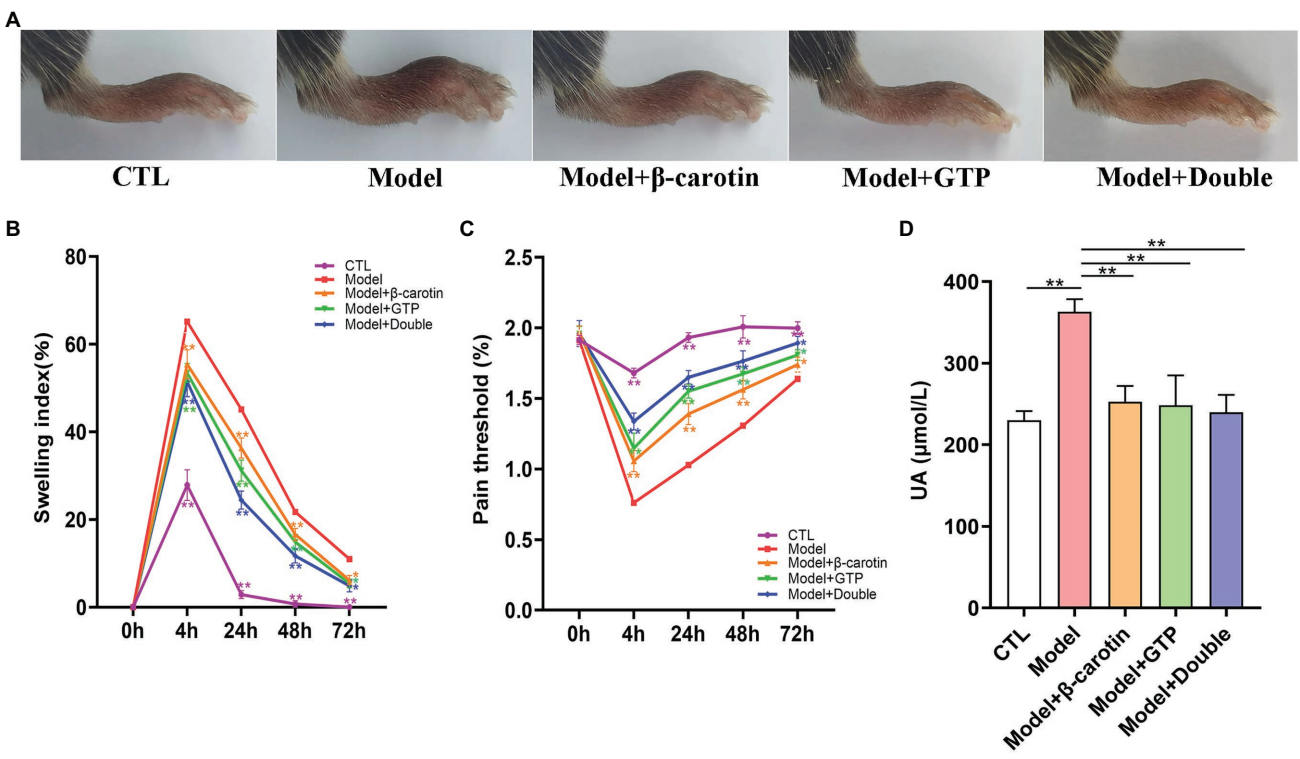

FIGURE 1 | Effects of β-carotin and green tea powder on alleviating the symptoms of gout in mice. **(A)** Representative images of foot joints in five groups of mice. **(B)** Level of footpad swelling in five groups of mice. **(C)** Level of footpad pain threshold in five groups of mice. **(D)** Level of serum uric acid (UA) in five groups of mice. *$p < 0.05$, **$p < 0.01$.

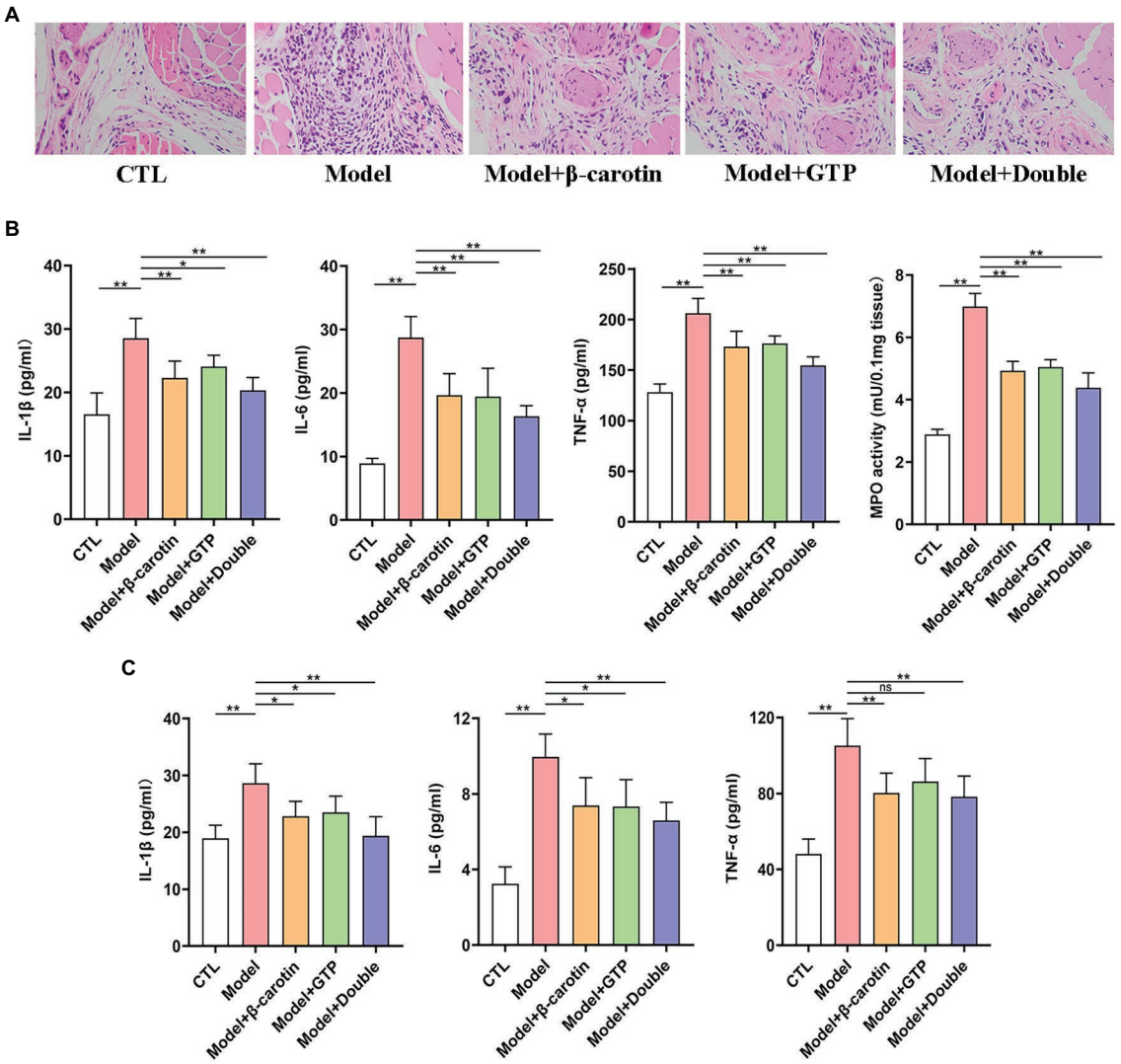

FIGURE 2 | Effects of β-carotin and green tea powder on the improvement of gout-related inflammation markers in mice. **(A)** HE analysis of the footpad. **(B)** Level of cytokines [i.e., interleukin-1β (IL-1β), interleukin-6 (IL-6), and tumor necrosis factor-α (TNF-α)] and myeloperoxidase (MPO) activity in the foot joint tissues of five groups of mice based on ELISA. **(C)** Level of cytokines (i.e., IL-1β, IL-6, and TNF-α) in the serum of five groups of mice based on ELISA. $^{*}p < 0.05$, $^{**}p < 0.01$, and "ns" represents no statistical significance.

The expression levels of three pro-inflammatory cytokines (i.e., IL-1β, IL-6, and TNF-α) associated with gout were further investigated in serum (**Figure 2C**). Compared with the CTL group, the levels of IL-1β, IL-6, and TNF-α in serum were significantly increased in the Model group, but decreased in mice fed with β-carotin and green tea powder (**Figure 2C**).

Effect of β-Carotin and Green Tea Powder on Purine Metabolism in Hepatic Tissue of Mice

The results of XOD and ADA activities measured in the hepatic tissues showed that both activities were not significantly elevated in the Model group compared with that of the CTL group (**Figures 3A,B**). It was noted that although feeding β-carotin and green tea powder to mice resulted in a decrease in the activities of both XOD and ADA, the differences were not statistically significant (**Figures 3A,B**).

Alterations of Gut Microbiota

To investigate the effects of β-carotin and green tea powder on the taxonomic composition of gut microbiota in mice, we collected the fecal samples from mice for 16S rRNA sequencing analysis. The results showed that species richness based on the ACE and Chao1 indices was significantly decreased in mice with gout, while the microbial diversity as assessed by Shannon and Simpson indices showed a significant decrease in mice with gout (**Figure 4A**). The application of β-carotin and green tea powder normalized the ACE, Chao1, Shannon, and Simpson indices (**Figure 4A**). The analysis of OTUs in feces showed that there were a total of 107 OTUs among the

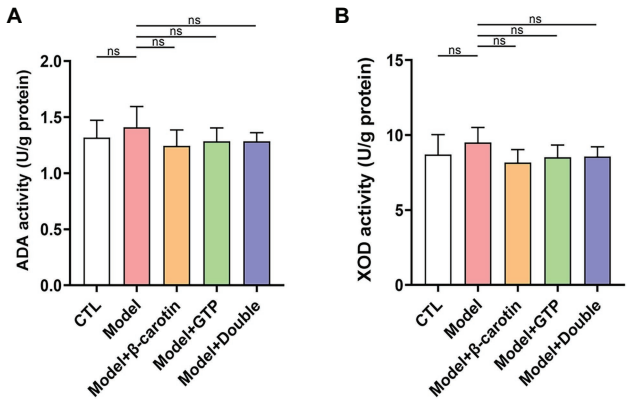

FIGURE 3 | Effects of β-carotin and green tea powder on enzymatic activities related to purine metabolism in mouse hepatic tissue. **(A)** Level of adenosine deaminase (ADA) activity in the hepatic tissue of five groups of mice based on ELISA. **(B)** Level of xanthine oxidase (XOD) activity in the hepatic tissue of five groups of mice based on ELISA. "ns" represents no statistical significance.

five groups of mice, with 3, 29, 19, 3, and 2 OTUs unique to the CTL, the Model, the Model + β-carotin, the Model + GTP, and the Model + Double groups, respectively (**Figure 4B**). For the Beta diversity, the results of PCoA revealed significant differences in gut microbiota between the CTL and Model groups, while the gut microbiota of mice fed with β-carotin and green tea powder was significantly similar to that of mice in the CTL group (**Figure 4C**). At the phylum level, analysis of the composition of the gut microbiota in five groups of mice showed that Firmicutes and Bacteroidetes were the dominant bacterial taxa (**Figure 4D**). The relative abundance of Bacteroidetes was significantly lower in the Model group compared to the CTL group, and feeding mice with β-carotin and green tea powder normalized the abundance of Bacteroidetes (**Figure 4D**). At the genus level, the relative abundance of microorganisms, such as *Muribaculaceae*, *Ruminococcaceae_UCG-014*, and *Lachnospiraceae_NK4A136_group* was decreased in the Model group compared to the CTL group, and feeding mice with β-carotin and green tea powder increased the relative abundance of these microorganisms (**Figure 4E**).

At the genus level, bacteria with relative abundance greater than 1% between the Model and CTL groups were compared to show that *Muribaculaceae*, *Lactobacillus*, *Ruminococcaceae_UCG-014*, *Lachnospiraceae_NK4A136_group*, *Akkermansia Parasutterella*, and *Prevotellaceae_UCG-001* were identified as the main taxa in the gut microbiota of both groups of mice (**Figure 5A**). Bacteria with relative abundance greater than 1% were presented in the volcano plots (**Figure 5B**). Compared with the CTL group, the relative abundance of *Muribaculaceae*, *Bacteroides*, and *Lachnospiraceae* in the Model group was significantly lowered (**Figure 5B**). A heat map showing the relative abundance of key bacteria in each sample was presented in **Figure 5C**. These results revealed that the relative abundance of *Muribaculaceae*, *Bacteroides*, and *Lachnospiraceae* was significantly decreased in the Model group compared to the CTL group, while feeding β-carotin and green tea powder to mice increased the relative abundance of these three taxa (**Figure 5C**).

Interaction of Gut Microbiota

Microorganisms with abundance TOP: 50 were selected to further investigate the correlation between gut microorganisms with the |Spearman correlation| ≥ 0.1 and $q \leq 0.05$ set as the filtering parameters. Due to space constraints, only bacteria numbers 1–10 are listed. The results revealed strong interactions among gut microbes (**Figure 6**). The interactions among the intestinal microorganisms were reduced in the Model group of mice compared to the CTL group (**Figures 6A,B**), while feeding β-carotin and green tea powder to mice significantly increased the interactions between gut microbes (**Figures 6C–E**). For example, *Lachnoclostridium* (28) was positively correlated with both *Blautia* (1) and *Ruminococcaceae* (2) in the CTL group (**Figure 6A**). In the Model group, *Lachnoclostridium* (32) was only negatively correlated with *Ureaplasma* (14; **Figure 6B**), while in the Model + β-carotin group, *Lachnoclostridium* (30) interacted positively with *Candidatus_Soleaferrea* (29; **Figure 6C**). In the Model + GTP group, *Lachnoclostridium* (28) was positively correlated with *Candidatus_Saccharimonas* (9), *Ruminiclostridium_9* (10), and *Ruminiclostridium* (22; **Figure 6D**), whereas in the Model + Double group, *Lachnoclostridium* (30) interacted positively with *Candidatus_Saccharimonas* (10; **Figure 6E**). Furthermore, the most significant increase in the level of interaction between gut microbes in mice was observed after the addition of combined β-carotin and green tea powder to their diets, showing a predominantly positive correlation (**Figure 6E**).

Metabolic Functions of the Gut Microbiota

PICRUSt was used to predict the functions of gut microbiota based on 16S rRNA sequencing and the KEGG database (**Figure 7**). The results showed that compared with the CTL group, the levels of ribosomal synthesis, pyrimidine metabolism, purine metabolism, and aminoacyl-tRNA biosynthetic metabolic pathways of the gut microbiota in the mice of the model group were increased (**Figure 7A**), while feeding mice with β-carotin and green tea powder significantly reduced the activities of these metabolic pathways (**Figure 7B**).

Correlation Between Key Gut Microbes and Pro-inflammatory Cytokines, Metabolites, and Metabolic Pathways in Mice

A heat map analysis of Spearman rank correlation coefficients was performed to determine the correlations between key bacterial taxa and the levels of IL-1β, IL-6, TNF-α, UA, activities of MPO, XOD, and ADA, and purine and pyrimidine metabolisms (**Figure 8**). The results showed that *Bacteroides* and *Lachnospiraceae* were negatively correlated with the levels of IL-1β, IL-6, TNF-α, UA, and MPO activity, but not significantly

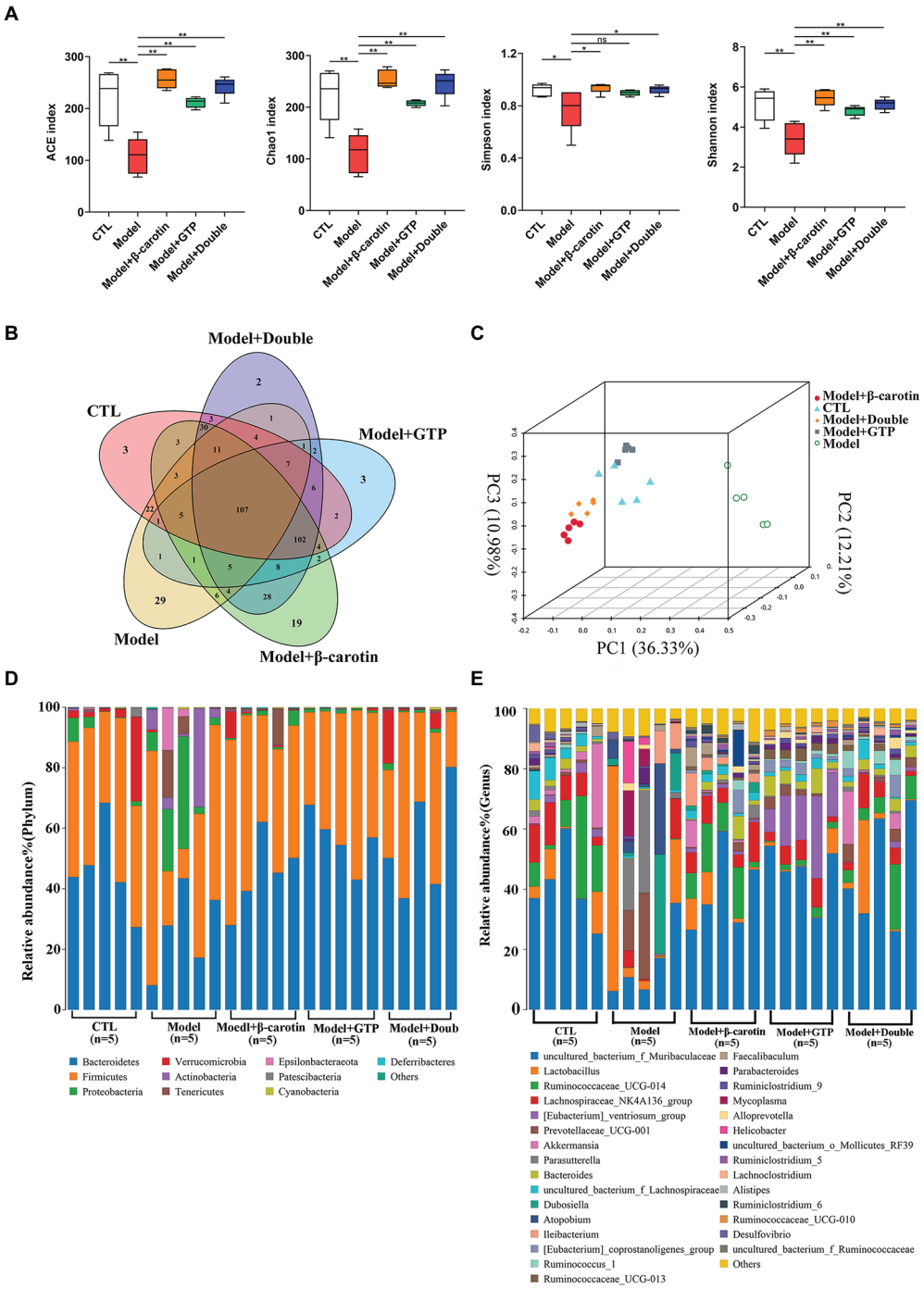

FIGURE 4 | Alterations in gut microbiota among five groups of mice. **(A)** Alpha diversity analysis. **(B)** Venn diagram of operational taxonomic units (OTUs). **(C)** Principal coordinate analysis (PCoA) of the gut microbiome. **(D)** Composition of the gut microbiota at the phylum level among the five groups of mice. **(E)** Composition of the gut microbiota at the genus level among the five groups of mice. *$p < 0.05$, **$p < 0.01$, and "ns" indicates no statistical significance.

correlated with the levels of XOD and ADA activities (**Figure 8A**). *Muribaculaceae* was negatively correlated with the levels of IL-1β, IL-6, TNF-α, and the activities of MPO and XOD, but not significantly correlated with the levels of ADA activity and UA (**Figure 8A**). *Bacteroides* was negatively correlated with both pyrimidine and purine metabolisms, *Lachnospiraceae* was negatively correlated with purine metabolism (**Figure 8B**), while *Muribaculaceae* was not significantly correlated with either pyrimidine metabolism or purine metabolism (**Figure 8B**).

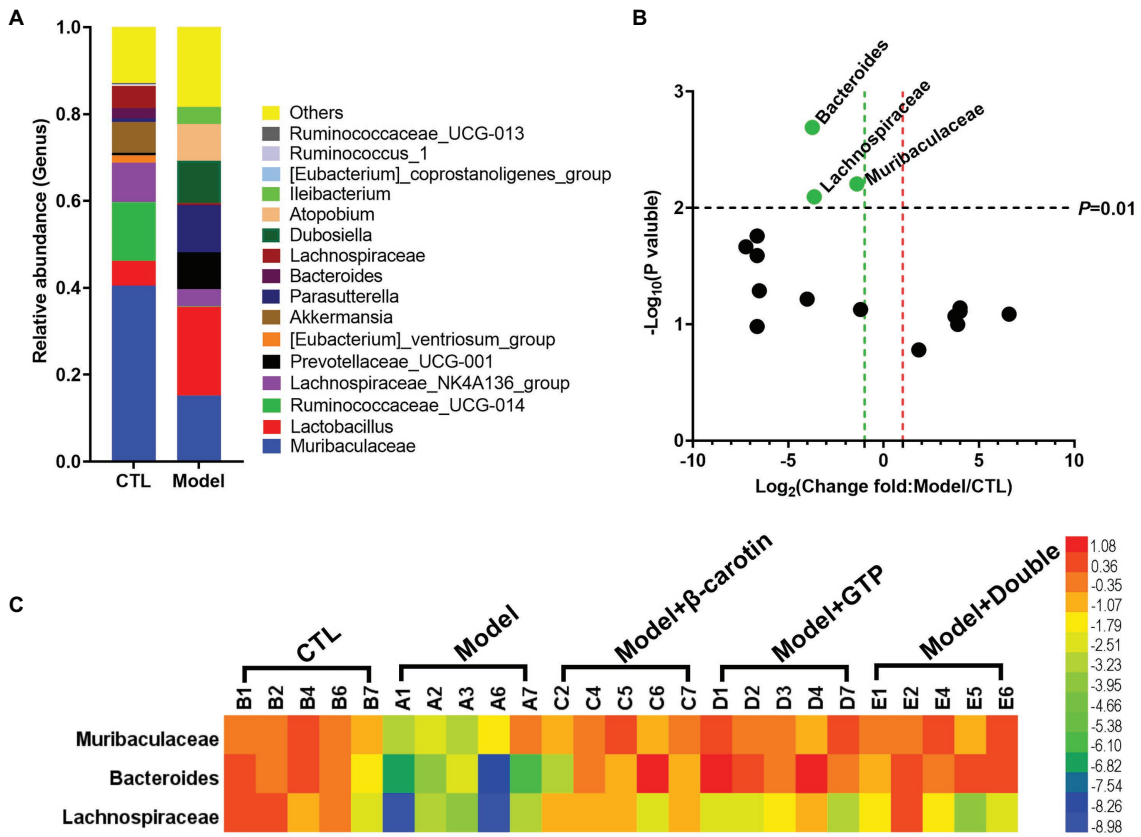

FIGURE 5 | Comparative analysis of key bacteria at the genus level in five groups of mice. **(A)** Comparison of microbial differences between the mice in Model and control group (CTL) groups showing the microbial taxa with the average relative abundance >1%. **(B)** Volcano graph analysis of changes in the gut microbiota of mice in Model and CTL groups. The *p* value is based on the *t*-test. Bacteria with a relative abundance >1% in **(A)** are selected as key bacteria. **(C)** The heat map showing the relative abundance of key bacteria in each sample of the five groups of mice.

DISCUSSION

With the increased prevalence of gout risk factors, such as obesity, hypertension, kidney disease, and hyperlipidemia (Elfishawi et al., 2018), the incidence, hospitalization, and health care costs related to gout have increased significantly and the gout has emerged as a public health problem, causing severe socioeconomic burden (Kuehn, 2018). However, the traditional treatments of gout are generally ineffective with severe side effects. Therefore, it is extremely important to identify novel strategies to prevent the development of gouty arthritis. In the present study, our results showed that the addition of β-carotin and green tea powder to the diets of mice effectively improved the symptoms of gout induced by the combination of MSU crystals and HFD and improved the gut microbiota profile of mice with gout.

Green tea powder contains a variety of nutritional and functional components, including phenols, catechins, and dietary fiber (Onakpoya et al., 2014; Wang et al., 2020), which not only prevents tooth decay, but also reduces the absorption of cholesterol and lipids in the gastrointestinal tract (Koo and Cho, 2004). The polyphenolic compounds in green tea have the effect of scavenging oxygen and nitrogen free radicals, and can also reduce serum UA concentration by regulating urinary UA excretion in mice with hyperuricemia (Frei and Higdon, 2003; Chen et al., 2015). In addition, the catechins in green tea have the potential to increase UA excretion (Kawakami et al., 2021). Numerous studies have shown that dietary fiber promotes the growth of beneficial microbes and inhibits the development of harmful microbes, helping maintain the balance of gut microbiota (Wang et al., 2020). As one type of important natural pigment in plants with multiple physiological functions (Wang et al., 2017), β-carotin is generally considered a safe form of vitamin A due to its highly-regulated intestinal absorption (Shete and Quadro, 2013). Studies have shown that β-carotin acts mainly as a type of effective antioxidant in scavenging peroxyl radicals (Jomova and Valko, 2013).

Gout is a disease with the disorders of purine metabolism involved in its development (Kuo et al., 2015), while the gut microbiota play an important role in purine metabolism (Chiaro et al., 2017). Furthermore, the gut microbiota play numerous functions in the development of the immune system and in maintaining the integrity of the intestinal barrier (O'Hara and Shanahan, 2006). Healthy gut microbiota show an important impact on the overall health of the host, while

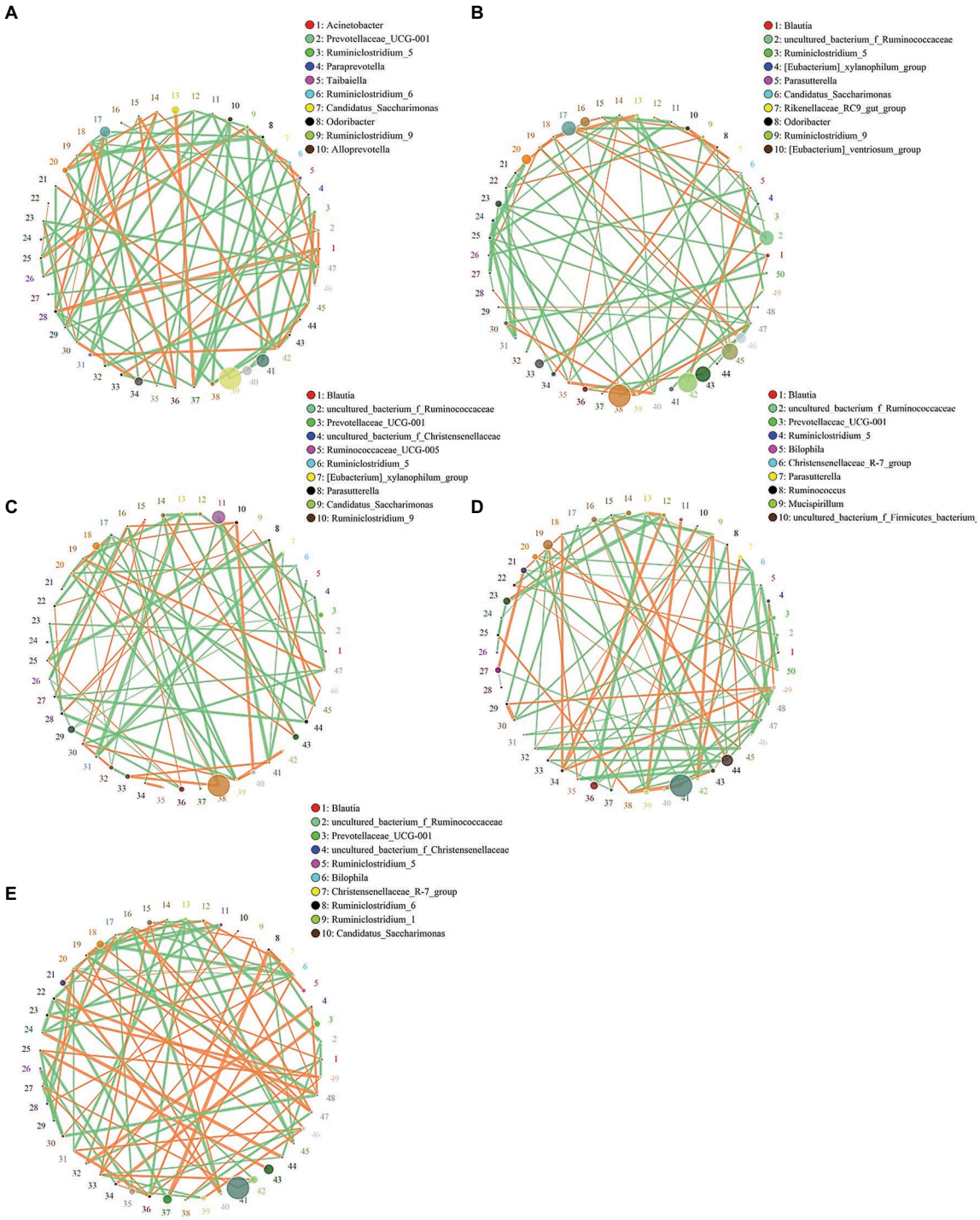

FIGURE 6 | Correlation of microbiota at genus level in the intestines of five groups of mice, including the CTL group **(A)**, the Model group **(B)**, the Model + β-carotin group **(C)**, the Model + GTP group **(D)**, and the Model + Double group **(E)**. The size of the circle represents the relative abundance, the line represents the correlation between the two taxa at both end of the line, the thickness of the line represents the strength of the correlation, the orange line represents positive correlation, and the green line represents negative correlation.

the alterations in the gut microbial community lead to disease susceptibility (Compare et al., 2016). Studies have shown that the gut microbiota is involved in the response to MSU crystals in a gout model of mice, whereas the germ-free mice or mice treated with antibiotics do not respond to the injections of MSU crystals (Vieira et al., 2015). Based on

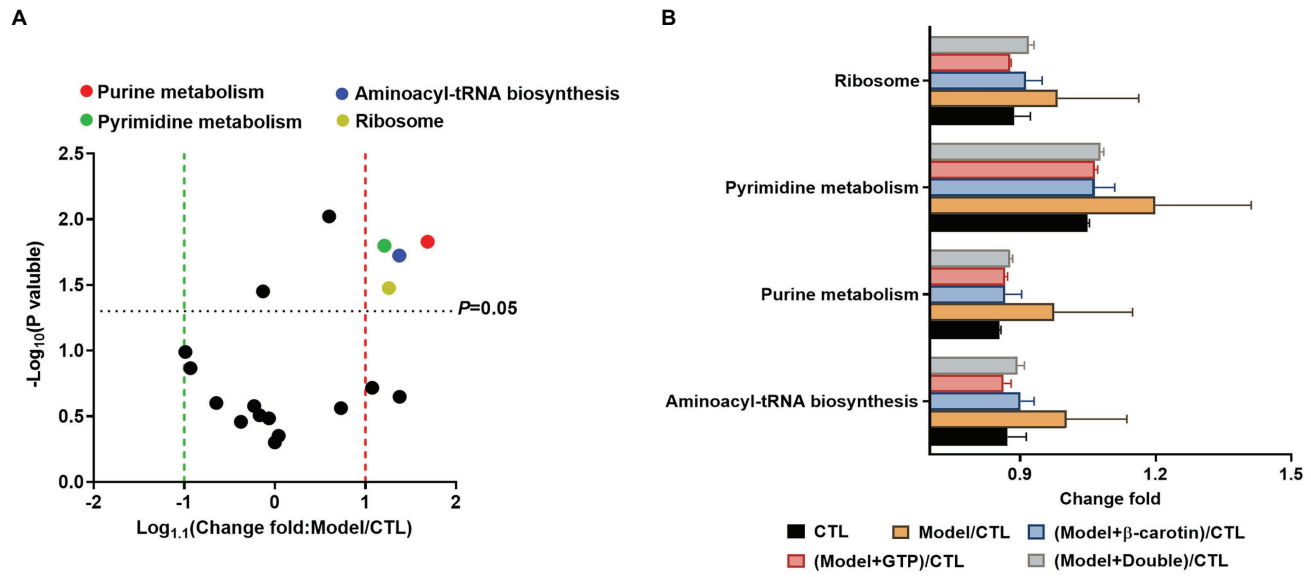

FIGURE 7 | Comparison of the relative abundance of the functional profiles of the gut microbiota based on PICRUSt among the five groups of mice. **(A)** Volcano plot analysis of altered Kyoto Encyclopedia of Genes and Genomes (KEGG) pathways with an average relative abundance >1% between the mice in CTL and Model groups. The *p* value is based on a two-tailed and paired *t*-test. **(B)** Distinct gene categories selected based on significant differences in gene categories at level 2 (*t*-test, $p < 0.05$).

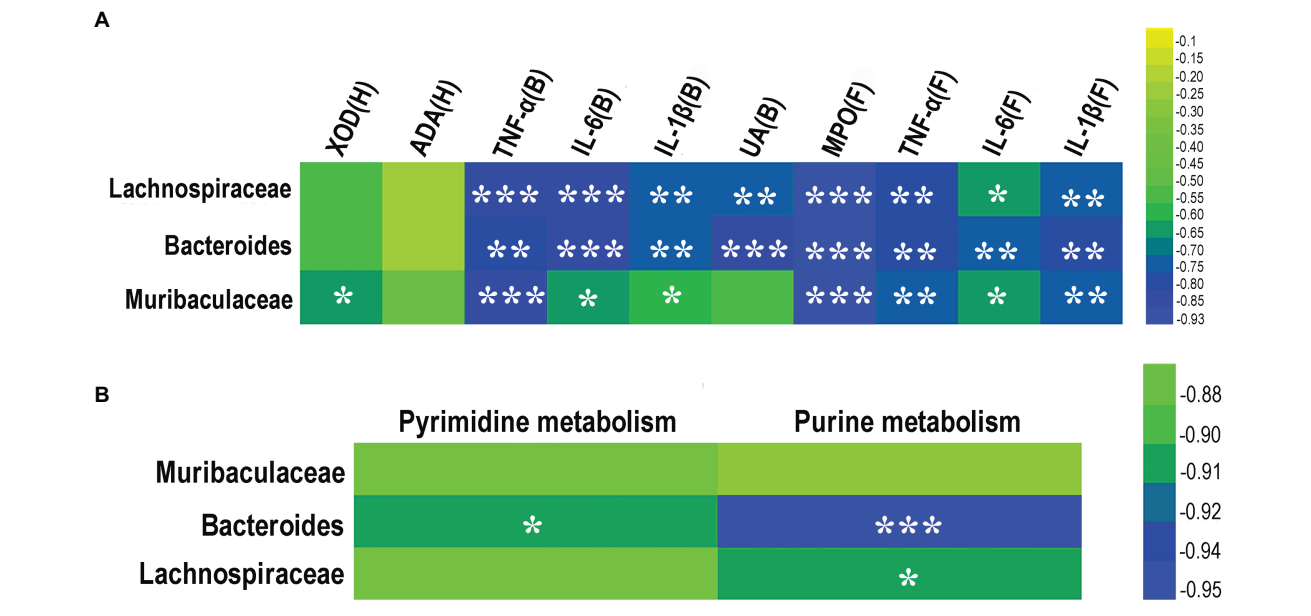

FIGURE 8 | Correlation between key gut microbes and pro-inflammatory cytokines, enzymes, and metabolic pathways from three taxa of gut microbes (i.e., *Lachnospiraceae*, *Bacteroides*, and *Muribaculaceae*). **(A)** Correlation among pro-inflammatory cytokines and enzymes. **(B)** Correlation between purine and pyrimidine metabolic pathways. The color of the cell indicates the relative *R* values ranging from −0.95 to 0 (i.e., blue to green). B, blood; H, hepatic tissue; and F, foot joint tissues. $^{*}p < 0.05$, $^{**}p < 0.01$, and $^{***}p < 0.001$.

the 16S rRNA sequencing (Lin et al., 2020b), the top three relatively dominant phyla of the mouse gut microbiota were Firmicutes, Bacteroidetes, and Proteobacteria. In our study, the relatively dominant phyla of the mouse gut microbiota were Firmicutes and Bacteroidetes, while the MSU crystals and HFD altered the composition of the gut microbiota mainly by decreasing the relative abundance of Bacteroidetes. At the genus level, MSU crystals and HFD significantly reduced the relative abundance of *Muribaculaceae*, *Bacteroides*, and *Lachnospiraceae*.

Studies have shown that members of *Lachnospiraceae* are the main producers of butyrate (Wen et al., 2021). Furthermore, studies have revealed the anti-inflammatory effects of butyrate by inhibiting class I histone deacetylase and MSU-induced cytokine production in patients with gout (Cleophas et al., 2016, 2017). Previous studies have shown that members of *Lachnospiraceae* associated with the production of SCFAs are depleted in patients with gout (Shao et al., 2017). Moreover, members of *Lachnospiraceae* can prevent human colon cancer by producing butyric acid (Langille et al., 2014). In this study, similar results were revealed showing the decreased relative abundance of *Lachnospiraceae* and the significantly negative correlation between the relative abundance of *Lachnospiraceae* and the levels of UA, IL-1β, IL-6, TNF-α, MPO activity, and purine metabolism in mice with gout.

Muribaculaceae are the dominant microbiota in the mouse gut (Seedorf et al., 2014) and are closely associated with the production of SCFAs (Wen et al., 2021). Studies have shown that genes involved in carbohydrate metabolism are upregulated in members of *Muribaculaceae* (Chung et al., 2020). Recent studies have reported that HFDs decrease the relative abundance of *Muribaculaceae* in the fecal samples of mice (Mu et al., 2020). In our study, injection of MSU crystals and feeding with HFD resulted in a decrease in the relative abundance of *Muribaculaceae* in the gut microbiota with a negative correlation observed between *Muribaculaceae* and the levels of IL-1β, IL-6, TNF-α, and XOD and MPO activities, whereas no association was observed between the relative abundance of *Muribaculaceae* and purine metabolism, which is closely related to the development of gout.

Bacteroides are the common and abundant bacterial components of the gut microbiota that maintain complex and generally beneficial relationships with their hosts (Wexler, 2007). *Bacteroides* can digest glycans derived from plants and hosts to produce healthy metazoans (Singh, 2019). Previous studies have shown that primary gout is closely associated with the overall alteration in intestinal *Bacteroides* (Xing et al., 2015), while an impaired jejunal intestinal barrier and a significant reduction in the amount of *Bacteroides* at the genus level were revealed in geese with gout (Ma et al., 2021). In our study, injection of MSU crystals and feeding with HFD caused a decrease in the relative abundance of *Bacteroides*, which was significantly negatively correlated with the levels of UA, IL-1β, IL-6, TNF-α, MPO activity, and purine and pyrimidine metabolisms in mice with gout. Therefore, it is speculated that both *Bacteroides* and *Lachnospiraceae* may promote gout production by affecting purine metabolism.

The balance of microbial interactions plays an important role in maintaining tissue homeostasis and human health (Li et al., 2020b). For example, *Lactococcus lactis* produces the lactic acid streptococcal peptides that inhibit pathogens such as *Staphylococcus aureus* through population sensing of their own populations (Abisado et al., 2018). In our study, results showed that combined feeding of β-carotin and green tea powder to mice with gout significantly increased the interactions between gut microbes, with predominantly positive correlations. These positive effects may play a positive role in alleviating the gout symptoms. It is noted that further studies are necessary to verify the findings revealed in our study. In addition, we have observed that combined feeding of β-carotin and green tea powder to mice with gout did not achieve our expected goal of preventing gout. This suggests that the combination of the two has no synergistic effect on the prevention of gout, but our study shows that the combination of the two enhanced the interaction of gut microbiota, especially the positive effect.

Furthermore, the activities of ADA and XOD were evaluated in the hepatic tissue of mice to further investigate the mechanism underlying the decreased purine metabolism. The results showed that feeding both the β-carotin and green tea powder reduced the activities of ADA and XOD, but the difference was not statistically significant, probably due to the insufficient treatment time. Although the reduction of ADA and XOD activity levels is not significant, we have observed that the gout symptoms of mice have been significantly improved. It may be that β-carotin and green tea powder reduce the serum uric acid level by affecting the gut microbiota, thereby further improving the symptoms of gout.

CONCLUSION

In conclusion, our results suggested that both β-carotin and green tea powder were effective in alleviating the inflammatory response to gout induced by the MSU crystals and feeding of HFD and improving the gut microbiota structure in mice with gout. Our study provides the strong experimental evidence to support the application of both β-carotin and green tea powder diet as a dietary adjustment strategy to prevent gouty arthritis in mice.

DATA AVAILABILITY STATEMENT

The datasets presented in this study can be found in online repositories. The names of the repository/repositories and accession number(s) can be found in the article/supplementary material.

ETHICS STATEMENT

The animal study was reviewed and approved by China Council for Animal Care and Utilization Committee of Shandong University, China.

AUTHOR CONTRIBUTIONS

DW conceived this study. YF and YY collected the data and drafted the manuscript. XB, YS, ZC, LW, and JM carried out the experiments and performed data analyses. All authors contributed to the article and approved the submitted version.

FUNDING

This study was financially supported by the National Natural Science Foundation of China (Grant/Award Numbers: 81972057, 81670942, 82070540, and 82172313), the Special Funds for Taishan Scholar Project (Grant/Award Number: tsqn202103180), and the Major Innovation Project of Shandong Province (Grant/Award Number: 2021GXGC011305).

REFERENCES

Abhishek, A., Roddy, E., and Doherty, M. (2017). Gout—a guide for the general and acute physicians. *Clin. Med.* 17, 54–59. doi: 10.7861/clinmedicine.17-1-54

Abisado, R. G., Benomar, S., Klaus, J. R., Dandekar, A. A., and Chandler, J. R. (2018). Bacterial quorum sensing and microbial community interactions. *mBio.* 9, e02331–e02317. doi: 10.1128/mBio.02331-17

Amaral, F. A., Bastos, L. F., Oliveira, T. H., Dias, A. C., Oliveira, V. L., Tavares, L. D., et al. (2016). Transmembrane TNF-α is sufficient for articular inflammation and hypernociception in a mouse model of gout. *Eur. J. Immunol.* 46, 204–211. doi: 10.1002/eji.201545798

Brinkworth, G. D., Noakes, M., Clifton, P. M., and Bird, A. R. (2009). Comparative effects of very low-carbohydrate, high-fat and high-carbohydrate, low-fat weight-loss diets on bowel habit and faecal short-chain fatty acids and bacterial populations. *Br. J. Nutr.* 101, 1493–1502. doi: 10.1017/S0007114508094658

Cavalcanti, N. G., Marques, C. D., Lins, T. U. L. E., Pereira, M. C., Rêgo, M. J., Duarte, A. L., et al. (2016). Cytokine profile in gout: inflammation driven by IL-6 and IL-18? *Immunol. Investig.* 45, 383–395. doi: 10.3109/08820139.2016.1153651

Chaplan, S. R., Bach, F. W., Pogrel, J. W., Chung, J. M., and Yaksh, T. L. (1994). Quantitative assessment of tactile allodynia in the rat paw. *J. Neurosci. Methods* 53, 55–63. doi: 10.1016/0165-0270(94)90144-9

Chen, G., Tan, M. L., Li, K. K., Leung, P. C., and Ko, C. H. (2015). Green tea polyphenols decreases uric acid level through xanthine oxidase and renal urate transporters in hyperuricemic mice. *J. Ethnopharmacol.* 175, 14–20. doi: 10.1016/j.jep.2015.08.043

Chiaro, T. R., Soto, R., Zac Stephens, W., Kubinak, J. L., Petersen, C., Gogokhia, L., et al. (2017). A member of the gut mycobiota modulates host purine metabolism exacerbating colitis in mice. *Sci. Transl. Med.* 9:eaaf9044. doi: 10.1126/scitranslmed.aaf9044

Chung, Y. W., Gwak, H. J., Moon, S., Rho, M., and Ryu, J. H. (2020). Functional dynamics of bacterial species in the mouse gut microbiome revealed by metagenomic and metatranscriptomic analyses. *PLoS One* 15:e0227886. doi: 10.1371/journal.pone.0227886

Clemente, J. C., Ursell, L. K., Parfrey, L. W., and Knight, R. (2012). The impact of the gut microbiota on human health: an integrative view. *Cell* 148, 1258–1270. doi: 10.1016/j.cell.2012.01.035

Cleophas, M. C., Crişan, T. O., and Joosten, L. A. (2017). Factors modulating the inflammatory response in acute gouty arthritis. *Curr. Opin. Rheumatol.* 29, 163–170. doi: 10.1097/BOR.0000000000000366

Cleophas, M. C., Crişan, T. O., Lemmers, H., Toenhake-Dijkstra, H., Fossati, G., Jansen, T. L., et al. (2016). Suppression of monosodium urate crystal-induced cytokine production by butyrate is mediated by the inhibition of class I histone deacetylases. *Ann. Rheum. Dis.* 75, 593–600. doi: 10.1136/annrheumdis-2014-206258

Compare, D., Rocco, A., Sanduzzi Zamparelli, M., and Nardone, G. (2016). The gut bacteria-driven obesity development. *Digest. Dis.* 34, 221–229. doi: 10.1159/000443356

Elfishawi, M. M., Zleik, N., Kvrgic, Z., Michet, C. J. Jr., Crowson, C. S., Matteson, E. L., et al. (2018). The rising incidence of gout and the increasing burden of comorbidities: a population-based study over 20 years. *J. Rheumatol.* 45, 574–579. doi: 10.3899/jrheum.170806

Frei, B., and Higdon, J. V. (2003). Antioxidant activity of tea polyphenols in vivo: evidence from animal studies. *J. Nutr.* 133, 3275S–3284S. doi: 10.1093/jn/133.10.3275S

Guo, Z., Zhang, J., Wang, Z., Ang, K. Y., Huang, S., Hou, Q., et al. (2016). Intestinal microbiota distinguish gout patients from healthy humans. *Sci. Rep.* 6:20602. doi: 10.1038/srep20602

Hills, R. D. Jr., Pontefract, B. A., Mishcon, H. R., Black, C. A., Sutton, S. C., and Theberge, C. R. (2019). Gut microbiome: profound implications for diet and disease. *Nutrients* 11:1613. doi: 10.3390/nu11071613

Holscher, H. D. (2017). Dietary fiber and prebiotics and the gastrointestinal microbiota. *Gut Microbes* 8, 172–184. doi: 10.1080/19490976.2017.1290756

Jomova, K., and Valko, M. (2013). Health protective effects of carotenoids and their interactions with other biological antioxidants. *Eur. J. Med. Chem.* 70, 102–110. doi: 10.1016/j.ejmech.2013.09.054

Kawakami, Y., Yasuda, A., Hayashi, M., Akiyama, M., Asai, T., Hosaka, T., et al. (2021). Acute effect of green tea catechins on uric acid metabolism after alcohol ingestion in Japanese men. *Clin. Rheumatol.* 40, 2881–2888. doi: 10.1007/s10067-021-05625-7

Koo, M. W., and Cho, C. H. (2004). Pharmacological effects of green tea on the gastrointestinal system. *Eur. J. Pharmacol.* 500, 177–185. doi: 10.1016/j.ejphar.2004.07.023

Kuehn, B. M. (2018). Chronic disease approaches needed to curb gout's growing burden. *JAMA* 319, 1307–1309. doi: 10.1001/jama.2018.0547

Kuo, C. F., Grainge, M. J., Zhang, W., and Doherty, M. (2015). Global epidemiology of gout: prevalence, incidence and risk factors. *Nat. Rev. Rheumatol.* 11, 649–662. doi: 10.1038/nrrheum.2015.91

Langille, M. G., Meehan, C. J., Koenig, J. E., Dhanani, A. S., Rose, R. A., Howlett, S. E., et al. (2014). Microbial shifts in the aging mouse gut. *Microbiome* 2:50. doi: 10.1186/s40168-014-0050-9

Langille, M. G., Zaneveld, J., Caporaso, J. G., McDonald, D., Knights, D., Reyes, J. A., et al. (2013). Predictive functional profiling of microbial communities using 16S rRNA marker gene sequences. *Nat. Biotechnol.* 31, 814–821. doi: 10.1038/nbt.2676

Li, Y., Li, W., Wang, X., Ding, C., Liu, J., Li, Y., et al. (2020a). High-salt diet-induced gastritis in C57BL/6 mice is associated with microbial dysbiosis and alleviated by a buckwheat diet. *Mol. Nutr. Food Res.* 64:e1900965. doi: 10.1002/mnfr.201900965

Li, H., Zang, Y., Wang, C., Li, H., Fan, A., Han, C., et al. (2020b). The interaction between microorganisms, metabolites, and immune system in the female genital tract microenvironment. *Front. Cell. Infect. Microbiol.* 10:609488. doi: 10.3389/fcimb.2020.609488

Lin, X., Shao, T., Huang, L., Wen, X., Wang, M., Wen, C., et al. (2020a). Simiao decoction alleviates gouty arthritis by modulating proinflammatory cytokines and the gut ecosystem. *Front. Pharmacol.* 11:955. doi: 10.3389/fphar.2020.00955

Lin, X., Shao, T., Wen, X., Wang, M., Wen, C., and He, Z. (2020b). Combined effects of MSU crystals injection and high fat-diet feeding on the establishment of a gout model in C57BL/6 mice. *Adv. Rheumatol.* 60:52. doi: 10.1186/s42358-020-00155-3

Lou, X. J., Wang, Y. Z., Lei, S. S., He, X., Lu, T. T., Zhan, L. H., et al. (2020). Beneficial effects of macroporous resin extract of *Dendrobium candidum* leaves in rats with hyperuricemia induced by a high-purine diet. *Evid. Based Complement. Alternat. Med.* 2020:3086106. doi: 10.1155/2020/3086106

Ma, W., Zhou, L., Li, Y., Xia, D., Chen, J., Chen, J., et al. (2021). Persistent purine metabolic abnormality induces the aggravation of visceral inflammation and intestinal microbiota dysbiosis in Magang goose. *Front Vet. Sci.* 8:737160. doi: 10.3389/fvets.2021.737160

Matsumoto, M., Suganuma, H., Ozato, N., Shimizu, S., Katashima, M., Katsuragi, Y., et al. (2021). Association between serum concentration of carotenoid and visceral fat. *Nutrients* 13:912. doi: 10.3390/nu13030912

Mu, H., Zhou, Q., Yang, R., Zeng, J., Li, X., Zhang, R., et al. (2020). Naringin attenuates high fat diet induced non-alcoholic fatty liver disease and gut bacterial dysbiosis in mice. *Front. Microbiol.* 11:585066. doi: 10.3389/fmicb.2020.585066

Mullin, G. E. (2010). Search for the optimal diet. *Nutr. Clin. Pract.* 25, 581–584. doi: 10.1177/0884533610385705

O'Hara, A. M., and Shanahan, F. (2006). The gut flora as a forgotten organ. *EMBO Rep.* 7, 688–693. doi: 10.1038/sj.embor.7400731

Onakpoya, I., Spencer, E., Heneghan, C., and Thompson, M. (2014). The effect of green tea on blood pressure and lipid profile: a systematic review and

meta-analysis of randomized clinical trials. *Nutr. Metab. Cardiovasc. Dis.* 24, 823–836. doi: 10.1016/j.numecd.2014.01.016

Rees, F., Hui, M., and Doherty, M. (2014). Optimizing current treatment of gout. *Nat. Rev. Rheumatol.* 10, 271–283. doi: 10.1038/nrrheum.2014.32

Roddy, E., and Doherty, M. (2010). Epidemiology of gout. *Arthritis Res. Ther.* 12:223. doi: 10.1186/ar3199

Ruiz-Miyazawa, K. W., Staurengo-Ferrari, L., Mizokami, S. S., Domiciano, T. P., Vicentini, F., Camilios-Neto, D., et al. (2017). Quercetin inhibits gout arthritis in mice: induction of an opioid-dependent regulation of inflammasome. *Inflammopharmacology* doi: 10.1007/s10787-017-0356-x [Epub ahead of print].

Scott, K. P., Gratz, S. W., Sheridan, P. O., Flint, H. J., and Duncan, S. H. (2013). The influence of diet on the gut microbiota. *Pharmacol. Res.* 69, 52–60. doi: 10.1016/j.phrs.2012.10.020

Seedorf, H., Griffin, N. W., Ridaura, V. K., Reyes, A., Cheng, J., Rey, F. E., et al. (2014). Bacteria from diverse habitats colonize and compete in the mouse gut. *Cell* 159, 253–266. doi: 10.1016/j.cell.2014.09.008

Shao, T., Shao, L., Li, H., Xie, Z., He, Z., and Wen, C. (2017). Combined signature of the fecal microbiome and metabolome in patients with gout. *Front. Microbiol.* 8:268. doi: 10.3389/fmicb.2017.00268

Shete, V., and Quadro, L. (2013). Mammalian metabolism of β-carotene: gaps in knowledge. *Nutrients* 5, 4849–4868. doi: 10.3390/nu5124849

Singh, R. P. (2019). Glycan utilisation system in *Bacteroides* and Bifidobacteria and their roles in gut stability and health. *Appl. Microbiol. Biotechnol.* 103, 7287–7315. doi: 10.1007/s00253-019-10012-z

So, A. K., and Martinon, F. (2017). Inflammation in gout: mechanisms and therapeutic targets. *Nat. Rev. Rheumatol.* 13, 639–647. doi: 10.1038/nrrheum.2017.155

Vieira, A. T., Macia, L., Galvão, I., Martins, F. S., Canesso, M. C., Amaral, F. A., et al. (2015). A role for gut microbiota and the metabolite-sensing receptor GPR43 in a murine model of gout. *Arthritis Rheum.* 67, 1646–1656. doi: 10.1002/art.39107

Wang, J., Li, P., Liu, S., Zhang, B., Hu, Y., Ma, H., et al. (2020). Green tea leaf powder prevents dyslipidemia in high-fat diet-fed mice by modulating gut microbiota. *Food Nutr. Res.* 64:3672. doi: 10.29219/fnr.v64.3672

Wang, Y., Xing, J., and Chen, H. (2017). Progress in metabolic engineering of β-carotene synthesis. *Sheng Wu Gong Cheng Xue Bao* 33, 578–590. doi: 10.13345/j.cjb.160356

Wen, X., Lou, Y., Song, S., He, Z., Chen, J., Xie, Z., et al. (2021). Qu-Zhuo-Tong-bi decoction alleviates gouty arthritis by regulating butyrate-producing bacteria in mice. *Front. Pharmacol.* 11:610556. doi: 10.3389/fphar.2020.610556

Wexler, H. M. (2007). Bacteroides: the good, the bad, and the nitty-gritty. *Clin. Microbiol. Rev.* 20, 593–621. doi: 10.1128/CMR.00008-07

Xing, S. C., Meng, D. M., Chen, Y., Jiang, G., Liu, X. S., Li, N., et al. (2015). Study on the diversity of *Bacteroides* and *Clostridium* in patients with primary gout. *Cell Biochem. Biophys.* 71, 707–715. doi: 10.1007/s12013-014-0253-5

Yang, G., Lee, H. E., Moon, S. J., Ko, K. M., Koh, J. H., Seok, J. K., et al. (2020). Direct binding to NLRP3 pyrin domain as a novel strategy to prevent NLRP3-driven inflammation and gouty arthritis. *Arthritis Rheum.* 72, 1192–1202. doi: 10.1002/art.41245

Yang, Y. J., Sheu, B. S., Yang, H. B., Lu, C. C., and Chuang, C. C. (2012). Eradication of *Helicobacter pylori* increases childhood growth and serum acylated ghrelin levels. *World J. Gastroenterol.* 18, 2674–2681. doi: 10.3748/wjg.v18.i21.2674

Conflict of Interest: The authors declare that the research was conducted in the absence of any commercial or financial relationships that could be construed as a potential conflict of interest.

Publisher's Note: All claims expressed in this article are solely those of the authors and do not necessarily represent those of their affiliated organizations, or those of the publisher, the editors and the reviewers. Any product that may be evaluated in this article, or claim that may be made by its manufacturer, is not guaranteed or endorsed by the publisher.

frontiers in Microbiology

ORIGINAL RESEARCH
published: 10 February 2022
doi: 10.3389/fmicb.2021.811272

Alteration of Porcine Intestinal Microbiota in Response to Dietary Manno-Oligosaccharide Supplementation

*En Yu[1,2], Daiwen Chen[1,2], Bing Yu[1,2], Zhiqing Huang[1,2], Xiangbing Mao[1,2], Ping Zheng[1,2], Yuheng Luo[1,2], Heng Yin[3], Jie Yu[1,2], Junqiu Luo[1,2], Hui Yan[1,2] and Jun He[1,2]**

[1] Institute of Animal Nutrition, Sichuan Agricultural University, Chengdu, China, [2] Key Laboratory of Animal Disease-Resistant Nutrition, Chengdu, China, [3] Dalian Institute of Chemical Physics, Chinese Academy of Sciences, Dalian, China

Manno-oligosaccharide (MOS) is a prebiotic derived from natural plants or yeasts. Here, we explored the response of intestinal microbiota and epithelial functions after ingestion of MOS in a porcine model. Sixteen pigs were randomly assigned into two treatments and fed with basal or MOS-containing (0.3% MOS) diet for 21 days. Results showed that MOS supplementation increased the cecal acetate content and ileal 16S rRNA gene copies ($p < 0.05$). Importantly, MOS decreased the abundance of phylum Proteobacteria in cecal digesta ($p < 0.05$). Moreover, MOS elevated the expression level of SCL5A8 and GPR109A but decreased the expression levels of HDAC1 and TNF-α in the ileal and cecal mucosa ($p < 0.05$). MOS upregulated the expression levels of tight-junction protein (ZO-1, claudin-1, and occludin) and IGF-1 in the ileum and cecum ($p < 0.05$). This study presents the alteration of intestinal microbiota composition and intestinal barrier function after MOS administration, and facilitates our understanding of the mechanisms behind the dietary MOS-modulated intestinal microbiota and health.

Keywords: manno-oligosaccharide, weaned pigs, intestinal microbiota, microbial metabolites, intestinal health

OPEN ACCESS

Edited by:
Xiaodong Xia,
Dalian Polytechnic University, China

Reviewed by:
Geetha Samak,
DVS College of Arts and Science, India
Jinming You,
Jiangxi Agricultural University, China

***Correspondence:**
Jun He
hejun8067@163.com

Specialty section:
This article was submitted to Food Microbiology, a section of the journal Frontiers in Microbiology

Received: *08 November 2021*
Accepted: *17 December 2021*
Published: *10 February 2022*

Citation:
Yu E, Chen D, Yu B, Huang Z, Mao X, Zheng P, Luo Y, Yin H, Yu J, Luo J, Yan H and He J (2022) Alteration of Porcine Intestinal Microbiota in Response to Dietary Manno-Oligosaccharide Supplementation. Front. Microbiol. 12:811272. doi: 10.3389/fmicb.2021.811272

INTRODUCTION

Oligosaccharides are composed of monosaccharide units (2–20) with low molecular weight and low degree of polymerization, which have been looked as prebiotics because of their beneficial effects on intestinal microbiota (Delzenne, 2003; Mussatto and Mancilha, 2007). Oligosaccharides are resistant to digestion in the upper intestinal tract, but can be fermented by certain microorganisms in large bowel to produce short-chain fatty acids (SCFAs) (Garro et al., 2004; Mussatto and Mancilha, 2007; Quintero-Villegas, 2014). A previous study indicated that oligosaccharide-derived SCFAs not only promoted proliferation and differentiation of the intestinal epithelial cells (Blottier et al., 1999) but also promoted the growth of beneficial microorganisms such as *Bifidobacterium* and *Lactobacillus* species (He et al., 2021). Manno-oligosaccharide (MOS) is a non-digestible oligosaccharide isolated from sugar polymers present in the cell wall of yeast, which is composed of glucose and mannose units through β-1,4 glycosidic bonds (Yu et al., 2020). Owing to MOS's special structures similar to the surface of intestinal mucosal (mannose), it may act as a guardian in the intestinal tract under subclinical infection (PC et al., 2000; Miguel et al., 2004). The health benefits of oligosaccharides have long been appreciated, and a diet containing MOS has been reported to increase the abundance of beneficial bacteria, enhance individual immunity, and maintain the

intestinal epithelium integrity of poultry and pigs (Baurhoo et al., 2007; Castillo et al., 2008; Che et al., 2011).

Intestinal microbiota plays a vital role in maintaining intestinal homeostasis of humans and animals (Ma et al., 2017; Shi et al., 2017). However, the gastrointestinal tract of the fetus is sterile; therefore, early colonization of the infant gastrointestinal tract is crucial for the overall health of the infant (Wall et al., 2009; O'Toole and Claesson, 2010). Besides, intestinal microbiota is dynamic and easily affected by various factors (physiological and environmental); dietary strategies are effective approaches to modulate the composition of the intestinal microbiota for maintaining host health (Wan et al., 2020). A study revealed that dietary supplementation with prebiotics has a positive effect on enteric microbiota by selectively promoting growth of beneficial bacteria (Wall et al., 2009).

This study aimed to investigate the alteration of porcine intestinal microbiota in response to dietary MOS supplementation in weaned pigs. Pig is one of the excellent used model animals in biomedical studies, which has high similarity with humans involved in anatomy, genetics, and physiology (Meurens et al., 2011). Our study will be helpful to understand the mechanisms underlying the positive effect of MOS on modulating gut health.

MATERIALS AND METHODS

Studies involving animals were conducted according to the Regulations for the Administration of Affairs Concerning Experimental Animals (Ministry of Science and Technology, China, revised in June 2004). Sample collection was approved by the Institutional Animal Care and Use Committee of Sichuan Agricultural University, Sichuan, China (No. 20181105).

Animal Housing and Sample Collection

Sixteen crossbred (Duroc × Landrace × Yorkshire) weaned pigs with an average initial body weight of 6.48 ± 0.14 kg were randomly allocated to two groups (n = 8). Pigs were kept individually and fed with a basal diet (BD) or BD containing 0.3% MOS. The diets (**Supplementary Table 1**) were formulated to meet the nutrient recommendations of the National Research Council 2012, and the chemical composition of the diet was analyzed using the AOAC method. Pigs were fed *ad libitum* and given free access to water. After 21 days, pigs were sacrificed by exsanguination under deep anesthesia *via* intravenous injection of sodium pentobarbital (200 mg/kg BW), and the intestinal tissues and mucosa samples were collected immediately. In addition, approximately 4 g digesta from the middle section of the ileum and cecum was transferred into sterile tubes and immediately frozen at −80°C for analysis of the SCFA concentration and the bacterial community.

Metabolite Concentrations in Colonic Contents

The SCFA (acetic acid, propionic acid, and butyric acid) concentrations were determined using a gas chromatograph system (VARIAN CP-3800, Varian, Palo Alto. CA, United States; capillary column 30 m × 0.32 mm × 0.25 μm film thickness) following the previous method (Franklin et al., 2002). After vortex, the digesta was centrifuged at 4°C for 10 min (12,000 × g), and the supernatant (1 ml) was then transferred into an Eppendorf tube (2 ml) and mixed with 0.2 ml metaphosphoric acid. After 30 min of incubation at 4°C, the tubes were centrifuged at 4°C for 10 min (12,000 × g) and aliquots of the supernatant (1 μl) were analyzed using the GC with a flame ionization detector and an oven temperature of 100–150°C. The polyethylene glycol column was operated with highly purified N_2 as the carrier gas at 1.8 ml/min.

Measurements of the Cecal Digesta pH Values

Immediately after the pigs were killed, approximately 5 g of digesta was collected into the ice-bathed sterile centrifugal tube, and then the pH value of each sample was determined using a PHS-3C pH meter (Shanghai, China).

Analysis of the Bacterial Community

Nucleic acids were extracted from 0.5 g of digesta sample using the Stool DNA kit (TIANGEN, China) according to the manufacturer's instructions. Quantitative Insights Into Microbial Ecology (QIIME) software package was used to analyze the diversity and composition of the bacterial community of these samples (Caporaso et al., 2010). PCR amplifications were used to amplify the V3–4 region of the 16S rRNA gene; the primer sequences used the 515F/806R primer set (341F: 5′-CCTAYGGGRBGCASCAG-3′; 806R: 5′-GGACTACNNGGGTATCTAAT-3′). The amplification procedures were based on a previously published protocol (Caporaso et al., 2011). Briefly, the PCR conditions used were 5 min at 95°C, 35 cycles of 30 s at 94°C, 30 s at 55°C, and 90 s at 72°C, followed by 10 min at 72°C. Amplification was carried out using a Verity Thermocycler (Applied Biosystems). The PCR products derived from amplification of specific 16S rRNA gene hypervariable regions were purified by electrophoretic separation on a 1.5% agarose gel and the use of a Wizard SV Gen PCR Clean-Up System (Promega), followed by a further purification step involving the Agencourt AMPure XP DNA purification beads (Beckman Coulter Genomics GmbH, Bernried, Germany) to remove primer dimers. The sequencing was conducted on an Illumina MiSeq 2000 platform (Personal Biotechnology, Shanghai).

Pairs of reads from the original DNA fragments were merged using Fast Length Adjustment of Short reads (FLASH) (Magoč and Salzberg, 2011), which can quickly and accurately merge the paired-end reads. Sequencing reads were assigned to each sample based on the unique barcode. Sequences were analyzed with the QIIME software package and UPARSE pipeline (Edgar, 2013), in addition to custom Perl scripts to analyze alpha (within sample) and beta (between sample) diversity. UPARSE was used to pick operational taxonomic units (OTUs). Sequences were assigned to OTUs using 97% species-level sequence identity. The first sequence assigned to each OTU was used as the reference sequence for that OTU field. RDP classifier was used to assign

taxonomic data to each representative sequence (Wang et al., 2007). Rarefaction curves were generated by using QIIME, and this software was also used to calculate both weighted and unweighted UniFrac for principal coordinate analysis (PCoA) and unweighted pair group method with arithmetic mean (UPGMA) clustering.

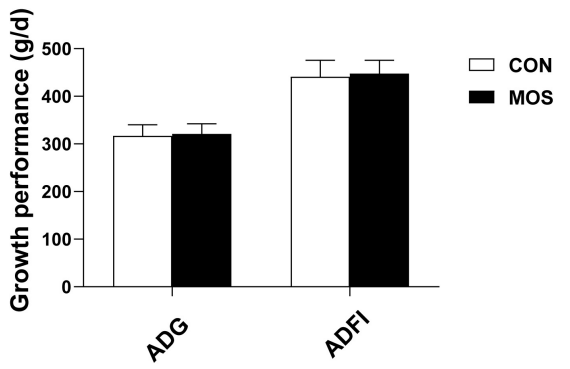

FIGURE 1 | Effects of MOS on growth performance of weaned pigs. ADG means average daily gain; ADFI means average daily feed intake.

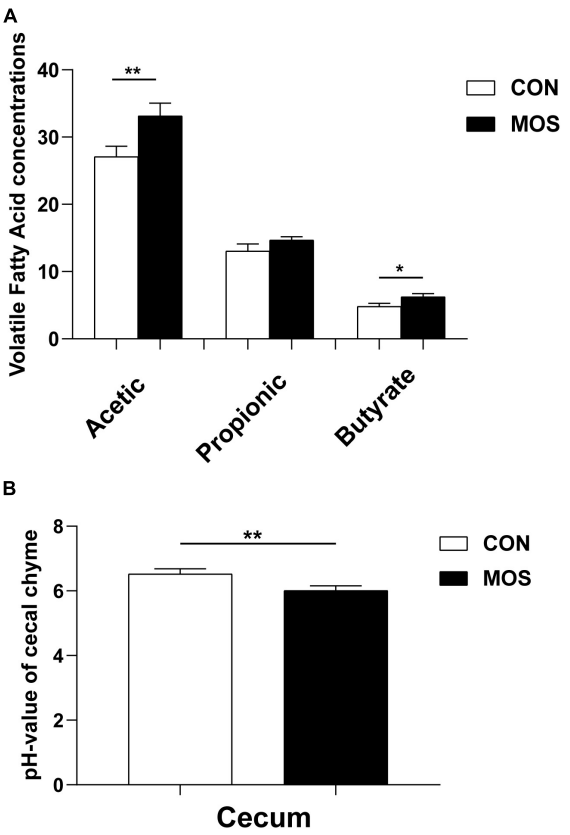

FIGURE 2 | Effects of MOS on microbial metabolites (VFA) **(A)** and pH values **(B)** of cecal digesta. Digesta samples were collected from pigs fed with the basal diet (CON) or a basal diet supplemented with 3 g/kg MOS (MOS) (n = 8). $^{**}p < 0.05$, $^{*}0.05 < p < 0.1$.

RNA Isolation, Reverse Transcription, and Real-Time Quantitative PCR

The frozen intestinal mucosa samples (about 0.1 g) were ground in liquid nitrogen and homogenized in 1 ml of RNAiso Plus (Takara Biotechnology Co., Ltd., Dalian, China) to extract total RNA following the manufacturer's instructions, and the purity and concentration of total RNA were detected by using a spectrophotometer (NanoDrop 2000; Thermo Fisher Scientific, Inc., Waltham, MA, United States); samples in which OD_{260}/OD_{280} ratio ranged from 1.8 to 2.0 were deemed appropriate. Subsequently, a volume equivalent to 1 μg total RNA from each duodenal, jejunal, and ileal sample was used for reverse transcription into cDNA, which is based on the protocol of PrimeScript RT reagent kit with gDNA Eraser (Takara Biotechnology Co., Ltd.). This process consists of two steps: I, 37°C for 15 min; II, 85°C for 5 s.

The expression level of the target gene [G protein-coupled receptor 41 (GPR41), GPR43, GPR109A, sodium-couple monocarboxylate transporter 1 (SLC5A8), histone deacetylase 1 (HDAC1), HDAC2, HDAC3, IL-1β, IL-10, TNF-α, NF-κB, ZO-1, zonula occludens-1, occludin, claudin-1, insulin-like growth factor (IGF-1), glucagon-like peptide (GLP-2), epidermal growth factor (EGF)] in intestinal mucosa was quantified using q-PCR, and the oligonucleotide primer sequences used in qPCR are presented in **Supplementary Table 2**. qPCR was performed

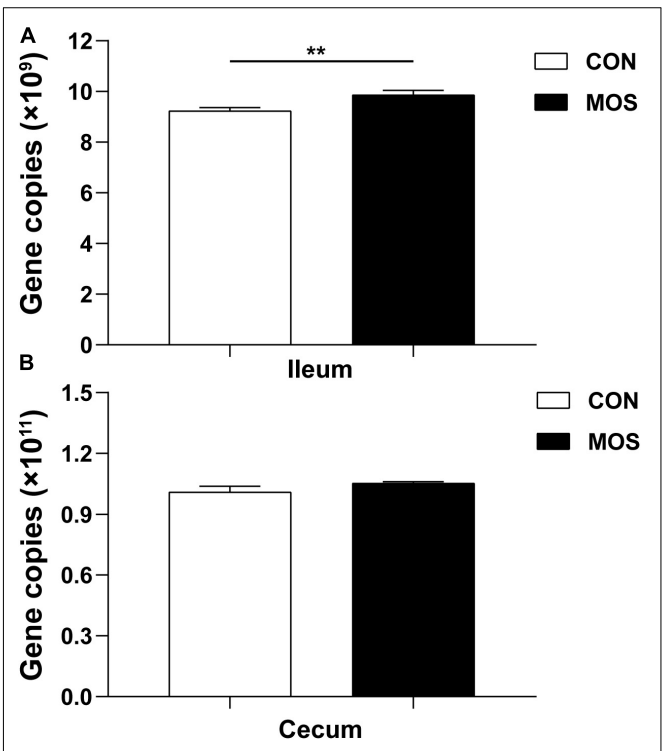

FIGURE 3 | Quantitative PCR analysis of 16S rRNA gene copy numbers in the intestinal digesta. Ileum **(A)** and cecum **(B)** digesta samples were collected from pigs fed with the basal diet (CON) or a basal diet supplemented with 3 g/kg MOS (MOS) (n = 8). $^{**}p < 0.05$.

with the SYBR Green PCR I PCR reagents (Takara Bio Inc., Dalian, China) using a CFX96 Real-Time PCR Detection System (Bio-Rad Laboratories, Hercules, CA, United States). All cDNA samples were detected in triplicate. The reaction mixture (10 μl) contained 5 μl SYBR Premix Ex Taq II (Tli RNaseH Plus), 0.5 μl forward primer, 0.5 μl reverse primer, 1 μl cDNA, and 3 μl RNase-free water. The protocol used in qPCR was as follows: 95°C for 30 s, followed by 40 cycles at 95°C for 5 s and 58°C for 34 s. The generated gene-specific amplification products were confirmed by melting curve analysis after each real-time quantitative PCR assay. The housekeeping gene β-actin was used to standardize the mRNA expression level of target genes, which was calculated based on the $2^{-\Delta\Delta Ct}$ method (Fleige et al., 2006).

RESULTS

Effect of Dietary Manno-Oligosaccharide Supplementation on Growth Performance and Microbial Metabolites

Figure 1 shows that MOS has no effect on growth performance of weaned pigs, and **Figure 2** reveals the effects of MOS

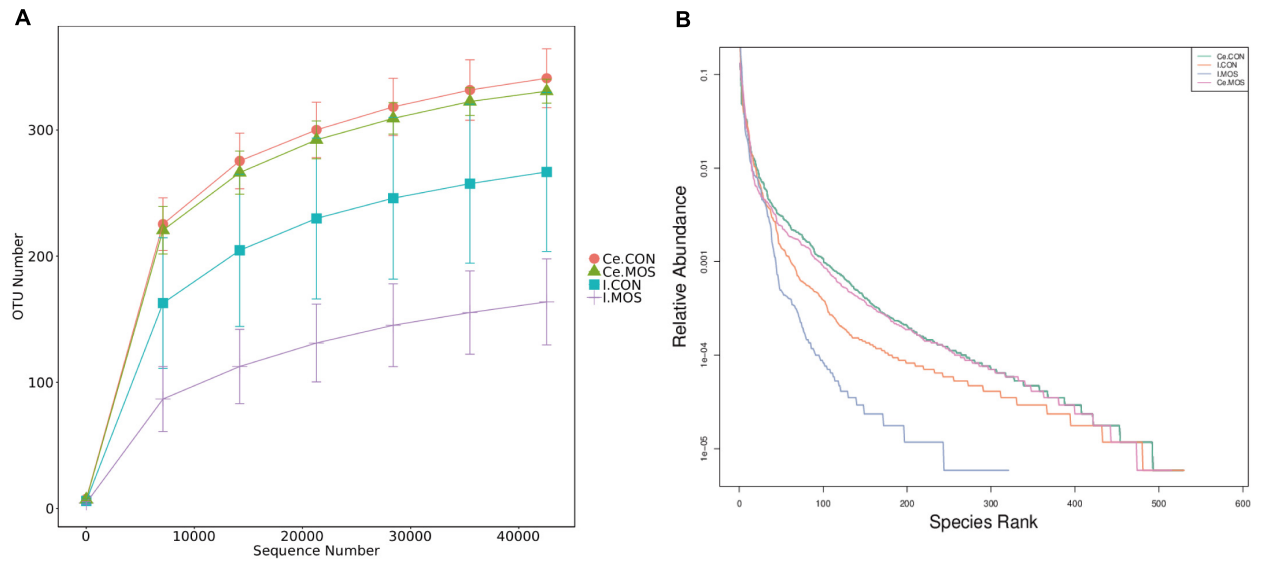

FIGURE 4 | Rarefaction **(A)** and rank–abundance **(B)** curves. I.CON means ileal digesta samples from pigs fed with the basal diet. I.MOS means ileal digesta samples from pigs fed with a basal diet supplemented with 3 g/kg MOS; Ce.CON means cecal digesta samples from pigs fed with the basal diet; Ce.MOS means cecal digesta samples from pigs fed with a basal diet supplemented with 3 g/kg MOS (n = 4).

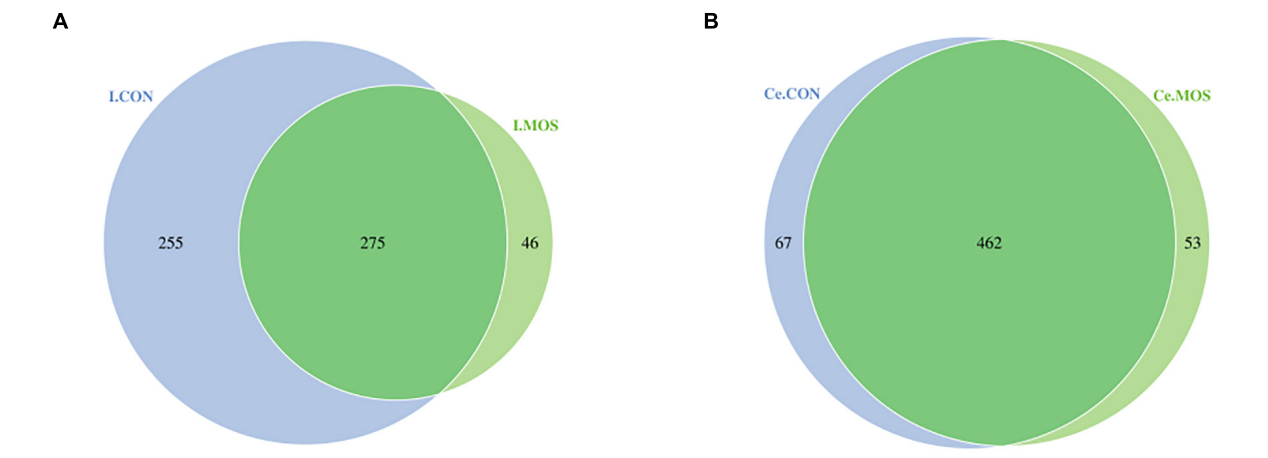

FIGURE 5 | Number of identified OTUs in various comparisons. **(A)** Venn diagram shows various comparisons of ileal OTUs at the genus level; **(B)** Venn diagram shows various comparisons of cecal OTUs at the genus level. I.MOS means ileal digesta samples from pigs fed with a basal diet supplemented with 3 g/kg MOS; Ce.CON means cecal digesta samples from pigs fed with the basal diet; Ce.MOS means cecal digesta samples from pigs fed with a basal diet supplemented with 3 g/kg MOS. For 16S rRNA analysis, two digesta samples in each group were pooled (n = 4).

supplementation on the SCFA content (A) and pH value of cecal digesta. Dietary MOS supplementation significantly increased the acetate content in cecal digesta compared with CON group ($p < 0.05$). Besides, MOS tended to increase the butyrate content in the cecal digesta ($p > 0.05$). Moreover, MOS significantly decreased the pH value (**Figure 2**) in the cecal digesta ($p < 0.05$).

Effect of Dietary Manno-Oligosaccharide Supplementation on Total 16S rRNA Gene Copies in the Ileum and Cecum

The 16S rRNA gene copies were determined using quantitative PCR, and equal volumes of the purified DNA of all samples were used in the assay. **Figure 3** shows that the average copy

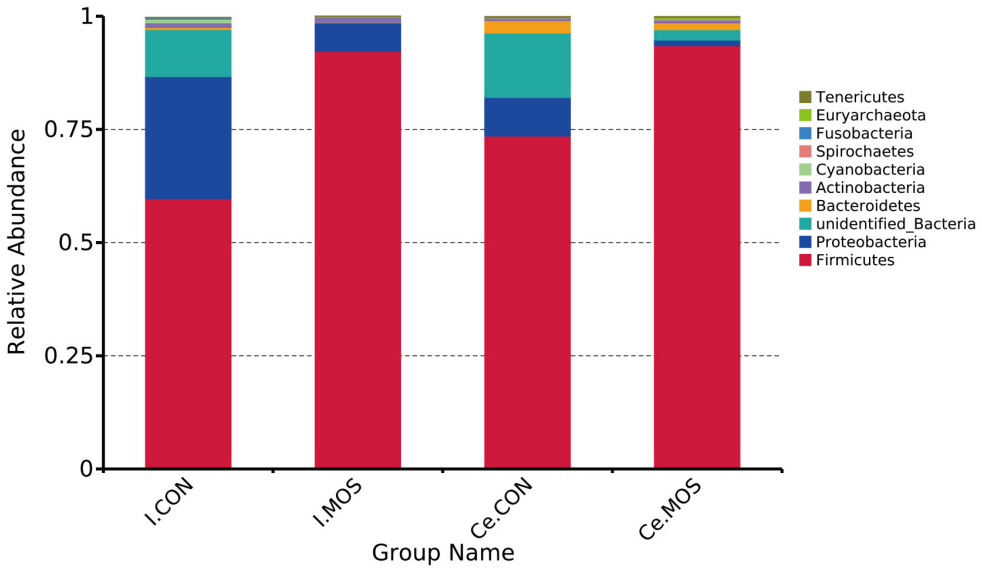

FIGURE 6 | Bar graph shows the phylum level composition of bacteria. Color-coded bar plot shows the relative abundance of bacterial phyla across the different groups. I.MOS means ileal digesta samples from pigs fed with a basal diet supplemented with 3 g/kg MOS; Ce.CON means cecal digesta samples from pigs fed with the basal diet; Ce.MOS means cecal digesta samples from pigs fed with a basal diet supplemented with 3 g/kg MOS. For 16S rRNA analysis, two digesta samples in each group were pooled ($n = 4$).

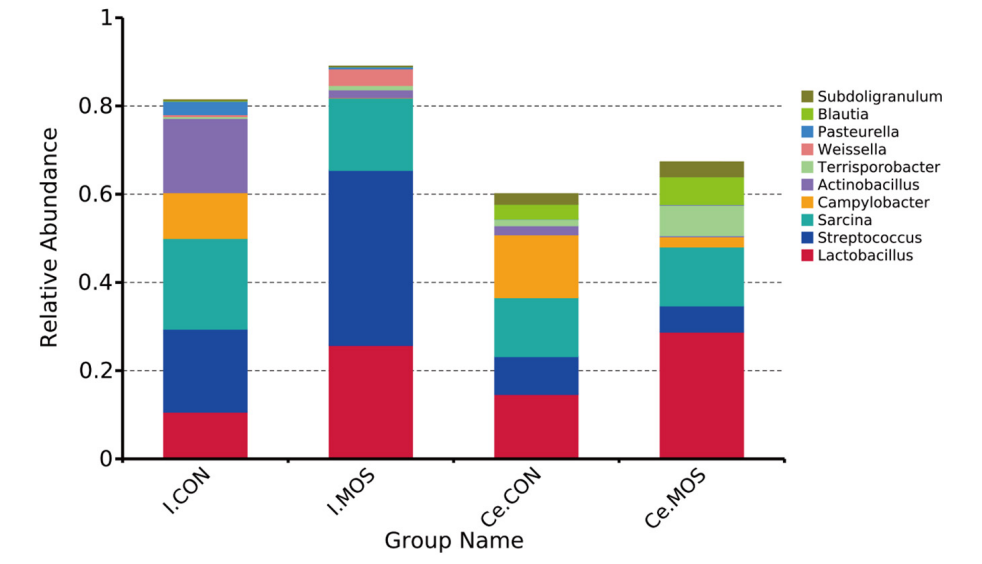

FIGURE 7 | Bar graph shows the genus-level composition of bacteria. Color-coded bar plot shows the relative abundance of bacterial phyla across the different groups. I.MOS means ileal digesta samples from pigs fed with a basal diet supplemented with 3 g/kg MOS; Ce.CON means cecal digesta samples from pigs fed with the basal diet; Ce.MOS means cecal digesta samples from pigs fed with a basal diet supplemented with 3 g/kg MOS. For 16S rRNA analysis, two digesta samples in each group were pooled ($n = 4$).

number in the cecal samples was higher than in the ileal samples. Dietary MOS supplementation had no significant influence on the total 16S rRNA gene copies in the cecal digesta. However, MOS significantly elevated the total 16S rRNA gene copies in the ileal digesta ($p < 0.05$).

Effect of Dietary Manno-Oligosaccharide Supplementation on Bacterial Community Structures

16S rRNA sequencing was used to compare digest samples based on the proportions of bacterial lineages in each specimen. Equal volumes of the purified DNA from each sample were amplified by PCR using bar-coded primers flanking the V3–4 region of the 16S rRNA gene, and samples were sequenced using the Illumina method. All sequencing information has been deposited in the National Center for Biotechnology Information (NCBI) and can be accessed in the Sequence Read Archive (SRA) under the accession number PRJNA768244. The rarefaction and rank–abundance curves directly indicated that the depth and the degree of evenness of sampling were adequate to assess the bacterial communities (**Figures 4A,B**). For the ileal samples, 46 OTUs were unique in the MOS group, whereas 255 OTUs were specifically identified in the CON group. A total of 275 OTUs were shared between two groups (**Figure 5A**). For cecal samples, 67 OTUs and 53 OTUs were specifically identified in the CON and MOS groups, respectively. Besides, the two groups shared 462 common OTUs (**Figure 5B**). In general, the number of OTUs identified in the cecum was higher than in the ileum.

We determined the similarity of microbiota communities by PCoA based on weighted UniFrac distance metrics

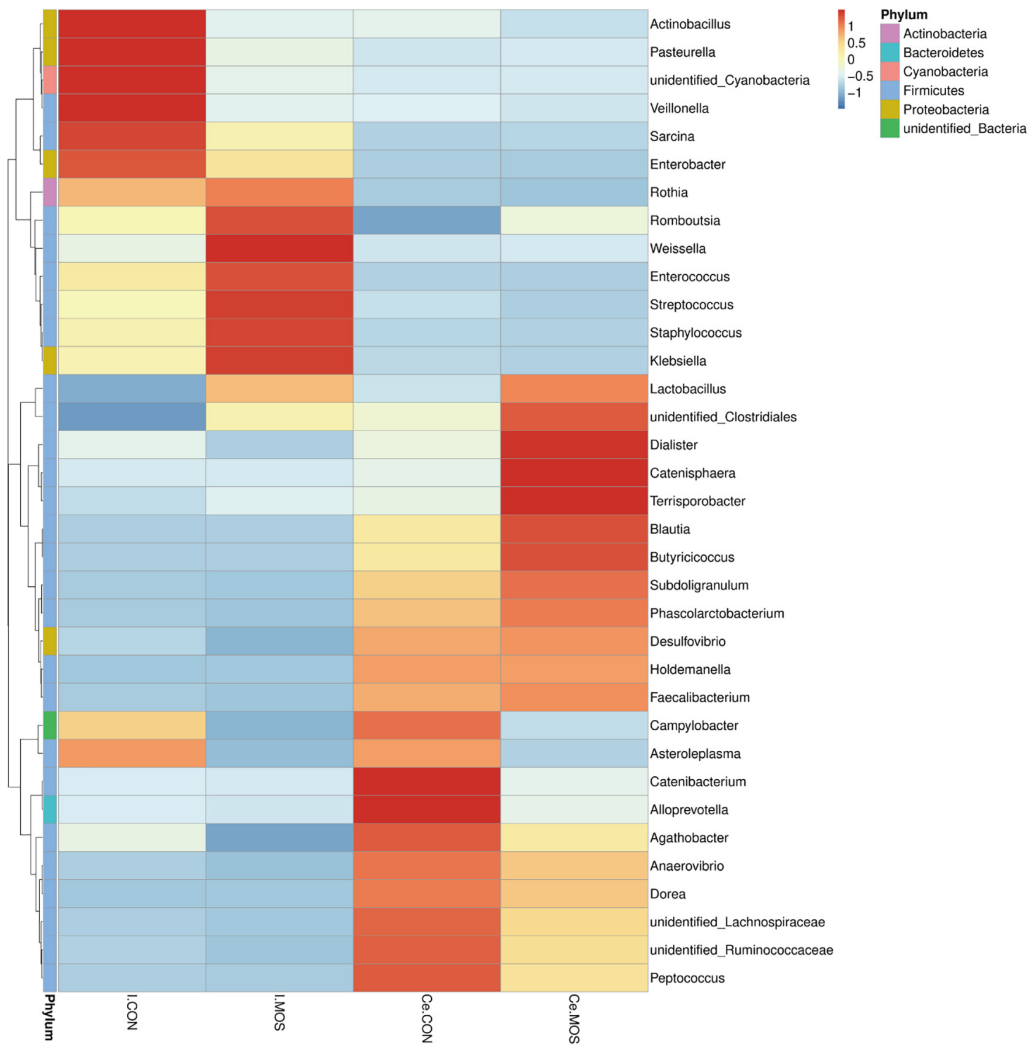

FIGURE 8 | Heatmap distribution of OTUs at phylum level. OTUs were arranged in rows and are clustered on the vertical axis. Samples are arranged vertically and are on the horizontal axis. Different colors indicate the relative abundance of taxons. I.MOS means ileal digesta samples from pigs fed with a basal diet supplemented with 3 g/kg MOS; Ce.CON means cecal digesta samples from pigs fed with the basal diet; Ce.MOS means cecal digesta samples from pigs fed with a basal diet supplemented with 3 g/kg MOS. For 16S rRNA analysis, two digesta samples in each group were pooled ($n = 4$).

(**Supplementary Figure 1**). The ileal microbiota from the MOS and CON groups was divided into disparate parts that were distinct in the PCoA. However, the cecal microbiota did not show significant differences between the two groups. In this study, all the qualified sequences from ileal and cecal samples were assigned to 18 and 16 known phyla, respectively. The relative abundant distribution of the top 10 intestinal bacterial at phylum and genus level between two groups of ileum and cecum are presented in **Figures 6**, **7**. Firmicutes (92.28%) is the predominant phyla identified in the MOS group, whereas Proteobacteria (26.95%) is the predominant phyla identified in the CON group of ileal samples. Similarly, Firmicutes (93.54%) is the predominant phyla identified in the MOS group of cecal samples (**Figure 6** and **Supplementary Table 3**). Compared with the CON group, MOS supplementation tends to elevate the abundance of Firmicutes ($p > 0.05$) in ileal and cecal samples, but significantly decreased the abundance of Proteobacteria ($p < 0.05$) in the cecal samples at phylum level. Furthermore, at genus level (**Figure 7** and **Supplementary Table 4**), *Lactobacillus* is the predominant genera in ileal (25.78%) and cecal (28.80%) samples of MOS group. MOS supplementation tends to elevate the *Blautia* abundance in cecal samples but decreased *Actinobacillus* in ileal samples ($p > 0.05$).

All sequences filtered from the ileal and cecal samples were assigned to 35 known genera and 20 known phyla (**Figures 8**, **9** and **Supplementary Tables 5, 6**). The heatmap exhibits the abundance of the selected genera and phyla across the samples, which directly revealed the significant differences in the phylum distribution between the CON and MOS groups (**Figures 8**, **9**). **Figure 9** (**Supplementary Table 6**) shows that dietary MOS supplementation significantly decreased the abundance of cecal Proteobacteria at phylum level ($p < 0.05$), but tends to elevate the abundance of ileal and cecal Firmicutes ($p > 0.05$).

Effect of Dietary Manno-Oligosaccharide Supplementation on Expression Levels of GPRs, HDACs, and Inflammatory-Related Genes

As shown in **Figure 10**, dietary MOS supplementation significantly elevated the expression level of SCL5A8 and GPR109A in the ileal and cecal mucosa ($p < 0.05$). Nevertheless, MOS not only significantly decreased the expression levels of HDAC1 and TNF-α expression levels in the ileal mucosa ($p < 0.05$) but also downregulated HDAC1, TNF-α, and NF-κB expression level in cecal mucosa ($p < 0.05$). Moreover, MOS tended to elevate the expression level of IL-10 in the ileal and cecal mucosa ($p > 0.05$).

Effect of Dietary Manno-Oligosaccharide Supplementation on Expression Levels of Critical Genes Related to Intestinal Barrier Functions

As shown in **Figure 11**, dietary MOS supplementation significantly elevated the expression levels of tight-junction proteins (ZO-1, claudin-1, and occludin) in the ileum and cecum

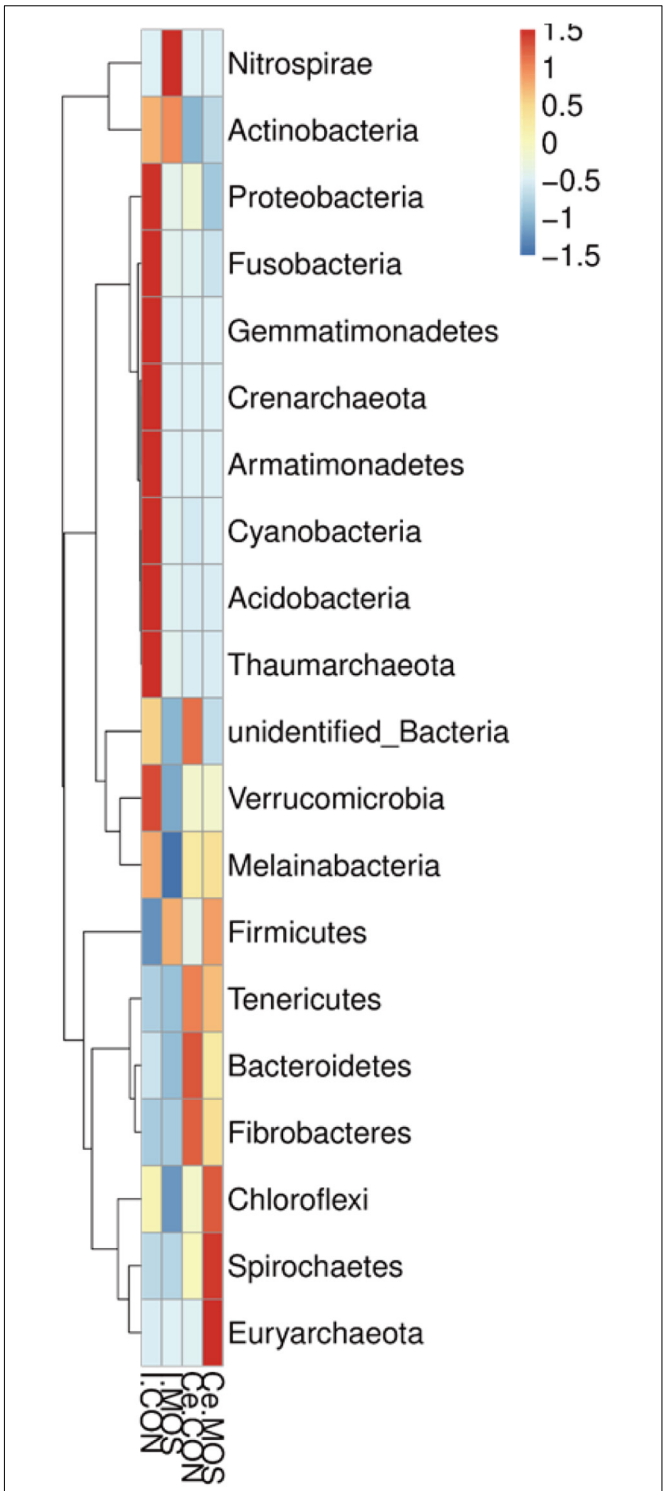

FIGURE 9 | Heatmap distribution of OTUs at genus level. OTUs were arranged in rows and are clustered on the vertical axis. Samples are arranged vertically and are on the horizontal axis. Different colors indicate the relative abundance of taxons. I.MOS means ileal digesta samples from pigs fed with a basal diet supplemented with 3 g/kg MOS; Ce.CON means cecal digesta samples from pigs fed with the basal diet; Ce.MOS means cecal digesta samples from pigs fed with a basal diet supplemented with 3 g/kg MOS. For 16S rRNA analysis, two digesta samples in each group were pooled ($n = 4$).

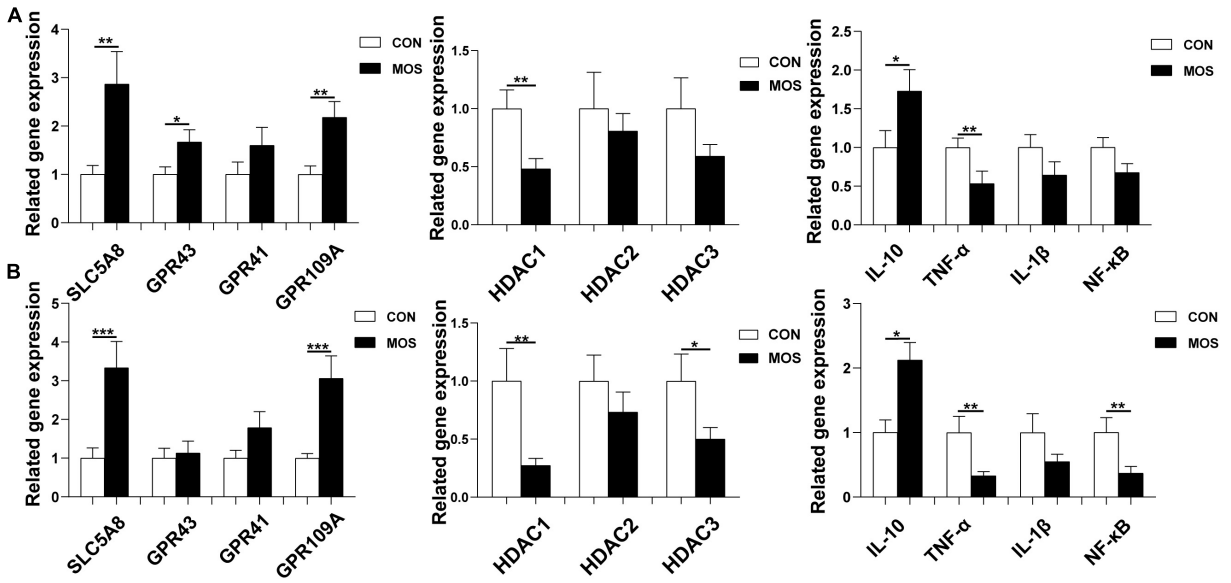

FIGURE 10 | Effect of MOS on expression levels of GPRs, HDACs, and inflammatory cytokines. Ileum **(A)** and cecum **(B)** digesta samples were collected from pigs fed with the basal diet (CON) or a basal diet supplemented with 3 g/kg MOS (MOS) ($n = 8$). *$0.05 < p < 0.1$; **$p < 0.05$, ***$p < 0.01$.

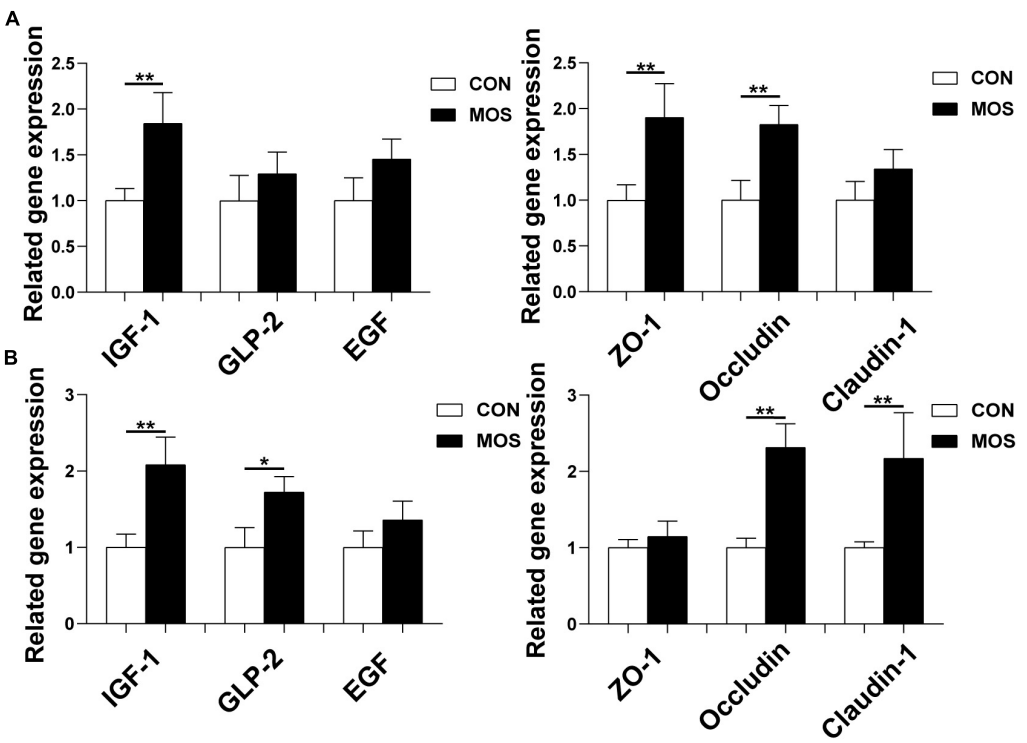

FIGURE 11 | Effect of MOS on expression levels of genes related to intestinal barrier functions. Ileum **(A)** and cecum **(B)** digesta samples were collected from pigs fed with the basal diet (CON) or a basal diet supplemented with 3 g/kg MOS (MOS) ($n = 8$). *$0.05 < p < 0.1$, **$p < 0.05$.

($p < 0.05$). Besides, MOS significantly elevated the expression level of IGF-1 in the ileum and cecum ($p < 0.05$). Moreover, MOS supplementation tended to elevate the expression level of GLP-2 in cecum ($p > 0.05$).

DISCUSSION

Gut microbiota refers to the complex community of microorganisms residing in or passing through the GI tract,

which plays an indispensable role in metabolic, physiological, and immunological processes in the body (Gerritsen et al., 2011). Previous studies have shown that oligosaccharides had dramatic influences on modulating the dysbiosis of the gut microbiota composition (Mitsuoka et al., 1987; Yang et al., 2008; Wan et al., 2020). In the present study, we explored the effect of dietary MOS on intestinal microbiota using a porcine model and found that MOS did not affect the growth performance of weaned pigs. SCFAs are the main end products of large bowel fermentation, which can serve as an energy source for intestinal epithelium and participate in regulation of cell growth, apoptosis, and various inflammatory responses (Havenaar, 2011; Lin et al., 2011; González-Herrera et al., 2019). Our results showed that dietary MOS supplementation elevated the SCFA content (acetate and butyrate) in the cecum. Previous studies have indicated the beneficial effect of SCFAs on improving glucose tolerance, maintaining the blood glucose homeostasis, and promoting the growth of probiotic bacteria (Puupponen-Pimiä et al., 2005; Yamashita et al., 2007; de Vadder et al., 2014). The elevated SCFA content is consistent with the decreased pH value in cecal digesta upon MOS supplementation. Both results indicated an antimicrobial potential of MOS in promoting the beneficial microbial fermentation in the intestine.

Previous studies suggested that dietary oligosaccharide supplementation significantly elevated the beneficial bacterial diversity in broiler chickens and weaned pigs (Baurhoo et al., 2007; Wan et al., 2020). In the present study, the 16S rRNA gene copy numbers were higher in the cecum than in the ileum, indicating that the large intestine is the main site of microbial fermentation. Interestingly, MOS significantly elevated the total copy numbers of the 16S rRNA gene in the ileum. A previous study indicated that the microbiota has the potential to regulate both the pro- and anti-inflammatory responses, and ecological imbalance in the intestinal flora may promote the development of various inflammatory bowel diseases (Round and Mazmanian, 2009). Firmicutes and Proteobacteria were the two dominant phyla identified in the ileum. The bacteria of phylum Firmicutes are involved in energy resorption (Chen et al., 2019), whereas the Proteobacteria are Gram-negative bacteria that includes numerous pathogenic species such as *Salmonella*, *Campylobacter*, and *Escherichia* (Patel and Pyrsopoulos, 2019). Importantly, high level of Proteobacteria may result in elevation of acetaldehyde, which increases intestinal permeability by disrupting the intestinal epithelium integrity (Arab and Martín-Mateos, 2017). Our result showed that MOS significantly decreased the abundance of Proteobacteria in the cecum, and tended to increase the abundance of Firmicutes in the ileum and cecum.

Actinobacillus species (belonging to the Proteobacteria phylum) are Gram-negative bacteria that can cause fatal pleuropneumonia in pigs (Rycroft and Garside, 2000). Our results showed that dietary MOS supplementation tended to decrease the abundance of *Actinobacillus* in the ileum. *Blautia* is a novel potential target/index against obesity and diabetes (Ozato et al., 2019). Moreover, *Blautia* is one of the most abundant genera in the intestine that can produce SCFAs (butyric acid and acetic acid) (Ozato et al., 2019). In the present study, MOS ingestion tended to elevate the abundance of *Blautia*. All these data suggested that MOS has a beneficial role of in regulating the intestinal microbiota.

Numerous studies indicated that SCFAs play an important role in maintaining gut health (Tan et al., 2014). A previous study indicated that SCFAs not only exert their effects by interacting with G-protein coupled receptors (e.g., FFAR2, FFAR3, OLFR78, and GPR109A) but also can serve as epigenetic regulators through inhibiting the histone deacetylase (HDAC) (Akhlaq, 2020). In the present study, we found that MOS ingestion significantly elevated the SLC5A8 and GPR109A expression level in the ileum and cecum. These results are consistent with the SCFA content, as the acetate and butyrate were found to activate the G protein-coupled receptors (SLC5A8 and GPR109A) (Singh et al., 2010). Interestingly, MOS supplementation decreased the HADC1 expression level, which is consistent with a previous report that butyrate and propionate not only inhibit HDAC but also can alter the expressions of specific genes *via* conformational changes in the active site of HDAC leading to its inactivation (Akhlaq, 2020). Furthermore, MOS decreased the expression levels of TNF-α in the ileum and cecum, indicating an anti-inflammatory potential of the oligosaccharides like with the MOS.

Tight junctions, consisting of cytoplasmic scaffold proteins such as ZO-1, claudins, and occluding, play a critical role in maintaining the intestinal barrier integrity and permeability (Citi and Cordenonsi, 1998; Yu et al., 2020). In the present study, the expression levels of occludin in the ileum and cecum were significantly elevated upon MOS supplementation. Moreover, MOS upregulated the expression of IGF-1 both in the ileum and cecum. IGF-I is a polypeptide hormone produced mainly by the liver in response to the endocrine GH stimulus, but it is also secreted by multiple tissues for autocrine/paracrine purposes (Puche and Castilla-Cortázar Larrea, 2012). Importantly, IGF-I is a trophic factor for the small intestine and exerts trophic effects on bowel mucosa, which showed beneficial effect in stimulating intestinal cell proliferate (Simmons et al., 1995).

CONCLUSION

In summary, our study revealed an alteration of porcine intestinal microbiota in response to dietary MOS supplementation. The altered microbiota and SCFA content may contribute to the changes in inflammatory response and intestinal barrier functions *via* activating G protein-coupled receptor and enhancing the tight junction proteins. Our findings will be also helpful for the understanding of the mechanisms behind the dietary MOS modulating intestinal health.

DATA AVAILABILITY STATEMENT

The datasets presented in this study can be found in online repositories. The names of the repository/repositories

and accession number(s) can be found in the article/ **Supplementary Material**.

ETHICS STATEMENT

The animal study was reviewed and approved by Institutional Animal Care and Use Committee of Sichuan Agricultural University, Sichuan, China (No.20181105).

AUTHOR CONTRIBUTIONS

JH conceived and designed the experiments. EY performed the experiments and wrote the manuscript. DC, BY, ZH, XM, PZ, YL, HY, JY, JL, and HY gave constructive comments for the results and discussion of the article. All authors have read and approved the final article.

FUNDING

This work was supported by the Key Research and Development Program of Sichuan Province (20ZDYF003) and the National Natural Science Foundation of China (31972599).

ACKNOWLEDGMENTS

We would like to thank Wang Huifen, Wu Fali, and Liu Lei for their help during the animal trial and sample collections.

SUPPLEMENTARY MATERIAL

The Supplementary Material for this article can be found online at: https://www.frontiersin.org/articles/10.3389/fmicb.2021.811272/full#supplementary-material

REFERENCES

Akhlaq, A. F. (ed.) (2020). "Chapter 1 - insulin resistance and obesity," in *Insulin Resistance as a Risk Factor in Visceral and Neurological Disorders*, (Academic Press), 1–70.

Arab, J., and Martín-Mateos, R. (2017). Gut-liver axis, cirrhosis and portal hypertension: the chicken and the egg. *Hepatol. Int.* 12:798. doi: 10.1007/s12072-017-9798-x

Baurhoo, B., Phillip, L., and Ruiz-Feria, C. (2007). Effects of purified lignin and mannan oligosaccharides on intestinal integrity and microbial populations in the ceca and litter of broiler chickens. *Poultry Sci.* 86, 1070–1078. doi: 10.1093/ps/86.6.1070

Blottier, H. M., Champ, M., Hoebler, C., Michel, C., Cherbut, C., Bonnet, C., et al. (1999). Les acides gras à chaîne courte : de la production colique aux effets physiologiques gastro-intestinaux. *Sci. Des. Aliments* 19, 269–290.

Caporaso, J., Kuczynski, J., Stombaugh, J., Bittinger, K., Bushman, F., Costello, E., et al. (2010). QIIME allows analysis of high-throughput community sequencing data. *Nat. Methods* 7, 335–336. doi: 10.1038/nmeth.f.303

Caporaso, J., Lauber, C., Walters, W., Berg-Lyons, D., Lozupone, C., Turnbaugh, P., et al. (2011). Global patterns of 16S rRNA diversity at a depth of millions of sequences per sample. *Proc. Natl. Acad. Sci. U.S.A.* 108(Suppl. 1), 4516–4522. doi: 10.1073/pnas.1000080107

Castillo, M., Martín-Orúe, S., Taylor-Pickard, J., Pérez, J., and Gasa, J. (2008). Use of mannan-oligosaccharides and zinc chelate as growth promoters and diarrhea preventive in weaning pigs: effects on microbiota and gut function. *J. Animal Sci.* 86, 94–101. doi: 10.2527/jas.2005-686

Che, T. M., Johnson, R. W., Kelley, K. W., van Alstine, W. G., Dawson, K. A., Moran, C. A., et al. (2011). Mannan oligosaccharide improves immune responses and growth efficiency of nursery pigs experimentally infected with porcine reproductive and respiratory syndrome virus1,2. *J. Animal Sci.* 89, 2592–2602. doi: 10.2527/jas.2010-3208

Chen, J., Yu, B., Chen, D. W., Zheng, P., Luo, Y., Huang, Z., et al. (2019). Changes of porcine gut microbiota in response to dietary chlorogenic acid supplementation. *Appl. Microbiol. Biotechnol.* 103, 10025–10028. doi: 10.1007/s00253-019-10025-8

Citi, S., and Cordenonsi, M. (1998). Tight junction proteins. *Biochim. Et Biophys. Acta* 1448, 1–11. doi: 10.1016/S0079-6107(02)00037-8

de Vadder, F., Kovatcheva-Datchary, P., Gonçalves, D., Vinera, J., Zitoun, C., Duchampt, A., et al. (2014). Microbiota-generated metabolites promote metabolic benefits via gut-brain neural circuits. *Cell* 156, 84–96. doi: 10.1016/j.cell.2013.12.016

Delzenne, N. (2003). Oligosaccharides: state of the art. *Proc. Nut. Soc.* 62, 177–182. doi: 10.1079/PNS2002225

Edgar, R. (2013). UPARSE: highly accurate OTU sequences from microbial amplicon reads. *Nat. Methods* 10:2604. doi: 10.1038/nmeth.2604

Fleige, S., Walf, V., Huch, S., Prgomet, C., Sehm, J., and Pfaffl, M. W. (2006). Comparison of relative mRNA quantification models and the impact of RNA integrity in quantitative real-time RT-PCR. *Biotechnol. Lett.* 28, 1601–1613. doi: 10.1007/s10529-006-9127-2

Franklin, M. A., Mathew, A. G., Vickers, J., and Clift, R. A. (2002). Characterization of microbial populations and volatile fatty acid concentrations in the jejunum, ileum, and cecum of pigs weaned at 17 vs 24 days of age. *J. Animal Sci.* 80, 2904–2910. doi: 10.2527/2002.80112904x

Garro, M., Font de Valdez, G., and Savoy, G. (2004). "Determination of oligosaccharides in fermented soymilk products by high-performance liquid chromatography," in *Environmental Microbiology: Methods and Protocols*, eds J. M. Walker, J. F. T. Spencer, and A. L. Ragout de Spencer (Humana Press), 135–138. doi: 10.1016/s0168-1605(98)00005-1

Gerritsen, J., Smidt, H., Rijkers, G., and de Vos, W. (2011). Intestinal microbiota in human health and disease: the impact of probiotics. *Genes Nut.* 6, 209–240. doi: 10.1007/s12263-011-0229-7

González-Herrera, S., Simental-Mendía, L., López, M. G., Rocha, N., Rutiaga-Quiñones, O., Rodriguez, R., et al. (2019). Effect of agave fructans on the production of short chain fatty acid in mice. *Food Sci. Biotechnol.* 28, 1493–1498. doi: 10.1007/s10068-019-00572-1

Havenaar, R. (2011). Intestinal health functions of colonic microbial metabolites: a review. *Beneficial Microbes* 2, 103–114. doi: 10.3920/BM2011.0003

He, J., Xie, H., Chen, D., Yu, B., Huang, Z., Mao, X., et al. (2021). Synergetic responses of intestinal microbiota and epithelium to dietary inulin supplementation in pigs. *Eur. J. Nut.* 60, 715–727. doi: 10.1007/s00394-020-02284-3

Lin, B., Gong, J., Wang, Q., Cui, S., Yu, H., and Huang, B. (2011). In-vitro assessment of the effects of dietary fibers on microbial fermentation and communities from large intestinal digesta of pigs. *Food Hydrocolloids* 25, 180–188. doi: 10.1016/j.foodhyd.2010.02.006

Ma, X., Wang, Q., Li, H., Xu, C., Cui, N., and Zhao, X. (2017). 16S rRNA genes illumina sequencing revealed differential cecal microbiome in specific pathogen free chickens infected with different subgroup of avian leukosis viruses. *Veterinary Microbiol.* 207:16. doi: 10.1016/j.vetmic.2017.05.016

Magoč, T., and Salzberg, S. L. (2011). FLASH: fast length adjustment of short reads to improve genome assemblies. *Bioinformatics* 27, 2957–2963. doi: 10.1093/bioinformatics/btr507

Meurens, F., Summerfield, A., Saif, L., and Gerdts, V. (2011). The pig: a model for human infectious diseases. *Trends Microbiol.* 20, 50–57. doi: 10.1016/j.tim.2011.11.002

Miguel, J., Rodriguez-Zas, S. L., and Pettigrew, J. (2004). Efficacy of biomos for improving nursery pig performance. *J. Swine Health Prod.* 12:296.

Mitsuoka, T., Hidaka, H., and Eida, T. (1987). Effect of fructooligosaccharides on intestinal microflora. *Die Nahrung* 31, 427–436.

Mussatto, S., and Mancilha, I. (2007). Non-digestible oligosaccharides: a review. *Carbohydrate Polymers* 68, 587–597. doi: 10.1016/j.carbpol.2006.12.011

O'Toole, P., and Claesson, M. (2010). Gut microbiota: changes throughout the lifespan from infancy to elderly. *Int. Dairy J.* 20, 281–291. doi: 10.1016/j.idairyj.2009.11.010

Ozato, N., Saito, S., Yamaguchi, T., Katashima, M., Tokuda, I., Sawada, K., et al. (2019). Blautia genus associated with visceral fat accumulation in adults 20–76 years of age. *NPJ Bio. Microb.* 5:101. doi: 10.1038/s41522-019-0101-x

Patel, K., and Pyrsopoulos, N. (2019). "The microbiome and metabolome in alcoholic liver disease," in *Microbiome and Metabolome in Diagnosis, Therapy, and other Strategic Applications*, ed. Citavi 6, (Elsevier), 271–277. doi: 10.1016/B978-0-12-815249-2.00028-2

PC, S., Wenk, C., Dawson, K., and Newman, K. E. (2000). The effects of dietary mannanoligosaccharides on cecal parameters and the concentrations of enteric bacteria in the ceca of *Salmonella*-challenged broiler chicks. *Poultry Sci.* 79, 205–211. doi: 10.1093/ps/79.2.205

Puche, J., and Castilla-Cortázar Larrea, I. (2012). Human conditions of insulin-like growth factor-I (IGF-I) deficiency. *J. Trans. Med.* 10:224. doi: 10.1186/1479-5876-10-224

Puupponen-Pimiä, R., Nohynek, L., Hartmann-Schmidlin, S., Kähkönen, M., Heinonen, M., Riihinen, K., et al. (2005). Berry phenolics selectively inhibit the growth of intestinal pathogens. *J. Appl. Microbiol.* 98, 991–1000. doi: 10.1111/j.1365-2672.2005.02547.x

Quintero-Villegas, M. I. (2014). Non-Digestible Oligosaccharides: Anti-Adherence and Other Biological Properties. Doctoral dissertation, The University of Nebraska-Lincoln

Round, J. L., and Mazmanian, S. K. (2009). The gut microbiota shapes intestinal immune responses during health and disease. *Nat. Rev. Immunol.* 9, 313–323. doi: 10.1038/nri2515

Rycroft, A., and Garside, L. (2000). Actinobacillus species and their role in animal disease. *Veterinary J.* 159, 18–36. doi: 10.1053/tvjl.1999.0403

Shi, N., Li, N., Duan, X., and Niu, H. (2017). Interaction between the gut microbiome and mucosal immune system. *Military Med. Res.* 4:122. doi: 10.1186/s40779-017-0122-9

Simmons, J. G., Hoyt, E. C., Westwick, J. K., Brenner, D. A., Pucilowska, J. B., and Lund, P. K. (1995). Insulin-like growth factor-I and epidermal growth factor interact to regulate growth and gene expression in IEC-6 intestinal epithelial cells. *Mol. Endocrinol.* 9, 1157–1165. doi: 10.1210/mend.9.9.7491108

Singh, N., Thangaraju, M., Prasad, P., Martin, P., Lambert, N., Boettger, T., et al. (2010). Blockade of dendritic cell development by bacterial fermentation products butyrate and propionate through a transporter (Slc5a8)-dependent inhibition of histone deacetylases. *J. Biol. Chem.* 285, 27601–27608. doi: 10.1074/jbc.M110.102947

Tan, J., Mckenzie, C., Potamitis, M., Thorburn, A., Mackay, C., and Macia, L. (2014). The role of short-chain fatty acids in health and disease. *Adv. Immunol.* 121, 91–119. doi: 10.1016/B978-0-12-800100-4.00003-9

Wall, R., Ross, R., Ryan, A. C., Hussey, S., Murphy, B., Fitzgerald, G., et al. (2009). Role of gut microbiota in early infant development. *Clin. Med. Pediatr.* 3, 45–54. doi: 10.4137/CMPed.S2008

Wan, J., Zhang, J., Chen, D. W., Yu, B., Huang, Z., Mao, X., et al. (2020). Alterations in intestinal microbiota by alginate oligosaccharide improve intestinal barrier integrity in weaned pigs. *J. Funct. Foods* 71:104040. doi: 10.1016/j.jff.2020.104040

Wang, Q., Garrity, G., Tiedje, J., and Cole, J. R. (2007). Naive bayesian classifier for rapid assignment of rRNA sequences into the new bacterial taxonomy. *Appl. Environ. Microbiol.* 73, 5264–5267. doi: 10.1128/AEM.00062-07

Yamashita, H., Fujisawa, K., Ito, E., Idei, S., Kawaguchi, N., Kimoto, M., et al. (2007). Improvement of obesity and glucose tolerance by acetate in type 2 diabetic otsuka long-evans tokushima fatty (OLETF) rats. *Biosci. Biotechnol. Biochem.* 71, 1236–1243. doi: 10.1271/bbb.60668

Yang, Y., Iji, P., Kocher, A., Thomson, E., Mikkelsen, L. L., and Choct, M. (2008). Effects of mannanoligosaccharide in broiler chicken diets on growth performance, energy utilisation, nutrient digestibility and intestinal microflora. *Br. Poultry Sci.* 49, 186–194. doi: 10.1080/00071660801998613

Yu, E., Chen, D. W., Yu, B., Huang, Z., Mao, X., Zheng, P., et al. (2020). Manno-oligosaccharide attenuates inflammation and intestinal epithelium injury in weaned pigs upon enterotoxigenic *Escherichia Coli* K88 challenge. *Br. J. Nut.* 126, 993–1002. doi: 10.1017/S0007114520004948

Conflict of Interest: The authors declare that the research was conducted in the absence of any commercial or financial relationships that could be construed as a potential conflict of interest.

Publisher's Note: All claims expressed in this article are solely those of the authors and do not necessarily represent those of their affiliated organizations, or those of the publisher, the editors and the reviewers. Any product that may be evaluated in this article, or claim that may be made by its manufacturer, is not guaranteed or endorsed by the publisher.

frontiers in Microbiology

ORIGINAL RESEARCH
published: 14 February 2022
doi: 10.3389/fmicb.2021.748594

Transcriptome and Gut Microbiota Profiling Revealed the Protective Effect of Tibetan Tea on Ulcerative Colitis in Mice

Ning Wang[1], Tao Wu[2], Di Du[3], Jie Mei[4], Huibo Luo[1], Zishan Liu[1], Muhammad Kashif Saleemi[5], Runhui Zhang[6], Candace Chang[7], Muhammad Aamer Mehmood[1,8] and Hui Zhu[1]**

[1] College of Bioengineering, Sichuan University of Science and Engineering, Zigong, China, [2] School of Food and Biological Engineering, Xihua University, Chengdu, China, [3] Process Technology Department, ExxonMobil Research and Engineering, Annandale, NJ, United States, [4] Sichuan Jixiang Tea Co., Ltd., Ya'an, China, [5] Department of Pathology, University of Agriculture, Faisalabad, Pakistan, [6] Department of Veterinary Medicine, College of Animal & Veterinary Sciences, Southwest Minzu University, Chengdu, China, [7] UCLA Microbiome Center, David Geffen School of Medicine at UCLA, Los Angeles, CA, United States, [8] Department of Bioinformatics and Biotechnology, Government College University Faisalabad, Faisalabad, Pakistan

OPEN ACCESS

Edited by:
Xiaodong Xia,
Dalian Polytechnic University, China

Reviewed by:
Umang Jain,
Washington University in St. Louis, United States
Zhaolai Dai,
China Agricultural University, China

***Correspondence:**
Muhammad Aamer Mehmood
draamer@gcuf.edu.pk
Hui Zhu
zhuhuiwn@outlook.com

Specialty section:
This article was submitted to Food Microbiology, a section of the journal Frontiers in Microbiology

Received: *28 July 2021*
Accepted: *15 December 2021*
Published: *14 February 2022*

Citation:
Wang N, Wu T, Du D, Mei J, Luo H, Liu Z, Saleemi MK, Zhang R, Chang C, Mehmood MA and Zhu H (2022) Transcriptome and Gut Microbiota Profiling Revealed the Protective Effect of Tibetan Tea on Ulcerative Colitis in Mice. Front. Microbiol. 12:748594. doi: 10.3389/fmicb.2021.748594

Traditionally, Ya'an Tibetan tea is routinely consumed by local people in the Tibet region. It is believed to possess promising anti-inflammatory benefits. This study was conducted to elucidate the protective impact of Tibetan tea extract (TTE) on dextran sodium sulfate (DSS)-induced colitis in mice. Mice were split into four groups: control (C) group, Tibetan tea (T) group, DSS-induced model (CD) group, and Tibetan tea + DSS (TD) group. The intake of TTE significantly reduced the clinical symptoms of ulcerative colitis (UC) by alleviating the impact of cellular damage and reducing glandular hypertrophy and the infiltration of inflammatory cells. UC led to a prominent shift of the microbial communities in the gut. Interestingly, the beneficial microbes, such as *Lactobacillus reuteri*, *Bifidobacterium choerinum*, and *Lactobacillus intestinalis*, were significantly increased in TTE-treated mice when compared to any other experimental group. The transcriptome analysis revealed that the positive effect of TTE on UC could be attributed to changes in the G alpha (i) signaling pathway and the innate immune system. The genes related to inflammation and immune system pathways were differentially expressed in the TTE-treated group. Moreover, the relative expression of genes linked to the inflammatory TLR4/MyD88/NF-κB signaling pathway was significantly downregulated toward the level of normal control samples in the TD group. Overall, this study revealed the modulatory effect by which TTE reversed the development and severity of chronic colon damage.

Keywords: ulcerative colitis, Tibetan tea, RNA-seq, gut microbiota, immune response

INTRODUCTION

Ulcerative colitis (UC) can trigger hemorrhagic diarrhea and passage of mucus and/or pus, which causes cramping in the abdominal during bowel movements (Ananthakrishnan et al., 2018). Due to the prolonged disease duration and recurrent attacks, the World Health Organization (WHO) has listed it among the modern refractory diseases (Caruso et al., 2020). It is believed that excessive

inflammation of the intestine occurs due to an imbalance in the gut microbiota and immunity of the mucosa, resulting in UC (Limdi and Vasant, 2015; Ajayi et al., 2018). Currently, the available drugs are inefficient in the remediation of the disease and cause several side effects. It is therefore essential to explore safer, more effective, and cost-effective alternatives to prevent dysbiosis (Oh et al., 2020).

Tibetans are at high risk of suffering from UC due to their extreme living environment and eating habits, being on a plateau, making it necessary for them to drink tea daily for its health benefits (Lewis and Abreu, 2017). Tibetan tea is a product of geographical indication exclusively produced in the Ya'an region in China. It is a type of black tea made from a mature small-leaf cultivar, which is picked from high up the mountains above 1,000 m (Zheng et al., 2020). Pile fermentation is the key process to achieving the characteristic features of Tibetan tea (Xu et al., 2020).

Microbial dysbiosis is among the major pathological factors of UC that affects host mucosal immunity (Franzosa et al., 2019; Liu et al., 2020; Lee and Chang, 2021). Pathogenic bacteria, along with opportunistic pathogens, interact with the gut mucosa either directly or indirectly by secreting toxins, which cause an improper mucosal immune response in the intestine (Qi et al., 2018). The dysregulated immune system responds in the form of inflammation, leading to the development of UC. Multiple immune cells, including T lymphocytes, macrophages, and neutrophils, are abnormally activated and do not only elicit acute colitis but also further damage the colon by upregulating the pro-inflammatory cytokines such as tumor necrosis factor alpha (TNF-α), interleukin 1 beta (IL-1β), and IL-6 (Sun et al., 2020). Thus, regulating the gut microbiota may be a promising strategy to preventing and/or treating UC (Petrella, 2016; Lee et al., 2018; Sun et al., 2018).

Based on the long-term consumption of Tibetan tea in the daily life of Tibetans, it was hypothesized that Tibetan tea polyphenols have preventive effects against UC. Accordingly, the current study evaluated the composition and anti-inflammatory effects of Tibetan tea extract (TTE) on dextran sodium sulfate (DSS)-induced colitis in mice. The impact of TTE on the expression of colonic genes and on the gut microbiota was elucidated using transcriptome combined with DNA sequencing analysis. These data were employed to identify the altered metabolic and immune pathways, as well as the key microbiota regulatory "hubs," that help elucidate the novel insights into the anti-inflammatory effects of TTE.

MATERIALS AND METHODS

Preparation of Tibetan Tea Extract

The Tibetan tea (*Camellia sinensis*) used in this study was of the first class and provided by Sichuan Jixiang Tea Co., Ltd. (Ya'an, China). It was made from tea with one bud and one leaf as raw materials and had been stored in a dry and ventilated warehouse at 24–28°C for 1 year. One hundred grams of Tibetan tea was pulverized and passed through an 80-mesh sieve. The powder was decocted in 50-fold volume using boiling water for 10 min. The supernatant was collected by centrifugation at 5,000 rpm for 10 min and was concentrated under reduced pressure using a rotary evaporator. TTE was lyophilized under 10 Pa at –55°C and stored at 4°C for further use.

Determination of the Major Compounds in Tibetan Tea

The total phenolic content (TPC) of the TTE samples was quantified using the Folin–Ciocalteu colorimetric assay. The results were expressed as milligrams of gallic acid equivalent (GAE) per 100 mg of dried extract. The total flavonoid content (TFC) was determined using the colorimetric method, and the results were expressed in milligrams rutin equivalent (RE) per 100 mg dry weight (Wu et al., 2016). The composition of Tibetan tea was evaluated with untargeted metabolomics as described previously (Li et al., 2021).

Ethics Statement

Mice were purchased from Vital River Laboratory Animal Technology Co. Ltd. (Beijing, China). All experiments were executed following the Guide for the Care and Use of Laboratory Animals by Sichuan University of Science and Engineering (Zigong, China), after seeking proper approval.

Experimental Setup to Induce UC in Mice

C57BL/6J mice (male, 18–22 g) were kept at 23 ± 1°C under a 12-h light/dark cycle. Unlimited standard rodent diet and water were provided. After 1 week, 32 mice were indiscriminately split into four experimental groups: the control (C) group, the Tibetan tea (T) group, the DSS model (CD) group, and the Tibetan tea + DSS (TD) group. Mice in the T and TD groups were orally administered 100 mg of TTE per kilogram body weight, while mice in the C and CD groups were treated with the same volume of ddH_2O (**Figure 1A**). After pretreatment for 7 days, the mice in the CD and TD groups were administered 3.5% DSS (MP Biochemicals, Irvine, CA, United States) in drinking water given *ad libitum* (days 8–14), as described (Fang et al., 2019). Body weight, stool blood, and the consistency of the stool (to calculate the Disease Activity Index, DAI) were recorded three times a day during the duration of the experiments (Jeengar et al., 2017).

Mice were sacrificed on day 21 (**Figure 1A**), and blood and cecum samples were collected for further study. The colons, taken from the ileocecal junction to the anal verge, were dissected and measured for weight and length before being longitudinally opened and washed using phosphate-buffered saline (PBS) at pH 7.4. Part of the colon tissues was fixed in 10% formalin (neutral-buffered) for subsequent histological analyses. The remaining colon samples were stored in liquid nitrogen until further use.

Histopathological Assays

The transverse rings of the colons were fixed in 4% buffered formalin and embedded in paraffin before staining with hematoxylin and eosin (H&E) (Leica Biosystems, Wetzlar, Germany). Goblet cells were observed with Alcian blue/periodic acid–Schiff (AB/PAS) straining. These sections were observed under a microscope (BX53M; Olympus, Tokyo, Japan) and were

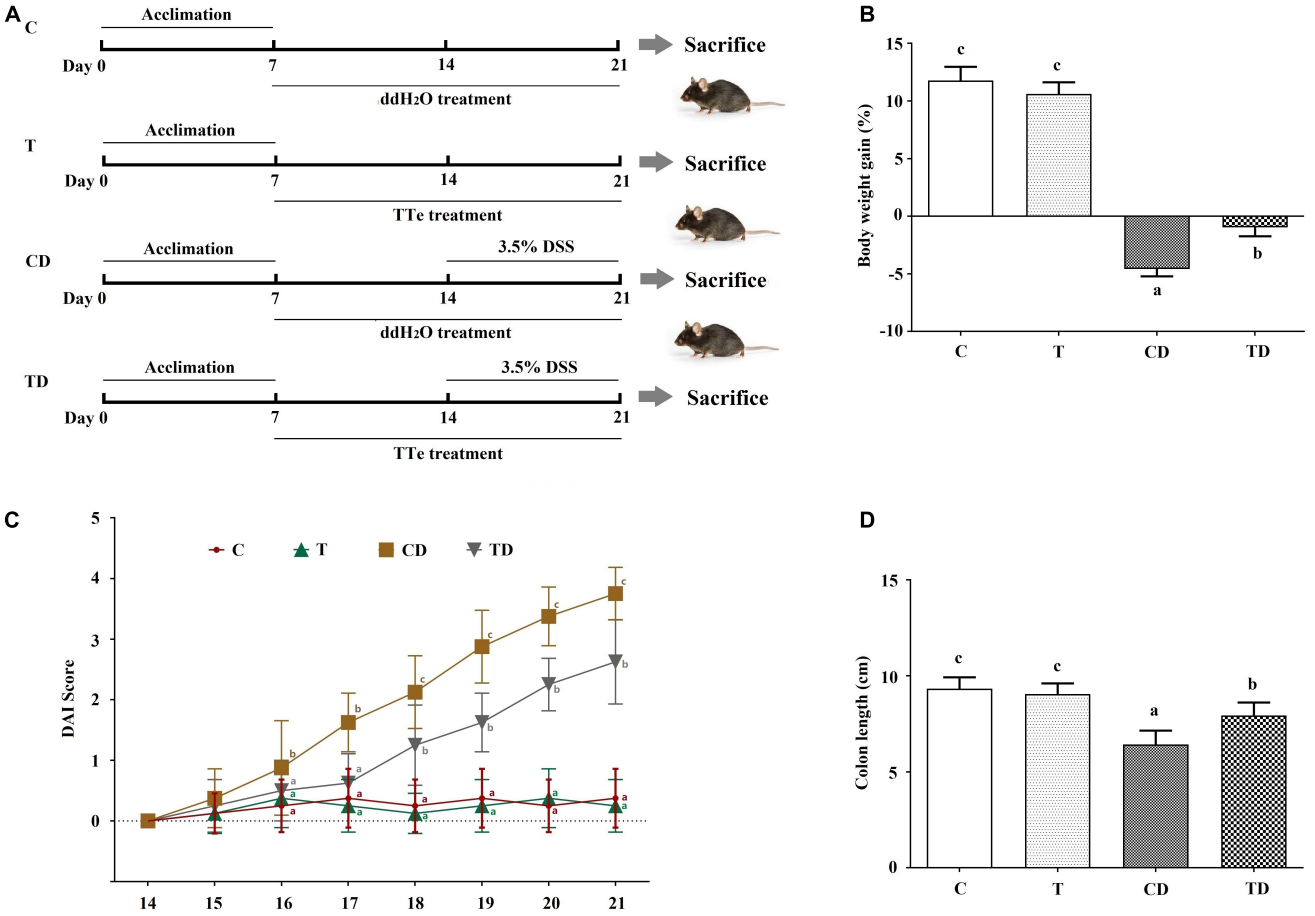

FIGURE 1 | Effect of Tibetan tea on the colon tissues of dextran sodium sulfate (DSS)-induced ulcerative colitis (UC) in mice. **(A)** Schema of the experimental design. **(B)** Body weight gain. **(C)** Disease Activity Index (DAI) scores during DSS treatment. **(D)** Colon length. Data were expressed as the mean ± SD. *Lowercase letters a–c* indicate significant differences in all treatment groups ($p < 0.05$). *C*, control group ($n = 8$); *T*, Tibetan tea group ($n = 8$); *CD,* DSS model group ($n = 8$); *TD*, Tibetan tea + DSS group ($n = 8$).

scored based on a four-point scale (0–4) upon examination for exudates, polymorphonuclear leukocyte invasions, epithelial damage, submucosal edema, and necrosis (Kuprys et al., 2020; Ma et al., 2020).

Immunohistochemical Analyses

Paraffin-embedded sections of the colonic tissues (5 mm thickness) were prepared and examined using mouse anti-myeloperoxidase (MPO) antibodies (NOVUS Biologicals, Littleton, CO, United States) as described previously (Lee et al., 2018). The positive rate of MPO cells (the number of positive cells/total cell number × 100) was calculated using HALO (Indica Labs, Albuquerque, NM, United States).

DNA Sequencing

Total DNA was extracted from all cecal digesta samples (75 mg sample was used) using the cetyltrimethyl ammonium bromide/sodium dodecyl sulfate (CTAB/SDS) method (Griffith et al., 2009). The quality and the quantity of the DNA were assessed using gel electrophoresis (1% agarose gel) and a NanoDrop Spectrophotometer (ND-1000; Thermo Fischer Scientific, Waltham, MA, United States), respectively. DNA was used as the template to amplify the V4 hypervariable region of the 16S ribosomal RNA (rRNA) gene and sequenced by Novogene Bioinformatics Technology Co. Ltd. (Beijing, China).

Sequence Analyses

Single-end reads were cleaned by removing the primer sequences and were subjected to quality filtration following the recommended quality control parameters in cutadapt V1.9.1 (Martin, 2011). Chimera sequences were removed using the SILVA reference database and the UCHIME algorithm (Edgar et al., 2011; Haas et al., 2011). The cleaned reads were analyzed by Uparse v7.0.1001, and sequences with ≥97% similarity were grouped into the same operational taxonomic units (OTUs). The SILVA database and the Mothur algorithm were employed for taxonomy assignment of the representative sequences of each OTU (Edgar, 2013). Finally, multiple sequence alignments were performed using MUSCLE v.3.8.31 (Edgar, 2004). Alpha

diversity and Jackknifed beta diversity analyses were performed as described previously (Schloss et al., 2009).

RNA Isolation for Library Construction

To further investigate the molecular mechanism of Tibetan tea in preventing DSS-induced UC in mice, colon samples were separately collected from the C, CD, and TD groups, and total RNA was extracted using the TriZol reagent as described by the manufacturer (Invitrogen, Carlsbad, CA, United States). After determining the RNA quality and quantity, the libraries were constructed and sequenced on the Illumina HiSeq X Ten platform. Subsequently, 150-bp paired-end reads were obtained.

RNA-Seq Analyses

The assembly and functional assignment of the RNA sequencing (RNA-seq) data were executed following a method described previously (Pandurangan et al., 2015). Two groups/conditions (in duplicate) were subjected to differential expression analyses using the DESeq2 R package (1.16.1). Gene Ontology (GO) analysis of differentially expressed genes (DEGs) was performed using the clusterProfiler R package, and gene length bias was corrected for. GO terms with corrected $p < 0.05$ were considered as enriched by DEGs. The statistical enrichment of DEGs in the Kyoto Encyclopedia of Genes and Genomes (KEGG) pathways was examined through the clusterProfiler R package.

Deseq2 (PMID: 25516281) was used to normalize the read counts in order to enable cross-sample comparisons. Accordingly, 2,526 genes showed differential expression between the CD and C groups, and 337 showed differential expression between the TD and CD groups.

Pathway Analyses

Pathway analyses were performed using the Reactome and KEGG databases. Protein–protein interactions were analyzed using STRING (PMID: 30476243) and were colored by the corresponding Reactome pathways. A KEGG gene–pathway clustered heatmap was calculated using Enrichr (PMID: 23586463 and PMID:27141961).

Real-Time Quantitative PCR

To further validate the key genes and pathways involved in the anti-inflammatory effects of TTE, real-time quantitative PCR (RT-qPCR) was performed to detect the relative expression levels of *IL-1*β, *IL-6*, *IL-10*, *MyD88*, *NF-κB*, *TLR4*, and *TNF-*α using the $2^{-\Delta\Delta Ct}$ method, while β-*actin* expression was used as the reference (**Supplementary Table 1**). The high-quality RNA extracted from the colon tissues was used as a template to synthesize complementary DNA (cDNA).

Statistical Analyses

All experiments were repeated three times, and data were shown as the mean ± SD. One-way ANOVA with Tukey's *post hoc* test was employed using GraphPad Prism 6.0 (San Diego, CA, United States). Data with *p*-values < 0.05 were considered significant.

RESULTS

Characterization of the Major Ingredients of Tibetan Tea

Tea polyphenols and flavonoids could be the major components responsible for the health benefits of TTE. Therefore, the contents of total polyphenols and total flavonoids in TTE were evaluated with spectroscopy, which were 70.24 ± 3.12 mg GAE/g and 104.57 ± 7.61 mg RE/g, respectively. Furthermore, the MS/MS fragment ions of TTE were analyzed using ultra-high-performance liquid chromatography/time-of-flight tandem mass spectrometry (UHPLC-TOF-MS/MS) (**Supplementary Table 2**). A total of 17 compounds were tentatively identified using MS-DIAL 4.6 software[1], including phenolic acids, flavonoids, and theaflavins. It is worth noting that the content of theaflavins in TTE was 3.3 times higher than that in Pu-erh tea (**Supplementary Figure 1**).

Tibetan Tea Extract Cured Dextran Sodium Sulfate-Induced Ulcerative Colitis

The DAI is a conventional index for evaluating colitis severity. Here, the DAI of the T group was little changed when compared to the DAI scores of mice in the C group. Administration of DSS resulted in apparent clinical symptoms such as diarrhea, weight loss, and fecal blood in mice of the CD and TD groups (**Figure 1B**). Accordingly, a significant increase in DAI was observed in the CD group on day 17 when compared to the control, and the maximum DAI was reached on day 21 (3.750 ± 0.433) (**Figure 1C**). Delayed and/or reduced symptoms, including reduced fecal occult blood and diarrhea, in response to TTE treatment were observed. The DAI of the TD group considerably decreased. These data demonstrated the protective effects of Tibetan tea against murine ulcerative colitis (**Figure 1C**). DSS administration also shortened the colonic length of mice from the CD group (6.43 ± 0.72 cm) when compared to mice in the C group (9.34 ± 0.59 cm, $p < 0.05$) (**Figure 1D** and **Supplementary Figure 2**), and TTE treatment was preventive against the shortening of the colon (7.94 ± 0.68 cm, $p < 0.05$) in DSS-administered mice. No of the experimental mice died during the experimental period.

Histopathology of the Colon and Calculation of the MPO-Positive Rate

Histopathological evaluation of the colons demonstrated that the TTE group also showed protective effects against DSS-induced colitis (**Figure 2**). Both the C and T groups showed normal colonic mucosa with the epithelium, crypts, and the submucosa intact. However, in the colons of the CD group, loss of epithelial and goblet cells along with severe neutrophil infiltration, deformation of the crypt structure, appearance of crypt abscesses, and ulcers were observed. Interestingly, mice treated with TTE showed alleviation of DSS-induced hemorrhage in the colon. After 7 days of DSS administration, the histological

[1]http://prime.psc.riken.jp/compms/msdial/main.html

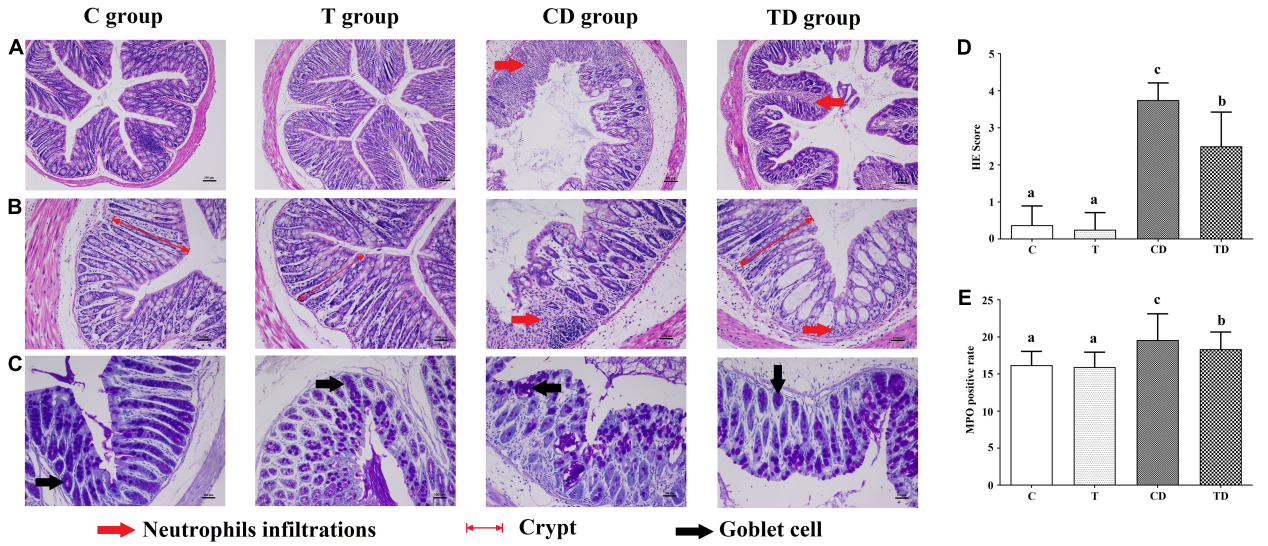

FIGURE 2 | Histopathological analysis of colon segments. **(A,B)** Staining of colon tissues of mice with hematoxylin–eosin (H&E), original magnifications of × 100 **(A)** and × 200 **(B)**. **(C)** Goblet cells observed with Alcian blue/periodic acid–Schiff (AB/PAS) staining. **(D)** Determination of the histological scores for the control (C), dextran sodium sulfate (DSS) model (CD), and Tibetan tea + DSS (TD) groups. **(E)** Sections immunostained with mouse anti-myeloperoxidase (MPO) antibody in each group, with the positive cells staining brown. The positive rate of MPO cells (the number of positive cells/total cell number × 100) was calculated using HALO. *Lowercase letters a–c* indicate significant differences in all treatment groups ($p < 0.05$).

scores were 3.75 ± 0.46 in the CD group and 2.50 ± 0.93 in the TD group (**Figure 2D**). In addition, the results of MPO protein immunohistochemistry showed that the MPO content in the colon tissues of mice in the CD group was substantially higher compared to that in the C group, but significantly decreased in the TD group (**Figure 2E**).

Tibetan Tea Extract Altered the Cecal Microbiota in Dextran Sodium Sulfate-Induced UC Mice

The IonS5TMXL platform was used to extract the single-end sequences of 16S rRNA genes, where a total of 1,844,712 high-quality reads remained, with an average of 76,863 reads per sample after deleting chimeras and low-quality reads. The overall effective rate of the quality control was 94.45%. These sequences were assigned to 875 OTUs based on similarity (≥97%). Among these, 440 (50.29%) OTUs were assigned to the genus level.

Comparison of the alpha diversity between the CD and TD groups showed that the Shannon and Simpson indices of the TD group were substantially lower than those of the CD group (Wilcoxon rank-sum test: $p < 0.05$) (**Figures 3A,B**). Obvious clustering was observed within the treatment groups in the principal coordinates analysis (PCoA) plot based on weighted and unweighted Unifrac and in the non-metric multidimensional scaling (NMDS) plot based on Bray–Curtis distances, suggesting that the CD and TD groups were composed of distinct bacterial communities (**Figures 3C–E**). Analysis of similarities (ANOSIM) also proved that differences in the community membership between both groups were statistically significant ($r = 0.6907$, $p = 0.001$). MetaStat was also used to look for bacterial taxa that show substantial differences in abundance (**Figure 4**). At the phylum level, the relative abundances of Bacteroidetes, Verrucomicrobia, Deferribacteres, and Melainabacteria decreased significantly ($p < 0.05$) in the TD group in comparison to the CD group. At the species level, the relative abundance of *Bacteroides dorei* decreased significantly ($p < 0.05$), while that of *Clostridium papyrosolvens* increased significantly ($p < 0.01$) in the TD group compared to the CD group. Comparison of the cecal microbiota of mice in the four groups revealed that beneficial microbes such as *Lactobacillus reuteri*, *Bifidobacterium choerinum*, and *Lactobacillus intestinalis* showed an "up–down–up" trend across the C, T, CD, and TD groups (**Figure 4C**).

The microbial community compositions of mice are shown in **Figure 4A**. MetaStat analysis was used to identify the differential distribution of the microbial taxa between groups at the phylum and species levels (**Figures 4B,C**). The relative abundances of the phyla Actinobacteria and Firmicutes in the CD group decreased significantly compared to those in the control group ($p < 0.01$), while those of the Proteobacteria, Bacteroidetes, Verrucomicrobia, and Deferribacteres increased significantly ($p < 0.05$). At the species level (top 10), the relative abundances of *L. reuteri*, *B. choerinum*, *Lactobacillus prophage* Lj928, *Dubosiella_newyorkensis*, and *Exiguobacterium undae* significantly reduced in the CD group compared to those in the control group ($p < 0.05$), whereas the relative abundances of *Parabacteroides merdae* and *Bacteroides dorei* significantly increased in the CD group ($p < 0.05$).

Transcriptome Data Analysis

To further elucidate the protective effects seen in TTE-treated mice, the colonic tissues of mice were subjected to

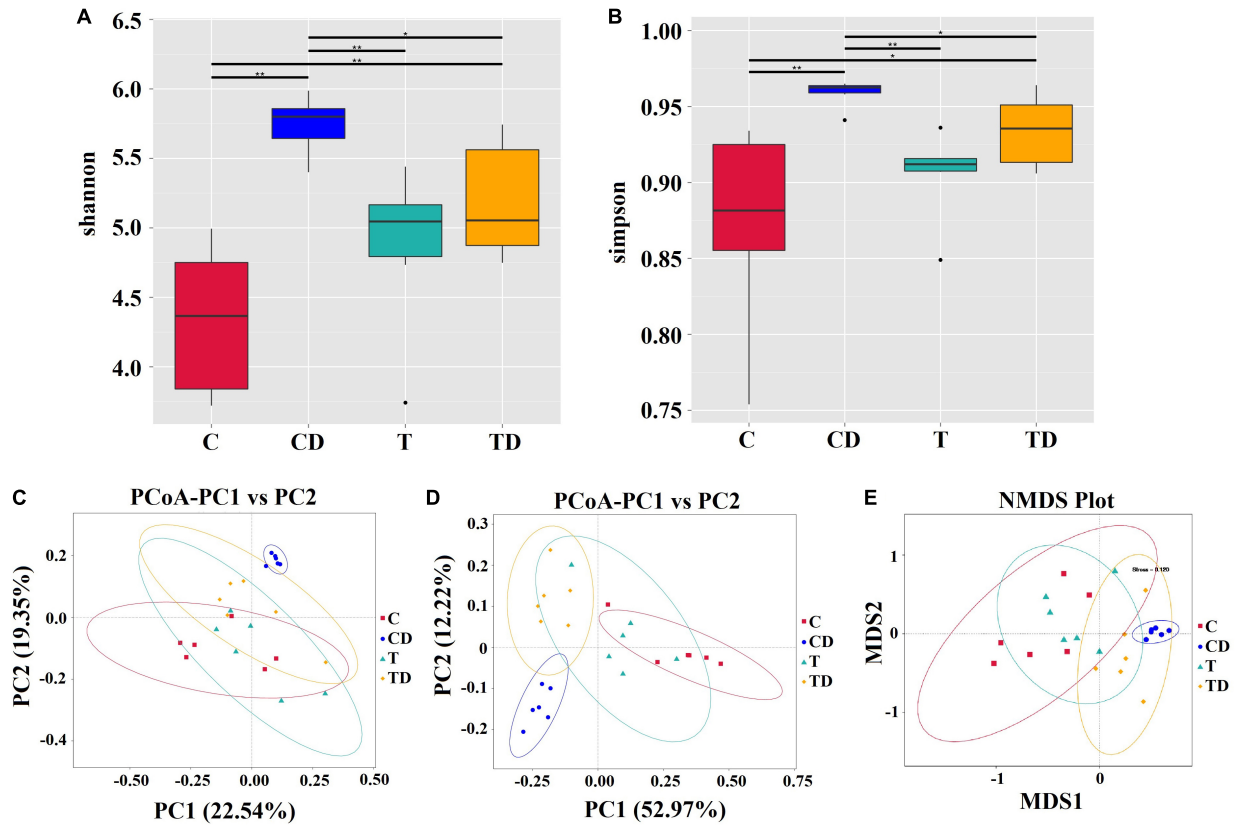

FIGURE 3 | Differences in the cecal microbiota of mice. **(A,B)** The diversity and richness of the microbiota of mice in different groups were measured by the Shannon **(A)** and Simpson **(B)** indices. *Asterisk above the box plots* indicates significant differences between age groups (Wilcoxon rank-sum test: $*p < 0.05$, $**p < 0.01$). **(C,D)** Principal coordinates analysis (PCoA) of microbial communities based on weighted **(C)** and unweighted **(D)** Unifrac distances. **(E)** Non-metric multidimensional scaling analysis.

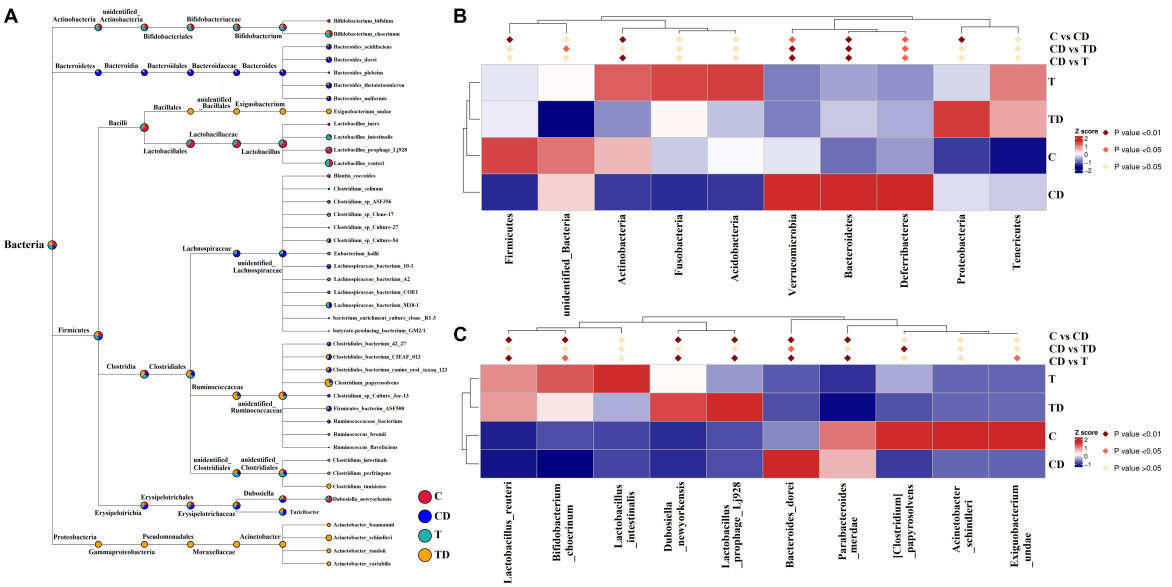

FIGURE 4 | Comparison of the microbial communities in mice. **(A)** Evolutionary tree of the top 100 genera. **(B)** Microbial taxa differentially distributed between groups at the phylum level. **(C)** Identification at the species level by MetaStat analysis.

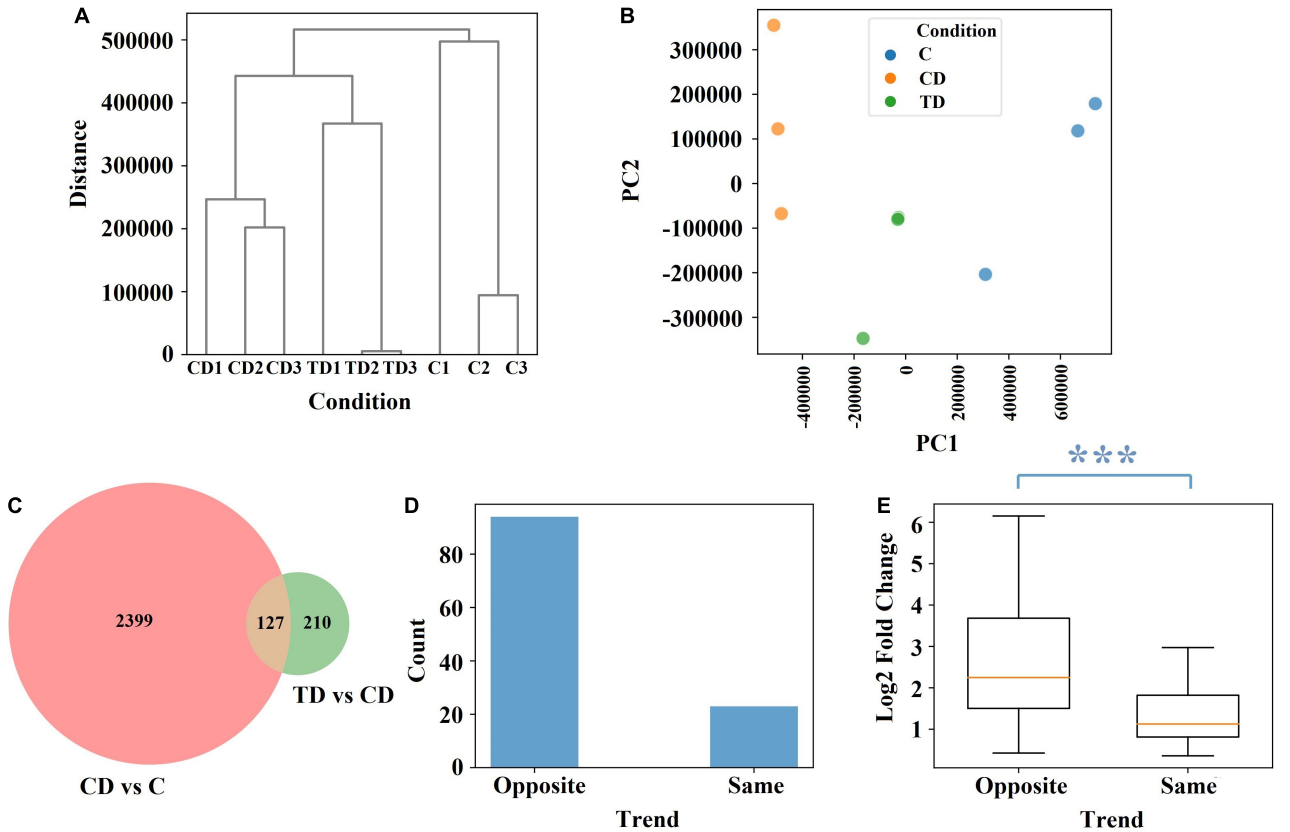

FIGURE 5 | The effect of Tibetan tea at the genetic level. **(A)** Hierarchical clustering dendrogram of normalized gene expression. **(B)** Principal component analysis of normalized gene expression. **(C)** Venn diagram of the differential expression between CD *vs*. C and between TD *vs*. CD. **(D)** Trend count of 127 common genes. **(E)** Log2 fold change of the 127 common genes. The difference between the two trends is characterized using the Mann–Whitney *U* test *p*-value. ***$p < 0.005$. *TD*, Tibetan tea + DSS; *CD*, dextran sodium sulfate-induced model; *C*, control.

transcriptomic analysis. Accordingly, a total of 1,224,984,344 raw sequence reads were generated from the colonic tissues of mice, and 1,172,856,536 clean reads were retained after filtering (**Supplementary Table 3**). The RNA-seq data were subjected to an unsupervised hierarchical clustering and principal component analysis (PCA; **Figures 5A,B**). The fact that all samples within each group were clustered together also validated the robustness of the data collection process. In the PCA model, the top 2 components explained 79 and 16% of the variance, respectively. After TTE treatment, the genetic profile in the TD group was shown to be closer to that of the C group, which confirmed that Tibetan tea had a positive effect on the induced UC at the genetic level.

Further comparisons of the different groups showed that 2,526 genes were differentially expressed between the CD and C groups and 337 genes between the TD and CD groups, among which 127 genes were common (**Figure 5C**). Among the 127 common genes, 94 showed an opposite trend across the C, CD, and TD groups, namely, upregulated at CD *vs*. C and downregulated at TD *vs*. CD or downregulated at CD *vs*. C and upregulated at TD *vs*. CD (**Figure 5D**). This finding verified that Tibetan tea is effective at reducing inflammation by regulating genes toward the level of normal control samples. It is worth noting that the 94 genes that showed the opposite trend across the C, CD, and TD groups also had significantly higher fold change values (**Figure 5E**).

Pathways Responsive to Tibetan Tea Extract Treatment

The protein–protein interactions of the DEGs between the TD and CD groups were analyzed and visualized in a network fashion (**Figure 6A**). The thickness of the edges represents the confidence of data support. Here, three Reactome pathways were identified—metabolism, G alpha (i) signaling events, and innate immune system—which covered most of the interaction networks with high-confidence edges. The relationship between these three pathways and their associated pathways that were within the top 20 pathways ranked by the false discovery rate are shown in **Figure 6B**. Two associated pathways of metabolism—amino acid metabolism and xenobiotics—were shown to be related to the differential expression between the TD and CD groups. The same analysis for the differential expression between CD and C (**Figure 6C**) was also performed. Several pathways, including signal transduction, innate immune system, hemostasis, and glycosaminoglycan metabolism, covered most of the interaction network with high-confidence edges between the CD and C

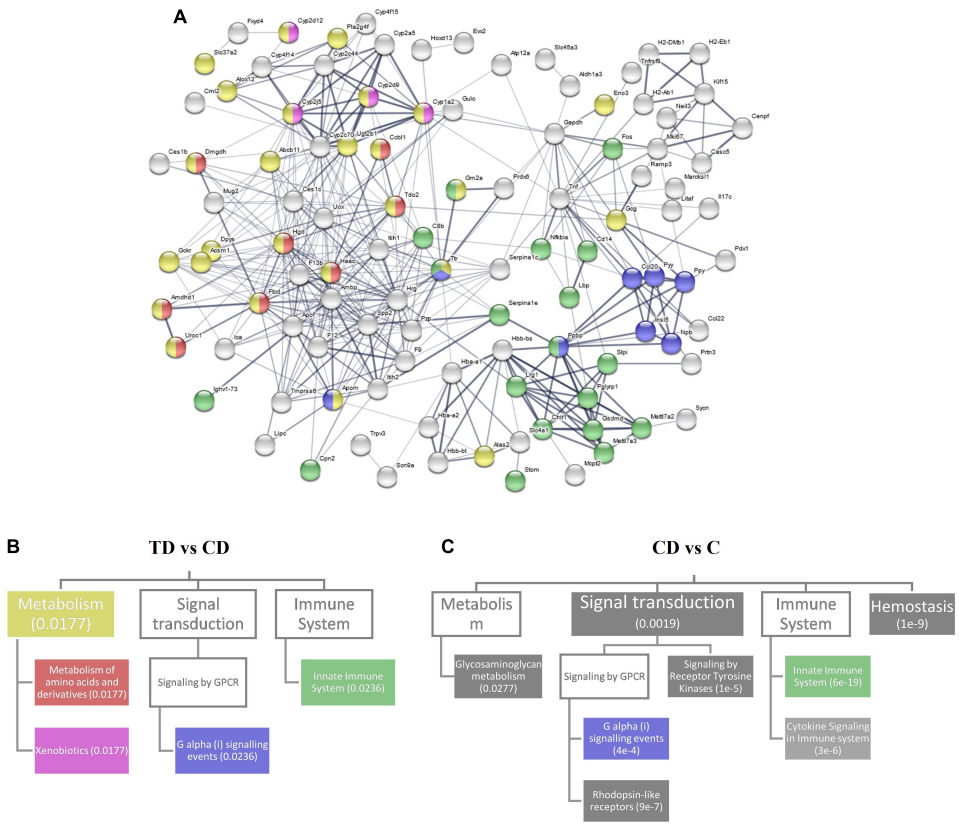

FIGURE 6 | Reactome pathway analysis. **(A)** Protein–protein interaction network for differential gene expression between TD and CD. **(B)** Top 20 related Reactome pathways for differential expression in TD and CD. The pathways are mapped in **(A)** with corresponding colors. **(C)** Top 20 related Reactome pathways for differential expression in CD and C. *Numbers within parentheses* represent the false discovery rate. *Boxes with no color* represent a false discovery rate >0.05. *TD*, Tibetan tea + DSS; *CD*, dextran sodium sulfate-induced model; *C*, control.

groups. A comparison between TD *vs.* CD and CD *vs.* C showed that the positive effect of TTE in controlling UC could be attributed to the changes in the G alpha (i) signaling pathway and the innate immune system. The fact that the xenobiotics pathway was highly differentially regulated in the TD *vs.* CD comparison, but not in the CD *vs.* C comparison, also confirmed that the changes in the pathways were due to exogenous compounds.

In addition to the Reactome pathways, the KEGG pathways associated with the differential expression between the TD and CD groups and those associated with the differential expression between the CD and C groups were also compared (**Figure 7**). The largest cluster in each comparison (boxed in blue) corresponding to several inflammation- and immune system-related pathways, including the intestinal immune network, Toll-like receptor signaling pathway, and IL-17 signaling pathway, were identified.

Gene Expression Involved in the TLR4/MyD88/NF-κB Signaling Pathway

We measured the relative mRNA expressions of the TLR4/MyD88/NF-κB signaling pathway-related genes (*IL-1*β, *IL-6*, *IL-10*, *MyD88*, *NF-κB*, *TLR4*, and *TNF-*α) in the colons. DSS administration significantly elevated the mRNA expressions of *IL-1*β, *IL-6*, *IL-10*, *MyD88*, *NF-κB*, *TLR4*, and *TNF-*α up to 4. 46–, 4. 16–, 2. 99–, 1. 52–, 10. 76–, 2. 69–, and 3.50-fold, respectively, in DSS-induced mice compared to mice in the C group ($p < 0.01$). The mRNA levels in mice with TTE pretreatment (TD group) were downregulated to nearly normal levels ($p > 0.05$) (**Figure 8**). These data confirmed that the anti-inflammatory impact of beneficial microbes correlated with the downregulation of the TLR4/MyD88/NF-κB signaling pathway.

DISCUSSION

Under muggy conditions with an abundance of environmental microorganisms, tea polyphenols go through oxidation, condensation, and hydrolysis, making Tibetan tea rich in a variety of phenolics, theaflavins, and thearubigins, among others. Pu-erh tea, a well-known black tea, is made from a large-leaf cultivar, whereas Tibetan tea is produced from local small-leaf cultivar. As a result, TTE contains high levels of theaflavins than Pu-erh tea. It was reported for the first time that the preventive effects of TTE on DSS-induced UC in mice were further explored comprehensively using transcriptome and DNA sequencing analyses.

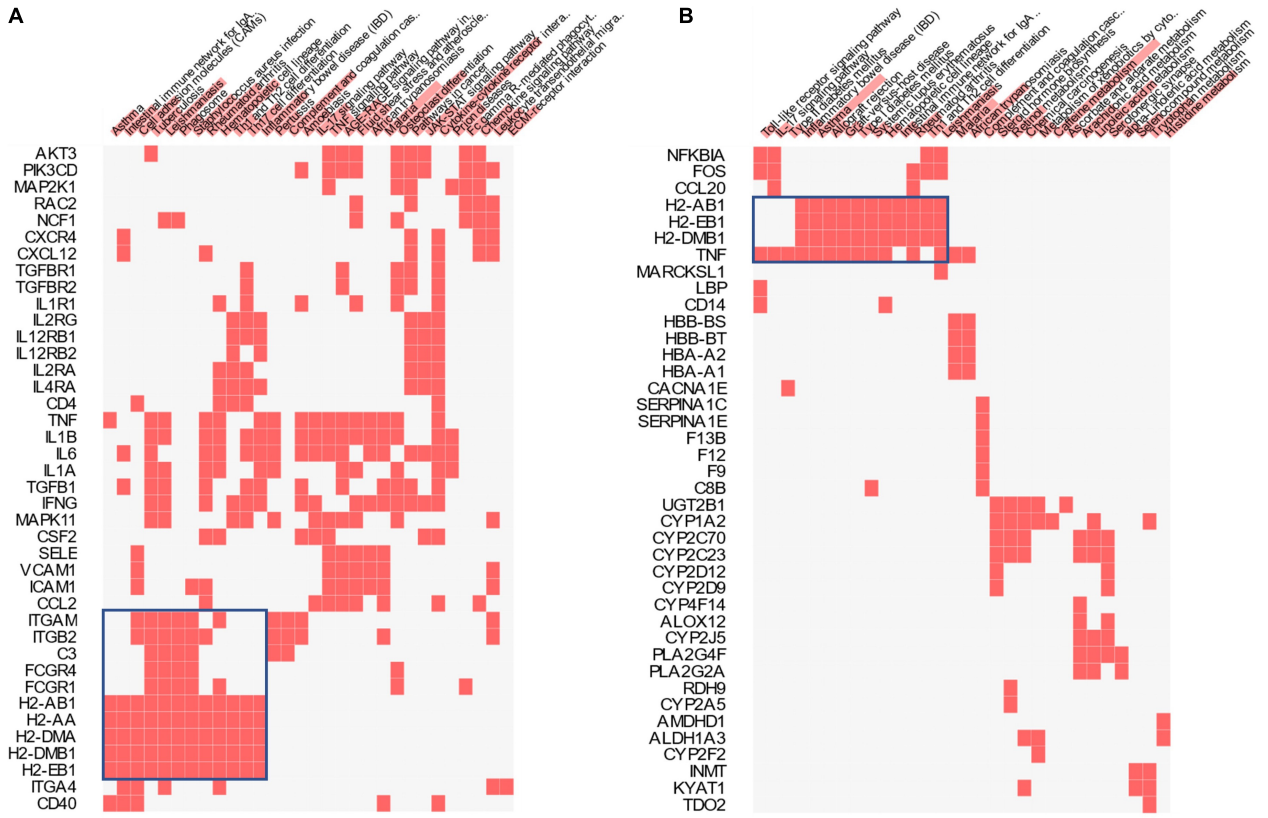

FIGURE 7 | Kyoto Encyclopedia of Genes and Genomes (KEGG) pathway analysis. Clustered heatmap of the KEGG genes and pathways for CD *vs*. C **(A)** and TD *vs*. CD **(B)**. *Color bars over the pathway names* represent the combined scores (*p*-values and *z*-scores) of the pathways. *TD*, Tibetan tea + DSS; *CD*, dextran sodium sulfate-induced model; *C*, control.

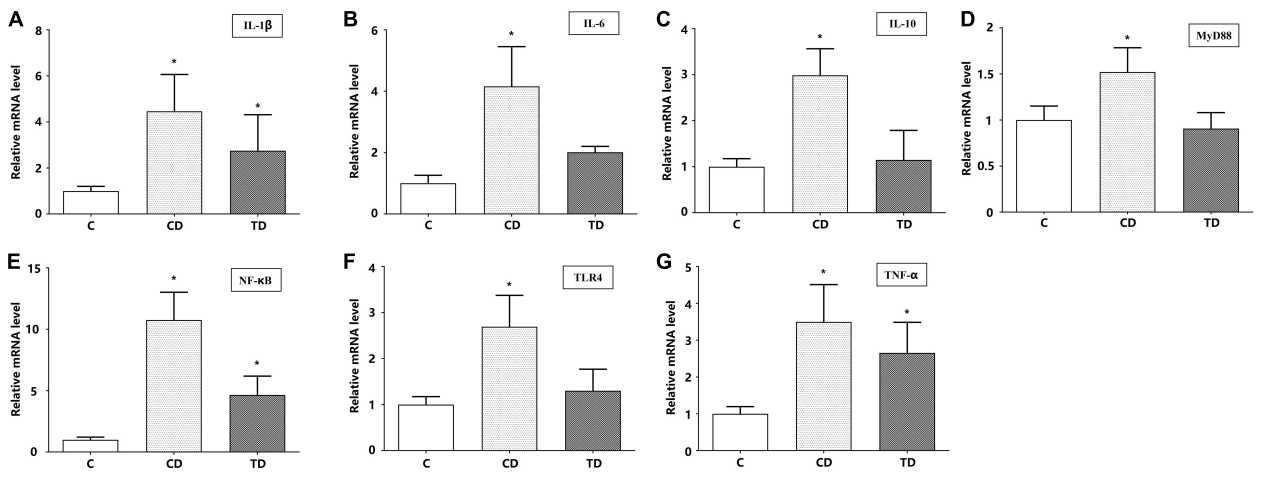

FIGURE 8 | The relative mRNA expression levels of IL-1β **(A)**, IL-6 **(B)**, IL-10 **(C)**, MyD88 **(D)**, NF-κB **(E)**, TLR4 **(F)**, and TNF-α **(G)** in colon tissues. *$p < 0.05$ vs. the control group.

In the current study, TTE intake significantly reduced the clinical symptoms of UC by alleviating the morphology of damaged cells and reducing glandular hypertrophy and the infiltration of inflammatory cells. An increase in the concentration of MPO is regarded as an index of the infiltration of neutrophils and inflammation (Choudhary et al., 2001). Herein, TTE significantly decreased the concentration of MPO when compared to non-treated DSS-administered mice.

There are two potential mechanisms of TTE preventing UC. The first mechanism is the indirect regulation of the gut microbiota. Pathogens damage or weaken the protective function of the intestinal mucosa, while beneficial microbes can counteract and/or fix such damage (Lee and Chang, 2021). When mice were treated with TTE, the relative abundance of Bacteroidetes, Verrucomicrobia, Deferribacteres, and Melainabacteria decreased significantly at the phylum level. These results indicated that TTE could alleviate UC by regulating the number of pathogenic bacteria in the gut microbiota. In the C, T, CD, and TD groups, beneficial microbes, such as *L. reuteri*, *B. choerinum*, and *L. intestinalis*, showed an "up–down–up" trend. It was demonstrated that TTE could significantly upregulate *Lactobacillus* and *Bifidobacterium* both in healthy and UC-induced mice and that these beneficial microbes were closely associated with colitis remission.

Bifidobacterium is one of the first beneficial microbes to colonize the intestines in babies and remains the major microbe of the intestines in adults (Ventura et al., 2014). It increases antioxidant activity and impedes the recurrence of UC. *Bifidobacterium breve* has been shown to reduce the apoptotic loss of epithelial cells in a MyD88-dependent fashion (Hughes et al., 2017). *Lactobacillus*, another beneficial commensal, has been shown to adjust the community of the gut microbiota along with inhibition of harmful bacteria *via* lowering the gut pH, producing short-chain fatty acids (SCFAs) and defensins (Durchschein et al., 2016). In addition, *Lactobacillus* prevents the colonization of harmful bacteria and the invasion of colon tissues and decreases the pro-inflammatory response of epithelial cells (Takamura et al., 2011). The probiotic *L. reuteri* produces reuterin, which contains hydroxy and aldehydic functional groups, and has been shown to have a robust repressive effect on intestinal pathogens (Takamura et al., 2011; Sun et al., 2018). Thus, it was expected that Tibetan tea could alleviate inflammatory reactions and prevent UC by increasing these beneficial microbes in the gut.

The second mechanism is the direct regulation of the host intestinal immune system to control inflammation. To explore the molecular mechanism of the protective effects of TTE on UC and to identify the key gene sets and pathways involved in this anti-inflammatory process, we focused on detecting changes in the C, CD, and TD groups. The colonic tissues of the mice from these three groups were subjected to transcriptomic and qPCR analyses. By analyzing the transcriptome, the positive effect of TTE on UC is likely attributed to the changes in the G alpha (i) signaling pathway and the innate immune system. The DEGs between the CD and TD groups were enriched in several inflammation- and immune system-related pathways (intestinal immune network, Toll-like receptor signaling pathway, IL-17 signaling pathway, etc.). The pathogenesis of inflammatory bowel disease (IBD) has been linked to an imbalanced and overactive immune response of the intestinal mucosa (Ramos and Papadakis, 2019). DSS damages the intestinal epithelial barrier; as a result, pathogens cross the mucosa and infect the epithelial cells, subsequently causing inflammation (Jeengar et al., 2017).

NF-κB, a key transcription factor, has been shown to be activated in the colon of IBD patients, where its activation level was shown to be correlated with disease severity (Meng et al., 2020). Therefore, modulating the NF-κB pathway could be an effective strategy to treat IBD. Interestingly, the positive impact of TTE on UC was attributed to changes in the innate immune system. Toll-like receptors (TLRs) elicit inflammatory reactions by triggering the inherent immune system (Alfonso-Loeches et al., 2010). For instance, TLR4 normalizes several inflammatory cytokines in IBD (Furuta et al., 2006). Furthermore, the relative expression of the genes linked to the TLR4/MyD88/NF-κB signaling pathway (*IL-1*β, *IL-6*, *IL-10*, *MyD88*, *NF-κB*, *TLR4*, and *TNF-*α) was verified in the colons of mice. The results clearly suggest that the anti-inflammatory impact of beneficial microbes is linked to the decreased expression of the TLR4/MyD88/NF-κB signaling pathway in the colonic tissues of mice.

CONCLUSION

Our data provided orthogonal evidence to confirm that TTE can regulate the immune system to reduce inflammation in UC. This was attributed to the effective regulation of the inflammatory signaling pathway (TLR4/MyD88/NF-κB) and the recovery of beneficial microbes belonging to the genera *Lactobacillus* and *Bifidobacterium*. This study advances the understanding of the protective effects of Tibetan tea in alleviating enteritis. Moreover, future investigations should focus on exploring the components of TTE that conferred the main anti-inflammatory impact.

DATA AVAILABILITY STATEMENT

The raw sequence data reported in this paper have been deposited in the Genome Sequence Archive (Genomics, Proteomics & Bioinformatics 2017) in National Genomics Data Center (Nucleic Acids Res 2021), China National Center for Bioinformation/ Beijing Institute of Genomics, Chinese Academy of Sciences, under accession number CRA004155 and CRA004148 that are publicly accessible at https://bigd.big.ac.cn/gsa.

ETHICS STATEMENT

The animal study was reviewed and approved by the Care and Use of Laboratory Animals by Sichuan University of Science and Engineering (Zigong, China).

AUTHOR CONTRIBUTIONS

NW and HZ conceived the study. NW and DD designed the study and wrote the first version of the manuscript. TW, HL, and ZL participated in its design and coordination and performed the statistical analysis. JM and RZ conceived the study and collected the experimental material. MS and MM collected and analyzed the raw data. MM revised the manuscript. HZ is responsible for this study, participated in its design and coordination, and helped draft the manuscript. All authors have read and approved the final manuscript.

FUNDING

This work was funded by grants from the Science and Technology Department of Sichuan Province (grant no. 2020YFH0130), the Talent Introduction Project of Sichuan University of Science & Engineering (grant no. 2019RC29), the Academician (Expert) Workstation Project of Sichuan University of Science & Engineering (grant no. 2018YSCZZ01), and the Innovation and Entrepreneurship Program for College Students (grant nos. S201910622061 and cx2020109).

SUPPLEMENTARY MATERIAL

The Supplementary Material for this article can be found online at: https://www.frontiersin.org/articles/10.3389/fmicb.2021.748594/full#supplementary-material

Supplementary Figure 1 | Comparison of theaflavins content between Tibetan tea **(A)** and Pu-erh tea **(B)** by UHPLC-Q-TOF.

Supplementary Figure 2 | Effects of TTE on colon length of mice after colitis induction. The arrow represents the site of colonic edema. Scale bars = 1 cm.

REFERENCES

Ajayi, B., Adedara, I., and Farombi, E. (2018). Protective mechanisms of 6-gingerol in dextran sulfate sodium-induced chronic ulcerative colitis in mice. *Hum. Exp. Toxicol.* 37, 1054–1068. doi: 10.1177/0960327117751235

Alfonso-Loeches, S., Pascual-Lucas, M., Blanco, A. M., Sanchez-Vera, I., and Guerri, C. (2010). Pivotal role of TLR4 receptors in alcohol-induced neuroinflammation and brain damage. *J. Neurosci.* 30, 8285–8295. doi: 10.1523/JNEUROSCI.0976-10.2010

Ananthakrishnan, A. N., Bernstein, C. N., Iliopoulos, D., Macpherson, A., Neurath, M. F., Ali, R. A. R., et al. (2018). Environmental triggers in IBD: a review of progress and evidence. *Nat. Rev. Gastroenterol. Hepatol.* 15, 39–49. doi: 10.1038/nrgastro.2017.136

Caruso, R., Lo, B. C., and Núñez, G. (2020). Host–microbiota interactions in inflammatory bowel disease. *Nat. Rev. Immunol.* 20, 411–426. doi: 10.1038/s41577-019-0268-7

Choudhary, S., Keshavarzian, A., Yong, S., Wade, M., Bocckino, S., Day, B. J., et al. (2001). Novel antioxidants zolimid and AEOL11201 ameliorate colitis in rats. *Dig. Dis. Sci.* 46, 2222–2230. doi: 10.1023/A:1011975218006

Durchschein, F., Petritsch, W., and Hammer, H. F. (2016). Diet therapy for inflammatory bowel diseases: the established and the new. *World J. Gastroenterol.* 22, 2179–2194. doi: 10.3748/wjg.v22.i7.2179

Edgar, R. C. (2004). MUSCLE: multiple sequence alignment with high accuracy and high throughput. *Nucleic Acids Res.* 32, 1792–1797. doi: 10.2460/ajvr.69.1.82

Edgar, R. C. (2013). Uparse: highly accurate OTU sequences from microbial amplicon reads. *Nat. Methods* 10, 996–1000. doi: 10.1038/NMETH.2604

Edgar, R. C., Haas, B. J., Clemente, J. C., Quince, C., and Knight, R. (2011). UCHIME improves sensitivity and speed of chimera detection. *Bioinformatics* 27, 2194–2200. doi: 10.1093/bioinformatics/btr381

Fang, W., Zhu, S., Niu, Z., and Yin, Y. (2019). The protective effect of syringic acid on dextran sulfate sodium-induced experimental colitis in BALB/c mice. *Drug Dev. Res.* 80, 731–740. doi: 10.1002/ddr.21524

Franzosa, E. A., Sirota-Madi, A., Avila-Pacheco, J., Fornelos, N., Haiser, H. J., Reinker, S., et al. (2019). Gut microbiome structure and metabolic activity in inflammatory bowel disease. *Nat. Microbiol.* 4, 293–305. doi: 10.1038/s41564-018-0306-4

Furuta, T., Kikuchi, T., Akira, S., Watanabe, N., and Yoshikawa, Y. (2006). Roles of the small intestine for induction of toll-like receptor 4-mediated innate resistance in naturally acquired murine toxoplasmosis. *Int. Immunol.* 18, 1655–1662. doi: 10.1093/intimm/dxl099

Griffith, G. W., Ozkose, E., Theodorou, M. K., and Davies, D. R. (2009). Diversity of anaerobic fungal populations in cattle revealed by selective enrichment culture using different carbon sources. *Fungal Ecol.* 2, 87–97. doi: 10.1016/j.funeco.2009.01.005

Haas, B. J., Gevers, D., Earl, A. M., Feldgarden, M., Ward, D. V., Giannoukos, G., et al. (2011). Chimeric 16S rRNA sequence formation and detection in Sanger and 454-pyrosequenced PCR amplicons. *Genome Res.* 21, 494–504. doi: 10.1101/gr.112730.110

Hughes, K. R., Harnisch, L. C., Alcon-Giner, C., Mitra, S., Wright, C. J., Ketskemety, J., et al. (2017). *Bifidobacterium breve* reduces apoptotic epithelial cell shedding in an exopolysaccharide and MyD88-dependent manner. *Open Biol.* 7:160155. doi: 10.1098/rsob.160155

Jeengar, M. K., Thummuri, D., Magnusson, M., Naidu, V. G. M., and Uppugunduri, S. (2017). Uridine ameliorates dextran sulfate sodium (DSS)-induced colitis in mice. *Sci. Rep.* 7:3924. doi: 10.1038/s41598-017-04041-9

Kuprys, P. V., Cannon, A. R., Shieh, J., Iftekhar, N., Park, S. K., Eberhardt, J. M., et al. (2020). Alcohol decreases intestinal ratio of *Lactobacillus* to *Enterobacteriaceae* and induces hepatic immune tolerance in a murine model of DSS-colitis. *Gut Microbes* 12:1838236. doi: 10.1080/19490976.2020.1838236

Lee, M., and Chang, E. B. (2021). Inflammatory bowel diseases (IBD) and the microbiome-searching the crime scene for clues. *Gastroenterology* 160, 524–537. doi: 10.1053/j.gastro.2020.09.056

Lee, W. T., Tung, Y. T., Wu, C. C., Tu, P. S., and Yen, G. C. (2018). Camellia oil (*Camellia oleifera Abel.*) modifies the composition of gut microbiota and alleviates acetic acid-induced colitis in rats. *J. Agric. Food Chem.* 66, 7384–7392. doi: 10.1021/acs.jafc.8b02166

Lewis, J. D., and Abreu, M. T. (2017). Diet as a trigger or therapy for inflammatory bowel diseases. *Gastroenterology* 152, 398–414.e6. doi: 10.1053/j.gastro.2016.10.019

Li, W., Liu, Y., Ye, Y., Che, Z., and Wu, T. (2021). Chemical profiling and metabolic mechanism of Pixian doubanjiang, a famous condiment in Chinese cuisine. *LWT* 145:111274. doi: 10.1016/j.lwt.2021.111274

Limdi, J. K., and Vasant, D. H. (2015). Anorectal dysfunction in distal ulcerative colitis: challenges and opportunities for topical therapy. *J. Crohns Colitis* 10, 503–503. doi: 10.1093/ecco-jcc/jjv217

Liu, Y., Wang, X., Chen, Q., Luo, L., Ma, M., Xiao, B., et al. (2020). Camellia sinensis and Litsea coreana ameliorate intestinal inflammation and modulate gut microbiota in dextran sulfate sodium-induced colitis mice. *Mol. Nutr. Food Res.* 64:1900943. doi: 10.1002/mnfr.201900943

Ma, Y., Hu, C., Yan, W., Jiang, H., and Liu, G. (2020). *Lactobacillus pentosus* increases the abundance of akkermansia and affects the serum metabolome to alleviate DSS-induced colitis in a murine model. *Front. Cell Dev. Biol.* 8:591408. doi: 10.3389/fcell.2020.591408

Martin, M. (2011). Cutadapt removes adapter sequences from high-throughput sequencing reads. *EMBnet J.* 17, 10–12. doi: 10.14806/ej.17.1.200

Meng, Q., Wu, W., Pei, T., Xue, J., Xiao, P., Sun, L., et al. (2020). miRNA-129/FBW7/NF-κB, a novel regulatory pathway in inflammatory bowel disease. *Mol. Ther. Nucleic Acids* 19, 731–740. doi: 10.1016/j.omtn.2019.10.048

Oh, W. S., Jung, J. C., Choi, Y. M., Mun, J. Y., Ku, S. K., and Song, C. H. (2020). Protective effects of fermented rice extract on ulcerative colitis induced by dextran sodium sulfate in mice. *Food Sci. Nutr.* 8, 1718–1728. doi: 10.1002/fsn3.1460

Pandurangan, A. K., Ismail, S., Saadatdoust, Z., and Esa, N. M. (2015). Allicin alleviates dextran sodium sulfate- (DSS-) induced ulcerative colitis in BALB/c mice. *Oxid. Med. Cell. Longev.* 2015:605208. doi: 10.1155/2015/605208

Petrella, C. (2016). *Lactobacillus reuteri* treatment and DSS colitis: new insight into the mechanism of protection. *Acta Physiol.* 217, 274–275. doi: 10.1111/apha.12719

Qi, Q., Liu, Y.-N., Jin, X.-M., Zhang, L.-S., Wang, C., Bao, C.-H., et al. (2018). Moxibustion treatment modulates the gut microbiota and immune function in a dextran sulphate sodium-induced colitis rat model. *World J. Gastroenterol.* 24, 3130–3144. doi: 10.3748/wjg.v24.i28.3130

Ramos, G. P., and Papadakis, K. A. (2019). Mechanisms of disease: inflammatory bowel diseases. *Mayo Clin. Proc.* 94, 155–165. doi: 10.1016/j.mayocp.2018.09.013

Schloss, P. D., Westcott, S. L., Ryabin, T., Hall, J. R., Hartmann, M., Hollister, E. B., et al. (2009). Introducing mothur: open-source, platform-independent, community-supported software for describing and comparing microbial communities. *Appl. Environ. Microbiol.* 75, 7537–7541. doi: 10.1128/AEM.01541-09

Sun, M., Liu, Y., Song, Y., Gao, Y., Zhao, F., Luo, Y., et al. (2020). The ameliorative effect of *Lactobacillus plantarum*-12 on DSS-induced murine colitis. *Food Funct.* 11, 5205–5222. doi: 10.1039/D0FO00007H

Sun, M. C., Zhang, F. C., Yin, X., Cheng, B. J., Zhao, C. H., Wang, Y. I., et al. (2018). *Lactobacillus reuteri* F-9-35 prevents DSS-induced colitis by inhibiting proinflammatory gene expression and restoring the gut microbiota in mice. *J. Food Sci.* 83, 2645–2652. doi: 10.1111/1750-3841.14326

Takamura, T., Harama, D., Fukumoto, S., Nakamura, Y., Shimokawa, N., Ishimaru, K., et al. (2011). *Lactobacillus bulgaricus* OLL1181 activates the aryl hydrocarbon receptor pathway and inhibits colitis. *Immunol. Cell Biol.* 89, 817–822. doi: 10.1038/icb.2010.165

Ventura, M., Turroni, F., Lugli, G. A., and van Sinderen, D. (2014). *Bifidobacteria* and humans: our special friends, from ecological to genomics perspectives. *J. Sci. Food Agric.* 94, 163–168. doi: 10.1002/jsfa.6356

Wu, T., Lv, H., Wang, F., and Wang, Y. (2016). Characterization of polyphenols from Lycium ruthenicum fruit by UPLC-Q-TOF/MSE and their antioxidant activity in Caco-2 cells. *J. Agric. Food Chem.* 64, 2280–2288. doi: 10.1021/acs.jafc.6b00035

Xu, J., Liang, X., Wang, W., Chen, S., and Tang, Q. (2020). Study on Anti-radiation effect of Ya'an Tibetan Tea. *J. Phys. Conf. Ser.* 1549:032049. doi: 10.1088/1742-6596/1549/3/032049

Zheng, Q., Li, W., Zhang, H., Gao, X., and Tan, S. (2020). Optimizing synchronous extraction and antioxidant activity evaluation of polyphenols and polysaccharides from Ya'an Tibetan tea (*Camellia sinensis*). *Food Sci. Nutr.* 8, 489–499. doi: 10.1002/fsn3.1331

Conflict of Interest: DD was employed by the company ExxonMobil Research and Engineering. JM was employed by Sichuan Jixiang Tea Co., Ltd.

The remaining authors declare that the research was conducted in the absence of any commercial or financial relationships that could be construed as a potential conflict of interest.

Publisher's Note: All claims expressed in this article are solely those of the authors and do not necessarily represent those of their affiliated organizations, or those of the publisher, the editors and the reviewers. Any product that may be evaluated in this article, or claim that may be made by its manufacturer, is not guaranteed or endorsed by the publisher.

frontiers in Microbiology

ORIGINAL RESEARCH
published: 16 February 2022
doi: 10.3389/fmicb.2022.846011

Multi-Omics Analysis After Vaginal Administration of *Bacteroides fragilis* in Chickens

Lu Chen[1†], Maosen Yang[1†], Wei Zhu[1†], Yuan Su[1], Diyan Li[1] and Tao Wang[2]**

[1]*Farm Animal Genetic Resources Exploration and Innovation Key Laboratory of Sichuan Province, Sichuan Agricultural University, Chengdu, China,* [2]*School of Pharmacy, Chengdu University, Chengdu, China*

The reproductive tract of chickens is an important organ for egg formation. The vagina is in close contact with the external environment, which may lead to the invasion of a variety of pathogenic bacteria, affect the internal and external quality of eggs, and even increase mortality and cause economic loss. In recent years, probiotics as a substitute for antibiotics have brought economic benefits in livestock and poultry production. In the present study, we investigated the effects of vaginal administration of *Bacteroides fragilis* on the cloacal microbiota, vaginal transcriptome and metabolomics of chickens and evaluated the beneficial potential of *B. fragilis*. The results showed that *B. fragilis* treatment could affect the microbial composition of the cloaca. Transcriptome analysis found that the immune-related genes *CCN3*, *HAS2*, and *RICTOR* were upregulated, that the inflammatory genes *EDNRB*, *TOX*, and *NKX2-3* were downregulated, and that DEGs were also enriched in the regulation of the inflammatory response, cellular metabolism, and synaptic response pathways. In addition, the differential metabolites were mainly related to steroid hormone biosynthesis, unsaturated fatty acid biosynthesis, and arachidonic acid metabolism, and we identified associations between specific differential metabolites and genes. Overall, this study provides a theoretical basis for the application of *B. fragilis* as a potential probiotic in livestock and poultry production.

Keywords: chicken, vagina, cloaca, *Bacteroides fragilis*, microbiota, transcriptome, metabolome

OPEN ACCESS

Edited by:
Fengjie Sun,
Georgia Gwinnett College, United States

Reviewed by:
Gong-Wei Zhang,
Southwest University, China
Zhixiong Pan,
Affiliated Hospital of Guilin Medical University, China

****Correspondence:***
Diyan Li
diyanli@sicau.edu.cn
Tao Wang
wanttao@hotmail.com

[†]These authors have contributed equally to this work

Specialty section:
This article was submitted to Food Microbiology, a section of the journal Frontiers in Microbiology

Received: *30 December 2021*
Accepted: *24 January 2022*
Published: *16 February 2022*

Citation:
Chen L, Yang M, Zhu W, Su Y, Li D and Wang T (2022) Multi-Omics Analysis After Vaginal Administration of Bacteroides fragilis in Chickens. Front. Microbiol. 13:846011. doi: 10.3389/fmicb.2022.846011

INTRODUCTION

The hen's reproductive tract is not as abundant in mammals; it is mainly used for egg formation (Sah and Mishra, 2018). Some pathogenic bacteria colonization of the oviduct can lead to egg pollution, such as *Salmonella strains* and *Gallibacterium anatis* (McWhorter and Chousalkar, 2016; Zhang et al., 2017). Therefore, the prevention of reproductive tract infection by pathogens is important for the safe production of eggs and the health of chickens. In recent years, with the rise of drug-resistant strains and adverse reactions after the use of antibiotics, probiotics have gradually entered poultry production, which can improve intestinal health, prevent disease, and promote nutrient absorption (Shini et al., 2013; Jeni et al., 2021).

Bacteroides fragilis is a gram-negative obligate anaerobe that often colonizes the oral cavity, intestinal tract, and female reproductive tract. A nontoxic *B. fragilis* (NTBF) strain uses dietary and host-derived polysaccharides as a source of carbon and energy (Spence et al., 2006). Moreover, *B. fragilis* has been shown to inhibit inflammation in the intestinal tract and cancer associated with enteritis (Lee et al., 2018; Zheng et al., 2020; Shao et al., 2021); it also participates in the immunomodulatory regulation of brain immunity through the gut-brain axis (Erturk-Hasdemir et al., 2021) and regulates inflammation in other areas (Johnson et al., 2018). The strain also suppressed pathogen infection, such as *Vibrio parahaemolyticus* and *Salmonella Heidelberg* (Li et al., 2017; Vernay et al., 2020). Although *B. fragilis* performed a variety of beneficial functions in other hosts, its effects in chickens remains unclear.

With the development of high-throughput sequencing technology, many studies are being conducted on multi-omics analysis. Previous studies have found that diet supplementation with the combination of *Bacillus* species for aging laying hens can reduce the number of *Escherichia coli* and increase *Lactobacillus* in the cecum (Yang et al., 2020). In addition, Wang et al. (2019b) found that oral administration of *Lactobacillus frumenti* can regulate lipid and amino acid metabolism and promote liver energy production in early weaned piglets. Recently, Chen et al. (2021) conducted a gavage experiment using germ-free mice that activated TLR4 and mTOR signaling pathways and increased the expression of fat-accumulating genes, leading to host inflammation. Although probiotics are generally treated using subcutaneous injection and intragastric administration, vaginal administration has been used to better study the effect of probiotics on the reproductive tract in recent years (Deng et al., 2014; Genís et al., 2017). Studies have found that using probiotics in the vagina can reduce the incidence of vaginal infections in women (Deng et al., 2014). In poultry, lactic acid bacteria by vaginal administration can safely colonize the vagina, eliminate some pathogens, and modulate the immune response (Reid and Bocking, 2003). Therefore, we attempted to explore the effects of intravaginal administration of *B. fragilis* on the microbiome, transcriptome, and metabolome of the chicken reproductive tract in this study.

MATERIALS AND METHODS

Bacterial Strains and Culture Conditions

Bacteroides fragilis ATCC25285 was obtained from the American Type Culture Collection (Manassas, VI, United States). The strain was anaerobically cultured on tryptic soy agar (TSA) supplemented with 5% sheep blood at 37°C under anaerobic workbench conditions containing 80% N_2, 10% CO_2, and 10% H_2. After purification and 16S rRNA gene sequencing identification, collected strains were prepared with cell pellets resuspended in phosphate-buffered saline (PBS) supplemented with 20% glycerol after centrifugation and preserved at −80°C. The bacterial solution was colony-forming unit (cfu) enumerated on TSA with 5% sheep blood before injection.

Animals and Experimental Design

This experiment was conducted in the poultry breeding base of Sichuan Agricultural University in Ya'an, China. Eleven 320-day-old green shell laying hens with the same weight and diet without antibiotics were randomly divided into a control group ($n = 5$) and a *B. fragilis* group ($n = 6$). The *B. fragilis* or vehicle (sterile PBS with 20% glycerin) were infused into the vaginal tract gently with 3-ml sterile pasteur pipettes (NEST, Wuxi, China). The control group was given 500 μl sterile PBS with 20% glycerin. The *B. fragilis* group was given 500 μl (1×10^{10} CFU/ml) of *B. fragilis* suspension by intravaginal administration. Injections were given every other day for a total of four times (Hsiao et al., 2013). Cloaca swabs were collected with cotton swabs after observation for 2 months (Mazmanian et al., 2005). Then, all chickens were sacrificed by cervical dislocation. Vaginal tissue samples were sampled from each experimental chicken for further RNA-seq and metabolome analysis. Storing all collected samples in a −80°C refrigerator.

DNA Extraction and Microbial 16S rRNA Sequencing Analysis

Cloacal microbial DNA was extracted using the Ezup Oral Swabs Genomic DNA Extraction Kit (Sangon Biotech, Shanghai, China) following the manufacturer's guidelines. The extracted DNA was quantified using a NanoDrop2000 spectrophotometer (Thermo Fisher Scientific, DE, United States), and the quality was assessed by 1% agarose gel electrophoresis. The V3-V4 hypervariable regions of the bacterial 16S rRNA gene were amplified used specific primer 341F (5′-CCTAYGGGRBGCASCAG-3′) and 806R (5′-GGACTACNNGGGTATCTAAT-3′). All PCRs were carried out with 15 μl of Phusion® High-Fidelity PCR Master Mix (New England Biolabs), 0.2 μM forward and reverse primers, and approximately 10 ng template DNA. Thermal cycling consisted of the initial denaturation at 98°C for 1 min, followed by 30 cycles of denaturation at 98°C for 10 s, annealing at 50°C for 30 s, and elongation at 72°C for 30 s, and then, finally 72°C for 5 min. PCR products were purified with a Qiagen Gel Extraction Kit (Qiagen, Germany). Sequencing libraries were generated using the TruSeq® DNA PCR-Free Sample Preparation Kit (Illumina, United States) following the manufacturer's recommendations, and index codes were added. The library quality was assessed on the Qubit@2.0 Fluorometer (Thermo Scientific) and Agilent Bioanalyzer 2100 system. Finally, the library was sequenced on an Illumina NovaSeq platform, and 250 bp paired-end reads were generated.

The raw 16S rRNA gene sequencing data were processed using QIIME2 (Bolyen et al., 2019). Then, these data were filtered to eliminate adapters and low-quality reads for clean reads. The high-quality representative feature sequences were used as the reference for taxonomic annotation with the Silva database (Quast et al., 2013).[1] Alpha diversity is represented by faith_ pd and evenness indices, and different groups were compared using the Kruskal–Wallis test. Principal coordinates analysis (PCoA) is represented by unweighted UniFrac distance, and PERMANOVA was used for intergroup significance tests.

[1]https://www.arb-silva.de/

RNA Extraction and Transcriptome Analysis

Total RNA was extracted from vaginal tissue using RNAiso Plus Total RNA extraction reagent (Takara) following the manufacturer's instructions, and RNA was detected with a NanoDrop2000 spectrophotometer (Thermo Fisher Scientific, DE, United States). The quantity of total RNA was determined using a Qubit 2.0 fluorimeter (Life Technologies, CA, United States), and the integrity of total RNA was analyzed using a Bioanalyzer 2100 system (Agilent Technologies, CA, United States). After the RNA samples were qualified, the eukaryotic mRNA was enriched by magnetic beads with oligo(dT). Then, cDNA was synthesized using mRNA as template. Second-strand cDNA was synthesized by buffer, dNTPs, DNA polymerase I and RNase H and purified using AMPure XP Beads. The purified double-stranded cDNA was end repaired; poly(A) was added, and the cDNA was ligated to a sequencing connector. After fragment selection and PCR amplification, a sequencing library was obtained and sequenced using DNBSEQ-T7 by Novogene (Beijing, China).

We removed low-quality reads and calculated the Q20, Q30, and GC contents of the clean reads to obtain high-quality clean reads. Clean data were mapped to the chicken reference genome (Gallus-6.0) using the STAR alignment tool (V2.7.6a). Then, Kallisto (V0.44.0) software was used to quantify gene expression as transcripts per million (TPM). Benjamini and Hochberg's procedure was used to adjust the value of p (Audic and Claverie, 1997; Benjamini and Yekutieli, 2001). The differentially expressed genes (DEGs) with an adjusted value of $p(Padj) < 0.05$ and $|\log2 \text{ (fold change)}| > 1$ identified by DESeq2 (v1.30.1) (Wang et al., 2010) were considered as differentially expressed. Functional enrichment including GO terms and KEGG pathways of differentially expressed genes was performed by Metascape (Zhou et al., 2019b), and $p < 0.05$ was considered as significant. Then, 10 randomly selected DEGs were used to verify the transcriptome results by quantitative real-time PCR (qRT–PCR). Total RNA was reverse transcribed into cDNA using the RT Easy™ II (with gDNase) kit (FOREGENE, Chengdu, China). Next, RT–qPCR amplification was performed using SYBR Green Master Mix, and the chicken β-actin gene was used as a housekeeping gene. The relative expression levels of validated genes were determined using the $2^{-\triangle\triangle Ct}$ method. Primer sequences are listed in **Supplementary Table 1**.

Metabolomic Analysis

Metabolic analysis was performed on vaginal tissue used in this study. Metabolome extraction and pretreatment were based on protocols followed by Novogene (Beijing, China) and mainly used liquid mass spectrometry (LC–MS) technology (Want et al., 2010; Dunn et al., 2011). After qualitative and quantitative analysis of metabolites, data quality control was carried out to ensure the accuracy and reliability of the data results. Then, multivariate statistical analysis, including principal component analysis (PCA) and partial least squares discriminant analysis (PLS-DA), was carried out for metabolites. The two parameters of variable importance in the projection value (VIP) > 1 and $p < 0.05$ were used as the criteria to screen differential metabolites. Finally, the biological significance of metabolites was explained by the functional analysis of metabolic pathways based on the Kyoto Encyclopedia of Genes and Genomes (KEGG) database.[2]

Transcriptome and Metabolome Association Analysis

To analyze the correlation between the relative abundance of specific DEGs and significantly different metabolites, the correlation coefficients rho and value p were calculated by Pearson's statistical methods.

RESULTS

Effects of the Vaginal Administration of *Bacteroides fragilis* on Cloacal Microbiota

We performed 16S rRNA sequencing on the cloacal microbiota. After quality control, up to 982,622 high-quality reads were generated from 11 samples with an average of 89,329 reads per sample (**Supplementary Table 2**). We then used evenness and faith_ pd indices to visualize the microbiota diversity in different groups. There was no significant alpha diversity in the *B. fragilis* group and control group (Kruskal–Wallis, $p > 0.05$), but principal coordinate analysis (PCoA) based on unweighted UniFrac distance showed a trend of separation, although the difference was not significant (**Supplementary Figure 1**; **Figure 1A**).

Next, we studied changes in the microbial composition of the two groups. At the phylum level (relative abundance >1%), Firmicutes, Actinobacteria, Proteobacteria, and Bacteroidetes were dominant phyla in the groups. However, Firmicutes and Actinobacteria represented a higher proportion of the phyla in the *B. fragilis* group, with relative abundances of 56.45 and 31.37%, respectively. Bacteroidetes (16.34%), Fusobacteria (9.25%), and Proteobacteria (7.72%) were more abundant in the control group (**Figure 1B**). At the genus level (relative abundance > 0.05%), taxa unclassified below the family level (43.14%) were the most abundant in the control group, but the most dominant genus in the *B. fragilis* group was *Romboutsia*, with a relative abundance of 20.38%, followed by *Actinomyces* (20.26%), *Corynebacterium 1* (10.62%), *Clostridium sensu stricto 1* (6.08%), *Fournierella* (5.14%), *unidentified_Lachnospiraceae* (4.31%), and *Anaerosporobacter* (3.12%), the abundance of these genera were higher than that of the control group (**Figure 1C**).

Transcriptome Analysis of Vagina Tissues After *Bacteroides fragilis* Treatment

To identify differentially expressed mRNAs of vaginal tissue in the control group and *B. fragilis* group, we carried out transcriptome sequencing. The results of transcriptome sequencing and quality parameters are shown in **Supplementary Table 3**. A total of 153.24 G of raw data was produced in this sequencing, and 149.69 G of clean data was obtained after filtration. The GC content of clean samples ranged from 47.89% to 50.32%, and

[2]https://www.kegg.jp/

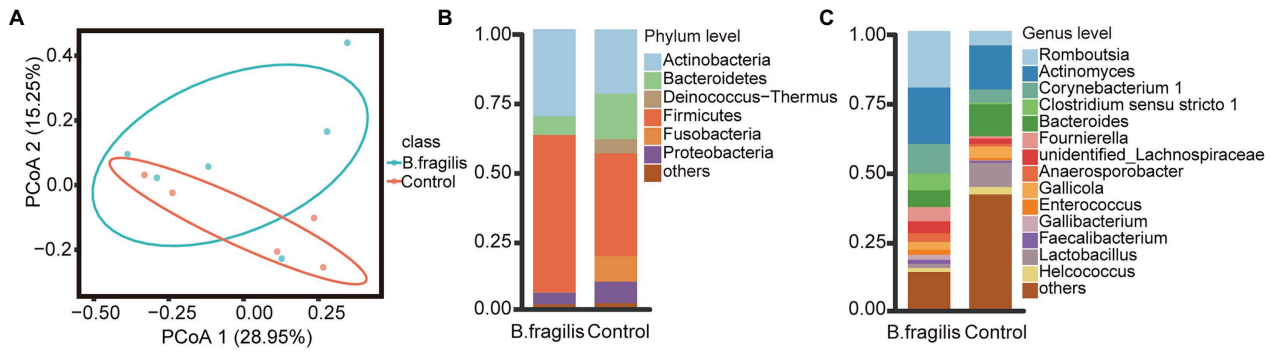

FIGURE 1 | Composition and distribution of the cloacal microbiota after the intravaginal administration of *Bacteroides fragilis* between the *Bacteroides fragilis* and control groups in chickens. **(A)** Principal coordinate analysis (PCoA) of bacterial community structures using the unweighted UniFrac method. **(B)** The relative abundances of the top seven phyla from cloaca samples. **(C)** The relative abundances of the top 15 genera in the microbiota.

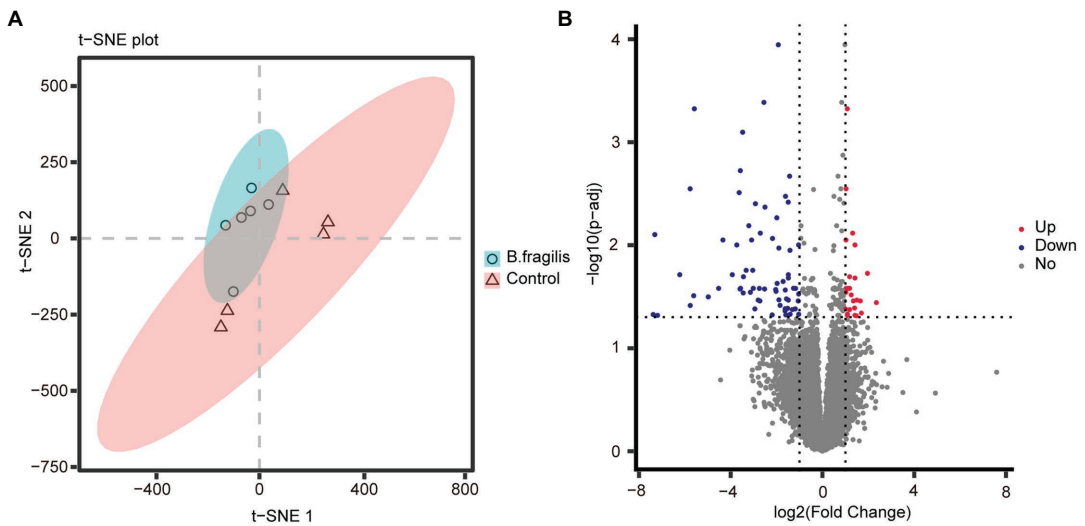

FIGURE 2 | Transcriptomic analysis of vaginal tissue between the *Bacteroides fragilis* group and the control group. **(A)** t-distributed stochastic neighbor embedding (t-SNE) based on gene expression as transcripts per million (TPM). **(B)** Volcano map of differentially expressed genes between the two groups.

the average percentage of Q20 bases in each sample was 95.53%. The high-quality reads were mapped to the chicken reference genome, and the average mapping was 95.78%.

Correlation analysis between samples was performed based on gene expression levels. Spearman correlation analysis showed that the 11 biological repeat samples were clustered, indicating that the sample selection was relatively reasonable (**Supplementary Figure 2**). t-SNE result revealed that there were significant differences between the *B. fragilis* and control groups (**Figure 2A**). A total of 16,776 genes were detected in both groups. Then, we screened 94 differentially expressed genes (DEGs) using *P*adj < 0.05 and | log2 (fold change) | > 1 as the standards, including 26 upregulated genes and 68 downregulated genes (**Figure 2B**). Then, we performed GO and KEGG enrichment analyses on these DEGs to study their biological functions. **Figure 3** shows the top 20 most enriched GO terms related to DEGs. The pathways related to immunity or inflammatory response terms mainly included the regulation of leukocyte cell–cell adhesion, the negative regulation of chemotaxis, and the regulation of inflammatory response and epithelial cell proliferation. The major DEGs involved in these GO terms included *CCN3*, *HAS2*, *RICTOR*, *TOX*, *EDNRB*, and *NKX2-3*. The remaining GO terms mainly included the metabolic process and cell and synaptic reactions, such as cellular response to hormone stimulus, cellular response to nitrogen compound, nucleoside bisphosphate metabolic process and cholesterol metabolic process, and chemical synaptic transmission. KEGG pathways enriched by DEGs mainly included the MAPK signaling pathway, calcium signaling pathway, and rheumatoid arthritis (**Supplementary Table 4**).

To validate the results of RNA-seq analysis, a total of 10 DEGs, including *CCN3*, *CTLA4*, *DIO2*, *ITPKA*, *PDK4*, *RICTOR*, *MYO5A*, *NPY*, *SEMA3c*, and *SYT12*, were subjected to quantitative reverse transcription-PCR (RT–qPCR; **Supplementary Table 5**). We found that the expression trend of RT–qPCR was consistent with the transcriptome through calculation, indicating the reliability of RNA-seq data.

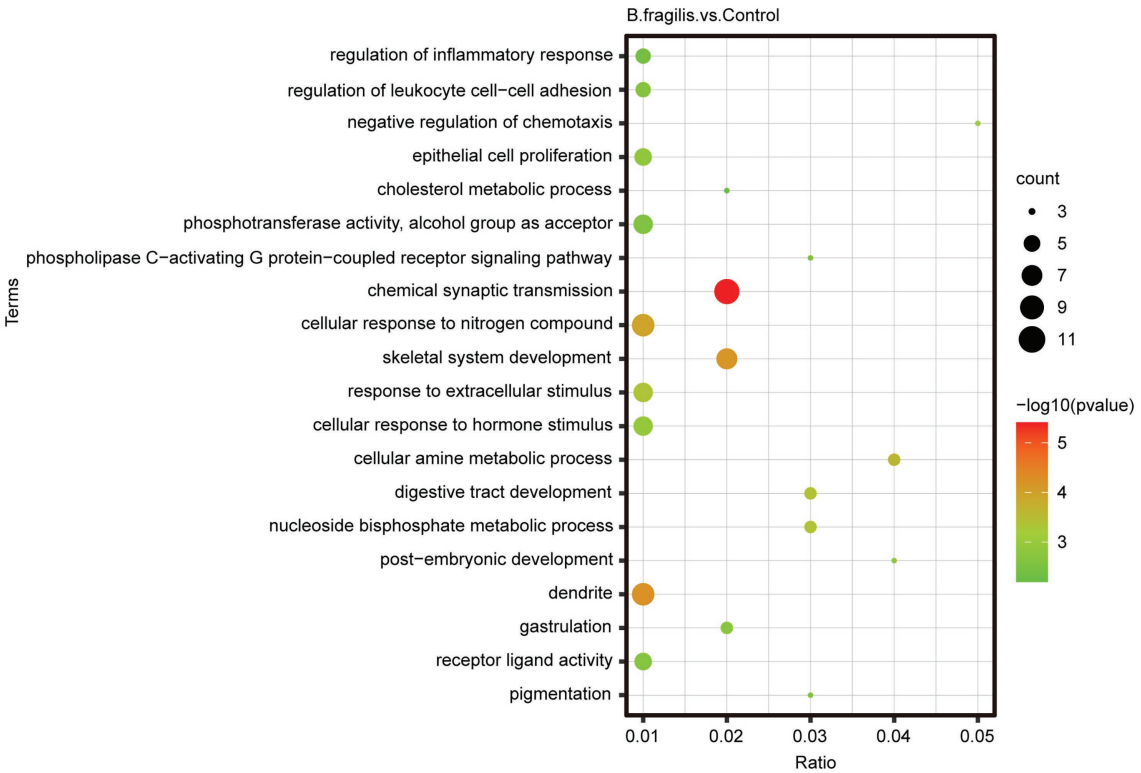

FIGURE 3 | Top 20 most enriched gene ontology (GO) terms of differentially expressed genes (DEGs). The X-axis shows the proportion of enriched genes to total genes in this term; the Y-axis shows the DEG-enriched GO term. The size and color of dots represent the number of genes and the value of *p*.

Metabolic Profiling of Vagina Tissues Following the Intravaginal Administration of *Bacteroides fragilis*

First, PLS-DA pattern analysis was performed on the control and *B. fragilis* groups to identify the overall metabolic differences between the two groups. According to the results in **Figure 4A**, we observed a significant trend toward separation of two groups in positive ion mode and negative ion mode. In addition, PCA showed excellent separation of metabolites between the two groups (**Supplementary Figure 3**).

The metabolomic analysis identified 38 metabolites with significant differences between the control and *B. fragilis* groups based on the value of VIP > 1.0 ($p < 0.05$). Among these metabolites are nine lipids and lipid-like molecules; the levels of these, except for estrone, palmitic acid, and prostaglandin F2alpha decreased; calcitriol, glycerol-3-phosphate, 7-ketocholesterol, corticosterone, 2-arachidonyl glycerol ether, and docosapentaenoic acid increased in the *B. fragilis* group compared with the control group. There were also eight organic acids and derivatives (**Supplementary Table 6**). At the same time, changes in these metabolites are shown in a volcano map and a heatmap generated by hierarchical clustering analysis (**Figures 4B,C**). Next, we used KEGG pathway enrichment to identify the most important biochemical metabolic pathways and signal transduction pathways involved in differential metabolites. Pathway enrichment analysis showed that the intravaginal administration of *B. fragilis* resulted in changes in lipid metabolism, including steroid hormone biosynthesis; the biosynthesis of unsaturated fatty acids; steroid biosynthesis; arachidonic acid metabolism; and the elongation, degradation, metabolism, and biosynthesis of fatty acids. The bacterial strain also regulated valine, leucine, and isoleucine degradation, tyrosine metabolism, and propanoate metabolism pathways (**Figure 5**).

Combined Analysis of Specific Differential Genes and Metabolites

To investigate the relationship between the vaginal transcriptome and metabolome after treatment with *B. fragilis*, we performed Pearson correlation analysis based on 24 differential genes and 37 differential metabolites. Calcitriol, methylmalonate, l-thyroxine, cysteinylglycine, and 7-ketocholesterol were positively correlated with most DEGs, such as *DRP2*, *ITPKA*, *STYK1*, and *HAS2* but were negatively correlated with *EDNRB*. Estrone, 3-indoxyl sulfate and bilirubin showed the opposite results, which were significantly negatively correlated with a majority of differential genes (**Figure 6**).

DISCUSSION

The chicken oviduct is an organ that receives ovulation from the ovary and completes egg formation; the vagina is located

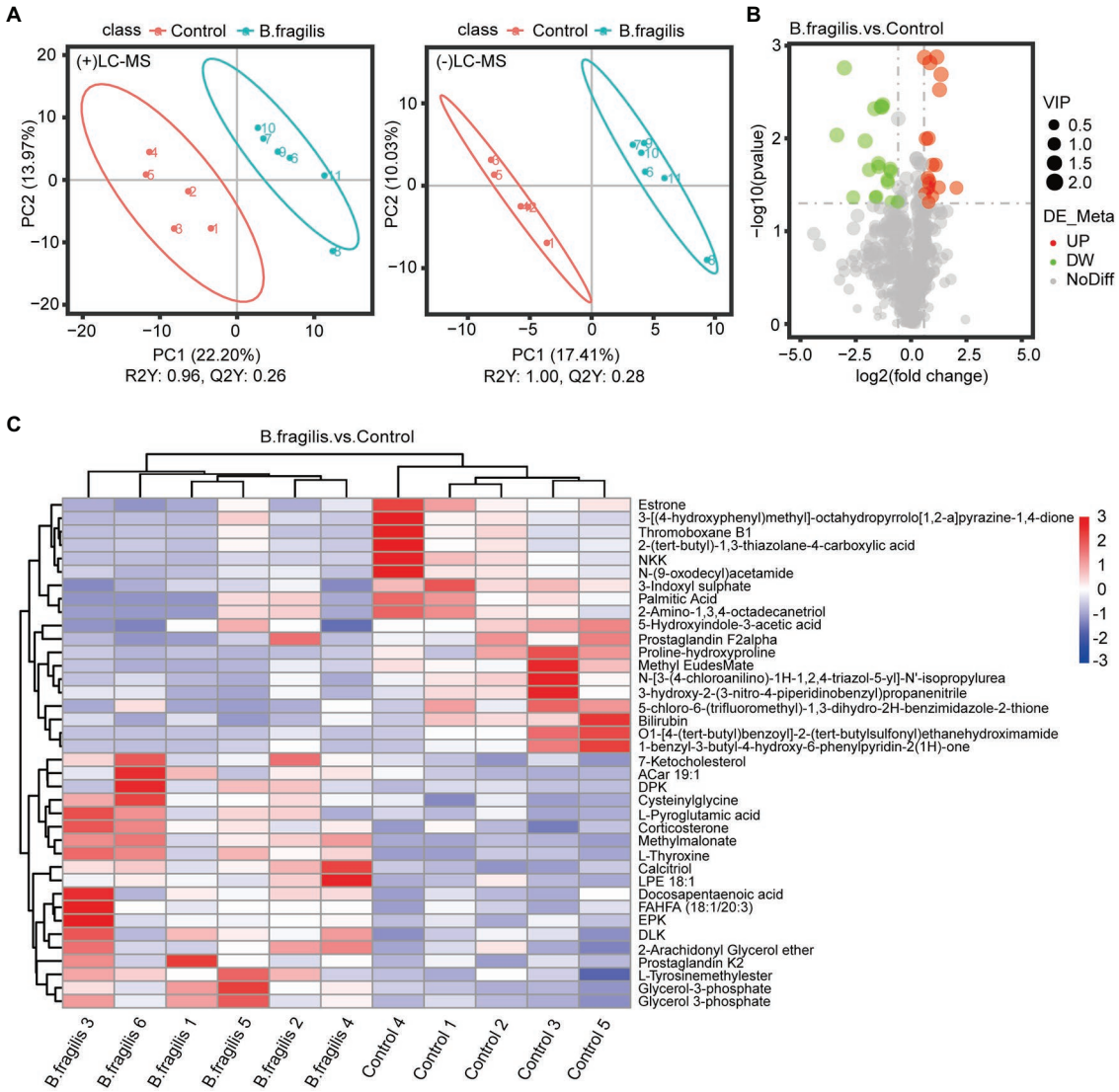

FIGURE 4 | Metabolomics analysis of vaginal differential metabolites between the two groups. **(A)** Score scatter plot of vaginal metabolites in the control and *Bacteroides fragilis* groups with *Bacteroides fragilis* treatment by PLS-DA in positive mode and negative mode. **(B)** Volcano plot of the differential metabolites. **(C)** The differential metabolite clustering heatmap. Each column represents a sample, and each row represents a metabolite.

in the lower part and contacts the environment (Abdel-Mageed et al., 2017). Hence, chicken vagina is easily infected by pathogenic bacteria, resulting in salpingitis, peritonitis and other reproductive tract diseases, which leads to lower egg production and even increased mortality (Bojesen et al., 2004; Allahghadry et al., 2021). Recent studies have shown that reproductive tract microbiota is the key factor affecting reproductive tract health and production performance of livestock and poultry. *Bacteroidetes* are the main bacterial communities in reproductive tract, among *B. fragilis ATCC 25285* (NCTC 9343) was one of the earliest to show beneficial effects on the host and played a vital role by releasing the main functional molecule polysaccharide A (PSA) (Tan et al., 2019). Our previous studies have shown that *B. fragilis* is significantly associated with a higher egg production. It may be that the immune system regulates reproductive activity in birds (Su et al., 2021). Similarly, the results of multiple omics in this study suggested that *B. fragilis* does affect immune function and metabolic homeostasis in the reproductive tract of chickens.

In this study, cloacal swabs were used for microbial analysis. The study found that the oviduct microbial composition is similar in chicken, and commensal bacteria from hens may be vertical transferred to the embryo (Lee et al., 2019). Moreover, intestinal tract and reproductive tract composition of microbiomes have a large overlap. This is mainly due to the physical results of chicken, the cloaca of chicken connects the intestinal tract and the reproductive tract (Shterzer et al., 2020). These findings suggested that the vagina and cloacal microbes may also communicate with each other.

Previous studies have shown that the oral administration of *B. fragilis* improves the offspring in a maternal immune activation

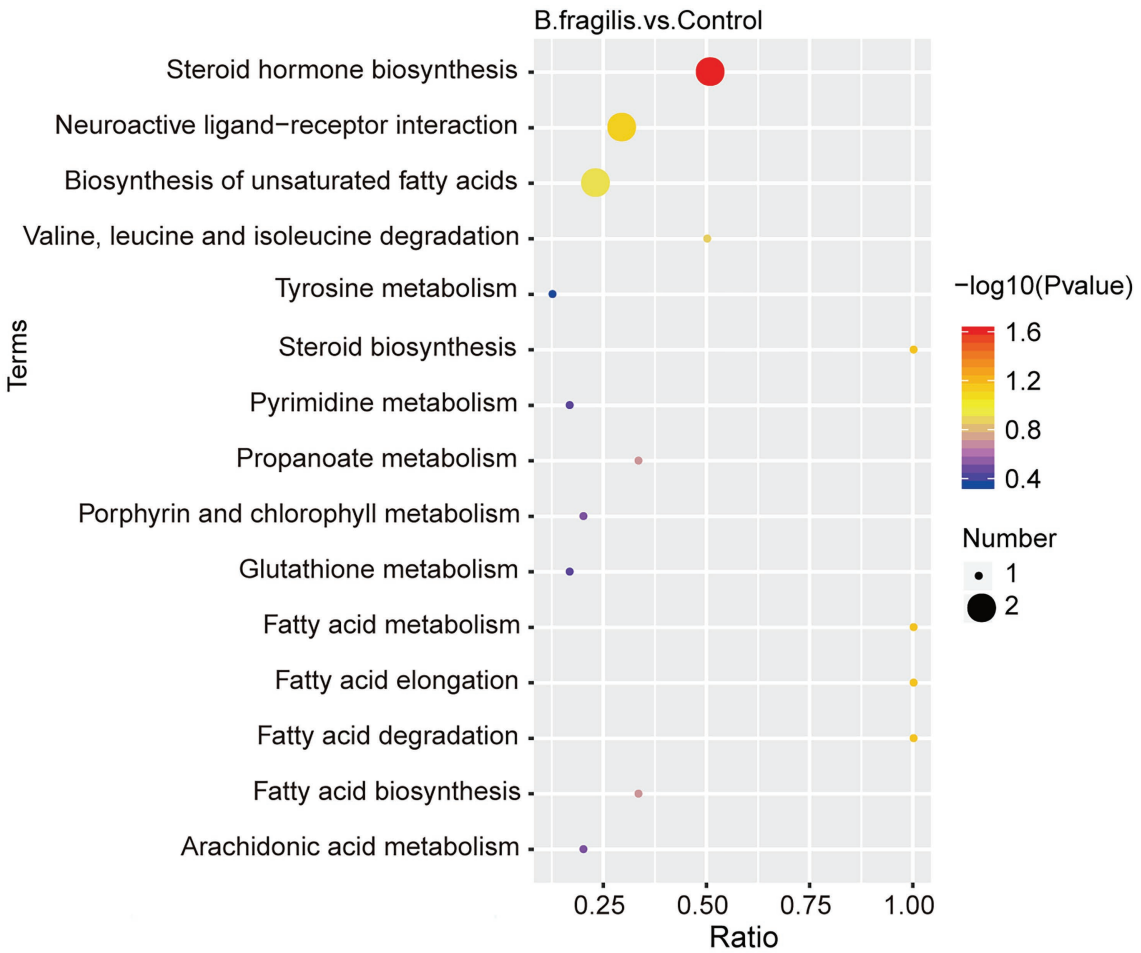

FIGURE 5 | KEGG pathway analysis of the altered metabolites in the vagina. The color of the points represents the value of *p* of the hypergeometric test, and the size of the points represents the number of differential metabolites in the corresponding pathway.

(MIA) model in mouse intestinal barrier integrity and microbial composition (Hsiao et al., 2013). In this study, no significant differences were observed following the *B. fragilis* treatment of the vagina in alpha diversity or in PCoA. However, vaginal administration altered the composition of the cloacal microbes, and the relative abundances of *Clostridium sensu stricto 1* and *Romboutsia* in the *B. fragilis* group were relatively high. Specific *Clostridium* has the potential to synthesize antibacterial compounds (Pahalagedara et al., 2020). Zhou et al. (2019a) found that *Clostridium butyricum WZ001* inhibited inflammation induced by *E. coli* and maintained vaginal microecological balance in mice. In addition, *Romboutsia* had the highest proportion in the *B. fragilis* group. A recent study showed that *Romboutsia* can be used as a predictor of egg production in chickens and that it reduces proinflammatory cytokines in the serum (Liang et al., 2016; Wen et al., 2021). These results suggest that *B. fragilis* is able to collectively improve reproductive tract health by altering microbial composition.

Vaginal transcriptome analysis showed that DEGs were enriched in inflammatory response regulation, regulation of leukocyte cell–cell adhesion, metabolic process, cellular response, and synaptic transmission. Our study indicated that the immune-related genes *CCN3*, *HAS2*, and *RICTOR* were upregulated in the *B. fragilis group*. *CCN3* participates in the functional regulation of regulatory T cells (Tregs) and hematopoietic stem cells; it can regulate angiogenesis and promote endothelial cell adhesion and survival (Lin et al., 2003; Peng et al., 2021). Studies have shown that *CCN3* loss leads to a significant increase in lipid uptake and foam cell formation in macrophages, while overexpression can inhibit atherosclerosis (Shi et al., 2017). Hyaluronan Synthase 2 (*HAS2*) has a protective effect on airway inflammation and emphysema induced by elastase in mice (Osawa et al., 2020). *RICTOR* has been found to play an important role in cell autophagy and metabolism (Zhao et al., 2020). Xu et al. (2018) demonstrated that enhanced *RICTOR* expression may reduce liver injury inflammation. This is consistent with our study showing that the high expression of this gene may influence vaginal cell metabolic and pathway responses.

In addition, genes associated with inflammation, such as *EDNRB*, *TOX*, and *NKX2-3*, were downregulated in the *B. fragilis group*. *EDNRB* is related to intestinal mucosal inflammation, and

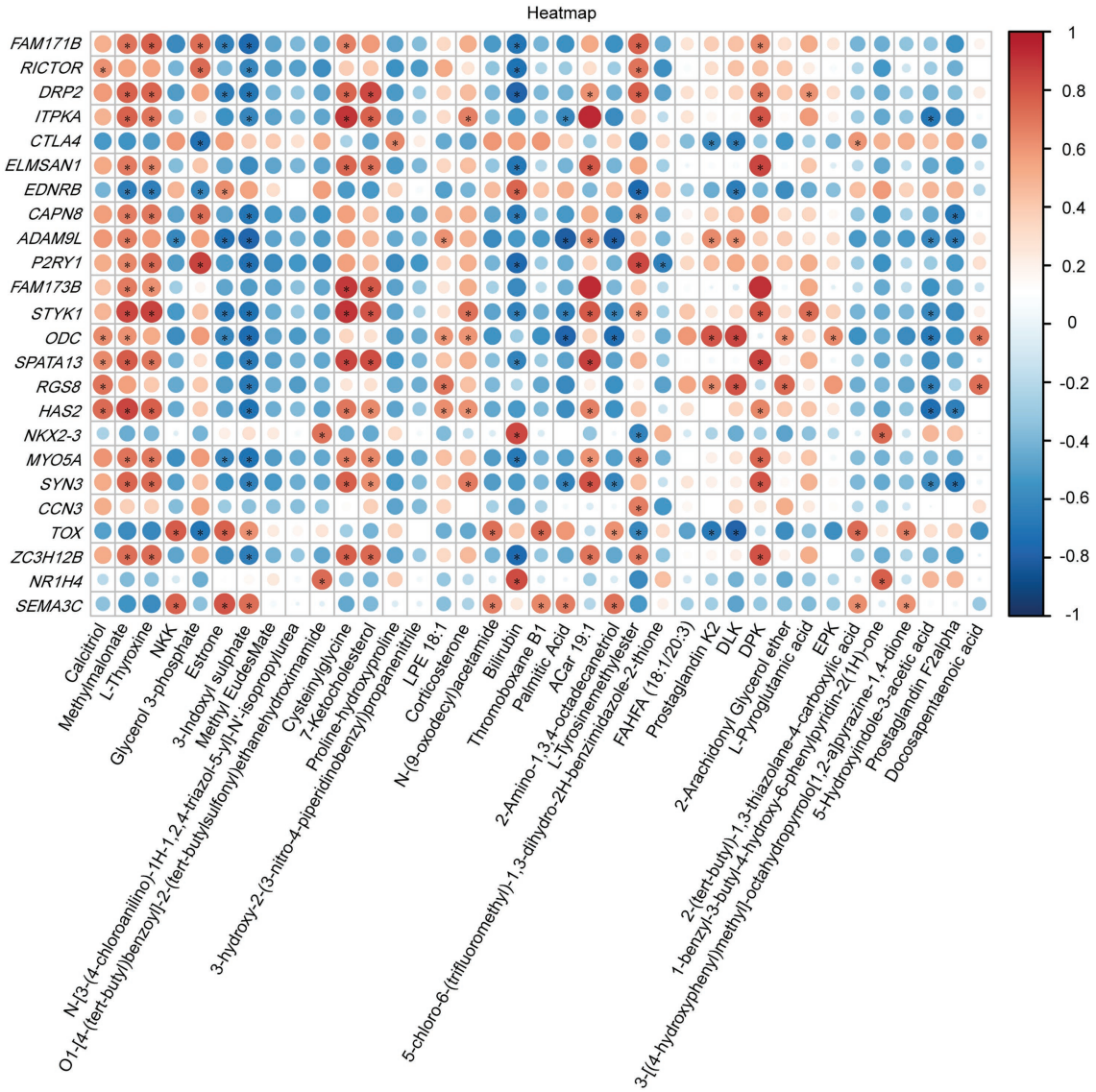

FIGURE 6 | Heatmap of specifically differentially expressed genes significantly associated with differential metabolites, as determined by Pearson's correlation analysis ($^{*}p < 0.05$).

probiotic treatment can downregulate the mRNA expression of this gene and exert anti-inflammatory effects by reducing macrophages and dendritic cells (Plaza-Díaz et al., 2017). *TOX* is a transcription factor in cancer progression, and it has been shown that the downregulation of *TOX* in CD8+ T cells can enhance the antitumor effect of cells (Wang et al., 2019a). *NKX2-3* is a transcription factor associated with inflammatory bowel disease (IBD), and its expression is increased in Crohn's disease (CD; Yu et al., 2012). Overall, these results suggest that *B. fragilis* treatment may exert its protective effect by upregulating immune genes and downregulating inflammation-related genes.

In the analysis of the metabolome of the intravaginal administration of *B. fragilis*, we found that there were significant differences in the differential metabolites between the *B. fragilis* group and the control group, including nine lipid-related molecules. Calcitriol is the active metabolite of vitamin D3; it has shown an anti-inflammatory effect on human corneal epithelial cells infected with *Pseudomonas aeruginosa* and suppresses the production of TNF-α and IL-1α (Kernacki and Berk, 1994; Xue et al., 2002). Meanwhile, calcitriol significantly inhibited the expression of NLRP3 inflammasome-related genes and IL-1β production in hyperosmotic stress (HS)-exposed cells (Dai et al., 2019). In addition, the combination of progesterone and calcitriol significantly inhibited the growth of endometrial and ovarian cancer cells (Paucarmayta et al., 2020). The results of our study showed that calcitriol levels in the *B. fragilis group* were significantly higher than those in the control group, and vaginal administration also significantly altered steroid and steroid hormone biosynthesis according to KEGG. Steroid hormones include sex hormones and adrenal

corticosteroids, which regulate innate and adaptive immunity and play an important role in reproduction (Czyzyk et al., 2017; Moulton, 2018; Cutolo and Straub, 2020).

Most of the differential metabolites were enriched in the metabolic pathways of fatty acids, including the biosynthesis of unsaturated fatty acids, arachidonic acid metabolism and various pathways of fatty acids. Arachidonic acid and docosapentaenoic acid are unsaturated fatty acids. Arachidonic acid is an essential dietary fatty acid that exists in the form of esterification in structural phospholipids in cell membranes throughout the body (Calder, 2007). In humans and other mammals, different enzymes cause membrane arachidonic (ARA) oxidation, resulting in the production of many proinflammatory and anti-inflammatory breakdown mediators (Hyde and Missailidis, 2009; Hanna and Hafez, 2018). In addition, docosapentaenoic acid (DPA) is more likely to be incorporated into inflammatory cells, resulting in a decrease in the synthetic substrates of pro-inflammatory eicosanes (PGE2 and LTB4), thereby regulating the production of inflammatory cytokines (Zheng et al., 2019). In this study, the increase in DPA levels induced by *B. fragilis* may be related to the immune regulation of vaginal cells.

On the other hand, *B. fragilis* produces short-chain fatty acids (SCFAs), mainly in the form of propionic acid. Our results showed that *B. fragilis* regulated propionic acid metabolic pathways. This is consistent with previous research, the oral administration of *B. fragilis* was found to significantly increase the concentration of SCFAs in the intestinal contents of *Salmonella*-infected rats, thereby further reducing inflammation and restoring the integrity of the intestinal barrier (Bukina et al., 2018). Furthermore, propionic acid metabolism can also induce the apoptosis of human colon cancer cells and avoid tumor formation (Cruz-Bravo et al., 2014). The production of SCFAs is closely related to the microbial community. Among *unidentified_Lachnospiraceae* and *Faecalibacterium* can produce SCFAs (Ma et al., 2020; Huang et al., 2021), and the abundance of these two genera in the *B. fragilis* group higher than the control group, suggesting that *B. fragilis* may also play a beneficial role by regulating microbial-metabolic processes. *B. fragilis* also regulated vaginal amino acid metabolism, we found that *B. fragilis* treatment modulated the valine, leucine, and isoleucine degradation pathway. Previous studies have shown that *P. copri* increased the concentration of metabolites of valine, leucine, and isoleucine biosynthesis in pig serum, leading to chronic inflammatory responses in the host (Chen et al., 2021). However, the opposite result was obtained in our study. These results suggest that vaginal injection with *B. fragilis* may have a positive effect on inhibiting vaginal inflammation in chickens. The combined transcriptome and metabolome analysis showed that some differential genes were significantly correlated with metabolites, which were consistent with the expression levels in this study. Such as, calcitriol was found to be a metabolite of vitamin D, which in turn is involved in *HAS2* regulation (Narvaez et al., 2020). This suggested that these differential genes and metabolites may interact to maintain the health of chicken reproductive tract after injection of *B. fragilis*. Meanwhile, this provided a reference for further exploring the possible mechanism of action after *B. fragilis* treatment.

CONCLUSION

In summary, our study suggested that the vaginal administration of *B. fragilis* could regulate cloacal microbial composition and affect the expression of vaginal immune and inflammatory genes and metabolism-related pathways. These results provide a theoretical basis for the application of *B. fragilis* as a potential probiotic in livestock and poultry production. In addition, the interaction mechanism between specific genes and metabolites needs to be further studied.

DATA AVAILABILITY STATEMENT

The datasets presented in this study can be found in online repositories. The names of the repository/repositories and accession number(s) can be found at: Bioproject, ID: PRJNA794049 and PRJNA792058.

ETHICS STATEMENT

The animal study was reviewed and approved by the Institutional Animal Care and Use Committee of Sichuan Agricultural University.

AUTHOR CONTRIBUTIONS

DL and TW conceived and designed the experiment. LC performed the experiments and wrote the manuscript. MY and WZ performed the bioinformatic analyses. YS participated in experimental design and sampling. All authors reviewed and approved the final manuscript.

FUNDING

This work was supported by grant from the Sichuan Science and Technology Program (2019JDTD0009).

ACKNOWLEDGMENTS

The authors would like to thank all members of the laboratory for their valuable comments on the manuscript. We also appreciate High-Performance Computing Platform of Sichuan Agricultural University for providing the powerful support for data analysis.

SUPPLEMENTARY MATERIAL

The Supplementary Material for this article can be found online at: https://www.frontiersin.org/articles/10.3389/fmicb.2022.846011/full#supplementary-material

REFERENCES

Abdel-Mageed, A. M., Nii, T., Isobe, N., and Yoshimura, Y. (2017). Modulatory roles of proinflammatory cytokines on the expression of cathelicidins in the lower regions of the oviduct of laying hens. *Cytokine* 99, 66–72. doi: 10.1016/j.cyto.2017.07.008

Allahghadry, T., Ng, D. Y. K., Dibaei, A., and Bojesen, A. M. (2021). Clonal spread of multi-resistant *Gallibacterium anatis* isolates among Iranian broilers and layers. *Vet. Res.* 52:27. doi: 10.1186/s13567-021-00894-1

Audic, S., and Claverie, J. M. (1997). The significance of digital gene expression profiles. *Genome Res.* 7, 986–995. doi: 10.1101/gr.7.10.986

Benjamini, Y., and Yekutieli, D. J. A. O. S. (2001). The control of the false discovery rate in multiple testing under dependency. *Ann. Stat.* 29, 1165–1188. doi: 10.1214/aos/1013699998

Bojesen, A. M., Nielsen, O. L., Christensen, J. P., and Bisgaard, M. (2004). In vivo studies of *Gallibacterium anatis* infection in chickens. *Avian Pathol.* 33, 145–152. doi: 10.1080/03079450310001652059

Bolyen, E., Rideout, J. R., Dillon, M. R., Bokulich, N. A., Abnet, C. C., Al-Ghalith, G. A., et al. (2019). Reproducible, interactive, scalable and extensible microbiome data science using QIIME 2. *Nat. Biotechnol.* 37, 852–857. doi: 10.1038/s41587-019-0209-9

Bukina, Y. V., Varynskyi, B. O., Voitovich, A. V., Koval, G. D., and Kamyshnyi, A. M. (2018). The definition of neutrophil extracellular traps and the concentration of short-chain fatty acids in salmonella-induced inflammation of the intestine against the background of vancomycin and *Bacteroides fragilis*. *For. Pathol.* 15, 10–17. doi: 10.14739/2310-1237.2018.1.128847

Calder, P. C. (2007). Dietary arachidonic acid: harmful, harmless or helpful? *Br. J. Nutr.* 98, 451–453. doi: 10.1017/s0007114507761779

Chen, C., Fang, S., Wei, H., He, M., Fu, H., Xiong, X., et al. (2021). Prevotella copri increases fat accumulation in pigs fed with formula diets. *Microbiome* 9:175. doi: 10.1186/s40168-021-01110-0

Cruz-Bravo, R. K., Guevara-González, R. G., Ramos-Gómez, M., Oomah, B. D., Wiersma, P., Campos-Vega, R., et al. (2014). The fermented non-digestible fraction of common bean (Phaseolus vulgaris L.) triggers cell cycle arrest and apoptosis in human colon adenocarcinoma cells. *Genes Nutr.* 9:359. doi: 10.1007/s12263-013-0359-1

Cutolo, M., and Straub, R. H. (2020). Sex steroids and autoimmune rheumatic diseases: state of the art. *Nat. Rev. Rheumatol.* 16, 628–644. doi: 10.1038/s41584-020-0503-4

Czyzyk, A., Podfigurna, A., Genazzani, A. R., and Meczekalski, B. (2017). The role of progesterone therapy in early pregnancy: from physiological role to therapeutic utility. *Gynecol. Endocrinol.* 33, 421–424. doi: 10.1080/09513590.2017.1291615

Dai, Y., Zhang, J., Xiang, J., Li, Y., Wu, D., and Xu, J. (2019). Calcitriol inhibits ROS-NLRP3-IL-1β signaling axis via activation of Nrf2-antioxidant signaling in hyperosmotic stress stimulated human corneal epithelial cells. *Redox Biol.* 21:101093. doi: 10.1016/j.redox.2018.101093

Deng, Q., Odhiambo, J. F., Farooq, U., Lam, T., Dunn, S. M., and Ametaj, B. N. (2014). Intravaginal lactic acid bacteria modulated local and systemic immune responses and lowered the incidence of uterine infections in periparturient dairy cows. *PLoS One* 10:e0124167. doi: 10.1371/journal.pone.0124167

Dunn, W. B., Broadhurst, D., Begley, P., Zelena, E., Francis-McIntyre, S., Anderson, N., et al. (2011). Procedures for large-scale metabolic profiling of serum and plasma using gas chromatography and liquid chromatography coupled to mass spectrometry. *Nat. Protoc.* 6, 1060–1083. doi: 10.1038/nprot.2011.335

Erturk-Hasdemir, D., Ochoa-Repáraz, J., Kasper, D. L., and Kasper, L. H. (2021). Exploring the gut-brain axis for the control of CNS inflammatory demyelination: immunomodulation by *Bacteroides fragilis*' polysaccharide A. *Front. Immunol.* 12:662807. doi: 10.3389/fimmu.2021.662807

Genís, S., Bach, À., and Arís, A. (2017). Effects of intravaginal lactic acid bacteria on bovine endometrium: implications in uterine health. *Vet. Microbiol.* 204, 174–179. doi: 10.1016/j.vetmic.2017.04.025

Hanna, V. S., and Hafez, E. A. A. (2018). Synopsis of arachidonic acid metabolism: a review. *J. Adv. Res.* 11, 23–32. doi: 10.1016/j.jare.2018.03.005

Hsiao, E. Y., McBride, S. W., Hsien, S., Sharon, G., Hyde, E. R., McCue, T., et al. (2013). Microbiota modulate behavioral and physiological abnormalities associated with neurodevelopmental disorders. *Cell* 155, 1451–1463. doi: 10.1016/j.cell.2013.11.024

Huang, L., Thonusin, C., Chattipakorn, N., and Chattipakorn, S. C. (2021). Impacts of gut microbiota on gestational diabetes mellitus: a comprehensive review. *Eur. J. Nutr.* 60, 2343–2360. doi: 10.1007/s00394-021-02483-6

Hyde, C. A., and Missailidis, S. (2009). Inhibition of arachidonic acid metabolism and its implication on cell proliferation and tumour-angiogenesis. *Int. Immunopharmacol.* 9, 701–715. doi: 10.1016/j.intimp.2009.02.003

Jeni, R. E., Dittoe, D. K., Olson, E. G., Lourenco, J., Corcionivoschi, N., Ricke, S. C., et al. (2021). Probiotics and potential applications for alternative poultry production systems. *Poult. Sci.* 100:101156. doi: 10.1016/j.psj.2021.101156

Johnson, J. L., Jones, M. B., and Cobb, B. A. (2018). Polysaccharide-experienced effector T cells induce IL-10 in FoxP3+ regulatory T cells to prevent pulmonary inflammation. *Glycobiology* 28, 50–58. doi: 10.1093/glycob/cwx093

Kernacki, K. A., and Berk, R. S. (1994). Characterization of the inflammatory response induced by corneal infection with Pseudomonas aeruginosa. *J. Ocul. Pharmacol.* 10, 281–288. doi: 10.1089/jop.1994.10.281

Lee, S., La, T. M., Lee, H. J., Choi, I. S., Song, C. S., Park, S. Y., et al. (2019). Characterization of microbial communities in the chicken oviduct and the origin of chicken embryo gut microbiota. *Sci. Rep.* 9:6838. doi: 10.1038/s41598-019-43280-w

Lee, Y. K., Mehrabian, P., Boyajian, S., Wu, W. L., Selicha, J., Vonderfecht, S., et al. (2018). The protective role of *Bacteroides fragilis* in a murine model of colitis-associated colorectal cancer. *mSphere* 3:e00587–18. doi: 10.1128/mSphere.00587-18

Li, Z., Deng, H., Zhou, Y., Tan, Y., Wang, X., Han, Y., et al. (2017). Bioluminescence imaging to track *Bacteroides fragilis* inhibition of vibrio parahaemolyticus infection in mice. *Front. Cell. Infect. Microbiol.* 7:170. doi: 10.3389/fcimb.2017.00170

Liang, G., Malmuthuge, N., Bao, H., Stothard, P., Griebel, P. J., and Guan le, L. (2016). Transcriptome analysis reveals regional and temporal differences in mucosal immune system development in the small intestine of neonatal calves. *BMC Genomics* 17:602. doi: 10.1186/s12864-016-2957-y

Lin, C. G., Leu, S. J., Chen, N., Tebeau, C. M., Lin, S. X., Yeung, C. Y., et al. (2003). CCN3 (NOV) is a novel angiogenic regulator of the CCN protein family. *J. Biol. Chem.* 278, 24200–24208. doi: 10.1074/jbc.M302028200

Ma, L., Ni, Y., Wang, Z., Tu, W., Ni, L., Zhuge, F., et al. (2020). Spermidine improves gut barrier integrity and gut microbiota function in diet-induced obese mice. *Gut Microbes* 12, 1832857–1832819. doi: 10.1080/19490976.2020.1832857

Mazmanian, S. K., Liu, C. H., Tzianabos, A. O., and Kasper, D. L. (2005). An immunomodulatory molecule of symbiotic bacteria directs maturation of the host immune system. *Cell* 122, 107–118. doi: 10.1016/j.cell.2005.05.007

McWhorter, A. R., and Chousalkar, K. K. (2016). In vitro invasive capacity of Salmonella strains into sections of the layer hen oviduct. *Vet. Microbiol.* 192, 135–144. doi: 10.1016/j.vetmic.2016.07.009

Moulton, V. R. (2018). Sex hormones in acquired immunity and autoimmune disease. *Front. Immunol.* 9:2279. doi: 10.3389/fimmu.2018.02279

Narvaez, C. J., Grebenc, D., Balinth, S., and Welsh, J. E. (2020). Vitamin D regulation of HAS2, hyaluronan synthesis and metabolism in triple negative breast cancer cells. *J. Steroid Biochem. Mol. Biol.* 201:105688. doi: 10.1016/j.jsbmb.2020.105688

Osawa, H., Kiwamoto, T., Sherpa, M.T., Tsunoda, Y., and Hizawa, N. (2020). "Hyaluronan Synthase 2 (HAS2) Mediates Elastase-Induced Airway Inflammation and Emphysema in Mice," in *American Thoracic Society 2020 International Conference*, May 15–20, 2020, Philadelphia, PA.

Pahalagedara, A., Flint, S., Palmer, J., Brightwell, G., and Gupta, T. B. (2020). Antimicrobial production by strictly anaerobic clostridium spp. *Int. J. Antimicrob. Agents* 55:105910. doi: 10.1016/j.ijantimicag.2020.105910

Paucarmayta, A., Taitz, H., McGlorthan, L., Casablanca, Y., Maxwell, G. L., Darcy, K. M., et al. (2020). Progesterone-calcitriol combination enhanced cytotoxicity of cisplatin in ovarian and endometrial cancer cells *in vitro*. *Biomedicine* 8:73. doi: 10.3390/biomedicines8040073

Peng, L., Wei, Y., Shao, Y., Li, Y., Liu, N., and Duan, L. (2021). The emerging roles of CCN3 protein in immune-related diseases. *Mediat. Inflamm.* 2021:5576059. doi: 10.1155/2021/5576059

Plaza-Díaz, J., Robles-Sánchez, C., Abadía-Molina, F., Morón-Calvente, V., Sáez-Lara, M. J., Ruiz-Bravo, A., et al. (2017). Adamdec1, Ednrb and Ptgs1/

Cox1, inflammation genes upregulated in the intestinal mucosa of obese rats, are downregulated by three probiotic strains. *Sci. Rep.* 7:1939. doi: 10.1038/s41598-017-02203-3

Quast, C., Pruesse, E., Yilmaz, P., Gerken, J., Schweer, T., Yarza, P., et al. (2013). The SILVA ribosomal RNA gene database project: improved data processing and web-based tools. *Nucleic Acids Res.* 41, D590–D596. doi: 10.1093/nar/gks1219

Reid, G., and Bocking, A. (2003). The potential for probiotics to prevent bacterial vaginosis and preterm labor. *Am. J. Obstet. Gynecol.* 189, 1202–1208. doi: 10.1067/s0002-9378(03)00495-2

Sah, N., and Mishra, B. (2018). Regulation of egg formation in the oviduct of laying hen. *Worlds Poult. Sci. J.* 74, 509–522. doi: 10.1017/S0043933918000442

Shao, X., Sun, S., Zhou, Y., Wang, H., Yu, Y., Hu, T., et al. (2021). *Bacteroides fragilis* restricts colitis-associated cancer via negative regulation of the NLRP3 axis. *Cancer Lett.* 523, 170–181. doi: 10.1016/j.canlet.2021.10.002

Shi, H., Zhang, C., Pasupuleti, V., Hu, X., Prosdocimo, D. A., Wu, W., et al. (2017). CCN3 regulates macrophage foam cell formation and atherosclerosis. *Am. J. Pathol.* 187, 1230–1237. doi: 10.1016/j.ajpath.2017.01.020

Shini, S., Shini, A., and Blackall, P. J. J. A. P. S. (2013). The potential for probiotics to prevent reproductive tract lesions in free-range laying hens. *Anim. Prod. Sci.* 53, 1298–1308. doi: 10.1071/AN12337

Shterzer, N., Rothschild, N., Sbehat, Y., Stern, E., Nazarov, A., and Mills, E. (2020). Large overlap Between the intestinal and reproductive tract microbiomes of chickens. *Front. Microbiol.* 11:1508. doi: 10.3389/fmicb.2020.01508

Spence, C., Wells, W. G., and Smith, C. J. (2006). Characterization of the primary starch utilization operon in the obligate anaerobe *Bacteroides fragilis*: regulation by carbon source and oxygen. *J. Bacteriol.* 188, 4663–4672. doi: 10.1128/jb.00125-06

Su, Y., Tian, S., Li, D., Zhu, W., Wang, T., Mishra, S. K., et al. (2021). Association of female reproductive tract microbiota with egg production in layer chickens. *Gigascience* 10:giab067. doi: 10.1093/gigascience/giab067

Tan, H., Zhai, Q., and Chen, W. (2019). Investigations of *Bacteroides* spp. towards next-generation probiotics. *Food Res. Int.* 116, 637–644. doi: 10.1016/j.foodres.2018.08.088

Vernay, T., Cannie, I., Gaboriau, F., Gall, S. D., Tamanai-Shacoori, Z., Burel, A., et al. (2020). *Bacteroides fragilis* prevents salmonella Heidelberg translocation in co-culture model mimicking intestinal epithelium. *Benef. Microbes* 11, 391–401. doi: 10.3920/bm2020.0004

Wang, L., Feng, Z., Wang, X., Wang, X., and Zhang, X. (2010). DEGseq: an R package for identifying differentially expressed genes from RNA-seq data. *Bioinformatics* 26, 136–138. doi: 10.1093/bioinformatics/btp612

Wang, X., He, Q., Shen, H., Xia, A., Tian, W., Yu, W., et al. (2019a). TOX promotes the exhaustion of antitumor CD8(+) T cells by preventing PD1 degradation in hepatocellular carcinoma. *J. Hepatol.* 71, 731–741. doi: 10.1016/j.jhep.2019.05.015

Wang, Z., Hu, J., Zheng, W., Yang, T., Wang, X., Xie, C., et al. (2019b). Lactobacillus frumenti mediates energy production via fatty acid β-oxidation in the liver of early-weaned piglets. *J. Anim. Sci. Biotechnol.* 10:95. doi: 10.1186/s40104-019-0399-5

Want, E. J., Wilson, I. D., Gika, H., Theodoridis, G., Plumb, R. S., Shockcor, J., et al. (2010). Global metabolic profiling procedures for urine using UPLC-MS. *Nat. Protoc.* 5, 1005–1018. doi: 10.1038/nprot.2010.50

Wen, C., Li, Q., Lan, F., Li, X., Li, G., Yan, Y., et al. (2021). Microbiota continuum along the chicken oviduct and its association with host genetics and egg formation. *Poult. Sci.* 100:101104. doi: 10.1016/j.psj.2021.101104

Xu, D., Zhu, J., Jeong, S., Li, D., Hua, X., Huang, L., et al. (2018). Rictor deficiency aggravates hepatic ischemia/reperfusion injury in mice by suppressing autophagy and regulating MAPK signaling. *Cell. Physiol. Biochem.* 45, 2199–2212. doi: 10.1159/000488165

Xue, M. L., Zhu, H., Thakur, A., and Willcox, M. (2002). 1 alpha,25-Dihydroxyvitamin D3 inhibits pro-inflammatory cytokine and chemokine expression in human corneal epithelial cells colonized with Pseudomonas aeruginosa. *Immunol. Cell Biol.* 80, 340–345. doi: 10.1046/j.1440-1711.80.4august.1.x

Yang, J., Zhan, K., and Zhang, M. (2020). Effects of the use of a combination of two bacillus species on performance, egg quality, small intestinal mucosal morphology, and Cecal microbiota profile in aging laying hens. *Probiotics Antimicrob. Proteins* 12, 204–213. doi: 10.1007/s12602-019-09532-x

Yu, W., Hegarty, J. P., Berg, A., Kelly, A. A., Wang, Y., Poritz, L. S., et al. (2012). PTPN2 is associated with Crohn's disease and its expression is regulated by NKX2-3. *Dis. Markers* 32, 83–91. doi: 10.3233/dma-2011-0867

Zhang, X. P., Lu, C. J., Li, Y. T., Yang, X., Wang, X. W., Chang, H. T., et al. (2017). In vitro adherence and invasion of primary chicken oviduct epithelial cells by *Gallibacterium anatis*. *Vet. Microbiol.* 203, 136–142. doi: 10.1016/j.vetmic.2017.02.009

Zhao, D., Jiang, M., Zhang, X., and Hou, H. (2020). The role of RICTOR amplification in targeted therapy and drug resistance. *Mol. Med.* 26:20. doi: 10.1186/s10020-020-0146-6

Zheng, Z., Dai, Z., Cao, Y., Shen, Q., and Zhang, Y. (2019). Docosapentaenoic acid (DPA, 22:5n-3) ameliorates inflammation in an ulcerative colitis model. *Food Funct.* 10, 4199–4209. doi: 10.1039/c8fo02338g

Zheng, L., Luo, M., Kuang, G., Liu, Y., Liang, D., Huang, H., et al. (2020). Capsular polysaccharide from *Bacteroides fragilis* protects against ulcerative colitis in an undegraded form. *Front. Pharmacol.* 11:570476. doi: 10.3389/fphar.2020.570476

Zhou, Y., Xu, W., Hong, K., Li, H., Zhang, J., Chen, X., et al. (2019a). Therapeutic effects of probiotic *Clostridium butyricum* WZ001 on bacterial vaginosis in mice. *J. Appl. Microbiol.* 127, 565–575. doi: 10.1111/jam.14329

Zhou, Y., Zhou, B., Pache, L., Chang, M., Khodabakhshi, A. H., Tanaseichuk, O., et al. (2019b). Metascape provides a biologist-oriented resource for the analysis of systems-level datasets. *Nat. Commun.* 10:1523. doi: 10.1038/s41467-019-09234-6

Conflict of Interest: The authors declare that the research was conducted in the absence of any commercial or financial relationships that could be construed as a potential conflict of interest.

Publisher's Note: All claims expressed in this article are solely those of the authors and do not necessarily represent those of their affiliated organizations, or those of the publisher, the editors and the reviewers. Any product that may be evaluated in this article, or claim that may be made by its manufacturer, is not guaranteed or endorsed by the publisher.

frontiers in Microbiology

ORIGINAL RESEARCH
published: 22 February 2022
doi: 10.3389/fmicb.2022.843045

Differential Effect of Dietary Fibers in Intestinal Health of Growing Pigs: Outcomes in the Gut Microbiota and Immune-Related Indexes

Yuheng Luo[1,2,3,4†], Yang Liu[1,2,3,4†], Hua Li[1,2,3,4†], Yao Zhao[1,2,3,4†], André-Denis G. Wright[5], Jingyi Cai[1,2,3,4], Gang Tian[1,2,3,4] and Xiangbing Mao[1,2,3,4]*

[1] Key Laboratory of Animal Disease-Resistant Nutrition, Ministry of Education, Sichuan Agricultural University, Chengdu, China, [2] Key Laboratory of Animal Disease-Resistant Nutrition and Feed, Ministry of Agriculture and Rural Affairs, Sichuan Agricultural University, Chengdu, China, [3] Key Laboratory of Animal Disease-Resistant Nutrition, Sichuan Agricultural University, Chengdu, China, [4] Animal Nutrition Institute, Sichuan Agricultural University, Chengdu, China, [5] University of Oklahoma, Norman, OK, United States

OPEN ACCESS

Edited by:
Zheng Ruan,
Nanchang University, China

Reviewed by:
Naschla Gasaly,
Universidad de Chile, Chile
Junhua Liu,
Nanjing Agricultural University, China
Miao Yu,
Institute of Animal Science,
Guangdong Academy of Agricultural Sciences, China

***Correspondence:**
Yuheng Luo
luoluo212@126.com

[†] These authors have contributed equally to this work

Specialty section:
This article was submitted to Food Microbiology, a section of the journal Frontiers in Microbiology

Received: 24 December 2021
Accepted: 14 January 2022
Published: 22 February 2022

Citation:
Luo Y, Liu Y, Li H, Zhao Y, Wright A-DG, Cai J, Tian G and Mao X (2022) Differential Effect of Dietary Fibers in Intestinal Health of Growing Pigs: Outcomes in the Gut Microbiota and Immune-Related Indexes. Front. Microbiol. 13:843045. doi: 10.3389/fmicb.2022.843045

Although dietary fibers (DFs) have been shown to improve intestinal health in pigs, it is unclear whether this improvement varies according to the type/source of DF. In the current study, we investigated the impact of dietary supplement (15%) of pea-hull fiber (PF), oat bran (OB), and their mixture (MIX, PF, and OB each accounted for 7.5%) in the growth performance as well as intestinal barrier and immunity-related indexes in growing pigs. Twenty-four cross-bred pigs (32.42 ± 1.95 kg) were divided into four groups: CON (basal diet with no additional DF), PF, OB, and MIX. After 56 days of feeding, we found that the growth performance of PF pigs was decreased ($p < 0.05$) compared with pigs in other groups. Results of real-time polymerase chain reaction and Western blot showed that the improvement of immune-related indexes (e.g., interleukin 10 [*IL-10*]) in OB and MIX pigs mainly presented in the ileum, whereas the improvement of intestinal barrier–related indexes (e.g., *MUC1* and *MUC2*) mainly presented in the colon. Whether in the ileum or colon, such improvement of immune function may be dependent on NOD rather than TLR-associated pathways. Amplicon sequencing results showed that PF and MIX pigs shared a similar bacterial community, such as lower abundance of ileal Clostridiaceae and colonic *Streptoccocus* than that of CON pigs ($p < 0.05$). Our results indicate that OB and MIX, rather than PF, benefit the intestinal health in growing pigs, and multiple-sourced DF may reduce the adverse effect of single-soured DF on the growth performance and gut microbiota in pigs.

Keywords: dietary fibers, growing pig, gut microbiota, intestinal barrier, intestinal immunity

INTRODUCTION

Dietary fiber (DF) was originally regarded as a component of the plant cell wall that is indigestible by human and animals (Hipsley, 1953; Trowell, 1976), and the high level of DF in the diet of pig may play an antinutritional role, such as the inhibition in the absorption of macronutrients and micronutrients (Campbell and Taverner, 1986; Zhou et al., 2013). However, recent studies show

that the supplementation of some DF, such as beet pulp (Yan et al., 2017) and wheat bran (Zhao et al., 2018), may not have negative impact on the growth of animals. This might be associated with the structure of DF, which is regarded to be closely related to the intestinal development, peristalsis, homeostasis, and microbiota (Lange et al., 2010; Bach Knudsen et al., 2012).

The integrity of intestinal barrier is crucial for the maintenance of gut health. An intestinal injury rat model showed that supplementation of multiple DF reduced intestinal permeability and prevented endotoxin from entering the portal vein blood (Gao et al., 2015). Diets with high levels of high-viscosity soluble dietary fibers (SDFs), such as wheat bran and pea-hull fiber (PF), may increase the expression of mucin gene (*MUC*) and the secretion of mucin in the distal small intestine of pigs by increasing the number of goblet cells (El Kaoutari et al., 2013). However, in a rat model, the stimulation of mucin secretion by dietary supplement of low-viscosity SDF may not be related to the number of goblet cells, but was reported to be associated with an enhanced expression of *MUC* expression (Ito et al., 2009). These results indicate that DF may be important for the maintenance of mucosal barrier by regulating the number of goblet cells or the expression of *MUC*.

Although the role of DF in intestinal health has been discussed extensively, few reports focused on the comparison of different sourced DF on the intestinal barrier and immune function of animals. Most DF can be fermented by microorganisms in the hindgut of monogastric animals to produce large amounts of short-chain fatty acids (SCFAs) (El Kaoutari et al., 2013; Sonnenburg and Sonnenburg, 2014). Therefore, the effect of DF on gut health is recognized to be associated with their impact on gut microbial communities (Conlon and Bird, 2014) and the indirect physiological effects of microbial metabolites (Bach Knudsen et al., 2012).

The effects of DF on microbial composition in the gut of human or animal models have been well studied. The utilization of DF by microorganisms in human gut was considered to take place in the large intestine. However, the microbial fermentation of DF might begin early even at distal small intestine (Venema et al., 2007), which suggests that microbes in small intestine, such as ileum, should be also considered when evaluating the influence of DF on gut microbial community.

In the current study, we selected two sourced DF, PF, and oat bran (OB). The main non-starch polysaccharides (NSPs) in PF are cellulose and rhamnogalacturonan, whereas the NSPs in OB mainly are β-glucan and cellulose (Knudsen, 1997; Sajilata et al., 2006; Stephen and Phillips, 2016). In our previous study in BALB/c mice, the dietary supplement of mixed DF (half of each β-glucan and microcrystalline cellulose) had a particular impact on the colonic bacterial community and phenotype of mice compared with the sole supplement of β-glucan or microcrystalline cellulose (Luo et al., 2017). Accordingly, we attempted to investigate whether there was a similar effect of the equivalent supplement of PF and OB. Results of current study may help to further understand the underlying mechanism of different sourced DF affecting the intestinal health of pigs or other animals with similar anatomical physiology.

MATERIALS AND METHODS

All experimental procedures and animal care were performed in accordance with the Guide for the Care and Use of Laboratory Animals prepared by the Institutional Animal Care and Use Committee of Sichuan Agricultural University, and all animal protocols were approved by the Animal Care and Use Committee of Sichuan Agricultural University under permit number DKYB20131704.

Experimental Design and Animal Feeding Management

A total of 24 cross-bred (Duroc × Landrace × Yorkshire) pigs, with an initial body weight of 32.42 ± 1.95 kg, were selected and randomly divided into four groups with six replicates in each group and one pig per replicate. Pigs in the control group (CON) were fed with basal diet without additional DF. Pigs in the other three groups were fed a basal diet with 15% PF, 15% OB, or a mixture (MIX) of OB (7.5%) and PF (7.5%), respectively. The preparation of corn-soybean meal diet was prepared according to the nutrient requirements of swine of the National Research Council (NRC) 2012 (National Research Council, 2012) and the Feeding Standard of Swine (China, NY/T65-2004) (**Supplementary Table 1**). The PF and OB were purchased from Shaanxi Ciyuan Biotechnology Co., Ltd. (Xi'an, China). The measured values of main nutrients including SDF and IDF of the two fibrous raw materials are shown in **Supplementary Table 2**. All pigs were raised in individual cages and fed three times a day (8:00 AM, 1:00 PM, and 6:00 PM). The trial lasted for 56 days, and water was available *ad libitum* during the entire experimental period.

Reverse Transcription Real-Time Polymerase Chain Reaction Analysis of Expression of the Genes Related to Immune and Barrier Functions in the Intestinal Mucosa

At the end of the trial, all pigs were weighed before being euthanized by a lethal injection of sodium pentobarbital (200 mg/kg body weight). Digesta and mucosal samples from the middle ileum and colon of each pig were collected and stored at −80°C. Approximately 0.5 g of each mucosal sample was thawed, and total RNA was extracted using Trizol (TAKARA, Japan), and mRNA was reversely transcribed into cDNA with PrimeScript^{TM} RT reagent kit (TAKARA, Japan). The SYBR Green–based real-time polymerase chain reaction (PCR) reaction mixture included 1.0 μL cDNA, 0.4 μL forward primer, 0.4 μL reverse primer, 5 μL SYBR Green PCR Master Mix (TAKARA, Japan), 0.2 μL correction fluid ROX (TAKARA, Japan), and 3 μL double-distilled water. Forty cycles of PCR were conducted as follows: predenaturation at 95°C for 10 s followed by 5 s of denaturation at same temperature, annealing at 60°C for 20 s, and extension at 72°C for 15 s (ABI 7900, United States). Three housekeeping genes, β-actin, 18S rRNA, and GAPDH, were selected as internal references, and relative quantity of each target gene in each sample was calculated according to

the method (Larionov et al., 2005). The sequences of primers and the length of the PCR product for each gene are shown in **Supplementary Table 3**.

Western Blotting Analysis of TLR4 and Nuclear Factor κB Expression in the Intestinal Mucosa

The proteins from each mucosal sample were extracted according to described method (Kim et al., 2012). Expression of targeting proteins, TLR4 and nuclear factor κB (NF-κB), was analyzed using Western blotting as previously described (Finamore et al., 2014) with β-actin as the internal reference. The bands were analyzed with Bio-Rad image analysis system, and the formula of separating and concentrated gel is shown in **Supplementary Table 4**.

Analysis of the Bacterial Community and Concentrations of Short-Chain Fatty Acids in the Digesta Samples

Procedures for the extraction of genomic DNA, analysis of microbial community, and the measurement of SCFAs concentrations have been previously described (Luo et al., 2015). Briefly, pairs of reads from the original DNA fragments were first merged using FLASH (Fast Length Adjustment of SHort reads) (Magoč and Salzberg, 2011). Diversity was analyzed using the QIIME (Quantitative Insights Into Microbial Ecology) software (Caporaso et al., 2010) after removal of chimeric sequences using USEARCH (Edgar et al., 2011). Operational taxonomic units (OTUs) for the sequences were picked using the *de novo* OTU picking protocol with a 97% similarity threshold. The bacterial taxa differentially represented between groups were identified using LEfSe [linear discriminant analysis (LDA) coupled with effect size] (Segata et al., 2011). All reads were deposited in the BIG Data Center in Beijing Institute of Genomics and can be accessed in the Genome Sequence Archive under accession number CRA001323[1]. The concentration of acetate, propionate, and butyrate in the digesta samples was measured using a gas chromatograph (GC) (GC-14B, Shimadzu, Japan; capillary column: 30 m × 0.32 mm × 0.25-μm film thickness), and the minimal detectable limit for each SCFA was 0.01 mmol/L.

Statistical Analysis

Data on the growth performance, expression of related genes and proteins, concentrations of SCFAs, and the relative abundance of main bacterial phyla and genera were first checked for normal distribution using the Descriptive Statistics (Explore) module of software SPSS 16.0 (SPSS Inc., Chicago, IL, United States). For those data with normal distribution, one-way analysis of variance was used to analyze the difference among groups, and the *post hoc* multiple-comparisons test was then performed using the Bonferroni method. The homogeneity of variance was tested using Duncan analysis, whereas Kruskal–Wallis non-parametric test was used to analyze the difference between groups for those skewed data. The correlation between the SCFA concentration and bacterial species was calculated using a Pearson correlational analysis, and the results were visualized using vegan, ggcor, and dplyr packages in R 4.0.1. Differences were considered to be significant when $p < 0.05$ and not significant when $p \geq 0.05$.

[1]https://ngdc.cncb.ac.cn/gsa/browse/CRA001323

RESULTS

The Growth Performance of Pigs in Different Groups

At the beginning of the experiment, there was no significant difference in the initial weight of pigs among the four groups ($p > 0.05$, **Supplementary Table 5**), indicating the rationality of grouping by body weight. Compared with CON, OB, and MIX pigs, the final body weight, feed intake, and body weight gain of PF pigs were decreased ($p < 0.05$).

The Expression of Genes Related to Intestinal Barrier and Immune Function of Pigs in Different Groups

For the ileal mucosa, we did not find any difference in the expression of the five intestinal barrier–related genes between CON group and fiber supplemented group ($p > 0.05$, **Figure 1A**), but the expression of *MUC2* in PF pigs was higher than that in OB pigs ($p < 0.05$, **Figure 1A**). For the colonic mucosa, the expression of *MUC1* in PF and MIX pigs, as well as the expression of *MUC2* in MIX pigs, was increased compared with CON pigs ($p < 0.05$, **Figure 1B**), whereas the expression of *ZO-1* in OB pigs was lower than that in CON and MIX pigs ($p < 0.05$, **Figure 1B**).

For the investigated genes related to immune function, we found the expression of *IRAK4* in the ileum of OB and MIX pigs, and the expression of *TRAF6* in the ileum of OB pigs was decreased compared with CON pigs ($p < 0.05$, **Figure 1C**), whereas the expression of *IL-10* in the ileum of OB and MIX pigs was increased compared with CON and PF pigs ($p < 0.05$, **Figure 1C**). Interestingly, the expression of *NOD2* in the ileum of OB pigs was higher than that of PF pigs ($p < 0.05$, **Figure 1C**), but the expression of *IRAK4* in the ileum of OB and MIX pigs was lower than that of PF pigs ($p < 0.05$, **Figure 1C**). However, only the expression of *RIPK2* in OB and MIX pigs was found higher than that in CON pigs ($p < 0.05$, **Figure 1D**) in the colon.

The Abundance of Protein TLR4 and NF-κB in the Ileum and Colon of the Pigs in Different Groups

No difference in the abundance of protein TLR4 was found in both ileum and colon of pigs among the four groups ($p > 0.05$, **Figures 2A–F**). Compared with CON pigs, the abundance of NF-κB–p65 in the ileum of PF and MIX pigs was decreased ($p < 0.05$, **Figure 2B**), whereas its abundance in the colon of PF, OB, and MIX pigs was increased ($p < 0.05$, **Figure 2E**). Moreover, the abundance of NF-κB–p65 protein in the ileum of OB pigs tended to be lower than that of CON pigs ($P = 0.07$, **Figure 2B**).

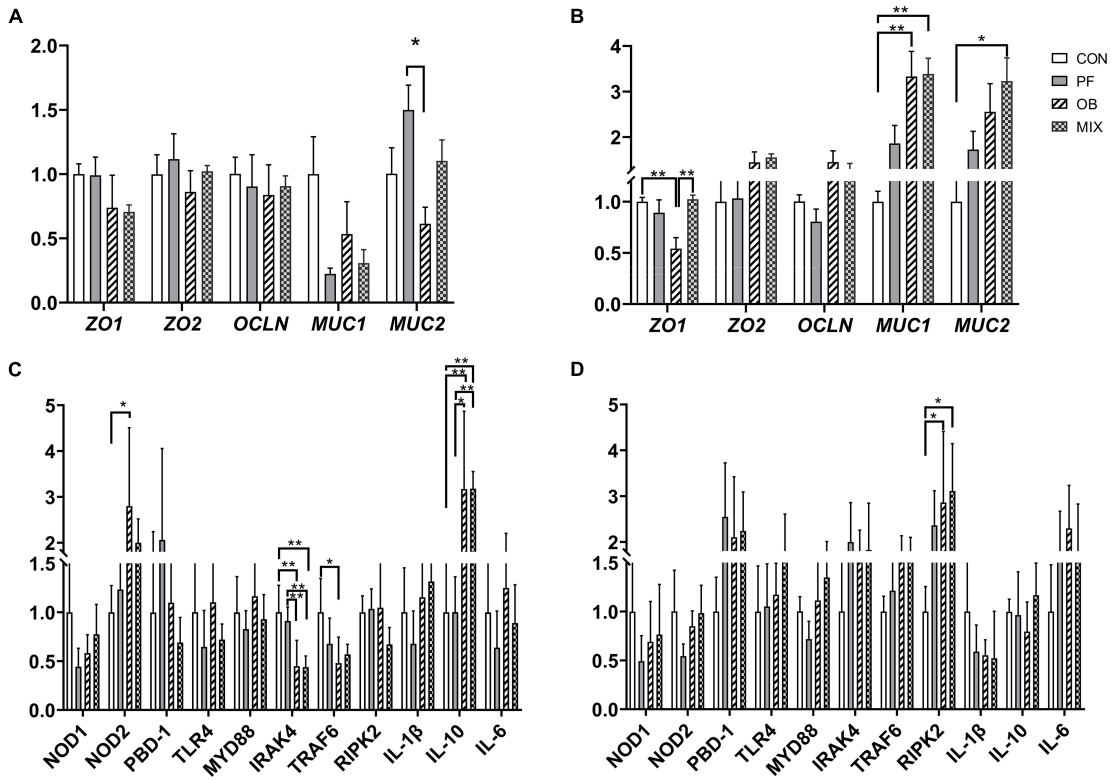

FIGURE 1 | The relative expression of intestinal barrier and immunity-related genes in the ileum and colon of pigs fed different diets. **(A)** The expression of genes encoding tight junction proteins and mucin in the ileal mucosa. **(B)** The expression of genes encoding tight junction proteins and mucin in the colonic mucosa. **(C)** The expression of key genes associated with TLR4 and NOD pathways in the ileal mucosa. **(D)** The expression of key genes associated with TLR4 and NOD pathways in the colonic mucosa. $^{*}p < 0.05$, $^{**}p < 0.01$. CON, control group; PF, 15% pea-hull fiber in the diet; OB, 15% oat bran in the diet; MIX, 7.5% pea-hull fiber and 7.5% oat bran in the diet.

The Concentration of Short-Chain Fatty Acids in the Ileal and Colonic Digesta of Pigs in Different Groups

Results of GC analysis showed that changes in the concentration of SCFAs induced by DF supplement were concentrated in the ileum (**Figure 3A**) rather than the colon (**Figure 3B**). In detail, when compared with CON pigs, the concentration of acetate and total SCFAs (TSCFAs, the sum of acetate, propionate, and butyrate concentrations) in the ileum of OB pigs was increased ($p < 0.05$), whereas the concentration of acetate, butyrate, and TSCFAs in the ileum of PF pigs, as well as the concentration of butyrate in the ileum of MIX pigs, was decreased ($p < 0.05$, **Figure 3A**). On the contrary, no difference in the concentration of SCFAs was found in the colon of the pigs among groups ($p > 0.05$, **Figure 3B**). Interestingly, the ratio of each SCFA to TSCFAs showed no difference ($p > 0.05$, **Figures 3A,B**), whether in ileum or colon.

The Bacterial Community in the Ileal and Colonic Digesta of Pigs in Different Groups

No significant difference was found in the Shannon index of microbial community in both ileal and colonic digesta of pigs among the four groups ($p > 0.05$, **Table 1**). Alternatively, the unweighted-Unifrac distance of ileal samples in PF pigs was higher than that in MIX pigs ($p < 0.05$). Compared with CON pigs, the unweighted-Unifrac distance of colonic samples in MIX pigs was higher ($p < 0.05$).

At phylum level (**Supplementary Table 6** and **Supplementary Figure 1**), only the relative abundance of phylum WPS-2 in the colonic digesta of PF pigs was increased compared with pigs in other groups ($p < 0.01$). Beyond that, the abundance of other phyla in the ileal and colonic digesta of pigs was not different among groups ($p > 0.05$).

At genus level, we found that the abundance of *Turicibacter* in PF pigs and the abundance of an unidentified genus belonging to Clostridiaceae in the ileal digesta of PF and MIX pigs were decreased compared with CON pigs ($p < 0.05$, **Supplementary Table 7**). And compared with OB pigs, the abundance of an unidentified genus belonging to Clostridiaceae was decreased in PF and MIX pigs ($p < 0.01$). In the colonic digesta, the abundance of CF231 and *Streptococcus* in PF and MIX pigs showed a decrease compared with CON pigs ($p < 0.05$). In addition, the abundance of an unidentified genus belonging to Clostridiaceae was also decreased in PF pigs than that in OB pigs ($p < 0.05$).

According to the results of LDA and LEfSe analysis, a total of 12 bacterial taxa in ileal digesta and 9 bacterial taxa in colonic

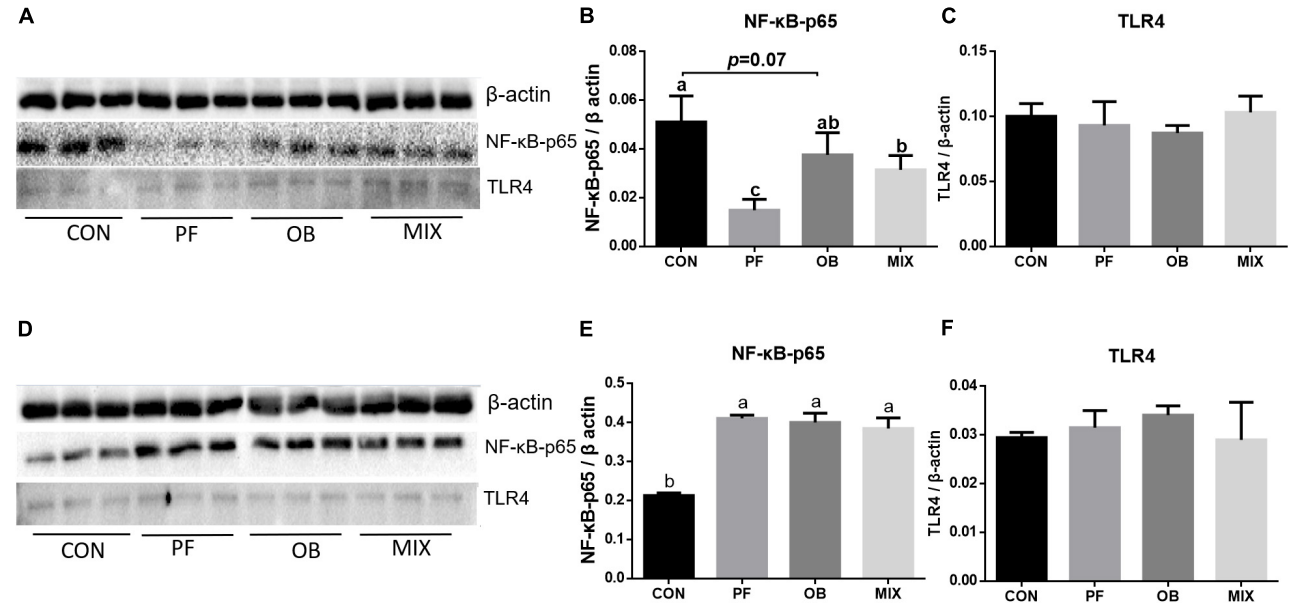

FIGURE 2 | The expression of TLR4 and NF-κB proteins in the ileal and colonic tissues of growing pigs in CON, PF, OB, and MIX groups. **(A)** The profile of sodium dodecyl sulfate–polyacrylamide gel electrophoresis (SDS-PAGE) of β-actin, NF-κB–p65, and TLR4 proteins in the ileal mucosa. **(B)** The average relative abundance (fold) of protein NF-κB–p65 to β-actin in the ileal mucosa. **(C)** The average relative abundance (fold) of protein TLR4 to β-actin in the ileal mucosa. **(D)** The profile of SDS-PAGE of β-actin, NF-κB–p65, and TLR4 proteins in the colonic mucosa. **(E)** The average relative abundance (fold) of protein NF-κB–p65 to β-actin in the colonic mucosa. **(F)** The average relative abundance (fold) of protein TLR4 to β-actin in the colonic mucosa. Different lowercase letters in the bar graphs indicate significant differences between two groups ($p < 0.05$, $n = 3$). CON, control group; PF, 15% pea-hull fiber in the diet; OB, 15% oat bran in the diet; MIX, 7.5% pea-hull fiber and 7.5% oat bran in the diet.

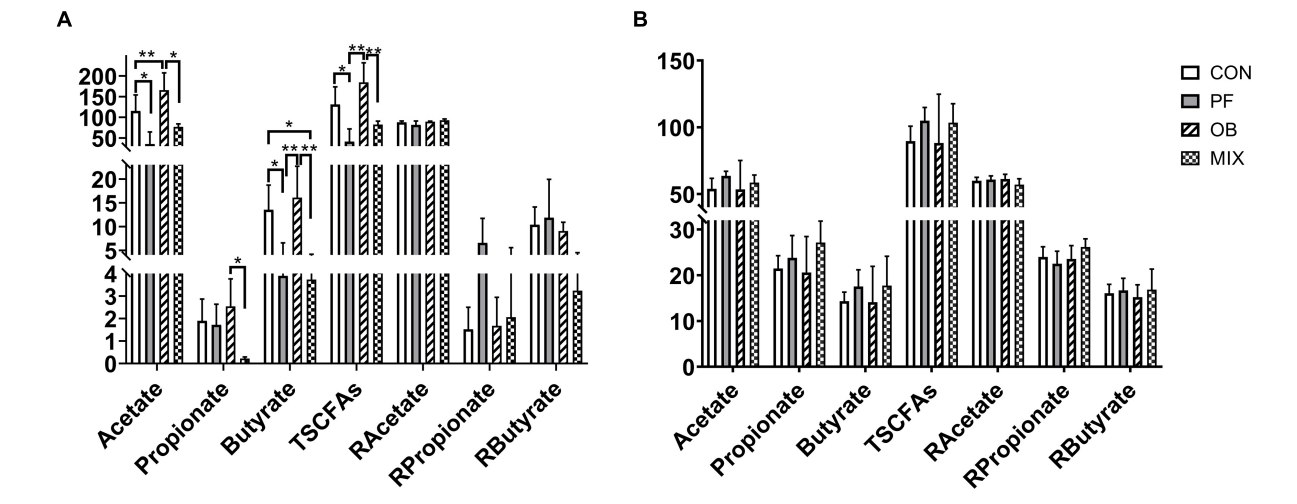

FIGURE 3 | The concentration and proportion of SCFAs in the ileal and colonic digesta of pigs in different groups. **(A)** The concentration and proportion of SCFAs in the ileum of the pigs. **(B)** The concentration and proportion of SCFAs in the colon of the pigs. *$p < 0.05$, **$p < 0.01$. CON, control group; PF, 15% pea-hull fiber in the diet; OB, 15% oat bran in the diet; MIX, 7.5% pea-hull fiber and 7.5% oat bran in the diet; TSCFAs, total SCFAs; R, ratio of each SCFA to TSCFAs.

digesta were different in relative abundance (α = 0.01, LDA score > 3.0) in pigs among different groups. In the ileal digesta, the genus *Turicibacter* and an unknown genus of Clostridiaceae were more abundant in CON pigs than in other pigs ($p < 0.05$, **Supplementary Figure 2**), whereas the order Lactobacillales and genus *Candidatus Arthromitus* were more abundant in PF pigs compared with those in pigs of other groups ($p < 0.05$, **Supplementary Figure 2**). In the colonic digesta, the families Streptococcaceae and Paraprevotellaceae, as well as the genera *Streptococcus* and CF231, showed more enriched in CON pigs compared with other pigs ($p < 0.05$, **Supplementary Figure 3**). Compared with CON, OB, and MIX pigs, the genus *Lachnospira*

TABLE 1 | The α- and β-diversity of microbial community in the digesta samples from ileum and colon of pigs in CON, PF, OB, and MIX groups[1].

Item	Ileum						Colon					
	CON	PF	OB	MIX	SEM	*p*-value	CON	PF	OB	MIX	SEM	*p*-value
Shannon index	4.19	3.65	3.20	3.66	0.14	0.10	7.63	7.25	7.81	7.55	0.12	0.42
Unweighted-unifrac distance	0.650^{ab}	0.661^{a}	0.599^{ab}	0.588^{b}	0.01	0.02	0.563^{b}	0.588^{ab}	0.589^{ab}	0.606^{a}	0.01	0.03

[1] *The variant alphabetical superscript in the same row indicates significant difference between groups when p < 0.05, n = 6. CON, control group; PF, 15% pea-hull fiber in the diet; OB, 15% oat bran in the diet; MIX, 7.5% pea-hull fiber and 7.5% oat bran in the diet; SEM, standard error of mean.*

was more abundant in PF pigs ($p < 0.05$), whereas the family Clostridiaceae and phylum WPS were enriched in OB pigs compared with other pigs ($p < 0.05$, **Supplementary Figure 3**).

Correlation Between the Concentration of Short-Chain Fatty Acids and the Abundance of the Main Bacterial Groups

Many species of bacteria in swine gut can ferment complex carbohydrates to produce SCFAs. The results above indicate that dietary supplement of DF may alter the concentrations and ratio of SCFAs in the gut, especially in the ileum, of the growing pigs. To further clarify the relationship between the changes in SCFAs and the composition of microbiota, a Pearson correlation analysis was conducted. We found that the abundance of the main bacterial genera (top 20 and significantly different genera) in ileal digesta of the pigs showed an extensive correlation with the concentration of acetate, butyrate, and propionate, as well as the ratio of each SCFA (**Figure 4**). For example, six bacterial groups, including *Lactobacillus*, *Clostridium*, and SMB53, were correlated with the concentration of acetate, whereas another six genera, including *Lactobacillus*, *Prevotella*, and *Pseudomonas*, were related to the concentration of butyrate (**Figure 1A**). In a word, several known genera such as *Turicibacter*, *Lactobacillus*, *Clostridium*, *Prevotella*, *Bacillus*, and SMB53 presented strong correlations with the concentration or ratio of SCFAs in the ileum. Unlike that, we found only two genera that might be associated with the concentration of butyrate (**Figure 4B**).

DISCUSSION

Although DFs have been regarded beneficial to humans and animals by reducing the incidence of many diseases, such as diabetes, cardiovascular disease, colorectal cancer, and obesity (King, 2005; Papathanasopoulos and Camilleri, 2010; Xu et al., 2014), few studies have focused on the mechanisms of different-sourced DF acting on the intestinal mucosal immunity and barrier functions. The current study revealed that the body weight gain of growing pigs was reduced by the dietary supplement of PF. However, the finally measured digestible energy of PF-containing diet (3.96 MJ/kg) was even slightly higher than that of control diet (3.78 MJ/kg), indicating that the decrease in weight gain of these animals may be due to the decline of feed intake, which probably resulted from the high concentration (15%) of PF. Despite the adverse impact of PF on the weight gain of the pigs, the intestinal barrier or immunity-related indexes of the pigs were, more or less, improved by the high-level supplement of these DF. Interestingly, the effect of these DF was different, depending on the intestinal segment.

We also investigated the relative expression of five intestinal barrier–related genes. We found that in the ileum of the pigs, none of these genes were differently expressed in pigs fed DF-containing diets compared with control pigs. Alternatively, the expression of several genes involved in the mucosal immunity was changed in the intestine of these animals. The transmembrane TLR4 and NOD are two proteins important in recognizing the pathogen-associated molecular patterns to regulate the innate immune responses (Liu et al., 2013). Binding of TLR4 or NOD with ligands can ultimately activate NF-κB and in turn induce the expression of inflammatory mediators (Fukata et al., 2009), such as IL-1β, IL-6, and IL-10. Appropriate levels of IL-1β can participate in immune regulation, but its high expression may induce tissue damage (Dionne et al., 1998). IL-10 can promote differentiation and proliferation of B cells, secretion of antibodies, and inhibition of inflammatory and cellular immune responses and also can enhance the tolerance associated with adaptive immunity and immune clearance (Antosz et al., 2015). In the current study, although the mRNA level of IL-6 in all mucosal samples kept stable, the expression of *IL-10* in the ileal mucosa was remarkably increased in those pigs fed OB and mixed DF-containing diets. Further analysis showed that the expression of *NOD2*, one of the key genes on NOD-associated pathway, in the ileal mucosa of pigs fed OB-containing diet was increased. Meanwhile, the expression of *TRAF6* and *IRAK4*, two key genes on TLR4-associated pathway, in the ileum of pigs fed OB and/or mixed fiber–containing diets was decreased, which was not accompanied by changes in the abundance of proteins TLR4 and NF-κB–p65. These results indicate that the improvement of ileal immune function by OB or mixed fibers may depend on NOD2-associated signal pathway rather than TLR4-associated pathway. Both bacteria and fungi in animal gut are the ligands of TLR and NOD (Creagh and O'Neill, 2006; Wolf et al., 2011; Netea et al., 2015). Microbes in the gastrointestinal tract are the main subjects for utilization of DF. In the current study, although the Shannon index of microbial community in the ileal digesta of the pigs fed DF-containing diets was observed to be decreased without a statistical difference, the range of decline varied from 12.6 to 23.6%, especially in those pigs fed OB-containing diet. This consequently suggests that the reduction of specific microorganisms may contribute to the decreased expression of genes associated with NOD signaling pathways, which in turn resulted in the increased expression of anti-inflammatory cytokine *IL-10*. On the other hand, the decline in the diversity or even the quantity of ileal microorganisms may

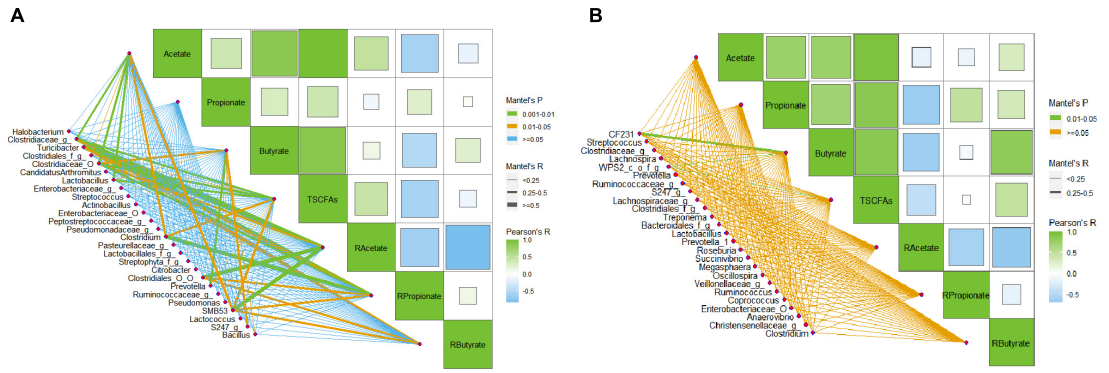

FIGURE 4 | Pearson correlation between the relative abundance of main bacteria and SCFAs in the ileal and colonic digesta of the growing pigs. **(A)** Correlation between the abundance of main bacteria (top 20 bacterial genera and bacteria with significant difference between groups) and SCFA concentrations and ratios in the ileal digesta of the pigs; **(B)** correlation between the abundance of main bacteria (top 20 bacterial genera and bacteria with significant difference between groups) and SCFA concentrations and ratios in the colonic digesta of the pigs. The lowercase letters o, f, and g following the Latin names of bacteria mean order, family, and genus, respectively.

be beneficial to the intestinal health of host. A large number of reports have confirmed that eliminating small bowel bacterial overgrowth can alleviate some intestinal inflammation including irritable bowel syndrome (Ghoshal et al., 2017). Sequencing results showed that the abundance of certain bacterial groups, such as Clostridiaceae, the major acetate producers in the hindgut of human and monogastric animals (Rey et al., 2010; Louis et al., 2014), decreased in the ileal digesta of pigs fed PF or mixed fiber–containing diets, which might directly lead to the decrease in the absolute concentration of ileal acetate and butyrate in these pigs. However, this decline may be compensated for the increase in some other SCFA-producing bacteria, such as Lactobacillales, to keep the ratio of these SCFAs to TSCFAs invariable. Interestingly, we not only found a greater change in the concentration of SCFAs in the ileum than that in the colon of those pigs fed DF-containing diets, but also revealed a stronger correlation between such change with the abundance of specific bacterial groups, such as *Lactobacillus*, *Prevotella*, and *Clostridium*. The results indicate that these bacteria may probably be the contributors of the changes in SCFA concentration coursed by DF-containing diets. Different from that observed in the ileum, both the expression of *MUC1* and *MUC2* in the colonic mucosa of pigs fed OB and/or mixed fiber–containing diets were increased compared with control pigs, indicating an enhanced barrier function in the colon. In addition, the expression of NF-κB protein, but not TLR, in the colonic mucosa of pigs fed DF-containing diets was markedly increased than control pigs. Our further analysis showed that the expression of *RIPK2* on the NOD-associated pathway increased in the colon of pigs fed diets with OB or mixed DF, suggesting that the increased expression of NF-κB protein may be mediated by the genes involved in NOD signaling pathway in the colon. Accordingly, both the α-diversity and β-diversity of the microbial community in the colonic digesta of pigs fed DF-containing diets were increased. It is worth mentioning the abundance of genus *Lachnospira* in the colon of pigs fed PF and mixed fiber–containing diets, accompanied by the decrease in *Streptococcus*, whereas the supplement of OB in the diet specifically increased the abundance of Clostridiaceae. It is reported that genus *Lachnospira* exists widely in the gastrointestinal tract and can utilize some DF such as pectin (Dusková and Marounek, 2001). Bacteria categorized as family *Lachnospiraceae*, including *Lachnospira*, *Butyrivibrio*, and *Roseburia*, are generally regarded as beneficial microorganisms producing butyrate and propionate (Cotta and Forster, 2006). In this respect, PF-containing diet may promote the proliferation of potential probiotics and inhibit the growth of specific conditional pathogens in the colon of pigs, which may have a positive effect on the intestinal health of these animals.

In summary, our results showed that the dietary supplement (15%) of OB or the equivalent mixtures of PF and OB, rather than the sole supplement of PF, may benefit the gut health in growing pigs. However, such positive effects may vary, depending on the intestinal segment; that is, the immune-related indexes are mainly improved in the ileum, whereas the intestinal barrier–related indexes are mainly improved in the colon. What needs to be pointed out is that the improvement of immune function in these pigs seems to be dependent on NOD rather than TLR-associated pathways, whether in the ileum or colon. Although the polysaccharides from DF can only be degraded by microorganisms in gastrointestinal tract, the supplement of these DF had limited effects on the microbial diversity in the ileum and colon of experimental pigs. Despite that, bacterial groups that specifically responded to each DF in the ileal or colonic digesta were identified. Contrary to general cognition, the impact of these DF on the concentration of SCFAs in the ileal digesta of the pigs was greater than that in the colon. Although the absolute concentration of acetate, propionate, and butyrate was decreased in the ileum of pigs fed diets with DF, the proportion of these SCFAs was not changed. In addition, a direct correlation between the change of microbial community and the expression of genes associated with intestinal barrier and immunity was not found. In terms of microbial community and composition, PF and mixed DF rather than OB showed similar effects.

DATA AVAILABILITY STATEMENT

The datasets presented in this study can be found in online repositories. The names of the repository/repositories and accession number(s) can be found below: https://ngdc.cncb.ac.cn/gsa/browse/CRA001323, CRA001323.

ETHICS STATEMENT

The animal study was reviewed and approved by all experimental procedures and animal care were performed in accordance with the Guide for the Care and Use of Laboratory Animals prepared by the Institutional Animal Care and Use Committee of Sichuan Agricultural University, and all animal protocols were approved by the Animal Care and Use Committee of Sichuan Agricultural University under permit number DKYB20131704.

AUTHOR CONTRIBUTIONS

YhL designed the experiments, wrote the manuscript, and had primary responsibility for the final content. YL helped to write the manuscript and analyzed part of the data. HL conducted the data analysis of sequencing and flow cytometry. YZ conducted the animal trial, real-time PCR analysis, and Western blot. A-DW helped to collect references and revised the manuscript. JC, GT, and XM helped to analyze the data. All authors contributed to the article and approved the submitted version.

FUNDING

This work was supported by the National Natural Science Foundation of China (Grant Numbers 31872369 and 31301987) and Sichuan Science and Technology Project (Grant Number 2014HH0051).

SUPPLEMENTARY MATERIAL

The Supplementary Material for this article can be found online at: https://www.frontiersin.org/articles/10.3389/fmicb.2022.843045/full#supplementary-material

REFERENCES

Antosz, H., Wojciechowska, K., Sajewicz, J., Choroszyńska, D., Marzec-Kotarska, B., Osiak, M., et al. (2015). IL-6, IL-10, c-Jun and STAT3 expression in B-CLL. *Blood Cells Mol. Dis.* 54, 258–265. doi: 10.1016/j.bcmd.2014.11.006

Bach Knudsen, K. E., Hedemann, M. S., and Lærke, H. N. (2012). The role of carbohydrates in intestinal health of pigs. *Anim. Feed Sci. Technol.* 173, 41–53. doi: 10.1016/j.anifeedsci.2011.12.020

Campbell, R. G., and Taverner, M. R. (1986). The effects of dietary fibre, source of fat and dietary energy concentration on the voluntary food intake and performance of growing pigs. *Anim. Sci.* 43, 327–333. doi: 10.1017/S0003356100002518

Caporaso, J. G., Kuczynski, J., Stombaugh, J., Bittinger, K., Bushman, F. D., Costello, E. K., et al. (2010). QIIME allows analysis of high-throughput community sequencing data. *Nat. Methods* 7, 335–336. doi: 10.1038/nmeth.f.303

Conlon, M. A., and Bird, A. R. (2014). The impact of diet and lifestyle on gut microbiota and human health. *Nutrients* 7, 17–44. doi: 10.3390/nu7010017

Cotta, M., and Forster, R. (2006). The family Lachnospiraceae, including the genera Butyrivibrio, Lachnospira and Roseburia. *Prokaryotes* 4, 1002–1021.

Creagh, E. M., and O'Neill, L. A. J. (2006). TLRs, NLRs and RLRs: a trinity of pathogen sensors that co-operate in innate immunity. *Trends Immunol.* 27, 352–357. doi: 10.1016/j.it.2006.06.003

Dionne, S., D'Agata, I. D., Hiscott, J., Vanounou, T., and Seidman, E. G. (1998). Colonic explant production of IL-1and its receptor antagonist is imbalanced in inflammatory bowel disease (IBD). *Clin. Exp. Immunol.* 112, 435–442. doi: 10.1046/j.1365-2249.1998.00595.x

Dusková, D., and Marounek, M. (2001). Fermentation of pectin and glucose, and activity of pectin-degrading enzymes in the rumen bacterium Lachnospira multiparus. *Lett. Appl. Microbiol.* 33, 159–163. doi: 10.1046/j.1472-765x.2001.00970.x

Edgar, R. C., Haas, B. J., Clemente, J. C., Quince, C., and Knight, R. (2011). UCHIME improves sensitivity and speed of chimera detection. *Bioinformatics* 27, 2194–2200. doi: 10.1093/bioinformatics/btr381

El Kaoutari, A., Armougom, F., Gordon, J. I., Raoult, D., and Henrissat, B. (2013). The abundance and variety of carbohydrate-active enzymes in the human gut microbiota. *Nat. Rev. Microbiol.* 11, 497–504. doi: 10.1038/nrmicro3050

Finamore, A., Roselli, M., Imbinto, A., Seeboth, J., Oswald, I. P., and Mengheri, E. (2014). Lactobacillus amylovorus inhibits the TLR4 inflammatory signaling triggered by enterotoxigenic *Escherichia coli* via modulation of the negative regulators and involvement of TLR2 in intestinal Caco-2 cells and pig explants. *PLoS One* 9:e94891. doi: 10.1371/journal.pone.0094891

Fukata, M., Vamadevan, A. S., and Abreu, M. T. (2009). Toll-like receptors (TLRs) and Nod-like receptors (NLRs) in inflammatory disorders. *Semin. Immunol.* 21, 242–253. doi: 10.1016/j.smim.2009.06.005

Gao, L., Chen, L., Huang, Q., Meng, L., Zhong, R., Liu, C., et al. (2015). Effect of dietary fiber type on intestinal nutrient digestibility and hindgut fermentation of diets fed to finishing pigs. *Livest. Sci.* 174, 53–58. doi: 10.1016/j.livsci.2015.01.002

Ghoshal, U. C., Shukla, R., and Ghoshal, U. (2017). Small intestinal bacterial overgrowth and irritable bowel syndrome: a bridge between functional organic dichotomy. *Gut Liver* 11, 196–208. doi: 10.5009/gnl16126

Hipsley, E. H. (1953). Dietary "fibre" and pregnancy toxaemia. *Br. Med. J.* 2, 420–422.

Ito, H., Satsukawa, M., Arai, E., Sugiyama, K., Sonoyama, K., Kiriyama, S., et al. (2009). Soluble fiber viscosity affects both goblet cell number and small intestine mucin secretion in rats. *J. Nutr.* 139, 1640–1647. doi: 10.3945/jn.109.110171

Kim, K.-A., Gu, W., Lee, I.-A., Joh, E.-H., and Kim, D.-H. (2012). High fat diet-induced gut microbiota exacerbates inflammation and obesity in mice via the TLR4 signaling pathway. *PLoS One* 7:e47713. doi: 10.1371/journal.pone.0047713

King, D. E. (2005). Dietary fiber, inflammation, and cardiovascular disease. *Mol. Nutr. Food Res.* 49, 594–600. doi: 10.1002/mnfr.200400112

Knudsen, K. E. B. (1997). Carbohydrate and lignin contents of plant materials used in animal feeding. *Anim. Feed Sci. Technol.* 67, 319–338.

Lange, C. F. M., de Pluske, J., Gong, J., and Nyachoti, C. M. (2010). Strategic use of feed ingredients and feed additives to stimulate gut health and development in young pigs. *Livest. Sci.* 134, 124–134. doi: 10.1016/j.livsci.2010.06.117

Larionov, A., Krause, A., and Miller, W. (2005). A standard curve based method for relative real time PCR data processing. *BMC Bioinformatics* 6:62. doi: 10.1186/1471-2105-6-62

Liu, Y., Chen, F., Li, Q., Odle, J., Lin, X., Zhu, H., et al. (2013). Fish oil alleviates activation of the hypothalamic-pituitary-adrenal axis associated with inhibition of TLR4 and NOD signaling pathways in weaned piglets after a lipopolysaccharide challenge. *J. Nutr.* 143, 1799–1807. doi: 10.3945/jn.113.179960

Louis, P., Hold, G. L., and Flint, H. J. (2014). The gut microbiota, bacterial metabolites and colorectal cancer. *Nat. Rev. Microbiol.* 12, 661–672. doi: 10.1038/nrmicro3344

Luo, Y., Zhang, L., Li, H., Smidt, H., Wright, A.-D. G., Zhang, K., et al. (2017). Different types of dietary fibers trigger specific alterations in composition and predicted functions of colonic bacterial communities in BALB/c mice. *Front. Microbiol.* 8:966. doi: 10.3389/fmicb.2017.00966

Luo, Y.-H., Yang, C., Wright, A.-D. G., He, J., and Chen, D.-W. (2015). Responses in ileal and cecal bacteria to low and high amylose/amylopectin ratio diets in growing pigs. *Appl. Microbiol. Biotechnol.* 99, 10627–10638. doi: 10.1007/s00253-015-6917-2

Magoč, T., and Salzberg, S. L. (2011). FLASH: fast length adjustment of short reads to improve genome assemblies. *Bioinformatics* 27, 2957–2963. doi: 10.1093/bioinformatics/btr507

National Research Council (2012). *Nutrient Requirements of Swine*. Washington, DC: The National Academies Press.

Netea, M. G., Joosten, L. A., van der Meer, J. W., Kullberg, B. J., and van de Veerdonk, F. L. (2015). Immune defence against Candida fungal infections. *Nat. Rev. Immunol.* 15, 630–642. doi: 10.1038/nri3897

Papathanasopoulos, A., and Camilleri, M. (2010). Dietary fiber supplements: effects in obesity and metabolic syndrome and relationship to gastrointestinal functions. *Gastroenterology* 138, 65–72.e1-2. doi: 10.1053/j.gastro.2009.11.045

Rey, F. E., Faith, J. J., Bain, J., Muehlbauer, M. J., Stevens, R. D., Newgard, C. B., et al. (2010). Dissecting the *in vivo* metabolic potential of two human gut acetogens. *J. Biol. Chem.* 285, 22082–22090. doi: 10.1074/jbc.m110.117713

Sajilata, M. G., Singhal, R. S., and Kulkarni, P. R. (2006). Resistant starch–a review. *Compr. Rev. Food Sci. Food Saf.* 5, 1–17.

Segata, N., Izard, J., Waldron, L., Gevers, D., Miropolsky, L., Garrett, W. S., et al. (2011). Metagenomic biomarker discovery and explanation. *Genome Biol.* 12:R60. doi: 10.1186/gb-2011-12-6-r60

Sonnenburg, E. D., and Sonnenburg, J. L. (2014). Starving our microbial self: the deleterious consequences of a diet deficient in microbiota-accessible carbohydrates. *Cell Metab.* 20, 779–786. doi: 10.1016/j.cmet.2014.07.003

Stephen, A. M., and Phillips, G. O. (2016). *Food Polysaccharides and their Applications*. Boca Raton, FL: CRC press.

Trowell, H. (1976). Definition of dietary fiber and hypotheses that it is a protective factor in certain diseases. *Am. J. Clin. Nutr.* 29, 417–427. doi: 10.1093/ajcn/29.4.417

Venema, K., Graaf, A. A., de Deutz, N. E. P., Salovaara, H., Gates, F., and Tenkanen, M. (2007). "Metabolic conversions of dietary carbohydrates by gut microbes," in *Dietary Fibre: Components and Functions*, eds H. Salovaara, F. Gates and M. Tenkanen (Wageningen: Wageningen Academic Publishers), 145–156.

Wolf, A. J., Arruda, A., Reyes, C. N., Kaplan, A. T., Shimada, T., Shimada, K., et al. (2011). Phagosomal degradation increases TLR access to bacterial ligands and enhances macrophage sensitivity to bacteria. *J. Immunol.* 187, 6002–6010. doi: 10.4049/jimmunol.1100232

Xu, H., Huang, X., Risérus, U., Krishnamurthy, V. M., Cederholm, T., Ärnlöv, J., et al. (2014). Dietary fiber, kidney function, inflammation, and mortality risk. *Clin. J. Am. Soc. Nephrol.* 9, 2104–2110.

Yan, C. L., Kim, H. S., Hong, J. S., Lee, J. H., Han, Y. G., Jin, Y. H., et al. (2017). Effect of Dietary sugar beet pulp supplementation on growth performance, nutrient digestibility, fecal Microflora, blood profiles and Diarrhea incidence in weaning pigs. *J. Anim. Sci. Technol.* 59:18. doi: 10.1186/s40781-017-0142-8

Zhao, J. B., Liu, P., Huang, C. F., Liu, L., Li, E. K., Zhang, G., et al. (2018). Effect of wheat bran on apparent total tract digestibility, growth performance, fecal microbiota and their metabolites in growing pigs. *Anim. Feed Sci. Technol.* 239, 14–26. doi: 10.1016/j.anifeedsci.2018.02.013

Zhou, X., Oryschak, M. A., Zijlstra, R. T., and Beltranena, E. (2013). Effects of feeding high- and low-fibre fractions of air-classified, solvent-extracted canola meal on diet nutrient digestibility and growth performance of weaned pigs. *Anim. Feed Sci. Technol.* 179, 112–120. doi: 10.1016/j.anifeedsci.2012.12.002

Conflict of Interest: The authors declare that the research was conducted in the absence of any commercial or financial relationships that could be construed as a potential conflict of interest.

Publisher's Note: All claims expressed in this article are solely those of the authors and do not necessarily represent those of their affiliated organizations, or those of the publisher, the editors and the reviewers. Any product that may be evaluated in this article, or claim that may be made by its manufacturer, is not guaranteed or endorsed by the publisher.

frontiers in Microbiology

ORIGINAL RESEARCH
published: 04 March 2022
doi: 10.3389/fmicb.2022.841397

Portulaca oleracea Polysaccharides Modulate Intestinal Microflora in Aged Rats *in vitro*

Qiang Fu[1,2], Siyi Zhou[1,2], Mengting Yu[1,2], Yang Lu[1,2], Genhe He[3], Xiaoliu Huang[1,2] and Yushan Huang[4]**

[1] College of Medicine, Jinggangshan University, Ji'an, China, [2] Ji'an Key Laboratory of Biomedicine, Ji'an, China, [3] School of Life Sciences, Jinggangshan University, Ji'an, China, [4] Center for Evidence Based Medical and Clinical Research, First Affiliated Hospital of Gannan Medical University, Ganzhou, China

To explore the effect of *Portulaca oleracea* polysaccharides (POP) in regulating intestinal microflora in aged rats *in vitro*, its intestinal microbial composition was analyzed by 16 S rDNA high-throughput sequencing, and the level of short-chain fatty acids in fermentation broth was determined by LC-MS. POP significantly upregulated the relative abundance of *Lactobacillus*, *Eggerthella*, and *Paraprevotella* and significantly downregulated *Escherichia_Shigella*, *Bacteroides*, and *Eubacterium nodatum* groups. The pH value and ammonia nitrogen level decreased significantly in the POP-treated group, resulting in a more short-chain fatty acid consumption which changed the acid–base environment of the fermentation broth. In conclusion, POP is beneficial to aged rats because it can regulate intestinal flora, promote the growth of probiotics, and inhibit the reproduction of pathogenic bacteria.

Keywords: *Portulaca oleracea* polysaccharides, *in vitro* fermentation, aged rats, intestinal microflora, probiotics

OPEN ACCESS

Edited by:
Fengjie Sun,
Georgia Gwinnett College,
United States

Reviewed by:
Zhaofei Wang,
Shanghai Jiao Tong University, China
Xiaolong Yang,
Nantong University, China

****Correspondence:***
Xiaoliu Huang
huangxl1976@163.com
Yushan Huang
3218680@qq.com

Specialty section:
This article was submitted to Food Microbiology, a section of the journal Frontiers in Microbiology

Received: *22 December 2021*
Accepted: *13 January 2022*
Published: *04 March 2022*

Citation:
Fu Q, Zhou S, Yu M, Lu Y, He G, Huang X and Huang Y (2022) Portulaca oleracea Polysaccharides Modulate Intestinal Microflora in Aged Rats in vitro. Front. Microbiol. 13:841397. doi: 10.3389/fmicb.2022.841397

INTRODUCTION

The intestinal flora of mammals are colonized by a large number of microflora, whose homeostasis is of great significance to the physiological functions of the organism (Simpson and Campbell, 2015; Zhou et al., 2020). However, with aging, the intestinal flora of the organism also changes, with a decrease in the stability of the dominant species, especially in the elderly population of human beings, thus threatening their health (Salazar et al., 2020). Studies have shown that intestinal flora are closely linked to the development of aging-related diseases, which correlate with reduced intestinal probiotics (Zhou et al., 2020; Chu et al., 2021). In addition, several studies have provided scientific evidence that the abundance of *Bifidobacteria* decreased, whereas *Firmicutes* and *Enterobacteriaceae* increased in the intestines of elderly individuals compared with young individuals (O'Callaghan and van Sinderen, 2016). Studies have also found that the proportions of *Bacteroidetes*, *Firmicutes*, and *Verrucomicro* phyla in the intestinal tract diminished with age (Vemuri et al., 2017; Yu et al., 2017; Lee et al., 2018). The intestinal flora plays an important symbiotic function by producing short-chain fatty acids through fermenting low- or non-digestible carbohydrates that are not easily absorbed by the small intestine (Zhu et al., 2021).

Polysaccharides are complex carbohydrates made up of more than 10 monosaccharide molecules polymerized by glycosidic bonds. In recent years, abundant evidence has demonstrated that polysaccharides can be used as a carbon source of intestinal flora to promote the reproduction of probiotics and consequently regulate intestinal flora through its metabolites, which are vital

in reshaping the diversity of intestinal microecology, making it a useful prebiotic (Fang et al., 2019). One of the resistant starches, amylose–lipid complex RS5, was reported to be helpful in regulating the microecology of human intestinal flora by promoting the production of butyric acid during *in vitro* fermentation, where the relative abundance of *Bifidobacterium*, *Dialister*, *Collinsella*, *Romboutsia*, and *Megamonas* increased significantly (Qin et al., 2021). In fact, acetic acid, propionic acid, and butyric acid regulate intestinal flora by reducing pH, inhibiting the excessive growth of pathogenic bacteria, such as *Escherichia coli*, and stimulating the growth of probiotics such as *Firmicutes* (Ghosh et al., 2011; Zimmer et al., 2012). Short-chain fatty acid production is considered a marker of interactions between host and intestinal flora, which also uncovers the causality between accelerated aging and flora dynamics in elderly individuals (Mangiola et al., 2018).

Purslane, a medicinal plant, is widely used in Traditional Chinese Medicine (Zhou et al., 2015). As a common homology of medicine and food, it also has a variety of indications (Iranshahy et al., 2017). Purslane is rich in bioactive substances, multiple flavonoids, alkaloids, polysaccharides, fatty acids, terpenoids, steroids, and proteins and is high in vitamins and minerals (Hu et al., 2018; Miao et al., 2019). Polysaccharides are the main active ingredients that have been widely studied. Results of the structural analysis show that glucose and galactose are the main monosaccharide molecules of *Portulaca oleracea* polysaccharide (POP). Research has demonstrated that POP exhibits antitumor and antimicrobial activities, improves diabetes, and promotes oxidation resistance (Dong et al., 2010; Hu et al., 2018). Our recently published study revealed that POP significantly improved the gut microbiota composition of weaned rats and promoted colonization probiotics such as *Lactobacilli* and *Bifidobacteria*, thus affecting the metabolic function of rats (Huang et al., 2021). This suggests that POP may play a role as a prebiotic in promoting the reproduction of intestinal probiotics and modulating the diversity of intestinal microecology. However, there are limited studies on the effect of POP as a prebiotic in gut microbiota homeostasis of aging individuals. The *in vitro* fermentation model is also considered to be an effective tool for investigating colon microflora in a highly controlled environment. Therefore, in the present study, based on our former results, we explored the effect of POP on regulating intestinal microflora of elderly rats *in vitro*, which provides potential insight into the development and utilization of POP as food.

MATERIALS AND METHODS

Reagents

Purslane polysaccharides (≥50%) are purchased from Lanzhou Wotelaisi Biotechnology Co., Ltd. (Wotls, Lanzhou, China). Methanol, distilled deionized water, formic acid, and acetonitrile (HPLC grade) were purchased from Thermo Fisher Scientific (Waltham, MA, United States); 3-NPH, EDC, and standard products (HPLC grade) were purchased from Sigma-Aldrich (St. Louis, MO, United States). Related analytical reagents were purchased from Sinopharm Chemical Reagent Co., Ltd (Shanghai, China). The basic medium was prepared as the methodology reported by Mandalari et al. (2008) with minor modifications (2 g/l peptone, 2 g/l yeast extract, 0.1 g/l NaCl, 0.04 g/l K_2HPO_4, 0.04 g/l KH_2PO_4, 0.01 g/l $MgSO_4{\cdot}7H_2O$, 0.01 g/l $CaCl_2{\cdot}6H_2O$, 2 g/l $NaHCO_3$, 2 ml Tween 80, 0.02 g/l hemin, 10 μl vitamin K_1, 0.5 g/l cysteine HCl, and 0.5 g/l bile salts, pH 7.0).

In vitro Fermentation of Purslane

Fecal samples collected by aseptic manipulation from five healthy Sprague-Dawley (SD) aged (21-month-old) rats were pooled with equal amounts and immediately placed inside an anaerobic chamber. 5 g of fecal samples was taken, and 20 times of the fecal weight of sterile saline was added to the anaerobic chamber, and the mixtures were fully shaken. The mixtures were filtered with eight layers of sterile gauze and transferred into another sterile sample bottle and then seeded into the basic medium to a final volume of 1 l for bacteria fermentation. The experiments were divided into six groups: Con1 (control group, fermented for 24 h), Con2 (control group, fermented for 48 h), LPOP1 (low-dose group of purslane polysaccharide fermented for 24 h), LPOP2 (low-dose group of purslane polysaccharide fermented for 48 h), HPOP1 (high-dose group of purslane polysaccharide fermented for 24 h), and HPOP2 (high-dose group of purslane polysaccharide fermented for 48 h). The fermentation volume of all groups was in 10 ml fermentation solution, the Con groups contained no POP, the LPOP groups contained POP (0.02 g/ml), and the HPOP groups contained POP (0.03 g/ml). Each group was repeated with five independent experiments. Gas production of the anaerobic cultures was recorded at 0, 12, 24, 36, and 48 h post inoculation (hpi), and the fermentation culture was collected at 24 and 48 hpi. Supernatants of the culture were separated by centrifugation for detection of pH, ammonia nitrogen, and short-chain fatty acid levels. The precipitates were stored at −80°C for further DNA extraction.

Analysis of Ammonia

For ammonia analysis, 2.5 ml phenol chromogenic agent was added into a 10-ml tube, and 10 μl fermentation supernatants was added later. Then, 2.0 ml hypochlorite solution was also added into the tube. After shaking and mixing, the tube was incubated in water bath at 40°C for 15 min then cooled to room temperature to measure the absorbance value (OD_{625}), and the ammonia content was calculated according to the standard curve.

Determination of Short-Chain Fatty Acids

Short-chain fatty acids were analyzed by LC-MS/MS. A volume of 100 μl supernatant was added with 100 μl 50% acetonitrile-aqueous solution (v/v), and then grinding for 3 min. After that, the samples were sonicated in an ice water bath for 10 min and then centrifuged for 10 min, at 4°C, 12,000 rpm, followed by sample derivation and stored at −80°C for further analysis. The 5-μl samples were added into a high-performance liquid chromatograph (Nexera UHPLC LC-30A, Shimazin, Japan) with a color matching column (ACQUITY UPLC BEH C18 100 m × 2.1 mm × 1.7 μm, Waters) and a high-resolution mass

spectrometer (AB SCIEX QTRAP 5500, AB SCIEX). The mass spectrum conditions are as follows: 0.1% formic acid-aqueous solution (A) and acetonitrile (B) are used as mobile phase, mass flow rate is 0.35 ml/min; curtain gas: 35 (psi); collision-activated dissociation (CAD) parameters: medium; negative ion spray voltage: −4,500 (V); ion source temperature: 450(°C); column temperature: 40(°C), ion source: gas 1:50 (psi); gas 2:60 (psi). Various short-chain fatty acids were determined according to the retention time, and the concentrations were calculated based on the standard curve.

DNA Extraction and Gene Amplification

Cecal content samples of the rats were collected and quick-frozen, then stored at −80°C for further analysis. Total genomic DNA was extracted using the DNA Extraction Kit (Magen, Guangzhou, China) according to the manufacturer's instructions. The concentration of DNA was verified with a NanoDrop 2000 spectrophotometer (Thermo Fisher Scientific, Waltham, MA, United States) and agarose gel electrophoresis, respectively. All DNA samples were stored at −20°C for further study. PCR amplification of the V3–V4 hypervariable regions of the bacterial 16S rRNA gene was carried out with a 25-μl reaction mixture using universal primers (343F: 5′-TACGGRAGGCAGCAG-3′; 798R: 5′-AGGGTATCTAATCCT-3′). The reverse primer contained a sample barcode, and both primers were connected with an Illumina sequencing adapter.

Library Construction and Sequencing

The amplicon quality was visualized by gel electrophoresis. The PCR products were purified with Agencourt AMPure XP beads (Beckman Coulter Co., Brea, CA, United States) and quantified using the Qubit dsDNA assay kit. The concentrations were then adjusted for sequencing. Sequencing was performed on an Illumina NovaSeq 6000 with two paired-end read cycles of 250 bases each (Illumina Inc., San Diego, CA, United States; Oe Biotech Company, Shanghai, China).

Bioinformatic Analysis

Paired-end reads were preprocessed with Trimmomatic software (Bolger et al., 2014) to detect and cut off ambiguous bases (N). It also cut off low-quality sequences with an average quality score below 20 using a sliding window trimming approach. After trimming, paired-end reads were assembled using FLASH software (Reyon et al., 2012). Parameters of assembly were 10 bp of minimal overlapping, 200 bp of maximum overlapping, and 20% of maximum mismatch rate. Further denoising of sequences was performed as follows: reads with ambiguous, homologous sequences or below 200 bp were abandoned. Reads with 75% of bases above Q20 were retained by QIIME software (version 1.8.0) (Caporaso et al., 2010). After that, reads with chimera were detected and removed using VSEARCH (Rognes et al., 2016). Clean reads were subjected to primer sequence removal and clustering to generate operational taxonomic units (OTUs) using VSEARCH software with a 97% similarity cutoff (Rognes et al., 2016). The representative read of each OTU was selected using the QIIME package. All representative reads were annotated and blasted against Silva database (Version 132) using the RDP classifier (confidence threshold was 70%) (Wang et al., 2007). The microbial diversity in cecal content samples was estimated using the alpha diversity that includes Chao1 index, Shannon index, Observed-species, Simpson, Goods-coverage, and PD-whole-tree. The UniFrac distance matrix performed by QIIME software was used for unweighted UniFrac principal coordinate analysis (PCoA) and phylogenetic tree construction. The 16S rRNA gene amplicon sequencing and analysis were conducted by Oe Biotech Co., Ltd. (Shanghai, China).

Statistical Analysis

Experimental data in the study are reported as mean ± standard deviation (SD) of at least biological duplicates. One-way analysis of variance (ANOVA) and Duncan's multiple-range tests were employed to analyze significant differences in gas production, NH_3-N value, pH value, short-chain fatty acid (SCFA), and α-diversity ($p < 0.05$) between groups using SPSS version 19.0 (SPSS Inc., Chicago, IL, United States). Gas, NH_3-N, pH, and SCFA profiles were plotted in the GraphPad Prism version 8.0 (GraphPad Software, Inc., La Jolla, CA, United States).

RESULTS

Gas Production, NH_3-N Value, and pH Value Analysis

As fermentation time increased, gas production in the HPOP and LPOP groups changed significantly compared with that in the Con group. Moreover, gas production in the HPOP group was significantly higher than in the LPOP and Con groups (**Figure 1A**). At the 24- and 48-h fermentation points, both ammonia nitrogen (NH_3-N) and pH values were significantly higher in the Con group than in the HPOP and LPOP groups (**Figures 1B,C**).

The results also showed that POP inhibited the production of short-chain fatty acids in the fermentation broth. After 24 and 48 h of fermentation, the concentrations of acetic acid (**Figure 2A**), butyric acid (**Figure 2B**), propionic acid (**Figure 2C**), and isovalerate (**Figure 2D**) in the fermentation broth of POP groups (both low- and high-dose groups) significantly decreased compared with Con groups; however, there was no difference between the LPOP and HPOP groups (**Figure 2**).

Effects of *Portulaca oleracea* Polysaccharides on Microbial Community Distribution

The Good's coverage indices in the six groups were all greater than 99%, which indicated that most of the bacteria present in the samples were identified (**Table 1**). Purslane polysaccharides were found to significantly decrease fecal microbiota richness (Shannon, Simpson, and PD-whole-tree) and diversity (Chao1 and observed-species) after 24 or 48 h of *in vitro* fermentation compared to the control groups (**Table 1**). In addition, POP altered bacterial β-diversity (**Figure 3**). Principal component analysis (PCA) revealed the distinct clustering of

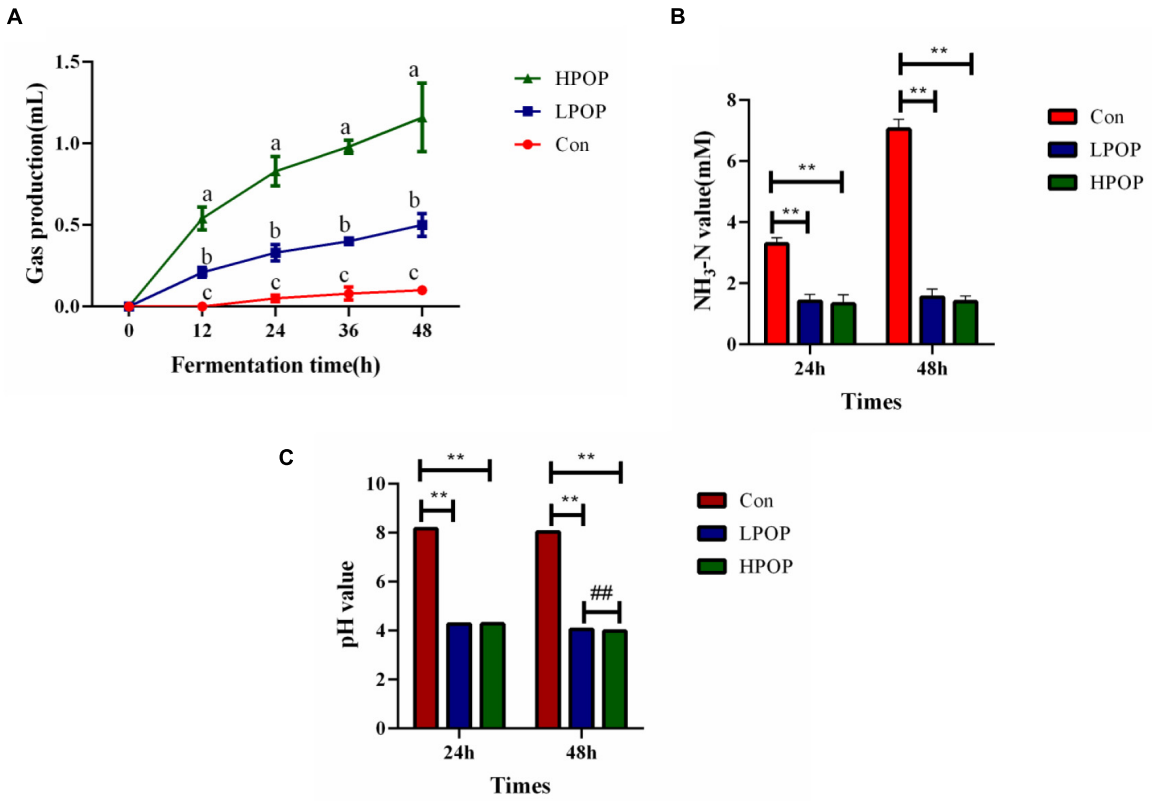

FIGURE 1 | Gas production of the anaerobic cultures was recorded at 0, 12, 24, 36, and 48 h post inoculation (hpi), and the fermentation culture was collected at 24 and 48 hpi. Supernatants of the culture were separated by centrifugation for detection of pH and ammonia nitrogen levels. Gas production, NH_3-N, and pH value during 48 h *in vitro* fecal fermentation with POP. **(A)** Gas production. **(B)** NH_3-N. $^{**}P < 0.01$ and $^{\#\#}P < 0.01$ vs different groups, respectively. **(C)** pH value.

microbiota compositions for the six groups. The microbiota compositions of LPOP1, LPOP2, HPOP1, and HPOP2 were not comparable; however, Con1 and Con2 were significantly comparable, but Con groups differed greatly from POP groups in the PC1 analysis, which was 16.1% of the total variation (**Figure 3**).

Microbial Composition at Phylum and Genus Levels

Microflora in fermentation cultures of different groups are mainly composed of *Firmicutes*, *Bacteroidetes*, *Proteobacteria*, and *Actinobacteriota* when categorized at the phylum level. Nine and six different phyla were observed with ANOVA analysis after 24 and 48 h of fermentation, respectively. Compared with the Con1 group, the abundance of *Firmicutes* in the LPOP1 and HPOP1 groups was significantly upregulated, while *Bacteroidetes*, *Proteobacteria*, *Fusobacteriota*, *Desulfobacterota*, *Actinobacteriota*, *Acidobacteriota*, *Cyanobacteria*, and others showed a significant decrease (**Figure 4A**). In addition, compared with the Con2 group, the relative abundance of *Firmicutes* in the LPOP2 and HPOP2 groups was significantly upregulated, whereas the relative abundance of *Proteobacteria*, *Desulfobacterota*, *Bacteroidota*, *Fusobacteriota*, and others was significantly decreased (**Figure 5A**).

At the genus level, *Escherichia-Shigella* and *Lactobacillus* were dominant in the Con and POP groups, respectively. After fermentation for 24 and 48 h, ANOVA analysis showed that 87 and 78 different bacterial genera were observed, respectively. Compared with the Con1 group, the relative abundance of *Lactobacillus* in the LPOP1 and HPOP1 groups increased significantly. However, other genera of microflora such as *Escherichia-Shigella*, *Parasutterella*, and *Klebsiella* decreased significantly (**Figure 4B**). Compared with the Con2 group, the relative abundance of *Lactobacillus* in the LPOP2 and HPOP2 groups was much higher. Conversely, the relative abundance of *Escherichia-Shigella*, *Parasutterella*, *Phascolarctobacterium*, *Eubacterium nodatum*_group, and *Klebsiella* decreased significantly (**Figure 5B**).

Screening of Different Species Between Groups

To identify specific microflora associated with POP, the linear discriminant analysis effect size (LEfSe) method was used to compare the differences in microflora between the Con and POP-treated groups after fermentation. The cladding diagrams of fermentative microorganisms and dominant bacteria composition are presented in **Figures 6B**, **7B**. The most differentially abundant taxa are shown in **Figures 6A**, **7A**.

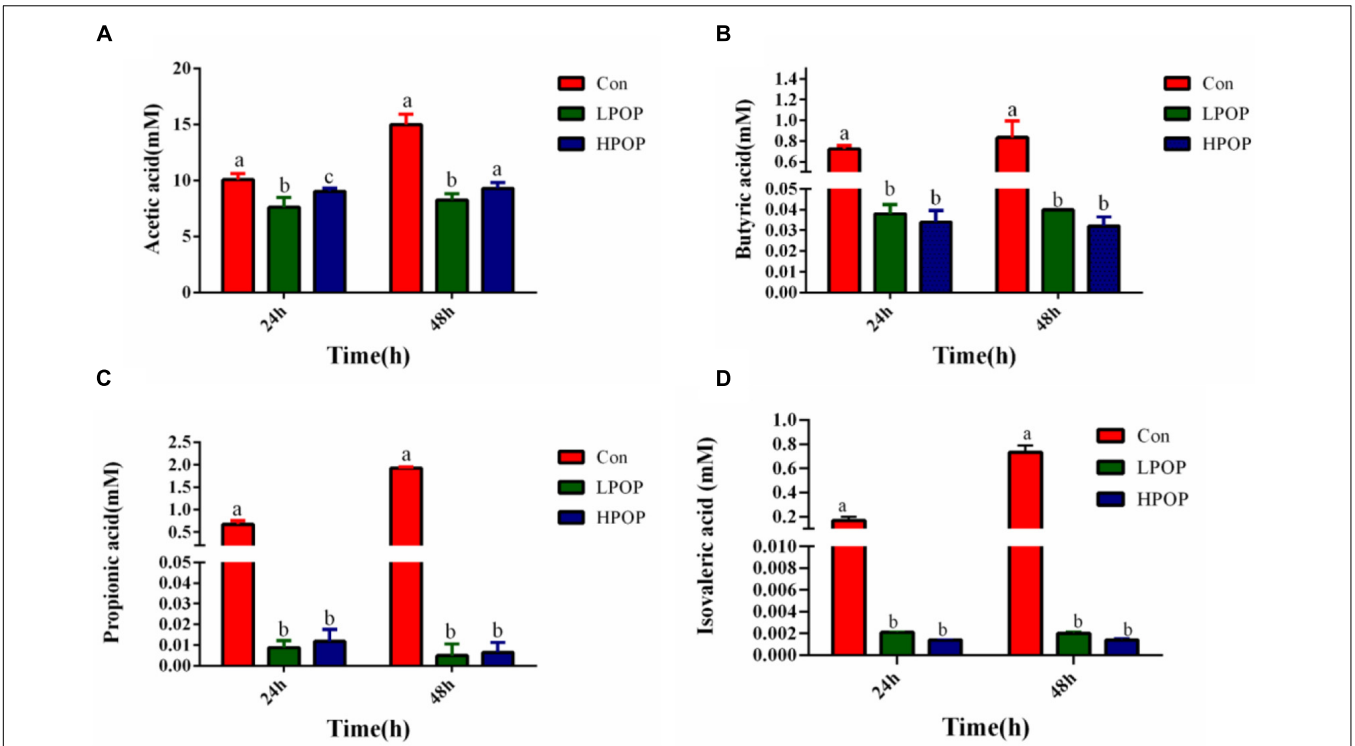

FIGURE 2 | Acetic acid **(A)**, butyric acid **(B)**, propionic acid **(C)**, and isovaleric acid **(D)** production after 24 and 48 h *in vitro* fecal fermentation of POP.

TABLE 1 | α-Diversity after 24 and 48 h *in vitro* fecal fermentation of POP.

Sample	Chao1	Observed-species	Shannon	Simpson	Goods-coverage	PD-whole-tree
Con1	762.89 ± 16.74^{a}	614.36 ± 25.81^{a}	3.21 ± 0.31^{a}	0.668 ± 0.074^{b}	0.9968 ± 0.0001^{a}	24.23 ± 0.84^{a}
LPOP1	576.20 ± 41.15^{b}	428.04 ± 36.33^{b}	2.68 ± 0.11^{b}	0.679 ± 0.042^{b}	0.9973 ± 0.0002^{b}	18.62 ± 1.56^{b}
HPOP1	538.11 ± 18.94^{b}	370.18 ± 40.07^{c}	3.06 ± 0.42^{ab}	0.778 ± 0.070^{a}	0.9975 ± 0.0001^{b}	16.51 ± 1.54^{c}
Con2	765.34 ± 45.08	620.08 ± 42.26	3.59 ± 0.12	0.711 ± 0.033	0.9971 ± 0.0001	23.97 ± 1.72
LPOP2	528.94 ± 64.93*	382.30 ± 48.16*	2.57 ± 0.11*	0.686 ± 0.012	0.9976 ± 0.0004*	16.82 ± 1.96*
HPOP2	529.33 ± 41.76*	371.58 ± 35.76*	2.64 ± 0.44*	0.705 ± 0.072	0.9976 ± 0.0002*	16.47 ± 1.55*

Values are mean ± SD.
*Significant ($p < 0.05$) differences among 24 h are indicated with different letters, *$p < 0.05$ means v Con2.*

After 24 h of fermentation, the relative abundance of *Bacilli–Lactobacillus*, *Eggerthella*, and *Firmicutes* in the LPOP1 group was significantly increased, and in the HPOP1 group, the relative abundance of other bacteria was also significantly increased. In addition, the *Escherichia–Shigella*, *Bacteroides*, *Clostridium sensu stricto* 13, *Enterobacter*, *Intestinimonas*, *Gardnerella*, *Proteus*, *Ruminococcus torques group*, *Eubacterium_nodatum group*, *Prevotella*, *Clostridium sensu stricto* 18, *Caldibacillus*, and *Eisenbergiella* in the Con1 group showed a significant increasing trend (**Figure 6A**). Furthermore, when the fermentation time was extended to 48 h, compared with the Con group, the relative abundance of *Bacilli–Lactobacillus* and *Firmicutes* in the LPOP2 group and *Paraprevotella* in the HPOP2 group showed a significant increasing trend. In the Con2 group, the relative abundance of several other phyla (i.e., *Escherichia–Shigella*, *Bacteroides*, *Parasutterella*, *Enterobacter*, *Veillonella*, *Clostridium sensu stricto* 13, *Marinobacter*, *Parabacteroides*, *Erysipelotrichaceae UCG-003*, *Ruminococcus_torques_group*, *Tyzzerella*, *Mobiluncus*, *Gardnerella*, and *Clostridium sensu stricto* 18) also significantly increased (**Figure 7A**).

Functional Properties Inherent to the Microbiomes Using Phylogenetic Investigation of Communities by Reconstruction of Unobserved States

Phylogenetic Investigation of Communities by Reconstruction of Unobserved States (PICRUSt) is designed to predict metagenome functional content from marker gene surveys and full genomes. The marker gene of 16s rRNA was used to amplify the subsequence to estimate the metabolomic function spectrum of a microbial community. According to the PICRUSt results, there were significant differences in metabolic potential between the Con and POP groups (**Figure 8**).

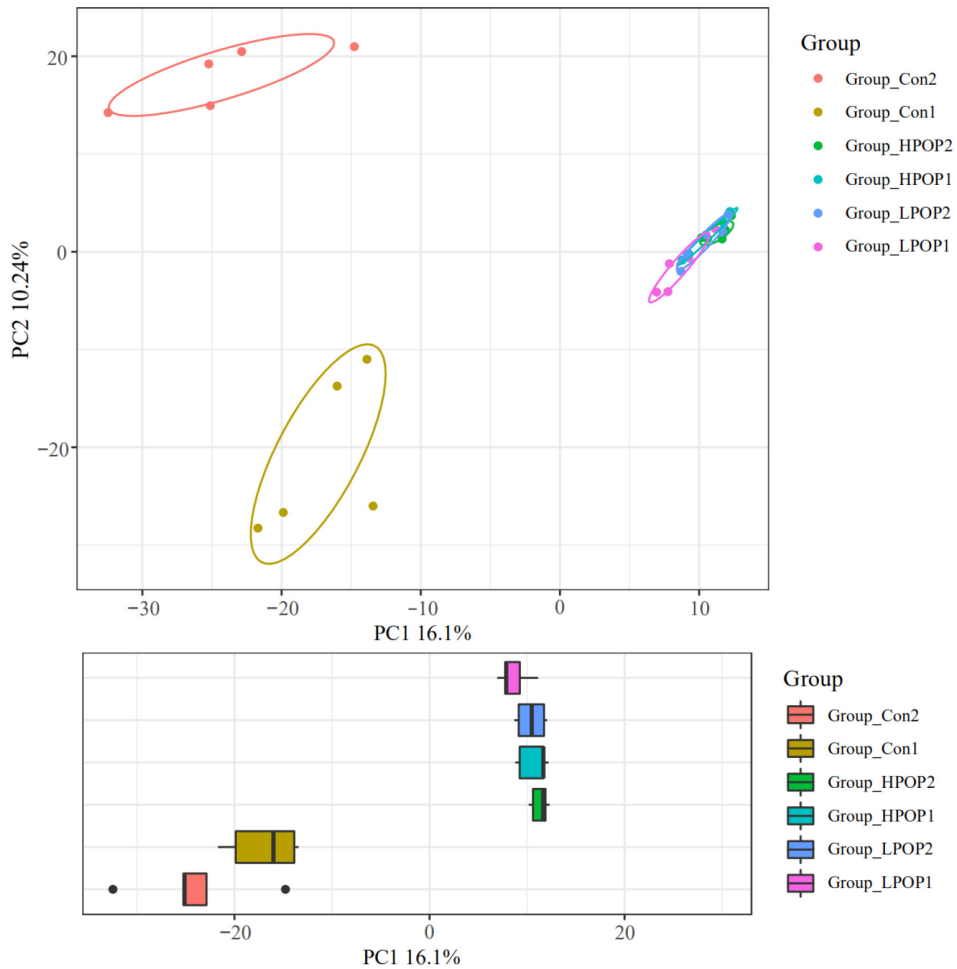

FIGURE 3 | Principal component analysis (PCA) of the microbial community composition after 24 and 48 h *in vitro* fecal fermentation with POP.

Compared with the POP-treated group, the Con groups showed an increasing trend in the expression of genes associated with environmental adaptation, xenobiotics biodegradation and metabolism, metabolism of cofactors and vitamins, metabolism of terpenoids and polyketides, lipid metabolism, metabolism of amino acids, carbohydrate metabolism, glycan biosynthesis and metabolism, energy metabolism, folding, sorting and degradation, transport and catabolism, cellular processes, signaling and metabolism, membrane transport, cell motility, biosynthesis of other secondary metabolites, cancers, metabolic diseases, cardiovascular diseases, neurodegenerative diseases, infectious diseases, circulatory system, digestive system, immune system, endocrine system, enzyme families, poorly characterized transcription, signal transduction, and genetic information processing. Conversely, the expression of genes involved in cell growth and death, translation, immune system diseases, signaling molecules, and interaction decreased.

Regarding fermentation time, in both LPOP1 and LPOP2 groups, genes of replication and repair, nucleotide metabolism, excretory system, nervous system, cell growth and death, translation, immune system diseases, xenobiotics biodegradation and metabolism, metabolism of cofactors, cell communication, and sensory system showed a noticeable change in expression level. The expression of genes for environmental adaptation, replication, and repair in the HPOP1 and HPOP2 groups was also significantly changed.

DISCUSSION

The gut microbiome plays a crucial role in human health (Gomaa, 2020). There is increasing evidence that natural products and their bioactive compounds have aroused interest in their diverse bioactivities (Kim and Kim, 2018; Xu et al., 2018). Polysaccharides are functional natural products that have been widely studied. Studies have shown that polysaccharides that are hard to digest can improve sugar metabolism and prevent diseases by altering the composition of the gut microbiome (Wang H. et al., 2018; Wang M. et al., 2018). Our results demonstrate that the pH values of fermentation cultures in the LPOP and HPOP groups are significantly lower than those in the Con group at 24 and 48 h of fermentation. The alteration in the

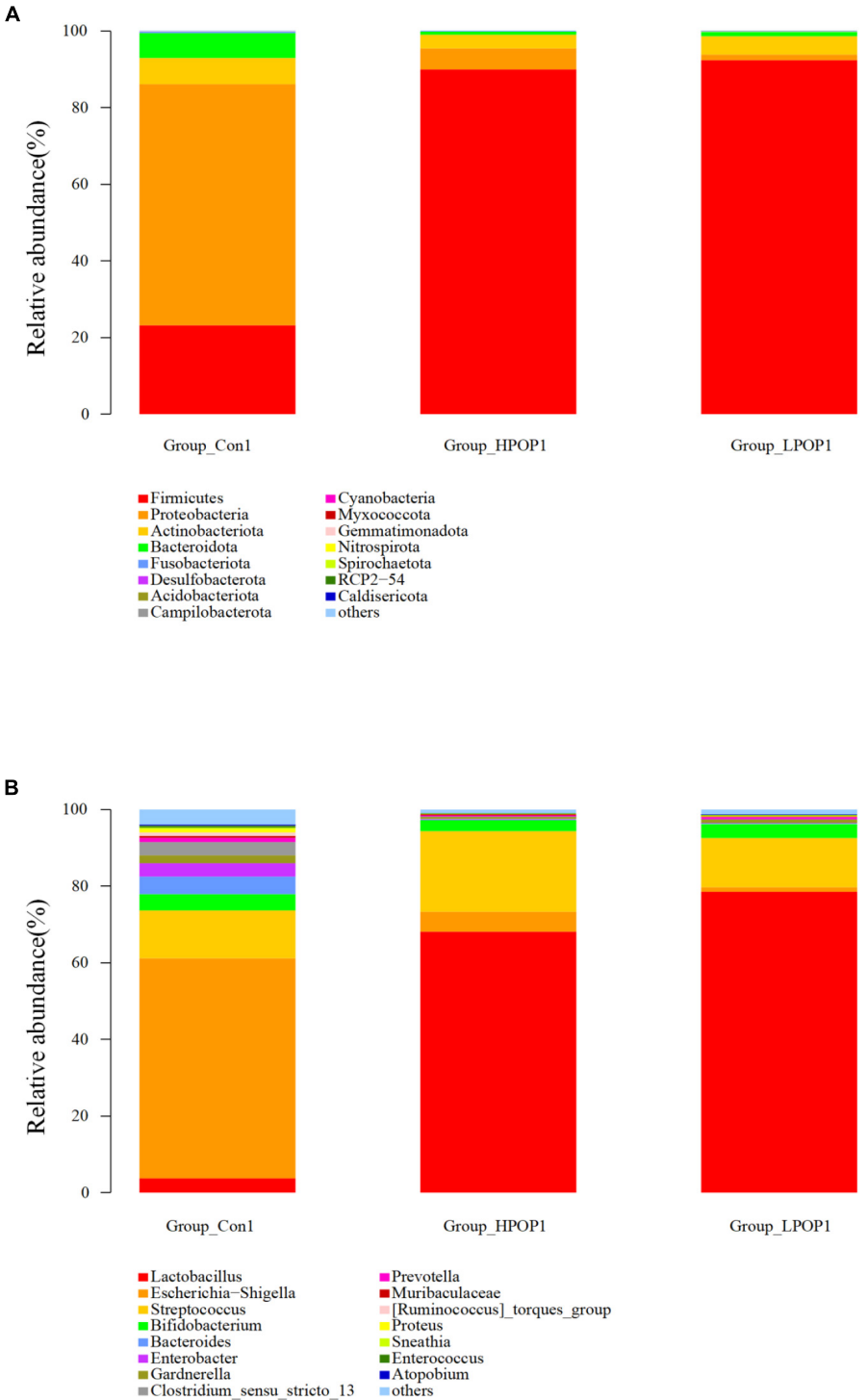

FIGURE 4 | Effects of POP on microbial composition of the fermentation (phylum and genus levels). Changes of microbiota composition at phylum **(A)** and genus **(B)** levels at 24 h *in vitro* fecal fermentation with POP.

pH value is an indicator of the rate of the fermentation reaction. Thus, POP can accelerate the speed of fermentation, which is consistent with changes in gas production in the fermentation system. At each time point, the gas production in the POP groups is significantly higher than that of the Con groups. Moreover, with the increase in polysaccharide concentration, gas production also significantly increased, which indicates that POP is a good carbon source. NH_3-N is a harmful metabolite generated by

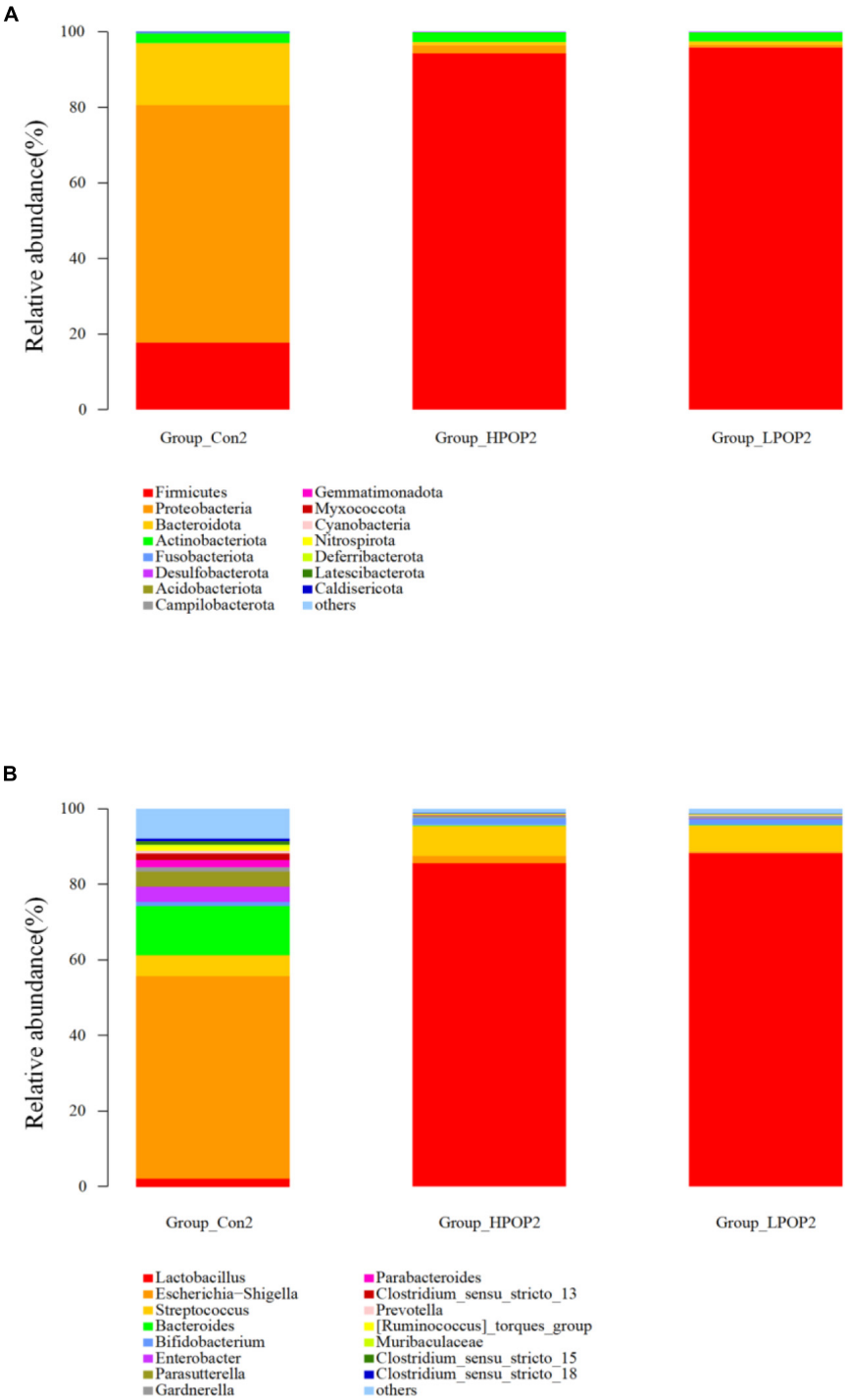

FIGURE 5 | Effects of POP on microbial composition of the fermentation (phylum and genus levels). Changes of microbiota composition at phylum **(A)** and genus **(B)** levels at 48 h *in vitro* fecal fermentation with POP.

intestinal flora. Excessive NH_3-N concentration leads to an increased ammonia metabolic load or ammonia poisoning (Luo et al., 2013). We found that NH_3-N levels reduced significantly in POP-treated groups, which indicates that POP has a positive role in NH_3-N emissions.

Furthermore, the α diversity and species richness of fecal flora decreased with POP fermentation at both low and high doses. Low α diversity may be associated with several processes, including efficient metabolism of POP, and/or increase in the relative abundance of the intestinal flora subgroup by POP

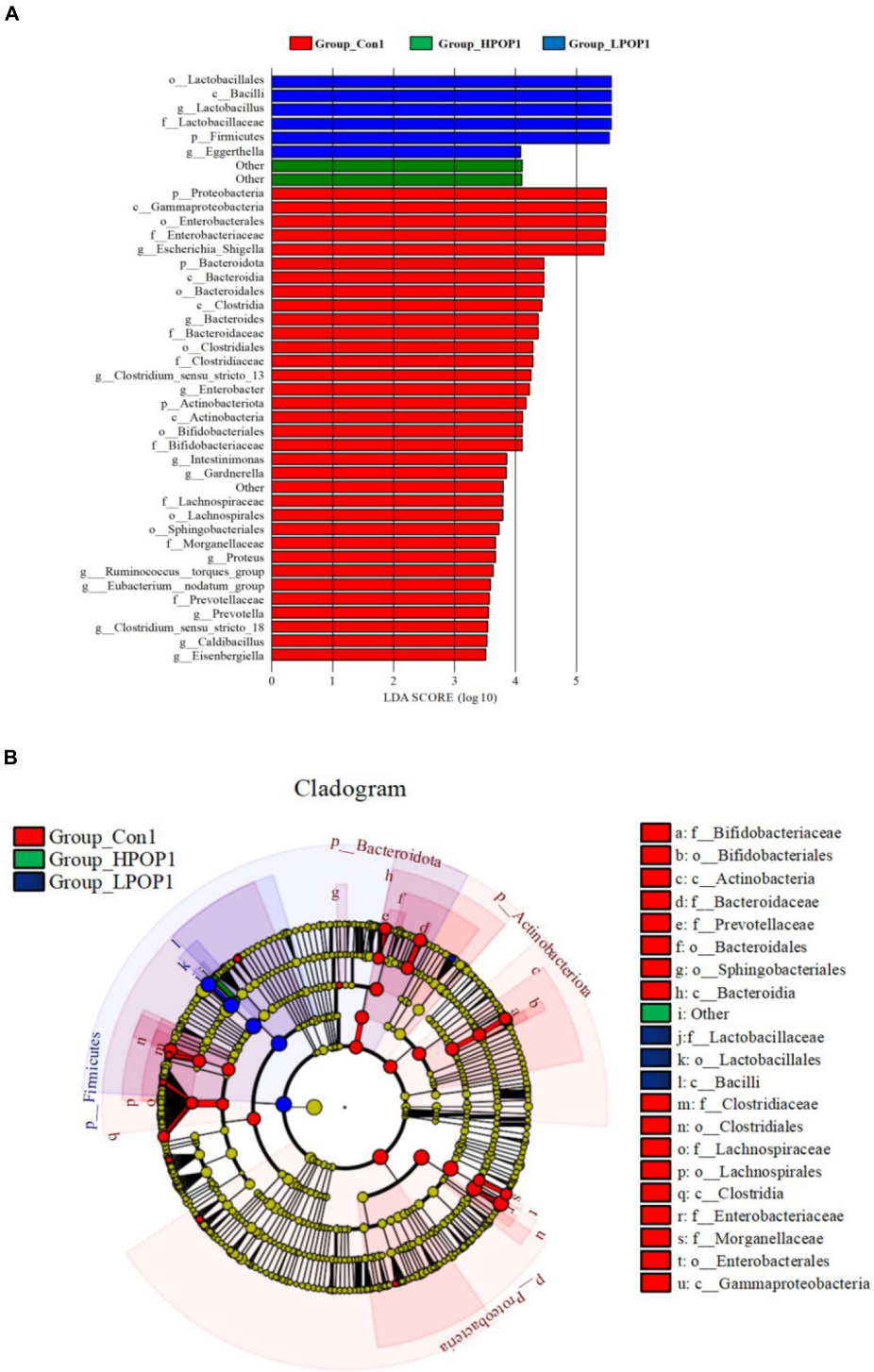

FIGURE 6 | LEfSe analysis showing the most differentially abundant taxa (LDA score >3.0) after 24 h *in vitro* fecal fermentation with POP. **(A)** Histogram of the LDA scores. **(B)** Taxonomic cladogram of all differentially abundant taxa across all taxonomic levels [from the inner to outer rings, phylum (p), class (c), order (o), family (f), and genus (g)].

degradation products, or suppression of the growth of flora that is sensitive to a low-pH environment (Duncan et al., 2009; Bendiks et al., 2020). With the decrease in overall microbial gene richness, the level of short-chain fatty acids in the POP groups decreased significantly. Compared with the Con groups, the yields of acetic acid, butyric acid, propionic acid, and isovaleric

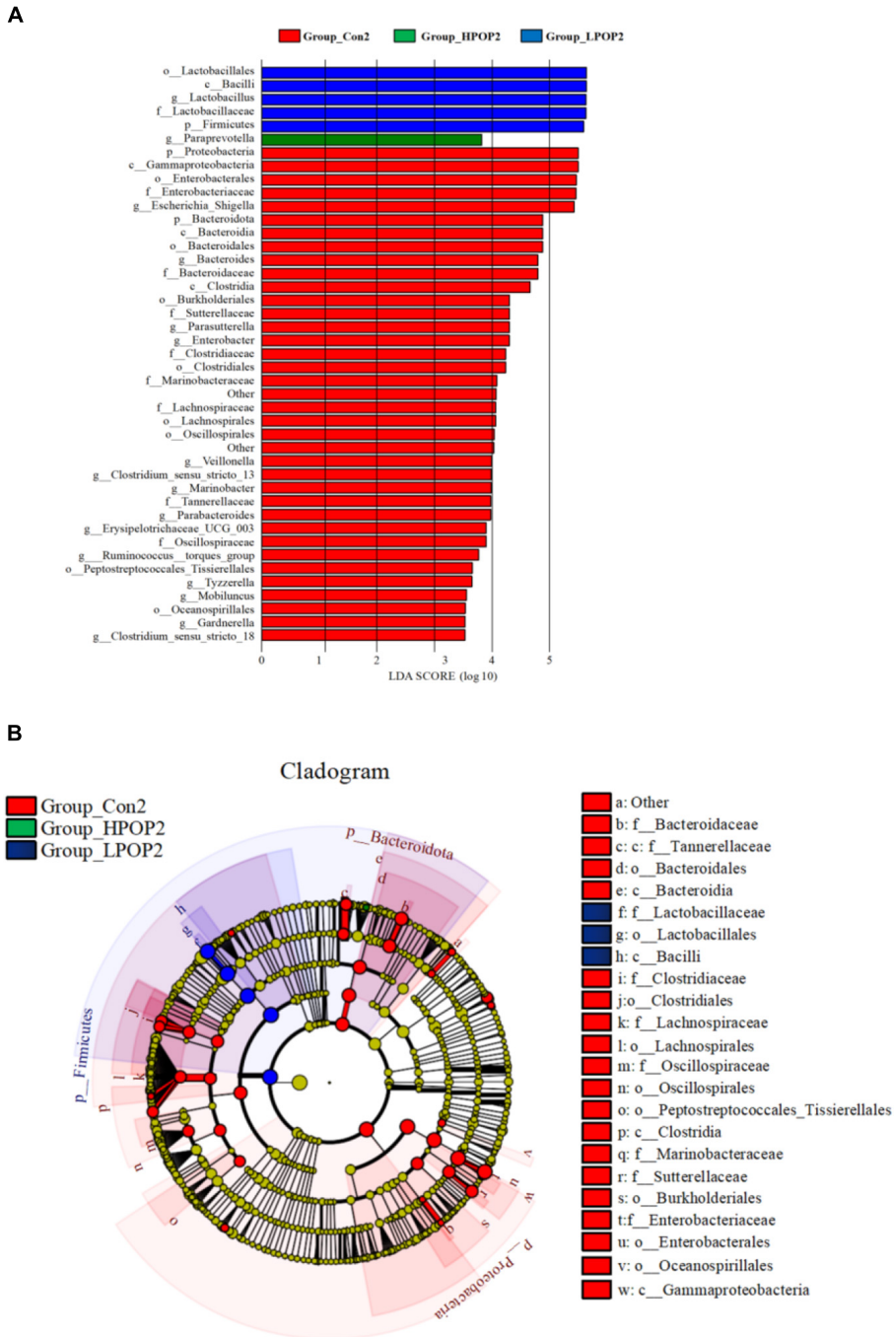

FIGURE 7 | LEfSe analysis showing the most differentially abundant taxa (LDA score >3.0) after 48 h *in vitro* fecal fermentation with POP. **(A)** Histogram of the LDA scores. **(B)** Taxonomic cladogram of all differentially abundant taxa across all taxonomic levels [from the inner to outer rings, phylum (p), class (c), order (o), family (f), and genus (g)].

acid in POP groups were also significantly reduced at 24 and 48 h of fermentation time. A recent study found that the yield of SCFAs increased significantly in the first 12 h of resistant starch fermentation then decreased in the following 12 h (Qin et al., 2021). Similar results were also observed in the *in vitro* fermentation of other forms of dietary fiber (Carlson et al., 2017). Thus, we infer that the increase in fermentation time and the rapid proliferation of bacteria in the POP group result in nutrient and short-chain fatty acid consumption.

Consistent with the structure of the main flora in the human intestinal tract, the four phyla of *Bacteroidetes*, *Firmicutes*, *Proteobacteria*, and *Actinobacteria* are the most important in

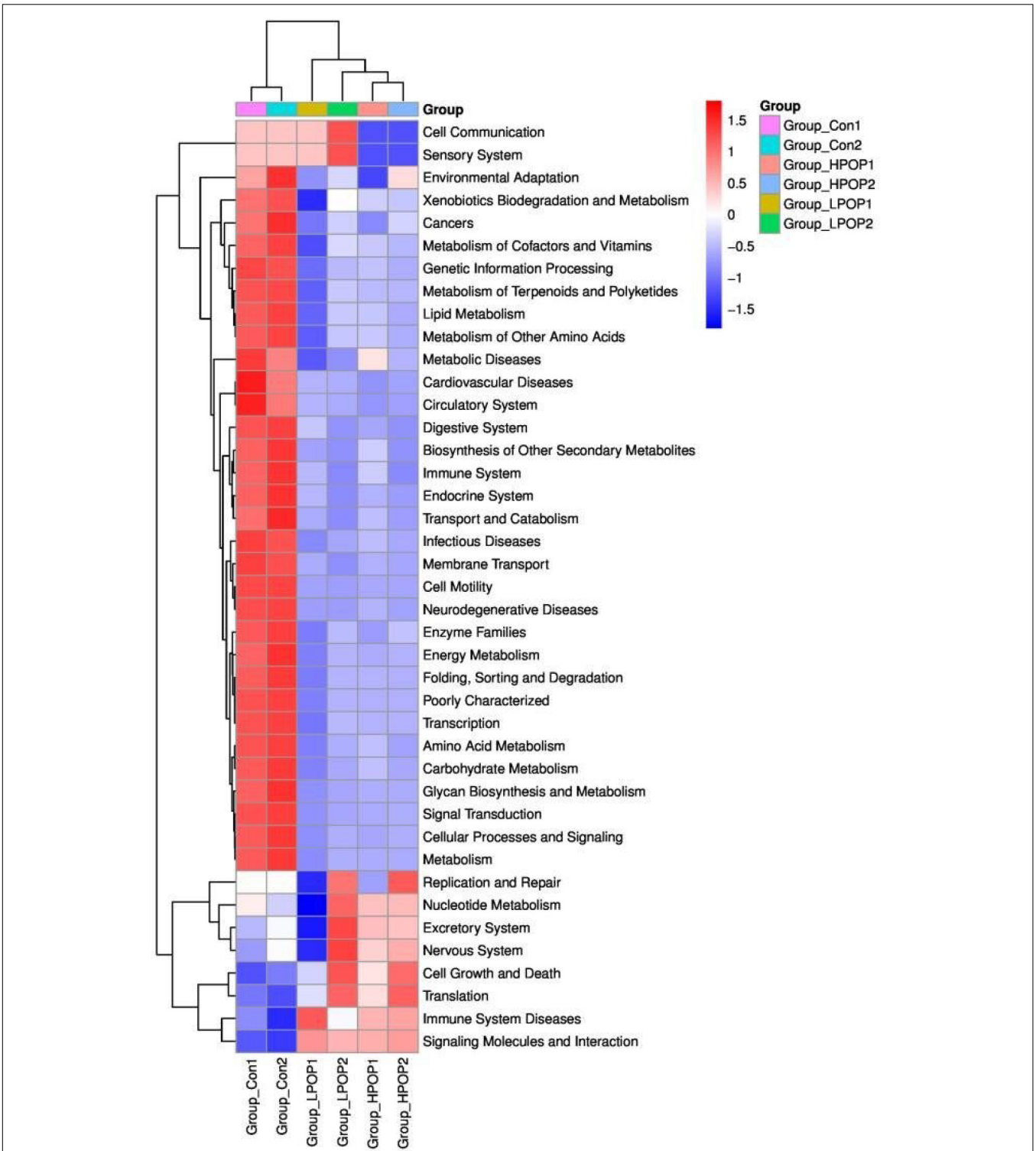

FIGURE 8 | The heatmap showing the PICRUSt-predicted KEGG ortholog (KO) functions among the Con1, Con2, LPOP1, LPOP2, HPOP1, and HPOP2 groups in *in vitro* fermentation.

the intestinal tract of elderly rats in this study (Simpson and Campbell, 2015; Binda et al., 2018). *Firmicutes* and *Bacteroidetes* account for more than 90% of the relative abundance of intestinal flora, and interactions between these two phyla are vital in maintaining intestinal homeostasis (Simpson and Campbell, 2015; Binda et al., 2018). Actinomycetes and Proteobacteria

account for the remaining 10% (Arumugam et al., 2011; Segata et al., 2012). *Firmicutes* are a phylum of gut microbiota and are composed of many different gram-positive bacteria. It is the main producer of butyrate in the gut and degrades indigestible polysaccharides. *Bacteroidetes* are mainly composed of gram-negative bacteria which are important in carbohydrate metabolism (Graf et al., 2015). *Proteobacteria* are composed of a variety of pathogenic bacteria, such as *Escherichia coli*, *Salmonella*, *Vibrio cholerae*, and *Helicobacter pylori*, which indicates a microecological disorder and is a potential diagnostic indicator of intestinal diseases (Shin et al., 2015; Rizzatti et al., 2017). Actinobacteria are mainly composed of gram-positive bacteria, including three major families of anaerobic bacteria (*Bifidobacteria*, *Propionibacteria*, and *Corynebacteria*) and one family of aerobic bacteria (*Streptomyces*) (Binda et al., 2018). Our present study demonstrates that POP treatment significantly promoted the relative abundance of *Firmicutes* while reducing the relative abundance of *Bacteroidetes*, *Actinobacteria*, and *Proteobacteria*, among which *Proteobacteria* showed the most significant decrease. These data suggest that POP can regulate the composition and function of intestinal flora by affecting the abundance of Firmicutes, which is consistent with the findings on the effects of POP on intestinal flora in weaned rats in our previous study.

To identify the specific microflora associated with POP effects, LEfSe analysis with a standard LDA score >3.0 was used to compare the microflora composition after 24 and 48 h of fermentation, to determine the group characteristics of microorganisms in each fermentative substrate. In contrast, the abundance of *Lactobacillus* dominated in the POP groups, while *Escherichia–Shigella* accounted for a high proportion in the Con groups. *Lactobacillus* belongs to the *Firmicutes* phylum, *Bacilli* class, and *Lactobacillus* family, acting as an essential regulator of homeostasis in the intestinal tract (O'Callaghan and O'Toole, 2013). It has an important role in reducing cholesterol, inhibiting the proliferation of harmful intestinal bacteria, promoting immunity, and facilitating the absorption of minerals and energy conversion (Shinohara et al., 2010; Pessione, 2012). *Paraprevotella*, a gram-negative anaerobe, was found to be significantly reduced in primary hypothyroidism patients (Su et al., 2020). Other studies have reported a high abundance of *Paraprevotella* and *Eggerthella* in patients with depression and an increased abundance of pro-inflammatory *Escherichia–Shigella* in patients with cognitive impairment and brain amyloidosis (Barandouzi et al., 2020). Likewise, our results show that POP can promote probiotic Lactobacillus in the intestinal flora of elderly rats and inhibit the reproduction of pro-inflammatory *Escherichia–Shigella*, which suggest that the intake of POP may be beneficial to the health of aging individuals.

The results from the PICRUSt analysis also reveal that after 48 h of fermentation, the proportion of genes associated with replication and repair, cell growth and death, translation, nucleotide metabolism, and excretory and nervous systems is relatively high. There is probably a connection with the increased relative abundance of *Firmicutes*, which metabolize starch, galactose, and butyric acid, especially with low-dose POP. However, the expression of genes associated with infectious diseases, metabolic diseases, cardiovascular diseases, cancers, and neurodegenerative diseases in the Con groups was significantly higher than that in the POP groups, which is consistent with the results that *Escherichia–Shigella* was the dominant flora in the Con groups.

CONCLUSION

Firmicutes, *Bacteroidetes*, *Proteobacteria*, and *Actinobacteriota* are the main phyla of gut microbiota in elderly rats. However, the diversity and composition of rat gut microbiota are significantly altered after POP treatment. The intake of POP reduces the pH and NH_3-N levels of fermentation substrates and consumes more short-chain fatty acids, which in turn promotes probiotics such as Lactobacillus and inhibits colonization of pathogenic bacteria such as *Escherichia–Shigella*.

This study provides new insights into the potential use of POP as a bioactive ingredient to maintain intestinal microbiota in a balanced state. Further studies should be conducted to investigate the potential physiological effects of POP fermentation on colon microecological health.

DATA AVAILABILITY STATEMENT

The datasets presented in this study can be found in online repositories. The names of the repository/repositories and accession number(s) can be found below: https://www.ncbi.nlm.nih.gov/, PRJNA789821.

ETHICS STATEMENT

The animal study was reviewed and approved by the Committee on the Ethics of Animal Experiments of the Jinggangshan University.

AUTHOR CONTRIBUTIONS

QF and XH conceived, designed the experiment, and drafted the manuscript. SZ, MY, and YL performed the experiments and collected the data. GH, XH, and YH provided resources and reviewed the manuscript. All authors contributed to the article and approved the submitted version.

FUNDING

This work was supported by grants from the National Natural Science Foundation of China (31860711 and 41867032), the Key Projects of Ji'an Science and Technology Bureau (JCJZ2020-83) and the Local Service Project of Jinggangshan University (JFD202108 and JFD202107), the Science and Technology Foundation of Jiangxi Education Department (GJJ211006 and GJJ201509).

REFERENCES

Arumugam, M., Raes, J., Pelletier, E., Le Paslier, D., Yamada, T., Mende, D. R., et al. (2011). Enterotypes of the human gut microbiome. *Nature* 473, 174–180.

Barandouzi, Z. A., Starkweather, A. R., Henderson, W. A., Gyamfi, A., and Cong, X. S. (2020). Altered Composition of Gut Microbiota in Depression: a Systematic Review. *Front. Psychiatry* 11:541. doi: 10.3389/fpsyt.2020.00541

Bendiks, Z. A., Knudsen, K. E. B., Keenan, M. J., and Marco, M. L. (2020). Conserved and variable responses of the gut microbiome to resistant starch type 2. *Nutr. Res.* 77, 12–28. doi: 10.1016/j.nutres.2020.02.009

Binda, C., Lopetuso, L. R., Rizzatti, G., Gibiino, G., Cennamo, V., and Gasbarrini, A. (2018). Actinobacteria: a relevant minority for the maintenance of gut homeostasis. *Dig. Liver Dis.* 50, 421–428. doi: 10.1016/j.dld.2018.02.012

Bolger, A. M., Lohse, M., and Usadel, B. (2014). Trimmomatic: a flexible trimmer for Illumina sequence data. *Bioinformatics* 30, 2114–2120. doi: 10.1093/bioinformatics/btu170

Caporaso, J. G., Kuczynski, J., Stombaugh, J., Bittinger, K., Bushman, F. D., Costello, E. K., et al. (2010). QIIME allows analysis of high-throughput community sequencing data. *Nat. Methods* 7, 335–336. doi: 10.1038/nmeth.f.303

Carlson, J. L., Erickson, J. M., Hess, J. M., Gould, T. J., and Slavin, J. L. (2017). Prebiotic Dietary Fiber and Gut Health: comparing the in Vitro Fermentations of Beta-Glucan. Inulin and Xylooligosaccharide. *Nutrients* 9:1361. doi: 10.3390/nu9121361

Chu, C.-Q., Yu, L.-l., Chen, W., Tian, F.-W., and Zhai, Q.-X. (2021). Dietary patterns affect Parkinson's disease via the microbiota-gut-brain axis. *Trends Food Sci. Technol.* 116, 90–101. doi: 10.3748/wjg.v21.i37.10609

Dong, C. X., Hayashi, K., Lee, J. B., and Hayashi, T. (2010). Characterization of structures and antiviral effects of polysaccharides from Portulaca oleracea L. *Chem. Pharm. Bull.* 58, 507–510. doi: 10.1248/cpb.58.507

Duncan, S. H., Louis, P., Thomson, J. M., and Flint, H. J. (2009). The role of pH in determining the species composition of the human colonic microbiota. *Environ. Microbiol.* 11, 2112–2122. doi: 10.1111/j.1462-2920.2009.01931.x

Fang, Q., Hu, J., Nie, Q., and Nie, S. (2019). Effects of polysaccharides on glycometabolism based on gut microbiota alteration. *Trends Food Sci. Technol.* 92, 65–70. doi: 10.3389/fimmu.2020.588079

Ghosh, S., Dai, C., Brown, K., Rajendiran, E., Makarenko, S., Baker, J., et al. (2011). Colonic microbiota alters host susceptibility to infectious colitis by modulating inflammation, redox status, and ion transporter gene expression. *Am. J. Physiol. Gastrointest. Liver. Physiol.* 301, G39–G49. doi: 10.1152/ajpgi.00509.2010

Gomaa, E. Z. (2020). Human gut microbiota/microbiome in health and diseases: a review. *Antonie Van Leeuwenhoek* 113, 2019–2040. doi: 10.1007/s10482-020-01474-7

Graf, D., Di Cagno, R., Fak, F., Flint, H. J., Nyman, M., Saarela, M., et al. (2015). Contribution of diet to the composition of the human gut microbiota. *Microb. Ecol. Health Dis.* 26:26164. doi: 10.3402/mehd.v26.26164

Hu, Q., Li, Y., Liu, C., Huang, L. P., Zeng, L., Wang, S., et al. (2018). Effects of polysaccharide from Portulaca oleracea L. on voltage-gated Na(+) channel of INS-1 cells. *Biomed. Pharmacother.* 101, 572–578. doi: 10.1016/j.biopha.2018.02.136

Huang, X., Luo, H., Huang, Y., Xu, D., Deng, X., and Wang, W. (2021). Effects of Portulacea oleracea L. Polysaccharide on Intestinal Flora in Weaned Rats. *Chin. J. Anim. Nutr.* 33, 4694–4707.

Iranshahy, M., Javadi, B., Iranshahi, M., Jahanbakhsh, S. P., Mahyari, S., Hassani, F. V., et al. (2017). A review of traditional uses, phytochemistry and pharmacology of Portulaca oleracea L. *J. Ethnopharmacol.* 205, 158–172. doi: 10.1016/j.jep.2017.05.004

Kim, C., and Kim, B. (2018). Anti-Cancer Natural Products and Their Bioactive Compounds Inducing ER Stress-Mediated Apoptosis: a Review. *Nutrients* 10:1021. doi: 10.3390/nu10081021

Lee, H., Lee, Y., Kim, J., An, J., Lee, S., Kong, H., et al. (2018). Modulation of the gut microbiota by metformin improves metabolic profiles in aged obese mice. *Gut Microbes* 9, 155–165. doi: 10.1080/19490976.2017.1405209

Luo, X., Cai, L., Ruan, Z., Huang, X., Liu, S., and OuoYang, C. (2013). Fermentation Characteristics of Four Kinds Foodstuff in Vitro. *Food Res. Dev.* 34, 4–8.

Mandalari, G., Nueno-Palop, C., Bisignano, G., Wickham, M. S., and Narbad, A. (2008). Potential prebiotic properties of almond (Amygdalus communis L.) seeds. *Appl. Environ. Microbiol.* 74, 4264–4270. doi: 10.1128/AEM.00739-08

Mangiola, F., Nicoletti, A., Gasbarrini, A., and Ponziani, F. R. (2018). Gut microbiota and aging. *Eur. Rev. Med. Pharmacol. Sci.* 22, 7404–7413.

Miao, L., Tao, H., Peng, Y., Wang, S., Zhong, Z., El-Seedi, H., et al. (2019). The anti-inflammatory potential of Portulaca oleracea L. (purslane) extract by partial suppression on NF-kappaB and MAPK activation. *Food. Chem.* 290, 239–245. doi: 10.1016/j.foodchem.2019.04.005

O'Callaghan, A., and van Sinderen, D. (2016). Bifidobacteria and Their Role as Members of the Human Gut Microbiota. *Front. Microbiol.* 7:925. doi: 10.3389/fmicb.2016.00925

O'Callaghan, J., and O'Toole, P. W. (2013). Lactobacillus: host-microbe relationships. *Curr. Top. Microbiol. Immunol.* 358, 119–154.

Pessione, E. (2012). Lactic acid bacteria contribution to gut microbiota complexity: lights and shadows. *Front. Cell. Infect. Microbiol.* 2:86. doi: 10.3389/fcimb.2012.00086

Qin, R., Wang, J., Chao, C., Yu, J., Copeland, L., Wang, S., et al. (2021). RS5 Produced More Butyric Acid through Regulating the Microbial Community of Human Gut Microbiota. *J. Agric. Food Chem.* 69, 3209–3218. doi: 10.1021/acs.jafc.0c08187

Reyon, D., Tsai, S. Q., Khayter, C., Foden, J. A., Sander, J. D., and Joung, J. K. (2012). FLASH assembly of TALENs for high-throughput genome editing. *Nat. Biotechnol.* 30, 460–465. doi: 10.1038/nbt.2170

Rizzatti, G., Lopetuso, L. R., Gibiino, G., Binda, C., and Gasbarrini, A. (2017). *Proteobacteria*: a Common Factor in Human Diseases. *Biomed. Res. Int.* 2017:9351507. doi: 10.1155/2017/9351507

Rognes, T., Flouri, T., Nichols, B., Quince, C., and Mahe, F. (2016). VSEARCH: a versatile open source tool for metagenomics. *PeerJ.* 4:e2584. doi: 10.7717/peerj.2584

Salazar, N., Gonzalez, S., Nogacka, A. M., Rios-Covian, D., Arboleya, S., Gueimonde, M., et al. (2020). Microbiome: effects of Ageing and Diet. *Curr. Issues Mol. Biol.* 36, 33–62. doi: 10.21775/cimb.036.033

Segata, N., Haake, S. K., Mannon, P., Lemon, K. P., Waldron, L., Gevers, D., et al. (2012). Composition of the adult digestive tract bacterial microbiome based on seven mouth surfaces, tonsils, throat and stool samples. *Genome Biol.* 13:R42. doi: 10.1186/gb-2012-13-6-r42

Shin, N. R., Whon, T. W., and Bae, J. W. (2015). *Proteobacteria*: microbial signature of dysbiosis in gut microbiota. *Trends Biotechnol.* 33, 496–503. doi: 10.1016/j.tibtech.2015.06.011

Shinohara, K., Ohashi, Y., Kawasumi, K., Terada, A., and Fujisawa, T. (2010). Effect of apple intake on fecal microbiota and metabolites in humans. *Anaerobe* 16, 510–515. doi: 10.1016/j.anaerobe.2010.03.005

Simpson, H. L., and Campbell, B. J. (2015). Review article: dietary fibre-microbiota interactions. *Aliment Pharmacol. Ther.* 42, 158–179. doi: 10.1111/apt.13248

Su, X., Zhao, Y., Li, Y., Ma, S., and Wang, Z. (2020). Gut dysbiosis is associated with primary hypothyroidism with interaction on gut-thyroid axis. *Clin. Sci.* 134, 1521–1535. doi: 10.1042/CS20200475

Vemuri, R. C., Gundamaraju, R., Shinde, T., and Eri, R. (2017). Therapeutic interventions for gut dysbiosis and related disorders in the elderly: antibiotics, probiotics or faecal microbiota transplantation? *Benef. Microbes* 8, 179–192. doi: 10.3920/BM2016.0115

Wang, H., Zhang, X., Wang, S., Li, H., Lu, Z., Shi, J., et al. (2018). Mannan-oligosaccharide modulates the obesity and gut microbiota in high-fat diet-fed mice. *Food Funct.* 9, 3916–3929. doi: 10.1039/c8fo00209f

Wang, M., Chen, Y., Wang, Y., Li, Y., Zheng, H., Ma, F., et al. (2018). The effect of probiotics and polysaccharides on the gut microbiota composition and function of weaned rats. *Food Funct.* 9, 1864–1877. doi: 10.1039/c7fo01507k

Wang, Q., Garrity, G. M., Tiedje, J. M., and Cole, J. R. (2007). Naive Bayesian classifier for rapid assignment of rRNA sequences into the new bacterial taxonomy. *Appl. Environ. Microbiol.* 73, 5261–5267. doi: 10.1128/AEM.00062-07

Xu, L., Li, Y., Dai, Y., and Peng, J. (2018). Natural products for the treatment of type 2 diabetes mellitus: pharmacology and mechanisms. *Pharmacol. Res.* 130, 451–465. doi: 10.1016/j.phrs.2018.01.015

Yu, M., Jia, H. M., Zhou, C., Yang, Y., Sun, L. L., and Zou, Z. M. (2017). Urinary and Fecal Metabonomics Study of the Protective Effect of Chaihu-Shu-Gan-San on Antibiotic-Induced Gut Microbiota Dysbiosis in Rats. *Sci. Rep.* 7:46551. doi: 10.1038/srep46551

Zhou, B., Yuan, Y., Zhang, S., Guo, C., Li, X., Li, G., et al. (2020). Intestinal Flora and Disease Mutually Shape the Regional Immune System in the Intestinal Tract. *Front. Immunol.* 11:575. doi: 10.3389/fimmu.2020.00575

Zhou, Y. X., Xin, H. L., Rahman, K., Wang, S. J., Peng, C., and Zhang, H. (2015). Portulaca oleracea L.: a review of phytochemistry and pharmacological effects. *Biomed. Res. Int.* 2015:925631. doi: 10.1155/2015/925631

Zhu, K., Fan, H., Zeng, S., Nie, S., Zhang, Y., Tan, L., et al. (2021). Polysaccharide from Artocarpus heterophyllus Lam. (jackfruit) pulp modulates gut microbiota composition and improves short-chain fatty acids production. *Food Chem.* 364:130434. doi: 10.1016/j.foodchem.2021.130434

Zimmer, J., Lange, B., Frick, J. S., Sauer, H., Zimmermann, K., Schwiertz, A., et al. (2012). A vegan or vegetarian diet substantially alters the human colonic faecal microbiota. *Eur. J. Clin. Nutr.* 66, 53–60. doi: 10.1038/ejcn.2011.141

Conflict of Interest: The authors declare that the research was conducted in the absence of any commercial or financial relationships that could be construed as a potential conflict of interest.

Publisher's Note: All claims expressed in this article are solely those of the authors and do not necessarily represent those of their affiliated organizations, or those of the publisher, the editors and the reviewers. Any product that may be evaluated in this article, or claim that may be made by its manufacturer, is not guaranteed or endorsed by the publisher.

frontiers in Microbiology

ORIGINAL RESEARCH
published: 10 March 2022
doi: 10.3389/fmicb.2022.865396

Scorias spongiosa Polysaccharides Promote the Antioxidant and Anti-Inflammatory Capacity and Its Effect on Intestinal Microbiota in Mice

*Yingyin Xu[1,2,3], Zhiyuan Zhang[1,2,3], Huiyu Feng[4], Jie Tang[1,2,3], Weihong Peng[1,2,3], Ying Chen[1,2,3], Jie Zhou[1,2,3] and Yong Wang[1,2,3]**

[1]Sichuan Institute of Edible Fungi, Chengdu, China, [2]National-Local Joint Engineering Laboratory of Breeding and Cultivation of Edible and Medicinal Fungi, Chengdu, China, [3]Scientific Observing and Experimental Station of Agro-microbial Resource and Utilization in Southwest China, Ministry of Agriculture, Chengdu, China, [4]College of Food and Biological Engineering, Chengdu University, Chengdu, China

OPEN ACCESS

Edited by:
Zheng Ruan,
Nanchang University, China

Reviewed by:
Xueran Geng,
Shanxi Agricultural University, China
Jinyan Zhang,
Huazhong Agricultural University, China
Cheng Zhang,
Anhui Agricultural University, China

***Correspondence:**
Yong Wang
yongwang3729@163.com

Specialty section:
This article was submitted to Food Microbiology, a section of the journal Frontiers in Microbiology

Received: *29 January 2022*
Accepted: *21 February 2022*
Published: *10 March 2022*

Citation:
Xu Y, Zhang Z, Feng H, Tang J, Peng W, Chen Y, Zhou J and Wang Y (2022) Scorias spongiosa Polysaccharides Promote the Antioxidant and Anti-Inflammatory Capacity and Its Effect on Intestinal Microbiota in Mice. Front. Microbiol. 13:865396. doi: 10.3389/fmicb.2022.865396

Scorias spongiosa, as an edible fungus, has multiple health benefits. However, the effects of *S. spongiosa* on intestinal health are rarely explored. Hence, our study aims to elaborate on the influences of *S. spongiosa* polysaccharides (SSPs) on antioxidant, anti-inflammatory, and intestinal microflora in C57BL/6J mice. In the present study, 18 male mice were randomly distributed into three groups: (1) Control group (CON); (2) Low dose SSPs group (LSSP); (3) High dose SSPs group (HSSP). After 14-day administration, the jejunum and serum samples were collected for detection. The results showed that SSPs exert no effects on the growth performance of mice regardless of doses. Meanwhile, SSPs administration reduced the serum pro-inflammatory cytokines and elevated the anti-inflammatory cytokines. Moreover, the antioxidant capacity was elevated by SSPs administration, as evidenced by the increased contents of T-AOC, GSH-Px, and the decreased content of MDA. Mechanistically, the administration of SSPs enhanced the protein abundances of p-Nrf2, Keap1, and HO-1 in mice. The results of 16S rDNA demonstrated that the microbial community and composition were altered by SSPs administration. To summarize, SSPs benefit intestinal health in C57BL/6J mice *via* a mechanism that involves elevating antioxidant and anti-inflammatory activities and regulating intestinal microbiota.

Keywords: ***Scorias spongiosa*** **polysaccharides, antioxidant, anti-inflammatory, intestinal microbiota, mice**

INTRODUCTION

The intestinal microbiota is considered to be a dynamic organ that plays an important role in maintaining host health, which includes Firmicutes, Bacteroidetes, Actinobacteria, Fusobacteria, and so on (Cheng et al., 2020; Wu et al., 2022). The microbiota can regulate the proliferation and differentiation of intestinal epithelial cells (IECs) and be conducive

to intestinal absorption of digestible nutrients (Lin et al., 2021; Chen et al., 2021a). Moreover, intestinal flora can promote the secretion of SIgA, a very important immunoglobulin in intestinal mucosal immunity, to prevent bacterial adhesion and invasion and to maintain the integrity of the intestinal mucosal layer (Bain and Cerovic, 2020). However, studies have indicated that the disturbance of intestinal microbiota may participate in the process of disease development, such as diabetes mellitus (DM), obesity, inflammatory bowel disease (IBD), cardiovascular disease (CVD), tumor, and mental diseases (Dong et al., 2019; Villeger et al., 2019; Alvarez-Vieites et al., 2020; Suslov et al., 2021). Therefore, finding effective natural bioactive ingredients to keep the balance of intestinal microbiota is of utmost interest.

The edible basidiomycete *Scorias spongiosa*, which belongs to the genus *Scorias Fr.*, (1825), was discovered by He in 2011 and is considered as a new record species after a pure culture experiment and internal transcribed spacer (ITS) sequence analysis (Zhong et al., 2020). *Scorias spongiosa* polysaccharides (SSPs), a chemical bioactive compound, were secreted through various stimulating agents, such as surfactants and organic solvents (Wu et al., 2018). Due to the large multitude of pharmacological activities of polysaccharides, studies have revealed that polysaccharides from natural plants have multiple effects including antioxidation, anti-inflammation, antitumor, bacteriostatic, and immune regulation (Mei et al., 2020; Wang and Liu, 2020; Ye et al., 2021; Chen et al., 2021b). However, the effect of the SSPs in alleviating gut dysbiosis has not been explored. Especially, How SSPs alter and reshape the gut microbiota remain unknown.

In the present study, we concentrated on the anti-oxidative and anti-inflammatory effects of SSPs in mice and evaluated the intestinal microbiota by 16S rDNA.

MATERIALS AND METHODS

Animals

Male C57BL/6J mice (aged 6–7 weeks, weighing 21–25 g) were purchased from Chengdu Dashuo Laboratory Animal. Animals were housed in groups of six mice with a temperature (22°C ± 3°C), humidity (55% ± 15%), and lighting (12 h light/dark cycle) with *ad libitum* access to food and water. All animals must adapt to conditions for at least 7 days after they arrived. All experimental procedures were approved by the Animal Care and Use Committee of the Sichuan Academy of Agricultural Sciences (Chengdu, China) and were conducted following the academy's animal experiment guidelines.

Experimental Design and SSPs Administration

In a 14-day experiment, 18 mice were randomly distributed into three treatment groups with six individuals per group: (1) Control group (CON), gavaged with saline once a day; (2) Low dose SSPs group (LSSP), gavaged with 200 uL SSPs once a day; (3) High dose SSPs group (HSSP), gavaged with 400 uL SSPs once a day. At the end of the experiment, all mice were sacrificed *via* anesthesia using pentobarbital sodium to collect the samples for subsequent determination.

Enzyme-Linked Immunosorbent Assay

The interleukin-1β (IL-1β), IL-6, IL-10, tumor necrosis factor-α (TNF-α), and interferon-gamma (IFN-γ) in serum and glutathione peroxidase (GSH-Px), superoxide dismutase (SOD), malondialdehyde (MDA), and total antioxidant capacity (T-AOC) contents were determined using spectrophotometric kits according to the manufacturer's instructions (Nanjing Jiancheng Bioengineering Institute, China).

Western Blotting

Frozen jejunal samples (approximately 0.1 g) were homogenized using 1 ml RIPA buffer. Following this, ultrasonication was performed to break the cells. The lysates were then centrifuged at 10,000 rcf for 20 min at 4°C. The proteins in the supernatant were diluted with 4× Laemmli sample buffer (Bio-RAD, United States) and denatured in a 98°C metal bath for 10 min. Equal amounts of samples were then subjected to SDS-PAGE, and the abundances of phospho-nuclear factor-E2-related factor 2 (p-Nrf2; Catalog#EP1809Y, Abcam), heme oxygenase-1 (HO-1; Catalog#10701-1-AP, Proteintech), Kelch-like ECH-associated protein 1 (Keap1; Catalog#8047S, Cell Signaling Technology) and GAPDH (Catalog#60004-1-Ig, Proteintech) proteins were assessed by western blot using the indicated antibodies. The expression level of GAPDH was assessed to ensure equal protein sample loading.

Gut Microbiota Analysis

Samples of the mice's intestinal contents were collected immediately after sacrifice. The cetyltrimethylammonium bromide/sodium dodecyl sulfate extraction method was employed to obtain the total DNA from the intestinal content. The extracted DNA was subjected to 16S amplification using primers designed to incorporate both the Illumina adapters and a sample barcode sequence, allowing directional sequencing that covers the variable region V4 (primers: 515 F [GTGCCAGCMGCCGCGGTAA] and 806 R [GGACTACHVGGGTWTCTAAT]). Phusion® High-Fidelity PCR Master Mix (New England Biolabs, United States) was used for the PCR reactions.

Sequencing libraries were produced using an Ion Plus Fragment Library Kit 48 rxns (Thermo Scientific, United States) according to the manufacturer's recommendations. Libraries were sequenced on an Ion S5TM XL platform and 400/600 bp single-end reads were generated. The data were based on sequenced reads and operational taxonomic units (OTUs). UPARSE software (v7.0.1001) was used to carry out the analysis. Sequences that have similarities ≥97% are regarded as the same OTUs. The Silva database was employed to annotate the taxonomic information based on the Mothur algorithm (Xu et al., 2021b).[1]

[1]https://www.arb-silva.de/

Statistical Analysis

All results were analyzed statistically by one-way analysis of variance (ANOVA) tests using IBM SPSS Statistics version 20.0 (IBM, United States) followed by Tukey's multiple comparison test. The data are expressed in the form of mean ± standard deviation (SD) and $p < 0.05$ was considered to imply statistical difference.

RESULTS

Effects of SSPs Administration on the Growth Performance of Mice

To determine whether the SSPs administration influences the growth performance of mice, we assessed the body weight (BW) at the beginning and end of the experiment. As shown in **Figure 1**, there were no significant changes among the three treatment groups ($p > 0.05$), indicating that the growth performance of mice was not affected by SSPs administration.

Effects of SSPs Administration on Intestinal Inflammation

To verify the anti-inflammatory capacity of SSPs, some inflammatory cytokines were determined by ELISA. The anti-inflammatory cytokines IL-10 (**Figure 2C**) increased by HSSPs administration ($p < 0.01$). Moreover, the pro-inflammatory cytokines including IL-1β (**Figure 2A**), IL-6 (**Figure 2B**), and TNF-α (**Figure 2D**) decreased by SSPs in a dose-dependent manner ($p < 0.01$).

Effects of SSPs Administration on Intestinal Anti-Oxidant Capacity

From the results of **Figure 3A**, it is found that SSPs administration increased ($p < 0.01$) the jejunal protein abundances of Keap1, HO-1, and p-Nrf2 in C57BL/6J mice. Subsequently, we detected the biomarkers of membrane lipid peroxidation and protein oxidative injury. Compared with the control group, SSPs administration decreased the content of MDA and increased the content of GSH-Px and T-AOC.

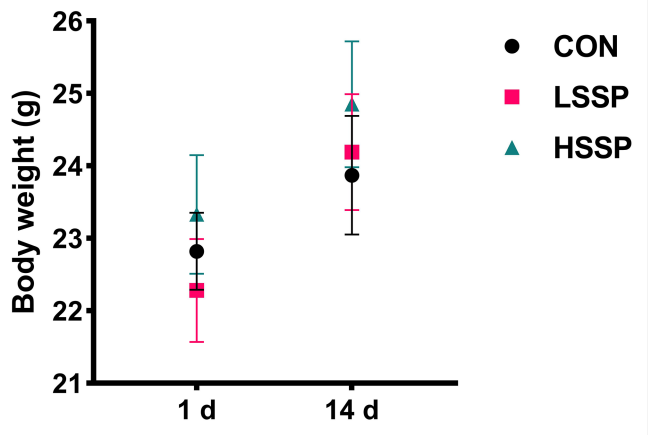

FIGURE 1 | Effect of SSPs on the bodyweight of C57BL/6J mice. CON: control group; LSSP: low dose *Scorias spongiosa* polysaccharide; HSSP: high dose *Scorias spongiosa* polysaccharide.

Effects of SSPs Administration on Intestinal Microbial Diversity

As shown in **Figure 4A**, SSPs increased ($p < 0.05$) the Chao1 index, dominance index and observed_otus index of bacteria in mice. Meanwhile, HSSPs decreased ($p < 0.05$) the Shannon index, Simpson index and pielou_e index of bacteria in mice. In addition, the PCoA analysis revealed that microbial community was significantly altered by HSSPs administration, with an evident separation ($p < 0.05$) compared with the control group.

Effects of SSPs Administration on Intestinal Microbiota Composition

The bacterial composition was analyzed at different taxonomic levels (**Figure 5**). At the phylum level, the dominant bacteria were Firmicutes, Bacteroidota, and Verrucomicrobiota, followed by Proteobacteria, Actinobacteria, Desulfobacterota, Deferribacteres, Patescibacteria, Campilobacterota, and Cyanobacteria. SSPs administration increased the abundances of Firmicutes, Campilobacterota, Desulfobacterota, Proteobacteria, Actinobacteria, and Fusobacteria, Bacteroidetes, and Verrucomicrobia, decreased the abundances of Verrucomicrobiota, Bacteroidota, Patescibacteria, and Synergistota.

DISCUSSION

Edible fungi, which belong to the phylum fungi, can form large fleshy (or colloidal) fruiting bodies or sclerotia tissues and can be used for food or medicine (Guo et al., 2021). Polysaccharides extracted and purified from the fruiting body or mycelium have multiple physiological functions. It is reported that *premna microphylla* turcz leaves polysaccharides (pPMTLs) showed high anti-inflammation activity *via* various pathways including antimicrobial peptides (AMPs) expression pathway, immunodeficiency (IMD) pathway, target of rapamycin (TOR) pathway and intestinal autophagy pathway (Song et al., 2021). Moreover, *Morchella importuna* polysaccharides (MIPs) attenuate CCl_4-induced hepatic inflammatory injury *via* decreasing pro-inflammatory cytokine production through inhibiting the TLR4/NF-κB signaling pathway (Wen et al., 2019; Xu et al., 2021a). However, the anti-inflammatory activity of the newly found SSPs has not been evaluated. In the present study, the SSPs administration increased the anti-inflammatory cytokines content (IL-10). Contrary to the anti-inflammatory cytokines, IL-1β, IL-6, and TNF-α, as pro-inflammatory cytokines which have been reported in the intestinal inflammation occurrence (Singh et al., 2020; Kim et al., 2021), were dose-dependently decreased by SSPs administration. The results suggested that the anti-inflammation activity of SSPs was relevant to keeping the balance of pro- and anti-inflammatory cytokines.

MDA, as an indirect indicator of the degree of tissue peroxidation, can promote the infiltration of inflammatory cells

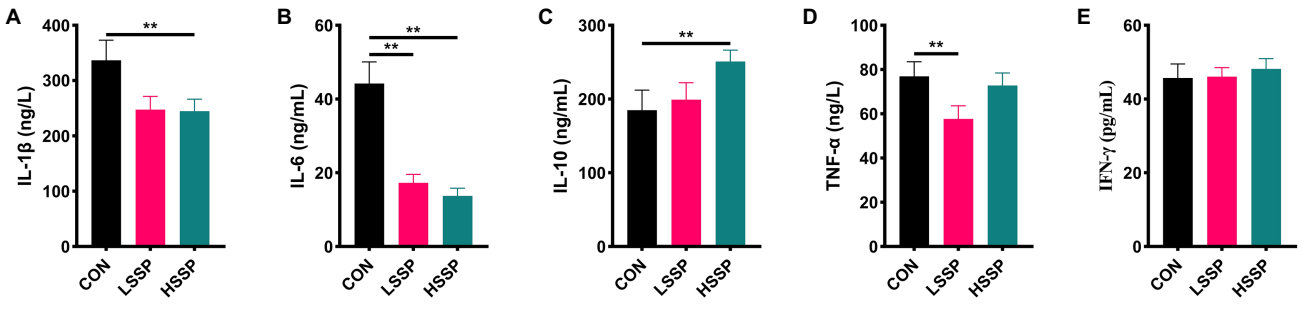

FIGURE 2 | Effect of SSPs on the inflammatory cytokines of C57BL/6J mice. The contents of IL-1β **(A)**, IL-6 **(B)**, IL-10 **(C)**, TNF-α **(D)**, and IFN-γ **(E)** were detected by ELISA. CON: control group; LSSP: low dose *Scorias spongiosa* polysaccharide; HSSP: high dose *Scorias spongiosa* polysaccharide. *Compared with the CON group, $^{**}p < 0.01$.

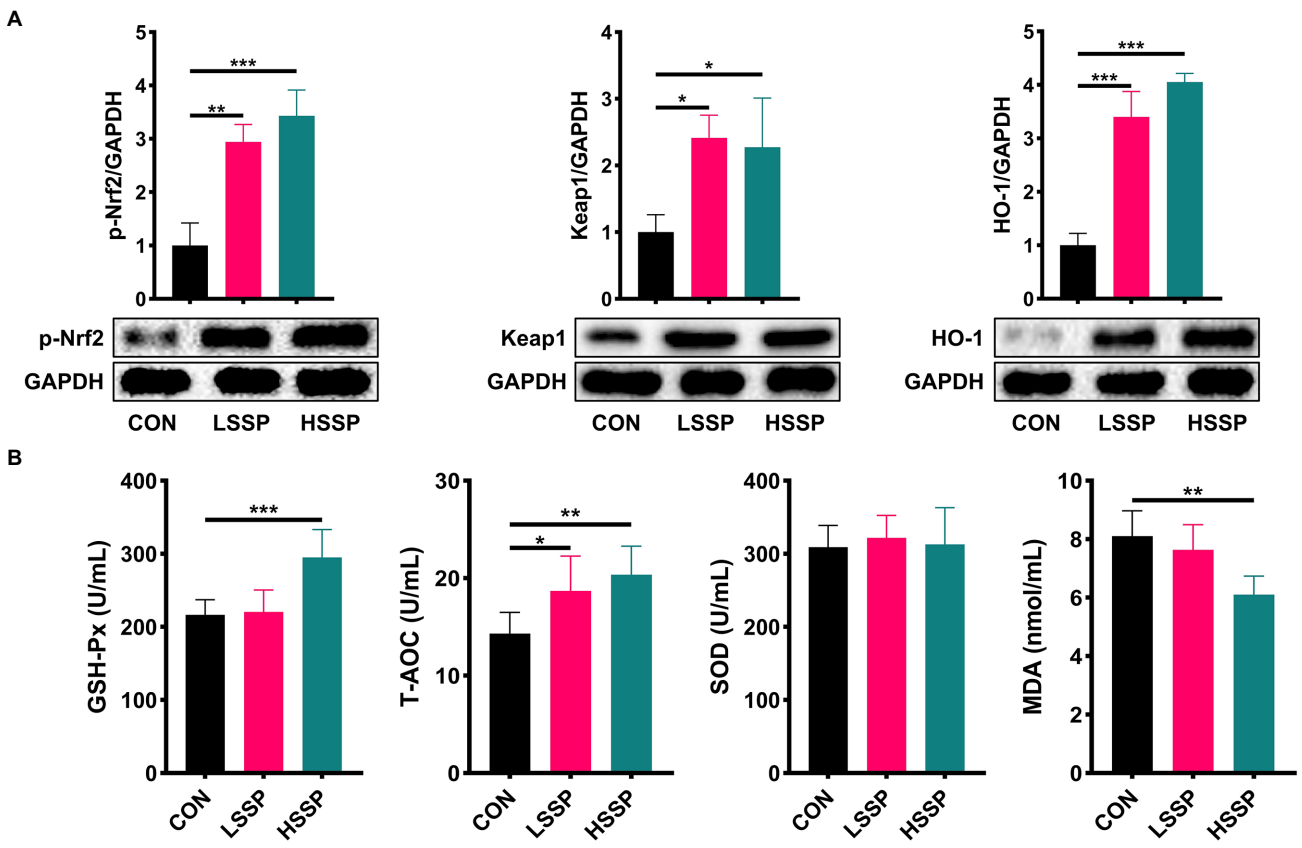

FIGURE 3 | Effect of SSPs on the anti-oxidant capacity of C57BL/6J mice. The protein abundances of p-Nrf2, Keap1 and HO-1 were detected by western blotting **(A)**. The contents of MDA, T-AOC, SOD, and GSH-Px were detected by ELISA **(B)**. CON: control group; LSSP: low dose *Scorias spongiosa* polysaccharide; HSSP: high dose *Scorias spongiosa* polysaccharide. *Compared with the CON group, $^{*}p < 0.05$, $^{**}p < 0.01$, and $^{***}p < 0.01$.

and even promote the expression of myeloperoxidase (MPO), while SOD, as an antioxidant enzyme, has the opposite effect (Tsikas, 2017; Rosa et al., 2021). GSH-Px is an important enzyme that catalyzes the decomposition of hydrogen peroxide and can specifically catalyze the reduction reaction of GSH to hydrogen peroxide, which plays an important role in protecting cells and tissues from oxidative stress injury (Pu et al., 2022). In our study, the results showed that SSPs administration significantly downregulated the content of MDA and upregulated the content of GSH-Px and T-AOC. To elucidate the molecular mechanisms by which SSPs promoted the anti-oxidative capacity, we investigated the Keap1-Nrf2-ARE signaling pathway-related protein expression.

Oxidative stress refers to that when the body is stimulated, the content of reactive oxygen species (ROS) or reactive nitrogen species (RNS) free radicals exceeds the range that can be cleared

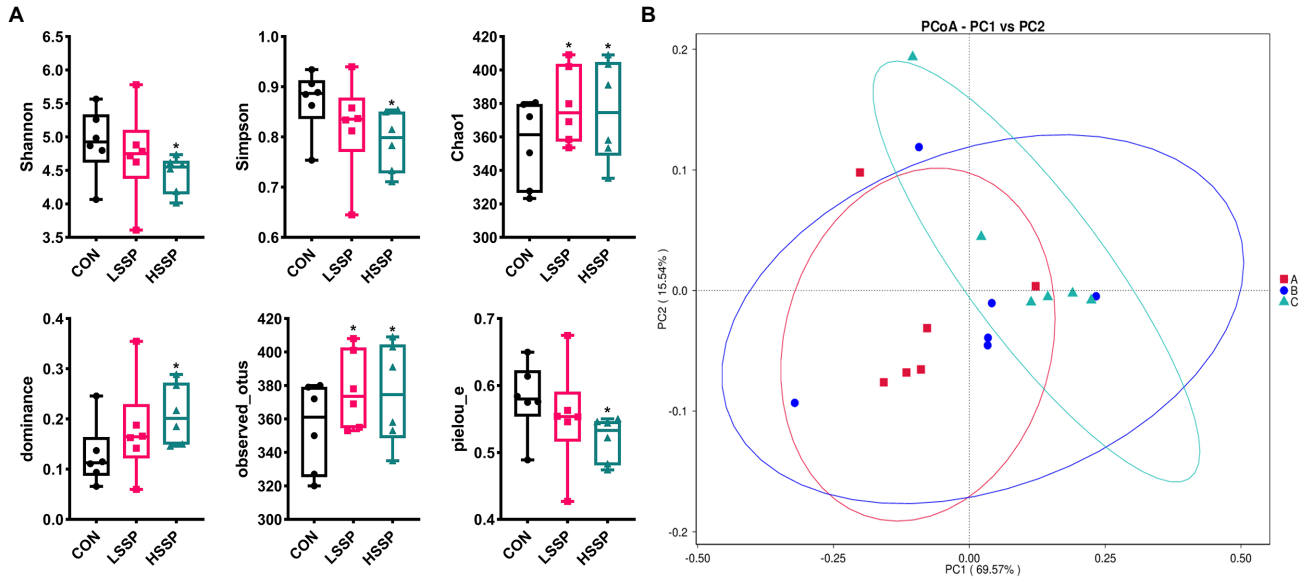

FIGURE 4 | Effect of SSPs on the intestinal bacteria diversity of C57BL/6J mice. The alpha diversity of intestinal bacteria in C57BL/6J mice were detected by 16S rDNA **(A)**. The PCoA **(B)** score plots demonstrate complete separation of the jejunal samples among the groups. A (CON): control group; B (LSSP): low dose *Scorias spongiosa* polysaccharide; C (HSSP): high dose *Scorias spongiosa* polysaccharide. *Compared with the CON group, $^{*}p < 0.05$.

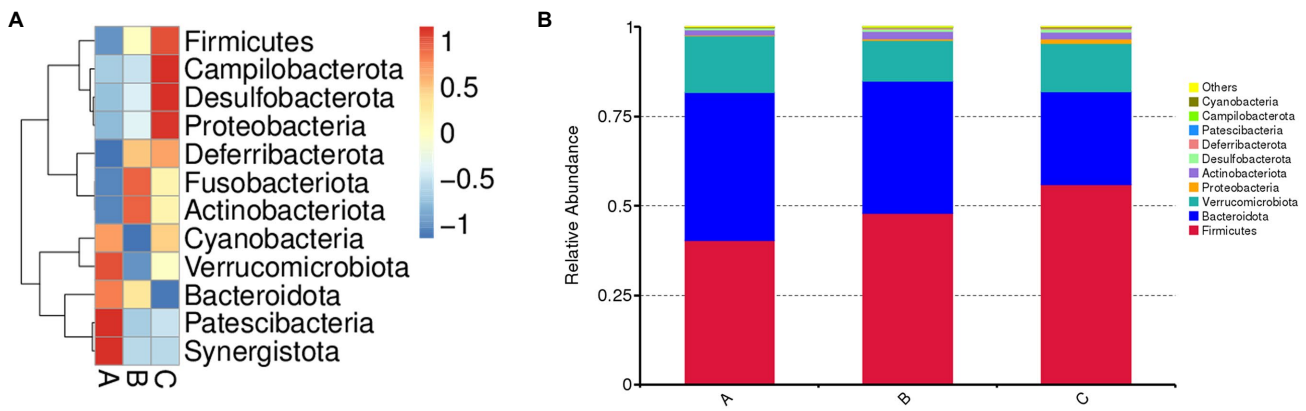

FIGURE 5 | Effect of SSPs on the intestinal bacteria composition of C57BL/6J mice. Microbial composition of the CON, LSSP, and HSSP groups at the phylum level **(A)**. Relative abundances of microbial composition among three groups at the phylum level **(B)**. A (CON): control group; B (LSSP): low dose *Scorias spongiosa* polysaccharide; C (HSSP): high dose *Scorias spongiosa* polysaccharide.

by itself, resulting in the imbalance of redox balance and tissue damage, and eventually lead to a series of diseases. In response to oxidative stress, body-self-expression produces a series of endogenous antioxidant factors, including antioxidant molecules and detoxifying enzymes. Among them, the Keap1-Nrf2-ARE signaling pathway plays a crucial role in mediating endogenous antioxidant factors. The results of western blotting indicated that the SSPs administration enhanced the protein level of p-Nrf2, Keap1, and HO-1, implying that SSPs possess a strong anti-oxidant capacity *via* regulating the antioxidant factor production through activating the Keap1-Nrf2-ARE signaling pathway.

The human gastrointestinal (GI) tract is a huge and complex micro-ecosystem, hosting trillions of microorganisms including but not limited to bacteria, fungi, and viruses (Watanabe et al., 2021). The interactions and homeostasis among gut microorganisms, nutrient metabolism and epithelium of the GI tract are critical to host health (Motta et al., 2021). Disrupting the composition of GI microbiota may result in the development and progression of diseases. Numerous studies have demonstrated that the dysbiosis of gut bacteria may interrupt intestinal and systemic immune homeostasis, leading to the development of various kinds of diseases (Baumler and Sperandio, 2016; Sittipo et al., 2018; Chakaroun et al., 2020).

As food-derived nutrients could directly interact with gut microbiota and alter the composition, diversity and function of gut bacteria, we found that SSPs-administered mice exhibit more diversity of evenness and richness than those in control mice, as they have higher Chao1 and observed_otu indices. Furthermore, the results of intestinal microbiota composition demonstrated that *Firmicutes* and *Bacteroidota* which is dominated in the gut microbiota were altered by SSPs administration. These species matter as they play a role in the body's energy-balance mechanism as they affect energy transformation, nutrient absorption, and glucose metabolism. The *Firmicutes*/*Bacteroidetes* ratio is raised in the groups treated with SSPs. These results suggested that SSPs may regulate intestinal diversity and composition to benefit gut health.

CONCLUSION

Taken together, our study showed that SSPs are instrumental in intestinal health by enhancing the anti-inflammation and anti-oxidative capacity. Furthermore, the diversity and composition of intestinal microbiota were enriched by SSPs administration. Our findings provided a deep understanding of the benefit of polysaccharides from edible fungi as bioactive materials to intestinal health.

DATA AVAILABILITY STATEMENT

The datasets presented in this study can be found in online repositories. The names of the repository/repositories and accession number(s) can be found at: NCBI BioProject—PRJNA808190.

ETHICS STATEMENT

The animal study was reviewed and approved by the Animal Care and Use Committee of the Sichuan Provincial People's Hospital (Chengdu, China).

AUTHOR CONTRIBUTIONS

YX, WP, and YW conceived and designed the experiments. ZZ, HF, JT, and YX conducted the experiments. YX and YW wrote the paper. YX, YC, and JZ analyzed the data. All authors contributed to the article and approved the submitted version.

FUNDING

This work was financially supported by the China Agriculture Research System of MOF and MARA (CARS-20).

REFERENCES

Alvarez-Vieites, E., Lopez-Santamarina, A., Miranda, J. M., Del Carmen Mondragon, A., Lamas, A., Cardelle-Cobas, A., et al. (2020). Influence of the intestinal microbiota on diabetes management. *Curr. Pharm. Biotechnol.* 21, 1603–1615. doi: 10.2174/1389201021666200514220950

Bain, C. C., and Cerovic, V. (2020). Interactions of the microbiota with the mucosal immune system. *Immunology* 199, 9–11. doi: 10.1111/cei.13400

Baumler, A. J., and Sperandio, V. (2016). Interactions between the microbiota and pathogenic bacteria in the gut. *Nature* 535, 85–93. doi: 10.1038/nature18849

Chakaroun, R. M., Massier, L., and Kovacs, P. (2020). Gut microbiome, intestinal permeability, and tissue bacteria in metabolic disease: perpetrators or bystanders? *Nutrients* 12:1082. doi: 10.3390/nu12041082

Chen, T., Liu, H., Liu, J., Li, J., An, Y., Zhu, M., et al. (2021b). Carboxymethylation of polysaccharide isolated from alkaline peroxide mechanical pulping (APMP) waste liquor and its bioactivity. *Int. J. Biol. Macromol.* 181, 211–220. doi: 10.1016/j.ijbiomac.2021.03.125

Chen, O., Mah, E., Dioum, E., Marwaha, A., Shanmugam, S., Malleshi, N., et al. (2021a). The role of oat nutrients in the immune system: a narrative review. *Nutrients* 13:1048. doi: 10.3390/nu13041048

Cheng, Y., Ling, Z., and Li, L. (2020). The intestinal microbiota and colorectal cancer. *Front. Immunol.* 11:615056. doi: 10.3389/fimmu.2020.615056

Dong, L. N., Wang, M., Guo, J., and Wang, J. P. (2019). Role of intestinal microbiota and metabolites in inflammatory bowel disease. *Chin. Med. J.* 132, 1610–1614. doi: 10.1097/CM9.0000000000000290

Guo, Y., Chen, X., and Gong, P. (2021). Classification, structure and mechanism of antiviral polysaccharides derived from edible and medicinal fungus. *Int. J. Biol. Macromol.* 183, 1753–1773. doi: 10.1016/j.ijbiomac.2021.05.139

Kim, J., Park, H., Saravanakumar, G., and Kim, W. J. (2021). Polymer/Aptamer-integrated gold nanoconstruct suppresses the inflammatory process by scavenging ROS and capturing pro-inflammatory cytokine TNF-alpha. *ACS Appl. Mater. Interfaces* 13, 9390–9401. doi: 10.1021/acsami.0c15727

Lin, D., Yang, L., Wen, L., Lu, H., Chen, Q., and Wang, Z. (2021). Crosstalk between the oral microbiota, mucosal immunity, and the epithelial barrier regulates oral mucosal disease pathogenesis. *Mucosal Immunol.* 14, 1247–1258. doi: 10.1038/s41385-021-00413-7

Mei, X., Yang, W., Huang, G., and Huang, H. (2020). The antioxidant activities of balsam pear polysaccharide. *Int. J. Biol. Macromol.* 142, 232–236. doi: 10.1016/j.ijbiomac.2019.09.168

Motta, J. P., Wallace, J. L., Buret, A. G., Deraison, C., and Vergnolle, N. (2021). Gastrointestinal biofilms in health and disease. *Nat. Rev. Gastroenterol. Hepatol.* 18, 314–334. doi: 10.1038/s41575-020-00397-y

Pu, X., Li, F., Lin, X., Wang, R., and Chen, Z. (2022). Oxidative stress and expression of inflammatory factors in lung tissue of acute mountain sickness rats. *Mol. Med. Rep.* 25:49. doi: 10.3892/mmr.2021.12565

Rosa, A. C., Corsi, D., Cavi, N., Bruni, N., and Dosio, F. (2021). Superoxide dismutase administration: a review of proposed human uses. *Molecules* 26:1844. doi: 10.3390/molecules26071844

Singh, M., Mastana, S., Singh, S., Juneja, P. K., Kaur, T., and Singh, P. (2020). Promoter polymorphisms in IL-6 gene influence pro-inflammatory cytokines for the risk of osteoarthritis. *Cytokine* 127:154985. doi: 10.1016/j.cyto.2020.154985

Sittipo, P., Lobionda, S., Lee, Y. K., and Maynard, C. L. (2018). Intestinal microbiota and the immune system in metabolic diseases. *J. Microbiol.* 56, 154–162. doi: 10.1007/s12275-018-7548-y

Song, G., Chen, F., Chen, S., and Ye, S. (2021). Polysaccharides from Premna microphylla turcz ameliorate inflammation via the enhancement of intestinal resistance in host. *J. Ethnopharmacol.* 276:114208. doi: 10.1016/j.jep.2021.114208

Suslov, A. V., Chairkina, E., Shepetovskaya, M. D., Suslova, I. S., Khotina, V. A., Kirichenko, T. V., et al. (2021). The neuroimmune role of intestinal microbiota in the pathogenesis of cardiovascular disease. *J. Clin. Med.* 10:1995. doi: 10.3390/jcm10091995

Tsikas, D. (2017). Assessment of lipid peroxidation by measuring malondialdehyde (MDA) and relatives in biological samples: analytical and biological challenges. *Anal. Biochem.* 524, 13–30. doi: 10.1016/j.ab.2016.10.021

Villeger, R., Lopes, A., Carrier, G., Veziant, J., Billard, E., Barnich, N., et al. (2019). Intestinal microbiota: a novel target to improve anti-tumor treatment? *Int. J. Mol. Sci.* 20:4584. doi: 10.3390/ijms20184584

Wang, W., and Liu, J. (2020). Efficient extraction, antioxidant activities, and anti-inflammation of polysaccharides from Notopterygium franchetii Boiss. *Carbohydr. Polym.* 248:116783. doi: 10.1016/j.carbpol.2020.116783

Watanabe, D., Guo, Y., and Kamada, N. (2021). Interaction between the inflammasome and commensal microorganisms in gastrointestinal health and disease. *EMBO Mol. Med.* 13:e13452. doi: 10.15252/emmm.202013452

Wen, Y., Peng, D., Li, C., Hu, X., Bi, S., Song, L., et al. (2019). A new polysaccharide isolated from morchella importuna fruiting bodies and its immunoregulatory mechanism. *Int. J. Biol. Macromol.* 137, 8–19. doi: 10.1016/j.ijbiomac.2019.06.171

Wu, Y., Li, T., Jia, X., Liu, H., Li, Z., Huang, D., et al. (2018). Effect of tween 80 and chloroform on the secretion, structure and cytotoxic activities of exopolysaccharides from *scorias spongiosa*. *J. Biol. Act. Prod. Nat.* 8, 312–318. doi: 10.1080/22311866.2018.1538815

Wu, W., Zhou, J., Xuan, R., Chen, J., Han, H., Liu, J., et al. (2022). Dietary kappa-carrageenan facilitates gut microbiota-mediated intestinal inflammation. *Carbohydr. Polym.* 277:118830. doi: 10.1016/j.carbpol.2021.118830

Xu, Y., Xie, L., Tang, J., He, X., Zhang, Z., Chen, Y., et al. (2021a). *Morchella importuna* polysaccharides alleviate carbon tetrachloride-induced hepatic oxidative injury in mice. *Front. Physiol.* 12:669331. doi: 10.3389/fphys.2021.669331

Xu, Y., Xie, L., Zhang, Z., Zhang, W., Tang, J., He, X., et al. (2021b). *Tremella fuciformis* polysaccharides inhibited colonic inflammation in dextran sulfate sodium-treated mice via foxp3+ T cells, gut microbiota, and bacterial metabolites. *Front. Immunol.* 12:648162. doi: 10.3389/fimmu.2021.648162

Ye, G., Li, J., Zhang, J., Liu, H., Ye, Q., and Wang, Z. (2021). Structural characterization and antitumor activity of a polysaccharide from Dendrobium wardianum. *Carbohydr. Polym.* 269:118253. doi: 10.1016/j.carbpol.2021.118253

Zhong, S., Yu, H., Nong, X., and Liu, C. (2020). A mini-review of distribution, growth environment and nutrient composition from Scorias spongiosa (bamboo Bird's Nest). *IOP Conf. Ser.: Mater. Sci. Eng.* 782:042040. doi: 10.1088/1757-899X/782/4/042040

Conflict of Interest: The authors declare that the research was conducted in the absence of any commercial or financial relationships that could be construed as a potential conflict of interest.

Publisher's Note: All claims expressed in this article are solely those of the authors and do not necessarily represent those of their affiliated organizations, or those of the publisher, the editors and the reviewers. Any product that may be evaluated in this article, or claim that may be made by its manufacturer, is not guaranteed or endorsed by the publisher.

frontiers in Microbiology

REVIEW
published: 25 March 2022
doi: 10.3389/fmicb.2022.823902

Mechanisms Underlying the Interaction Between Chronic Neurological Disorders and Microbial Metabolites *via* Tea Polyphenols Therapeutics

Mengyu Hong[1], Lu Cheng[2], Yanan Liu[1], Zufang Wu[1], Peng Zhang[3]* and Xin Zhang[1]**

[1] Department of Food Science and Engineering, Ningbo University, Ningbo, China, [2] Department of Food Science, Rutgers, The State University of New Jersey, New Brunswick, NJ, United States, [3] Department of Student Affairs, Xinyang Normal University, Xinyang, China

OPEN ACCESS

Edited by:
Xiaodong Xia,
Dalian Polytechnic University, China

Reviewed by:
Leandro Dias Teixeira,
University of Florida, United States
Guijie Chen,
Nanjing Agricultural University, China
Simin Feng,
Zhejiang University of Technology, China

***Correspondence:**
Lu Cheng
lc894@scarletmail.rutgers.edu
Peng Zhang
zp017083@163.com
Xin Zhang
zhangxin@nbu.edu.cn

Specialty section:
This article was submitted to Food Microbiology, a section of the journal Frontiers in Microbiology

Received: *28 November 2021*
Accepted: *24 February 2022*
Published: *25 March 2022*

Citation:
Hong M, Cheng L, Liu Y, Wu Z, Zhang P and Zhang X (2022) Mechanisms Underlying the Interaction Between Chronic Neurological Disorders and Microbial Metabolites via Tea Polyphenols Therapeutics. Front. Microbiol. 13:823902. doi: 10.3389/fmicb.2022.823902

The number of hydroxyl groups and existence of characteristic structural groups in tea polyphenols (TP) make them have antioxidant activity, which gives TP anti-inflammatory effects, toward protecting the intestinal flora and brain neurons. Host-associated microbial metabolites are emerging as dominant modifiers of the central nervous system. As yet, the investigations on host-microbiota crosstalking remain challenging, studies focusing on metabolites such as serotonin, short-chain fatty acids, and others have pinpointed multiple actionable signaling pathways relevant to host health. However, there are still complexities and apparent limitations inherent in transforming complex human diseases to corresponding animal models. Here, we choose to discuss several intestinal metabolites with research value, as crucial areas for assessing TP-mediated chronic brain diseases interactions with microbial.

Keywords: tea polyphenols, intestinal metabolites, host health, chronic brain diseases, interaction

INTRODUCTION

Tea, coffee, and cocoa are collectively known as the three major beverages in the world. According to the different fermentation levels of contemporary tea, people divide tea into six categories, namely green tea, white tea, yellow tea, oolong tea, black tea, and dark tea. Green tea and white tea belong to unfermented tea. Green tea contains a variety of substances, such as tea polyphenols (TP), proteins, amino acids, vitamins and others (Han et al., 2016). Yellow tea is lightly fermented, oolong tea is semi-fermented, black tea is fermented and dark tea is post-fermented (Zhu et al., 2020).

Tea contains a wide range of compounds, but the substances with antioxidant and beneficial effects are mainly polyphenols (PPs). PPs are a large group of phytochemicals, containing one or more hydroxyl aromatic rings. They exist as secondary plant metabolites in most fruits and vegetables, as well as herbs and spices (Saric et al., 2016). PPs have attracted much attention for their anti-cancer, antioxidant, antibacterial, anti-inflammatory, and prevention of chronic diseases such as diabetes, obesity, neurodegenerative diseases and cardiovascular diseases (Ohishi et al., 2021). PPs with higher molecular weight, due to their chemical complexity, will not be absorbed in the small intestine. It has been proven that only 5–10% of the total intake of PPs can be absorbed by

the small intestine, which depends largely on their structure and combination with sugar moieties (Zhou et al., 2020).

Tea catechins account for about 70–80% of the total PPs. Catechins belong to flavanols and are a derivative of 2-phenylbenzopyran. Catechins mainly include (−)-epigallocatechin-3-gallate (EGCG), (−)-epicatechin (EC), (−)-epigallocatechin (EGC) and (−)-epicatechin-3-gallate (ECG). Among them, the content of EGCG is the most abundant, accounting for about 50 ∼ 80% of the total catechins. Growing evidence suggest that EGCG reshapes gut microbiota architecture. Remely et al. (2017) stated that EGCG interventions reduced *Clostridium* spp., increased *Bacteroides*, and altered propensity of *Bifidobacterium* and *Prevotella* in the murine gut. Research is currently underway to reveal that the microbiota can impact the brain through the microbiota-gut-brain (MGB) axis (Sampson et al., 2016). Understanding how this MGB axis communication may lead to disease and homeostasis in the body is the key to human health and well-being. Consistent with observations those neurological diseases patients are conventionally accompanied by intestinal symptoms, their microbial compositions are distinct from healthy participants, since microbial transplantation alters the disease pathophysiology (Jameson et al., 2020). Intestinal flora has some relations with neurological diseases, wherein gut dysbiosis reduce the rescue effect of EGCG. Therefore, the intestinal microbial structure is not only related to the progression of a series of body diseases, but also mediates the nutritional intervention of active compounds *in vivo*.

5-hydroxytryptamine (5-HT) is a brain-gut peptide and neurotransmitter widely distributed in the central nervous system (CNS) and gastrointestinal (GI) tract. Its anabolic and physiological functions are regulated by the intestinal flora. Intestinal flora can regulate the strength of intestinal motility by interfering with the balance of 5-HT in the intestine (Reynaud et al., 2016). Both of them play an important role in the pathogenesis of intestinal diseases and CNS diseases such as inflammatory bowel syndrome (IBS), Alzheimer's disease (AD) and depression (Fung et al., 2019).

Henceforth, in this contribution, we discuss the overview of TP-mediate for the effective treatment of CNS disorders and intestine-related diseases. As an essential neurotransmitter, 5-HT plays a significant role in the signal pathway of the MGB axis. It is important to note, this complex interaction between TP, intestinal flora, 5-HT, and brain seem to underlie the development of intestinal inflammation, psychiatric and neurodevelopmental disorders, and may inform the safe use of TP therapy.

TEA POLYPHENOLS AND THE BIOCHEMICAL PROPERTIES

Tea polyphenols is a general term for a class of phenolic compounds contained in tea. A large number of experimental studies *in vitro* have shown that TP has strong antioxidant activity (Musial et al., 2020). The antioxidant function of individual TP depends on its molecular structure, the position of the hydroxyl group and other substituents (Yan et al., 2020). TP can provide active hydrogen through hydroxyl to generate more stable phenolic free radicals to scavenge active oxygen and free radicals. TP displays the ability of broad-spectrum and strong antibacterial properties, and certain inhibitory effects on hundreds of bacteria in nature (Wang et al., 2020). There are many metal ions in the bacteria, some of which are coenzymes and others are essential elements. TP with polyhydroxyl structure can react with iron, calcium and other metal ions to form cyclic chelates, resulting in the formation of precipitation, thus affecting bacterial enzymes, activity and the growth and reproduction of sensitive microorganisms (Chen et al., 2016). The phenolic hydroxyl group and benzene ring in the structure of TP can also form hydrogen bonds or hydrophobic structures with proteins, which affect the normal expression of proteins, thereby inhibiting the activity of bacteria. Studies have also shown that the antibacterial effect of TP is related to its degree of polymerization. Compared with the monomers of TP, its oligomers show stronger antibacterial properties (Sasaki et al., 2004) (**Figure 1A**).

In addition to anti-oxidative, scavenging free radicals, chelating metal ions, anti-cancer, anti-inflammatory and anti-apoptotic properties, TP also has potential therapeutic potential in preventing neurodegenerative diseases (Yan et al., 2021). A large number of studies have reported that TP possesses a protective effect against brain damage in a variety of animal models of Parkinson's disease (PD) (Liu et al., 2013). TP extract and monomer EGCG can reduce striatal dopamine consumption and substantia nigra dopaminergic neuron apoptosis. Abundant animal models indicate that TP such as EGCG and EC can pass through the blood–brain barrier. After the rats ingested EGCG (500 $mg \cdot kg^{-1}$), the concentration of EGCG in the brain reached 0.5 $nmol \cdot g^{-1}$ and localized in the brain tissue (Sun et al., 2021). These findings indicate that TP have potentially bioactive substances with neuroprotective and neuromodulating effects (**Figure 1B**).

The antioxidant effect of TP may protect the dopamine system against free radicals, anionic superoxide and intracellular hydroxydopamine-induced neuronal apoptosis (Khan and Mukhtar, 2018). In the CNS, TP can inhibit lipid oxidation and the accumulation of divalent iron complexes, which may be the main mechanism of its neuroprotective effect. The inhibitory effect of TP on lipid peroxidation includes the scavenging of inorganic free radicals. First, TP participates in the initial reaction, effectively scavenging reactive oxygen species such as oxygen ions, and preventing the initiation of lipid peroxidation; secondly, it reacts with lipid free radicals of lipid peroxidation, resulting in chain breakage. The combination of these two effects made TP show significant anti-lipid oxidation function (Tian et al., 2021). In mitochondria, TP may stimulate cellular energy expenditure, thereby reducing weight gain. At the same time, in the nucleus, TP may inhibit the expression of fatty acid synthase gene by down-regulating EGF-receptor/PI3K/Akt/AP-1 signal transduction pathways, thus inhibiting blood lipids and cell growth (Lin and Lin-Shiau, 2006). EGCG is an important antioxidant and iron chelating substance (Zhang et al., 2021). The 3′, 4′-dihydroxy group and gallate group in the B-ring may reduce the divalent iron ions to inactive iron atoms and thus protect cells from oxidative stress damage. EGCG inhibits more

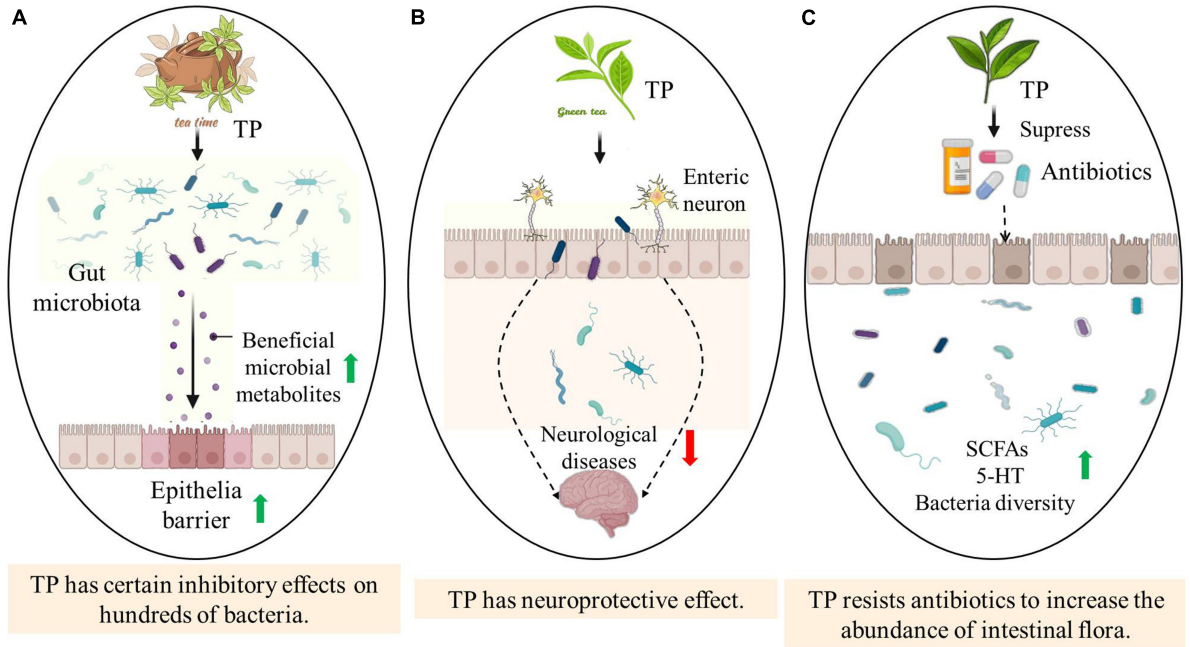

FIGURE 1 | The impact of the multiple biodiversity of tea polyphenols on the host. Panel **(A)** describes that when tea polyphenols is ingested by the host, tea polyphenols interacts with intestinal flora, thereby increasing some beneficial metabolites that enhance the epithelial barrier and thus resist pathogenic bacteria. Panel **(B)** shows that TP has a certain regulatory effect on the enteric nervous system, so as to prevent, cure or at least alleviate neurological diseases. As shown by Panel **(C)**, TP significantly increases the richness and diversity of intestinal flora after antibiotic treatment, improves the imbalance of intestinal flora, and increases the level of SCFAs and 5-HT.

than 90% of DNA damage mediated by chelating metal ions (Perron et al., 2008, 2010). Therefore, the protective effect of TP is partly due to free radical scavenging or metal chelation.

THE ESSENTIAL ROLES OF INTESTINAL MICROBIOTA ON THE BODY

Humans can be divided into three different "enterotypes" based on the type and number of bacteria in the intestine. Researchers named these three enterotypes as *Bacteroides*, *Prevotella,* and *Ruminoccus* type to reflect the dominant bacteria in each ecosystem (Romo-Vaquero et al., 2019). The bacteria in the *Bacteroides* type system mainly obtain energy from carbohydrates and proteins; the *Prevotella* system is good at digesting glycoproteins in the intestines, and this tendency is the same as the rumen cocci system (Costea et al., 2018). Although the knowledge of enterotypes is far less than the understanding of blood type, scientists believe that the information of enterotypes can also provide a reference for the diagnosis and treatment of diseases. The type and number of flora in the intestine reflect the digestive ability, immune ability and response of different people to drugs.

Each species or strain of gut mutualistic bacteria performs unique biological functions, and therefore, their balance is essential for maintaining GI homeostasis. Importantly, through cooperation and competition, the colonization of each type of bacteria restricts and influences each other (Fassarella et al., 2021). Different types or strains of symbiotic bacteria in the intestine harbor different nutritional preferences and are used to adapt to the intestinal environment.

Furthermore, another species of *Lactobacillus* named as *Lactobacillus plantarum* can be used as probiotics, which contributes to the host health. For example, *L. plantarum* has beneficial effect against metabolic syndromes, diabetes, and brain diseases (Liu Y. W. et al., 2018). Wang et al. (2013) found that *L. plantarum* strain ZLP001 could fortify the intestinal barrier function by reinforcing the intestinal epithelium and modulating gut microbiota composition. In addition, the probiotics contained in healthy microbiota can elicit host protective immunity or anti-inflammatory immunity, thereby helping to combat pathogens and promote the recovery of inflammatory damage (Guo et al., 2020). Rats prone to diabetes were fed with *Lactobacillus johnsonii* N6.2 and/or rosmarinic acid. After a period of time, it was found that the early gastrointestinal inflammation in rats was effectively alleviated. As a potential probiotic, *L. johnsonii* N6.2 can reduce the level of pro-inflammatory cytokines, such as interleukin (IL)-1β and lower levels of interferon (IFN)-γ transcription (Teixeira et al., 2018).

Studies have observed that alterations in intestinal flora are capable of promoting the occurrence and progression of chronic diseases, and the progress of chronic diseases can also aggravate the disorder of intestinal flora (Liu et al., 2010). The bacteria in the intestine are mainly composed of *Firmicutes* (F) and *Bacteroides* (B). The ratio of F/B in the intestine not only

affects carbohydrate metabolism, but also alters the production of short-chain fatty acids (SCFAs). There are strong tight junction proteins between the intestinal epithelium of normal people, which connect the intestinal epithelial cells together. However, high blood sugar in diabetic patients can elicit intestinal barrier damage, leading to microbial metabolites entering the body, promoting the proliferation, transferring of pathogenic bacteria, and worsening intestinal infection status (Gong et al., 2017).

Intestinal flora dysregulation is not narrowly defined as a disorder of bacteria in the intestinal tract, and also includes conversions of fungi and viruses in the bowel (Elson and Cong, 2012). Li et al. (2018) demonstrated that intestinal fungal disorders caused by anti-fungal treatment or inoculation of some typical rare fungi would cause excessive immune response, which illustrated the significant role of intestinal fungi in immune homeostasis. Research by Sartor and Wu (2017) indicated specific changes in the intestinal fungi of Crohn's disease, which implicated that the unique intestinal environment of Crohn's disease might be instrumental in fungi, whereas impaired the growth and reproduction of bacteria and promoted the perturbation of intestinal flora. Accordingly, the disorder of the intestinal flora is a complex, including different degrees and types of dysfunction forms. When studying chronic diseases and intestinal flora disorders, it should not be simply considered as alterations in the structure and richness of bacteria, which also includes flora metabolism, fungi, viruses, and others.

GUT MICROBIOTA-DERIVED METABOLITES AND THEIR EFFECTS ON HOST HEALTH

In the past 15 years, scientists have proved that gut microbes are involved in nutrient absorption, substance metabolism, immune defense and other important physiological processes, associated with a variety of diseases, such as diabetes, heart disease, allergy and depression (Qi et al., 2021). Metabolism is the common basis of all cellular processes involved in the host, host microbiota, and invading pathogens. One of the main ways for intestinal flora to interact with host is through metabolites, which are intermediate or final products of microbial metabolism (Troha and Ayres, 2020). These metabolites are derived from dietary digestion, modification of host molecules, such as bile acids, or directly from bacteria. These metabolic signals affect immune maturation, immune homeostasis, host energy metabolism and mucosal integrity. One of the reasons why these tiny organisms have such a big impact is that they secrete metabolites into the blood circulation (Oliphant and Allen-Vercoe, 2019). The existence of MGB axis makes the intestinal tract and brain of the host communicate closely. MGB axis functional changes are involved in the occurrence of a variety of gastrointestinal diseases, such as IBS and related functional gastrointestinal diseases. Studies have also found that MGB axis disorders are also involved in many brain diseases, including autism, PD, depression and chronic pain. Intestinal microorganisms and their metabolites can regulate gastrointestinal function by affecting intestinal permeability, mucosal immune function, gastrointestinal motility and enteric nervous system (ENS) activity; intestinal microorganisms and their metabolites are also involved in regulating behavior and brain processes, including stress response, emotional behavior, pain regulation, feeding behavior and brain biochemistry (Raskov et al., 2016; Liang et al., 2018).

Host can directly detect the metabolites of microorganisms and coordinate the process and physiology of the host. The intestine of a mammal consists of a single epithelial layer that physically isolates the microbiota from the rest of the body and prevents excess solutes, microorganisms and lumen antigens from entering the body (Laukoetter et al., 2008). Intestinal epithelium directly senses microbial metabolites and induces the host's response, further promotes the integrity of the barrier. For example, in order to maintain a homeostatic relationship with the intestinal microbiota, the barrier integrity of the intestinal epithelial layer must be maintained (McCarville et al., 2020). Intestinal barrier includes physical barrier, chemical barrier, microbial barrier and immune barrier. The epithelial cell layer and the internal and external mucin layer constitute the physical barrier, while the mucus, digestive juice produced by the epithelial cells and the bacteriostatic substances secreted by normal bacteria are chemical barriers, and the mucosal flora and intestinal microflora form a multi-level intestinal microbial barrier. Intestinal associated lymphocyte tissue and diffuse immune cells form immune barrier (Ghosh et al., 2020). If the intestinal barrier is broken, lipopolysaccharide (LPS) is transported through the blood to LPS-binding proteins or lipoproteins, and CD14 as a cofactor interacts with surface receptors on immune cells, such as toll-like receptor 4, to initiate inflammatory response, which in turn activates NF-κB pathway, resulting in increased transcription of pro-inflammatory cytokines such as tumor necrosis factor (TNF)-α, IL-1β and IL-6 (Lu et al., 2008).

The SCFAs are organic fatty acids with carbon chain length less than 6, mainly including acetic acid, propionic acid, butyric acid and valeric acid, and is one of the metabolites with the highest microbial content in the intestinal lumen (Zhao et al., 2016). Studies have shown that the use of probiotics *Lactobacillus johnsonii* N6.2 and phenols may be an effective way to improve metabolic syndrome related diseases caused by high-fat diet, help to maintain the healthy and steady state of the intestinal tract, and thus promote the metabolic production of SCFAs (Teixeira et al., 2021). SCFAs can enhance the health of the host by reducing inflammation, improving autoimmune diseases and allergies, maintaining the intestinal barrier and mediating the colonization resistance of intestinal pathogens to enhance the health of the host and regulate the functions of multiple systems, such as the intestines, nerves, endocrine and blood systems (Overby and Ferguson, 2021). A large amount of evidence shows that SCFAs plays a vital role in maintaining intestinal health, preventing and improving a variety of non-communicable diseases, including cancer, and are one of the most important intermediates between disease, nutrition and intestinal flora (Van Treuren and Dodd, 2020). As an essential medium, it directly or indirectly plays an important physiological role in multiple organs and tissues of the body (**Figure 2**). More and more studies have shown that the

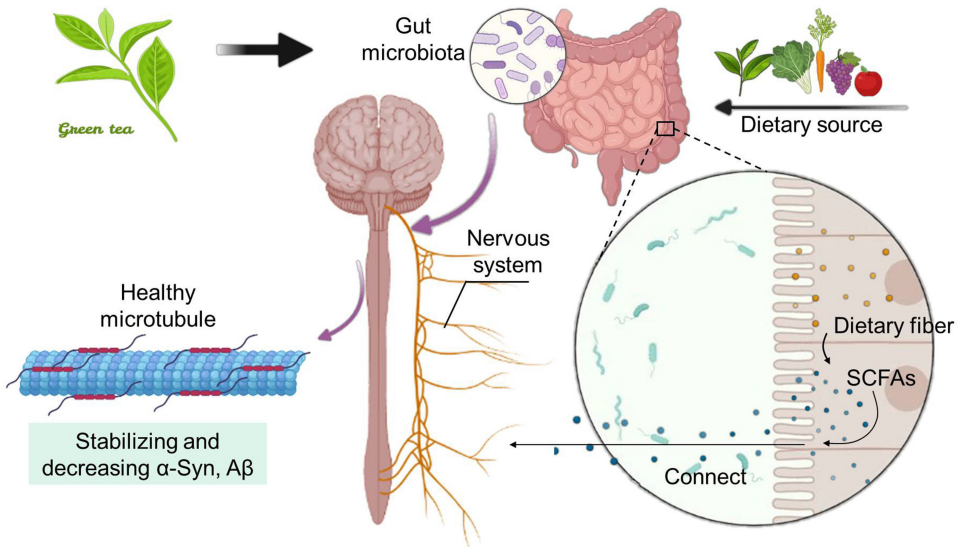

FIGURE 2 | Dietary fiber-produced SCFAs and tea polyphenols-mediated intestinal flora work together to establish a connection with the host nervous system. The intake of TP and dietary fiber can increase the amount of SCFAs, a metabolite in the intestinal tract. The pathway between the intestinal tract and the brain makes SCFAs as a transmission medium, which can effectively improve neurological diseases.

SCFAs produced by dietary fiber under the action of microflora can act not only on the intestinal tract, but also on the distal part of the brain. As one of the receptors of SCFAs, Gpr41 is widely expressed in the peripheral nervous system in addition to ENS, such as sympathetic ganglia, vagus nerve, dorsal root and trigeminal ganglia. One of the effects of SCFAs on the brain is that during intravenous administration, a small amount of acetic acid is absorbed across the blood-brain barrier and activates hypothalamic neurons, resulting in a sense of satiety (Koh et al., 2016; Makki et al., 2018).

Tryptophan is an important amino acid, which affects the metabolism of the host through metabolites produced by the three main fermentation pathways of the intestinal flora and GI cells (Keszthelyi et al., 2009). Tryptophan can be broken down by the intestinal flora into indole and its derivatives called aryl hydrocarbon receptor ligand; it is metabolized by the kynurenine pathway in immune and epithelial cells, and its activity is regulated by the gut flora; it also produces 5-HT by tryptophan hydroxylase 1 in enterochromaffin cell (Gheorghe et al., 2019). Since animal cells cannot produce tryptophan, humans rely on exogenous, mainly dietary intake, including bananas, milk, peanuts and others. The tryptophan metabolism pathway has been identified in the intestinal flora of some people, such as *Clostridium sporogenes*, which can achieve decarboxylation and lead to the production of the neurotransmitter tryptamine. Tryptamine (a tryptophan metabolite produced by *C. sporogenes* and *Ruminococcus gnavus*) is a β-arylamine neurotransmitter that is involved in intestinal health (Jenkins et al., 2016). In the intestine, tryptamine induces the release of the neurotransmitter 5-HT through enterochromaffin cells (ECs) located on the mucosal surface, and 5-HT stimulates GI motility by means of neurons in the enteric nervous system (Okaty et al., 2019). 5-HT is an inhibitory neurotransmitter with high content in the cerebral cortex and nerve synapses (**Figure 3**). It can enhance memory and protect neurons from "excitatory neurotoxin" damage and is generally considered to be a contributor to happiness.

INFLUENCES OF INTESTINAL BACTERIA DISORDER ON THE BODY

The perturbation of this balance "so-called gut dysbiosis" triggers or exacerbates various GI diseases, such as inflammatory bowel diseases (IBD). There is also ample evidence that dysbiosis can increase intestinal inflammation. For example, a decrease in strict anaerobes and an increase in facultative anaerobes lead to increased intestinal inflammation (David et al., 2014). In addition, decreased numbers of SCFA-producing microorganisms, such as *Clostridium* spp. has been observed in IBD patients (Nagao-Kitamoto and Kamada, 2017). Microbial-derived SCFAs, especially butyrate, promote the production of regulatory T cells and intestinal mucus to block inflammatory signal transduction pathways and strengthen the epithelial barrier function (Thibault et al., 2010). Another feature of the IBD microbiome is the reduction of tryptophan metabolism. The tryptophan metabolite indole acrylic acid produced by several species of *Peptostreptococcus* spp. promotes mucosal barrier function and reduces inflammation (Nikolaus et al., 2017). Intestinal inflammation caused by pathogens significantly changes the intestinal microenvironment, which in turn affects the adaptability and stability of GI bacteria, thus forming a structure of resident microbial communities.

Factors involved in the development of an unhealthy state of the gut microbiome include drastic changes in dietary patterns, microbial infections and frequent use of medications, especially

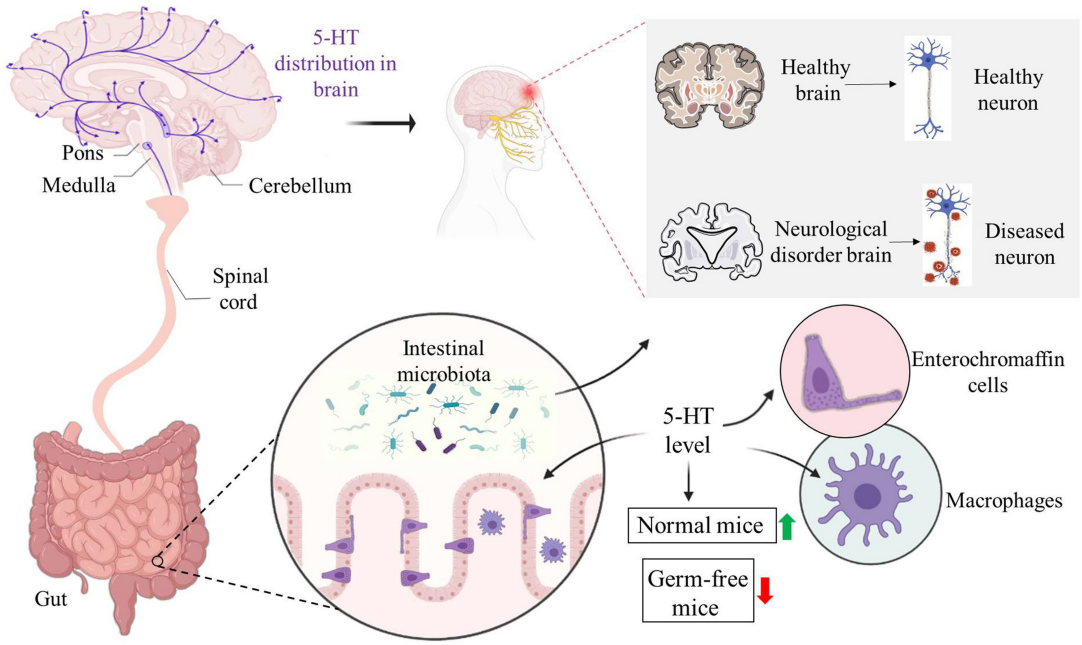

FIGURE 3 | Distributions of 5-HT in the brain and intestine affect the brain nerves. The distribution of 5-HT in the brain affects the state of the brain, which is different between health and neurological diseases. Enterochromaffin cells and macrophages can promote the secretion of 5-HT in the intestine. Compared with normal flora colonized mice, the level of 5-HT in germ-free mice was lower. The level of 5-HT may also regulate the intestinal microecological environment, which can affect the function of the central nervous system and is associated with neurological diseases.

antibiotics (Matsuoka and Kanai, 2015). External disturbances can cause the stable microbial ecosystem to be pushed into an unstable state, after which it may return to its original state. Nevertheless, they may also lead to another healthier and more stable state. A stable microbial community can resist the invasion and expansion of non-native bacteria and pathogens, resulting in the phenomenon known as colonization resistance (Ding and Schloss, 2014). The interactions between the host and the gut microbes need to actively maintain a dynamic equilibrium in order to achieve a healthy and stable state.

TEA POLYPHENOLS AND THE BENEFICIAL EFFECTS ON INTESTINAL MICROBIOTA

The regulation of TP on the composition and function of the intestinal flora was generally dose-dependent, and different doses of TP could dramatically change the relative abundance of *Lactobacillus* after antibiotic action. Low-dose TP (daily dose of 90 mg/kg) apparently antagonized the decrease in the abundance of *Lactobacillus* caused by antibiotics, even significantly higher than the normal group (only received distilled water) (Li et al., 2021). However, the influence of TP on the intestinal microflora depended on the microbial strains, TP structure and testing dose. High doses of TP (daily dose of 360 mg/kg) might adversely affect probiotics, leading to inactivation of *Lactobacillus* (Li et al., 2021). Because excessive intake of TP may cause damage to the liver of animals, produce certain toxic side effects, and the probiotics will also be affected (Patel et al., 2013). Therefore, in order to avoid the possible negative effects of high-dose TP on the intestinal flora and maintain the balance of the intestinal flora, the intake of TP at an appropriate dose probably plays an effective role.

Antibiotics have been used to treat or alleviate certain diseases, nevertheless, antibiotics tremendously alter the composition and metabolic activity of the intestinal microflora (Kim et al., 2017). TP significantly increases the richness and diversity of the gut microflora after antibiotics treatment, improves the imbalance of the intestinal microflora, increases the level of SCFAs, and reduces the risk of cancer, obesity, diabetes and other diseases caused by antibiotics (Pérez-Burillo et al., 2021). The modulation of intestinal microflora by TP may be one of the mechanisms of its anti-tumor, anti-obesity, immune regulation and other biological activities. Accordingly, TP has a potential to be a functional food additive to reduce the negative effects of antibiotics (Gowd et al., 2019) (**Figure 1C**).

Several types of studies have shown that TP can regulate the intestinal microbial community by exerting a probiotic-like effect or antibacterial activity on intestinal pathogenic bacteria (Zhang et al., 2020). TP has been considered as a natural source of antibacterial agents, which can inhibit the growth of some pathogenic bacteria such as *Escherichia coli* (*E. coli*), *Streptococcus, Bacteroides,* and *Parasutterella* (Liu Z. et al., 2018). TP can inhibit the production of pro-inflammatory factors and reduce the incidence of colorectal cancer by decreasing the synthesis of bacterial lipopolysaccharide and the abundance of functional pathways related to cancer (Huang et al., 2021). By increasing the abundance of *Akkermansia* and

butyric acid production, the intestinal flora composition and metabolism of EGCG-mediated colitis mice were significantly changed, and the symptoms of colitis were alleviated. After oral administration of EGCG, the levels of proinflammatory cytokines IL-6, IL-1β, and TNF-α in colon decreased significantly, the level of antioxidation increased, and eight kinds of probiotic genera such as *Bifidobacterium* and *Faecalibaculum* were enriched (Wu et al., 2021). Various researches also reported about the bioavailability of PPs and its impact on the host, which depended on their biotransformation into specific compounds by the action of gut microbiota (Cardona et al., 2013; Duda-Chodak et al., 2015; Roopchand et al., 2015). In the rat intestinal microflora, bacteria such as *Enterobacter aerogenes* and *Raoultella planticola* can decompose the chemicals in tea and then be absorbed by the body. And then enrich *Faecalibacterium*, *Bifidobacterium*, *Lactococcus*, *Coprococcus,* and other bacteria in the intestinal tract (Gan et al., 2018).

Following the transformation, the TP biological activity can be enhanced. The human small intestine cannot fully absorb TP. Most of the TP is considered to be left in the intestine and converted into lactic acid type I metabolites (lactones, phenolic and aromatic acids, and simple phenols) and type II metabolites (glucuronate, sulfate, and oxymethyl derivatives). After which they are converted into intermediate metabolites propelled by colonic bacterial enzyme glycosylation, intestinal microbial dehydroxylation and demethylation (Zeng et al., 2019). There is further conversion into small molecular compounds, which enter the liver-intestine circulation or systemic circulation and exert various physiological functions, and finally metabolites are excreted from the body through urine or feces (Gowd et al., 2019).

CHEMICAL SIGNALS BETWEEN THE INTESTINE AND THE BRAIN

Short-Chain Fatty Acids and Enteric Neurons

Intestinal microbes influence the brain and behavior through immune, neuronal and metabolic pathways. In particular, emerging evidence shows that certain members of the microbiota are able to synthesize and/or modulate many neurochemical substances whereby regulate neurotransmission, as well as many other metabolites that can directly or indirectly affect neuronal activity (Jameson et al., 2020). Neural pathways connect the intestines and the brain. Leading of these nerve pathways is the vagus nerve, which extends from the brainstem to the intestines and ENS (Strandwitz, 2018). The intestinal microbiota can help regulate the homeostasis and behavior of host through chemical communication with the nervous system (including direct and indirect signals) (Fassarella et al., 2021). As an example of direct signal transmission, SCFAs are lipids produced by intestinal microbes through fermentation of dietary fiber, emphasizing the close connection between the intestinal microbiota and nerve function (Morais et al., 2021) (**Figure 2**).

Although some animal experiments have emphasized microbial regulation of appetite is the basis for the difference in weight gain, we are very much in the dark how microbial regulation of SCFAs affects the host feeding behaviors. SCFA free fatty acid receptors 2 and 3 are expressed in the ENS, portal nerve and various sensory ganglia, prompting that activation of the nervous system plays a role in regulating these functions (Czajkowska and Szponar, 2018).

INTESTINAL MICROBIOTA INDUCE NEURONAL 5-HT PRODUCTION

5-HT, also known as serotonin, is approximately 95% derived from the gut and synthesized by the ECs and the myenteric plexus, while the remaining 5% is synthesized in central 5-HT neurons. Tryptophane in the intestine is catalyzed by tryptophane hydroxylase 1 in ECs to produce 5-hydroxytryptophan, which then tryptophan decarboxylase catalyzes the production of 5-HT (Rhoades et al., 2019).

In addition to being an important neurotransmitter, 5-HT is also a secretagogue, a crucial regulator for vast biofunctionals residing in the digestive tract, comprising the regulation seen in intestinal secretion and exercise. The majority of 5-HT are released from ECs, which not only regulate the diversified physiological functions in GI, but also have the function of modulating immunity and interacting intimately with mucosal immune cells (Li et al., 2016).

Immune cells are associated with various 5-HT receptors, including lymphocytes, monocytes, macrophages, T cells and B cells. 5-HT levels may be affected by gut microbes. In germ-free (GF) mice, the concentration of 5-HT was significantly reduced compared with the control group colonized by conventional flora. Spore-forming bacteria from healthy individuals promote the biosynthesis of 5-HT in colon ECs and then release it to the mucosa and lumen, thereby increasing the level of 5-HT (Meneses and Liy-Salmeron, 2012). One of the regulatory mechanisms of hypothalamic energy balance involves the 5-HT energy system. Its pharmacological stimulation can cause anorexia in humans and rodents, while inhibiting it increases food intake. Long-term consumption of high-fat foods will reduce postprandial insulin and 5-HT in the extracellular area of the hypothalamus, resulting in disorders of energy metabolism and increased inflammatory response. TP can improve high fat diet-induced hypothalamic inflammation, without affecting the 5-HT energy system (Okuda et al., 2014). 5-HT can change intestinal sensitivity and motility, and affect the pathophysiological process of IBS. Drugs acting on 5-HT receptors can relieve intestinal smooth muscle spasm, reduce visceral sensitivity, regulate intestinal motility, and improve abdominal pain and intestinal function in patients with IBS (Mikocka-Walus et al., 2020). Patients with IBS are usually accompanied by mental disorders, such as depression, anxiety and tension. People's emotions are mainly controlled by the limbic system of the brain, which can regulate endocrine and autonomic nervous functions at the same time. Antidepressants act on the limbic system of the

brain to improve mental state while relieving IBS symptoms (Macedo et al., 2017).

Furthermore, selected bacterial strains, such as *Bacteroides fragilis*, *Brucella* and altered *Schaedler* flora modify the levels of 5-HT in the colon and serum. *Corynebacterium*, *Streptococcus* and *E. coli* synthesize 5-HT through tryptophan *in vivo* (Nagao-Kitamoto and Kamada, 2017). Microbial mediation of alterations in 5-HT also has a regulatory effect on intestinal microenvironment in turn. Disturbance of the intestinal flora can cause imbalance of 5-HT levels, while the use of probiotics alleviates the symptoms of 5-HT dysfunction. Therefore, targeted bacteria can be used as a preferred method to regulate the bioavailability of peripheral 5-HT and treat disease symptoms (Jenkins et al., 2016) (**Figure 3**).

INTERACTIONS BETWEEN THE MICROBIOTA AND 5-HT ARE NEUROPROTECTIVE

5-HT, as a major neurotransmitter, plays an important role in the MGB axis signaling pathway. The ENS is an irreplaceable and important hub in the physiological functions of the intestine, such as enterocinesia, secretion of digestive juice, intestinal blood flow, etc. (Furness, 2012). As we all know, the intestine contains trillions of bacteria, which modulate the host's production of a variety of signal molecules including 5-HT, together with other hormones and neurotransmitters. 5-HT is widely present in mammalian tissues, with a high content in the synapses of the cerebral cortex, which can affect the human body's mood, energy and memory. About 90% of 5-HT come from the intestinal tract. The activation of 5-HT_4 receptor in the ENS is related to adult nerve formation and neuroprotection (Rebholz et al., 2018). 5-HT is a significant research substance, due in part to its diverse roles as a neurotransmitter in both the GI tract (that is, in processes such as peristalsis, secretion and absorption) and the CNS (that is, in regulation of pain modulation, sleep and mood) (Ochoa-Repáraz and Kasper, 2016).

5-HT is believed to play a non-negligible role in neurogenesis and improving the survival rate of nerve cells. De Vadder et al. (2018) confirmed that colonization of GF mice partially restored serum levels of 5-HT, likely by inducing *de novo* 5-HT synthesis by increasing the expression of the rate-limiting enzyme for 5-HT synthesis, *Tph1*, in the mucosa. Furthermore, depletion of the microbiota with antibiotics reduced circulating 5-HT levels.

Alzheimer's disease, which represents the most common form of dementia in the elderly. It is clinically manifested as a large number of neuron reduction, brain structure atrophy, amyloid beta peptides (Aβ) deposition in the brain, senile plaque appears as well as neurofibrillary tangles (Włodarek, 2019). PD is a common neurodegenerative disorder along with midbrain substantia dopamine neuron necrosis in middle-aged and elderly people, huge reduced striatal dopamine, occurrence of α-Synuclein (α-Syn) aggregates in cells as well as formation of Lewy Body-predominant in neurons (Włodarek, 2019).

Alzheimer's disease and PD are the most common causes of cognitive impairment in the elderly, both neurodegenerative diseases characterized by progressive memory loss and cognitive decline. AD, PD and all neurological diseases occur within a tissue separated from blood by the blood-brain barrier. Our understanding of this disease is still far from complete. The factors trigger this disease occurring may have a correlation with the individual's resistance at many levels, such as intestinal flora colonization, 5-HT levels, etc. (Galts et al., 2019; Correia et al., 2021; Ou et al., 2021).

Research by Cirrito et al. (2011) shed light on utilizing selective serotonin reuptake inhibitor (SSRI) or directly augmenting the amount of extracellular 5-HT can apparently reduce the Aβ content in mouse brain tissue fluid by 25%. An increasing body of evidence has suggested that SSRI suppress 5-HT re-uptake, enhance the concentration of 5-HT in the brain, and diminish Aβ aggregation by reacting with receptors (Yao et al., 2020).

Holmqvist et al. (2014) injected α-Syn into the intestinal wall of rats and found that the protein was finally found in the brain, indicating that α-Syn could be spread from the intestinal neuron and microtubules associated with transportation to the brain, in turn PD occurs. The latest study, implanting gut flora of PD, AD patients and normal flora, respectively, into GF mice, and it was found that the former had motor deficits, weakened GI function and constipation, which further indicated that intestinal bacteria may be correlated to PD and AD diseases (Sampson et al., 2016). TP can penetrate the blood-brain barrier, thereby improving the cognitive impairment of the brain. EGCG has been shown to play a neuroprotective role in a series of cellular and animal models of neurological diseases. The spatial learning and memory ability of 5-HT gene deficient mice was impaired, and the plasma 5-HT concentration of stress mice with poor cognitive ability decreased significantly, while under the regulation of TP, the 5-HT concentration of stress mice increased and the cognitive function was improved (Chen et al., 2010).

Accordingly, modulating intestinal flora homeostasis, applying TP and SSRI to improve the concentration of 5-HT in the hippocampus of the brain, and weakening the accumulation of Aβ and α-Syn are expected to become a new therapeutic option for the management of neurological conditions (Mostert et al., 2008).

INTESTINAL FLORA-5-HT AND DEPRESSION, AUTISM

Depression is an affective disorder that accompanied by symptoms of low emotions, inattention, together with decreased volition and behavior. It also includes symptoms like inappropriate suicidal thoughts, insomnia, and anorexia (Bair et al., 2003). Modern studies have shown that depression is directly related to 5-HT, and the production of modern antidepressants mainly focus on elevating 5-HT concentration in the brain or inhibiting 5-HT uptake by platelets (Morais et al., 2021). Oral L-theanine can increase the levels of 5-HT and dopamine in striatum, hypothalamus and hippocampus (Zhu et al., 2012). Abnormal structure of the intestinal flora induce inflammation with the production of various inflammatory factors, whereby entering the CNS through circulatory pathway,

activating microglia in the glial cells, and promoting depressive episodes. Emerging evidence suggests that implantation the flora of depression and normal people into GF mice, respectively, showing the former had depression-like behaviors, flora diversity had changed and was highly similar to that of depressive patients (Zheng et al., 2016). MGB axis connects the emotions of the brain with the peripheral control and function of the intestine. 5-HT is a key element of this axis, acting as a neurotransmitter in the CNS and the ENS of the intestinal wall. *Lactobacillus* and *Bifidobacterium* are the two major probiotics, attenuating immune inflammatory factors, restoring the integrity of the intestinal barrier, regulating tryptophan metabolism, influencing 5-HT and mood.

The effect of 5-HT on mood has been studied through an acute tryptophan depletion technique whereby reducing dietary tryptophan leads to a lowering in brain 5-HT levels, which acquires analysis for 5-HT dependent behavior. The subjects ate food rich and lack in tryptophan, respectively, and then used pictures to exacerbate indignation of the subjects, ultimately utilized magnetic resonance imaging technology to observe the brain's response (Alkhalaf and Ryan, 2015). The results show that when tryptophan-deficient causing a decrease in the level of 5-HT in the body, the anger responses derived from brain are uneasy to suppress, meanwhile the signaling communications between the frontal lobe of the brain and the amygdala are reduced (Okaty et al., 2019). The frontal lobe is responsible for controlling emotions such as anger, while the amygdala is anger-related, yielding the view when deficient in 5-HT, the rational frontal lobe is unable to control the angry amygdala (Récamier-Carballo et al., 2017).

Autism, is a common disease of infants and young children with congenital developmental disorders. After treatment with *Bacteroides fragilis* or *Bacteroides polymorpha*, the structure of autism model mice changed close to normal mice (Iovene et al., 2017), and their autism symptoms were improved. Recent research also demonstrates that *Lactobacillus* has the ability to maintain intestinal homeostasis and facilitate the therapeutics of autism (Sgritta et al., 2019). The antidepressant effect of TP may be due to its ability to block the reuptake of the neurotransmitter 5-HT by the presynaptic membrane of nerve endings and increase the concentration of monoamines in the synaptic space (Wei et al., 2015). In addition, TP inhibited the activity of monoamine oxidase B and increased the level of monoamine in rat C6 astrocytes in a dose-dependent manner, indicating that monoamines play an important role in the pathophysiology of depression (Zhu et al., 2012; Frolkis et al., 2019). All of these indicate that the colonization of intestinal flora impact host behavior and the occurrence of related diseases.

INTESTINAL FLORA-5-HT AND IMMUNE DISEASE LIKE INFLAMMATORY BOWEL SYNDROME

Inflammatory bowel syndrome is a clinically common GI dysfunction disease along with manifestations such as abdominal pain, bloating, and changes in bowel habits, accompanied by anxiety, depression, irritability and other mental problems (Fond et al., 2014). These phenomena are considered to be hypersensitivity reactions of the MGB system. Studies have shown that the intestinal flora can elicit mononuclear macrophages and mast cells, release 5-HT, produce changes in IL-10, IL-6, IL-1β, TNF-α, and IFN-γ, and inhibit intestinal motility (Liu et al., 2009).

Experimental studies have shown that as the main body of ECs, mucosal mast cells are activated after acute stress, and they increase or approach the enteric nerve after chronic stress (Albert-Bayo et al., 2019). These mast cells release neuropeptides, namely 5-HT, proteases and pro-inflammatory cytokines, which are known to cause modifications in IBS intestinal sensory, motor, secretory and osmotic media. The amount of 5-HT in neonates increases after acute stress, while the increased 5-HT is closely related to the occurrence of IBS.

It is well known that stress-related can trigger alterations in intestinal motility, visceral sensitivity and intestinal secretion, as well as the occurrence of many extra-intestinal stress-related diseases (such as anxiety, depression or chronic pain syndrome), whereas 5-HT is a non-negligible therapeutic strategy in the treatment of stress-related diseases.

Usage of probiotics to ameliorate the intestinal environment of IBS and related mental problems may become an effective intervention. It is possible to renovate the diversity and stability of the intestinal flora as target, using intestinal prebiotics, antibiotics and fecal bacteria transplantation to elevate the abundance of symbiotic microorganisms, with decreasing flora ratio that can ameliorate IBS symptoms (such as *Clostridium*, *E. coli*, *Salmonella*, *Shigella*, and *Pseudomonas*), to achieve the purpose of treating IBS and other 5-HT-related MGB axis perturbations (Currò et al., 2017).

At present, studies have shown that there is a certain relationship between theanine and PPs in tea and 5-HT. TP not only produces neuroactive microbial metabolites, but also inhibits harmful bacteria, providing a source of nutrition for antidepressant-related probiotics. As a potential antidepressant, TP can treat inflammation in IBS, inhibit the activation of kynurenine pathway, promote digestive system and stop diarrhea (Mikocka-Walus et al., 2020; Cao et al., 2021). Under treatment such as antidepressants or psychotherapy, neurons may grow again. The study found that the level of brain-derived neurotrophic factor before neurogenesis increased with the treatment of antidepressants, and this increase seemed to be related to the degree of recovery of depression (Brunoni et al., 2008).

NEUROPROTECTIVE AND ANTI-INFLAMMATORY EFFECTS OF TEA POLYPHENOLS

Vascular dementia (VD) is a brain function disease with intellectual disability triggered by insufficient blood and oxygen supply to the brain owing to various diseases (Romay et al., 2019). It is the second largest dementia disease after AD. Hippocampus is a crucial structure that participates in the body's

spatial learning and memory. Cerebral ischemia and hypoxia can easily stimulate hippocampal neuronal apoptosis and decrease cognitive function. Several observational studies have indicated that after TP-intervention, the morphology of neurons in the CA1 area of the hippocampus of VD rats tended to be normal, and the deposition of Aβ decreased, illustrating that it has a protective effect on neurons (Simão et al., 2012; Libro et al., 2016; Fernando et al., 2017).

The PPs compounds may exert neuroprotective effects through anti-aggregation properties. TP inhibit the formation of wild-type α-Syn filamentous aggregates and depolymerize the fibrous α-Syn. EGCG can effectively restrain the formation of α-Syn filaments, and also convert large toxic α-Syn filaments into small non-toxic and non-fixed shape protein aggregates. Green tea intake can prevent the decrease of glutathione peroxidase, indicating that green tea has a protective effect on age-related oxidative damage. A wealth of evidence now implicates that TP is potentially bioactive substances with neuroprotective and neuromodulating activities (Wang Y. et al., 2021).

Studies have shown that interfere with EGCG in high-fat diet rats can significantly control the expression level of C-reactive protein, alleviate the red blood cell sedimentation rate and total white blood cell count, as well as inhibit the formation of atherosclerosis through anti-inflammatory effects (Song et al., 2021). In the insulin-resisting rat model, TP prevents the expression of inflammatory cytokines, enhance the production of anti-inflammatory proteins, and relieve the damage of chronic inflammation to the myocardium by regulating signaling communication associated with insulin, lipid metabolism and inflammation (Xia et al., 2019). In a LPS-induced rat model of acute lung injury, EGCG diminishes the expression of inflammatory factors by managing signal pathways, attenuates the accumulation of neutrophils in the lungs, and has a protective effect on lung injury (Wang M. et al., 2021).

While a small number of studies have reported the intake and brain distribution of edible TP, there are still great uncertainties in the dosage, absorption, metabolism, tissue distribution, and intracellular accumulation and excretion of TP (Hong et al., 2021). Therefore, these aspects may be the focus of future research.

CONCLUSION

Tea polyphenols, especially EGCG has been the focus of research owing to it multiple protective effects on various diseases of the host. A wealth of epidemiological studies and clinical trials has shown that appropriate supplementation of TP has obvious protective effects on chronic neurological diseases and related immune diseases. As such the low bioavailability of oral administration of TP, clinical application meets many as-yet-uncharacterized challenges. It is still unclear how to effectively deliver EGCG to the target site. Increasing information from both clinical and preclinical fields presents convincing evidence that crosstalk between the gut microbiota and associated metabolism along with the mammalian nervous system shapes dysregulated and stable neural processes. As the vast metabolites among gut microbes, SCFAs and 5-HT are proposed as a kind of transmission media, which establishes the inextricable connection between brain neurons and enteric neurons. Therefore, the co-evolution of host with their related microbial communities and metabolites seems to have led to complex biological communication between the intestine and the brain. This is a fascinating prospect that requires more research in the future, but also provides a promising new way for the regulation of mental and neurological diseases.

AUTHOR CONTRIBUTIONS

MH: conceptualization, validation, and writing – original draft. LC and PZ: supervision and writing – original draft. YL: conceptualization and validation. ZW: writing – original draft. XZ: supervision and writing – review and editing. All authors contributed to the article and approved the submitted version.

FUNDING

This work was sponsored by Zhejiang Provincial Key Research and Development Program (2020C02037) and People-benefit Project of Ningbo (202002N3078).

REFERENCES

Albert-Bayo, M., Paracuellos, I., González-Castro, A. M., Rodríguez-Urrutia, A., Rodríguez-Lagunas, M. J., Alonso-Cotoner, C., et al. (2019). Intestinal mucosal mast cells: key modulators of barrier function and homeostasis. *Cells* 8:135. doi: 10.3390/cells8020135

Alkhalaf, L. M., and Ryan, K. S. (2015). Biosynthetic manipulation of tryptophan in bacteria: pathways and mechanisms. *Chem. Biol.* 22, 317–328. doi: 10.1016/j.chembiol.2015.02.005

Bair, M. J., Robinson, R. L., Katon, W., and Kroenke, K. (2003). Depression and pain comorbidity: a literature review. *Arch. Intern. Med.* 163, 2433–2445. doi: 10.1001/archinte.163.20.2433

Brunoni, A. R., Lopes, M., and Fregni, F. (2008). A systematic review and meta-analysis of clinical studies on major depression and BDNF levels: implications for the role of neuroplasticity in depression. *Int. J. Neuropsychopharmacol.* 11, 1169–1180. doi: 10.1017/S1461145708009309

Cao, P. Q., Li, X. P., Ou-Yang, J., Jiang, R. G., Huang, F. F., Wen, B. B., et al. (2021). The protective effects of yellow tea extract against loperamide-induced constipation in mice. *Food Funct.* 12, 5621–5636. doi: 10.1039/d0fo02969f

Cardona, F., Andrés-Lacueva, C., Tulipani, S., Tinahones, F. J., and Queipo-Ortuño, M. I. (2013). Benefits of polyphenols on gut microbiota and implications in human health. *J. Nutr. Biochem.* 24, 1415–1422. doi: 10.1016/j.jnutbio.2013.05.001

Chen, I. J., Liu, C. Y., Chiu, J. P., and Hsu, C. H. (2016). Therapeutic effect of high-dose green tea extract on weight reduction: a randomized, double-blind, placebo-controlled clinical trial. *Clin. Nutr.* 35, 592–599. doi: 10.1016/j.clnu.2015.05.003

Chen, W. Q., Zhao, X. L., Wang, D. L., Li, S. T., Hou, Y., Hong, Y., et al. (2010). Effects of epigallocatechin-3-gallate on behavioral impairments induced by psychological stress in rats. *Exp. Biol. Med.* 235, 577–583. doi: 10.1258/ebm.2010.009329

Cirrito, J. R., Disabato, B. M., Restivo, J. L., Verges, D. K., Goebel, W. D., Sathyan, A., et al. (2011). Serotonin signaling is associated with lower amyloid-β levels and plaques in transgenic mice and humans. *Proc. Natl. Acad. Sci. U.S.A.* 108, 14968–14973. doi: 10.1073/pnas.1107411108

Correia, A. S., Cardoso, A., and Vale, N. (2021). Highlighting immune system and stress in major depressive disorder, Parkinson's, and Alzheimer's Diseases, with a connection with serotonin. *Int. J. Mol. Sci*. 22:8525. doi: 10.3390/ijms22168525

Costea, P. I., Hildebrand, F., Arumugam, M., Bäckhed, F., Blaser, M. J., Bushman, F. D., et al. (2018). Enterotypes in the landscape of gut microbial community composition. *Nat. Microbiol.* 3, 8–16. doi: 10.1038/s41564-017-0072-8

Currò, D., Ianiro, G., Pecere, S., Bibbò, S., and Cammarota, G. (2017). Probiotics, fibre and herbal medicinal products for functional and inflammatory bowel disorders. *Br. J. Pharmacol*. 174, 1426–1449. doi: 10.1111/bph.13632

Czajkowska, A., and Szponar, B. (2018). Short chain fatty acids (SCFA), the products of gut bacteria metabolism and their role in the host. *Postep. Hig. Med. Dosw.* 72, 131–142. doi: 10.5604/01.3001.0011.6468

David, L., Babin, A., Picos, A., and Dumitrascu, D. L. (2014). Small intestinal bacterial overgrowth is associated with intestinal inflammation in the irritable bowel syndrome. *Clujul. Med*. 87, 163–165. doi: 10.15386/cjmed-303

De Vadder, F., Grasset, E., Mannerås Holm, L., Karsenty, G., Macpherson, A. J., Olofsson, L. E., et al. (2018). Gut microbiota regulates maturation of the adult enteric nervous system via enteric serotonin networks. *Proc. Natl. Acad. Sci. U.S.A*. 115, 6458–6463. doi: 10.1073/pnas.1720017115

Ding, T., and Schloss, P. D. (2014). Dynamics and associations of microbial community types across the human body. *Nature* 509, 357–360. doi: 10.1038/nature13178

Duda-Chodak, A., Tarko, T., Satora, P., and Sroka, P. (2015). Interaction of dietary compounds, especially polyphenols, with the intestinal microbiota: a review. *Eur. J. Nutr*. 54, 325–341. doi: 10.1007/s00394-015-0852-y

Elson, C. O., and Cong, Y. (2012). Host-microbiota interactions in inflammatory bowel disease. *Gut Microbes* 3, 332–344. doi: 10.4161/gmic.20228

Fassarella, M., Blaak, E. E., Penders, J., Nauta, A., Smidt, H., and Zoetendal, E. G. (2021). Gut microbiome stability and resilience: elucidating the response to perturbations in order to modulate gut health. *Gut* 70, 595–605. doi: 10.1136/gutjnl-2020-321747

Fernando, W., Somaratne, G., Goozee, K. G., Williams, S., Singh, H., and Martins, R. N. (2017). Diabetes and Alzheimer's disease: can tea phytochemicals play a role in prevention? *J. Alzheimers Dis.* 59, 481–501. doi: 10.3233/JAD-161200

Fond, G., Loundou, A., Hamdani, N., Boukouaci, W., Dargel, A., Oliveira, J., et al. (2014). Anxiety and depression comorbidities in irritable bowel syndrome (IBS): a systematic review and meta-analysis. *Eur. Arch. Psychiatry Clin. Neurosci*. 264, 651–660. doi: 10.1007/s00406-014-0502-z

Frolkis, A. D., Vallerand, I. A., Shaheen, A. A., Lowerison, M. W., Swain, M. G., Barnabe, C., et al. (2019). Depression increases the risk of inflammatory bowel disease, which may be mitigated by the use of antidepressants in the treatment of depression. *Gut* 68, 1606–1612. doi: 10.1136/gutjnl-2018-317182

Fung, T. C., Vuong, H. E., Luna, C., Pronovost, G. N., Aleksandrova, A. A., Riley, N. G., et al. (2019). Intestinal serotonin and fluoxetine exposure modulate bacterial colonization in the gut. *Nat. Microbiol.* 4, 2064–2073. doi: 10.1038/s41564-019-0540-4

Furness, J. B. (2012). The enteric nervous system and neurogastroenterology. *Nat. Rev. Gastroenterol. Hepatol*. 9, 286–294. doi: 10.1038/nrgastro.2012.32

Galts, C., Bettio, L., Jewett, D. C., Yang, C. C., Brocardo, P. S., Rodrigues, A., et al. (2019). Depression in neurodegenerative diseases: common mechanisms and current treatment options. *Neurosci. Biobehav. Rev.* 102, 56–84. doi: 10.1016/j.neubiorev.2019.04.002

Gan, R. Y., Li, H. B., Sui, Z. Q., and Corke, H. (2018). Absorption, metabolism, anti-cancer effect and molecular targets of epigallocatechin gallate (EGCG): an updated review. *Crit. Rev. Food Sci. Nutr.* 58, 924–941. doi: 10.1080/10408398.2016.1231168

Gheorghe, C. E., Martin, J. A., Manriquez, F. V., Dinan, T. G., Cryan, J. F., and Clarke, G. (2019). Focus on the essentials: tryptophan metabolism and the microbiome-gut-brain axis. *Curr. Opin. Pharmacol*. 48, 137–145. doi: 10.1016/j.coph.2019.08.004

Ghosh, S. S., Wang, J., Yannie, P. J., and Ghosh, S. (2020). Intestinal barrier dysfunction, LPS translocation, and disease development. *J. Endocr. Soc.* 4:bvz039. doi: 10.1210/jendso/bvz039

Gong, J., Hu, M., Huang, Z., Fang, K., Wang, D., Chen, Q., et al. (2017). Berberine attenuates intestinal mucosal barrier dysfunction in type 2 diabetic rats. *Front. Pharmacol*. 8:42. doi: 10.3389/fphar.2017.00042

Gowd, V., Karim, N., Shishir, M. R. I., Xie, L. H., and Chen, W. (2019). Dietary polyphenols to combat the metabolic diseases via altering gut microbiota. *Trends Food Sci. Tech.* 93, 81–93. doi: 10.1016/j.tifs.2019.09.005

Guo, Y., Kitamoto, S., and Kamada, N. (2020). Microbial adaptation to the healthy and inflamed gut environments. *Gut Microbes*. 12:1857505. doi: 10.1080/19490976.2020.1857505

Han, Z. X., Rana, M. M., Liu, G. F., Gao, M. J., Li, D. X., Wu, F. G., et al. (2016). Green tea flavour determinants and their changes over manufacturing processes. *Food Chem.* 212, 739–748. doi: 10.1016/j.foodchem.2016.06.049

Holmqvist, S., Chutna, O., Bousset, L., Aldrin-Kirk, P., Li, W., Björklund, T., et al. (2014). Direct evidence of Parkinson pathology spread from the gastrointestinal tract to the brain in rats. *Acta Neuropathol.* 128, 805–820. doi: 10.1007/s00401-014-1343-6

Hong, M. Y., Ho, C. T., Zhang, X., Zhang, R. L., and Liu, Y. N. (2021). Dietary strategies may influence human nerves and emotions by regulating intestinal microbiota: an interesting hypothesis. *Int. J. Food. Sci. Tech.* 56, 3311–3321. doi: 10.1111/ijfs.14986

Huang, Y., Xing, K., Qiu, L., Wu, Q., and Wei, H. (2021). Therapeutic implications of functional tea ingredients for ameliorating inflammatory bowel disease: a focused review. *Crit. Rev. Food Sci. Nutr. [Online ahead of print]* doi: 10.1080/10408398.2021.1884532

Iovene, M. R., Bombace, F., Maresca, R., Sapone, A., Iardino, P., Picardi, A., et al. (2017). Intestinal dysbiosis and yeast isolation in stool of subjects with autism spectrum disorders. *Mycopathologia* 182, 349–363. doi: 10.1007/s11046-016-0068-6

Jameson, K. G., Olson, C. A., Kazmi, S. A., and Hsiao, E. Y. (2020). Toward understanding microbiome-neuronal signaling. *Mol. Cell.* 78, 577–583. doi: 10.1016/j.molcel.2020.03.006

Jenkins, T. A., Nguyen, J. C., Polglaze, K. E., and Bertrand, P. P. (2016). Influence of tryptophan and serotonin on mood and cognition with a possible role of the gut-brain axis. *Nutrients* 8:56. doi: 10.3390/nu8010056

Keszthelyi, D., Troost, F. J., and Masclee, A. A. (2009). Understanding the role of tryptophan and serotonin metabolism in gastrointestinal function. *Neurogastroenterol. Motil.* 21, 1239–1249. doi: 10.1111/j.1365-2982.2009.01370.x

Khan, N., and Mukhtar, H. (2018). Tea polyphenols in promotion of human health. *Nutrients* 11:39. doi: 10.3390/nu11010039

Kim, S., Covington, A., and Pamer, E. G. (2017). The intestinal microbiota: antibiotics, colonization resistance, and enteric pathogens. *Immunol. Rev*. 279, 90–105. doi: 10.1111/imr.12563

Koh, A., De Vadder, F., Kovatcheva-Datchary, P., and Bäckhed, F. (2016). From dietary fiber to host physiology: short-chain fatty acids as key bacterial metabolites. *Cell* 165, 1332–1345. doi: 10.1016/j.cell.2016.05.041

Laukoetter, M. G., Nava, P., and Nusrat, A. (2008). Role of the intestinal barrier in inflammatory bowel disease. *World J. Gastroenterol.* 14, 401–407. doi: 10.3748/wjg.14.401

Li, J., Chen, C., Yang, H., and Yang, X. (2021). Tea polyphenols regulate gut microbiota dysbiosis induced by antibiotic in mice. *Food Res. Int*. 141:110153. doi: 10.1016/j.foodres.2021.110153

Li, J., Chen, D., Yu, B., He, J., Zheng, P., Mao, X., et al. (2018). Fungi in gastrointestinal tracts of human and mice: from community to functions. *Microb. Ecol*. 75, 821–829. doi: 10.1007/s00248-017-1105-9

Li, Y., Zhong, W., Wang, D., Feng, Q., Liu, Z., Zhou, J., et al. (2016). Serotonin neurons in the dorsal raphe nucleus encode reward signals. *Nat. Commun*. 7:10503. doi: 10.1038/ncomms10503

Liang, S., Wu, X., and Jin, F. (2018). Gut-brain psychology: rethinking psychology from the microbiota-gut-brain axis. *Front. Integr. Neurosci.* 12:33. doi: 10.3389/fnint.2018.00033

Libro, R., Giacoppo, S., Soundara Rajan, T., Bramanti, P., and Mazzon, E. (2016). Natural phytochemicals in the treatment and prevention of dementia: an overview. *Molecules* 21:518. doi: 10.3390/molecules21040518

Lin, J. K., and Lin-Shiau, S. Y. (2006). Mechanisms of hypolipidemic and anti-obesity effects of tea and tea polyphenols. *Mol. Nutr. Food Res.* 50, 211–217. doi: 10.1002/mnfr.200500138

Liu, J. E., Zhang, Y., Zhang, J., Dong, P. L., Chen, M., and Duan, Z. P. (2010). Probiotic yogurt effects on intestinal flora of patients with chronic liver disease. *Nurs. Res*. 59, 426–432. doi: 10.1097/NNR.0b013e3181fa4dc6

Liu, M. T., Kuan, Y. H., Wang, J., Hen, R., and Gershon, M. D. (2009). 5-HT4 receptor-mediated neuroprotection and neurogenesis in the enteric nervous system of adult mice. *J. Neurosci.* 29, 9683–9699. doi: 10.1523/JNEUROSCI.1145-09.2009

Liu, Y., Jia, G., Gou, L., Sun, L., Fu, X., Lan, N., et al. (2013). Antidepressant-like effects of tea polyphenols on mouse model of chronic unpredictable mild stress. *Pharmacol. Biochem. Behav.* 104, 27–32. doi: 10.1016/j.pbb.2012.12.024

Liu, Y. W., Liong, M. T., and Tsai, Y. C. (2018). New perspectives of *Lactobacillus Plantarum* as a probiotic: the gut-heart-brain axis. *J. Microbiol.* 56, 601–613. doi: 10.1007/s12275-018-8079-2

Liu, Z., Bruins, M. E., Ni, L., and Vincken, J. P. (2018). Green and black tea phenolics: bioavailability, transformation by colonic microbiota, and modulation of colonic microbiota. *J. Agric. Food Chem.* 66, 8469–8477. doi: 10.1021/acs.jafc.8b02233

Lu, Y. C., Yeh, W. C., and Ohashi, P. S. (2008). LPS/TLR4 signal transduction pathway. *Cytokine* 42, 145–151. doi: 10.1016/j.cyto.2008.01.006

Macedo, D., Filho, A., Soares de Sousa, C. N., Quevedo, J., Barichello, T., Júnior, H., et al. (2017). Antidepressants, antimicrobials or both? Gut microbiota dysbiosis in depression and possible implications of the antimicrobial effects of antidepressant drugs for antidepressant effectiveness. *J. Affect. Disord.* 208, 22–32. doi: 10.1016/j.jad.2016.09.012

Makki, K., Deehan, E. C., Walter, J., and Bäckhed, F. (2018). The impact of dietary fiber on gut microbiota in host health and disease. *Cell Host Microbe* 23, 705–715. doi: 10.1016/j.chom.2018.05.012

Matsuoka, K., and Kanai, T. (2015). The gut microbiota and inflammatory bowel disease. *Semin. Immunopathol.* 37, 47–55. doi: 10.1007/s00281-014-0454-4

McCarville, J. L., Chen, G. Y., Cuevas, V. D., Troha, K., and Ayres, J. S. (2020). Microbiota metabolites in health and disease. *Annu. Rev. Immunol.* 38, 147–170. doi: 10.1146/annurev-immunol-071219-125715

Meneses, A., and Liy-Salmeron, G. (2012). Serotonin and emotion, learning and memory. *Rev. Neurosci.* 23, 543–553. doi: 10.1515/revneuro-2012-0060

Mikocka-Walus, A., Ford, A. C., and Drossman, D. A. (2020). Antidepressants in inflammatory bowel disease. *Nat. Rev. Gastroenterol. Hepatol.* 17, 184–192. doi: 10.1038/s41575-019-0259-y

Morais, L. H., Schreiber, H. L. 4th., and Mazmanian, S. K. (2021). The gut microbiota-brain axis in behaviour and brain disorders. *Nat. Rev. Microbiol.* 19, 241–255. doi: 10.1038/s41579-020-00460-0

Mostert, J. P., Koch, M. W., Heerings, M., Heersema, D. J., and De Keyser, J. (2008). Therapeutic potential of fluoxetine in neurological disorders. *CNS Neurosci. Ther.* 14, 153–164. doi: 10.1111/j.1527-3458.2008.00040.x

Musial, C., Kuban-Jankowska, A., and Gorska-Ponikowska, M. (2020). Beneficial properties of green tea catechins. *Int. J. Mol. Sci.* 21:1744. doi: 10.3390/ijms21051744

Nagao-Kitamoto, H., and Kamada, N. (2017). Host-microbial cross-talk in inflammatory bowel disease. *Immune Netw.* 17, 1–12. doi: 10.4110/in.2017.17.1.1

Nikolaus, S., Schulte, B., Al-Massad, N., Thieme, F., Schulte, D. M., Bethge, J., et al. (2017). Increased tryptophan metabolism is associated with activity of inflammatory bowel diseases. *Gastroenterology* 153, 1504.e2–1516.e2. doi: 10.1053/j.gastro.2017.08.028

Ochoa-Repáraz, J., and Kasper, L. H. (2016). The second brain: is the gut microbiota a link between obesity and central nervous system disorders? *Curr. Obes. Rep.* 5, 51–64. doi: 10.1007/s13679-016-0191-1

Ohishi, T., Fukutomi, R., Shoji, Y., Goto, S., and Isemura, M. (2021). The beneficial effects of principal polyphenols from green tea, coffee, wine, and curry on obesity. *Molecules* 26:453. doi: 10.3390/molecules26020453

Okaty, B. W., Commons, K. G., and Dymecki, S. M. (2019). Embracing diversity in the 5-HT neuronal system. *Nat. Rev. Neurosci.* 20, 397–424. doi: 10.1038/s41583-019-0151-3

Okuda, M. H., Zemdegs, J. C., de Santana, A. A., Santamarina, A. B., Moreno, M. F., Hachul, A. C., et al. (2014). Green tea extract improves high fat diet-induced hypothalamic inflammation, without affecting the serotoninergic system. *J. Nutr. Biochem.* 25, 1084–1089. doi: 10.1016/j.jnutbio.2014.05.012

Oliphant, K., and Allen-Vercoe, E. (2019). Macronutrient metabolism by the human gut microbiome: major fermentation by-products and their impact on host health. *Microbiome* 7:91. doi: 10.1186/s40168-019-0704-8

Ou, G. Y., Lin, W. W., and Zhao, W. J. (2021). Neuregulins in neurodegenerative diseases. *Front. Aging Neurosci.* 13:662474. doi: 10.3389/fnagi.2021.662474

Overby, H. B., and Ferguson, J. F. (2021). Gut microbiota-derived short-chain fatty acids facilitate microbiota: host cross talk and modulate obesity and hypertension. *Curr. Hypertens. Rep.* 23:8. doi: 10.1007/s11906-020-01125-2

Patel, S. S., Beer, S., Kearney, D. L., Phillips, G., and Carter, B. A. (2013). Green tea extract: a potential cause of acute liver failure. *World J. Gastroenterol.* 19, 5174–5177. doi: 10.3748/wjg.v19.i31.5174

Pérez-Burillo, S., Navajas-Porras, B., López-Maldonado, A., Hinojosa-Nogueira, D., Pastoriza, S., and Rufián-Henares, J. A. (2021). Green tea and its relation to human gut microbiome. *Molecules* 26:3907. doi: 10.3390/molecules26133907

Perron, N. R., Hodges, J. N., Jenkins, M., and Brumaghim, J. L. (2008). Predicting how polyphenol antioxidants prevent DNA damage by binding to iron. *Inorg. Chem.* 47, 6153–6161. doi: 10.1021/ic7022727

Perron, N. R., Wang, H. C., Deguire, S. N., Jenkins, M., Lawson, M., and Brumaghim, J. L. (2010). Kinetics of iron oxidation upon polyphenol binding. *Dalton Trans.* 39, 9982–9987. doi: 10.1039/c0dt00752h

Qi, C., Wang, P., Fu, T., Lu, M., Cai, Y., Chen, X., et al. (2021). A comprehensive review for gut microbes: technologies, interventions, metabolites and diseases. *Brief. Funct. Genomics*. 20, 42–60. doi: 10.1093/bfgp/elaa029

Raskov, H., Burcharth, J., Pommergaard, H. C., and Rosenberg, J. (2016). Irritable bowel syndrome, the microbiota and the gut-brain axis. *Gut Microbes* 7, 365–383.

Rebholz, H., Friedman, E., and Castello, J. (2018). Alterations of expression of the serotonin 5-HT4 receptor in brain disorders. *Int. J. Mol. Sci.* 19:3581. doi: 10.3390/ijms19113581

Récamier-Carballo, S., Estrada-Camarena, E., and López-Rubalcava, C. (2017). Maternal separation induces long-term effects on monoamines and brain-derived neurotrophic factor levels on the frontal cortex, amygdala, and hippocampus: differential effects after a stress challenge. *Behav. Pharmacol.* 28, 545–557. doi: 10.1097/FBP.0000000000000324

Remely, M., Ferk, F., Sterneder, S., Setayesh, T., Roth, S., Kepcija, T., et al. (2017). EGCG prevents high fat diet-induced changes in gut microbiota, decreases of DNA strand breaks, and changes in expression and DNA methylation of *Dnmt1* and *MLH1* in C57BL/6J male mice. *Oxid. Med. Cell Longev.* 2017:3079148. doi: 10.1155/2017/3079148

Reynaud, Y., Fakhry, J., Fothergill, L., Callaghan, B., Ringuet, M., Hunne, B., et al. (2016). The chemical coding of 5-hydroxytryptamine containing enteroendocrine cells in the mouse gastrointestinal tract. *Cell Tissue Res.* 364, 489–497. doi: 10.1007/s00441-015-2349-7

Rhoades, J. L., Nelson, J. C., Nwabudike, I., Yu, S. K., McLachlan, I. G., Madan, G. K., et al. (2019). ASICs mediate food responses in an enteric serotonergic neuron that controls foraging behaviors. *Cell* 176, 85.e14–97.e14. doi: 10.1016/j.cell.2018.11.023

Romay, M. C., Toro, C., and Iruela-Arispe, M. L. (2019). Emerging molecular mechanisms of vascular dementia. *Curr. Opin. Hematol.* 26, 199–206. doi: 10.1097/MOH.0000000000000502

Romo-Vaquero, M., Cortes-Martin, A., Loria-Kohen, V., Ramirez-de-Molina, A., Garcia-Mantrana, I., Collado, M. C., et al. (2019). Deciphering the human gut microbiome of urolithin metabotypes: association with enterotypes and potential cardiometabolic health implications. *Mol. Nutr. Food Res.* 63:e1800958. doi: 10.1002/mnfr.201800958

Roopchand, D. E., Carmody, R. N., Kuhn, P., Moskal, K., Rojas-Silva, P., Turnbaugh, P. J., et al. (2015). Dietary polyphenols promote growth of the gut bacterium akkermansia muciniphila and attenuate high-fat diet-induced metabolic syndrome. *Diabetes* 64, 2847–2858. doi: 10.2337/db14-1916

Sampson, T. R., Debelius, J. W., Thron, T., Janssen, S., Shastri, G. G., Ilhan, Z. E., et al. (2016). Gut microbiota regulate motor deficits and neuroinflammation in a model of Parkinson's disease. *Cell* 167, 1469.e1412–1480.e1412. doi: 10.1016/j.cell.2016.11.018

Saric, S., Notay, M., and Sivamani, R. K. (2016). Green tea and other tea polyphenols: effects on sebum production and acne vulgaris. *Antioxidants* 6:2. doi: 10.3390/antiox6010002

Sartor, R. B., and Wu, G. D. (2017). Roles for intestinal bacteria, viruses, and fungi in pathogenesis of inflammatory bowel diseases and therapeutic approaches. *Gastroenterology* 152, 327.e4–339.e4. doi: 10.1053/j.gastro.2016.10.012

Sasaki, H., Matsumoto, M., Tanaka, T., Maeda, M., Nakai, M., Hamada, S., et al. (2004). Antibacterial activity of polyphenol components in Oolong tea extract against streptococcus mutans. *Caries Res.* 38, 2–8. doi: 10.1159/000073913

Sgritta, M., Dooling, S. W., Buffington, S. A., Momin, E. N., Francis, M. B., Britton, R. A., et al. (2019). Mechanisms underlying microbial-mediated changes in

social behavior in mouse models of autism spectrum disorder. *Neuron* 101, 246.e6–259.e6. doi: 10.1016/j.neuron.2018.11.018

Simão, F., Matté, A., Pagnussat, A. S., Netto, C. A., and Salbego, C. G. (2012). Resveratrol prevents CA1 neurons against ischemic injury by parallel modulation of both GSK-3β and CREB through PI3-K/Akt pathways. *Eur. J. Neurosci.* 36, 2899–2905. doi: 10.1111/j.1460-9568.2012.08229.x

Song, D., Yang, C. S., Zhang, X., and Wang, Y. (2021). The relationship between host circadian rhythms and intestinal microbiota: a new cue to improve health by tea polyphenols. *Crit. Rev. Food Sci. Nutr*. 61, 139–148. doi: 10.1080/10408398.2020.1719473

Strandwitz, P. (2018). Neurotransmitter modulation by the gut microbiota. *Brain Res*. 1693, 128–133. doi: 10.1016/j.brainres.2018.03.015

Sun, Q. Y., Cheng, L., Zhang, X., Wu, Z. F., and Weng, P. F. (2021). The interaction between tea polyphenols and host intestinal microorganisms: an effective way to prevent psychiatric disorders. *Food Funct*. 12, 952–962. doi: 10.1039/d0fo02791j

Teixeira, L. D., Kling, D. N., Lorca, G. L., and Gonzalez, C. F. (2018). *Lactobacillus johnsonii* N6.2 diminishes caspase-1 maturation in the gastrointestinal system of diabetes prone rats. *Benef. Microbes* 9, 527–539. doi: 10.3920/BM2017.0120

Teixeira, L. D., Torrez Lamberti, M. F., DeBose-Scarlett, E., Bahadiroglu, E., Garrett, T. J., Gardner, C. L., et al. (2021). *Lactobacillus johnsonii* N6.2 and blueberry phytophenols affect lipidome and gut microbiota composition of rats under high-fat diet. *Front. Nutr.* 8:757256. doi: 10.3389/fnut.2021.757256

Thibault, R., Blachier, F., Darcy-Vrillon, B., de Coppet, P., Bourreille, A., and Segain, J. P. (2010). Butyrate utilization by the colonic mucosa in inflammatory bowel diseases: a transport deficiency. *Inflamm. Bowel Dis.* 16, 684–695. doi: 10.1002/ibd.21108

Tian, L., Kejing, Y., Zhang, S., Yi, J., Zhu, Z., Decker, E. A., et al. (2021). Impact of tea polyphenols on the stability of oil-in-water emulsions coated by whey proteins. *Food Chem.* 343:128448. doi: 10.1016/j.foodchem.2020.128448

Troha, K., and Ayres, J. S. (2020). Metabolic adaptations to infections at the organismal level. *Trends Immunol*. 41, 113–125. doi: 10.1016/j.it.2019.12.001

Van Treuren, W., and Dodd, D. (2020). Microbial contribution to the human metabolome: implications for health and disease. *Annu. Rev. Pathol*. 15, 345–369. doi: 10.1146/annurev-pathol-020117-043559

Wang, L. X., Liu, K., Gao, D. W., and Hao, J. K. (2013). Protective effects of two *Lactobacillus plantarum* strains in hyperlipidemic mice. *World J. Gastroenterol.* 19, 3150–3156. doi: 10.3748/wjg.v19.i20.3150

Wang, M., Zhong, H., Zhang, X., Huang, X., Wang, J., Li, Z., et al. (2021). EGCG promotes PRKCA expression to alleviate LPS-induced acute lung injury and inflammatory response. *Sci. Rep.* 11:11014. doi: 10.1038/s41598-021-90398-x

Wang, S. T., Cui, W. Q., Pan, D., Jiang, M., Chang, B., and Sang, L. X. (2020). Tea polyphenols and their chemopreventive and therapeutic effects on colorectal cancer. *World J. Gastroenterol.* 26, 562–597. doi: 10.3748/wjg.v26.i6.562

Wang, Y., Tong, Q., Ma, S. R., Zhao, Z. X., Pan, L. B., Cong, L., et al. (2021). Oral berberine improves brain dopa/dopamine levels to ameliorate Parkinson's disease by regulating gut microbiota. *Signal Transduct. Target. Ther*. 6:77. doi: 10.1038/s41392-020-00456-5

Wei, J., He, J. B., Chen, C. L., and Wang, X. K. (2015). A catechin-modified carbon paste electrode for electrocatalytic determination of neurotransmitters. *Anal. Methods* 7, 5641–5648. doi: 10.1039/c5ay00928f

Włodarek, D. (2019). Role of ketogenic diets in neurodegenerative diseases (Alzheimer's disease and Parkinson's disease). *Nutrients* 11:169. doi: 10.3390/nu11010169

Wu, Z., Huang, S., Li, T., Li, N., Han, D., Zhang, B., et al. (2021). Gut microbiota from green tea polyphenol-dosed mice improves intestinal epithelial homeostasis and ameliorates experimental colitis. *Microbiome* 9:184. doi: 10.1186/s40168-021-01115-9

Xia, H. M., Wang, J., Xie, X. J., Xu, L. J., and Tang, S. Q. (2019). Green tea polyphenols attenuate hepatic steatosis, and reduce insulin resistance and inflammation in high-fat diet-induced rats. *Int. J. Mol. Med.* 44, 1523–1530. doi: 10.3892/ijmm.2019.4285

Yan, R., Yang, C. S., and Zhang, X. (2021). Maintain host health with time-restricted eating and phytochemicals: a review based on gut microbiome and circadian rhythm. *Trends Food Sci. Technol.* 108, 258–268. doi: 10.1016/j.tifs.2021.01.007

Yan, Z., Zhong, Y., Duan, Y., Chen, Q., and Li, F. (2020). Antioxidant mechanism of tea polyphenols and its impact on health benefits. *Anim. Nutr.* 6, 115–123. doi: 10.1016/j.aninu.2020.01.001

Yao, X., Li, L., Kandhare, A. D., Mukherjee-Kandhare, A. A., and Bodhankar, S. L. (2020). Attenuation of reserpine-induced fibromyalgia via ROS and serotonergic pathway modulation by fisetin, a plant flavonoid polyphenol. *Exp. Ther. Med*. 19, 1343–1355. doi: 10.3892/etm.2019.8328

Zeng, J., Du, G., Shao, X., Feng, K. N., and Zeng, Y. (2019). Recombinant polyphenol oxidases for production of theaflavins from tea polyphenols. *Int. J. Biol. Macromol*. 134, 139–145. doi: 10.1016/j.ijbiomac.2019.04.142

Zhang, R., Liu, L. L., Wang, X. W., Guo, C. Y., and Zhu, H. (2020). Dietary tea polyphenols induce changes in immune response and intestinal microbiota in Koi carp, cryprinus carpio. *Aquaculture* 516:734636. doi: 10.1016/j.aquaculture.2019.734636

Zhang, Z., Zhang, Y., Li, J., Fu, C., and Zhang, X. (2021). The neuroprotective effect of tea polyphenols on the regulation of intestinal flora. *Molecules* 26:3692. doi: 10.3390/molecules26123692

Zhao, X., Jiang, Z., Yang, F., Wang, Y., Gao, X., Wang, Y., et al. (2016). Sensitive and simplified detection of antibiotic influence on the dynamic and versatile changes of fecal short-chain fatty acids. *PLoS One* 11:e0167032. doi: 10.1371/journal.pone.0167032

Zheng, P., Zeng, B., Zhou, C., Liu, M., Fang, Z., Xu, X., et al. (2016). Gut microbiome remodeling induces depressive-like behaviors through a pathway mediated by the host's metabolism. *Mol. Psychiatry* 21, 786–796. doi: 10.1038/mp.2016.44

Zhou, N., Gu, X., Zhuang, T., Xu, Y., Yang, L., and Zhou, M. (2020). Gut microbiota: a pivotal hub for polyphenols as antidepressants. *J. Agric. Food Chem*. 68, 6007–6020. doi: 10.1021/acs.jafc.0c01461

Zhu, M. Z., Li, N., Zhou, F., Ouyang, J., Lu, D. M., Xu, W., et al. (2020). Microbial bioconversion of the chemical components in dark tea. *Food Chem*. 312:126043. doi: 10.1016/j.foodchem.2019.126043

Zhu, W. L., Shi, H. S., Wei, Y. M., Wang, S. J., Sun, C. Y., Ding, Z. B., et al. (2012). Green tea polyphenols produce antidepressant-like effects in adult mice. *Pharmacol. Res.* 65, 74–80. doi: 10.1016/j.phrs.2011.09.007

Conflict of Interest: The authors declare that the research was conducted in the absence of any commercial or financial relationships that could be construed as a potential conflict of interest.

Publisher's Note: All claims expressed in this article are solely those of the authors and do not necessarily represent those of their affiliated organizations, or those of the publisher, the editors and the reviewers. Any product that may be evaluated in this article, or claim that may be made by its manufacturer, is not guaranteed or endorsed by the publisher.

frontiers | Frontiers in Microbiology

ORIGINAL RESEARCH
published: 07 April 2022
doi: 10.3389/fmicb.2022.862882

Dissecting the Effect of Berberine on the Intestinal Microbiome in the Weaned Piglets by Metagenomic Sequencing

Hong Hu[1], Kexing Xu[1], Kunping Wang[1], Feng Zhang[1,2] and Xi Bai[1]**

[1] College of Animal Science, Anhui Science and Technology University, Chuzhou, China, [2] Anhui Province Key Laboratory of Animal Nutrition Regulation and Health, Chuzhou, China

OPEN ACCESS

Edited by:
Zheng Ruan,
Nanchang University, China

Reviewed by:
Wei Zhang,
Institute of Animal Husbandry and Veterinary Medicine, Anhui Academy of Agricultural Sciences (CAAS), China
Hua Rong,
Yunnan Agricultural University, China

***Correspondence:**
Feng Zhang
zhangfeng@ahstu.edu.cn
Xi Bai
baixi1987326@163.com

Specialty section:
This article was submitted to Food Microbiology, a section of the journal Frontiers in Microbiology

Received: *26 January 2022*
Accepted: *11 February 2022*
Published: *07 April 2022*

Citation:
Hu H, Xu K, Wang K, Zhang F and Bai X (2022) Dissecting the Effect of Berberine on the Intestinal Microbiome in the Weaned Piglets by Metagenomic Sequencing. Front. Microbiol. 13:862882. doi: 10.3389/fmicb.2022.862882

This study aimed to investigate the microbial structure and function in the rectum of weaned piglets with berberine supplementation. Twelve healthy 21-day-old Duorc × (Landrace × Large White) weaned piglets (similar body weight) were evenly divided into control and berberine groups and were fed a basal diet supplemented with 0 and 0.1% berberine, respectively. After 21 days, metagenomic sequencing analysis was performed to detect microbial composition and function in the rectum of weaned piglets. Results showed that there were 10,597,721,931–14,059,392,900 base pairs (bp) and 10,186,558,171–15,859,563,342 bp of clean data in the control and berberine groups, respectively. The Q20s of the control and berberine groups were 97.15 to 97.7% and 96.26 to 97.68%, respectively. The microorganisms in the berberine group had lower ($p < 0.05$) Chao1, alternating conditional expectation, Shannon, and Simpson indices at the species levels than those in the control group. Analysis of similarity showed that there were significant differences ($p < 0.01$) between the control and berberine groups at the genus and species levels of the gut microorganisms. Dietary berberine significantly increased ($p < 0.05$) the abundance of *Subdoligranulum variabile*, but decreased ($p < 0.05$) the abundance of *Prevotella copri* compared with the control group. Carbohydrate-active enzymes analysis revealed that the levels of polysaccharide lyases and carbohydrate esterases were lower ($p < 0.05$) in the berberine group than that in the control group. Linear discriminant analysis effect size analysis showed that berberine supplementation could induce various significant Kyoto Encyclopedia of Genes and Genomes pathways, including carbohydrate metabolism, environmental information processing, and microbial metabolism in diverse environments. In conclusion, our findings suggest that berberine could improve the composition, abundance, structure, and function of gut microbiome in the weaned piglets, potentially providing a suitable approach for the application of berberine in human and animal health.

Keywords: weaned piglets, berberine, gut microbiota, metagenomic sequencing, microbial function

INTRODUCTION

Berberine is an isoquinoline alkaloid isolated from the traditional Chinese herb *Coptis chinensis*, which is widely used for its medicinal properties. Berberine has antidiarrheal, antibacterial, anti-inflammatory, antitumor, and hypoglycemic effects. It has good therapeutic effect on intestinal inflammation, diabetes, hypertension, and tumors (Fu et al., 2020; Huang et al., 2021; Patel, 2021). Specifically, the therapeutic effect of berberine on intestinal bacterial infection has been investigated for its potential use in clinical practice (Yu M. et al., 2020). Berberine helps in maintaining the intestinal health as it accumulates in the intestine easily and is beneficial in improving the imbalance in intestinal bacteria (Wu et al., 2020).

The intestinal microflora is a complex microbial system composed of a variety of microorganisms participating in numerous physiological processes of the body (Jin et al., 2019; Ma and Ma, 2019; Sun et al., 2020). The intestine harbors various microorganisms such as *Lactobacillus*, *Bacillus*, *Enterobacter*, *Bifidobacterium*, and *Enterococcus*. Initially, the gut microflora was thought to be closely related only to digestion and nutrient absorption; however, recent studies reported that it affects the body health by regulating metabolic diseases, such as obesity, diabetes, and cardiovascular diseases, as well as immune-related disorders (Schippa and Conte, 2014; Yadav and Jha, 2019). As the largest and most complex microecosystem of the body, intestinal microorganisms and their metabolites play an important role in animal health.

Limited studies have focused on the possible link between microbiome and function of gut microflora with berberine supplementation in weaned piglets. With the development of metagenomic high-throughput sequencing technology, it is possible to analyze a large number of microbial community species, abundance, and related biological information by performing total microbial DNA extraction from a specific environment and library construction (Fraher et al., 2012; Zhou et al., 2015; Quan et al., 2019). Thus, a large amount of information on non-culturable microbial flora can be obtained without the need of isolation and culture methods used in traditional microbial research (Guo et al., 2014; Walker et al., 2014). Currently, metagenomic sequencing technology has become an important tool to study intestinal environmental microorganisms. In the present study, this technique was used to characterize the microbial composition and function in the rectum of weaned pigs supplemented with berberine.

MATERIALS AND METHODS

Animals and Experimental Design

The animal experimental design was approved by the Animal Care and Use Committee of Anhui Science and Technology University. Twelve healthy 21-day-old Duorc × (Landrace × Large White) weaned piglets (similar body weight) were purchased from Qingxuan Agricultural Development Co., Ltd. (Bengbu, China), and equally divided into the control and berberine groups (six replicates and one pig/replicate). Pigs in the control and berberine groups were fed a basal diet supplemented with 0 and 0.1% berberine, respectively. Berberine chloride hydrate (purity ≥ 98%) was obtained from Aladdin Reagent Co., Ltd. (China). A basal diet (**Table 1**) was designed on the basis of National Research Council [NRC] (2012). Piglets could feed and drink water freely.

Sample Collection

After 21 days, the stool samples were collected from the rectum of all piglets by rectal massage. These samples were immediately stored in liquid nitrogen (−196°C) for further analysis and metagenomic sequencing.

Genomic DNA Extraction

Genomic DNA was isolated from stool samples using Magen HiPure Bacterial DNA Kits (Guangzhou, China). The quality of genomic DNA was verified using Qubit Fluorometric Quantification and Nanodrop Spectrophotometers (Thermo Fisher Scientific, Waltham, MA, United States).

Metagenomic Sequencing Analysis

Metagenomic sequencing analysis was performed as described by Liu et al. (2020). Briefly, 12 metagenomic DNA libraries

TABLE 1 | Composition and nutrient levels of basal diets (%, as-fed basis).

Items	Content (%)
Corn	37.50
Puffed corn	15.00
Soybean meal	15.00
Puffed soybean	10.0
Egg yolk power	2.00
Fish meal	2.50
Whey power	10.00
Sugar	2.00
Soybean oil	2.00
Vitamin and mineral premix*	4.00
Total	100.00
Nutrient levels	
CP	19.15
DE, MJ/kg	14.64
Lys	1.38
Thr	0.86
Met	0.41
Ca	0.65
AP	0.35

**Provided per kilogram of diet: Zn ($ZnSO_4 \cdot H_2O$), 100 mg; Cu ($CuSO_4 \cdot 5H_2O$), 125 mg; Mn ($MnSO_4 \cdot H_2O$), 60 mg; Fe ($FeSO_4 \cdot H_2O$), 120 mg; I [$Ca(IO_3)_2$], 0.6 mg; Se (Na_2SeO_3), 0.30 mg; vitamin A, 10,000 IU; vitamin D_3, 2,500 IU, vitamin 35 IU; vitamin K_3, 3.0 IU; vitamin B_5, 40 mg; nicotinic acid, 60 mg; folic acid, 1 mg; biotin, 0.2 mg; vitamin B_6, 4.0 mg; vitamin B_2, 7.5 mg; vitamin B_1, 5.0 mg; vitamin B_{12}, 0.08 mg.*

were constructed using NEBNext™ MLtra® DNA Library Prep Kit (NEB, Ipswich, MA, United States) for Illumina. Polymerase chain reaction was used to amplify 300- to 400-bp-long DNA fragments. Metagenomic sequencing was carried out on an Illumina Novaseq 6000 platform at Gene *Denovo* Biotechnology Co., Ltd. (Guangzhou, China). Clean data were obtained from raw data using FASTP 18.0 software (Chen et al., 2018), which was used for further genome assembly.

Bioinformatics Analysis

Bioinformatics analysis of the metagenomic sequence was performed as described by Liu et al. (2020). Gene assembly and prediction were performed using MEGAHIT 11.2 and MetaGeneMark 3.38, respectively.

α Diversity refers to the richness of species/functions in an intestinal microbial environment, which indicates the balance state and living conditions of the gut microorganisms. Analysis of α diversity with Chao1, alternating conditional expectation (ACE), Shannon, and Simpson parameters were performed using the Python scikit-bio package.

Analysis of similarity (ANOSIM) is a test method for analyzing microbial community structure, which is used to test whether the difference between groups is significantly greater than that within groups. ANOSIM test was performed using the vegan R package.

The Venn graph was plotted using VennDiagram package in R project. Welch *t* and analysis of variance (ANOVA) tests were used to show the species with significant differences between the two groups. Prediction of carbohydrate-active enzymes (CAZy) was performed using the CAZy databases. Kyoto Encyclopedia of Genes and Genomes (KEGG) pathway analysis was performed using the DIAMOND software in the KEGG databases. Linear discriminant analysis effect size (LEfSe) analysis was performed by LEfSe software. All bioinformatics analyses were performed using the R software, and $p < 0.05$ indicates statistical significance.

RESULTS

Analysis of the Intestinal Microbial Metagenomic Sequencing Data in Weaned Piglets

Twelve metagenomic DNA libraries constructed from the control and berberine groups were sequenced on the Illumina Novaseq 6000 platform. As shown in **Table 2**, there were 10,622,678,100–14,120,565,000 base pairs (bp) and 10,226,653,500–15,941,277,000 bp of raw data in the control and berberine groups, respectively. After filtering these data, 10,597,721,931–14,059,392,900 bp and 10,186,558,171–15,859,563,34 bp of clean data were obtained in the control and berberine groups, respectively (**Table 2**). The Q20s (%) of the control and berberine groups were 97.15 to 97.7% and 96.26 to 97.68%, respectively (**Table 2**). Furthermore, the GC contents (%) of the control and berberine groups were 43.86 to 47.3% and 42.94 to 49.59%, respectively (**Table 2**). Negligible *n* (%) content was found in both groups (**Table 2**).

Effect of Berberine on Microbiome Diversity (α-Diversity Analysis) of Pig Gut Microbiome

The microorganisms in the berberine group had lower ($p < 0.05$) Chao1, ACE, Shannon, and Simpson indices at the species levels than those in the control group (**Figure 1**).

Analysis of Similarity Between the Control and Berberine Groups

As shown in **Figure 2**, there was significant difference ($p < 0.01$) between the control and berberine groups at the genus and species levels of the gut microorganisms.

TABLE 2 | Sequencing data of intestinal microbial metagenomics in weaned piglets.

Sample	Raw data (bp)	Clean data (bp)	Q20 (%)	*n* (%)	GC (%)
Control1	10,814,343,000	10,785,737,116 (99.74%)	10,537,625,000 (97.7%)	288,590 (0.0%)	5,101,805,024 (47.3%)
Control2	10,622,678,100	10,597,721,931 (99.77%)	10,324,690,051 (97.42%)	293,195 (0.0%)	4,895,352,310 (46.2%)
Control3	10,826,112,300	10,795,693,976 (99.72%)	10,527,897,184 (97.52%)	298,263 (0.0%)	5,017,055,625 (46.47%)
Control4	11,016,380,100	10,987,285,740 (99.74%)	10,718,060,574 (97.55%)	260,469 (0.0%)	5,420,474,218 (49.33%)
Control5	11,120,942,100	11,088,979,787 (99.71%)	10,799,013,973 (97.39%)	274,779 (0.0%)	5,113,743,984 (46.12%)
Control6	14,120,565,000	14,059,392,900 (99.57%)	13,659,274,446 (97.15%)	150,051 (0.02%)	6,166,217,653 (43.86%)
Berberine1	10,226,653,500	10,186,558,171 (99.61%)	9,805,479,415 (96.26%)	169,146 (0.0%)	4,636,233,462 (45.52%)
Berberine2	10,891,334,700	10,867,882,674 (99.78%)	10,589,454,821 (97.44%)	276,217 (0.0%)	5,389,587,090 (49.59%)
Berberine3	10,629,873,300	10,609,483,224 (99.81%)	10,349,069,808 (97.55%)	281,753 (0.0%)	4,956,793,040 (46.72%)
Berberine4	10,745,099,400	10,720,204,112 (99.77%)	10,431,619,440 (97.31%)	299,057 (0.0%)	5,289,747,437 (49.34%)
Berberine5	15,941,277,000	15,859,563,342 (99.49%)	15,285,113,751 (96.38%)	169,138 (0.02%)	6,809,305,846 (42.94%)
Berberine6	10,531,396,200	10,507,346,266 (99.78%)	10,263,382,226 (97.68%)	384,034 (0.0%)	4,658,637,700 (44.34%)

Q20 (%) is the percentage of equal Q20 data in the clean data; n (%) is the percentage of N bases in the clean data. GC (%) is the percentage of G and C bases in clean data.

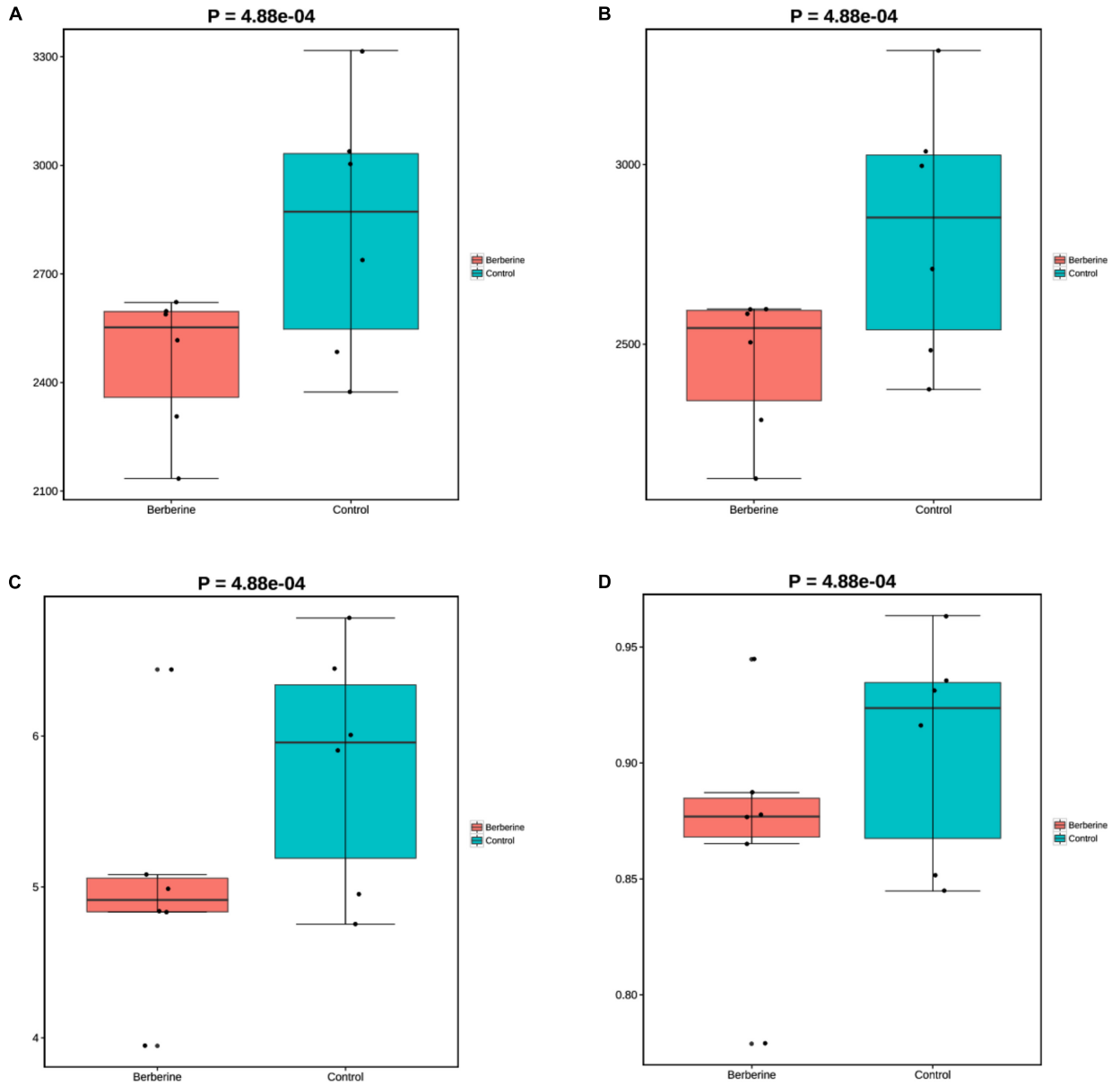

FIGURE 1 | Effects of berberine on microbiome diversity (α-diversity analysis) of pig gut microbiome (**A:** Chao1; **B:** ACE; **C:** Shannon; **D:** Simpson).

Species Venn Analysis Between the Control and Berberine Groups

The species distribution in microbial communities of the different treatment groups has a certain degree of similarity and specificity. In order to understand the species differences, Venn diagram was used to show the common and unique information between the different groups based on the species abundance information of samples. As shown in **Figure 3**, a total of 3,218 microbial species were common in both groups; however, 1,314 and 525 microbial species were unique in the control and berberine groups, respectively.

Effects of Berberine on Microbial Species of Pig Gut Microbiome

Welch *t*-test showed that berberine supplementation significantly increased ($p < 0.05$) the abundance of *Subdoligranulum variabile*, *Lactobacillus johnsonii*, *Parabacteroides distasonis*, *Fournierella massiliensis*, *Ruthenibacterium lactatiformans*, *Frisingicoccus caecimuris*, and *Gemmiger formicilis*, but significantly decreased ($p < 0.05$) the abundance of *Prevotella copri*, *Prevotella* sp. P2-180, *Prevotella* sp. P4-76, *Prevotella* sp. AM42-24, *Prevotella* sp. 885, *Prevotella* sp. P5-50, *Erysipelotrichaceae bacterium* YH-PanP20, *Prevotellaceae bacterium*, and *Phascolarctobacterium succinatutens* compared

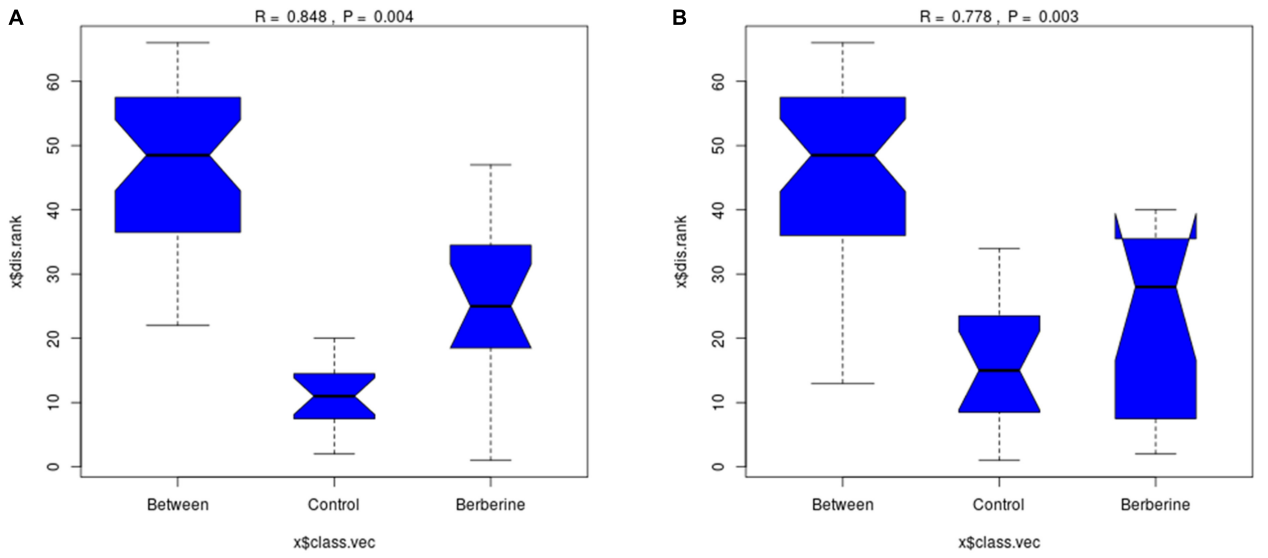

FIGURE 2 | Analysis of similarity analysis between control and berberine groups (**A:** genus levels; **B:** species levels).

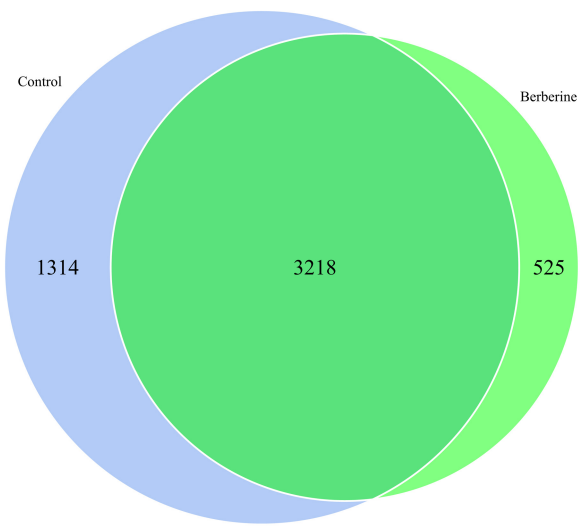

FIGURE 3 | Species Venn analysis between control and berberine groups.

with the control group (**Figure 4**). ANOVA test showed that berberine supplementation significantly increased ($p < 0.05$) the abundance of *S. variabile*, but significantly decreased ($p < 0.05$) the abundance of *P. copri* compared with the control group (**Figure 5**).

CAZy Analysis Between the Control and Berberine Groups

CAZy include glycoside hydrolases, glycosyl transferases, polysaccharide lyases (PLs), carbohydrate esterases (CEs), and auxiliary activities. As shown in **Figure 6**, PL and CE levels were lower in the berberine group than that in the control group.

Kyoto Encyclopedia of Genes and Genomes Analysis Between the Control and Berberine Groups

The results of LEfSe analysis in the berberine group were significantly associated with various KEGG pathways, including carbohydrate metabolism, environmental information processing, microbial metabolism in diverse environments, drug metabolism cytochrome P450, cellular community prokaryotes, dioxin degradation, xylene degradation, *Staphylococcus aureus* infection, starch and sucrose metabolism, toluene degradation, and so on (**Figure 7**).

DISCUSSION

Early weaning of piglets can shorten the slaughter cycle of pigs and improve the reproductive performance of sows. However, incomplete development of intestinal microbiota in early weaned piglets may lead to intestinal irritability and reduced production performance (Moeser et al., 2017; Upadhaya and Kim, 2021). Antibiotics can improve the above conditions, but the problem of antibiotic residues needs to be addressed (Yang et al., 2019). Berberine, a traditional Chinese herbal extract, has strong antibacterial effect and is an effective antibiotic substitute (Xu et al., 2020; Zhu et al., 2021). However, few studies have focused on the effect of berberine on the gut microbiota in early weaned piglets. In this work, the macrogenomics and high-throughput sequencing techniques were used to investigate the effects of berberine on intestinal microbiome and function of early weaned piglets (weaning age: 21 days).

Metagenomic analysis involves the DNA extraction from all microorganisms in environmental samples directly

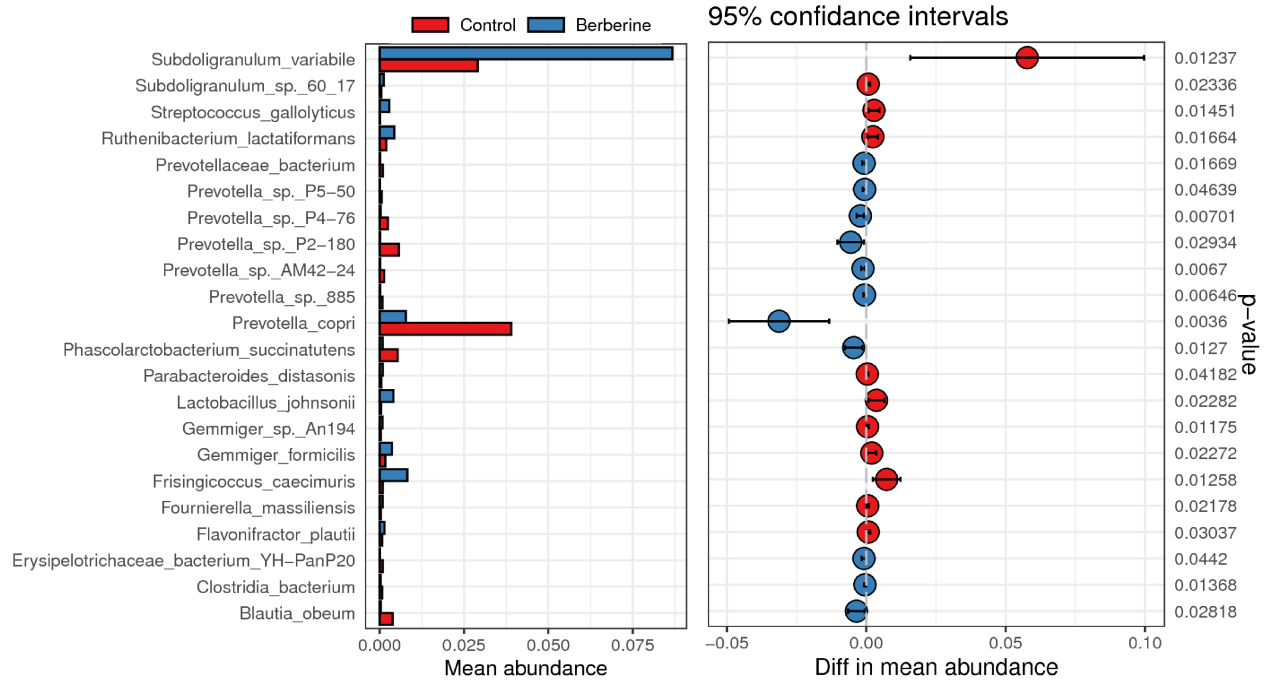

FIGURE 4 | Welch *t*-test of berberine on microbial species of pig gut microbiome.

followed by a metagenomic library construction and uses high-throughput sequencing technique to study the genetic composition and community functions of these microorganisms (Prayogo et al., 2020). Animal microbial population is distributed on the body surface, oral cavity, gastrointestinal tract, and reproductive tracts, but there are significant differences in the types and quantities of microorganisms based on dietary, species, sex, and age. The microbes in the gut are more numerous than the body's other organs. The complexity of the environment and microorganisms results in less rigorous data analysis using traditional methods; however, the development of metagenomics and high-throughput sequencing technology has promoted the study of gut microbes considerably (Walker et al., 2014; Guo et al., 2021). In the present study, a major part of raw data (>99%) contributed to the clean data, and the Q20 (%) was more than 96% in the gut microbiomes of the control and berberine groups. A total of 68.7 and 68.3 billion bp clean reads were obtained by conducting metagenomic sequencing of the control and berberine groups, respectively. ANOSIM revealed that the control and berberine groups had significant differences at the genus and species levels of intestinal microorganisms in weaned piglets. These results suggest that the metagenomic sequencing data were reliable and sufficient to investigate the effects of berberine on the gut microbial diversity and function in weaned piglets.

Nutritional digestion and absorption, physiology, metabolism, intestinal barrier, immune function, and disease onset are affected by the composition, diversity, and functional changes in intestinal microflora (Chang and Martinez-Guryn, 2019; Liu et al., 2019). Accordingly, the stability of microecological environment plays a crucial role in animal health regulation. Berberine shows a broad-spectrum antibacterial effect against a variety of gram-positive, gram-negative, and drug-resistant bacteria (Yue et al., 2019; Jamshaid et al., 2020). The effects of berberine influence intestinal infectious disease development and body health through the inhibition of intestinal bacteria (Zhu et al., 2021). Studies have shown that berberine can directly regulate the structure of intestinal microbiota by reducing the number of intestinal microbes in a dose-dependent manner (Zhang et al., 2019). In metagenomics research, Chao1, ACE, Shannon, and Simpson indices are used to study the gut microbiome diversity. We found that dietary 0.1% berberine significantly decreased these indices at the species level compared with those in the control group, suggesting toward the efficacy of berberine in reducing the richness and diversity of intestinal microbiome. Similarly, research conducted by Zhang et al. (2019) revealed that berberine decreased the diversity and quantity of the intestinal microflora in db/db mice.

Berberine is not easily absorbed after oral administration; thus, it can maintain a high concentration in the gastrointestinal tract, providing the necessary conditions required for inhibiting the intestinal bacterial growth (Cheng et al., 2021). In addition, as an antibacterial drug, it can inhibit a variety of pathogenic bacteria and change the structure of intestinal microflora (Habtemariam, 2020; Yu C. et al., 2020; Cheng et al., 2021). The most common mechanism of berberine-mediated regulation of intestinal flora is to change the original dominant intestinal bacteria to maintain the microecological

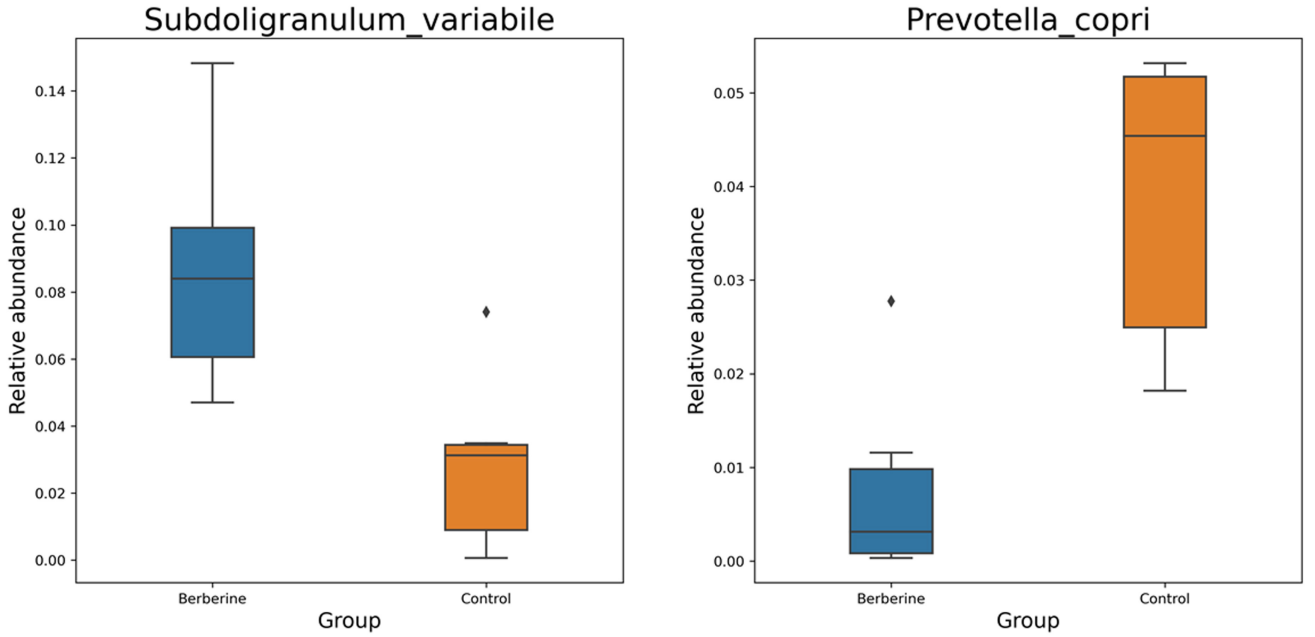

FIGURE 5 | ANOVA test of berberine on microbial species of pig gut microbiome.

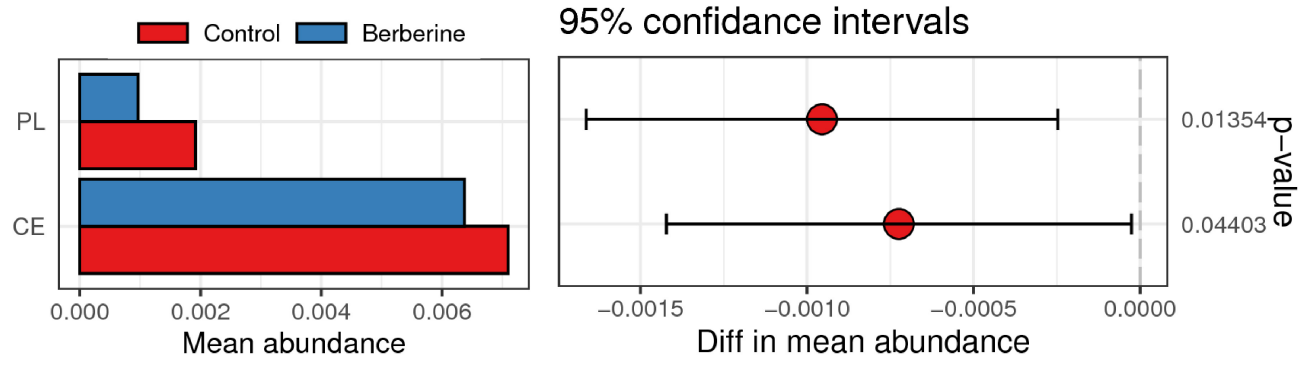

FIGURE 6 | Analysis of CAZy between control and berberine groups.

balance. Habtemariam (2020) suggested that the underlying mechanism for the multifunctional role of berberine was its regulation of gut microbiota. Zhang et al. (2012) showed that berberine with high-fat diet in rats could increase the abundance of *Allobaculum* and *Blautia* in the intestine. Dietary berberine also increased the abundance of beneficial bacteria including *S. variabile*, *L. johnsonii*, and *P. distasonis*, as shown in the present study. *S. variabile* improves gut mucosal immune response and inhibits food allergy in mice (Abdel-Gadir et al., 2019). *L. johnsonii* can promote growth, gut development, and intestinal microorganisms in pig, mice, and chicken, when used as a probiotic (Wang et al., 2017; He et al., 2019; Wang et al., 2020). The abundance of *P. distasonis* was negatively correlated with obesity, non-alcoholic fatty liver disease, diabetes, and other disease states, suggesting that it possibly plays a positive regulatory role in glucose and lipid metabolism (Wang et al., 2019). By contrast, dietary berberine decreased the abundance of *P. copri*, which leads to changes in microbiota metabolism and reduces interleukin-18 production. This aggravates the intestinal inflammation and may result in systemic autoimmunity (Ley, 2016).

Berberine can activate some signaling pathways and carbohydrate-related enzymes by improving intestinal microflora and health (Liao et al., 2020; Li et al., 2021). Findings from the present study revealed that berberine changed the structure, abundance, and function of gut microbiota in weaned piglets. Alterations in the gut microbiota lead to functional changes as well. Dietary berberine could markedly affect the CAZy activity of intestinal microflora. Similarly, Li et al. (2021) reported that berberine treatment affects the carbohydrate utilization by altering CAZy activity in the intestinal microflora. Alignment

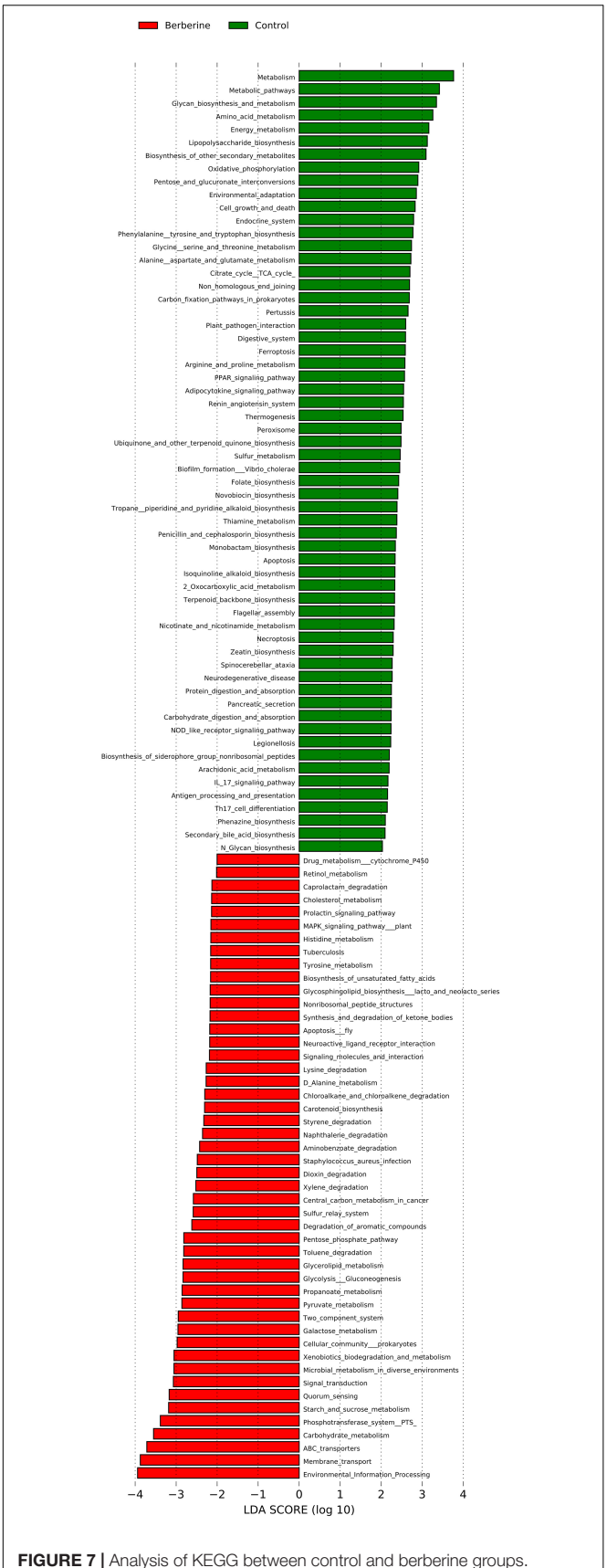

FIGURE 7 | Analysis of KEGG between control and berberine groups.

analysis based on KEGG database showed significantly enriched carbohydrate metabolism and environmental information processing pathways in the berberine group. Carbohydrate metabolism pathway mainly involves carbohydrate digestion to provide energy for microbial growth through fermentation in the large intestine, which leads to generation of volatile fatty acids and their derivatives to provide nutrition for the body (Tremaroli and Bäckhed, 2012). Environmental information processing pathway is related to the changes in intestinal microbiota (Arboleya et al., 2016).

CONCLUSION

In summary, there were microbial community and functional differences in the rectum of weaned piglets between the control and berberine groups. We demonstrated that berberine could improve the composition, abundance, structure, and function of gut microbiome in the weaned piglets. Our research might provide a novel scientific basis for the further development and application of berberine (such as replacing antibiotics) in the feed and food industries.

DATA AVAILABILITY STATEMENT

The raw sequencing data presented in the study are deposited in the National Center for Biotechnology Information (NCBI) Sequence Read Archive (SRA) repository, accession number PRJNA807368.

ETHICS STATEMENT

The animal study was reviewed and approved by the Animal Care and Use Committee of Anhui Science and Technology University.

AUTHOR CONTRIBUTIONS

HH and XB: data the collection and drafting the manuscript. HH, FZ, and XB: conceive and design the study. KX and KW: statistical analysis. FZ: critical revision of the manuscript. All authors contributed to the article and approved the submitted version.

FUNDING

This research was supported by the special Fund for Anhui Agriculture Research System (AGCYJSTX-05-15), the High-level Talents Introduction Foundation of Anhui Science and Technology University (DKYJ201802 and DKYJ202101), the Natural Science Key Foundation of Anhui Education Department (KJ2021A0868),the College Student Innovation and Entrepreneurship Project (202110879058; S202110879172), and Laboratory Open Project of Anhui Province Key Laboratory of Animal Nutrition Regulation and Health (APKLANRH202001).

REFERENCES

Abdel-Gadir, A., Stephen-Victor, E., Gerber, G. K., Rivas, M. N., Wang, S., Harb, H., et al. (2019). Microbiota therapy acts via a regulatory T cell MyD88/RORγt pathway to suppress food allergy. *Nat. Med.* 25, 1164–1174. doi: 10.1038/s41591-019-0461-z

Arboleya, S., Sánchez, B., Solís, G., Fernández, N., Suárez, M., Hernández-Barranco, A. M., et al. (2016). Impact of prematurity and perinatal antibiotics on the developing intestinal microbiota: a functional inference study. *Int. J. Mol. Sci.* 17:649. doi: 10.3390/ijms17050649

Chang, E. B., and Martinez-Guryn, K. (2019). Small intestinal microbiota: the neglected stepchild needed for fat digestion and absorption. *Gut Microbes* 10, 235–240. doi: 10.1080/19490976.2018.1502539

Chen, S., Zhou, Y., Chen, Y., and Gu, J. (2018). fastp: an ultra-fast all-in-one FASTQ preprocessor. *Bioinformatics* 34, 884–890. doi: 10.1093/bioinformatics/bty560

Cheng, H., Liu, J., Tan, Y., Feng, W., and Peng, C. (2021). Interactions between gut microbiota and berberine, a necessary procedure to understand the mechanisms of berberine. *J. Pharm. Anal.* 21, 117–119. doi: 10.1016/j.jpha.2021.10.003

Fraher, M. H., O'Toole, P. W., and Quigley, E. M. (2012). Techniques used to characterize the gut microbiota: a guide for the clinician. *Nat. Rev. Gastroenterol. Hepatol.* 9, 312–322. doi: 10.1038/nrgastro.2012.44

Fu, K., Xu, M., Zhou, Y., Li, X., Wang, Z., Liu, X., et al. (2020). The Satus quo and way forwards on the development of Tibetan medicine and the pharmacological research of Tibetan materia medica. *Pharmacol. Res.* 155:104688. doi: 10.1016/j.phrs.2020.104688

Guo, L., Zhang, D., Fu, S., Zhang, J., Zhang, X., He, J., et al. (2021). Metagenomic sequencing analysis of the effects of colistin sulfate on the pig gut microbiome. *Front. Vet. Sci.* 8:663820. doi: 10.3389/fvets.2021.663820

Guo, M., Huang, K., Chen, S., Qi, X., He, X., Cheng, W. H., et al. (2014). Combination of metagenomics and culture-based methods to study the interaction between ochratoxin A and gut microbiota. *Toxicol. Sci.* 141, 314–323. doi: 10.1093/toxsci/kfu128

Habtemariam, S. (2020). Berberine pharmacology and the gut microbiota: a hidden therapeutic link. *Pharmacol. Res.* 155:104722. doi: 10.1016/j.phrs.2020.104722

He, T., Zhu, Y. H., Yu, J., Xia, B., Liu, X., Yang, G. Y., et al. (2019). *Lactobacillus johnsonii* L531 reduces pathogen load and helps maintain short-chain fatty acid levels in the intestines of pigs challenged with *Salmonella enterica* infantis. *Vet. Microbiol.* 230, 187–194. doi: 10.1016/j.vetmic.2019.02.003

Huang, J., Feng, W., Li, S., Tang, H., Qin, S., Li, W., et al. (2021). Berberine exerts anti-cancer activity by modulating adenosine monophosphate-activated protein kinase (AMPK) and the phosphatidylinositol 3-kinase/protein kinase B (PI3K/AKT) signaling pathways. *Curr. Pharm. Des.* 27, 565–574. doi: 10.2174/1381612826666200928155728

Jamshaid, F., Dai, J., and Yang, L. X. (2020). New development of novel berberine derivatives against bacteria. *Mini Rev. Med. Chem.* 20, 716–724. doi: 10.2174/1389557520666200103115124

Jin, M., Qian, Z., Yin, J., Xu, W., and Zhou, X. (2019). The role of intestinal microbiota in cardiovascular disease. *J. Cell. Mol. Med.* 23, 2343–2350. doi: 10.1111/jcmm.14195

Ley, R. E. (2016). *Prevotella* in the gut: choose carefully. *Nat. Rev. Gastroenterol. Hepatol.* 13, 69–70. doi: 10.1038/nrgastro.2016.4

Li, X., Su, C., Jiang, Z., Yang, Y., Zhang, Y., Yang, M., et al. (2021). Berberine attenuates choline-induced atherosclerosis by inhibiting trimethylamine and trimethylamine-N-oxide production via manipulating the gut microbiome. *NPJ Biofilms Microbe* 7:36. doi: 10.1038/s41522-021-00205-8

Liao, Z., Xie, Y., Zhou, B., Zou, B., Xiao, D., Liu, W., et al. (2020). Berberine ameliorates colonic damage accompanied with the modulation of dysfunctional bacteria and functions in ulcerative colitis rats. *Appl. Microbiol. Biotechnol.* 104, 1737–1749. doi: 10.1007/s00253-019-10307-1

Liu, H., Hu, L., Han, X., Zhao, N., Xu, T., Ma, L., et al. (2020). Tibetan sheep adapt to plant phenology in alpine meadows by changing rumen microbial community structure and function. *Front. Microbiol.* 11:587558. doi: 10.3389/fmicb.2020.587558

Liu, J., Wang, H. W., Lin, L., Miao, C. Y., Zhang, Y., and Zhou, B. H. (2019). Intestinal barrier damage involved in intestinal microflora changes in fluoride-induced mice. *Chemosphere* 234, 409–418. doi: 10.1016/j.chemosphere.2019.06.080

Ma, N., and Ma, X. (2019). Dietary amino acids and the gut-microbiome-immune axis: physiological metabolism and therapeutic prospects. *Compr. Rev. Food Sci. Food Saf.* 18, 221–242. doi: 10.1111/1541-4337.12401

Moeser, A. J., Pohl, C. S., and Rajput, M. (2017). Weaning stress and gastrointestinal barrier development: implications for lifelong gut health in pigs. *Anim. Nutr.* 3, 313–321. doi: 10.1016/j.aninu.2017.06.003

National Research Council [NRC] (2012). *Nutrient Requirements of Swine*. Washington, DC: National Academy Press.

Patel, P. (2021). A bird's eye view on a therapeutically 'wonder molecule': berberine. *Phytomed. Plus* 1:100070. doi: 10.1016/j.phyplu.2021.100070

Prayogo, F. A., Budiharjo, A., Kusumaningrum, H. P., Wijanarka, W., Suprihadi, A., and Nurhayati, N. (2020). Metagenomic applications in exploration and development of novel enzymes from nature: a review. *J. Genet. Eng. Biotechnol.* 18:39. doi: 10.1186/s43141-020-00043-9

Quan, J., Cai, G., Yang, M., Zeng, Z., Ding, R., Wang, X., et al. (2019). Exploring the fecal microbial composition and metagenomic functional capacities associated with feed efficiency in commercial DLY pigs. *Front. Microbiol.* 10:52. doi: 10.3389/fmicb.2019.00052

Schippa, S., and Conte, M. P. (2014). Dysbiotic events in gut microbiota: impact on human health. *Nutrients* 6, 5786–5805. doi: 10.3390/nu6125786

Sun, M., Ma, N., He, T., Johnston, L. J., and Ma, X. (2020). Tryptophan (Trp) modulates gut homeostasis via aryl hydrocarbon receptor (AhR). *Crit. Rev. Food Sci.* 60, 1760–1768. doi: 10.1080/10408398.2019.1598334

Tremaroli, V., and Bäckhed, F. (2012). Functional interactions between the gut microbiota and host metabolism. *Nature* 489, 242–249. doi: 10.1038/nature11552

Upadhaya, S. D., and Kim, I. H. (2021). The impact of weaning stress on gut health and the mechanistic aspects of several feed additives contributing to improved gut health function in weanling piglets—a review. *Animals* 11:2418. doi: 10.3390/ani11082418

Walker, A. W., Duncan, S. H., Louis, P., and Flint, H. J. (2014). Phylogeny, culturing, and metagenomics of the human gut microbiota. *Trends. Microbiol.* 22, 267–274. doi: 10.1016/j.tim.2014.03.001

Wang, H., Ni, X., Qing, X., Zeng, D., Luo, M., Liu, L., et al. (2017). Live probiotic *Lactobacillus johnsonii* BS15 promotes growth performance and lowers fat deposition by improving lipid metabolism, intestinal development, and gut microflora in broilers. *Front. Microbiol.* 8:1073. doi: 10.3389/fmicb.2017.01073

Wang, H., Sun, Y., Xin, J., Zhang, T., Sun, N., Ni, X., et al. (2020). *Lactobacillus johnsonii* BS15 prevents psychological stress–induced memory dysfunction in mice by modulating the gut–brain axis. *Front. Microbiol.* 11:1941. doi: 10.3389/fmicb.2020.01941

Wang, K., Liao, M., Zhou, N., Bao, L., Ma, K., Zheng, Z., et al. (2019). *Parabacteroides distasonis* alleviates obesity and metabolic dysfunctions via production of succinate and secondary bile acids. *Cell Rep.* 26, 222–235. doi: 10.1016/j.celrep.2018.12.028

Wu, M., Yang, S., Wang, S., Cao, Y., Zhao, R., Li, X., et al. (2020). Effect of berberine on atherosclerosis and gut microbiota modulation and their correlation in high-fat diet-fed ApoE-/- mice. *Front. Pharmacol.* 11:223. doi: 10.3389/fphar.2020.00223

Xu, X., Yang, C., Chang, J., Wang, P., Yin, Q., Liu, C., et al. (2020). Dietary supplementation with compound probiotics and berberine alters piglet production performance and fecal microbiota. *Animals* 10:511. doi: 10.3390/ani10030511

Yadav, S., and Jha, R. (2019). Strategies to modulate the intestinal microbiota and their effects on nutrient utilization, performance, and health of poultry. *J. Anim. Sci. Biotechnol.* 10:2. doi: 10.1186/s40104-018-0310-9

Yang, H., Paruch, L., Chen, X., van Eerde, A., Skomedal, H., Wang, Y., et al. (2019). Antibiotic application and resistance in swine production in China: current situation and future perspectives. *Front. Vet. Sci.* 6:136. doi: 10.3389/fvets.2019.00136

Yu, C., Zhang, J., Qin, Q., Liu, J., Xu, J., and Xu, W. (2020). Berberine improved intestinal barrier function by modulating the intestinal microbiota in blunt snout bream (*Megalobrama amblycephala*) under dietary high-fat and high-carbohydrate stress. *Fish Shellfish Immunol.* 102, 336–349. doi: 10.1016/j.fsi.2020.04.052

Yu, M., Jin, X., Liang, C., Bu, F., Pan, D., He, Q., et al. (2020). Berberine for diarrhea in children and adults: a systematic review and meta-analysis. *Therap. Adv. Gastroenterol.* 13:1756284820961299. doi: 10.1177/1756284820961299

Yue, M., Tao, Y., Fang, Y., Lian, X., Zhang, Q., Xia, Y., et al. (2019). The gut microbiota modulator berberine ameliorates collagen-induced arthritis in rats by facilitating the generation of butyrate and adjusting the intestinal hypoxia and nitrate supply. *FASEB J.* 33, 12311–12323. doi: 10.1096/fj.201900425RR

Zhang, W., Xu, J. H., Yu, T., and Chen, Q. K. (2019). Effects of berberine and metformin on intestinal inflammation and gut microbiome composition in db/db mice. *Biomed. Pharmacother.* 118:109131. doi: 10.1016/j.biopha.2019.109131

Zhang, X., Zhao, Y., Zhang, M., Pang, X., Xu, J., Kang, C., et al. (2012). Structural changes of gut microbiota during berberine-mediated prevention of obesity and insulin resistance in high-fat diet-fed rats. *PLoS One* 7:e42529. doi: 10.1371/journal.pone.0042529

Zhou, J., He, Z., Yang, Y., Deng, Y., Tringe, S. G., and Alvarez-Cohen, L. (2015). High-throughput metagenomic technologies for complex microbial community analysis: open and closed formats. *mBio* 6:e02288-14. doi: 10.1128/mBio.02288-14

Zhu, C., Huang, K., Bai, Y., Feng, X., Gong, L., Wei, C., et al. (2021). Dietary supplementation with berberine improves growth performance and modulates the composition and function of cecal microbiota in yellow-feathered broilers. *Poult. Sci.* 100, 1034–1048. doi: 10.1016/j.psj.2020.10.071

Conflict of Interest: The authors declare that the research was conducted in the absence of any commercial or financial relationships that could be construed as a potential conflict of interest.

frontiers | Frontiers in Microbiology

ORIGINAL RESEARCH
published: 19 April 2022
doi: 10.3389/fmicb.2022.841662

Analgesic and Anxiolytic Effects of Gastrodin and Its Influences on Ferroptosis and Jejunal Microbiota in Complete Freund's Adjuvant-Injected Mice

Xin Chen[1,2†], Jinyue Wang[1†], Zhixian He[1], Xin Liu[1], Huawei Liu[2] and Xing Wang[1]*

[1]College of Medicine, Southwest Jiaotong University, Chengdu, China, [2]Department of Laboratory Medicine, The Affiliated Hospital of Southwest Jiaotong University, The Third People's Hospital of Chengdu, Chengdu, China

OPEN ACCESS

Edited by:
Zheng Ruan,
Nanchang University, China

Reviewed by:
Jian Du,
Huazhong Agricultural University, China
Hong Hu,
Anhui Science and Technology University, China

***Correspondence:**
Xing Wang
wshing@swjtu.edu.cn

†These authors have contributed equally to this work and share first authorship

Specialty section:
This article was submitted to Food Microbiology, a section of the journal Frontiers in Microbiology

Received: *22 December 2021*
Accepted: *11 February 2022*
Published: *19 April 2022*

Citation:
Chen X, Wang J, He Z, Liu X, Liu H and Wang X (2022) Analgesic and Anxiolytic Effects of Gastrodin and Its Influences on Ferroptosis and Jejunal Microbiota in Complete Freund's Adjuvant-Injected Mice. Front. Microbiol. 13:841662. doi: 10.3389/fmicb.2022.841662

This study investigated the effects of gastrodin (GAS) on analgesic, anxiolytic, ferroptosis, and jejunal microbiota in chronic inflammatory pain mice. The chronic inflammatory pain model of C57BL/6J mice was established by hindpaw injection of complete Freund's adjuvant (CFA). After GAS treatment, thermal hyperalgesia test, mechanical allodynia test, elevated plus-maze (EPMT), and open-field test (OFT) were performed to assess the behavioral changes of pain and anxiety. mRNAs of FTHI, GPX4, HO-1, and PTGS2 and jejunal microbiota were measured by qPCR. In CFA-injected C57BL/6 mice, we found that the mechanical and thermal pain threshold were increased with treatment of GAS. In EPMT, the number of entries in open arms and retention times of open arms were increased by GAS. In the OFT, the time spent in the central area was also increased. Furthermore, GAS enhanced mRNA expressions of FTHI, GPX4, and HO-1 but decreased the expression of PTGS2 in a dose-dependent manner. GAS is effective in the treatment of mice chronic inflammatory pain and anxiety-like behaviors. It may be exhibits potential neuroprotective effects through inhibition of ferroptosis independently of the intestinal microbiota.

Keywords: gastrodin, analgesic, anxiolytic, ferroptosis, microbiota

INTRODUCTION

Ferroptosis is a unique iron-dependent form of regulated cell death (Dixon et al., 2012). The accumulation of lipid peroxidation products and lethal reactive oxygen species (ROS) is the main characteristic of ferroptosis (Xie et al., 2016). Ferroptosis, as a way to promote cell death, may be implicated in the occurrence and development of many diseases. Studies have shown the importance of ferroptosis in many diseases of the central nervous system, such as Alzheimer's disease (AD), Parkinson's disease (PD), Huntington's disease (HD), amyotrophic lateral sclerosis (ALS), and traumatic brain injury (TBI; Wu et al., 2018).

Gastrodiae Rhizoma (Tianma), a notable Chinese herb, is dry tubers of *Gastrodia elata Blume* which belongs to Orchidaceae. *Gastrodiae Rhizoma* is considered a top-grade medicine

described to treat the hypertension of liver-yang hyperactivity in the tradition Chinese medicine. Studies have shown that the application of *gastrodia elatahas* biological activities of anticonvulsion, antioxidation, neuroprotection, anti-denguevirus, anti-cardio-cerebral-vascular diseases, and anti-inflammation (Ahn et al., 2007; Han et al., 2014; Zhan et al., 2016). The major active component and material basis of *Gastrodia elata* are Gastrodin (GAS). GAS, a chemical compound that known as 4-hydroxybenzyl alcohol-4O-β-D-glucopyranoside, is isolated from the rhizome of *Gastrodia elata*. Furthermore, the molecular formula of GAS is $C_{13}H_{18}O_7$, and its chemical structural formula is shown in **Figure 1**. GAS has numerous pharmacological activities including analgesic (Guo et al., 2013), antidepressant (Chen and Sheen, 2011), anxiolytic (Peng et al., 2013), anti-inflammatory (Kim et al., 2012), antiobesity (Park et al., 2011), and memory and retrieval improvements (Wu et al., 1996; Hsieh et al., 1997). Among them, analgesic, antioxidant, anti-inflammatory, and neuroprotective effects are the main research hotspots in recent years. Recent findings suggest that GAS exerts a protective effect on primary neural progenitor cells (NPCs) by resisting amyloidβ (Aβ; 1–42)-induced neurotoxicity (Li and Qian, 2016). In the meantime, GAS increased the expression of HO-1, Nrf2, and GPX4 protein in Rat Glioma Cell Line C6, which protected Rat Glioma Cell Line C6 from ferroptosis induced by H_2O_2 (Jiang et al., 2020). In recent years, several neuroprotective mechanisms of GAS have been fund. However, the study regarding to the effects of Gas on ferroptosis is rare. GAS was also reported to display powerful anti-inflammation properties. Based on the above research progress and analysis, it is speculated that GAS might be a potential therapeutic for the inhibition of ferroptosis. This study was designed to explore the analgesic, anti-inflammatory, and anxiolytic effects of GAS. We also examined whether GAS can exhibit neuroprotective effect through inhibition of ferroptosis, as well as its relation with intestinal microbiota.

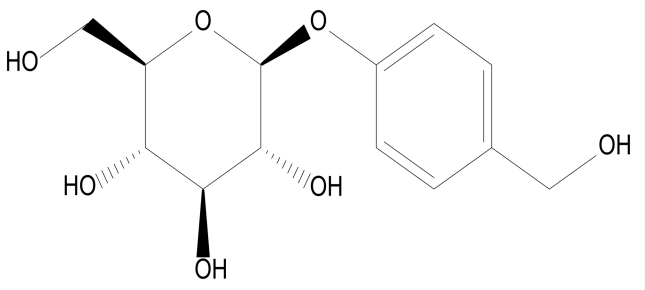

FIGURE 1 | The chemical structural formula of gastrodin (GAS).

Abbreviations: GAS, Gastrodin; CFA, Complete Freund's adjuvant; EPMT, Elevated plus-maze test; OFT, Open-field test; GPX4, Glutathione peroxidase; FTH1, Ferritin heavy chain 1; HO-1, The heme oxygenase-1; PTGS2, Prostaglandin-endoperoxide synthase2; ROS, Reactive oxygen species; ACC, Anterior cingulate cortex; Nrf2, Nuclear factor erythroid 2-relatedfactor2.

MATERIALS AND METHODS

Materials

Gastrodin was purchased from Nanjing Baide Biotechnology Co., Ltd. (>99% purity, Nanjing, China). Complete Freund's adjuvant (CFA) and Von Frey filaments were purchased from Sigma (St. Louis, MO). Elevated Plus-Maze Video Tracking System was purchased from Shanghai Xinruan Information Technology Co., Ltd. (Shanghai, China). YLS-6A Intelligent hot plate was purchased from Jinan Yiyan Technology Development Co., Ltd. (Shandong, China). ABI7500 Real-Time PCR Detection Systems were purchased from Bio-Rad (Hercules, California). AxyPrep™ Multisource Total RNA was purchased from AXYGEN (Silicon Valley, California). SYBR Green qPCR Mix (2×) was purchased from Beyotime Biotechnology (Shanghai, China). D7260 Prime Script™ RT Reagent Kit was purchased from TaKaRa (Liaoning, China); RR037A primer was purchased from Sangon Biotech (Shanghai, China).

Animals and Grouping

Male C57BL/6J mice (aged 8 weeks, weighing 21–25 g) were purchased from Chengdu Dashuo Laboratory Animal. Animals were housed in groups of six mice with a temperature (20 ± 2°C), humidity (55 ± 15%), and lighting (12 h light/dark cycle, lights on at 7:00 AM). All animals must adapt to conditions for at least 7 days after they arrived. Food and water were freely available. All experimental procedures were approved by the Animal Ethics Committee of Southwest Jiaotong University and were conducted in accordance with the university's animal experiment guidelines.

The rats were randomly divided into four groups of six individuals each as follows: Blank group [physiological saline (SAL)-treated group, $n = 6$], model group (The CFA-induced plus SAL-treated group, $n = 6$), the CFA-induced plus 100 mg/kg GAS-treated group (CFA + GAS 100 group, $n = 6$), and the CFA-induced plus 200 mg/kg GAS-treated group (CFA + GAS 200 group, $n = 6$).

Experimental Designs and GAS Treatment

A total of 10 μl CFA (50%) was injected intraplantar subcutaneously into the left hindpaws of mice to established chronic peripheral inflammatory pain. In the control group, the same volume of SAL was injected into the hindpaws of mice. GAS was dissolved in saline before use. The mice were intraperitoneally injected with GAS (100 and 200 mg/kg) after CFA insult GAS or saline was used repeatedly in mice once a day for 2 weeks.

Mechanical Allodynia

Mechanical allodynia was assessed with a set of von Frey filaments on day 1, 4, 7, and 14. Mice were placed on a wire mesh covered with organic glass and acclimated to the environment at least 30 min prior to test. Start with 0.4 mN (#2.44) filament and stimulate the center of left hindpaw until filament bending for 3 s, and the mice have reactions like licking foot or foot lifting.

TABLE 1 | Specific gene primes sequences.

Gene name	Forward prime (5′–3′)	Reverse prime (5′–3′)	Accession number
HO-1	AGACACCGCTCCTCCAGT	TCAGGTATCTCCCTCCATT	NM_010442
FTH1	GCAGGATATAAAGAAACCAGA	TCTCAATGAAGTCACATAAGT	NM_010239
GPX4	GTCTGGCAGGCACCATGT	GTGACGATGCACACGAAACC	NM_008162
PTGS2	TGGAGGCGAAGTGGGTTTTA	GAGTGGGAGGCACTTGCATT	NM_011198
GAPDH	GCAGAATTCCTGGCCAAGGTCATCCATGAC	GCAGGTACCGGGGCCATCCACAGTCTTCTG	NM_001289726

TABLE 2 | Primes for real-time PCR of bacteria.

Item	Primer sequence (5′–3′)	Amplicon length (bp)
Bacteroidetes	Forward: GGARCATGTGGTTTAATTCGATGAT Reverse: AGCTGACGACAACCATGCAG	126
Firmicutes	Forward: GGAGYATGTGGTTTAATTCGAAGCA Reverse: AGCTGACGACAACCATGCAC	126
Lactobacillus	Forward: AGCAGTAGGGAATCTTCCA Reverse: ATTCCACCGCTACACATG	345

Thermal Hyperalgesia

After 14 days of administration, the temperature of the hot plate was set to 55°C. The left hindpaw of mice was placed on the hot plate, and time was recorded when the mice had reactions like foot lifting.

Elevated Plus-Maze Test

Mice were placed in the central zone of the maze facing the closed arm, and the time was recorded for 5 min. Outcome measures: the number of entries in open arms, retention times of open arms, the number of entries in closed arms, and retention times of closed arms. The number of entries in open arms and retention times of open arms were negatively correlated with anxiety in mice.

Open-Field Test

Mice were placed in the center of the box, and the time of mice entering the central area was videotaped. The observation time is 5 min.

Intestinal Histomorphology

Specimens of cross-sections of jejunum were embedded in paraffin wax and cut into 5 μm thick histological sections for hematoxylin and eosin staining. An image processing and analysis system were used to measure tissue sections under a microscope. The villus height, crypt depth, and the ration of villus height to crypt depth (VC) of the jejunum were measured by Image-Pro Plus 6.0.

Real-Time Quantitative PCR

The total RNA was extracted from the ACC and the spinalcord of the rat lumbosacral enlargement (L4-5) using TRIZOL reagent (TaKaRa, Dalian, China). D7260 Prime Script™ RT Reagent Kit performed reverse transcription for the synthesis of cDNA. Reverse transcription was the performed *via* Real-Time PCR System in a 20 μl reaction mixture and while following the manufacturer's instructions. SYBR Green qPCR Mix (2×) was used for QRT-PCR. The primers utilized here are shown in (**Table 1**).

Jejunal Microbiota Analysis

Bacterial DNA was extracted from jejunal digesta using the QIAamp DNA Stool Kit (Qiagen, Hilden, Germany) according to the manufacturer's instructions. Bacterial DNA extracted from the jejunal digesta was used for gene sequence amplification by quantitative PCR using the primers specified in **Table 2**. Primer specificity was assessed on the basis of the 16S rRNA gene sequence. The reaction conditions for quantitative PCR were as follows: 50°C for 2 min, 95°C for 5 min and 40 cycles of denaturation at 94°C for 20 s, primer annealing at a species-specific temperature for 30 s, and primer extension at 60°C for 1 min.

Statistical Analysis

All results are presented as mean ± standard deviation (SD) and were analyzed using SPSS (Version 13.0, Chicago, United States). A p value <0.05 was considered to be statistically significant.

RESULTS

Effects of GAS on CFA-Induced Mechanical and Thermal Hypersensitivity

After CFA was injected into mice, mechanical thresholds were determined on day 1, 4, 7, and 14. As shown in **Figure 2**, on the first day after CFA injection, the mechanical pain threshold of the model group was significantly lower than blank group, and the left hindpaw of mice was obviously swollen, indicating that the chronic inflammatory pain model was successfully established. The paw withdrawal threshold of CFA-injected mice significantly decreased after CFA injection for 1–4 days. Meanwhile, the administration of GAS (100 and 200 mg/kg) increased the paw withdrawal threshold in CFA-injected mice. GAS also attenuated thermal hyperalgesia in CFA-injected mice (**Figure 3**). Moreover, GAS dose-dependently increased the mechanical and thermal pain threshold in mice.

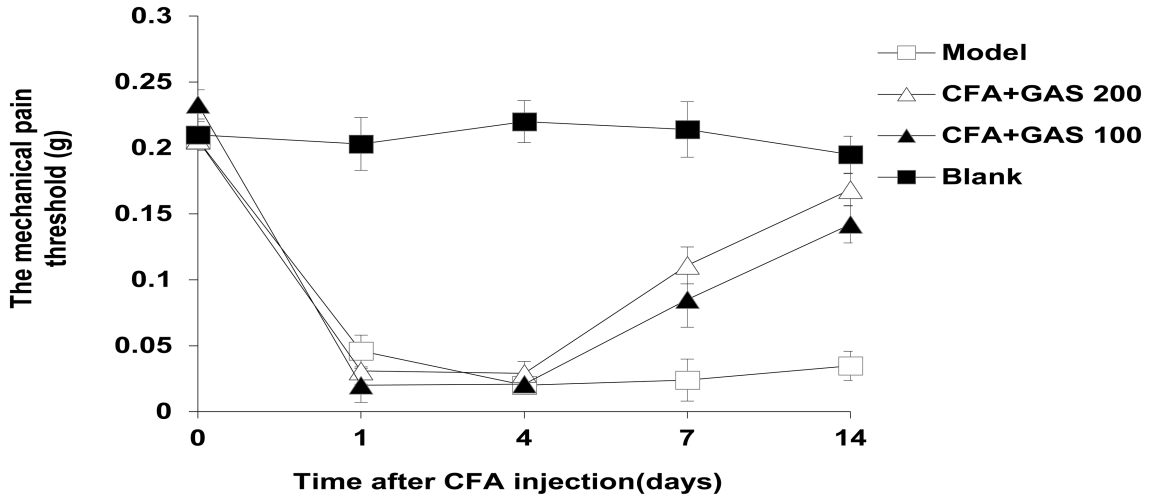

FIGURE 2 | Changes of the paw withdrawal threshold after complete Freund's adjuvant (CFA) injection.

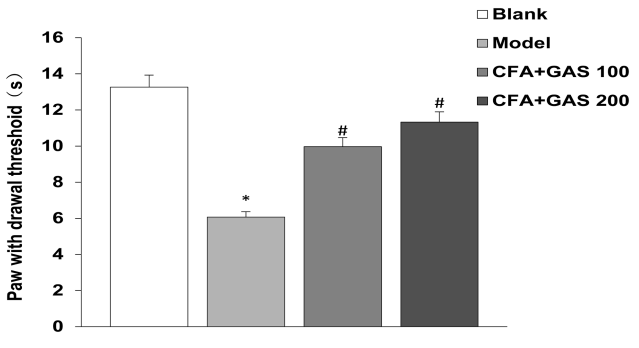

FIGURE 3 | The paw withdrawal latency of mice(s) ($^{*}p < 0.05$ compared with blank group; $^{\#}p < 0.05$ compared with model group).

Effects of GAS on CFA-Induced Anxiety-Like Behavior

Anxiety-like behaviors of animal are determined by EPMT and OFT. In EPMT, after CFA injection, the number of entries in open arms and retention times of open arms significantly decreased. Moreover, compared with the model group, the number of entries in open arms and retention times of open arms in the GAS-treated group were increased (**Figures 4A,B**). In the OFT, compared with the blank group, the time spent in the central area decreased in the model group, while the GAS (100 and 200 mg/kg) reversed the reduction caused by CFA (**Figure 5**). The results show that GAS attenuated CFA-induced anxiety-like behavior.

Effects of GAS on Ferroptosis-Related Gene Expression

The mRNA expressions of FTHI, GPX4, HO-1, and PTGS2 in the anterior cingulate cortex (ACC) and L4-5 of mice on day 14 after CFA injection were detected through qPCR. The relative expression levels of ferroptosis-related genes were shown in **Figure 6**. In the ACC and L4-5, both FTH1 and GPX4 were significantly decreased on the model group as compared with blank group. Meanwhile, we found that CFA elevated the expression levels of PTGS2 and HO-1. Compared with the model group, FTH1, GPX4, and HO-1 in GAS groups were significantly increased while PTGS2 decreased in a dose-dependent pattern. Taken together, GAS increased the FTHI, GPX4, HO-1, and PTGS2 mRNA expressions but did not change the jejunal microbiota.

Effects of GAS on Jejunal Structure and Microbiota

The effects of GAS jejunal morphological characteristics and microbiota are shown in **Figures 7, 8**, respectively. The jejunum villus length was decreased in the model group, whereas the villus length was increased in GAS groups (100 and 200 mg/kg). In addition, CFA decreased the Bacteroidetes and Firmicutes species without affecting *Lactobacillus* species. However, the jejunal microbiota did not change after GAS treatment.

DISCUSSION

Acute inflammatory pain induced by injection of CFA. In this process, rats were allergic to mechanical allodynia and thermal hyperalgesia, and the pain-induced anxiogenic effect lasted for more than 14 days (Nagakura et al., 2003). Clinically, it has been reported that chronic pain leads to mental problems such as anxiety and depression, which seriously reduces the quality of life of patients and hinders their normal life (Gallagher et al., 1995). GAS is a phenolic glucoside with significant analgesic and anti-inflammatory effects. In the CFA-induced chronic inflammatory pain model, we found that mechanical and thermal pain threshold were increased with treatment of

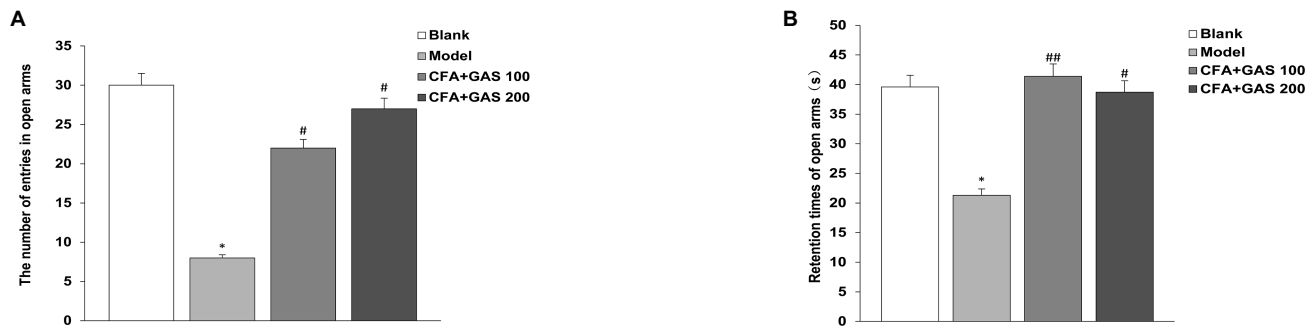

FIGURE 4 | Effect of GAS on results of Morris water maze test. **(A)** The number of entries in open arms. **(B)** Retention times of open arms ($^{*}p < 0.05$ compared with blank group; $^{\#\#}p < 0.01$ and $^{\#}p < 0.05$ compared with model group).

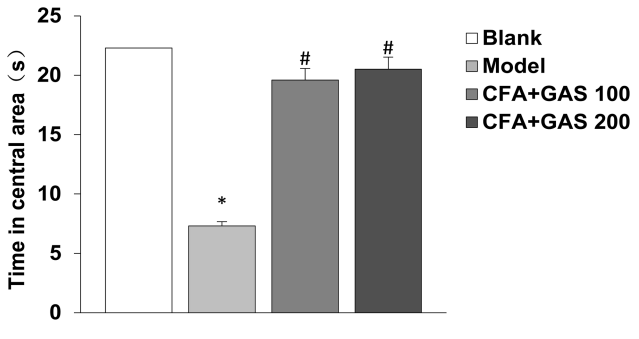

FIGURE 5 | Effect of GAS on results of OFT ($^{*}p < 0.05$ compared with blank group; $^{\#}p < 0.05$ compared with model group).

GAS in a dose-dependent pattern. In addition, the number of entries in open arms and retention times of open arms were increased by GAS. These studies further confirmed that GAS has powerful analgesic, anti-inflammatory, and anti-anxiety effects in the chronic inflammatory pain model of mice. GAS exerted analgesic and anti-inflammatory effects by decreasing the activation of astrocyte and microglia and the induction of TNF-α and IL-6 in the ACC (Sun et al., 2016). In a mouse model of chemotherapeutic agent-induced neuropathic pain, 5-HT 1A receptor can mediate the powerful antinociceptive of GAS (Guo et al., 2013).

Inflammatory disease (ID) is a series of diseases characterized by inflammatory response, and ferroptosis is closely related to inflammatory response (Andersen et al., 2020). There are some inflammatory factors related to the metabolism of peroxides and arachidonic acid in ferroptosis tissues (Stockwell et al., 2020). Studies have shown that both ferroptosis and inflammatory diseases have the depletion of Gx4 and GSH, the increase of lipid peroxidation products, and the interruption of iron metabolism (Mao et al., 2020). At present, although a variety of molecular mechanisms and signaling pathways can lead to ferroptosis, iron metabolism and lipid peroxidation signaling are the main way to regulate ferroptosis (Dixon et al., 2015). During iron metabolism, excessive iron leads to ferroptosis by producing ROS. Ferritin heavy chain 1 (FTH1), as an iron storage protein complex, is involved in the uptake of excessive iron (Xie et al., 2016). We found that GAS increased the expression of FTH1 and thus balanced intracellular iron levels. The heme oxygenase-1 (HO-1), a major intracellular source of iron (Kwon et al., 2015), plays an important role in ferroptosis and inflammation. It was reported that p38 MAPK phosphorylation could mediate the protective effect of GAS on H_2O_2-induced oxidative stress (Zhang et al., 2018). GAS could ameliorate MPP+-induced oxidative stress by regulating the expression of HO-1 in human dopaminergic cells (Jiang et al., 2014). We also demonstrated that GAS increases HO-1 expression, which accelerates the decomposition of heme and inhibits inflammation. In addition, the expressions of glutathione peroxidase4 (GPX4) and prostaglandin-endoperoxide synthase2 (PTGS2) are also important for the induction of ferroptosis.

In our experiments, GAS significantly upregulates the expression of FTH1 and GPX4, decreases PTGS2 expression, and suggests that GAS against ferroptosis by reducing lipid peroxidation. CFA-induced chronic inflammatory pain is accompanied by the ferroptosis of neuronal cells, and GAS has an inhibitory effect on ferroptosis, which is one of the possible mechanisms to protect neuronal cells.

DATA AVAILABILITY STATEMENT

The original contributions presented in the study are included in the article/supplementary material, further inquiries can be directed to the corresponding author.

ETHICS STATEMENT

All experimental procedures were approved by the Animal Ethics Committee of Southwest Jiaotong University and were conducted in accordance with the university's animal experiment guidelines.

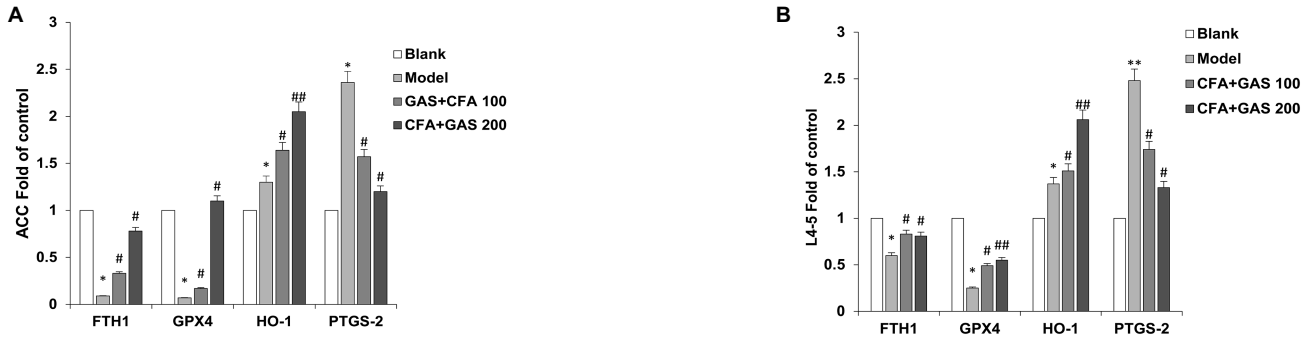

FIGURE 6 | $2^{-(\Delta\Delta Ct)}$ value of genes in ACC and L4-5. **(A)** $2^{-(\Delta\Delta Ct)}$ value of ferroptosis-related genes in ACC **(B)** $2^{-(\Delta\Delta Ct)}$ value value of ferroptosis-related genes in L4-5. $^{*}p<0.05$ and $^{**}p<0.01$ compared with blank group; $^{\#\#}p<0.01$ and $^{\#}p<0.05$ compared with model group.

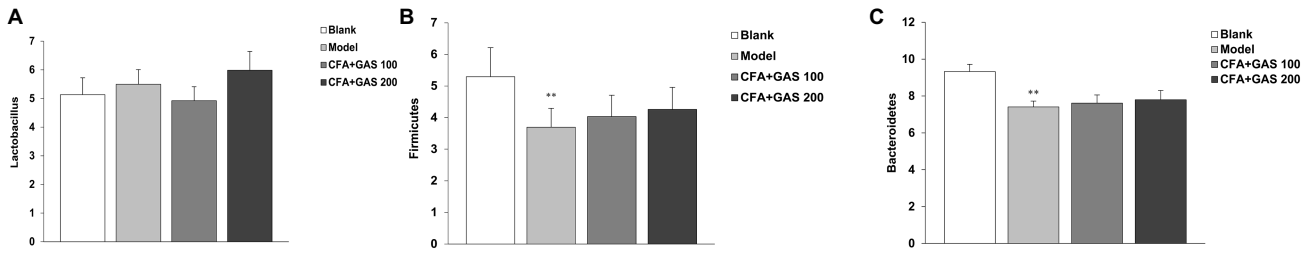

FIGURE 7 | Effect of GAS on jejunal microbiota. **(A)** Effect of GAS on Lactobacillus species. **(B)** Effect of GAS on Firmicutes species. **(C)** Effect of GAS on Bacteroidetes species. $^{**}p<0.01$ compared with blank group.

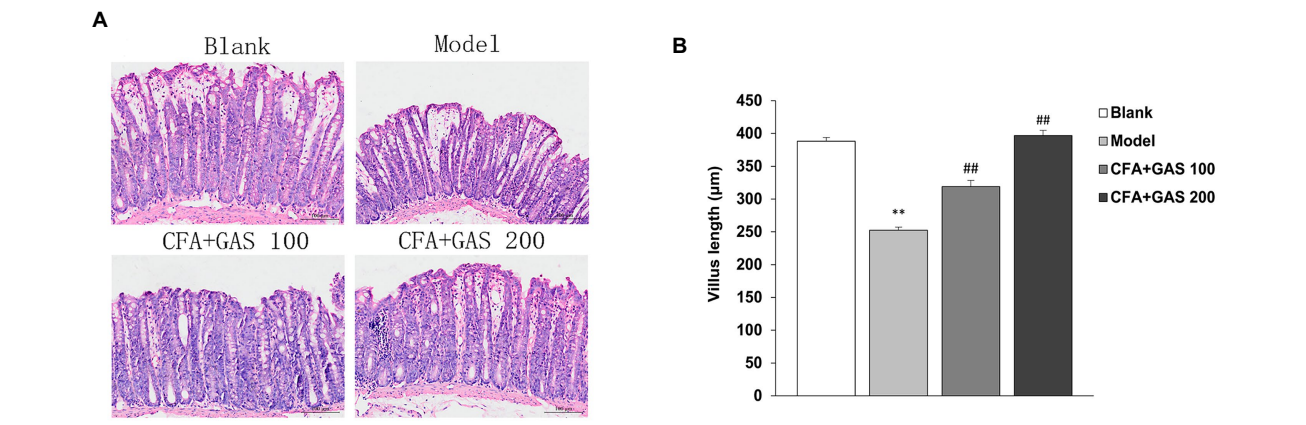

FIGURE 8 | Effect of GAS on jejunal microbiota. **(A)** Characteristics of jejunal villi of mice in each group. **(B)** Effect of GAS on jejunum villus length. $^{**}p<0.01$ compared with blank group; $^{\#\#}p<0.01$ compared with model group.

AUTHOR CONTRIBUTIONS

JW and ZH: data collection. XW and XL: conceive and design the study. JW and XL: statistical analysis. XC, JW, and ZH: drafting the manuscript. XC and HL: critical revision of the manuscript. All authors contributed to the article and approved the submitted version.

FUNDING

This work was supported by the Science and Technology Department of Sichuan Province (project no.: 2018FZ0096) and the Fundamental Research Funds for the Central Universities (project no.: A0920502052001-10).

REFERENCES

Ahn, E. K., Jeon, H. J., Lim, E.-J., Jung, H. J., and Park, E. H. (2007). Anti-inflammatory and anti-angiogenic activities of *Gastrodia elata* Blume. *J. Ethnopharmacol.* 110, 476–482. doi: 10.1016/j.jep.2006.10.006

Andersen, V., Mller, S., Jensen, P. B., Mller, F. T., and Green, A. (2020). Caesarean delivery and risk of chronic inflammatory diseases (inflammatory bowel disease, rheumatoid arthritis, coeliac disease, and diabetes mellitus): a population based registry study of 2,699,479 births in Denmark during 1973–2016. *Clin. Epidemiol.* 12, 287–293. doi: 10.2147/CLEP.S229056

Chen, P. J., and Sheen, L. Y. (2011). Gastrodiae Rhizoma (tiān má): a review of biological activity and antidepressant mechanisms. *J. Tradit. Complement. Med.* 1, 31–40. doi: 10.1016/S2225-4110(16)30054-2

Dixon, S. J., Lemberg, K. M., Lamprecht, M. R., Skouta, R., Zaitsev, E. M., Gleason, C. E., et al. (2012). Ferroptosis: an iron-dependent form of nonapoptotic cell death. *Cell* 149, 1060–1072. doi: 10.1016/j.cell.2012.03.042

Dixon, S. J., Winter, G. E., Musavi, L. S., Lee, E., Snijder, B., Rebsamen, M., et al. (2015). Human haploid cell genetics reveals roles for lipid metabolism genes in nonapoptotic cell death. *ACS Chem. Biol.* 10, 1604–1609. doi: 10.1021/acschembio.5b00245

Gallagher, R. M., Moore, P., and Chernoff, I. (1995). The reliability of depression diagnosis in chronic low back pain. A pilot study. *Gen. Hosp. Psychiatry* 17, 399–413. doi: 10.1016/0163-8343(95)00088-7

Guo, Z. G., Jia, X. P., Su, X. J., Li, P., and Hao, J. H. (2013). Gastrodin attenuates vincristine-induced mechanical hyperalgesia through serotonin 5-HT1A receptors. *Bangladesh J. Pharmacol.* 8, 414–419. doi: 10.3329/bjp.v8i4.16836

Han, Y. J., Je, J. H., Kim, S. H., Ahn, S. M., Kim, H. N., Kim, Y. R., et al. (2014). *Gastrodia elata* shows neuroprotective effects via activation of PI3K signaling against oxidative glutamate toxicity in HT22 cells. *Am. J. Chin. Med.* 42, 1007–1019. doi: 10.1142/S0192415X14500633

Hsieh, M. T., Wu, C. R., and Chen, C. F. (1997). Gastrodin and p-hydroxybenzyl alcohol facilitate memory consolidation and retrieval, but not acquisition, on the passive avoidance task in rats. *J. Ethnopharmacol.* 56, 45–54. doi: 10.1016/S0378-8741(96)01501-2

Jiang, T., Chu, J., Chen, H., Cheng, H., and Li, Q. (2020). Gastrodin inhibits H_2O_2-induced ferroptosis through its antioxidative effect in rat glioma cell line C6. *Biol. Pharm. Bull.* 43, 480–487. doi: 10.1248/bpb.b19-00824

Jiang, G., Hu, Y., Liu, L., Cai, J., Peng, C., and Li, Q. (2014). Gastrodin protects against MPP(+)-induced oxidative stress by up regulates heme oxygenase-1 expression through p38 MAPK/Nrf2 pathway in human dopaminergic cells. *Neurochem. Int.* 75, 79–88. doi: 10.1016/j.neuint.2014.06.003

Kim, B. W., Koppula, S., Kim, J. W., Lim, H. W., Hwang, J. W., Kim, I. S., et al. (2012). Modulation of LPS-stimulated neuroinflammation in BV-2 microglia by *Gastrodia elata*: 4-Hydroxybenzyl alcohol is the bioactive candidate. *J. Ethnopharmacol.* 139, 549–557. doi: 10.1016/j.jep.2011.11.048

Kwon, M. Y., Park, E., Lee, S. J., and Su, W. C. (2015). Heme oxygenase-1 accelerates erastin-induced ferroptotic cell death. *Oncotarget* 6, 24393–24403. doi: 10.18632/oncotarget.5162

Li, M., and Qian, S. (2016). Gastrodin protects neural progenitor cells against amyloid β (1–42)-induced neurotoxicity and improves hippocampal neurogenesis in amyloid β (1–42)-injected mice. *J. Mol. Neurosci.* 60, 21–32. doi: 10.1007/s12031-016-0758-z

Mao, H., Zhao, Y., Li, H., and Lei, L. (2020). Ferroptosis as an emerging target in inflammatory diseases. *Prog. Biophys. Mol. Biol.* 155, 20–28. doi: 10.1016/j.pbiomolbio.2020.04.001

Nagakura, Y., Okada, M., Kohara, A., Kiso, T., Toya, T., Iwai, A., et al. (2003). Allodynia and hyperalgesia in adjuvant-induced arthritic rats: time course of progression and efficacy of analgesics. *J. Pharmacol. Exp. Ther.* 306, 490–497. doi: 10.1124/jpet.103.050781

Park, S., Da, S. K., and Kang, S. (2011). *Gastrodia elata* Blume water extracts improve insulin resistance by decreasing body fat in diet-induced obese rats: vanillin and 4-hydroxybenzaldehyde are the bioactive candidates. *Eur. J. Nutr.* 50, 107–118. doi: 10.1007/s00394-010-0120-0

Peng, Z., Wang, H., Zhang, R., Chen, Y., Xue, F., Nie, H., et al. (2013). Gastrodin ameliorates anxiety-like behaviors and inhibits IL-1β level and p38 MAPK phosphorylation of hippocampus in the rat model of posttraumatic stress disorder. *Physiol. Res.* 62, 537–545. doi: 10.33549/physiolres.932507

Stockwell, B. R., Jiang, X., and Gu, W. (2020). Emerging mechanisms and disease relevance of ferroptosis. *Trends Cell Biol.* 30, 478–490. doi: 10.1016/j.tcb.2020.02.009

Sun, T., Wang, J., Li, X., Li, Y. J., Feng, D., Shi, W. L., et al. (2016). Gastrodin relieved complete Freund's adjuvant-induced spontaneous pain by inhibiting inflammatory response. *Int. Immunopharmacol.* 41, 66–73. doi: 10.1016/j.intimp.2016.10.020

Wu, C. R., Hsieh, M. T., Huang, S. C., Peng, W. H., and Chen, C. (1996). Effects of *Gastrodia elata* and its active constituents on scopolamine-induced amnesia in rats. *Planta Med.* 62, 317–321. doi: 10.1055/s-2006-957892

Wu, J. R., Qing-Zhang, T., and Lei, P. (2018). Ferroptosis, a recent defined form of critical cell death in neurological disorders. *J. Mol. Neurosci.* 66, 197–206. doi: 10.1007/s12031-018-1155-6

Xie, Y., Hou, W., Song, X., Yu, Y., Huang, J., Sun, X., et al. (2016). Ferroptosis: process and function. *Cell Death Differ.* 23, 369–379. doi: 10.1038/cdd.2015.158

Zhan, H. D., Zhou, H. Y., Du, X. L., Sui, Y. P., Wang, W. H., Dai, L., et al. (2016). The rhizome of *Gastrodia elata* Blume–an ethnopharmacological review. *J. Ethnopharmacol.* 189, 361–385. doi: 10.1016/j.jep.2016.06.057

Zhang, H., Yuan, B., Huang, H., Qu, S., Yang, S., and Zeng, Z. (2018). Gastrodin induced HO-1 and Nrf2 up-regulation to alleviate H_2O_2-induced oxidative stress in mouse liver sinusoidal endothelial cells through p38 MAPK phosphorylation. *Rev. Bras. Pesqui. Med. Biol.* 51, 51–61. doi: 10.1590/1414-431x20187439

Conflict of Interest: The authors declare that the research was conducted in the absence of any commercial or financial relationships that could be construed as a potential conflict of interest.

Advantages of publishing in Frontiers

OPEN ACCESS
Articles are free to read for greatest visibility and readership

FAST PUBLICATION
Around 90 days from submission to decision

HIGH QUALITY PEER-REVIEW
Rigorous, collaborative, and constructive peer-review

TRANSPARENT PEER-REVIEW
Editors and reviewers acknowledged by name on published articles

Frontiers
Avenue du Tribunal-Fédéral 34
1005 Lausanne | Switzerland

Visit us: www.frontiersin.org
Contact us: frontiersin.org/about/contact

REPRODUCIBILITY OF RESEARCH
Support open data and methods to enhance research reproducibility

DIGITAL PUBLISHING
Articles designed for optimal readership across devices

FOLLOW US
@frontiersin

IMPACT METRICS
Advanced article metrics track visibility across digital media

EXTENSIVE PROMOTION
Marketing and promotion of impactful research

LOOP RESEARCH NETWORK
Our network increases your article's readership